University of Nevada, Reno

Climate Change and Groundwater Use Impacts to Groundwater and Spring Hydrology, Amargosa Desert, Nevada and Death Valley National Park, California

A thesis submitted in partial fulfillment of the requirements for the degree of Master of Science in Hydrogeology

by

Terry T. Fisk

Dr. Greg Pohll/Thesis Advisor

August 2011

University of Nevada, Reno
Statewide • Worldwide

THE GRADUATE SCHOOL

We recommend that the thesis
prepared under our supervision by

TERRY T. FISK

entitled

Climate Change And Groundwater Use Impacts To Groundwater And Spring Hydrology Amargosa Desert, Nevada And Death Valley National Park, California

be accepted in partial fulfillment of the
requirements for the degree of

MASTER OF SCIENCE

Greg Pohll, Ph.D., Advisor

Donald Sada, Ph.D., Committee Member

Mark Stone, Ph.D., Graduate School Representative

Marsha H. Read, Ph. D., Associate Dean, Graduate School

August, 2011

Abstract

This project evaluates the affects of climate change, and to some degree groundwater pumping, on the magnitude and timing of changes in groundwater levels and spring discharge in the Amargosa Desert in southwest Nevada and a portion of Death Valley National Park in eastern California. This is important because, almost without exception, groundwater is the sole source of water for ecosystem and human needs in southern Nevada and Death Valley National Park. The research focused on how the groundwater flow system in the Amargosa Desert, Nevada and Furnace Creek area of Death Valley National Park will respond to climate change, and comparison of the magnitude of climate response to that of continued groundwater pumping. This research will assist in developing a quantitative understanding of groundwater – spring dynamics so that changes to aquatic ecosystems that depend on groundwater flow may be predicted. The U.S. Geological Survey transient groundwater model for the Death Valley Regional Flow System was used for this project. Impacts to the groundwater flow system corresponding to possible climate change scenarios were simulated by varying recharge in the model. Synthesized results of global circulation climate models downscaled to the Death Valley region indicate average temperature will increase by approximately 3.4°C and average precipitation will decline by approximately 0.33 millimeters per month during the 21st Century. Simulated groundwater head changes resulting from climate change relative to baseline 20th Century conditions ranged from an increase of 0.34 meters to a decline of 2 meters, depending on the recharge (climate) scenario. Simulated groundwater discharge changes relative to baseline conditions ranged from an increase of 369 m^3/day to a decline of 2,130 m^3/day. The primary conclusion of this project is that climate change will affect the Amargosa Desert and Death Valley groundwater system and will likely exacerbate conditions of limited water supply. However, local and regional groundwater pumping have and will continue to have much greater affect on the groundwater system. Even if climate

change results in increased precipitation and recharge, groundwater decline will continue as a result of pumping in the Death Valley regional groundwater flow system.

Acknowledgements

I would like to Acknowledge my Committee: Greg Pohll, Don Sada, and Mark Stone for their support of my thesis and overall graduate school endeavors. Greg is a superb advisor and I am indebted to him for his ability to pass on knowledge and willingness to take on a non traditional student. Don and Mark worked with me for many years before I returned to school, and their encouragement was a significant element in my decision to pursue a graduate degree.

This research was funded by the National Science Foundation, Nevada Experimental Program for the Stimulation of Competitive Research (EPSCoR), Agreement Number EPS-0814372. My appreciation goes out to the National Science Foundation and the Nevada EPSCoR program for their support.

I wish to thank Debra Hughson, Ph.D. of the Mojave National Preserve and Claudia Faunt, Ph.D. of the U.S. Geological Survey for their insight, and advice over the years and during this project. It is a pleasure to have their friendship.

Finally, Julia Fowler. My partner.

Table of Contents

Tables

Figures

1.0 Introduction

This project evaluates the effects of climate change, and to some degree groundwater pumping, on the magnitude and timing of changes in groundwater levels and spring discharge in the Amargosa Desert in southwest Nevada and a portion of Death Valley National Park in eastern California. Global and regional climate changes are expected to result in increased temperatures and reduced precipitation in southern Nevada and southeastern California (IPCC 2007). Anticipated climate change is therefore hypothesized to result in decreased groundwater recharge. Climate change effects will be superimposed on a system in which groundwater withdrawal has caused substantial declines in groundwater head in portions of southern Nevada, including the Amargosa Desert, and may exacerbate water supply conditions.

The Death Valley regional groundwater flow system and the Lower Carbonate Aquifer (Winograd and Thordarson 1975; Belcher and Sweetkind 2010) within the flow system are the primary focus of this study. The Death Valley regional flow system encompasses an area of approximately 45,000 square kilometers (km^2) and underlies much of southern Nevada, including the Amargosa Desert and a portion of Death Valley National Park. Numerous springs in Ash Meadows National Wildlife Refuge in the Amargosa Desert are intermediate discharge points from the Lower Carbonate Aquifer (Winograd and Thordarson 1975; Belcher and Sweetkind 2010). At least one dozen springs in the Furnace Creek area of Death Valley, including Nevares, Texas, and Travertine Springs are terminal discharge points from the Lower Carbonate Aquifer (Bredehoeft et al. 2005; Bedinger and Harrill 2008; Belcher and Sweetkind 2010). The second aquifer of interest, primarily in relation to pumping and groundwater levels, is the basin-fill aquifer overlying the Lower Carbonate Aquifer in the Amargosa Desert.

Groundwater withdrawal in the Amargosa Desert began in the 1950s and increased for the next decade or so (Walker and Eakin 1963). Based on research by the U.S. Geological Survey

(Fenelon and Moreo 2002), the average groundwater withdrawal rate in the Amargosa Desert (generally corresponding to the study area for this project) between 1966 and 2000 was approximately 33,000 cubic meters per day (m^3/day), equivalent to approximately 9,800 acre-feet per year. Between 1991 and 2000, the average pumping rate was approximately 42,000 m^3/day (12,400 acre-feet per year). Groundwater levels in the region of the primary pumping center in the Amargosa Desert have declined by approximately 10 meters as a result of pumping (Fenelon and Moreo 2002).

Springs are created where groundwater reaches the land surface through natural processes. They provide much of the aquatic wetland environment in arid lands as well as a substantial portion of regional aquatic and riparian biodiversity (Hubbs 1995; Anderson and Anderson 1997; Myers and Resh 1999). Arid land springs are distinct from springs in more mesic regions because they are typically isolated, more susceptible to climate change, and are strongly influenced by aquifer characteristics (Thomas et al. 1996). However, insight into how aquatic and riparian communities will respond to climate change is currently limited to speculation.

The Ash Meadows and Furnace Creek area springs support dense riparian vegetation and a diverse assemblage of endemic and widely distributed benthic macroinvertebrates (Sada and Herbst 2006). Ecological characteristics of these springs are reasonably well known and are representative of many southern Nevada springs. In the Furnace Creek area, Travertine springs were developed more than 100 years ago to supply water for mining and agriculture, and eventually tourism. Other large springs in the Furnace Creek area have been developed in the past 75 years. Development of these springs was by installation of collection devices that resulted in direct diversion from spring outlets with no provision for regulating the volume diverted. The diversions have led to dramatic changes in the aquatic environment of each spring and spring brook. Research by Sada and Herbst (2006) at Travertine Spring demonstrated that each species of benthic macroinvertebrate prefers a distinctive microhabitat that can be quantified in terms of

water depth, current velocity, and substrate. This suggests that benthic macroinvertebrate ecosystems are affected by changes in the available aquatic habitat that occurs when discharge rates are altered.

In 2009, Death Valley National Park changed the Furnace Creek water system so that direct diversion from Travertine Springs will be phased out gradually. Instead, potable water is now pumped from wells upgradient from the springs and irrigation water is collected from downgradient infiltration galleries. Therefore, changes to the Furnace Creek water supply system and knowledge of the Travertine Springs aquatic ecosystem provide a very suitable infrastructure to evaluate how aquifer dynamics, spring discharge, and aquatic ecosystems may be affected by climate change. Park data will be used to compare effects caused by pumping with those simulated to occur because of climate change.

The U.S. Geological Survey transient groundwater model for the Death Valley Regional Flow System (DVRFS) was used for this project. The DVRFS model was constructed by the USGS to simulate regional-scale groundwater flow; therefore, it can be used to evaluate regional hydrologic effects such as climate change. Changes to the groundwater flow system corresponding to possible climate change scenarios were simulated by varying recharge in the model. Simulated groundwater elevations and spring discharge resulting from changes in recharge during the future were compared to results from model runs extended into the future using current climate conditions. This project results in greater understanding of how groundwater conditions in the Death Valley Regional Groundwater Flow system may be altered by climate change.

2.0 Objectives

The objective of this project is to evaluate the effect of climate change on groundwater and spring flow within a portion of southern Nevada and Death Valley National Park. The primary research question is: How will the groundwater flow system in the Amargosa Desert, Nevada and Furnace Creek area of Death Valley National Park, California respond to climate change, and how will that response compare to effects of ongoing groundwater pumping? Information developed during this study will help answer a follow up question: Can a quantitative understanding of groundwater – spring dynamics be developed so that changes to aquatic ecosystems that depend on groundwater flow be predicted?

The hypothesis driving this study presumes that climate change in southern Nevada will result in decreased precipitation, increased temperature, and a decrease in recharge to the groundwater system (IPCC 2007). Further, it is hypothesized that a reduction in spring discharge will occur because of decreased groundwater recharge, and a reduction in discharge will affect dependent aquatic ecosystems. This is important because, except for Las Vegas' use of Colorado River water, groundwater is the sole source of water in southern Nevada and Death Valley National Park. Even the few perennial streams in the region depend entirely on spring discharge for their existence. Changes to the groundwater flow system caused by climate change may have far-reaching effects on aquatic ecosystems and human activity in the region. The locations of Amargosa Desert and Death Valley are shown in Figure 1. The study area is shown in Figure 2.

Figure 1. Location Map

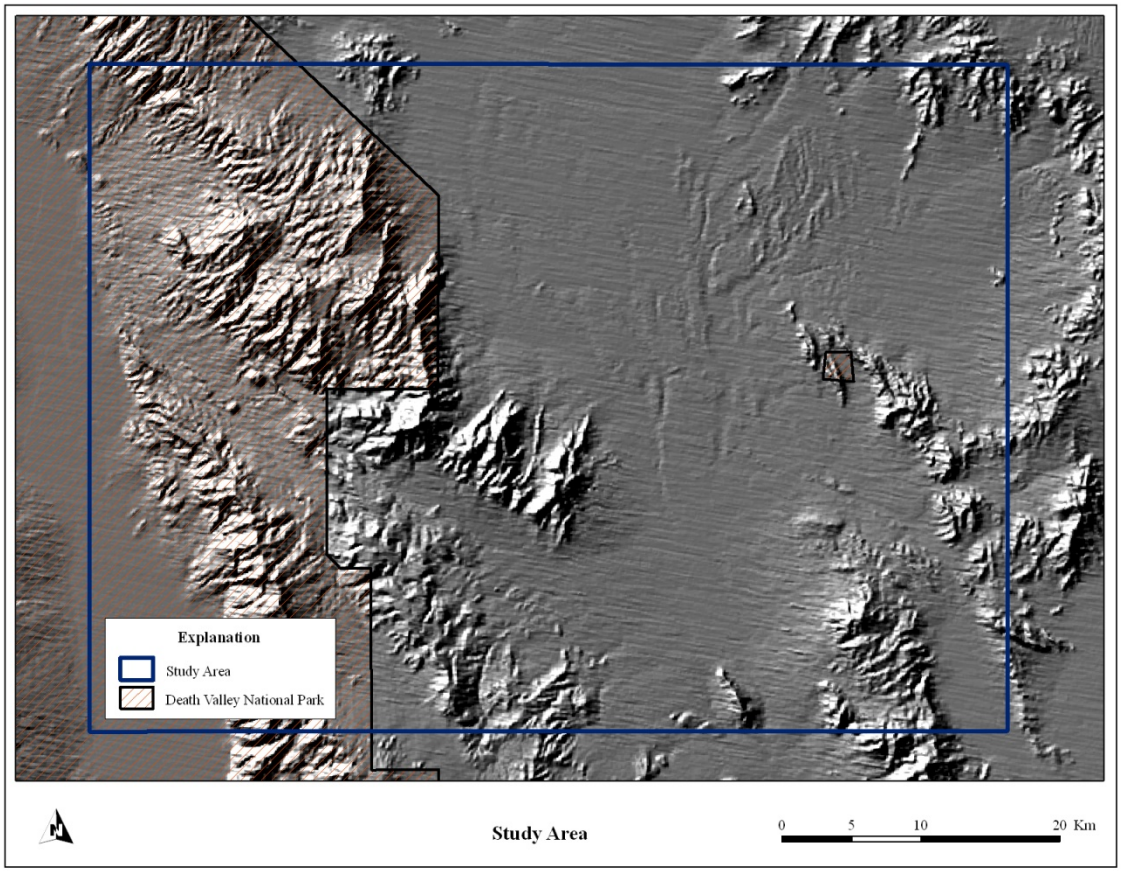

Figure 2. Study Area

3.0 Hydrogeology

The hydrogeology of Amargosa Desert and Death Valley is complex and exceedingly interesting. Water level and spring discharge data are widely available for the study area because of research related to the Nevada Test Site, proposed nuclear waste repository at Yucca Mountain, Nevada, Ash Meadows National Wildlife Refuge, Devils Hole, and Death Valley National Park. Scientists have spent decades refining the understanding of the area using tools ranging from extremely detailed field mapping to remote sensing to advanced geochemical techniques. Within the study area, the principal aquifers are Paleozoic carbonate rocks and Cenozoic basin-fill sediments, with volcanic rock aquifers of lesser importance (Winograd and Thordarson 1975). Groundwater flow is controlled by stratigraphic and structural relationships between aquifers and less permeable confining units.

The study area discussed in this report includes portions of two subbasins: the Ash Meadows subbasin and the Alkali Flat-Furnace Creek Ranch subbasins. The subbasins are shown in Figure 3. Each of these subbasins is part of the larger DVRFS. The subbasin boundaries are based on lithologic and structural controls on groundwater flow, areas of groundwater recharge, flow paths, and areas of groundwater discharge, and water chemistry (Fenelon and Moreo 2002).

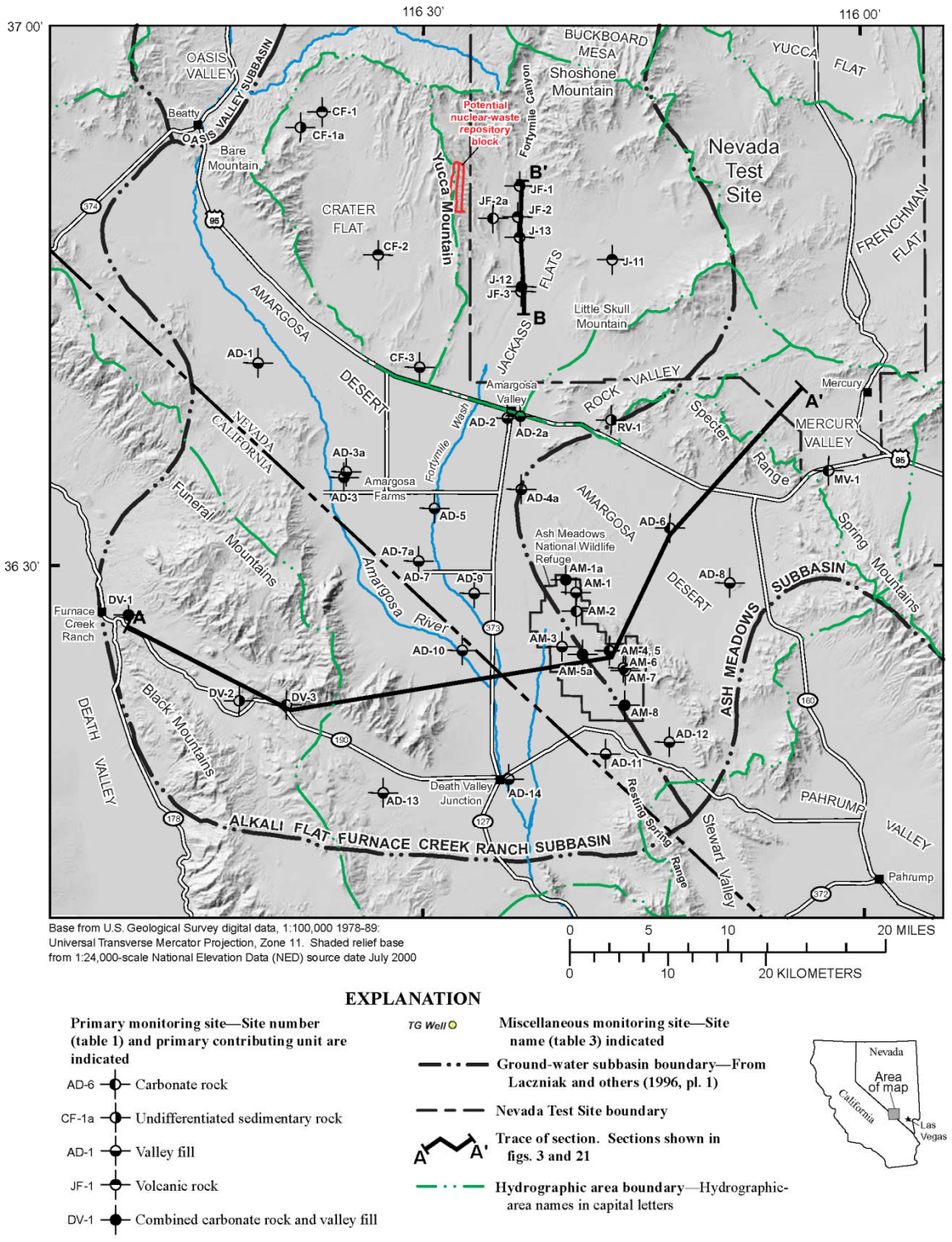

Figure 3. Ash Meadows and Alkali Flat-Furnace Creek Subbasins (adapted from Fenelon and Moreo 2002)

3.1 Stratigraphy

In general, the geologic units of interest are Tertiary and Quaternary basin-fill sedimentary deposits, Tertiary volcanic rocks, and Paleozoic carbonate rocks. During late Proterozoic through Devonian, the study area was characterized by deposition of a westward-thickening sequence of marine sedimentary rocks on a continental margin. Approximately 37,000 feet of marine sediments accumulated during the Proterozoic and Paleozoic (Winograd and Thordarson 1975). The base of the marine sequence, immediately above crystalline basement rocks, consists of siliciclastic and quartzite rocks of the Pahrump Group. From middle Cambrian through at least Devonian, the vast majority of rocks deposited were continental shelf limestone and dolomite. These units include the Carrara, Bonanza King and Nopah Formations, Pogonip Group, Ely Springs, Simonson, Sevy and Laketown dolomites and Devils Gate Limestone. Winograd and Thordarson (1975) termed these rocks the "Lower Carbonate Aquifer." The Proterozoic and early to middle Paleozoic carbonate rocks typically form and underlie the Funeral, Spring, Resting Spring and Nopah mountains in and around the study area. These carbonate rocks also underlie the Amargosa Desert, based on cross sections developed by the U.S. Geological Survey (Sweetkind et al. 2001).

Mesozoic rocks are not present in the study area with the exception of several granitic stocks. The study area was a topographic high during the Mesozoic and therefore, few rocks were deposited. After deposition of the Proterozoic and Paleozoic continental margin sedimentary rocks, the first major mountain building event (the Sevier Orogeny) occurred in the Mesozoic. This included substantial folding and thrust faulting of the Lower Carbonate Aquifer rocks. Mountain building was followed in middle to late Tertiary by strike-slip and normal faulting and eventual creation of today's Basin and Range topography (Winograd and Thordarson 1975).

Cenozoic rocks in and marginal to the study area are characterized by extensive volcanism and deposition of basin-fill sedimentary rocks. The center of volcanism gradually

migrated (in at least a relative sense) from northeast to southwest during the Cenozoic. The sequence began with volcanic fields north of the Nevada Test Site. The middle of the sequence forms the southwestern Nevada volcanic field in the Nevada Test Site and Yucca Mountain areas. The central Death Valley volcanic field in the Black Mountains and local younger lava flows are the most recent expressions of the volcanism (Belcher and Sweetkind 2010). Overall, the volcanic deposits, primarily tuffs, are about 13,000 feet thick.

As the Basin and Range topography developed in middle to late Miocene, increased deposition of sedimentary rocks occurred in the basins developing on the margins of the rising mountain blocks. The basins typically have a deep sequence of coarse orogenic-related clastic sediments shed from adjacent rising mountain ranges, followed by a series of younger alluvial fan, local channel, and playa deposits (Belcher and Sweetkind 2010). Currently, the buried relief of basins can equal or exceed the topographic relief between existing basins and the tops of adjacent ranges.

The thickness of basin-fill deposits in the Amargosa Desert west of Ash Meadows may range between 500 and 2,500 m (meters), based on gravity data (Blakely et al. 2005). The Amargosa Desert and Death Valley basins are filled with relatively young sedimentary deposits consisting of non-marine sedimentary and volcanic rocks. The deposits include fluvial conglomerate, sandstone, siltstone, lacustrine claystone, and limestone, volcanic ashes of various kinds and local lava flows. The upper part of the basin sediments consist of Quaternary period alluvial, playa and eolian deposits.

3.2 Structure

The structure of the study area is complex. The Amargosa Desert is a combination of several smaller basins created by regional strike-slip and extensional movement. The floor of the basin consists of the Paleozoic carbonate aquifer rocks, underlain by clastic confining units that

crop out in portions of the Funeral Mountains (Bredehoeft et al. 2005) and other basin-bounding ranges. The Furnace Creek area of Death Valley is a smaller basin within the overall Death Valley basin. Death Valley is formed from regional strike-slip faults, normal faults, and extensional tectonics. A general cross section of the study area is shown in Figure 4.

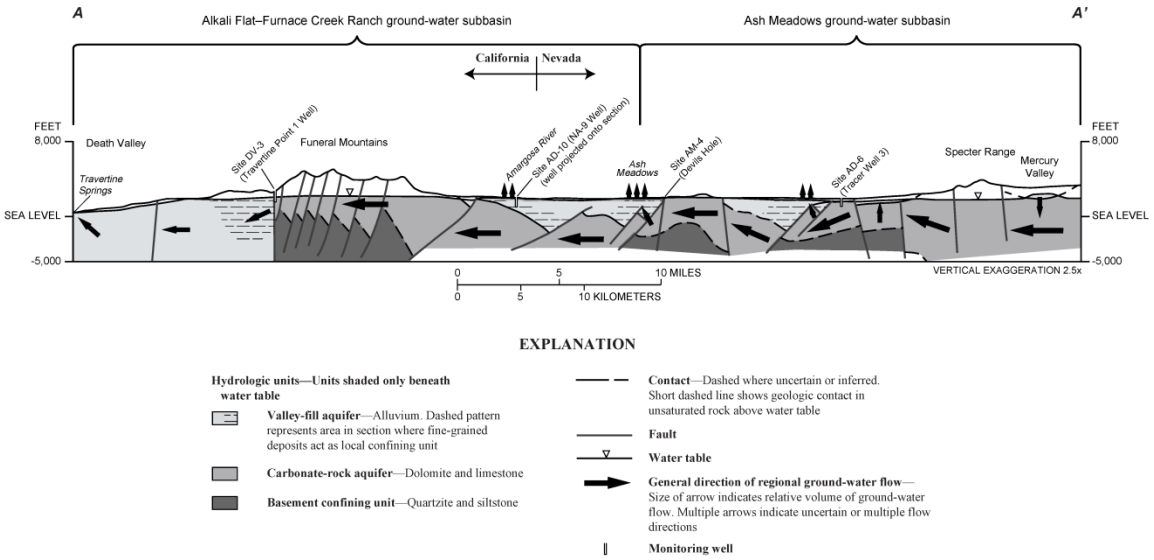

Figure 4. Cross Section: Ash Meadows to Furnace Creek (adapted from Fenelon and Moreo 2002)

The oldest substantial structural deformation is regional Mesozoic folding and thrust faults related to the Sevier Orogeny that has displaced older rocks on top of younger rocks. Displacement on the thrusts ranges from several thousand feet to several miles. In some cases, multiple thrusts have stacked repeated sequences of pre-Cenozoic rocks on top of each other (Winograd and Thordarson 1975). The thrust faults are interpreted to have been regionally continuous at one time; however, they have been disrupted by younger Cenozoic strike-slip and extensional normal faulting.

Although substantial deformation occurred during the Mesozoic, Cenozoic deformation has played the largest role in the current hydrogeologic-related structure of the area. Faulting

during the Cenozoic is characterized by (1) basin and range extension, (2) local extension along detachment faults, (3) development of strike-slip faults and trans tensional basins in the Walker Lane Belt, and (4) Cenozoic volcanism both preceding and concurrent with regional extension (Belcher and Sweetkind 2010). Much of the deformation is tied to tectonic forces acting on the Walker Lane Belt, a structural zone dominated by northwest trending large-offset right-lateral strike-slip faults such as the Pahrump Valley-Stewart Valley fault zone and Las Vegas Valley shear zone. The Pahrump-Stewart Valley fault zone extends into at least the west-central Amargosa Desert and is estimated to be as long as 150 km (kilometers). The fault is right-lateral strike-slip, and offsets Proterozoic era and Paleozoic era rocks between 20 and 30 km (Belcher and Sweetkind 2010).

Several structural zones trend in a northeast direction transverse to the shear zones. The Spotted Range-Mine Mountain zone extends from the Frenchman Flat area southwest to the southern Funeral Mountains. Ash Meadows is located on the southern margin of the zone (Winograd and Thordarson 1975; Belcher and Sweetkind 2010). Near Devils Hole, northeast trending faults and fractures control the location of Devils Hole and other collapse features because of regional extension in the northwest-southeast direction (Carr 1988). Large scale normal faulting in the study area began during the Miocene and continued into the Quaternary. Faulting disrupted both the Tertiary sedimentary and volcanic rocks, and the underlying Proterozoic and Paleozoic rocks, and resulted in basin and range structure of today. As the mountain ranges surrounding the Amargosa Desert and Death Valley rose along the normal faults, they shed their debris into the developing basins (Dudley and Larson 1976). Typical motion on the faults is an eastward rotation of mountain blocks with movement on steeply dipping west side down normal faults (Belcher and Sweetkind 2010). Displacement along the normal faults is generally less than 500 feet, but can be thousands of feet on some faults

(Winograd and Thordarson 1975). These large-offset normal faults juxtapose hydrogeologic units of different permeabilities against each other.

The so-called "gravity fault" that traverses Ash Meadows is an example of a normal fault that juxtaposes low permeability Tertiary basin-fill sedimentary rocks against the Lower Carbonate Aquifer (Belcher and Sweetkind 2010). The gravity fault generally denotes the western margin of Paleozoic exposures in the Amargosa Desert (Sweetkind and Workman 2006). The fault is called the gravity fault because it was identified by gravity survey and has been confirmed by subsequent gravity surveys. However, the fault is not only named because of gravity, but is the physical representation of gravity-driven collapse into the developing basin on its west side (Sweetkind and Workman 2006). Offset along the fault generally ranges from 1,500 feet in the north to several thousand feet in the southern Ash Meadows area (Winograd and Thordarson 1975; Blakely et al. 2005).

The Funeral Mountains are bounded by two regional-scale right-lateral strike-slip faults. The Furnace Creek fault forms the southwest front of the range and abuts the Furnace Creek basin. The Pahrump-Stewart Valley fault system is located northeast from the eastern flank of the range (Bredehoeft et al. 2005). The Pahrump-Stewart Valley fault underlies the active channel of the Amargosa River in the area. The internal structure of the southern Funeral Mountains includes extensional faults related to the Furnace Creek and Stateline faults, as well as the Cleary and Schwaub Peak Thrusts, which formed during the Sevier Orogeny (Bredehoeft et al. 2005). The thrust faults and the related folds are cut and tilted by the much younger extensional faults. Rocks exposed in the Funeral Mountains include an 8,000 m thick Lower Carbonate Aquifer section overlying sedimentary rocks of the Pahrump Group. The Furnace Creek basin, southwest from the Funeral Range, is comprised of Cenozoic basin-fill sediments that overlie rocks pre-dating the Lower Carbonate Aquifer sequence (Bredehoeft et al. 2005). A simplified geologic map of the southern Funeral Mountains is presented in Figure 5.

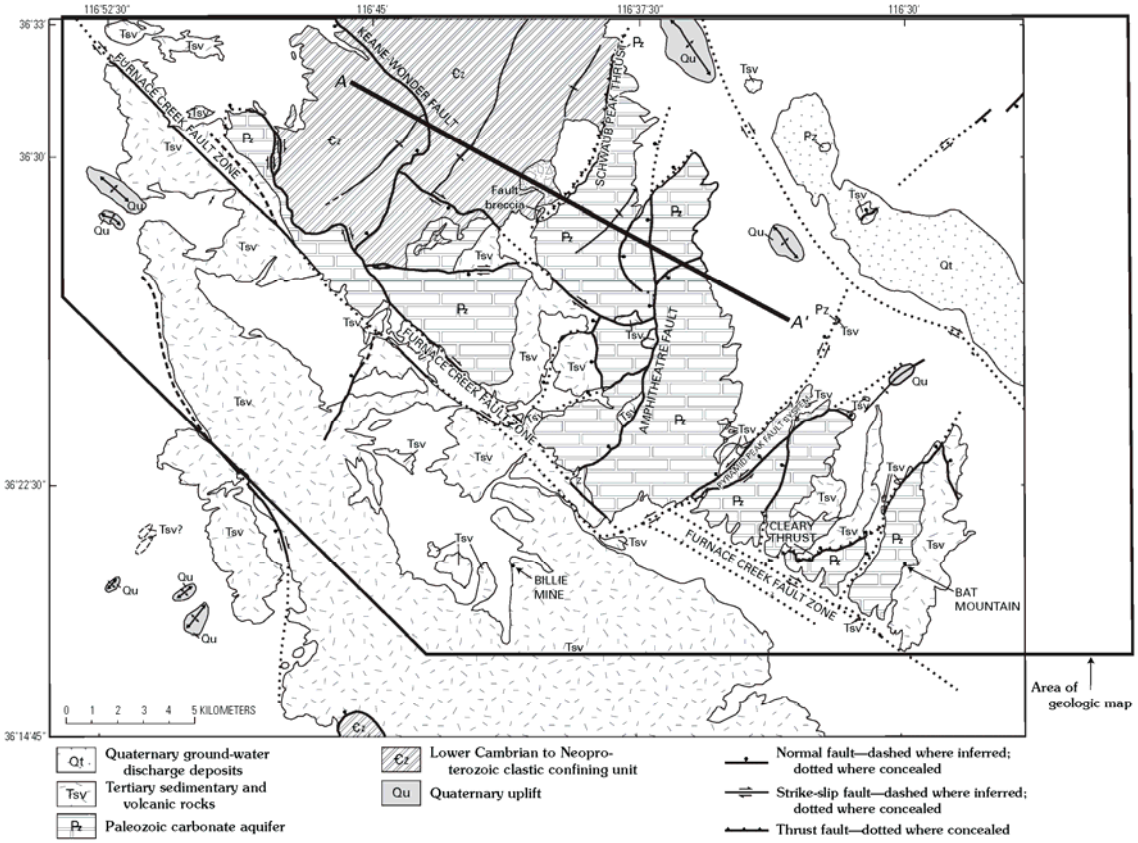

Figure 5. Geology of southern Funeral Mountains (adapted from Fridrich et al. 2008)

3.3 Lithology

The Proterozoic and early Paleozoic rocks are considered an aquitard forming the hydraulic basement in the region. The siltstone, shale, and sandstone of these units typically deform plastically, instead of in a brittle manner as do the overlying carbonates (Winograd and Thordarson 1975).

The carbonate rock aquifer throughout the study area consists of middle Cambrian through Devonian limestone and dolomite – the upper Carrara Formation, Bonanza King Formation, Nopah Formation, Pogonip Group, Eureka Quartzite, Nevada Formation dolomite, and Devils Gate Limestone. These rocks have an aggregate thickness approaching 8,000 m, although that thickness has been substantially changed by regional folding and faulting. These

rocks provide for interbasin flow where hydraulically connected, primarily in zones of secondary permeability caused by fractures, faults and solution channels (Belcher and Sweetkind 2010). The carbonate rocks have a significant density of joints, and the finer-grained rocks generally have a higher density of jointing and fracturing. Data suggest that at least the upper 1,500 feet of the carbonate aquifer contain open and interconnected fractures. In some areas, data indicate open and interconnected fractures, and fresh water, to depths of about 9,400 feet below the top of the carbonate aquifer rock sequence (Winograd and Thordarson 1975). Thin clastic strata present within the carbonates are commonly offset by normal and strike-slip faults of much greater displacement than the thickness of the clastic layers (Winograd and Thordarson 1975).

The carbonate rocks are overlain by Cenozoic consolidated and unconsolidated basin-fill, primarily volcanic and sedimentary rock units. In the study area, they range in age from Eocene to Holocene and include lavas, welded and nonwelded tuffs, alluvial, fluvial, colluvial, eolian, and lacustrine sediments. These units are lithologically diverse and are complexly interfingered in the Amargosa Desert and other basins (Belcher and Sweetkind 2010). Alluvial fan and wash deposits on the basin margins are usually coarser and interfinger with the basin deposits.

3.4 Groundwater Recharge, Discharge, and Flow

Walker and Eakin (1963) were the first to describe recharge to the Amargosa Desert groundwater system (Amargosa Desert Hydrographic Basin 230, Nevada and California). Amargosa Desert Basin 230 is shown in Figure 6. Their interpretation is that recharge is supplied by precipitation within the surface drainage area of the basin and by groundwater underflow from outside the Amargosa Desert basin. The surface drainage area (approximately 6,700 km^2) includes tributaries of the Amargosa Desert, such as Oasis Valley, Crater Flat, Fortymile Canyon, and Jackass Flats in hydrographic basins 225, 226, 227A, 227B, 229, and 228 (Figure 6).

Walker and Eakin estimated recharge from precipitation to the Amargosa Desert as a percentage of precipitation in each elevation zone within the basin. For elevations below 5,000 feet, recharge to the groundwater system is zero. For elevations between 5,000 and 6,000 feet, recharge is 1 percent of precipitation and precipitation was assumed to be from 8 to 12 inches. For elevations between 6,000 to 7,000 feet, recharge is 7 percent of precipitation and precipitation was assumed to be from 12 to 15 inches. For elevations above 7,000 feet, recharge is 15 percent of precipitation and precipitation was assumed to be from 15 to 20 inches. The total average annual recharge from precipitation to the Amargosa Desert surface drainage area was estimated at 1,500 ac-ft (acre-feet), 700 ac-ft from precipitation above 6,000 feet, and 800 ac-ft from precipitation between 5,000 and 6,000 feet (Walker and Eakin 1963).

However, Walker and Eakin (1963) stated that the majority of the recharge is provided by underflow through Paleozoic and possibly Tertiary rocks outside the drainage basin. The principal source for the underflow was interpreted to be recharge from the north and west slopes of the Spring Mountains and possibly areas to the northeast of the Amargosa Desert. Groundwater underflow into Amargosa Desert Basin 230 estimated by Walker and Eakin included 13,000 ac-ft/yr (acre-feet per year) from the Spring Mountains, 4,000 ac-ft/yr from the northeast, and 1,500 ac-ft/yr as upward flow from the carbonate aquifer into basin-fill sediments. Therefore, Walker and Eakin (1963) estimated annual recharge to the Amargosa Desert is approximately 20,000 ac-ft/yr.

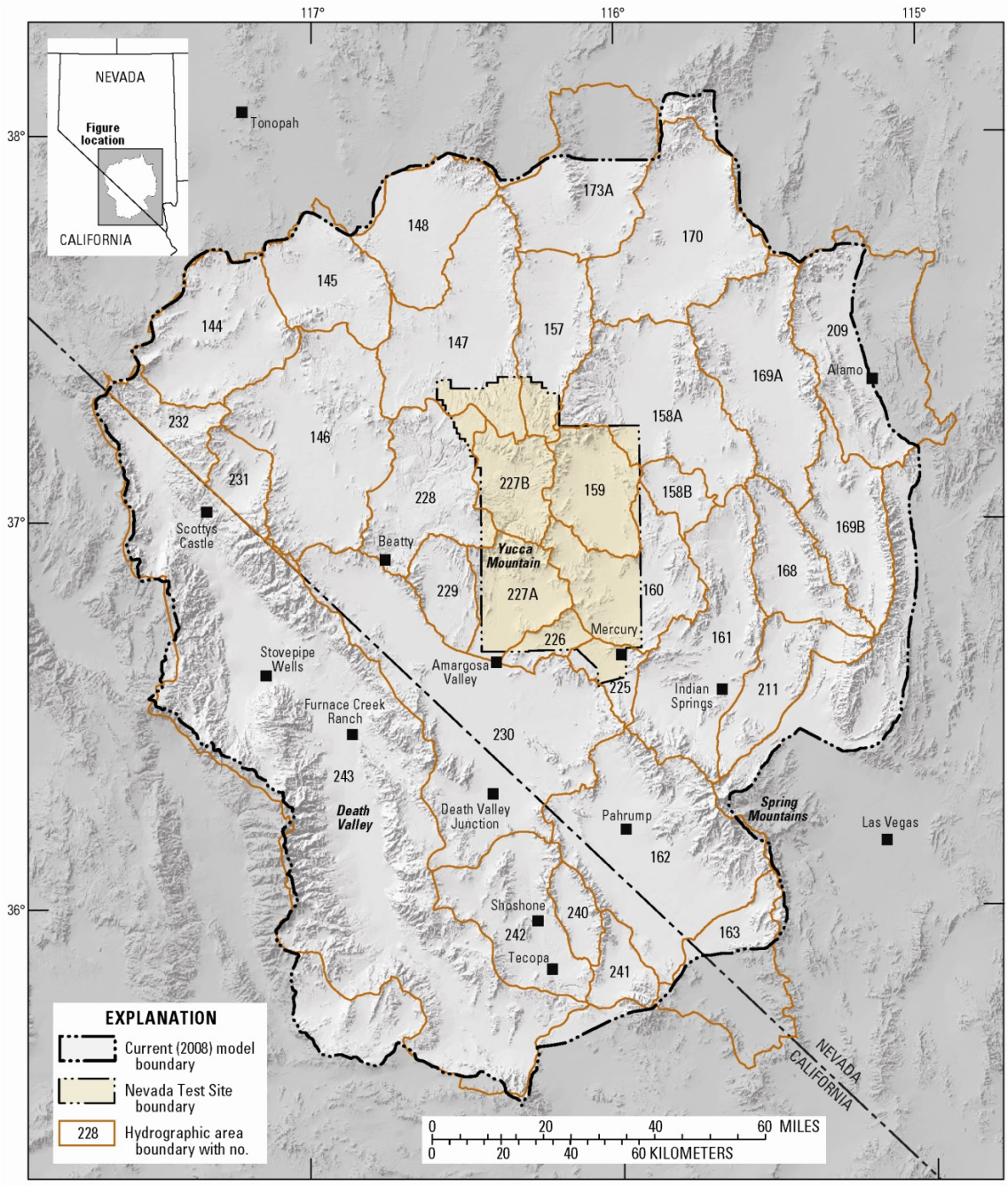

Figure 6. Amargosa Desert Basin 230 (adapted from Belcher and Sweetkind 2010)

Annual discharge from the basin was estimated at 24,000 ac-ft/yr by Walker and Eakin (1963). They estimated transpiration of 11,500 ac-ft/yr from vegetation, evaporation of 12,000 ac-ft/yr from surface water, and underflow and surface flow of 500 ac-ft/yr out of the basin-fill

sediments in the southern portion of the basin. Of the 23,500 ac-ft estimated to be discharged through evapotranspiration, Walker and Eakin (1963) estimated discharge from Ash Meadows springs accounted for 17,000 ac-ft of the total (Winograd and Thordarson [1975] estimated discharge from the springs at Ash Meadows as 17,100 ac-ft/yr). Although their estimates of recharge and discharge are not equal, Walker and Eakin (1963) suggested that discharge estimates were a more reasonable basis on which to determine the perennial yield of the basin.

Groundwater in the Lower Carbonate Aquifer moves from northeast to southwest, down the hydraulic gradient (Winograd and Thordarson 1975). Interbasin movement of groundwater occurs via the carbonate aquifer, and is greatly influenced by major geologic structures – folds that bring the lower clastic aquitard close to the surface and faults that juxtapose lower permeability units against the carbonate aquifer. Varying degrees of hydraulic compartmentalization of the carbonate aquifer are likely in the study area. Where the carbonate aquifer is only partially juxtaposed against lower permeability material or contains a fault zone barrier, a prominent difference in head will not preclude movement of important quantities of water across the barrier (Winograd and Thordarson 1975). Thin clastic strata within the carbonates do not substantially restrict flow or influence the depth of circulation because these clastic layers are commonly offset by normal and strike-slip faults of much greater displacement than the thickness of the clastic layers (Winograd and Thordarson 1975). The large-offset right-lateral strike-slip faults such as the Pahrump Valley-Stewart Valley fault zone and Furnace Creek fault trend in a northwest direction and are interpreted to be hydraulic barriers where they are perpendicular to the primary groundwater flow direction. Conversely, high permeability conduits in the Lower Carbonate Aquifer are related to northeast trending zones such as the Spotted Range-Mine Mountain zone. The Spotted Range-Mine Mountain zone between Frenchman Flat and the southern Funeral Mountains is very transmissive because of 5,000 to 8,000 feet of

saturated thickness in the carbonate aquifer and greater than usual fracturing (Winograd and Thordarson 1975).

Groundwater in consolidated and unconsolidated basin-fill of the Amargosa Desert is moving south-southeast, generally along the axis of the valley from north of Big Dune toward Death Valley Junction (Walker and Eakin 1963). In general, the depth to water in the basin-fill increases toward the north: the depth to water is several feet at Death Valley Junction, between 40 and 135 feet in the general area of Amargosa Farms, and greater than 350 feet at Lathrop Wells.

In the southern Funeral Mountains, the Lower Carbonate Aquifer contains only few and thin interbedded shale and sandstone units. These structurally dismembered interbeds have insufficient continuity to effectively interrupt groundwater flow through the highly permeable, fracture-flow-dominated Lower Carbonate Aquifer. The overlying Cenozoic rocks form a confining unit over the Lower Carbonate Aquifer. The Cenozoic section is lithologically diverse. Most units are low permeability, but some thin, highly permeable beds form local aquifers of limited extent. Extensive reconnaissance conducted by Dr. Chris Fridrich of the USGS (Bredehoeft et al. 2005) suggests that the carbonate aquifer passes through the southern Funeral Mountains via two “spillways.” The spillways are areas where carbonate rocks of the aquifer are not truncated by impermeable metamorphic rocks to the north or displaced by underlying siliciclastic rocks forming the regional aquitard at the base of the system. A structural contour map of the southern Funeral Mountains and the spillways is shown in Figure 7 (Bredehoeft et al. 2005).

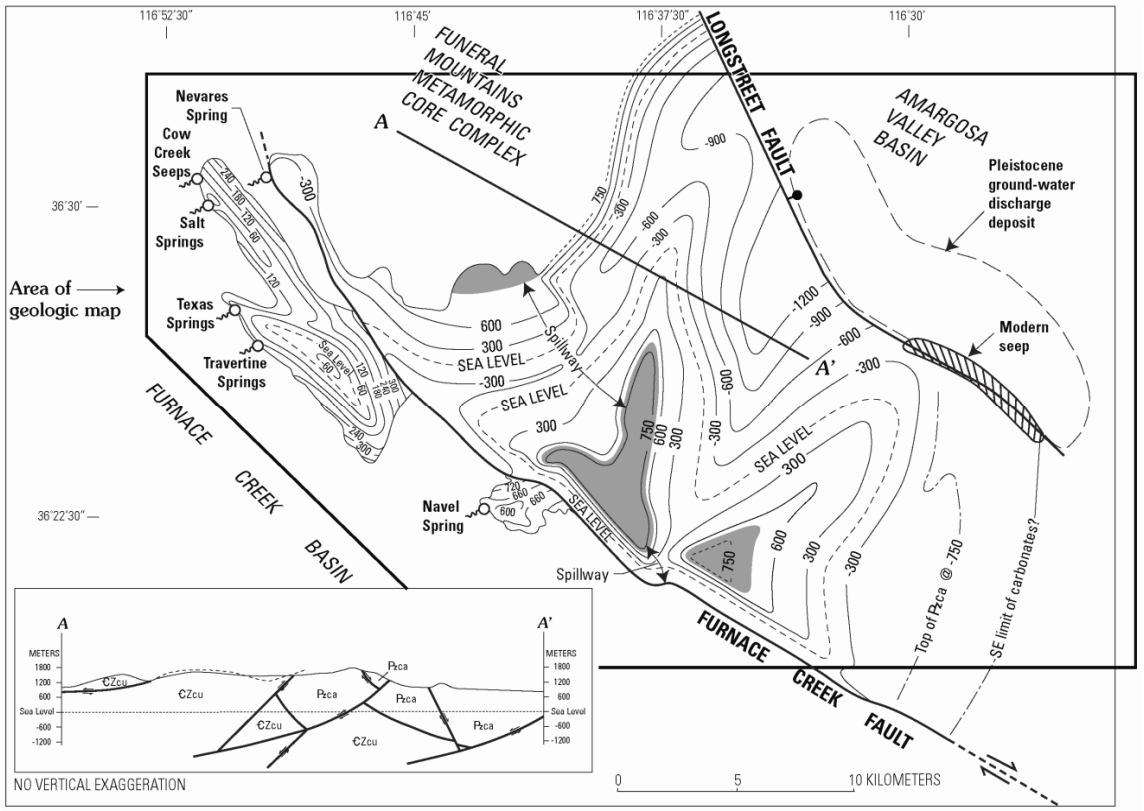

Figure 7. Structural Contour Map of southern Funeral Mountains (adapted from Fridrich et al. 2008)

Nevares, Travertine, and Texas springs in Death Valley are located at the southwest termination of the Lower Carbonate Aquifer system. The uppermost, poorly consolidated alluvium in the Furnace Creek basin, called the Funeral Formation, forms the local aquifer. In the Furnace Creek basin, the alluvial aquifer is juxtaposed against the Lower Carbonate Aquifer across the Furnace Creek fault. Groundwater in the Lower Carbonate Aquifer flows through the plane of the Furnace Creek fault into the Funeral Formation. All of the Furnace Creek area springs (e.g. Travertine, Texas) discharge from the Funeral Formation, rather than from the Lower Carbonate Aquifer. Travertine and Texas springs are located where the Funeral Formation is truncated by the underlying very low permeability Furnace Creek Formation. Nevares spring, to the north, discharges directly from the carbonate section (Bredehoeft et al. 2005).

4.0 Western United States Climate Change

In the western United States, there is a strong link between climate and the availability of water resources. Surface water volume and recharge to groundwater are based primarily on winter precipitation and snowpack. Climate change effects began in the mid-20th Century and are continuing (Barnett et al. 2008, Christensen et al. 2004). The effects of climate change between 1950 and 2000 include water shortages and changes in the timing of runoff. The principal factors being (1) a shift to more winter precipitation falling as rain instead of snow in mountainous regions, (2) earlier snow melt as a result of warming winter temperatures, and (3) associated increases in river flow in the spring and decreases in the summer and fall (Barnett et al. 2008). Recent work by researchers indicates climate change will continue to impact water resources in the southwestern United States (see, for example, Bates et al. 2008 and Seager et al. 2007).

For this project, a range of potential future climate conditions that could occur are described based on IPCC Emissions Scenarios A1B, B1, and A2. The A1 scenarios assume a future world of very rapid economic growth, global population that peaks in mid-century and declines thereafter, and the rapid introduction of new and more efficient technologies. Major themes are convergence among world regions and increased cultural and social interactions, with a substantial reduction in regional differences in per capita income (IPCC 2000). The A1 scenario family develops into three groups describing alternative directions of technological change in the energy system. The A1F1 pathway is fossil fuel intensive. The A1T pathway is based on non-fossil fuel energy sources. The A1B pathway is a balance across energy sources. The A1B scenario assumes carbon dioxide (CO_2) emissions rise from the 1990 baseline of about 8 gigatons of carbon per year (GtC/yr) to a peak at about 17 GtC/yr in 2050 and decline to about 14 GtC/yr in 2100 (IPCC 2000).

The A2 scenarios assume a very heterogeneous world. Major themes are self-reliance and preservation of local identities. Global population increases continuously. Economic development is primarily regionally oriented and per capita economic growth and technological change are more fragmented and slower than in other scenarios. The A2 scenario assumes carbon dioxide (CO_2) emissions rise continuously from the 1990 baseline to about 18 GtC/yr in 2050 and about 29 GtC/yr in 2100 (IPCC 2000).

The B1 scenarios assume global population that peaks in mid-century and declines thereafter as in scenarios for A1B. However the B1 scenarios describe rapid changes in economic structures toward a service and information economy, with reductions in material intensity, and the introduction of clean and resource-efficient technologies. The emphasis is on global solutions to economic, social, and environmental sustainability, without additional climate initiatives. The B1 scenario assumes carbon dioxide (CO_2) emissions rise from the 1990 baseline to a peak at about 12 GtC/yr in 2040 and decline to about 4 GtC/yr in 2100 (IPCC 2000).

Assessment reports of the Intergovernmental Panel on Climate Change (Bates et al. 2008; IPCC 2007) indicate the Southwestern U.S. faces general temperature increases during the next century, with the largest warming expected in the summer months. Christensen et al. (2004), and Christensen and Lettenmaier (2007) considered climate change effects in the Colorado River Basin relative to a baseline period from 1950 to 1999. The 2004 study used one global circulation model downscaled statistically to ⅛-degree resolution. The 2007 study used eleven global circulation models, also downscaled statistically to ⅛-degree (approximately 13 km) resolution. The authors evaluated temperature and other hydrologic-related parameters for three future periods: 2010 to 2039, 2040 to 2069, and 2070 to 2099. The results of the projections of temperature changes are shown in Table 1.

Table 1. Projected Temperature Increases in the Colorado River Basin: 2010 to 2099 (Christensen et al. 2004, Christensen and Lettenmaier 2007)

Study	Emissions Scenario	2010 to 2039	2040 to 2069	2070 to 2099
2004	"Business as Usual" (preceded but similar to A2)	1.0°C	1.7°C	2.4°C
2007	B1	1.3°C	2.1°C	2.7°C
2007	A2	1.2°C	2.6°C	4.4°C

Projected changes in precipitation are more difficult to model than temperature changes; however, the southwestern U.S. as a whole is expected to experience less overall precipitation. For the same three time periods (2010 to 2039, 2040 to 2069, and 2070 to 2099) Christensen et al. (2004), and Christensen and Lettenmaier (2007) considered how precipitation, evaporation, and runoff may change. Average changes throughout the Colorado River Basin are shown in Table 2. However, decreases in precipitation are greater (10 % to 15 %) in arid portions of the basin than in the mountainous portions.

Table 2. Projected Percentage Changes in Precipitation, Evaporation, and Runoff in the Colorado River Basin: 2010 to 2099 (Christensen et al. 2004, Christensen and Lettenmaier 2007)

Study	Emissions Scenario	2010 to 2039	2040 to 2069	2070 to 2099
Precipitation				
2004	"Business as Usual" (preceded but similar to A2)	-3 %	-3 %	-3 %
2007	B1	-3 %	-3 %	-3 %
2007	A2	-3 %	-3 %	-3 %
Evaporation				
2004	"Business as Usual" (preceded but similar to A2)	-3 %	-3 %	-3 %
2007	B1	-3 %	-3 %	-3 %
2007	A2	-3 %	-3 %	-3 %
Runoff				
2004	"Business as Usual" (preceded but similar to A2)	-3 %	-3 %	-3 %
2007	B1	-3 %	-3 %	-3 %
2007	A2	-3 %	-3 %	-3 %

Seager et al. (2007) evaluated an ensemble of global climate models using the A1B scenario and report a decrease in precipitation is expected in the 21st Century in the subtropics, including the southwestern United States. Almost all models simulate a drying trend in the American Southwest, and they consistently simulate drier conditions through time (Seager et al. 2007). For example, of the 49 individual projections conducted with 19 models only 3 projections simulate a shift to a wetter climate. The mean of the climate model ensemble indicates a transition to a sustained drier climate that begins in the late 20th and early 21st centuries. The analysis indicates both precipitation and evaporation will decrease and precipitation will decrease by a greater amount (Seager et al. 2007). These results are in accordance with those of Christensen and Lettenmaier (2007). In winter, precipitation decreases and evaporation is unchanged or increases slightly, whereas in summer, precipitation and evaporation decrease (Seager et al. 2007). The median reduction in precipitation simulated by the models suggests reductions in precipitation by about 0.1 millimeter per day (mm/day) by approximately 2050. This compares with a reduction in precipitation for the southwest of about 0.09 mm/day during the Dust Bowl years of 1932 through 1939, and about 0.13 mm/day during the Southwest drought of 1948 through 1957 (Seager et al. 2007).

5.0 Methods

5.1 USGS Death Valley Regional Groundwater Flow Model

The U.S. Geological Survey Death Valley Regional Groundwater Flow System Transient Groundwater Flow Model (Regional Model [Belcher and Sweetkind 2010]), spring discharge data, and groundwater level data were used for this project. The Regional Model is constructed using MODFLOW 2000, version 1.13. MODFLOW uses the following groundwater flow equation to describe transient three-dimensional groundwater flow (Harbaugh et al. 2000).

$$\frac{\partial}{\partial x}\left(K_{xx}\frac{\partial h}{\partial x}\right)+\frac{\partial}{\partial y}\left(K_{yy}\frac{\partial h}{\partial y}\right)+\frac{\partial}{\partial z}\left(K_{zz}\frac{\partial h}{\partial z}\right)+W=S_s\frac{\partial h}{\partial t}$$

Where;

- K_{xx}, K_{yy}, and K_{zz} represent hydraulic conductivity values along the x, y, and z coordinate axes and the axes are assumed parallel to the major axes of hydraulic conductivity (L/T);
- h represents the potentiometric head value (L);
- W is a volumetric flux representing sources and/or sinks of water, with negative values for flow out of the groundwater system, and positive values for flow into the groundwater system (T^{-1});
- S_S represents the specific storage of the porous material (L^{-1}); and
- t represents time (T).

MODFLOW simulates three-dimensional groundwater flow through porous media using the finite-difference method (Harbaugh et al. 2000). The code uses a nonlinear least-squares regression method to estimate aquifer parameters. MODFLOW-2000 uses several processes in its simulations and each process solves an equation, with the exception of the Global Process. The MODFLOW 2000 processes are (1) Global, (2) Groundwater Flow, (3) Observation, (4) Sensitivity, and (5) Parameter Estimation (Harbaugh et al. 2000).

The Global Process controls overall flow of the program, opens files, and reads global data. Input data files describe the model grid geometry, layers, time discretization, and program operation.

The Groundwater Flow Process contains the physical properties of the media and the groundwater flow system; input through a number of packages (e.g. hydrogeologic-unit flow, recharge, drain, and constant-head boundaries). The Groundwater Flow Process solves the groundwater flow equation and provides model output as hydraulic head solutions.

The Observation Process compares simulated values to observed data. The process also calculates observation sensitivities that can be used in sensitivity and regression analyses.

The Sensitivity Process calculates the sensitivity of hydraulic heads with respect to various parameters.

The Parameter Estimation Process adjusts parameters, selected by the user, to minimize the value of the weighted least-squares objective function. The sum of squared weighted residuals is used to evaluate the fit of simulated to observed values. Parameters are used to define the data values specified for each model cell. A parameter is a single value used to determine data values for multiple cells. Parameter definition includes a parameter name and value, and the cells for which the input values are calculated using that parameter.

The Regional Model was developed by the USGS for the U.S. Department of Energy and is based on numerous separate but inter-related investigations within the DVRFS. The investigations evaluated groundwater discharge occurring through evapotranspiration (ET) and spring flow, groundwater recharge, boundary conditions, hydraulic conductivity of hydrogeologic units, water levels within the DVRFS, and groundwater pumping. The original model included steady-state water levels before 1913, and transient water levels and pumping data between 1913 and 1998, and was presented in USGS Scientific Investigations Report 2004-5025 (Belcher et al. 2004). The current version of the model, and the version used in this project, incorporates water

level and pumping data for the period from 1998 through 2003 (Belcher and Sweetkind 2010). The area included in the Regional Model is shown in Figure 8.

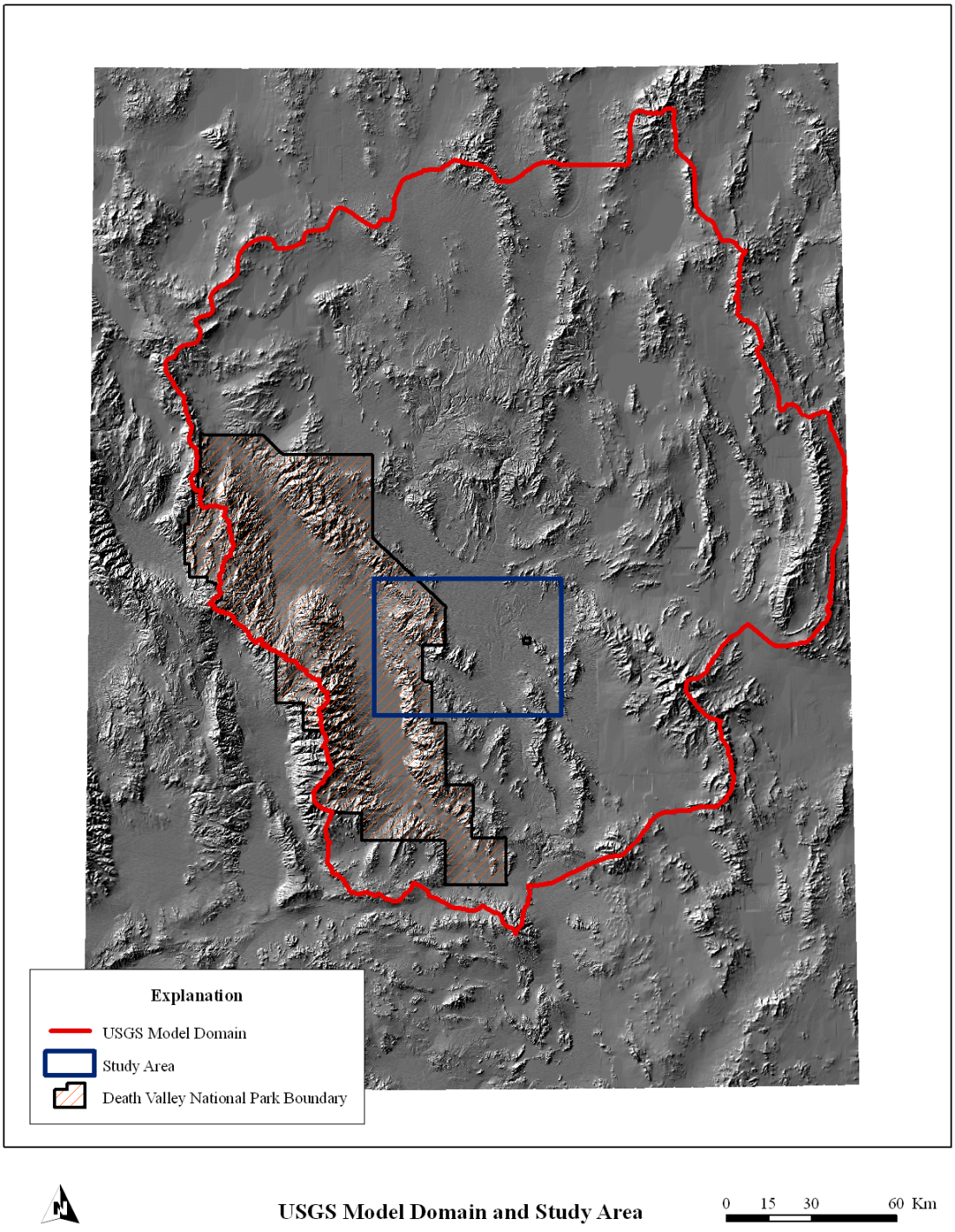

Figure 8. Study Area and USGS Death Valley Regional Groundwater Flow Model Domain

The model consists of 16 layers, and a block-centered finite-difference grid of 194 rows and 160 columns for 496,640 cells. The 16 layers range in thickness from 50 m to more than 300 m (Table 3). All model layers are simulated as confined. However, Layer 1, the uppermost layer, uses a storage coefficient equivalent to a value of specific yield in an unconfined aquifer. The top of Layer 1 is set to the simulated potentiometric surface of the aquifer system. Layer 1 is thick where low-permeability rocks, groundwater mounding, or steep hydraulic gradients are present. Layer 16, the basal layer, is thickest in the Spring Mountains and portions of the northeastern part of the domain. The upper model layers simulate relatively shallow flow through basin-fill sediments, volcanic rocks, and mountains. The lower layers simulate flow through the regional Lower Carbonate Aquifer beneath the basin-fill and mountain ranges (Belcher and Sweetkind 2010).

Table 3. Model Layer Thickness and Depth to Top of Layer

Model Layer	Layer Thickness (m)	Minimum Depth to Top of Layer (m)
1	1 to 850	--
2	50	50
3	50	100
4	100	150
5	100	250
6	100	350
7	100	450
8	100	550
9	100	650
10	100	750
11	150	850
12	200	1,000
13	250	1,200
14	250	1,450
15	300	1,700
16	1,800 to 5,000	2,000

The groundwater flow model uses a digital hydrogeologic framework model developed from digital elevation models, geologic maps, borehole information, cross sections, and earlier groundwater models to represent the geometry of hydrogeologic units in the DVRFS. The hydrogeologic framework represents the rock and basin-fill deposits of the DVRFS in 27 hydrogeologic units. Hydrogeologic units are the basis for assigning horizontal hydraulic conductivity, vertical anisotropy, depth decay of hydraulic conductivity, and storage characteristics of the cells. In model cells containing more than one hydrogeologic unit, hydraulic properties are averaged using the hydrogeologic-unit flow (HUF) package developed by the USGS. The 27 hydrogeologic units are combined into four major rock types: confining units, designated as K1; carbonate-rock aquifers, designated as K2; volcanic-rock units, designated as K3; and basin-fill units, designated as K4. Five of the 27 hydrogeologic units, including the Lower Carbonate Aquifer and regional confining units, cover extensive areas (Belcher and Sweetkind 2010).

Recharge in the model is from infiltration of precipitation in higher elevation mountain ranges, flux through wash bottoms during floods, and limited underflow from adjacent basins. Discharge is modeled as ET and spring flow (using the Drain Package, as discussed below), pumping, and limited underflow to adjacent basins. Groundwater discharge for spring flow and Inflow and outflow across the model boundary is specified using constant head boundaries in cells along the boundary positioned at or below the regional potentiometric surface. Therefore, constant heads occur in different model layers along different parts of the boundary (Belcher and Sweetkind 2010).

Depth decay of hydraulic conductivity is implemented in the model. Depth decay enables hydrogeologic units to be relatively permeable at shallow depths and less permeable at deeper depths. Vertical anisotropy also is defined for each hydrogeologic unit. Typically, basin-fill deposits have greater vertical anisotropy than the volcanic or carbonate rocks.

Simplifications and assumptions made by the USGS during model development include (Belcher and Sweetkind 2010):

1. Groundwater flow is through a porous medium. Even though much regional flow occurs through fractured bedrock, the scale is such that flow may be simulated as through a porous medium.
2. Horizontal hydraulic conductivity is isotropic within individual model cells. Heterogeneity is simulated by changing the horizontal hydraulic conductivity of adjacent cells. Anisotropy in the vertical plane is achieved by using a scaling factor, based on horizontal hydraulic conductivity values. Structural zones and substantial faults likely to be barriers to horizontal flow are represented in the model and introduce horizontal anisotropy.
3. Prepumping conditions are assumed to have been at equilibrium and to have represented average annual conditions so that system recharge equaled system discharge.
4. Groundwater pumping during the 1913 to 1998 transient simulation period is the only transient stress on the aquifer system. Therefore, all changes (decline) in water levels in the originally published model are attributed to pumping. The USGS considered that any water level decline from glacial water level maximums still occurring would be minimal and not affect the model. The USGS also considered seasonal and decadal fluctuations in groundwater levels to be noise and accounted for the noise during model calibration.

The model was calibrated initially to steady-state conditions, based on water level conditions before 1913. It is assumed that pre-1913 conditions represent conditions before appreciable groundwater pumping occurred in the DVRFS. Calibration to transient conditions was conducted for the 85-year period between 1913 and 1998. The model was calibrated to both steady-state and transient conditions using parameter-estimation techniques. The 85 years in the

transient simulation period (1913–1998) are divided into annual stress periods for which pumping is defined. Each stress period is divided into two time steps (Belcher and Sweetkind 2010).

Observations used for calibration of the model are hydraulic heads, changes in head over time because of pumping, and discharge by springs and ET. Estimates of natural discharge from springs and ET for discrete time periods are considered constant and not affected by pumping, except in the Pahrump Valley. Only water levels considered representative of regional groundwater conditions were used for head observations. Prepumping, steady-state head observations were developed at 700 wells. Head observations at these wells were computed as the average of all water-level measurements throughout the entire period of record. For transient stress periods, hydraulic-head observations were computed as average annual water levels from approximately 15,000 water-level measurements. Matching natural groundwater discharge from ET and springs was generally more difficult than matching hydraulic heads and head changes in wells but provided important information for calibration. The overall fit of simulated groundwater discharge and boundary flow to observations is unbiased (Belcher and Sweetkind 2010).

The USGS periodically updates the water level and pumping dataset for the DVRFS. The initial update (Moreo and Justet 2008) incorporated data through 2003. The most recent update (Pavelko 2010) includes data through 2007. Input files for the Regional Model incorporate the 2003 dataset, but do not yet include the 2007 data. Inclusion of data through 2003 into the model improves water use estimates for irrigation, and accounts for recharge to the groundwater system as return flow from irrigation water not consumptively used (Moreo and Justet 2008). The irrigation return flow is assigned a 7-year time lag, therefore is incorporated into the model from 1920 through 2010.

5.2 Study Area, Boundary Conditions, and Available Data

The study area for this project is a subset of the domain included in the Regional Model. The study area incorporates features of particular interest in the Amargosa Desert and Death Valley. These include Devils Hole (a detached portion of Death Valley National Park) and Ash Meadows National Wildlife Refuge in the eastern study area, and the Furnace Creek area of Death Valley National Park in the western study area. The study area is shown in Figure 8. Elevations within the study area range from approximately 1,700 m in the southern Funeral Mountains to sea level at the apex of the Furnace Creek alluvial fan. The study area includes 44 columns (columns 50 to 94) and 32 rows (rows 111 to 143) within the Regional Model. Boundary conditions were not altered from the current USGS model, except, of course, for recharge.

Data used to evaluate simulated changes to the groundwater flow system include water levels and spring flow (as drain cell discharge) at locations in the Amargosa Desert (eastern study area) and Death Valley National Park (western study area). Approximately 170 wells used by the USGS for steady-state and transient calibration are located in the study area. Nevares, Texas, and Travertine springs in the Furnace Creek area of Death Valley are included as specific discharge locations in the model. The Ash Meadows, Amargosa Flat, Amargosa River (Franklin Well), and Franklin Lake ET areas are within the Amargosa Desert portion of the study area. USGS monitoring locations in the Amargosa Desert and Furnace Creek are shown in Figure 9. In addition to wells included in the USGS database and model, Death Valley National Park has monitoring wells in the Furnace Creek area and Inyo County, California has a well near the southeast flank of the Funeral Mountains. Although these wells are not incorporated into the Regional Model, they are used to evaluate simulated water level changes in the Furnace Creek area, based on overall head changes in the model cells in which they are located. Locations of wells in the Furnace Creek area are shown in Figure 10.

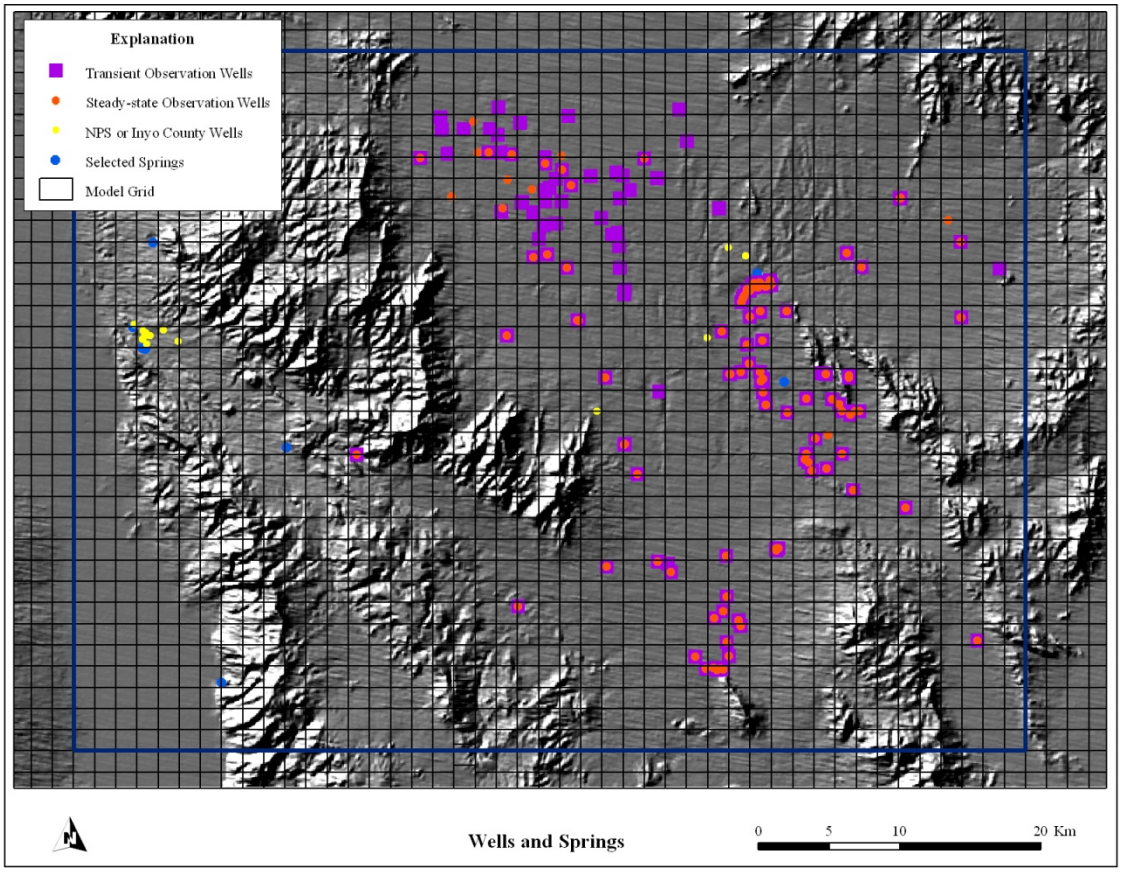

Figure 9. Study Area Springs and Wells

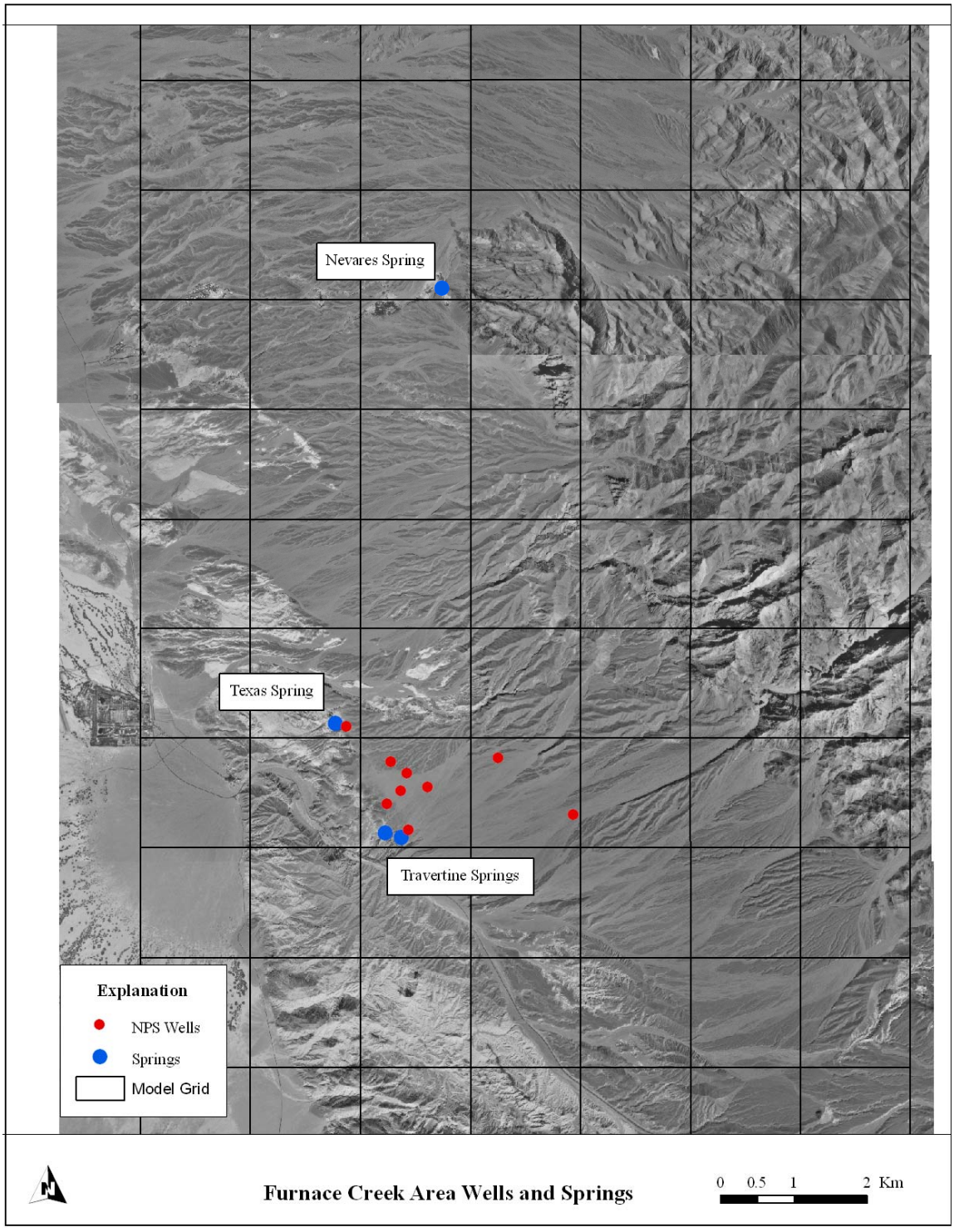

Figure 10. Furnace Creek Area Springs and Wells

5.3 Key Issues

Recharge and discharge as applied in the Regional Model were key issues examined during this project. The recharge and drain packages were of particular interest because these packages control values of recharge and ET that could be varied for model simulations. The Recharge Package (RCH) simulates areally distributed recharge to the groundwater system. The Drain Package (DRN) removes water from an aquifer through a head-dependent boundary such as a spring and is also used to simulate ET in the Regional Model.

5.3.1 Recharge

Groundwater recharge is water that infiltrates downward through the unsaturated zone to the water table. The source of recharge to groundwater in the DVRFS is precipitation. The amount of precipitation is closely related to elevation, and as precipitation increases with elevation, potential evapotranspiration decreases (Bedinger and Harrill 2008). The distribution and quantification of recharge in the DVRFS have been evaluated using empirical, water-balance, chloride mass-balance, and distributed-parameter methods (Belcher and Sweetkind 2010). As reported by Bedinger and Harrill (2008), in 1949 Maxey and Eakin developed an empirical relationship between elevation and recharge in the Great Basin of Nevada by assigning recharge as a percentage of precipitation at select elevation intervals. The intervals begin between the elevations of 1,524 m to 1,829 m, with three percent of precipitation becoming recharge (Bedinger and Harrill 2008). Maxey and Eakin assumed recharge from precipitation at elevations less than 1,524 m was negligible. Maxey and Eakin calibrated their method by balancing recharge estimates with measurements of discharge for single closed basins and multiple basin systems with interbasin flow. Water budgets have been estimated for most basins in Nevada using the Maxey-Eakin method.

A distributed-parameter method (Hevesi et al. 2003) for determining recharge was used in the Regional Model. The method uses a deterministic water-balance approach that includes the

distributed parameters of precipitation, potential evapotranspiration, soil and bedrock storage, and permeability. The net infiltration approach simulates surface water flow, snowmelt, transpiration, and groundwater drainage in the root zone. The method also uses an algorithm that simulates daily climate conditions in local watersheds. Topography, geology, soils, and vegetation data represent local drainage-basin characteristics. Uncertainties in using a net infiltration approach increase as the thickness and heterogeneity of the unsaturated zone increases (Hevesi et al. 2003).

Net infiltration is the sum of snowmelt, precipitation, and infiltrating surface water flow minus the sum of ET, surface water runoff, and changes in root-zone storage. The USGS used net-infiltration results to create a recharge input for the Regional Model that balances system discharges, the transmissivity of rock units at the water table, and the variable depth to the water table (Blainey et al. 2006). Based on the average annual net-infiltration rate and the relative permeability of rocks in the upper five model layers, recharge in the Regional Model was created using nine zones and five recharge parameters. Rock types are classified as predominantly (more than 50 percent) aquifer material with relatively higher permeability (basin-fill, volcanic-rock, and carbonate-rock aquifers) or relatively lower permeability rocks not identified as aquifers (Belcher and Sweetkind 2010). To fit recharge to observed discharge, recharge was adjusted using a multiplication array and recharge parameters based on the nine zones.

The infiltration model simulates the mass-balance equation within the unsaturated zone to a depth of 6 m, which the USGS selected as the depth where seasonal effects of ET become insignificant (Belcher and Sweetkind 2010). The simulation is completed on a daily time step for each cell in the infiltration model. Calibration of infiltration was accomplished by matching the simulated daily surface water discharge to streamflow records at 31 locations with gage records in the DVRFS (Hevesi et al. 2003). Because daily climate data and stream gage data are limited in the DVRFS, calibration was difficult and model results were constrained by prior estimates of recharge calculated using other methods (e.g. Maxey-Eakin).

The infiltration model simulates daily net infiltration from 1950 through 1999. This period was used because of the availability of climate and streamflow records. Recharge in the model is represented by average annual conditions, with rates ranging from 0 to 0.468 mm (millimeters) per day (0 to approximately 14.8 mm/month) depending on location (Belcher and Sweetkind 2010). An average annual net infiltration of 2.8 mm was estimated over the entire Regional Model domain by averaging simulated daily net infiltration over the 50-year simulation period. This estimate is less than 2 percent of the average annual precipitation computed for the same period (Hevesi and others, 2003). For the active cells comprising the model domain, 303,415 m^3/day was simulated as recharge, equivalent to approximately 125 million m^3/year for the active cells in the model domain. The average annual surface water runoff over the 50-year simulation period was 2.2 mm (Belcher and Sweetkind 2010).

For Amargosa Desert Basin 230, the model simulates 5,145 m^3/day recharge from precipitation compared to Walker and Eakins 1963 estimate of 5,066 m^3/day (Hevesi and others, 2003). Recharge cells within the study area are shown in Figure 11.

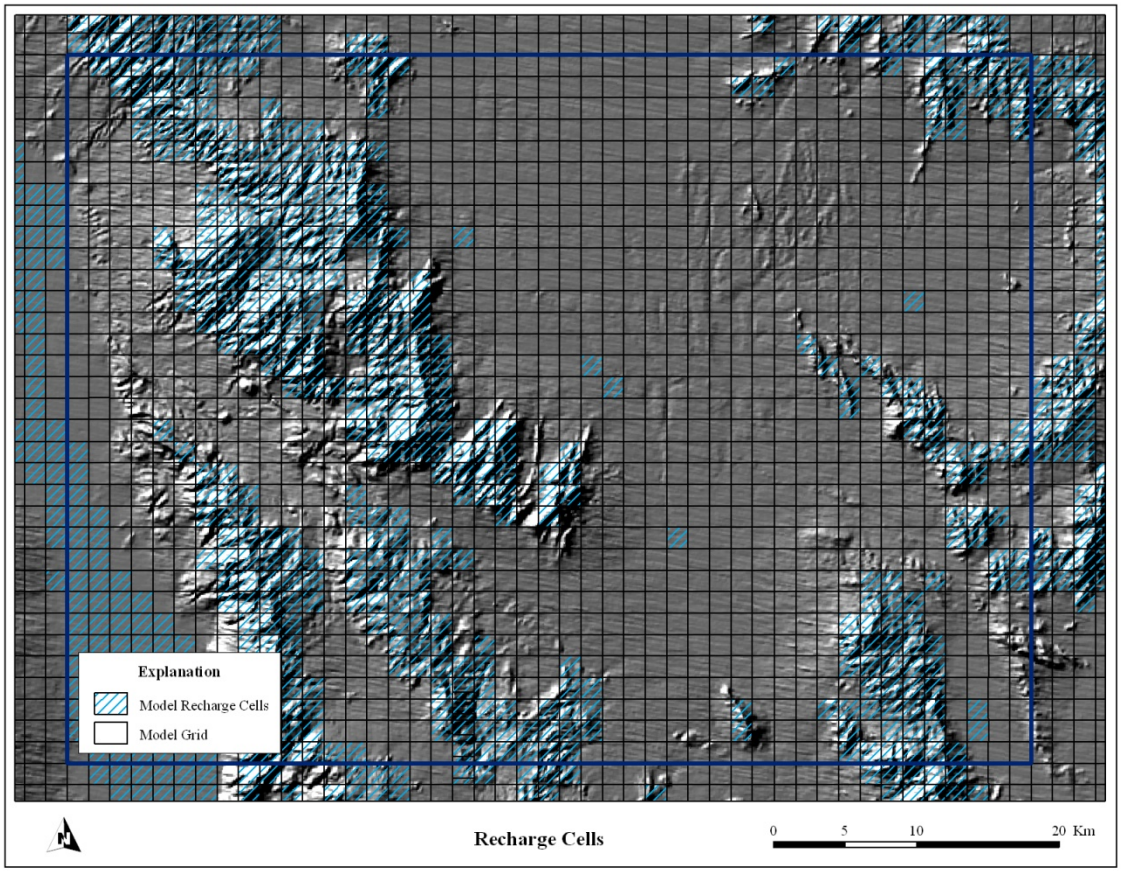

Figure 11. Study Area Recharge Cells

5.3.2 Discharge

Groundwater discharge for spring flow and ET is simulated in the Regional Model using the Drain package. Areas of discharge include wet playas, wetlands with free-standing water or surface flow, riparian corridors, and broad areas of phreatophytes. ET rates measured at Ash Meadows, Death Valley, and Oasis Valley (near Beatty, Nevada) are used to approximate discharge because most ground water discharging from springs and seeps is evaporated or transpired locally and is accounted for in estimates of ET (Blainey et al. 2006).

The Drain package simulates groundwater discharge using a head-dependent boundary. Drain conductance is defined using the hydraulic properties of the materials through which water flows to the surface. Simulated discharge is calculated as the conductance of the drain multiplied

by the difference in elevation between the simulated head and the drain. For cells containing a partial ET area, the area is specified in the Drain package. Only cells with ET areas greater than 4 percent of the cell area are included as drain cells, unless the cell also has a spring. Drain altitudes were set at 10 m below the land surface elevation for the cell (or group of cells) and the depth of 10 m represents the maximum extinction depth for ET (Belcher and Sweetkind 2010). For drain cells representing springs in the Regional Model, the drain at that location connects directly to the uppermost occurrence of the Lower Carbonate Aquifer, located between model layers 1 and 10 (Blainey et al. 2006). Drain cells within the study area are shown in Figure 12.

As discussed in Section 3.4, annual discharge from the basin was estimated at 24,000 ac-ft/yr by Walker and Eakin (1963). They equated annual discharge with perennial yield of the basin and stated that perennial yield could support 17,000 ac-ft/yr discharge from Ash Meadows and 7,000 ac-ft/year from groundwater pumping (Walker and Eakin 1963). Simulations conducted for this project were unable to provide an estimate of groundwater recharge into the study area or the Amargosa Desert Basin 230. However, the Regional Model does provide insight into groundwater discharge and pumping from locations within Amargosa Desert Basin 230. For Ash Meadows, the Regional Model (Belcher and Sweetkind 2010) uses an observed discharge of 17,865 ac-ft/yr (60,372 m^3/day) and simulates 1997 discharge at 18,080 ac-ft/yr (61,098 m^3/day). In 1998, pumping in the entire Amargosa Desert Basin 230 was estimated at 24,913 ac-ft (84,191 m^3/day) by the USGS (Belcher and Sweetkind 2010), and pumping in the portion of the Amargosa Desert roughly equivalent to the study area at approximately 15,000 ac-ft (50,690 m^3/day [Fenelon and Moreo 2002]).

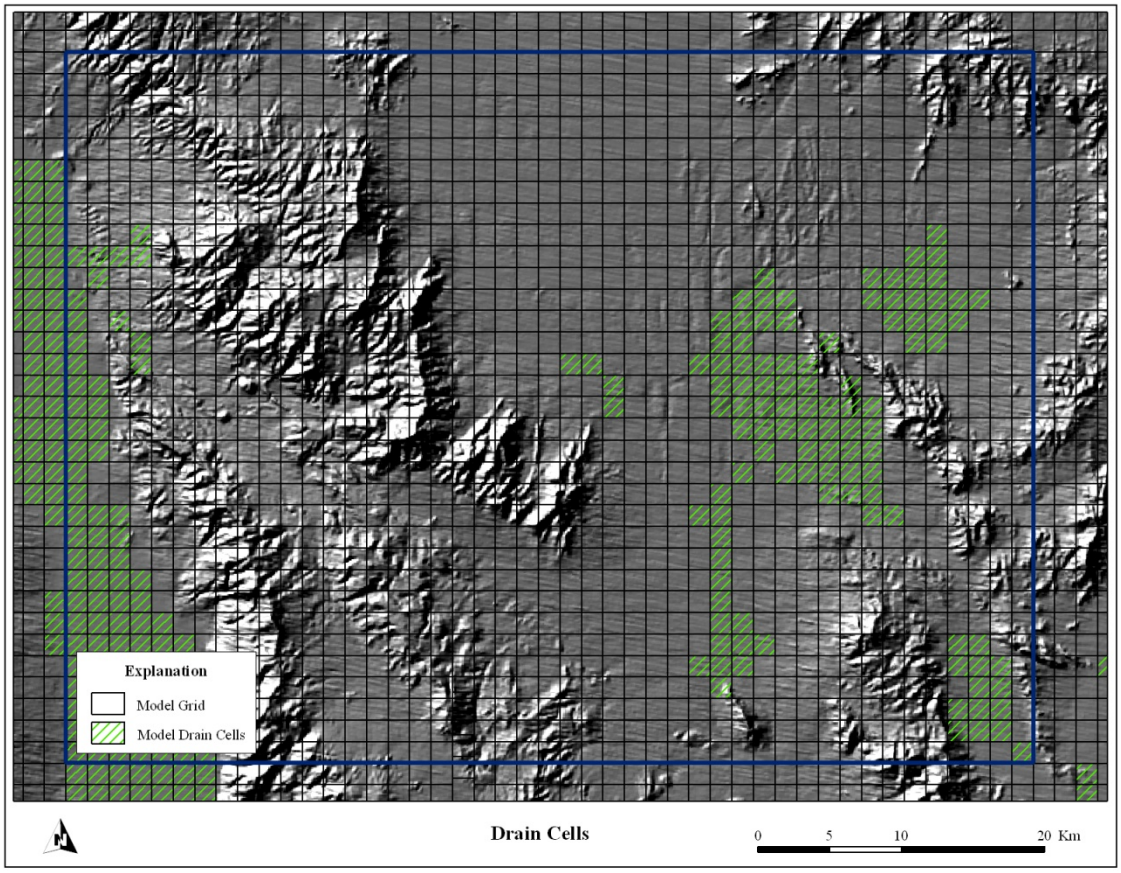

Figure 12. Study Area Drain Cells

5.4 Climate Change in Southern Nevada and Death Valley

Because of the aridity of southern Nevada, including the Amargosa Desert, and Death Valley, relatively small changes in temperature and precipitation may translate into significant alterations in evapotranspiration, runoff, and recharge. The climate change studies cited in Section 4.0 are focused primarily on changes that will effect surface water systems. However, changes in temperature and precipitation are also expected to change the amount of recharge to groundwater systems. Research suggests that groundwater recharge will decrease as (1) snowpack declines in areal extent and in thickness, (2) a greater percentage of winter precipitation falls as rain, and (3) snowlines migrate to progressively higher elevations (Lenert 2004).

For this project, temperature and precipitation data specific to the boundaries of the DVRFS were obtained using the World Climate Research Programme's Coupled Model Intercomparison Project phase 3 (CMIP3) multi-model dataset (Maurer et al. 2007).

Climate modeling groups have produced numerous simulations of past and future climates for the IPCC. The World Climate Research Programme helped coordinate modeling activities through the CMIP3 effort and worked to co-locate the simulations within a single archive hosted by the Lawrence Livermore National Laboratory Program for Climate Model Diagnosis and Intercomparison (PCMDI). The model archive is also supported by the U.S. Bureau of Reclamation Research and Development Office, U.S. Department of Energy National Energy Technology Laboratory, U.S. Army Corps of Engineers Institute for Water Resources, Santa Clara University Civil Engineering Department, Climate Central, and The Institute for Research on Climate Change and its Societal Impacts.

The model archive includes bias-corrected and spatially downscaled ⅛-degree resolution climate projections derived from CMIP3 data. The climate projections are available at the following website: *http://gdo-dcp.ucllnl.org/downscaled_cmip3_projections/dcpInterface.html#Welcome*, as described by Maurer et al (2007). The archive contains translations of 112 contemporary climate projections over the contiguous United States. The archive offers user-specified data retrieval options for geographic areas, specific climate models, emissions pathways, time periods, and projected variables. For this study, temperature and precipitation projections were specified from all available models. The output includes data from 112 downscaled datasets representing 40 CMIP3 models from 16 modeling groups and emissions scenarios A1B, A2, and B1. The models provide simulated changes in temperature and precipitation relative to 1950 to 1999 for three future time periods: 2000 through 2039, 2040 through 2069, and 2070 through 2099. The 16 CMIP3 modeling groups are shown in Table 4.

The geographic area of the climate projections is from latitude 35° to 38.125° north, and longitude 115° to 117.625° west, corresponding to the area of the Death Valley flow system.

Table 4. CMIP3 Models

Modeling Group	Model Name
Bjerknes Centre for Climate Research	BCCR-BCM 2.0
Canadian Centre for Climate Modeling and Analysis	CGCM 3.1 (T47)
Meteo-France/Center National de Recherches Meteorologiques	CNRM-CM 3
CSIRO Atmospheric Research, Australia	CSIRO-MK 3.0
US Dept. of Commerce/NOAA/Geophysical Fluid Dynamics Laboratory	GFDL-CM 2.0
US Dept. of Commerce/NOAA/Geophysical Fluid Dynamics Laboratory	GFDL-CM 2.1
NASA/Goddard Institute for Space Studies	GISS-ER
Institute for Numerical Mathematics, Russia	INM-CM 3.0
Institute Pierre Simon Laplace, France	IPSL-CM 4
Center for Climate System Research (University of Tokyo), National Institute for Environmental Studies, and Frontier Research Center for Global Change (JAMSTEC), Japan	MIROC 3.2 (medres)
Meteorological Institute of the University of Bonn, Meteorological Research Institute of KMA	ECHO-G
Max Planck Institute for Meteorology, Germany	ECHAM5/MPI-OM
Meteorological Research Institute, Japan	MRI-CGCM 2.3.2
National Center for Atmospheric Research, USA	CCSM 3
National Center for Atmospheric Research, USA	PCM
Hadley Centre for Climate Prediction and Research/Met Office, United Kingdom	UKMO-HadCM 3

Table 5 summarizes the combined results of the 112 model simulations for the Death Valley groundwater flow system, relative to the 1950 through 1999 reference period.

Table 5. CMIP3 Models: Projected Changes in Temperature and Precipitation 2000 to 2099

Change	2000 to 2039	2040 to 2069	2070 to 2099
Average Temperature	+1.1°C	+2.3°C	+3.4°C
Average Precipitation	-0.03 mm/month	-0.22 mm/month	-0.33 mm/month
Percent Precipitation	-0.20 %	-1.64 %	-2.53 %

Graphs of the relationship between mean annual precipitation and average temperature change for the period from 2000 through 2039, 2040 through 2069, and 2070 through 2099 relative to the reference period are shown in Figures 13 through 18.

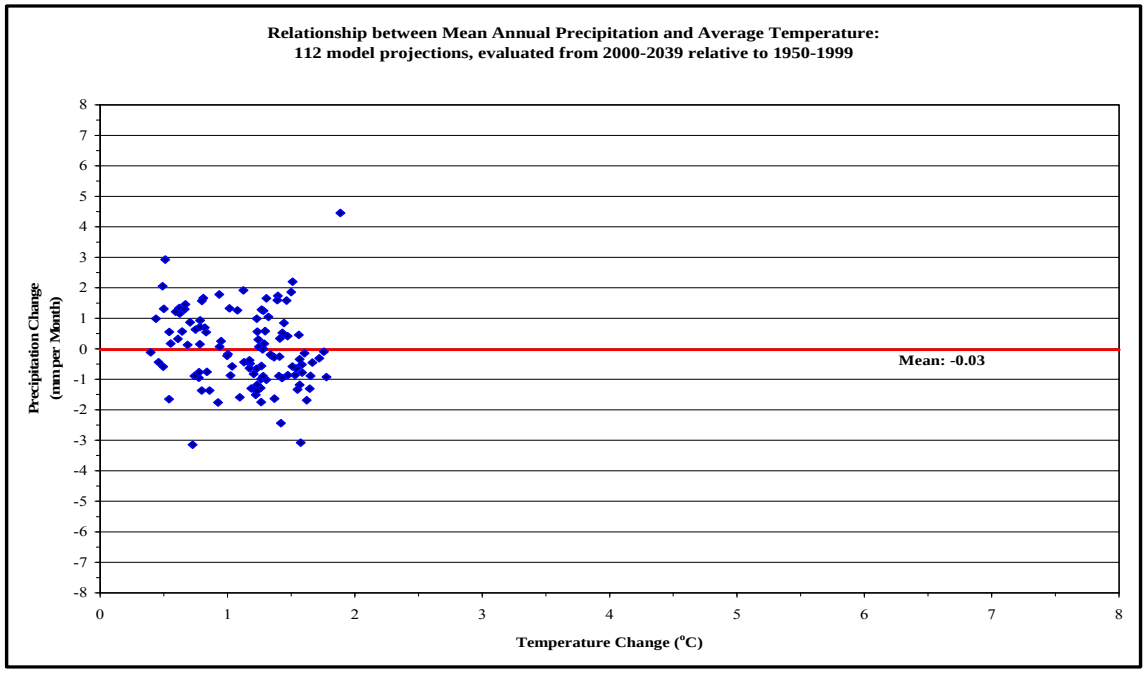

Figure 13. Simulated Temperature and Precipitation 2000 to 2039 (Maurer et al. 2007)

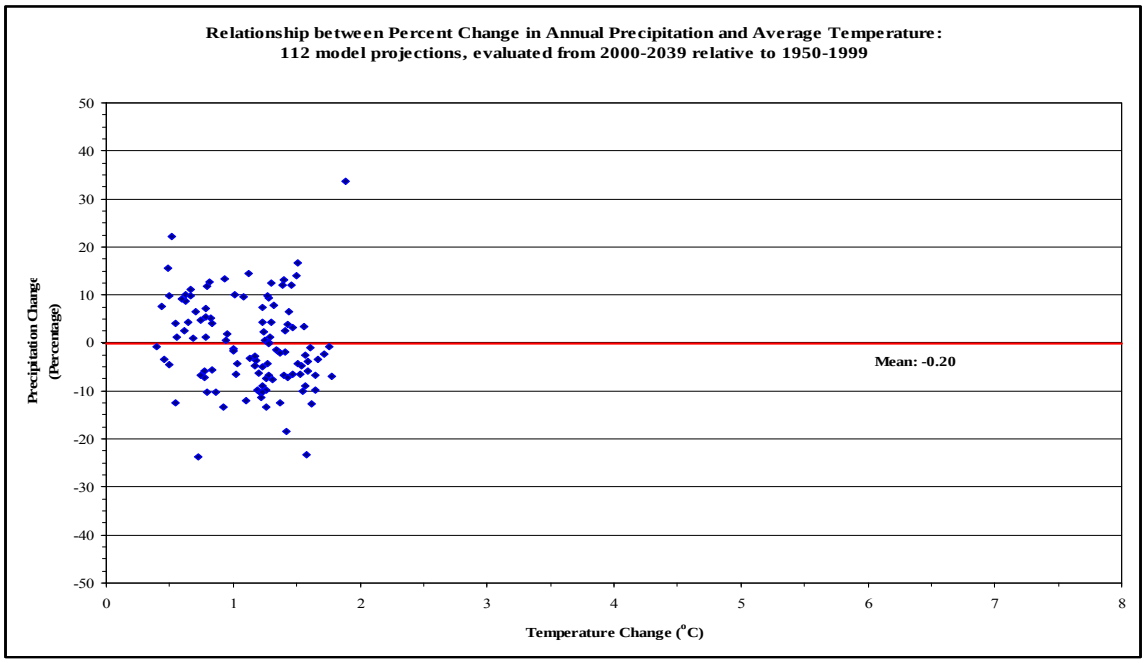

Figure 14. Simulated Percent Change in Precipitation 2000 to 2039 (Maurer et al. 2007)

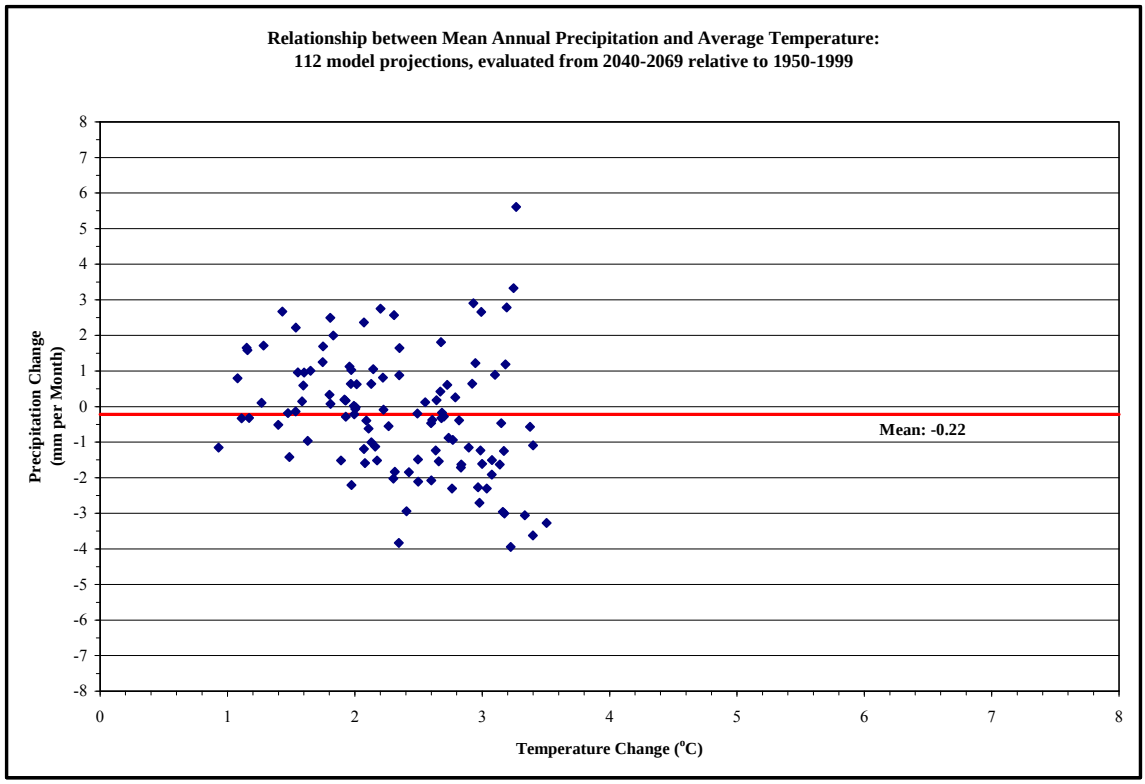

Figure 15. Simulated Temperature and Precipitation 2040 to 2069 (Maurer et al. 2007)

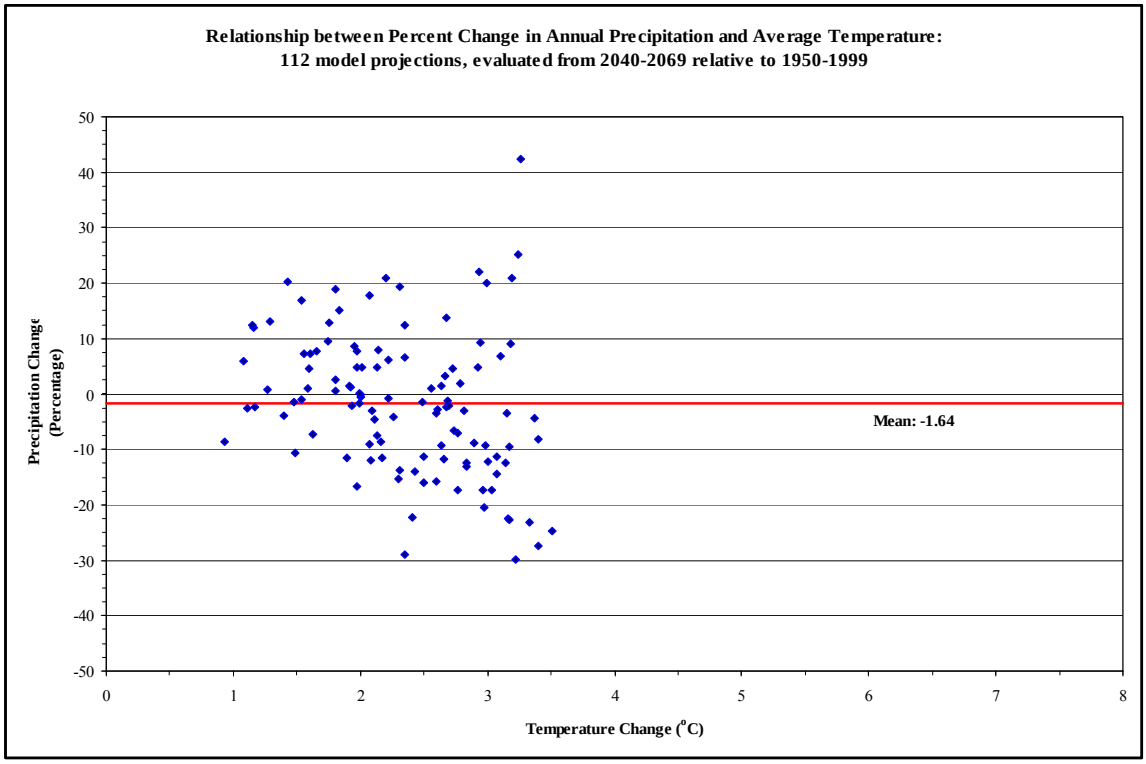

Figure 16. Simulated Percent Change in Precipitation 2040 to 2069 (Maurer et al. 2007)

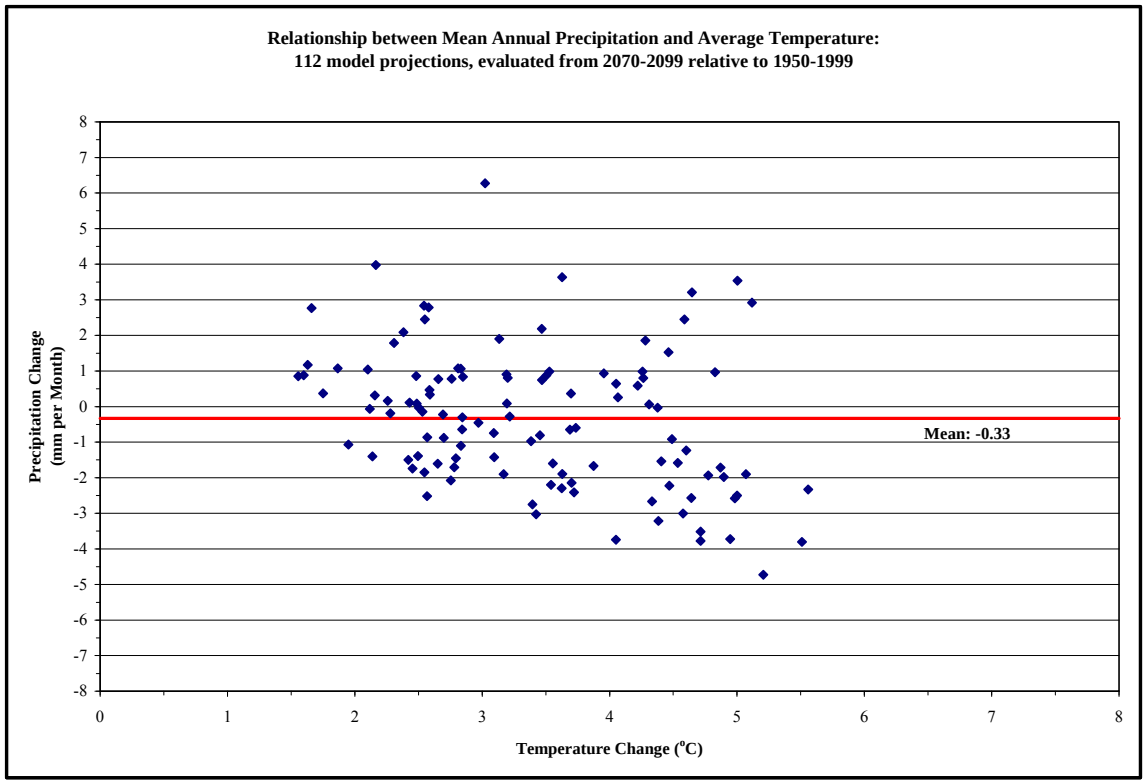

Figure 17. Simulated Temperature and Precipitation 2070 to 2099 (Maurer et al. 2007)

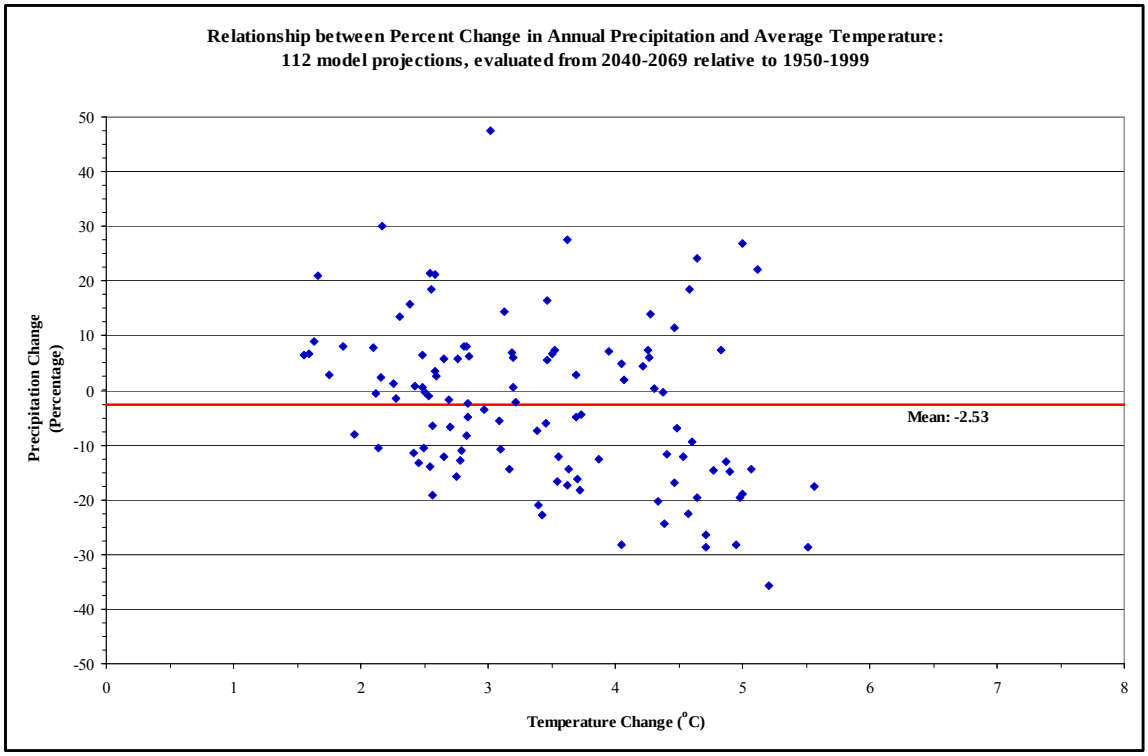

Figure 18. Simulated Percent Change in Precipitation 2070 to 2099 (Maurer et al. 2007)

Graphs of individual climate model runs are included in Appendix A.

5.5 Groundwater Model Simulations

5.5.1 General

Simulations for this project were run using the entire Regional Model. However, results are evaluated only for the study area (with the exception of water budgets for the entire model domain). The project was completed using the MODFLOW 2000, version 1.13 executable command line mode and editing applicable input files. Results from model runs were evaluated and displayed using the following programs:

- ZoneBudget, version 2.1 (public domain software available from the USGS)
- Model Viewer, version 1.4 (public domain software available from the USGS)
- GW_Chart, version 1.23.3.0 (public domain software available from the USGS)
- Groundwater Modeling System (GMS), version 7.1.8 (commercial software available from Aquaveo)

A number of simulation modes are available in MODFLOW 2000. For the Regional Model, four types of model simulation modes are considered most relevant (Blainey et al. 2006): (1) forward predictive with observations and parameter-value substitution, (2) parameter sensitivity with observations, (3) sensitivity analysis, and (4) parameter estimation mode. Forward predictive scenarios were run to evaluate changes in water level and discharge from springs and drain cells in the study area. Execution of forward (predictive) simulations generated head and water level drawdown arrays, and water-budget terms.

5.5.2 Modification of Regional Model Input Files

Running predictive scenarios with the Regional Model required editing several of the model input files, as follows:

Constant Head Package, CHD (chd_15reg_tr7.txt): The Regional Model modifies the traditional constant head package into a time-variant package that simulates specified head boundaries that may change within or between stress periods. The input file was modified for this project by adding stress periods 88 through 599 (1999 through the year 2510).

Discretization File, DIS (DIS_WT_CONFINED7.txt): This file specifies how data used in the models, including (1) the number of rows, columns, and layers, (2) cell dimensions, (3) quasi-3-dimensional confining layers, if any, and (4) time discretization into time steps and stress periods. The Regional Model uses a one-year stress period and two time steps per year. The input file was modified for this project by adding stress periods 88 through 599 (1999 through the year 2510).

Drain Package, DRN (drn_tr7.txt): This file simulates head-dependent flux boundaries. The Regional Model uses the drain package to represent springs and areas of evapotranspiration. The input file was modified for this project by adding stress periods 88 through 599.

Horizontal Flow Barrier, HFB (hfb_final_tr.txt): This package is used to simulate barriers to flow by reducing the conductance between individual pairs of cells. The Regional Model uses this package to simulate barriers such as faults and locations were geologic units of differing hydraulic conductivities are structurally juxtaposed against each other. The input file was modified for this project by adding stress periods 88 through 599.

Multi-Node Drawdown-Limited Well, MNW1 (New_mnw_03_7.txt): This package is used to simulate wells that intercept more than one cell, and in many cases more than one model layer. In the Regional Model this file lists each well used in calibrating the model, and incorporates the pumping rate for each well during each stress period. The Regional Model file includes pumping data through 2003. The input file was modified for this project by adding stress periods 88 through 599. Therefore, in simulations completed for this project, the pumping rate was constant from 2004 through 2510.

Output Control, OC (OC7.txt): This file specifies the head, drawdown, or water budget data that will be printed to a file or saved to a file. The input file was modified for this project by adding stress periods 88 through 599. For the simulations, head, drawdown, and water budget data were saved in time step two of stress period 1 (1912) and then in time step two of every 5th stress period between 1915 and 2310. These parameters were saved in time step two of every 10th stress period between 2320 and 2510.

Recharge Package, RCH (RCH_tr7.txt): The recharge package simulates a specified flux distributed in selected model layer 1 cells. MODFLOW-2000 multiplies the flux by the horizontal area of the cells to calculate volumetric flux rates. This file required most of the critical modifications to use the Regional Model for simulation climate change effects. As described in Section 5.3.1, recharge in the Regional Model was created using nine zones and five recharge parameters. To fit recharge to observed discharge, the USGS adjusted recharge using a recharge multiplication array and recharge parameters based on the nine zones. The input file for this project was modified by changing the array in the original USGS model to a single column of values where each value corresponds to a specific Layer 1 cell. During simulations completed for this project, the column of recharge values was multiplied by an appropriate factor to represent a change in recharge during any desired range of stress periods.

Well Package, WEL (new_irr_ret_03_7.txt): The wel package simulates a specified flux to individual cells through time. In the Regional Model this file is used to specify return flow of water pumped from irrigation wells that is not used consumptively. Return flow is credited as recharge to the uppermost groundwater surface in the model with a lag time of 7 years. The file lists each irrigation well used in calibrating the model, and incorporates the return flow rate for each well during each stress period. The Regional Model file includes pumping data through 2003. The input file was modified for this project by adding stress periods 88 through 599.

Therefore, in simulations completed for this project and accounting for the 7 year lag time, the return flow rate was constant from 2011 through 2510.

Name File (name7.txt): This file specifies the names of the input and output files, associates each file name with a unit number, and identifies the packages that will be used in the model. The name file also controls the parts of the model program that are active. This file was modified by renaming the CHD, DIS, DRN, MNW1, OC, RCH, and WEL packages, and adding a cell budget term for use with the ZoneBudget program.

5.5.2 Recharge-Related Command Files

In addition to modifying Regional Model input files, several new files were created to assist in changing recharge values, and running simulations in command line mode. The files are:

Recharge Multiplier (rech_perc.txt): This file is used in applying a recharge factor to input file containing recharge values for each Layer 1 cell in the Regional Model. The file applies a user-selected recharge factor for stress periods 1 through 599 (1912 – 2510).

Fortran File (rech_future.f90): This file contains the command codes that instruct the program to properly format and apply the values in the recharge multiplier file to the recharge input file.

Executable File (RECH_FUTURE.exe): This file executes the commands from the Fortran file and calculates the correct recharge applied to Layer 1 cells.

5.5.4 Simulating Climate Change

Simulations for this project were executed using the entire Regional Model. However, results were evaluated only for the study area (with the exception of water budgets for the entire model domain). Climate change effects on the groundwater flow system were evaluated by altering the recharge package in the Regional Model as described above. All simulations completed for this project assume that the percentage change in precipitation is matched by an equal percentage change in recharge to the groundwater system.

The initial simulation (100 % of 20th Century recharge) consisted of holding all parameters, including pumping and current recharge constant through the year 2510. The Climate Tracking Model and other simulations were produced by replacing the constant recharge values. Recharge was not modified from the USGS values through 2000. After 2000, recharge values were modified in accordance with the projected precipitation data from the downscaled climate models. New recharge values were obtained by multiplying the original value by a factor representing the percent change in recharge simulated by the aggregated climate models, as shown in Table 6. The climate models do not make projections past the year 2099. Therefore, the values of recharge projected by the climate models for the 2070 through 2099 period were extended through the year 2510.

The remaining simulations were conducted by adding or subtracting to the Climate Tracking Model recharge values. Simulations of additional recharge were conducted in increments of 3 percent up to 109 percent of the Climate Tracking Model. Simulations of lower recharge were conducted in increments of 3 percent to 85 percent of the Climate Tracking Model. Thereafter, recharge was reduced in increments of 5 percent or 10 percent to a low value of 50 percent of the Climate Tracking Model. The constants and the resulting recharge values for each simulation are shown in Table 6.

Table 6. Recharge Factors Applied to Simulations

	Period			
	1912 to 2000	2001 to 2039	2040 to 2069	2070 to 2510
Average Percent Change in Recharge	0	-0.200	-1.637	-2.528
	Recharge Factor			
100% of 20th Century Recharge	1	1	1	1
Climate Tracking Model	1	.9980	.9836	.9747
109% of Climate Model	1	1.0880	1.0736	1.0647
106% of Climate Model	1	1.0580	1.0436	1.0347
103% of Climate Model	1	1.0280	1.0136	1.0047
97% of Climate Model	1	.9680	.9536	.9447
94% of Climate Model	1	.9380	.9236	.9147
91% of Climate Model	1	.9080	.8936	.8847
88% of Climate Model	1	.8780	.8636	.8547
85% of Climate Model	1	.8480	.8336	.8247
80% of Climate Model	1	.7980	.7836	.7747
75% of Climate Model	1	.7480	.7336	.7247
70% of Climate Model	1	.6980	.6836	.6747
60% of Climate Model	1	.5980	.5836	.5747
50% of Climate Model	1	.4980	.4836	4747

Pumping was simulated as constant using current pumping rates throughout most simulations. However, one simulation was conducted with reduced pumping in the study area to evaluate the overall effects of pumping compared to climate change. Other boundary conditions also were held constant throughout the simulations, except those that may have changed in accordance with change in recharge values.

6.0 Results

Evaluating the results of model simulations included comparing changes in groundwater head in cells throughout the study area and head in multiple layers within cells, developing plots of groundwater contours in Layer 1, and comparing changes in discharge from drain cells.

6.1 Simulated Groundwater Head Change

Simulated changes in head in the study area were evaluated for the approximate 500-year period from 2000 to 2500. Data from the simulations were compared to the baseline condition in which 100 percent of 20th Century recharge was continued throughout entire period from 1912 to 2500. Analysis focuses on the years from 2000 to 2500 because this is the period in which recharge was changed in the model in accordance with projected changes in precipitation and temperature.

Groundwater head in the study area declined between 2000 and 2500 in all simulations and in all model layers, with one exception. The decline began in the mid-20th Century after pumping had occurred in the Amargosa Desert (and other areas of the DVRFS) for several decades. Simulations indicate that in all cases but one, head continues to decline through the year 2500, although the rate of decline typically moderates after about 2200. The decline in head is simulated as greater in the Amargosa Desert than in Death Valley. The locations of cells where changes in head were examined are shown in Figure 19. Additional groundwater head graphs are included in Appendix B.

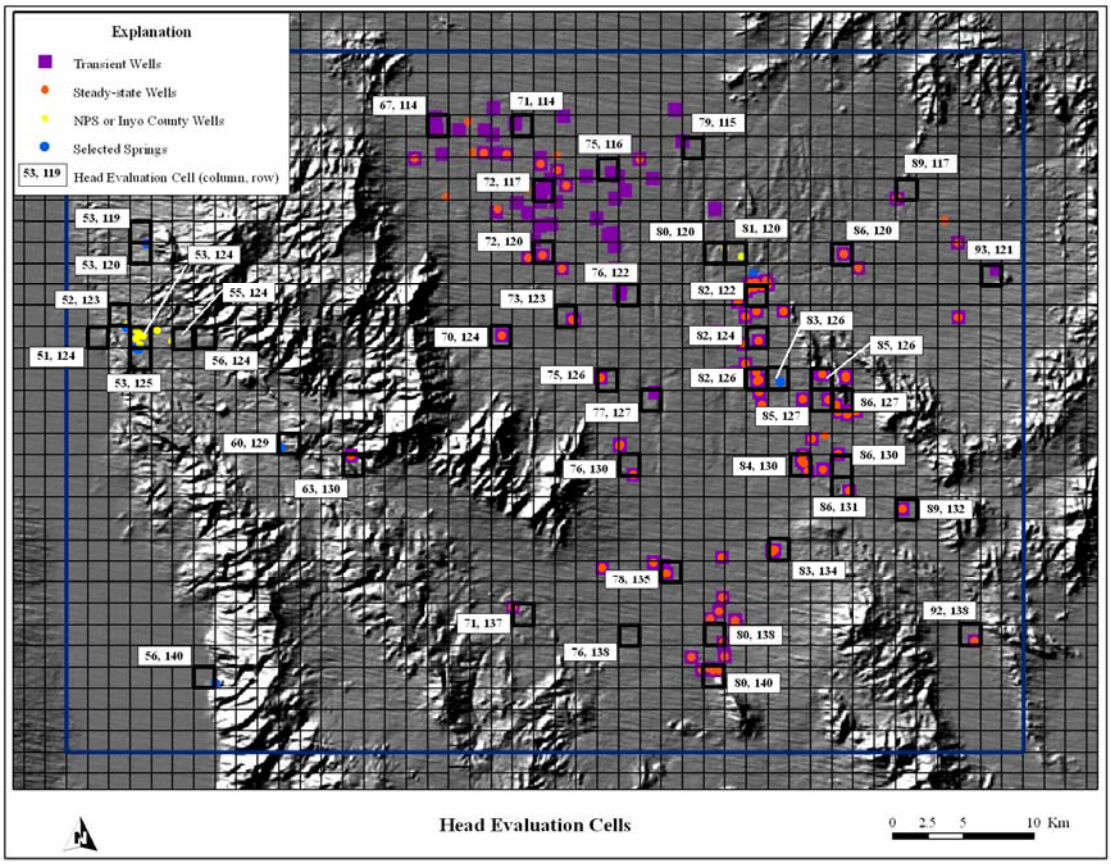

Figure 19. Cells for Evaluation of Groundwater Head Changes

6.1.1 Groundwater Head Change in the Amargosa Desert

Simulated declines in head in the Amargosa Desert in the baseline condition of 100 percent of 20th Century recharge ranged from zero to greater than 23 meters between 1912 and 2000. For the period from 2000 to 2500, the additional decline in simulated head ranged from 2 meters to greater than 41 meters, as shown in Table 7.

Table 7. Simulated Total Head Decline from 2000 to 2500: 100 % of 20th Century Recharge

	Average Decline in Head	
Location	All Layers Examined	Layer 1
Amargosa Central Pumping Area	21.2 meters	23.5 meters
Ash Meadows	7.3 meters	6.4 meters
Cells outside the central pumping area and outside Ash Meadows	6.8 meters	6.4 meters

The average simulated head decline between 2000 and 2500 in the pumping area of the Amargosa Desert (the Amargosa Farms agricultural area) was between 21 and 24 meters. In Ash Meadows and other areas of the Amargosa Desert, the decline was between 6 and 8 meters. The locations in Table 7 are shown in Figure 20. In Figure 20, Amargosa pumping area cells are shown in yellow, Ash Meadows cells in blue, and other cells in green. White cells are in the Death Valley portion of the study area and are not included in this analysis.

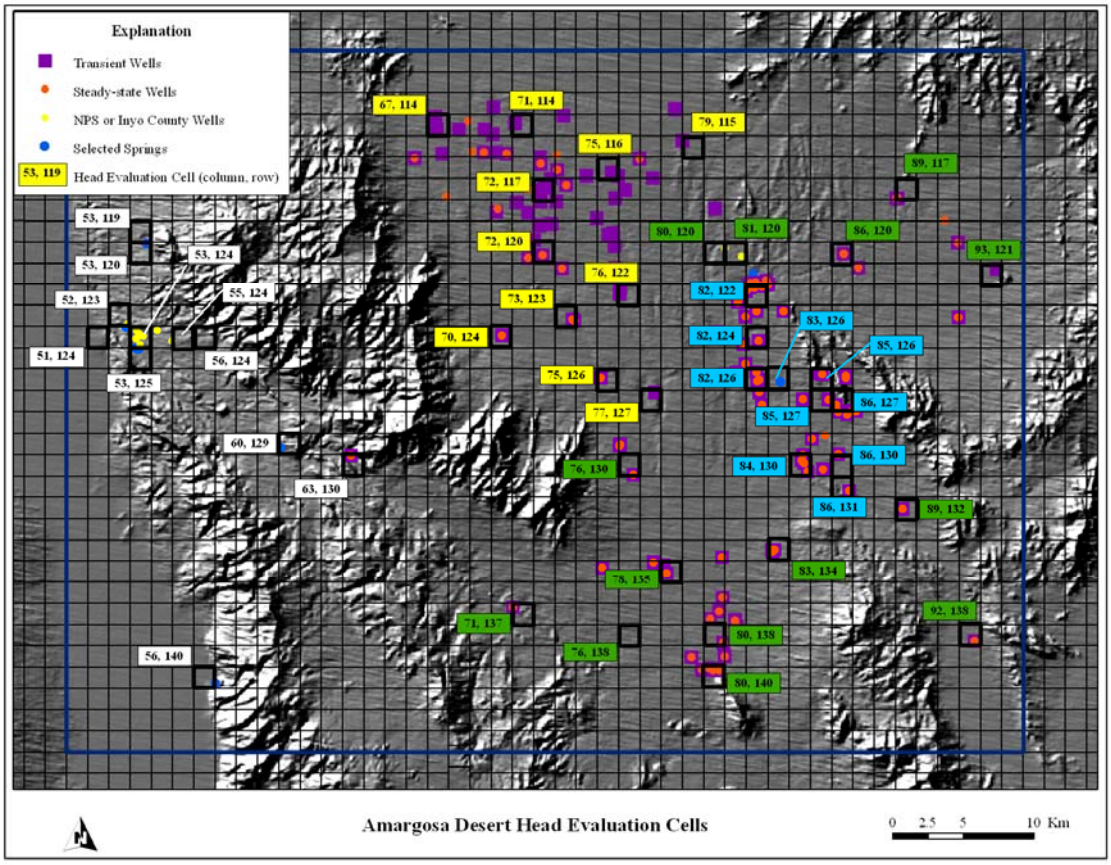

Figure 20. Amargosa Pumping Area, Ash Meadows, and Other Locations

For the model runs with recharge greater than the baseline scenario, simulations indicate head increases relative to baseline. For the period from 2000 to 2500, the increase in simulated head relative to baseline ranged from zero meters to 0.26 meters, depending on cell and layer. However, simulations also indicate an overall decline in head even when recharge is increased.

For the model runs with recharge less than the baseline scenario, simulations indicate head declines relative to baseline. For the period from 2000 to 2500, the decline in simulated head relative to baseline ranged from zero meters to 1.54 meters, depending on cell and layer.

Simulated changes in head for selected cells within the Amargosa Desert are shown in Figures 21 through 38. The hydrographs present the overall change in head from 1912 to 2500 and the relative range of head change for the scenarios of 109 percent of baseline recharge, the Climate Model, and 50 percent of baseline recharge. The bar graphs quantify head change in Layer 1 for each recharge scenario at each cell evaluated.

Figures are grouped by location as in Table 7: Amargosa Pumping Area, Ash Meadows, and Other locations. The figures include the USGS designated well name, and the model cell and layer. Cell locations are shown in Figure 20.

6.1.1.1 Amargosa Pumping Area

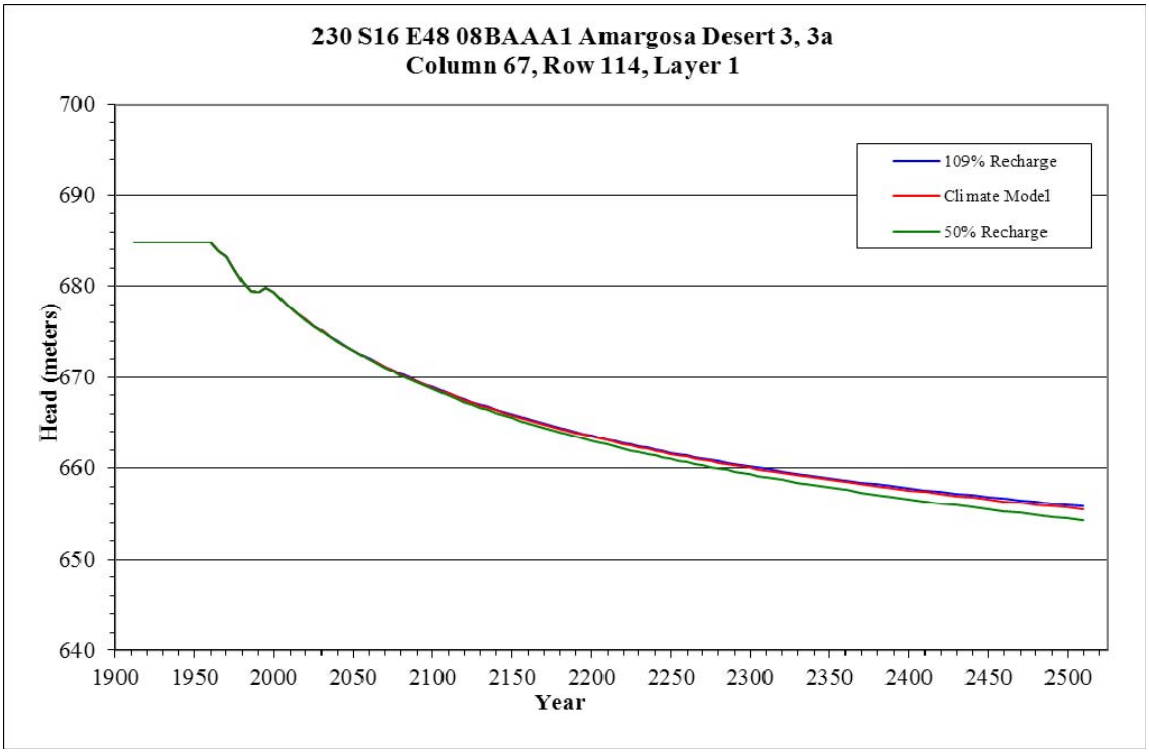

Figure 21. Head Change in Column 67, Row 114, Layer 1

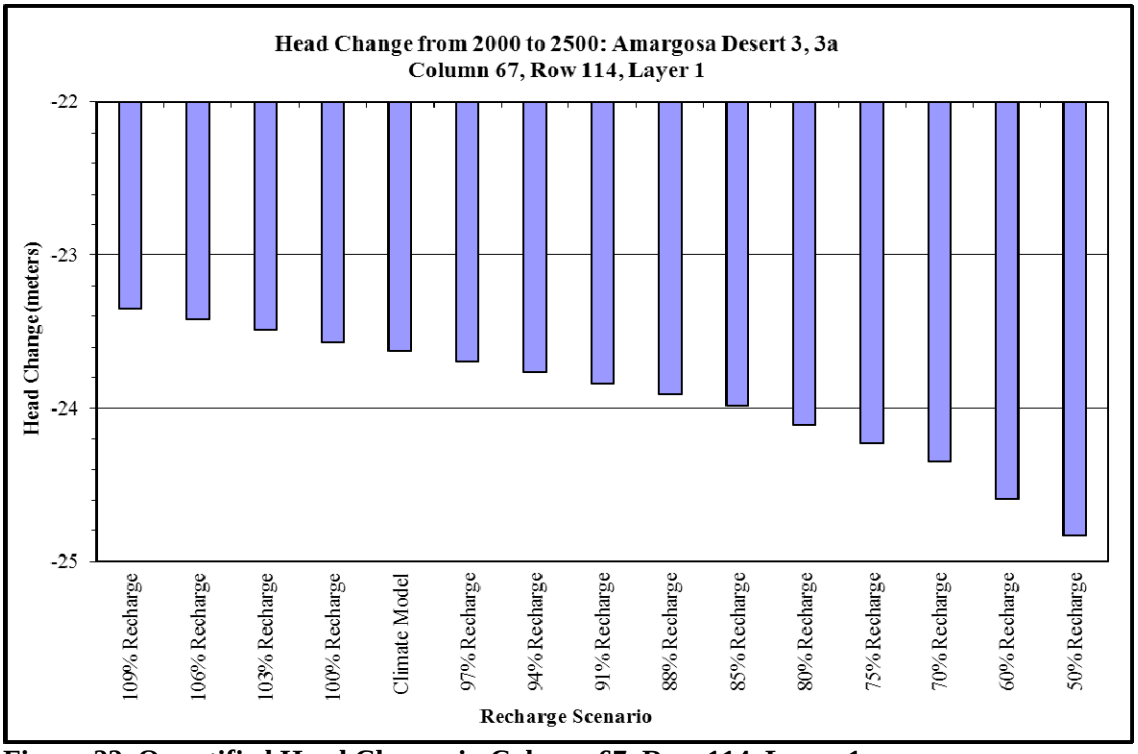

Figure 22. Quantified Head Change in Column 67, Row 114, Layer 1

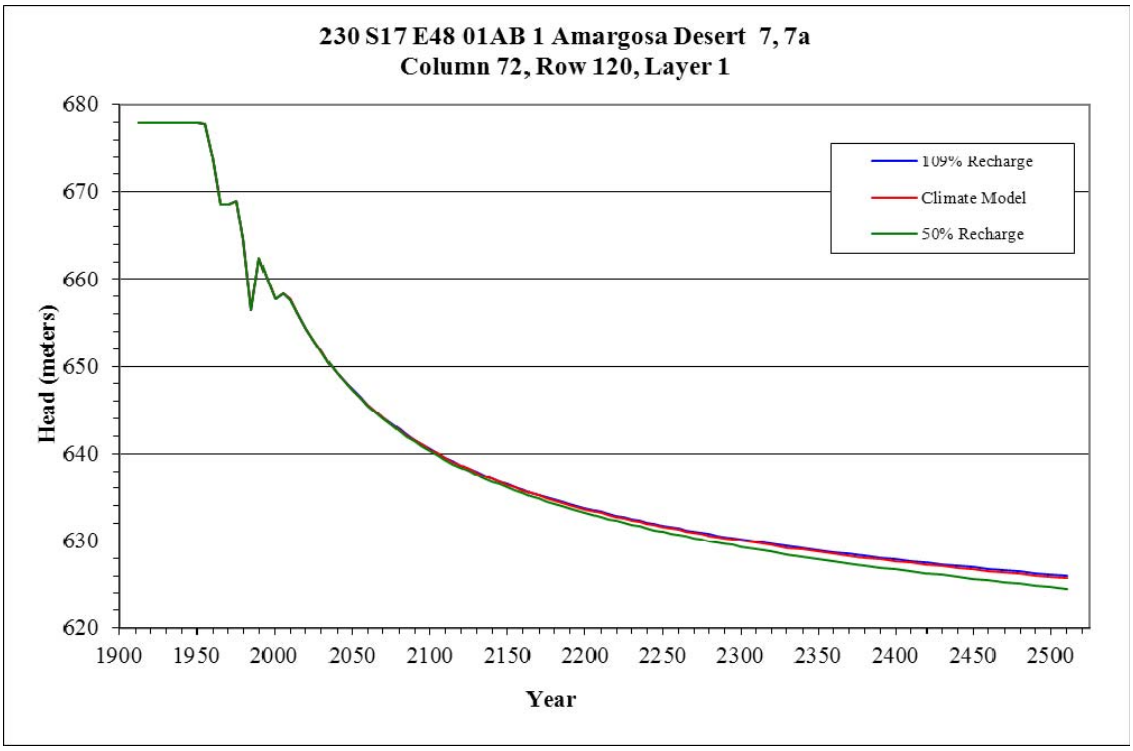

Figure 23. Head Change in Column 72, Row 120, Layer 1

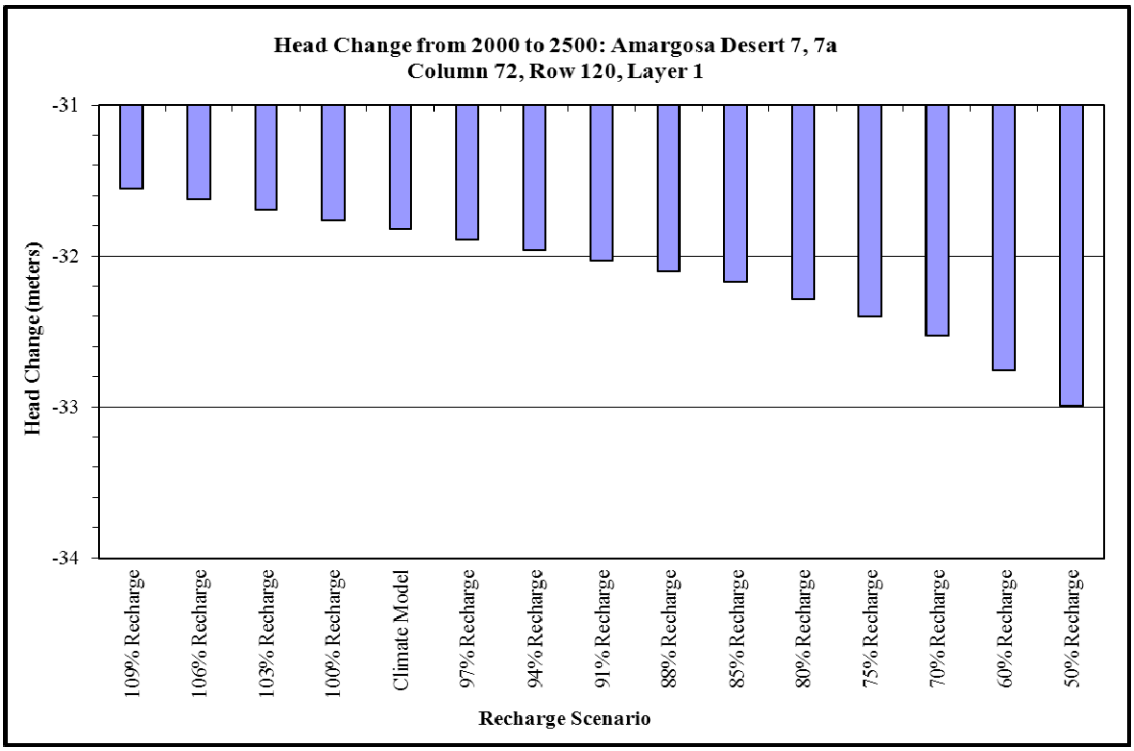

Figure 24. Quantified Head Change in Column 72, Row 120, Layer 1

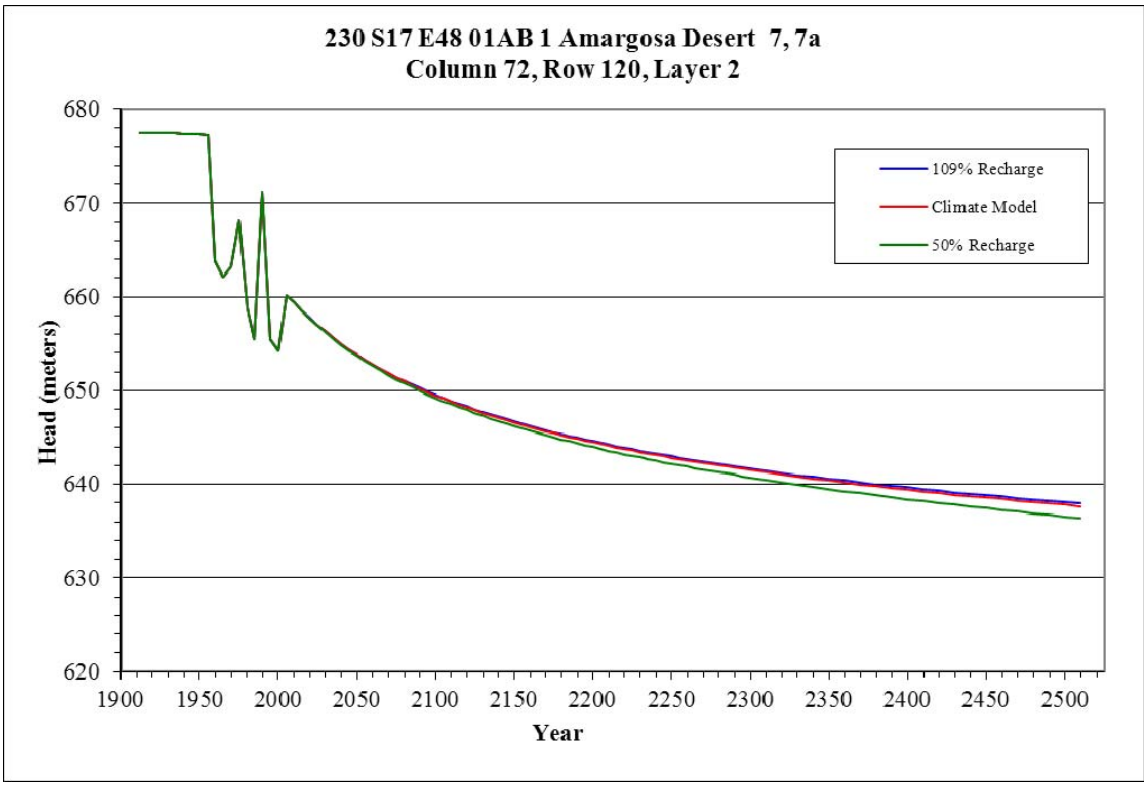

Figure 25. Head Change in Column 72, Row 120, Layer 2

6.1.1.2 Ash Meadows Area

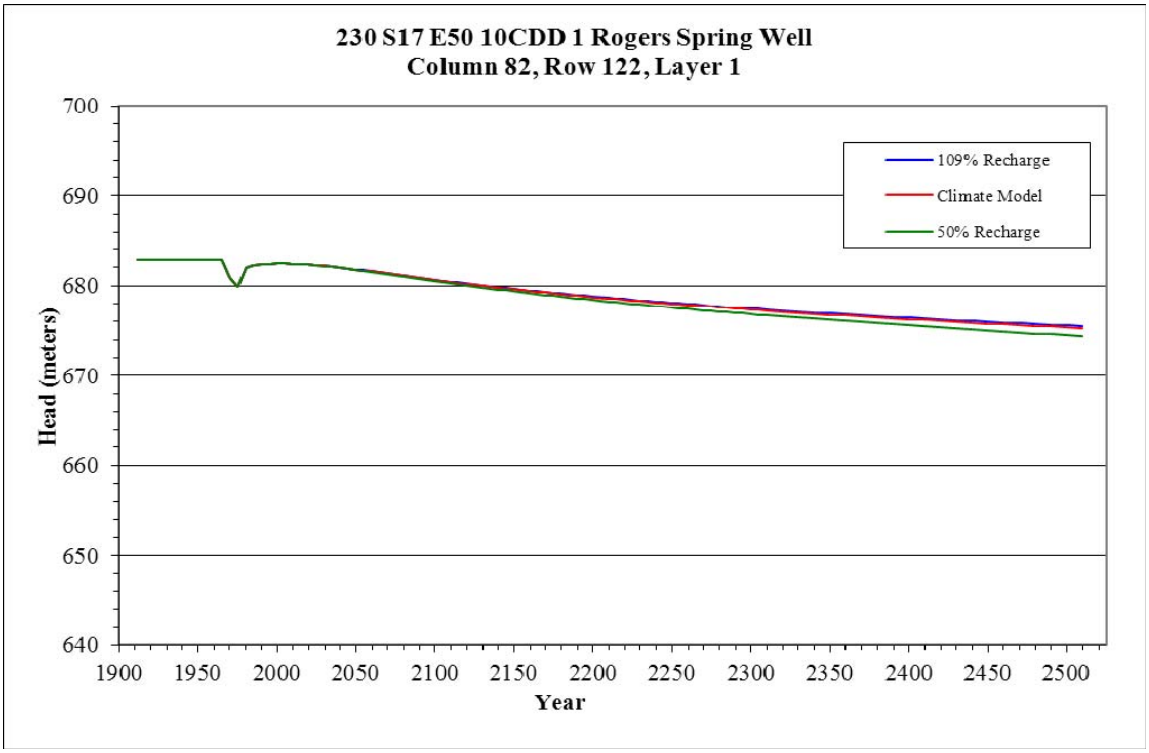

Figure 26. Head Change in Column 82, Row 122, Layer 1

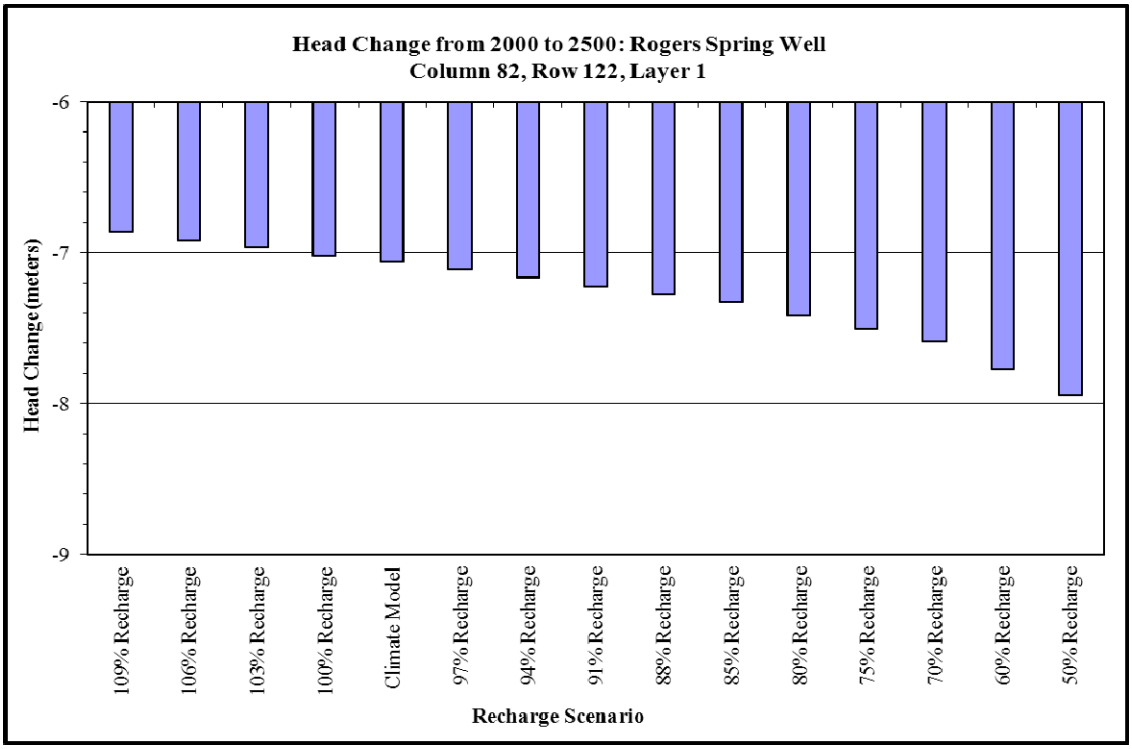

Figure 27. Quantified Head Change in Column 82, Row 122, Layer 1

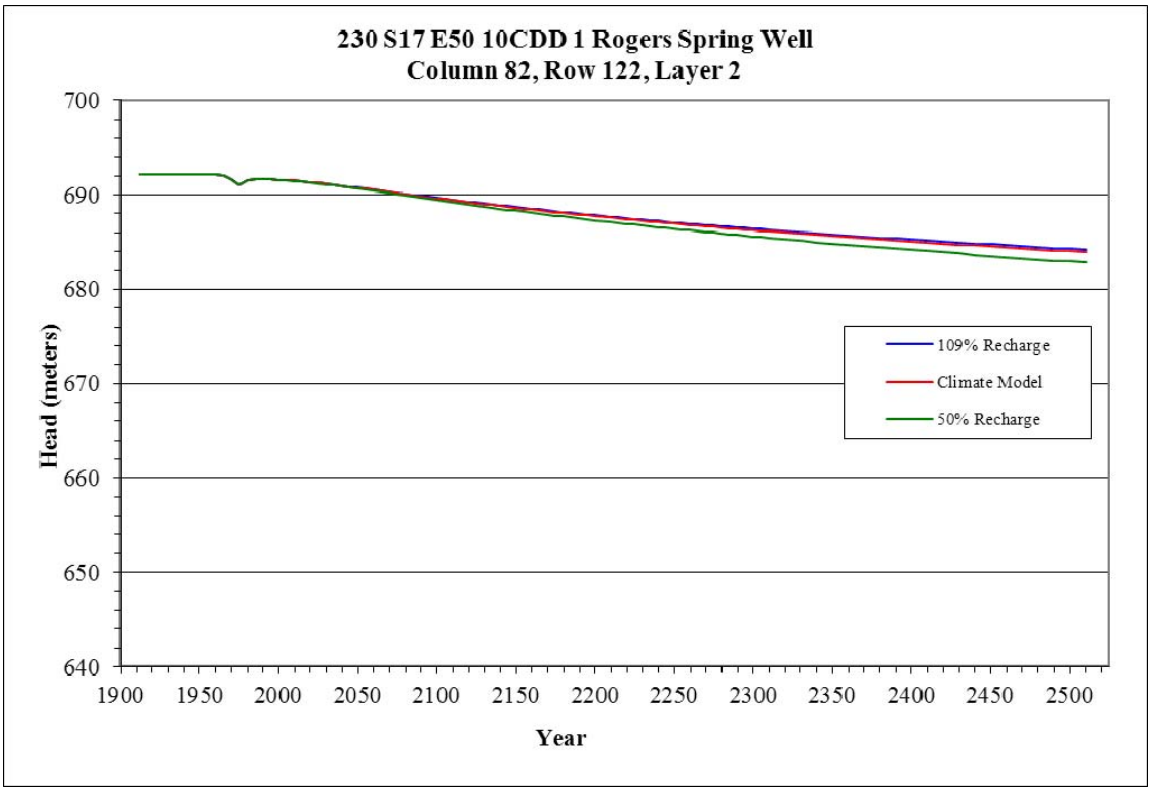

Figure 28. Head Change in Column 82, Row 122, Layer 2

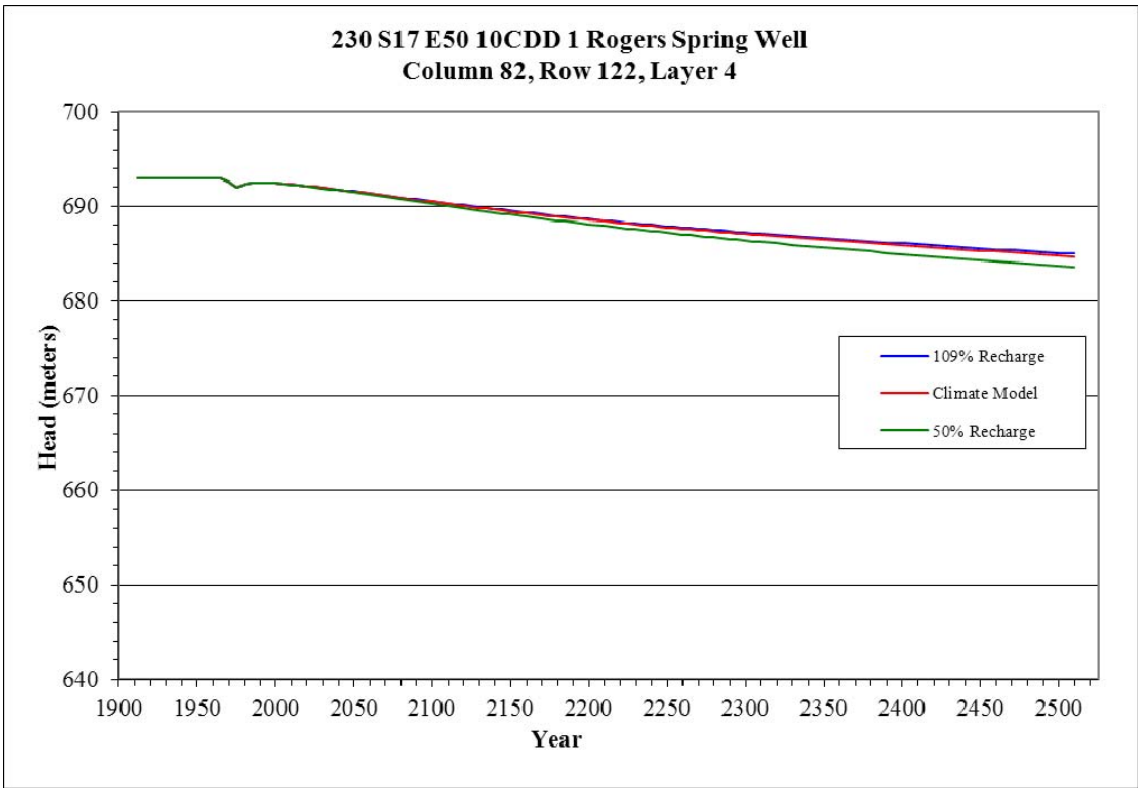

Figure 29. Head Change in Column 82, Row 122, Layer 4

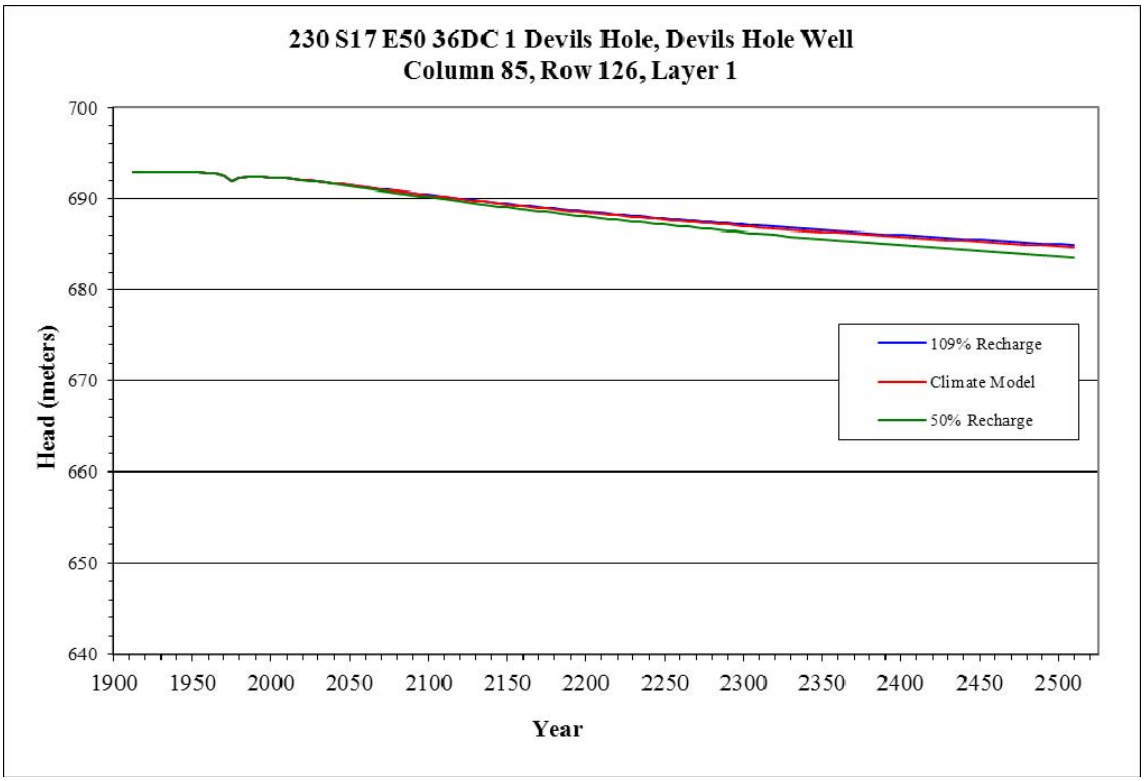

Figure 30. Head Change in Column 85, Row 126, Layer 1

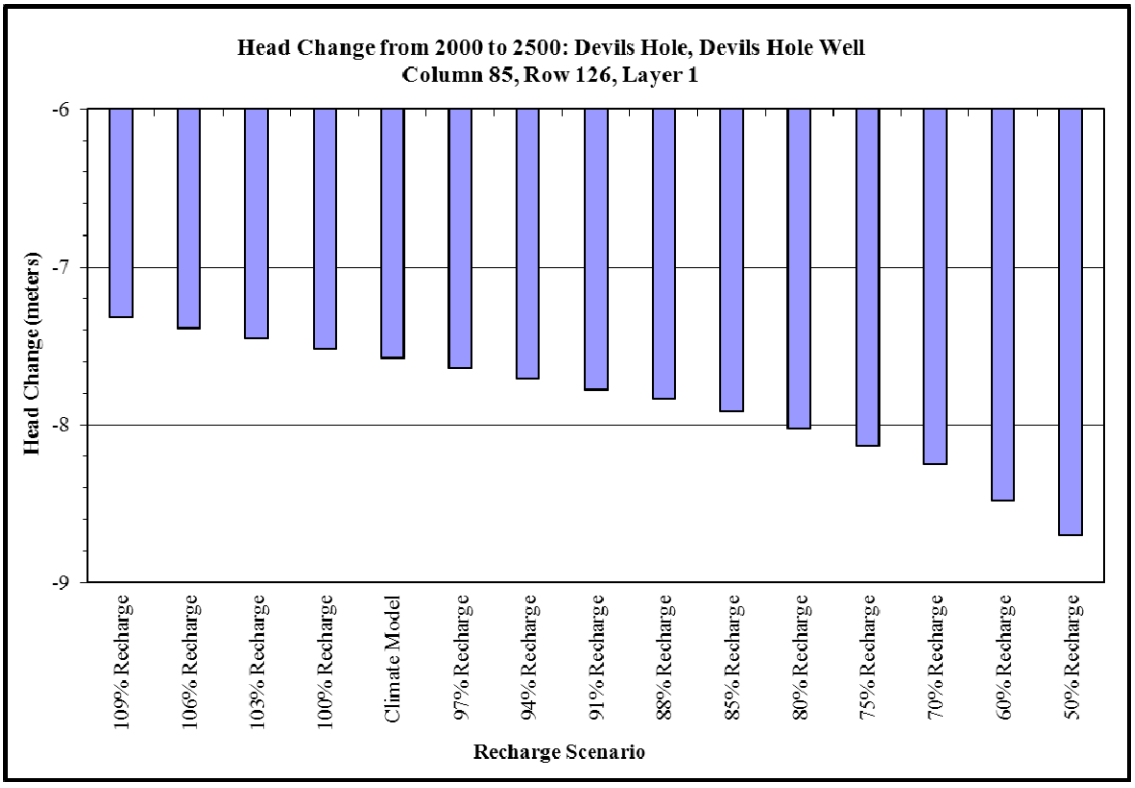

Figure 31. Quantified Head Change in Column 85, Row 126, Layer 1

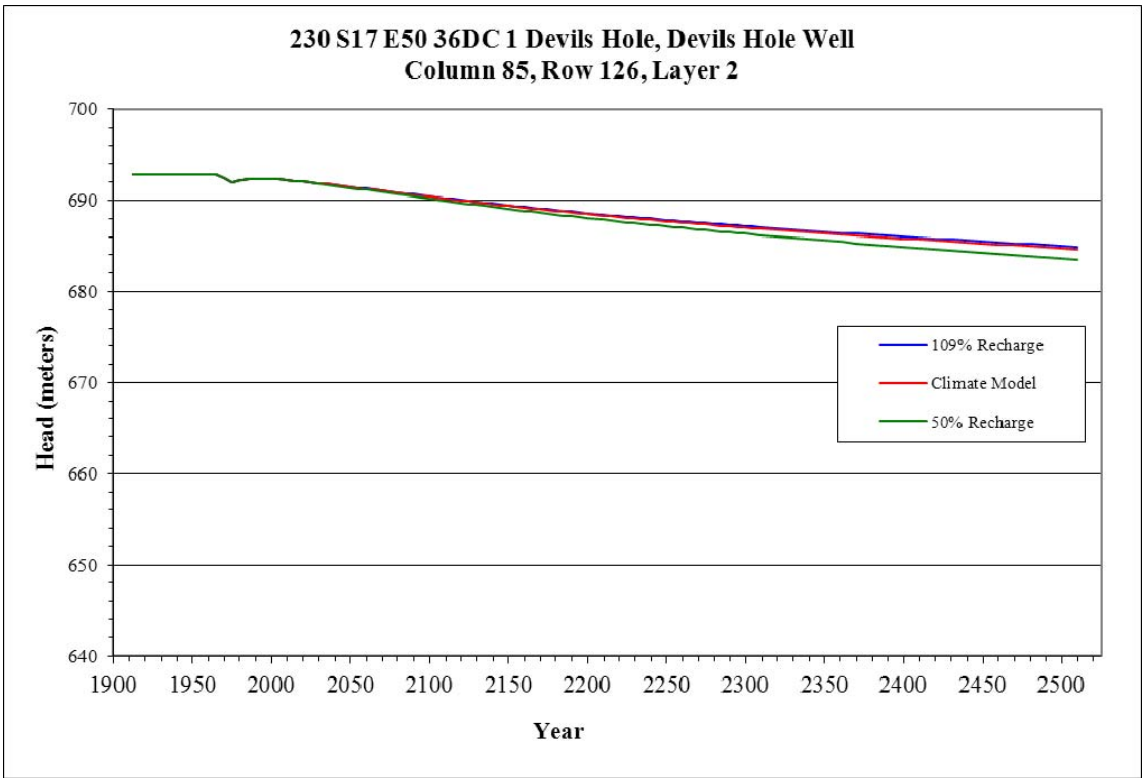

Figure 32. Head Change in Column 85, Row 126, Layer 2

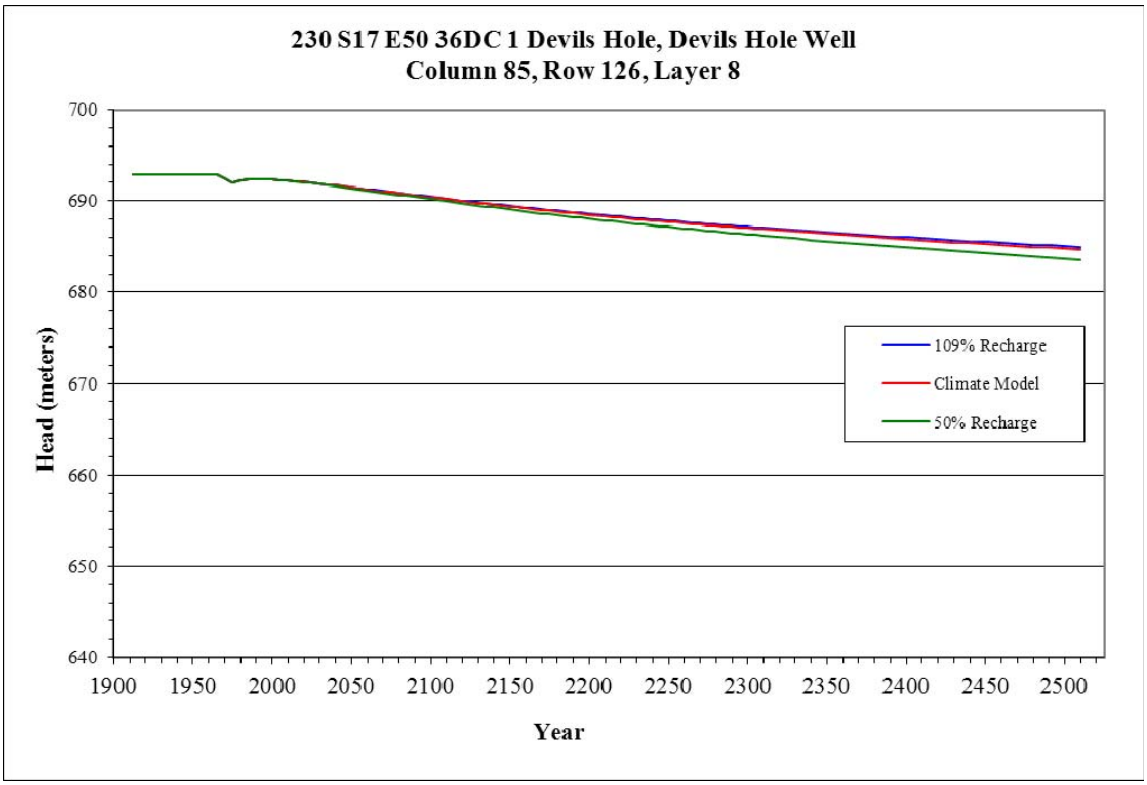

Figure 33. Head Change in Column 85, Row 126, Layer 8

6.1.1.3 Amargosa Desert, Excluding Amargosa Farms and Ash Meadows

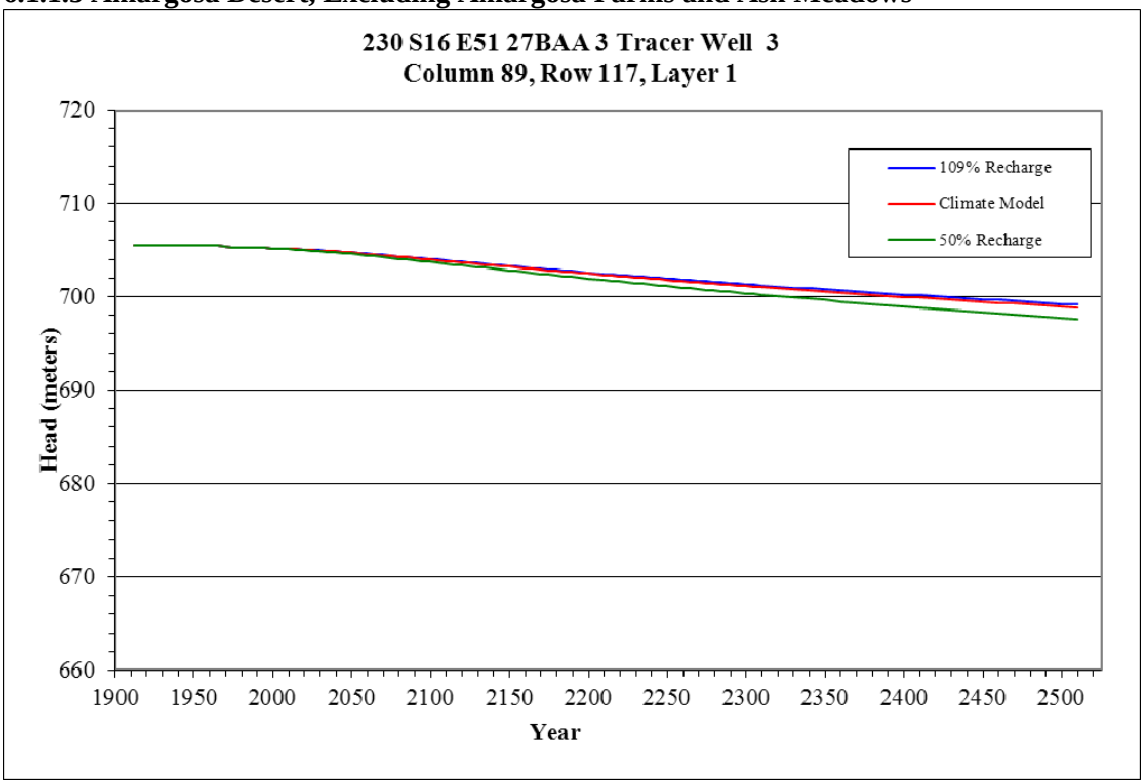

Figure 34. Head Change in Column 89, Row 117, Layer 1

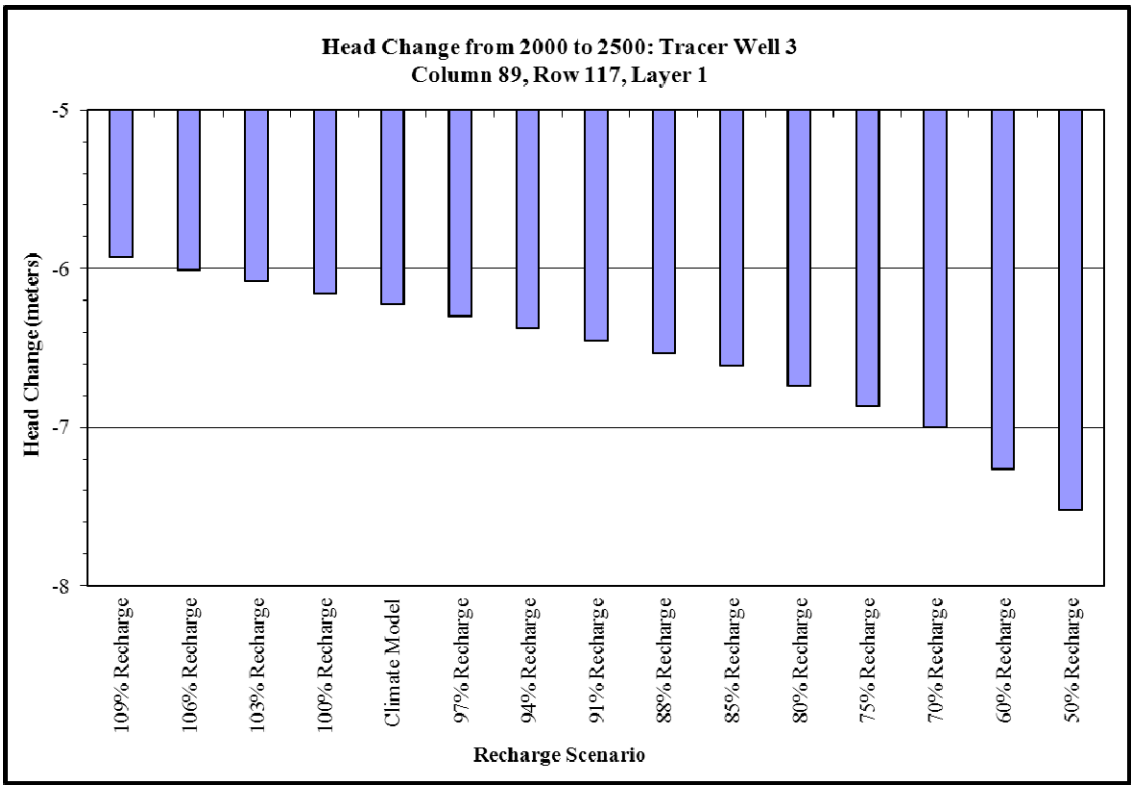

Figure 35. Quantified Head Change in Column 89, Row 117, Layer 1

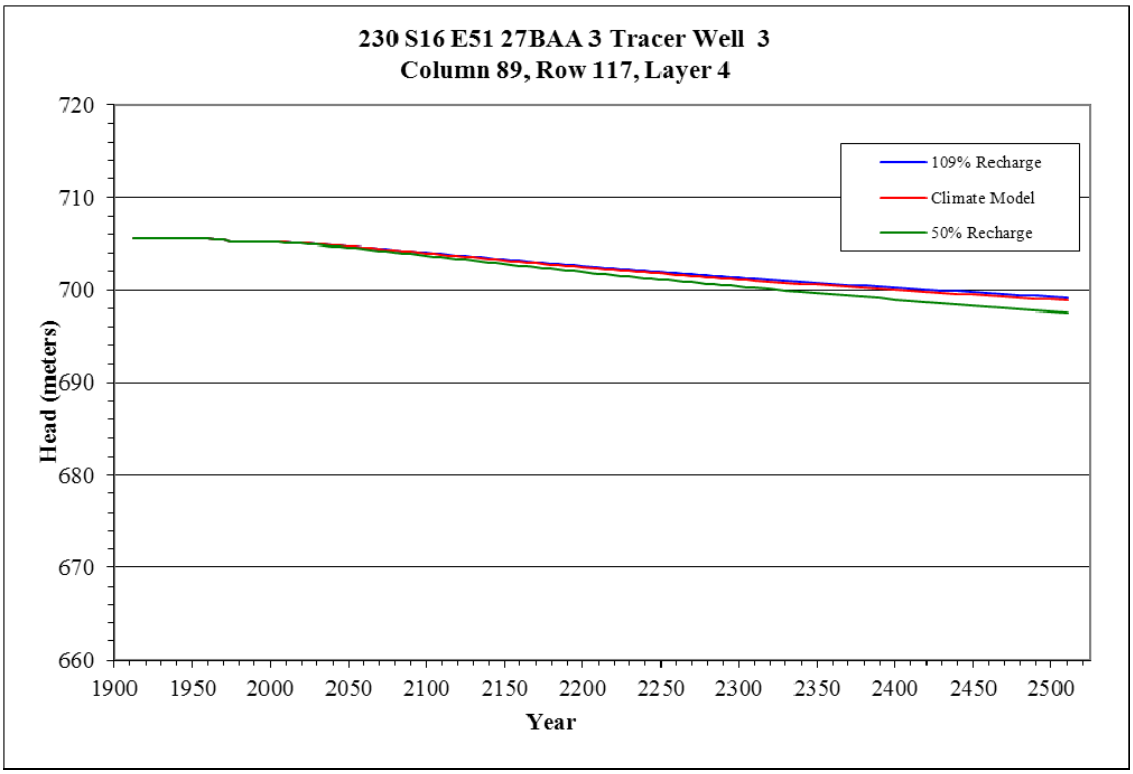

Figure 36. Head Change in Column 89, Row 117, Layer 4

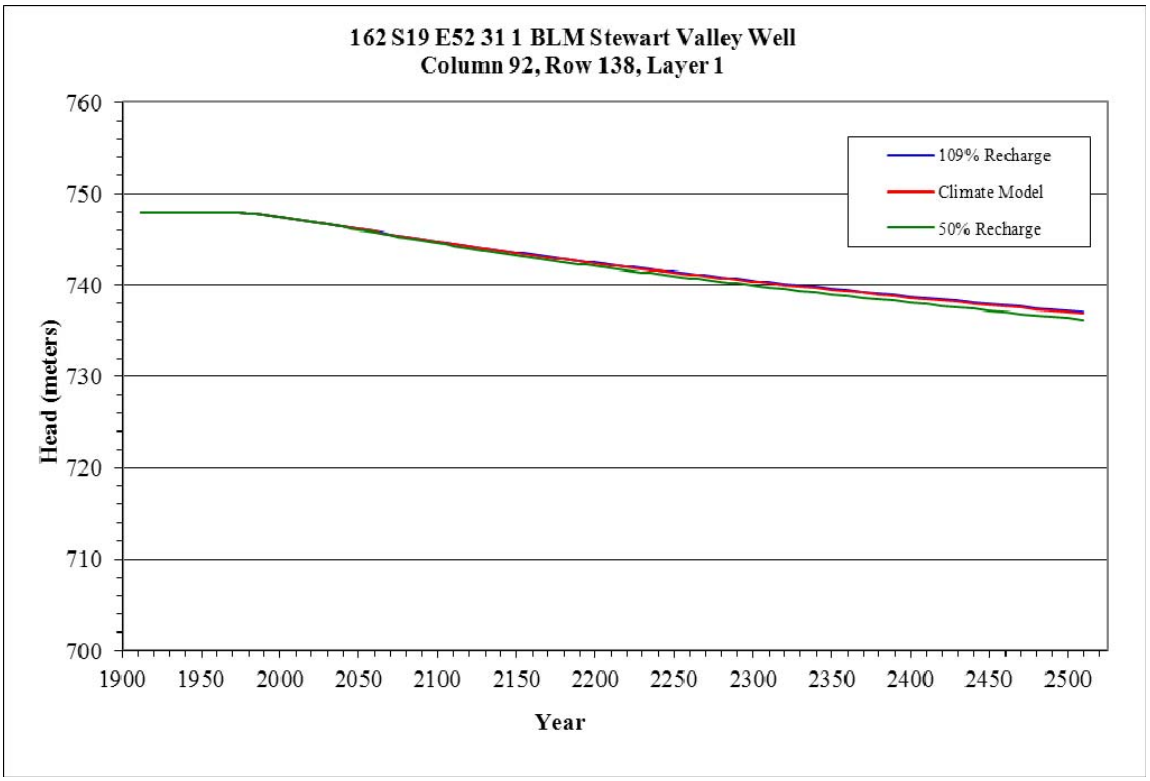

Figure 37. Head Change in Column 92, Row 138, Layer 1

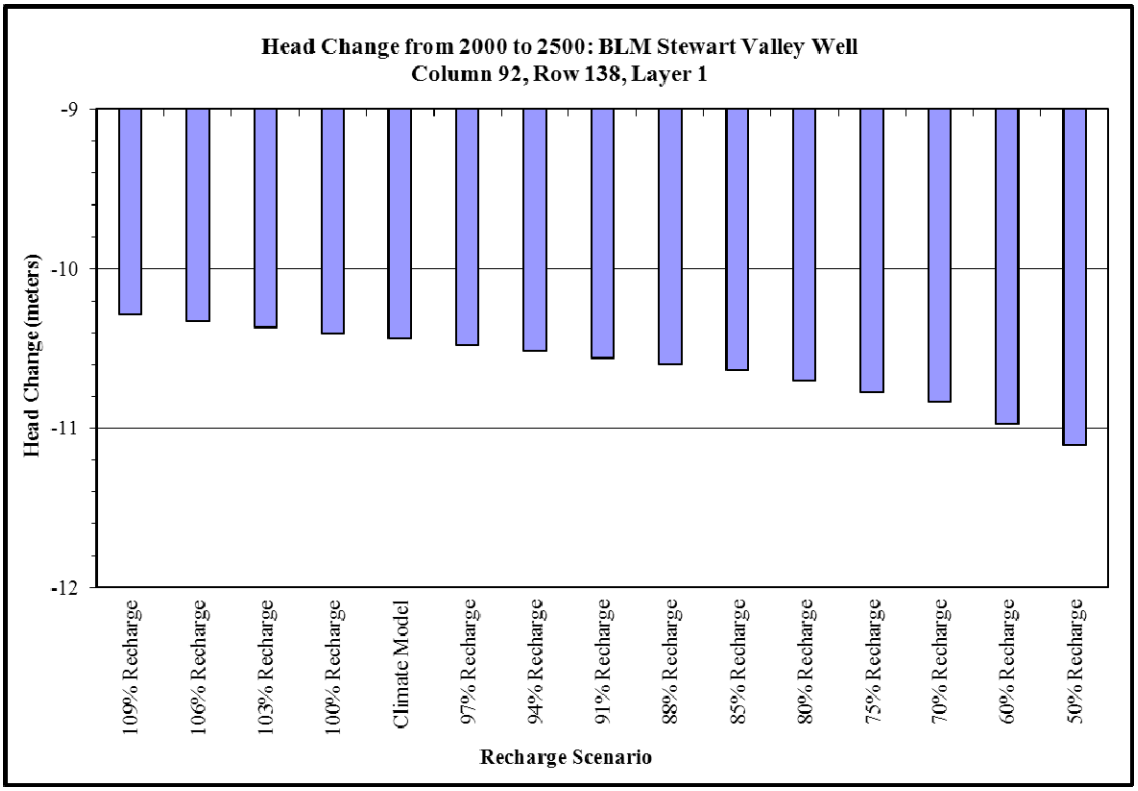

Figure 38. Quantified Head Change in Column 92, Row 138, Layer 1

6.1.2 Groundwater Head Change in Death Valley National Park

The simulated declines in head in Death Valley in the baseline condition of 100 percent of 20th Century recharge were essentially zero (less than 0.03) meters between 1912 and 2000. For the period from 2000 to 2500, the additional decline in simulated head ranged from zero to greater than 9 meters. Simulated declines greater than 5 meters were observed in cells (55,124; 56,124; 60,129; and 63,130) located along the southern flank of the Funeral Mountains and upgradient from the spring discharge area of Furnace Creek (Figure 39).

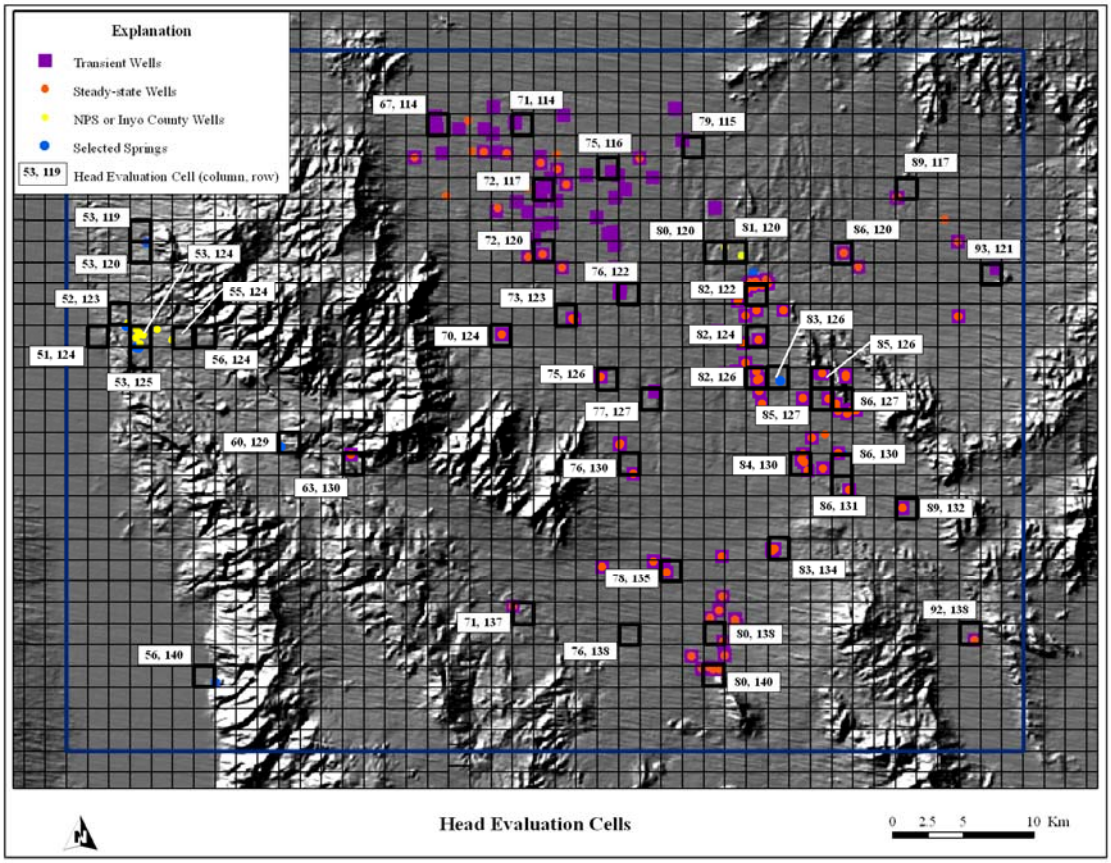

Figure 39. Cells for Evaluation of Groundwater Head Changes

For the model runs with recharge greater than the baseline scenario, simulations indicate head increases relative to baseline. However, simulations also indicate overall decline in head

even when recharge is increased. For the period from 2000 to 2500, the increase in simulated head relative to baseline ranged from zero to 0.34 meters.

For the model runs with recharge less than the baseline scenario, simulations indicate head declines relative to baseline. For the period from 2000 to 2500, the decline in simulated head relative to baseline ranged from zero to 2 meters.

Simulated changes in head for selected cells within Death Valley are shown in Figures 40 through 51. The hydrographs present the overall change in head from 1912 to 2500 and the relative range of head change for the scenarios of 109 percent of baseline recharge, the Climate Model, and 50 percent of baseline recharge. The bar graphs quantify head change in Layer 1 for each recharge scenario at each cell evaluated.

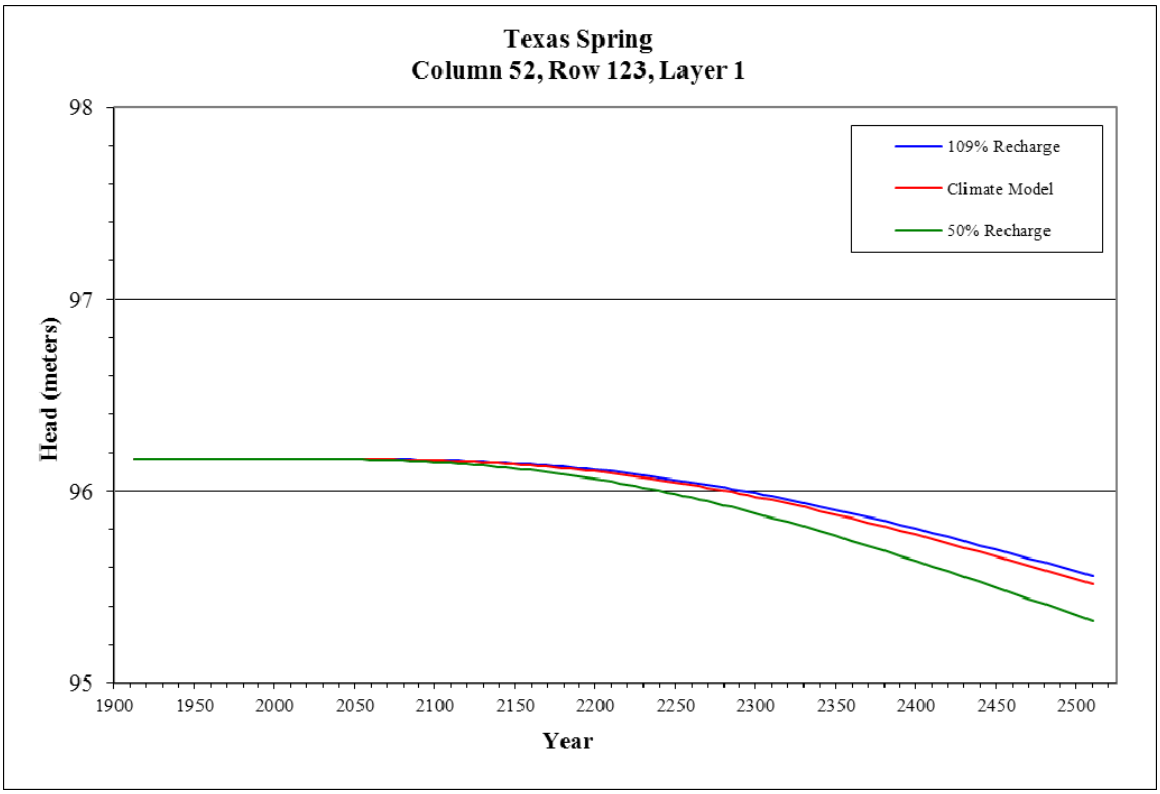

Figure 40. Head Changes in Column 52, Row 123, Layer 1

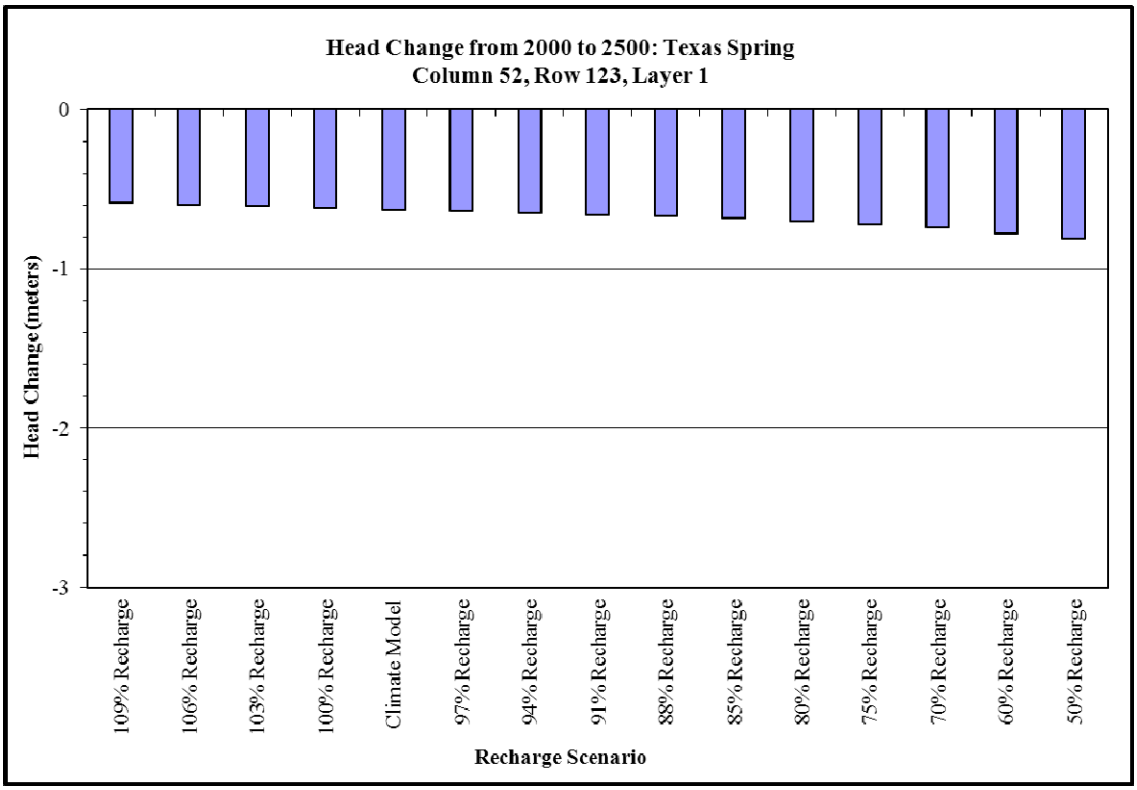

Figure 41. Quantified Head Change in Column 52, Row 123, Layer 1

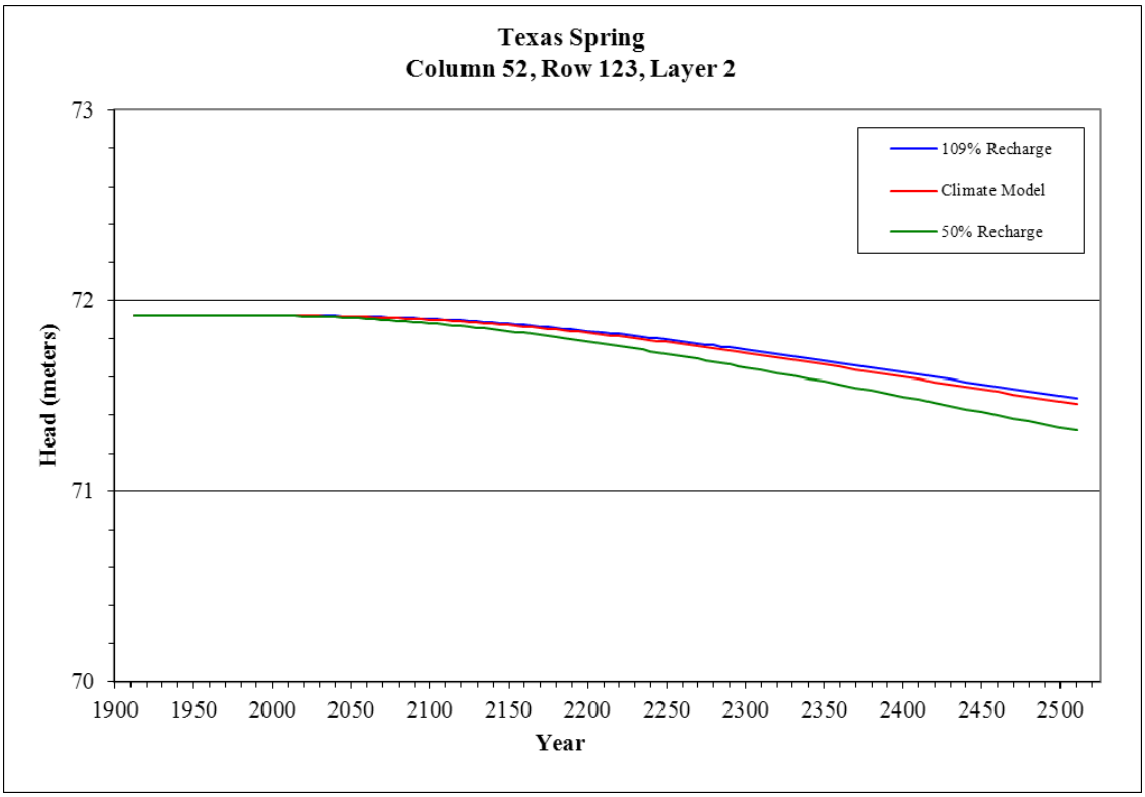

Figure 42. Head Changes in Column 52, Row 123, Layer 2

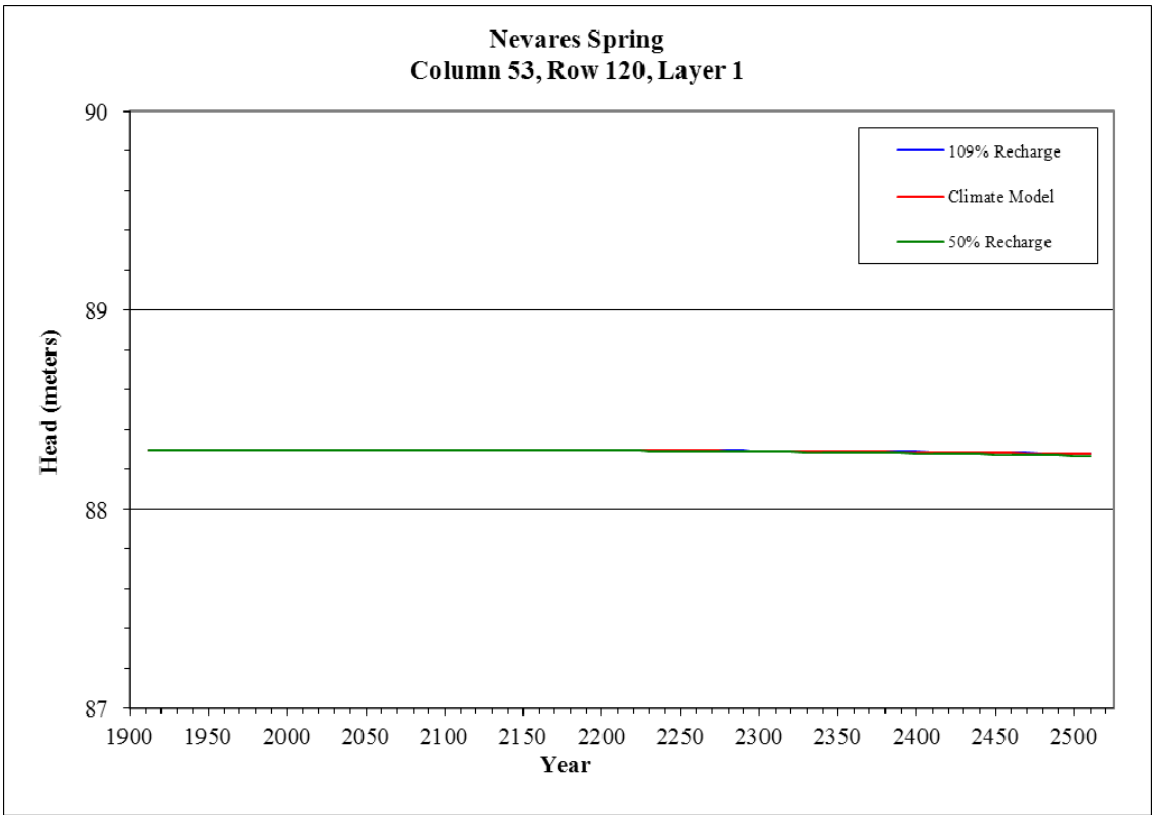

Figure 43. Head Change in Column 53, Row 120, Layer 1

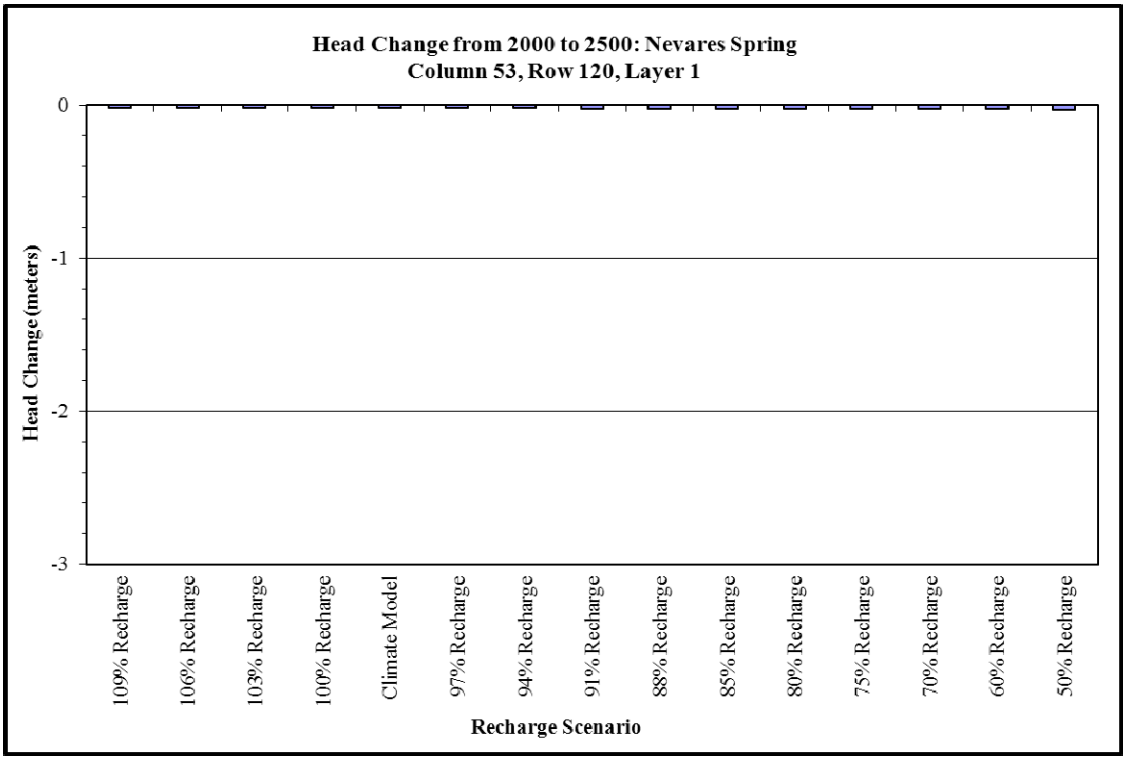

Figure 44. Quantified Head Change in Column 53, Row 120, Layer 1

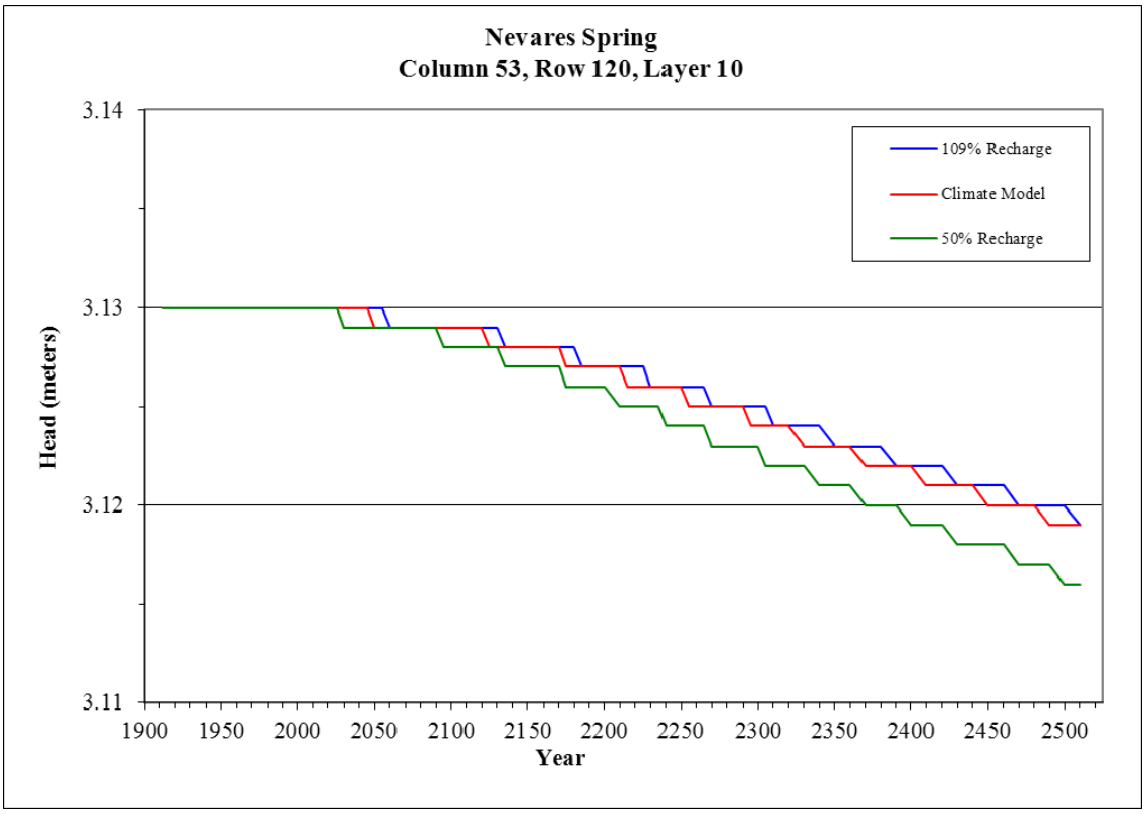

Figure 45. Head Change in Column 53, Row 120, Layer 10

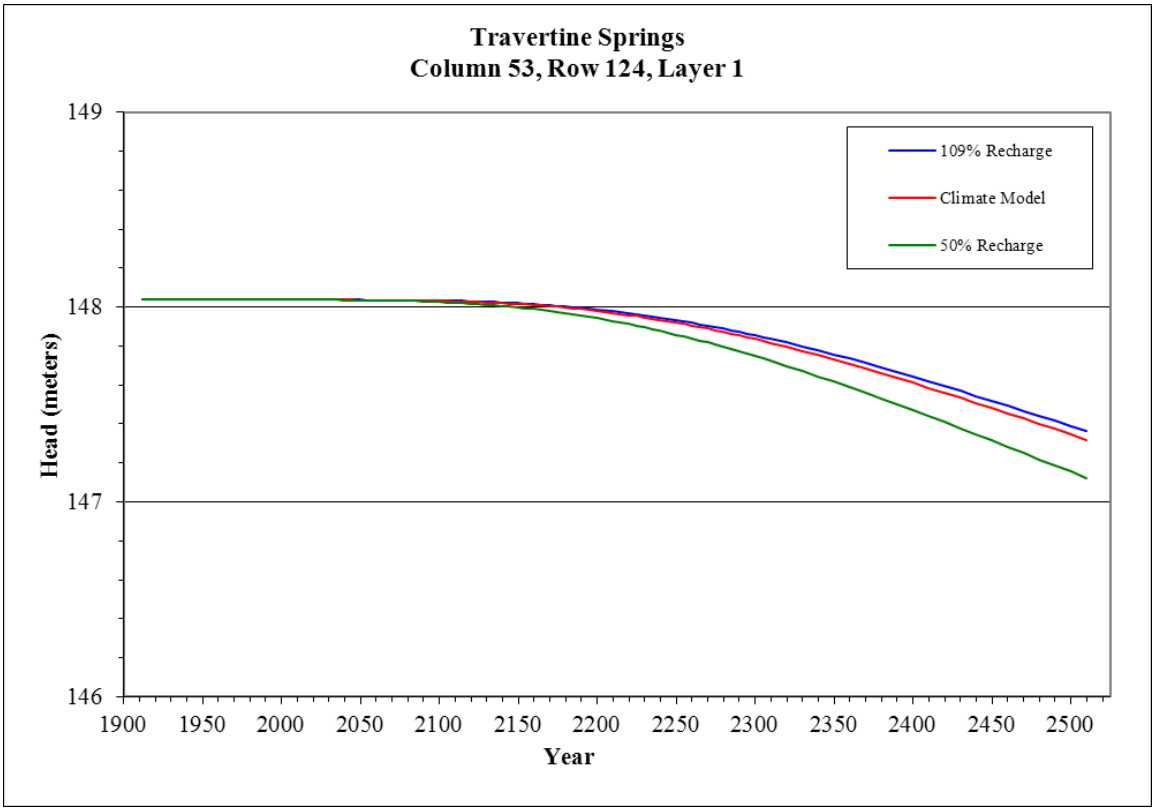

Figure 46. Head Change in Column 53, Row 124, Layer 1

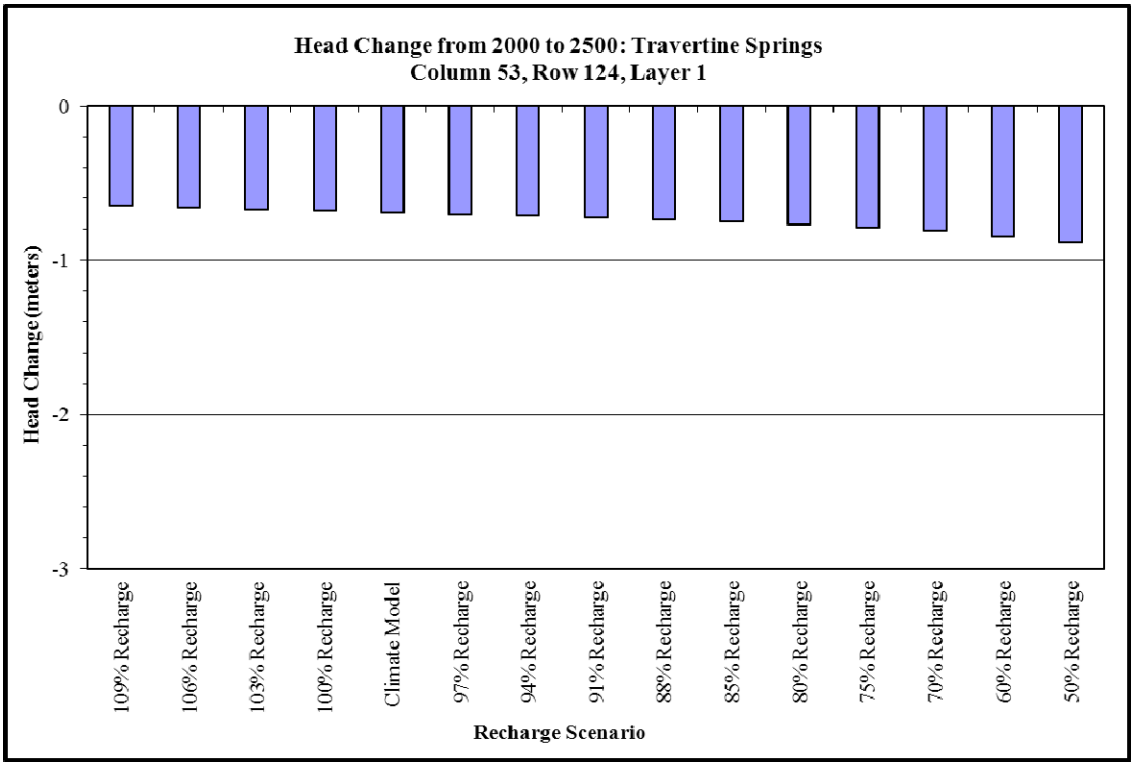

Figure 47. Quantified Head Change in Column 53, Row 124, Layer 1

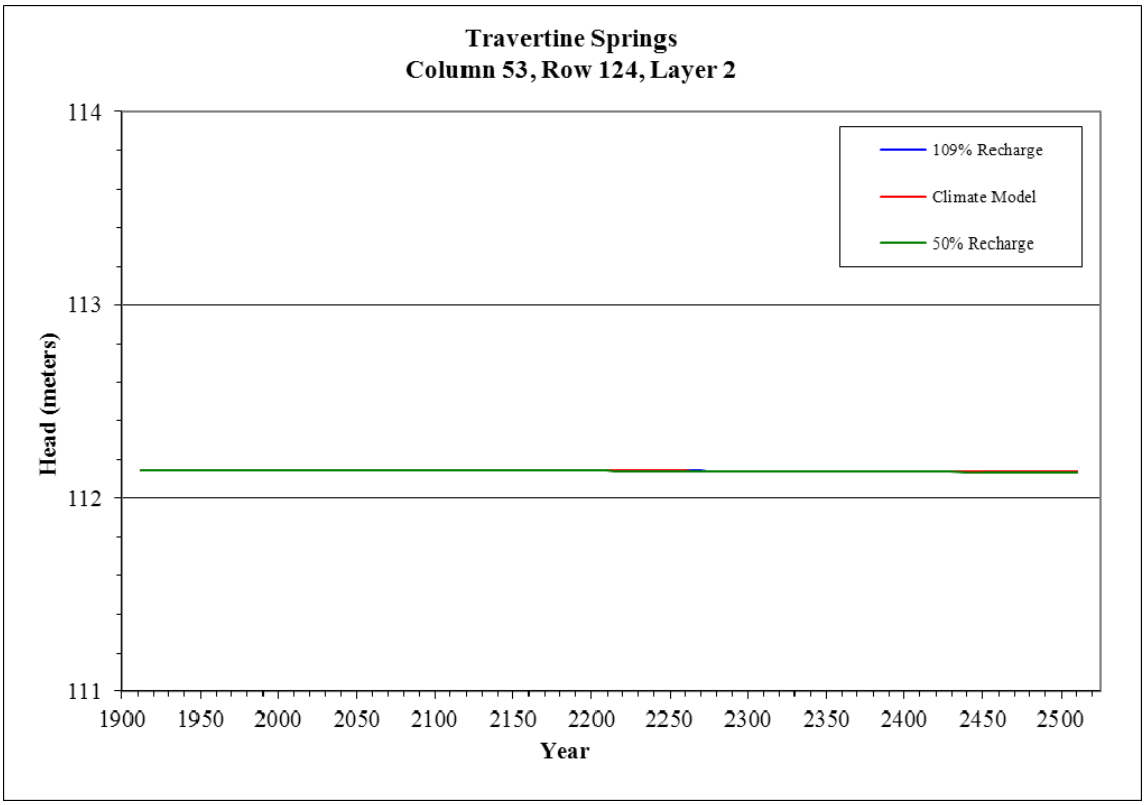

Figure 48. Head Changes in Column 53, Row 124, Layer 2

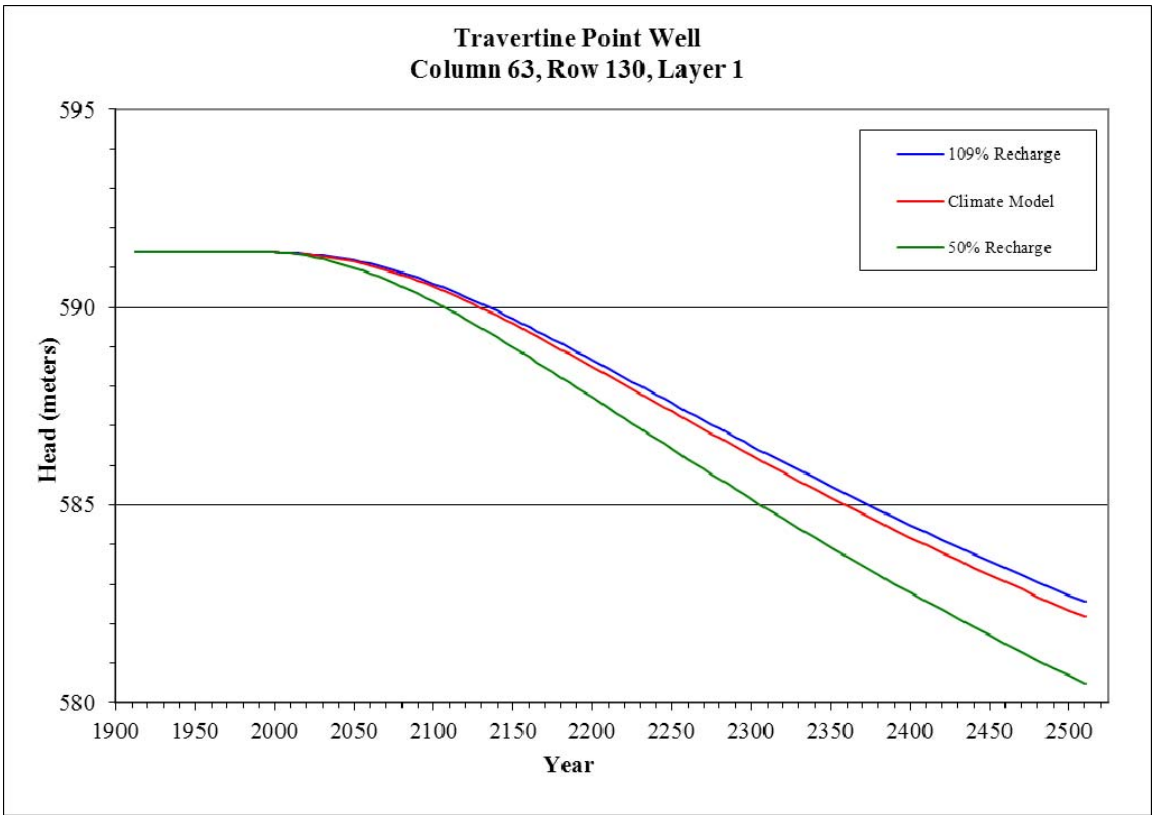

Figure 49. Head Change in Column 63, Row 130, Layer 1

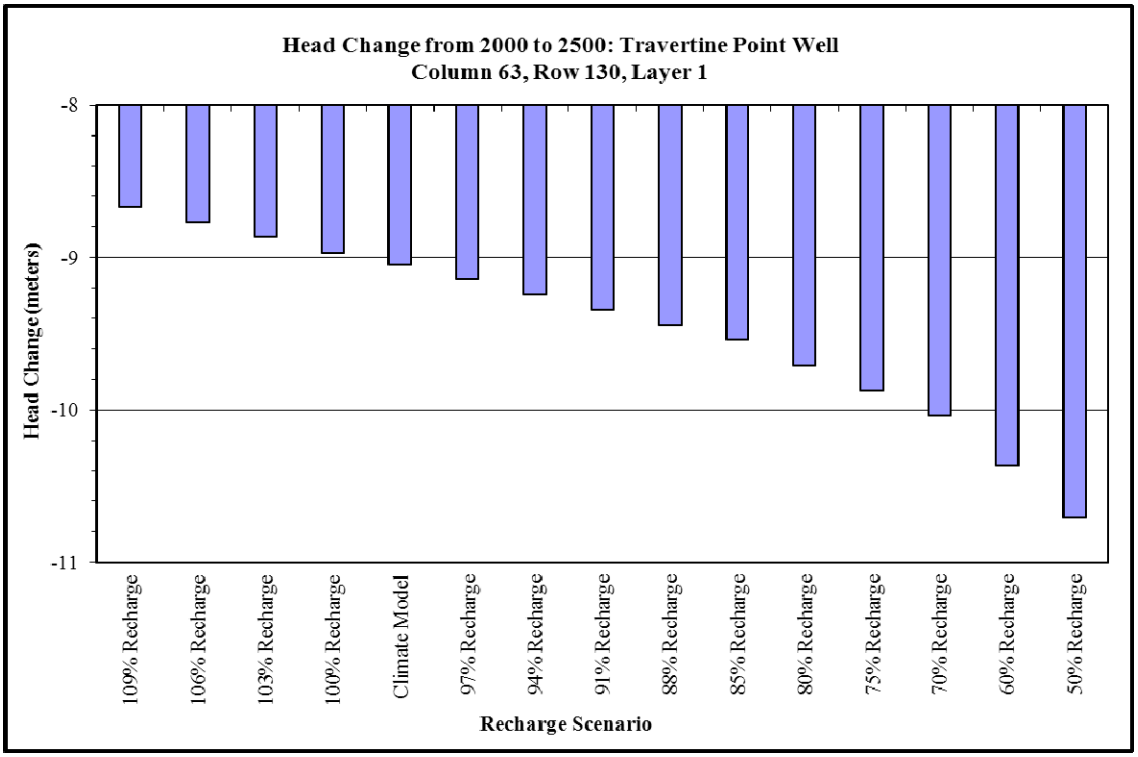

Figure 50. Quantified Head Change in Column 63, Row 130, Layer 1

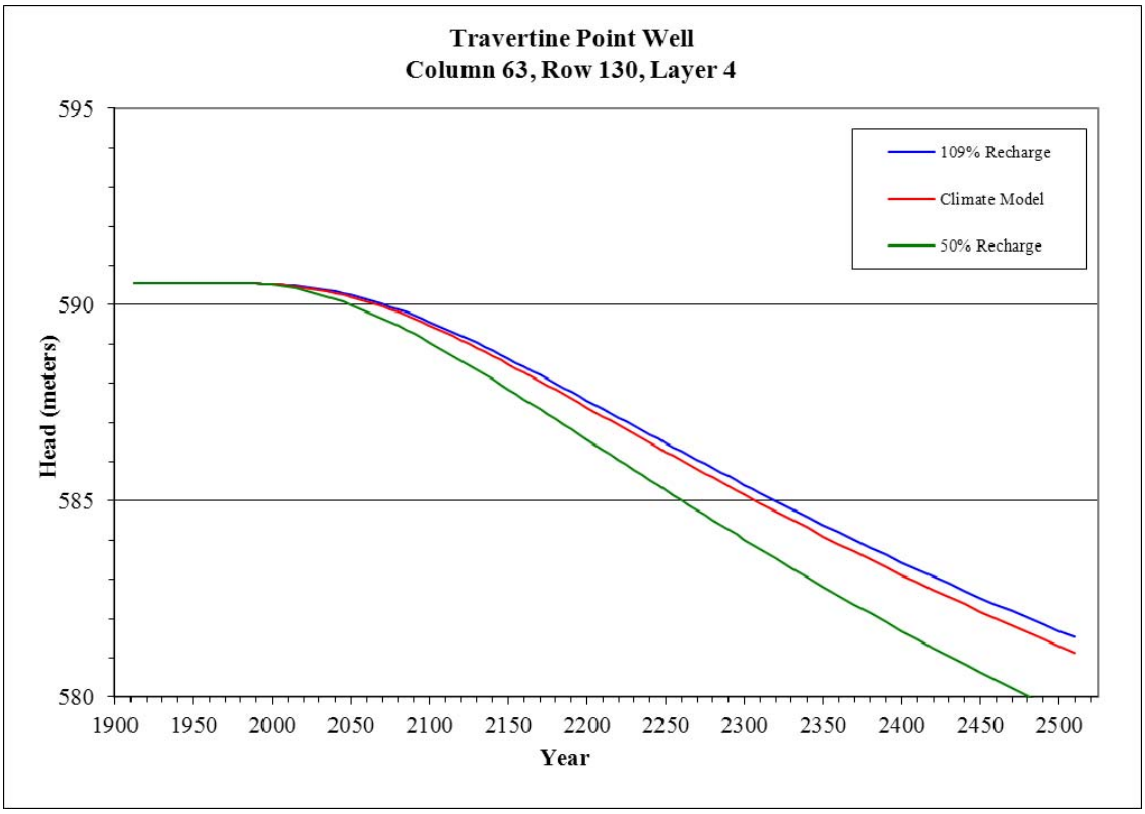

Figure 51. Head Change in Column 63, Row 130, Layer 4

6.1.3 Effects of Pumping versus Recharge

The data summarized above suggest that a factor other than climate change is responsible for the simulated decline in head over time because (1) head declines occurred before recharge was simulated to be reduced, (2) heads decline in the simulations in which recharge is held at or increased relative to 20th Century levels, and (3) in many simulations the overall head decline is substantially greater than the range of decline caused by a change in recharge.

To evaluate how groundwater discharge through pumping may be affecting the groundwater flow system compared to changes in recharge, one simulation was conducted in which groundwater pumping in the study area was minimized. The reduced pumping simulation used the baseline 100 percent of 20th Century recharge scenario. Pumping was reduced only

within the study area and was not changed in other areas of the model domain, such as north of Las Vegas, the Nevada Test Site, and Pahrump Valley. For the simulation, two input files were modified:

New_mnw_03_7.txt was modified by reducing pumping from wells in the study area in 2001, 2002, and 2003, and continuing the reduced pumping rate into the future. For the model run, pumping rates greater than 27.5 m^3/day (approximately 5 gallons per minute) no matter how large, were arbitrarily reduced to a pumping rate of 27.5 m^3/day. This is not a realistic scenario of possible future pumping rates in the study area, however the simulation does serve to evaluate the effects of pumping in the Amargosa Desert on groundwater conditions as compared to simulated changes in recharge. The reductions were 47,147 m^3/day less pumping in 2001, 51,588 m^3/day less pumping in 2002, and 59,268 m^3/day less pumping in 2003. The reduced pumping conditions in 2003 were carried into the future through the end of simulations in 2510.

new_irr_ret_03_7.txt was modified by eliminating return flow from pumping wells in the study area in 2008, 2009, and 2010. The USGS calculated a return flow lag time of 7 years from irrigation wells (Belcher and Sweetkind 2010). Therefore, wells in which the pumping rate was reduced in 2001, 2002, or 2003 would not see a decline in return flow until beginning in 2008. Return flow rates in other areas of the model domain were not changed. Return flows eliminated were 9,509 m^3/day in 2001, 10,416 m^3/day in 2002, and 11,968 m^3/day in 2003. The return flow conditions in 2010 were carried into the future through the end of simulations in 2510.

The results of the simulation of reduced pumping indicate that pumping is a greater stress on the groundwater flow system than the projected effects of climate change. The locations of cells where changes in head were graphed are shown in Figure 52. Select graphs in which the results of the model run simulating minimized pumping compared with current pumping are shown in Figures 53 through 74.

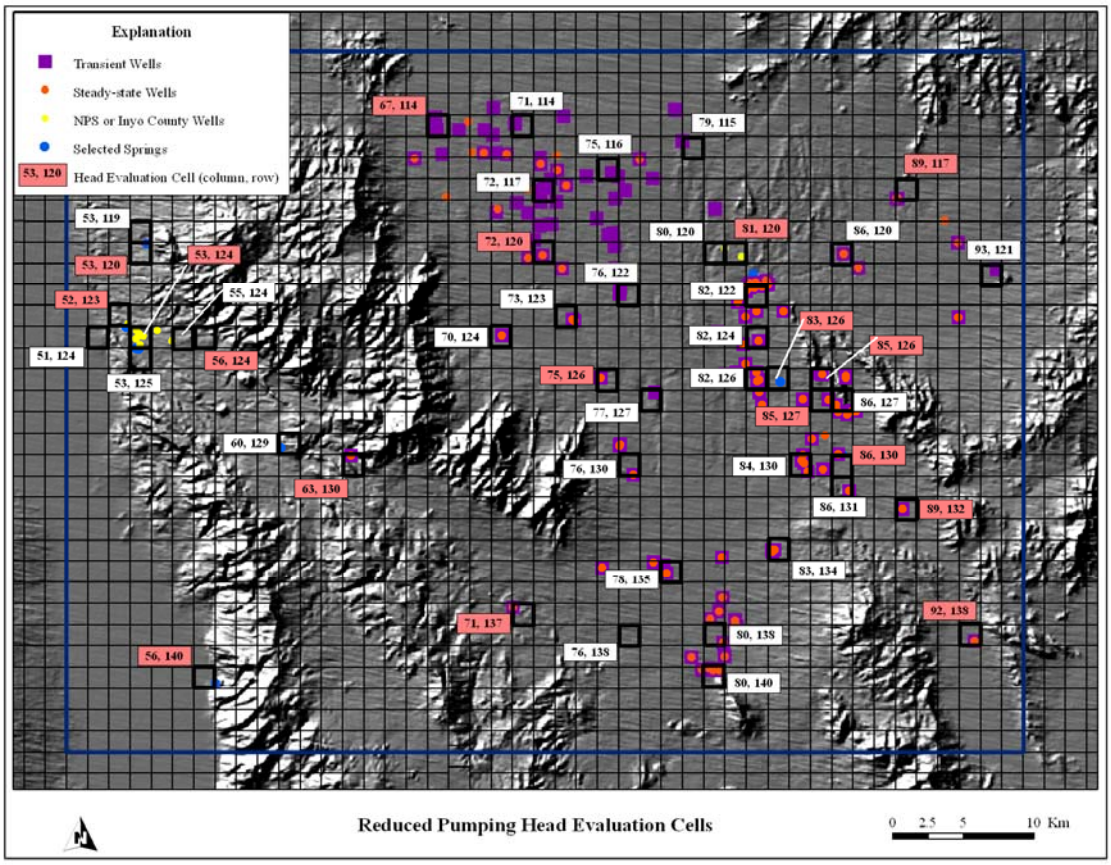

Figure 52. Cells for Evaluation of Reduced Amargosa Desert Pumping Head Change

6.1.3.1 Amargosa Desert Comparison

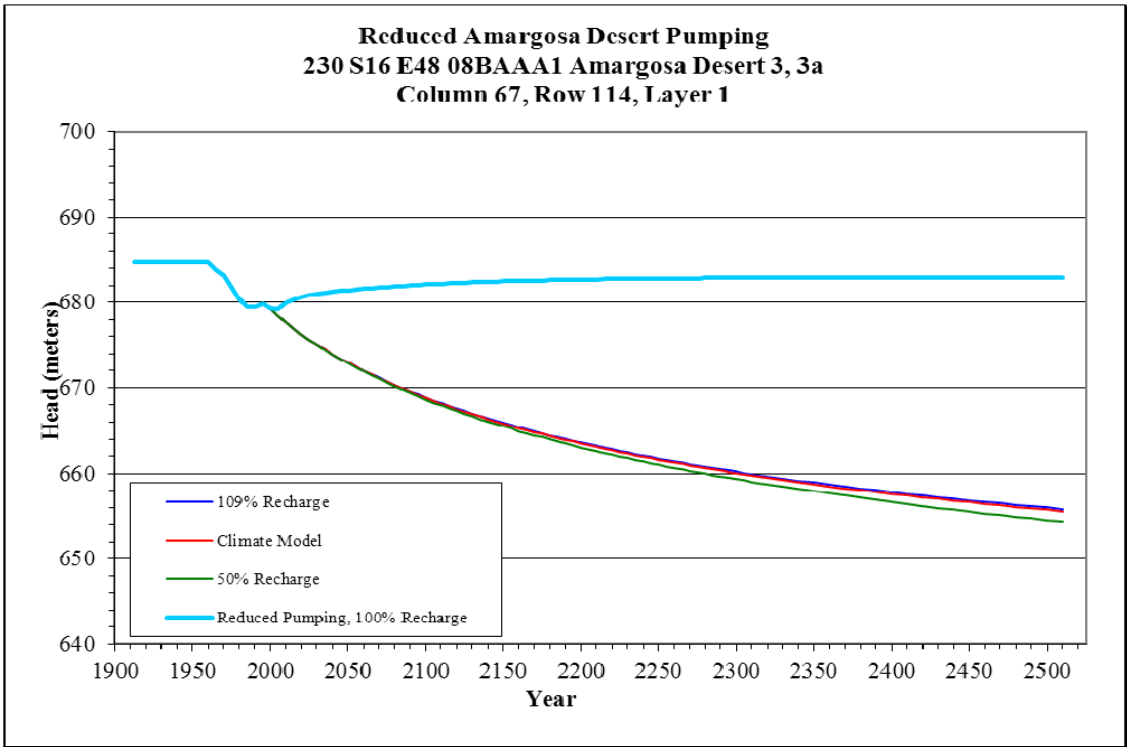

Figure 53. Head Changes with Pumping Minimized: Column 67, Row 114, Layer 1

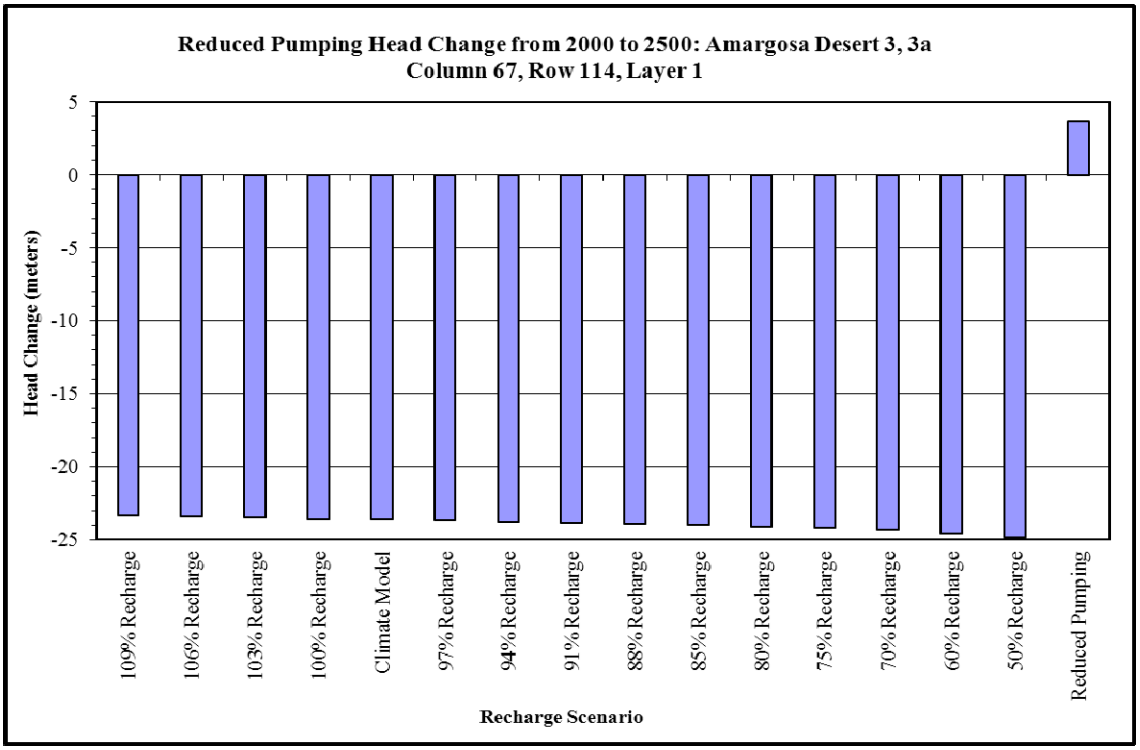

Figure 54. Quantified Head Change: Pumping Minimized: Column 67, Row 114, Layer 1

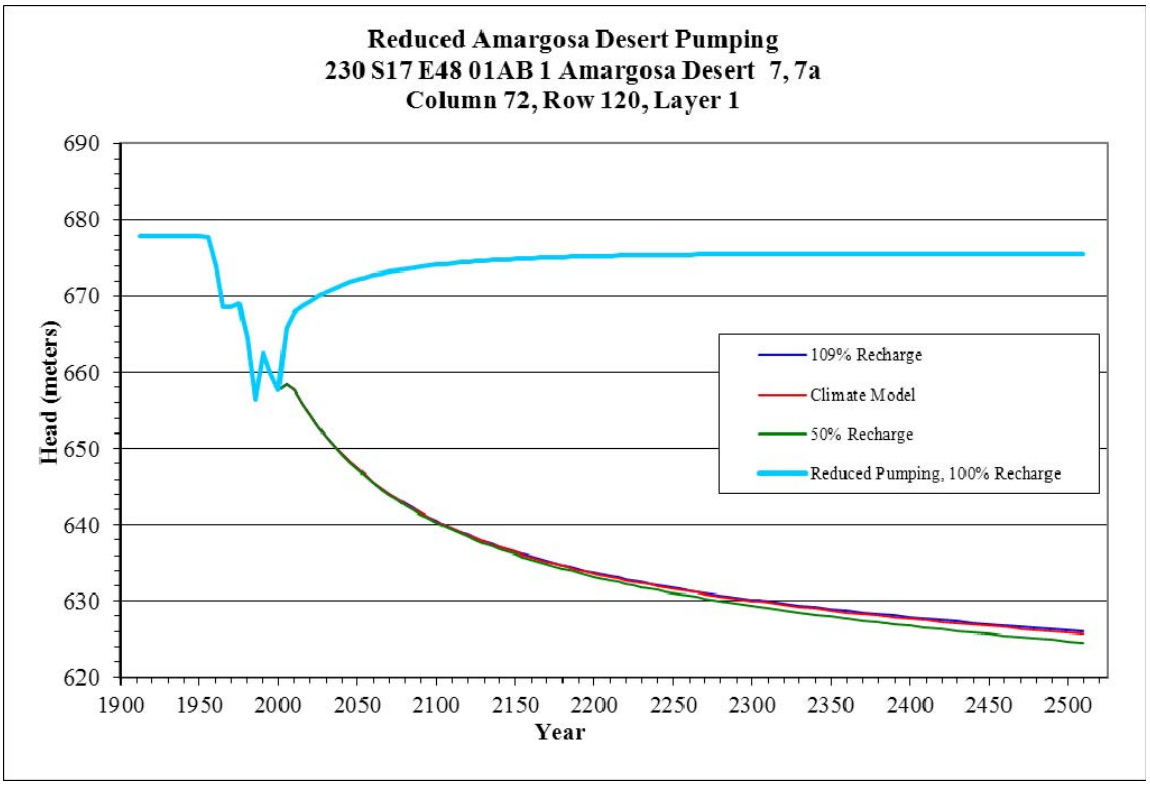

Figure 55. Head Changes with Pumping Minimized: Column 72, Row 120, Layer 1

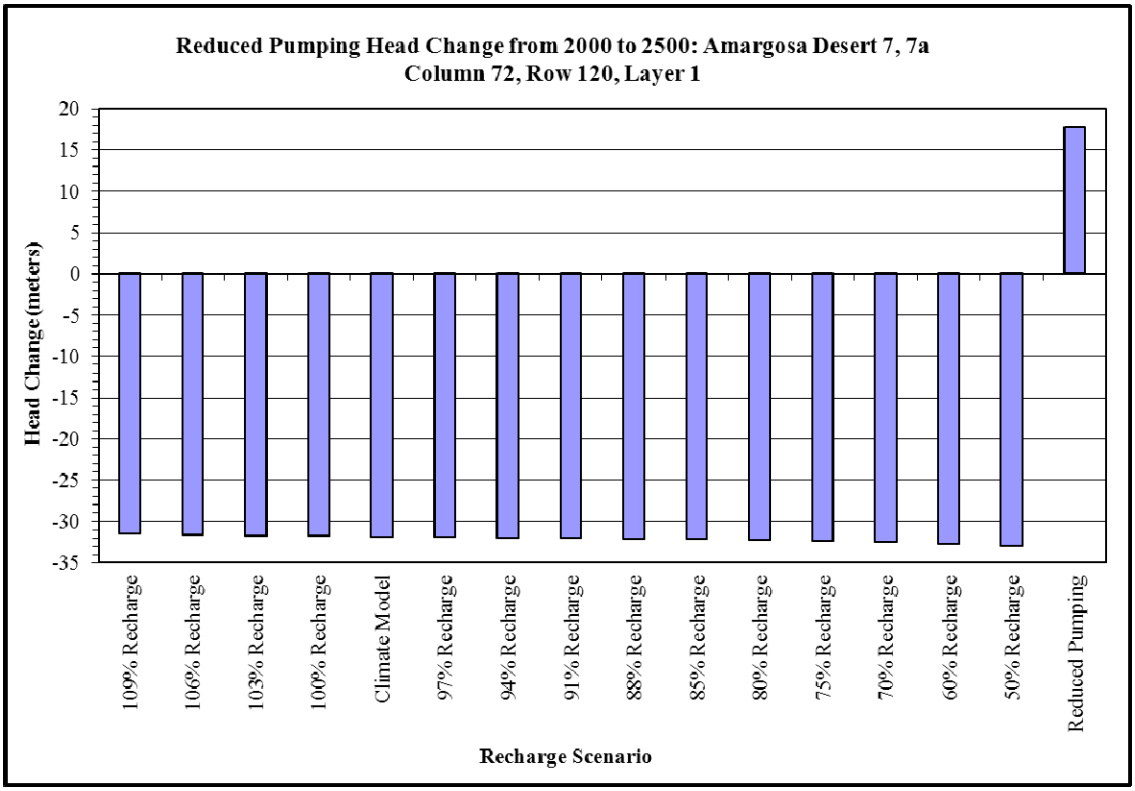

Figure 56. Quantified Head Change: Pumping Minimized: Column 72, Row 120, Layer 1

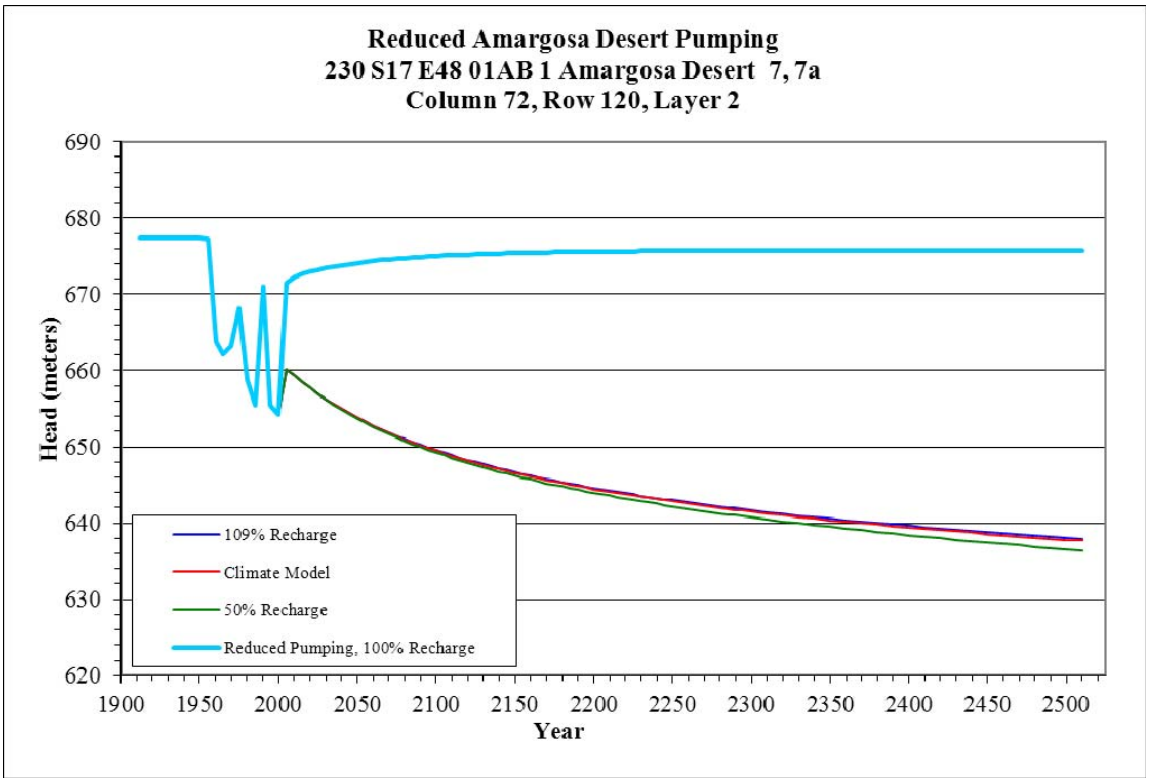

Figure 57. Head Change with Pumping Minimized: Column 72, Row 120, Layer 2

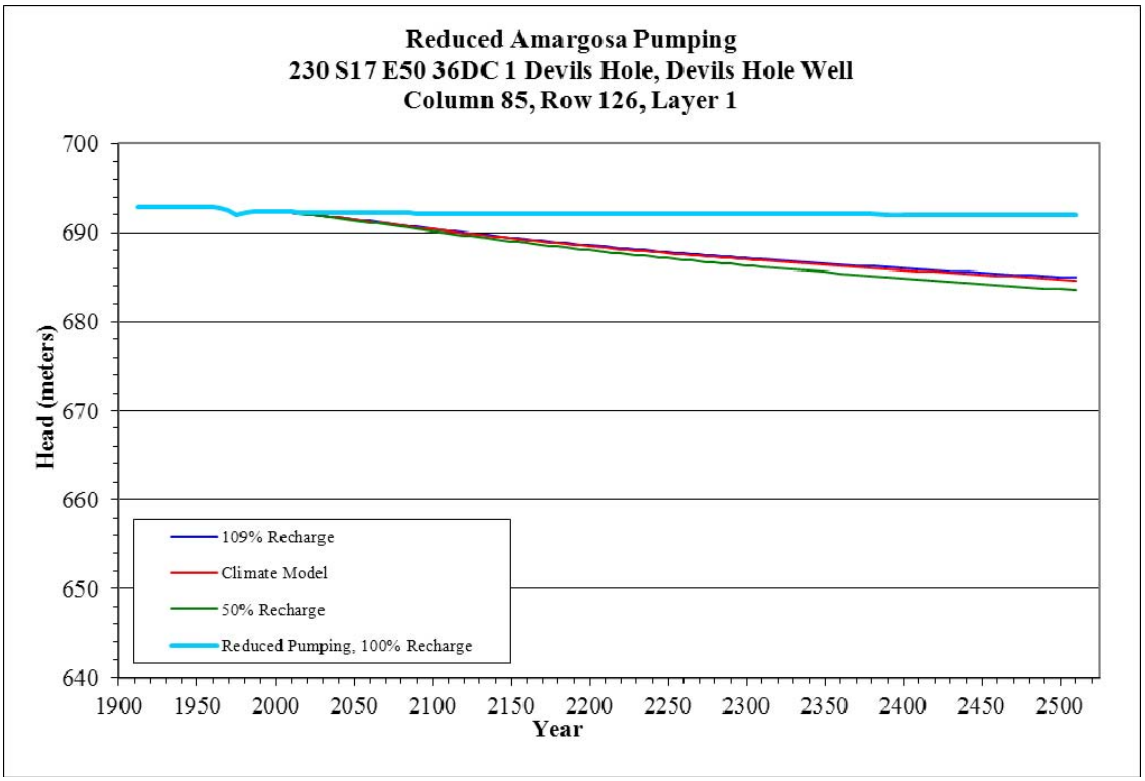

Figure 58. Head Change with Pumping Minimized: Column 85, Row 126, Layer 1

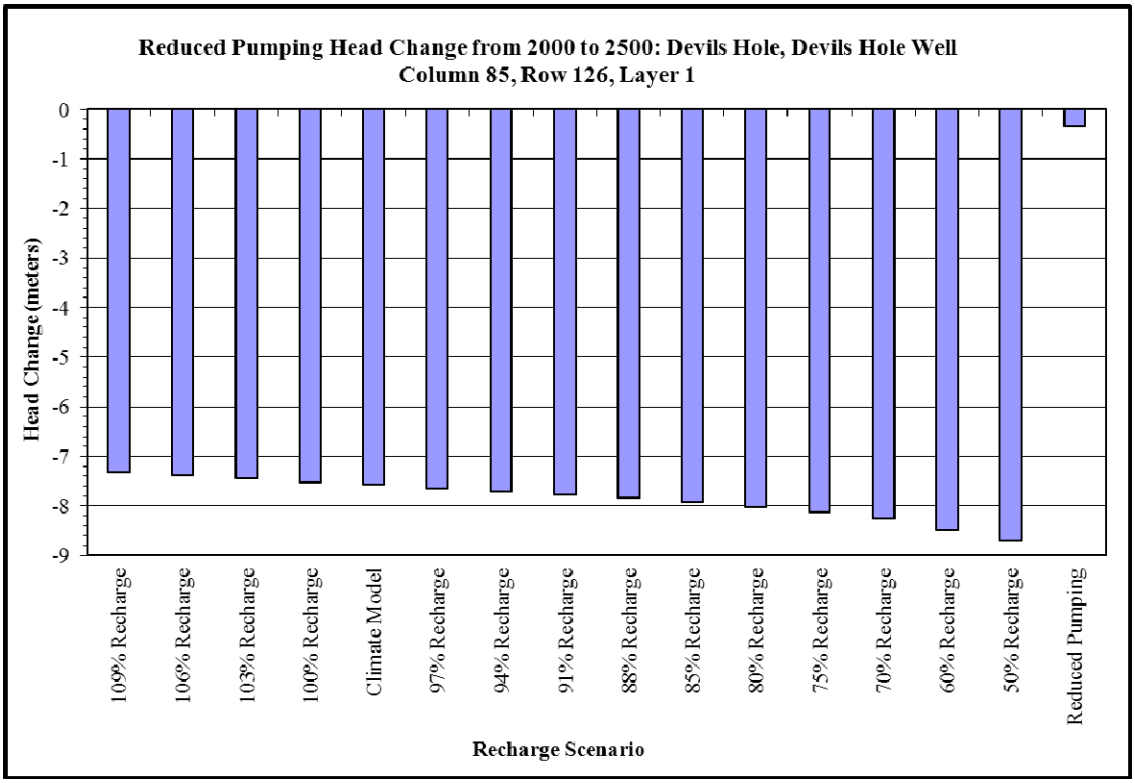

Figure 59. Quantified Head Change: Pumping Minimized: Column 85, Row 126, Layer 1

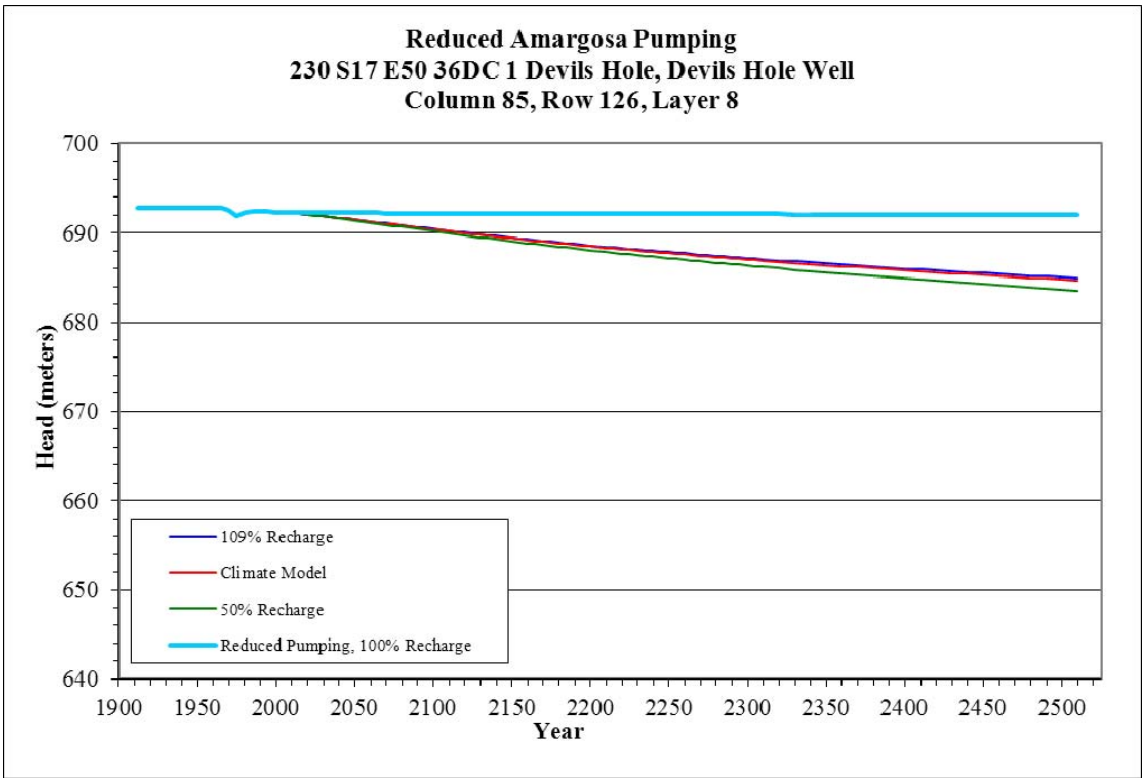

Figure 60. Head Change with Pumping Minimized: Column 85, Row 126, Layer 8

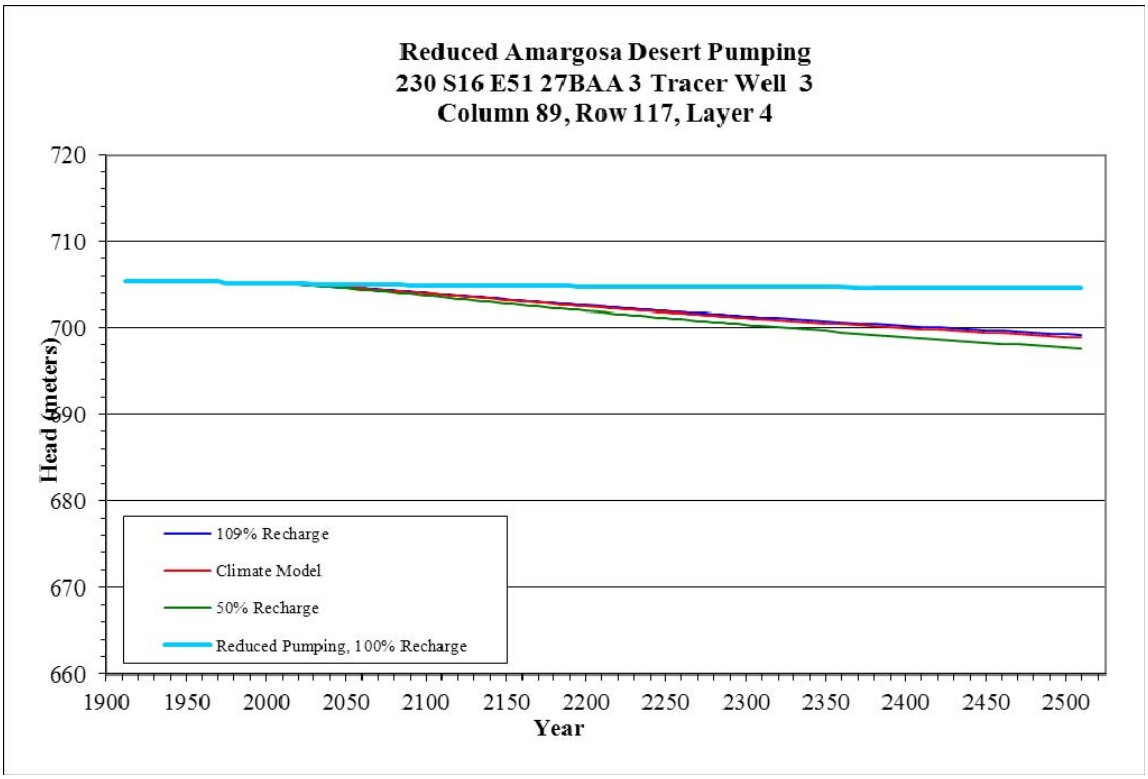

Figure 61. Head Changes with Pumping Minimized: Column 89, Row 117, Layer 4

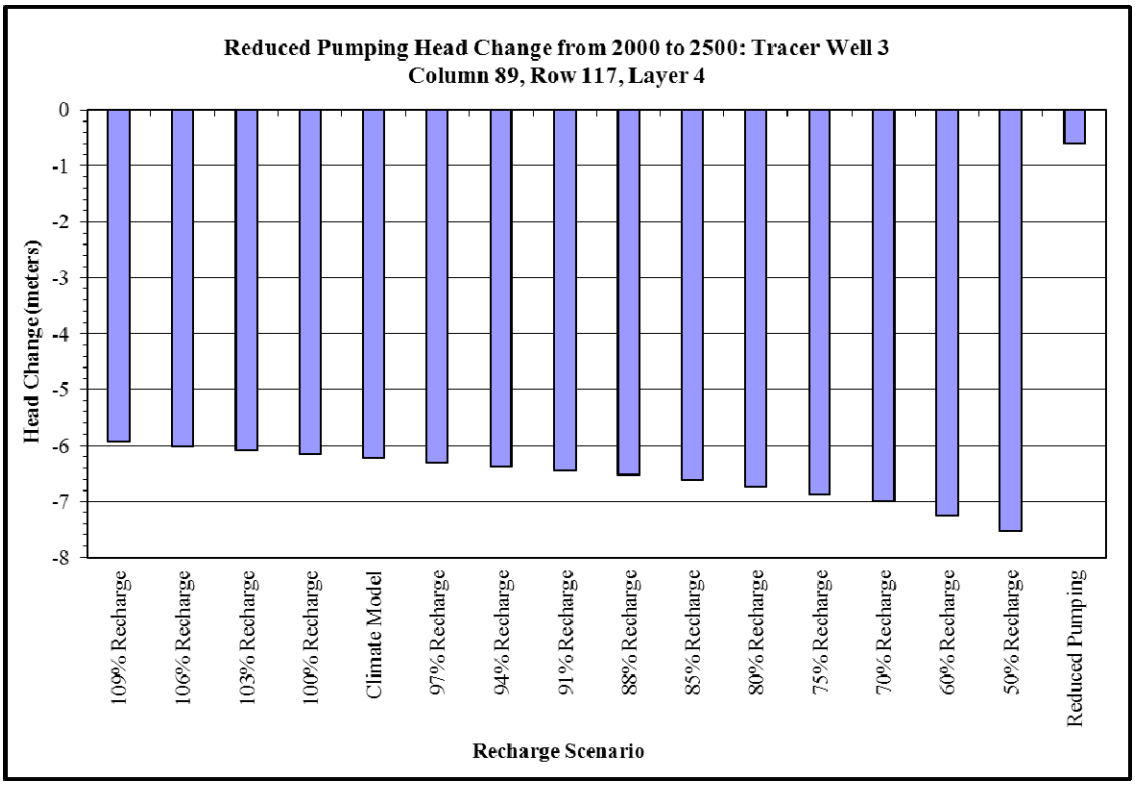

Figure 62. Quantified Head Change: Pumping Minimized: Column 89, Row 117, Layer 4

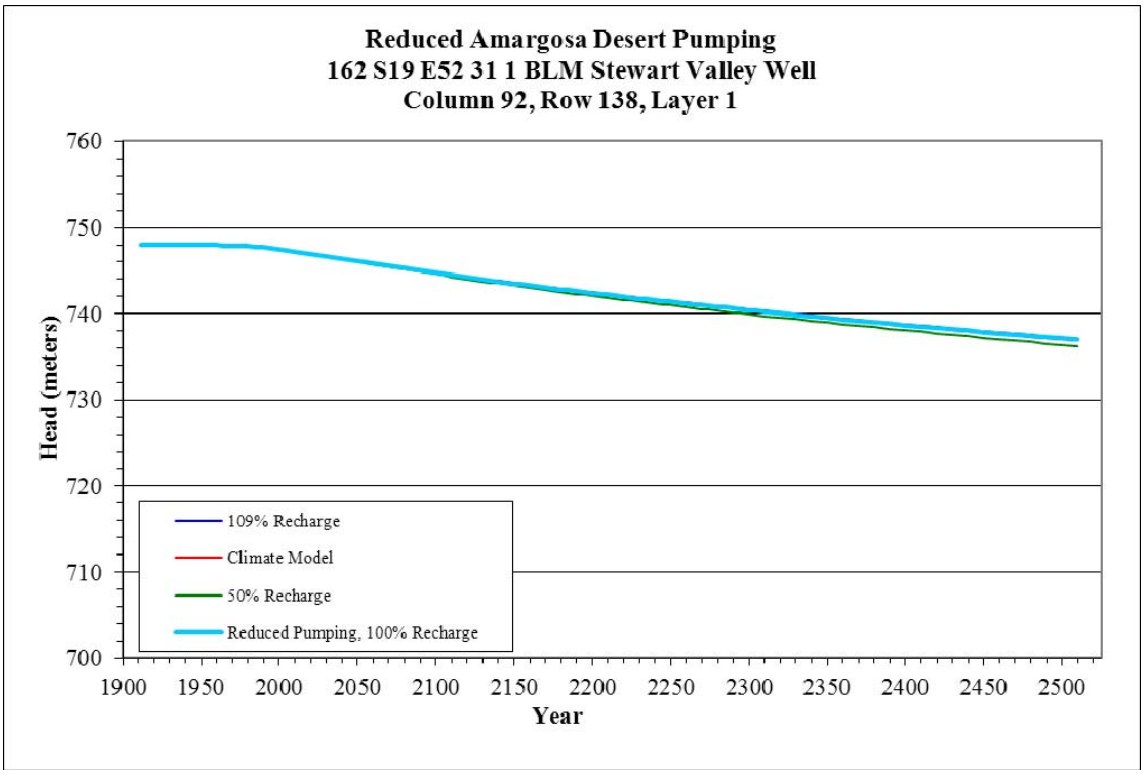

Figure 63. Head Change with Pumping Minimized: Column 92, Row 138, Layer 1

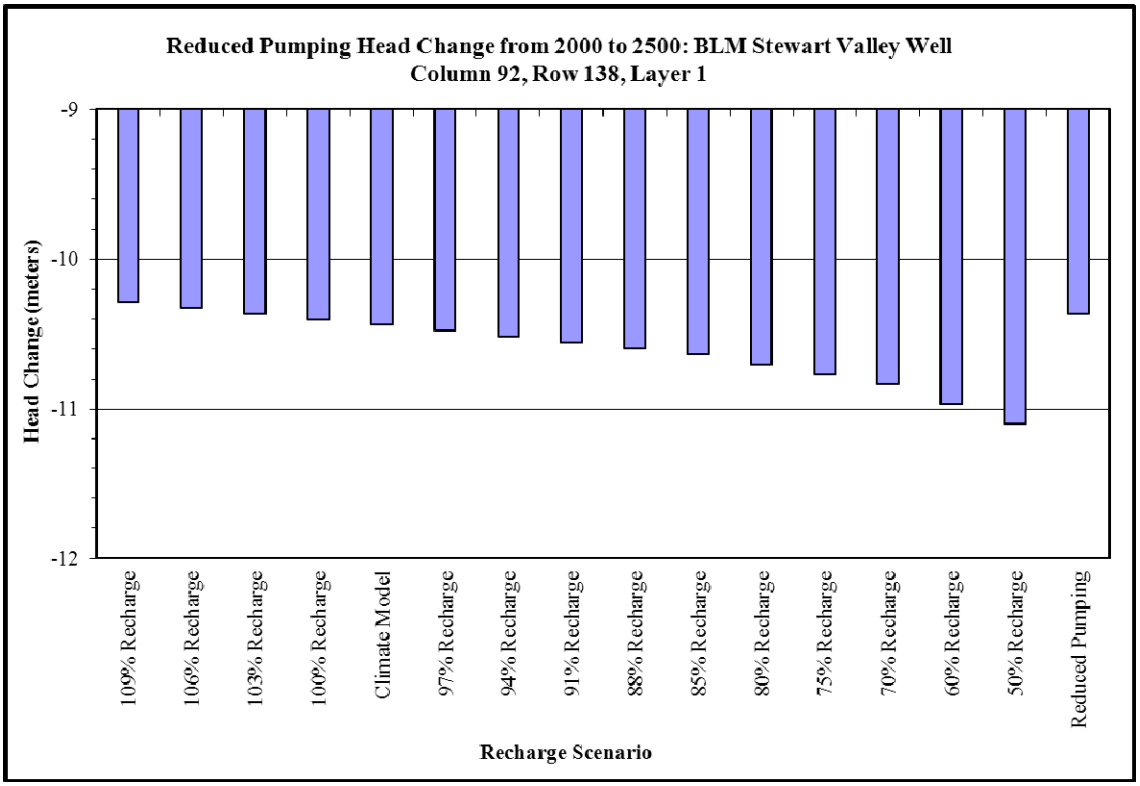

Figure 64. Quantified Head Change: Pumping Minimized: Column 92, Row 138, Layer 1

6.1.3.2 Death Valley Comparison

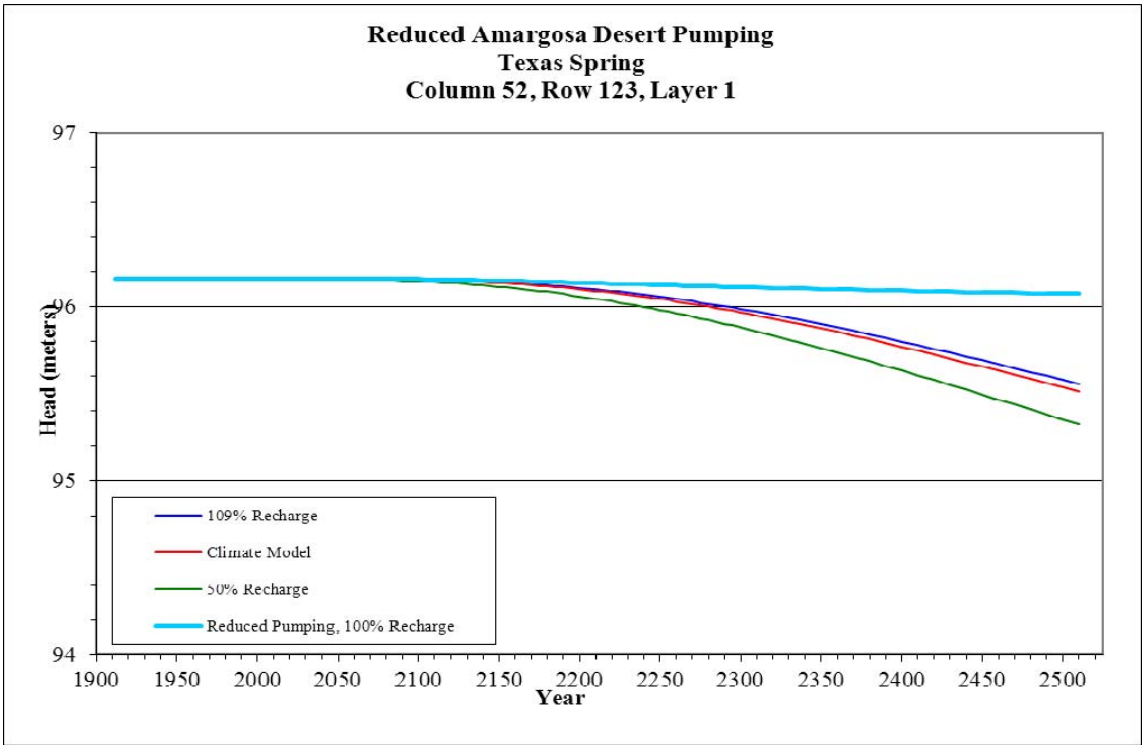

Figure 65. Head Changes with Pumping Minimized: Column 52, Row 123, Layer 1

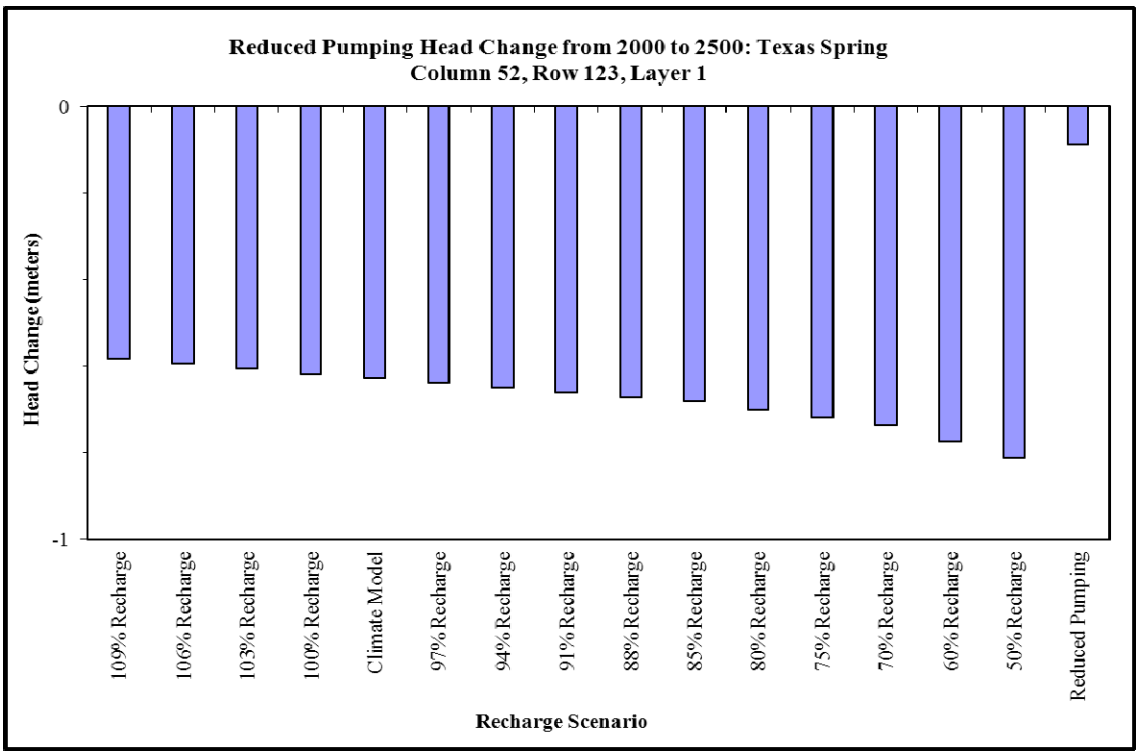

Figure 66. Quantified Head Change: Pumping Minimized: Column 52, Row 123, Layer 1

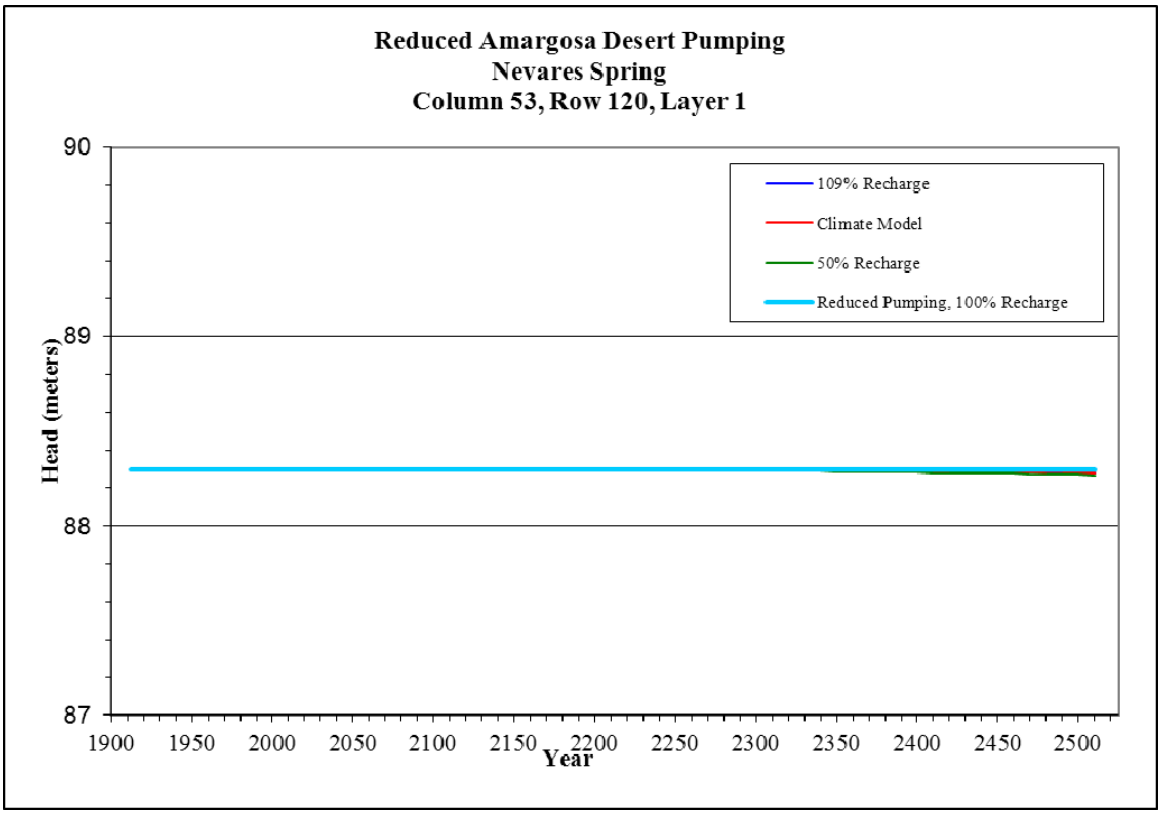

Figure 67. Head Changes with Pumping Minimized: Column 53, Row 120, Layer 1

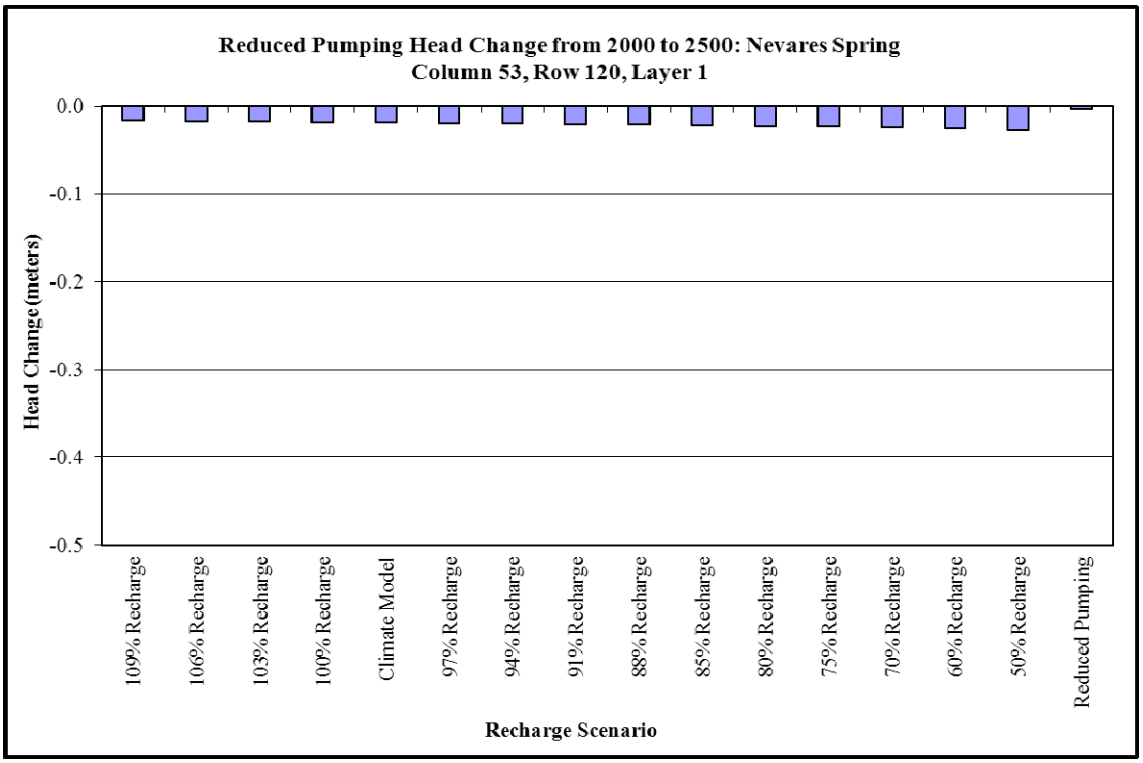

Figure 68. Quantified Head Change: Pumping Minimized: Column 53, Row 120, Layer 1

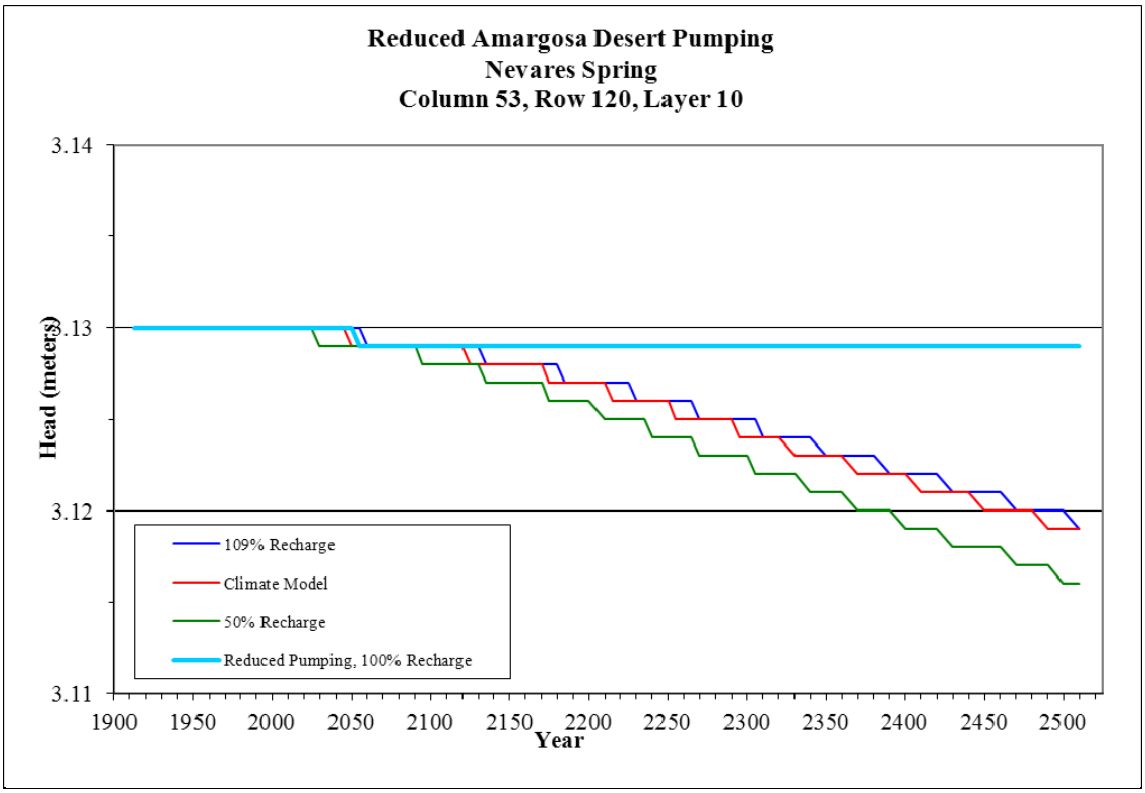

Figure 69. Head Change with Pumping Minimized: Column 53, Row 120, Layer 10

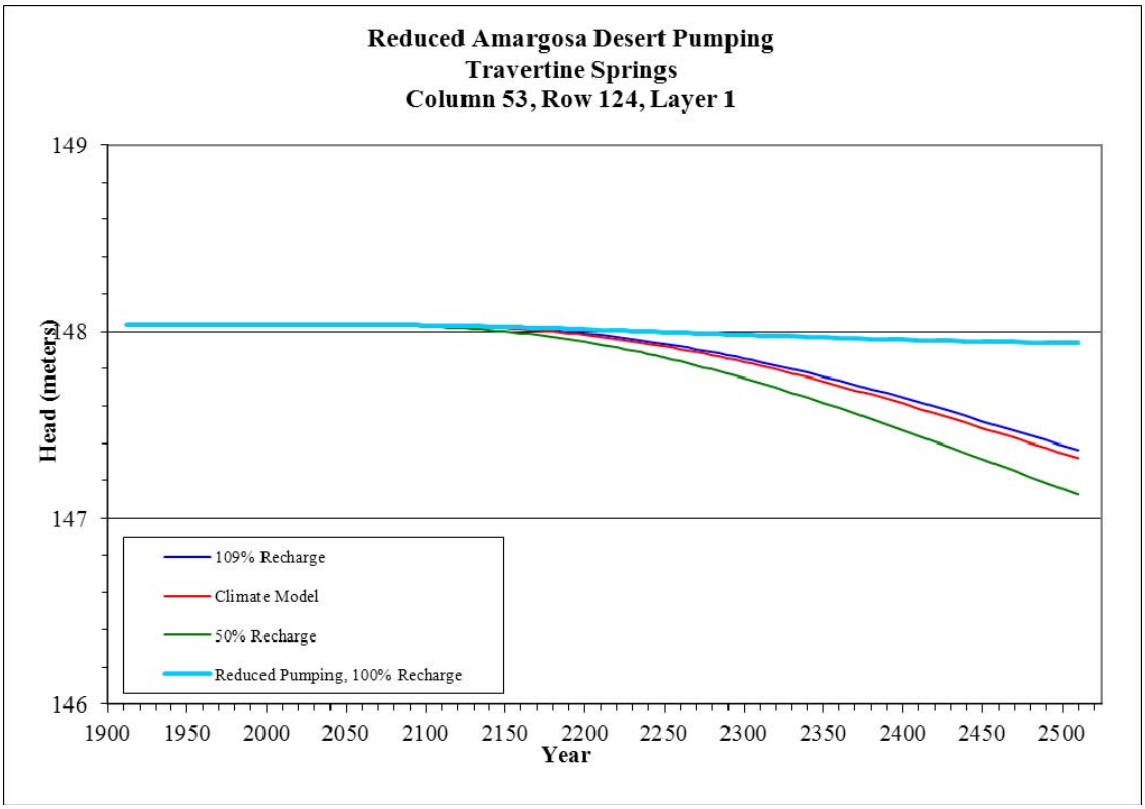

Figure 70. Head Change with Pumping Minimized: Column 53, Row 124, Layer 1

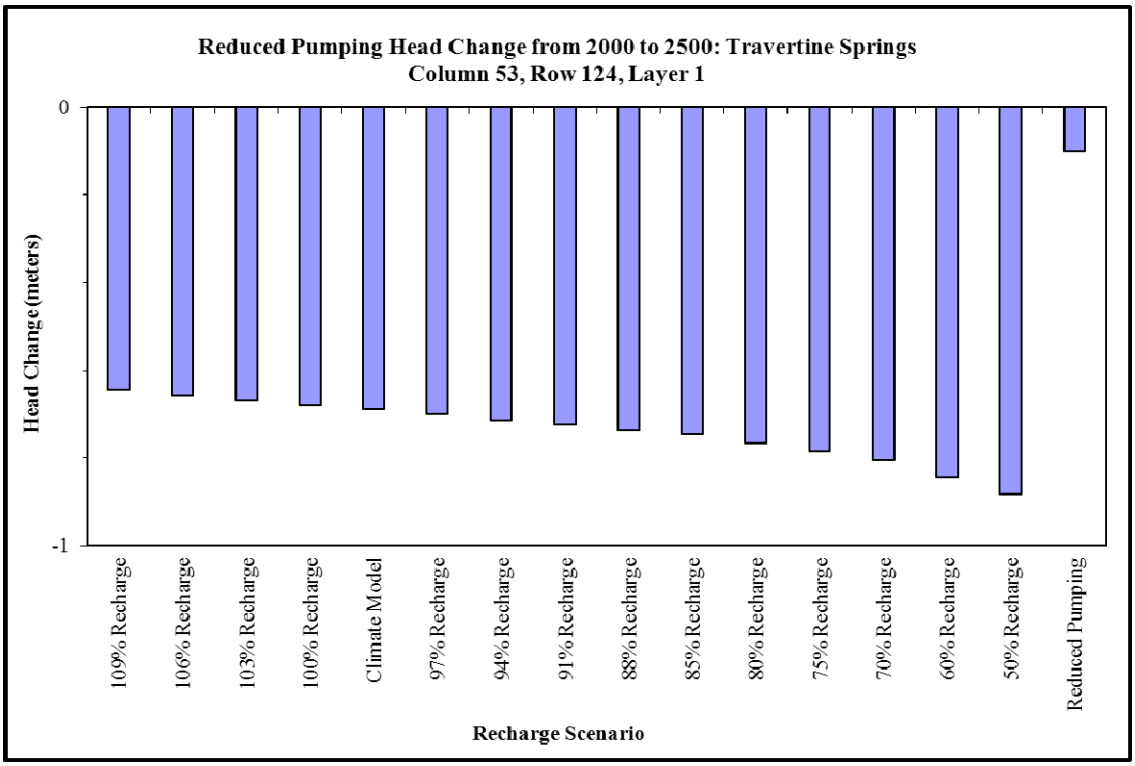

Figure 71. Quantified Head Change: Pumping Minimized: Column 53, Row 124, Layer 1

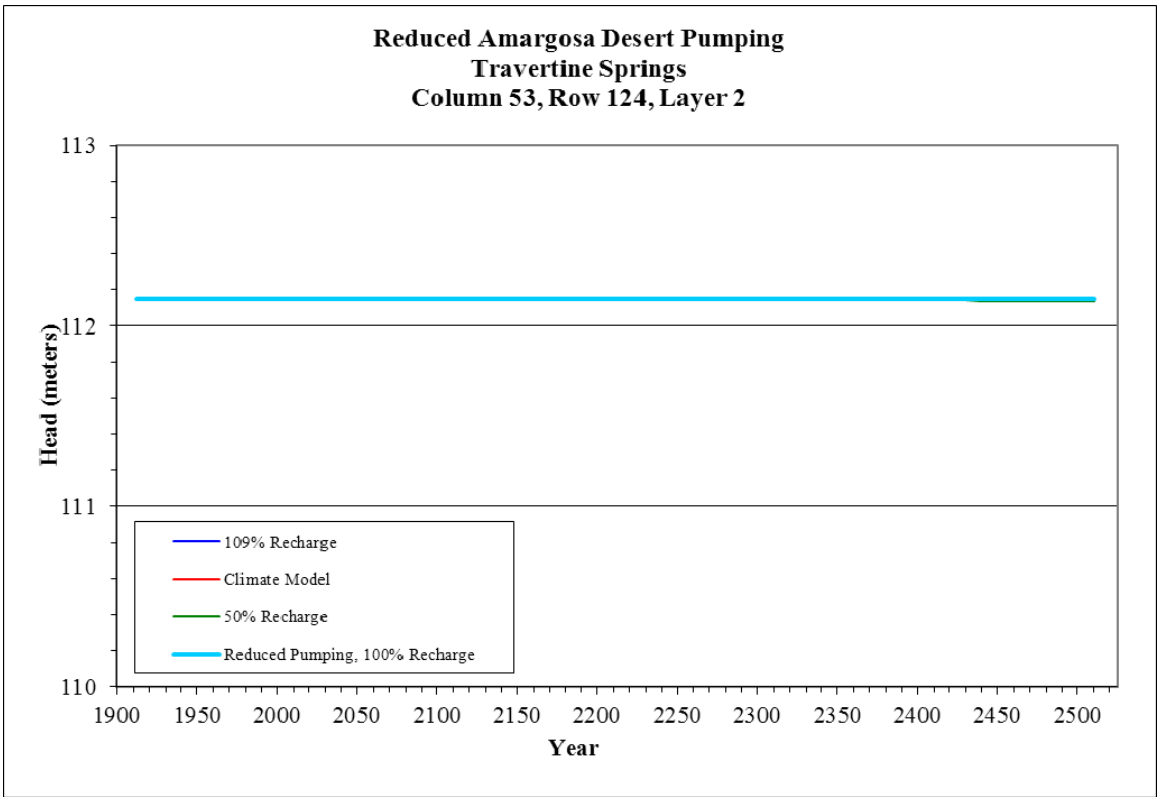

Figure 72. Head Changes with Pumping Minimized: Column 53, Row 124, Layer 2

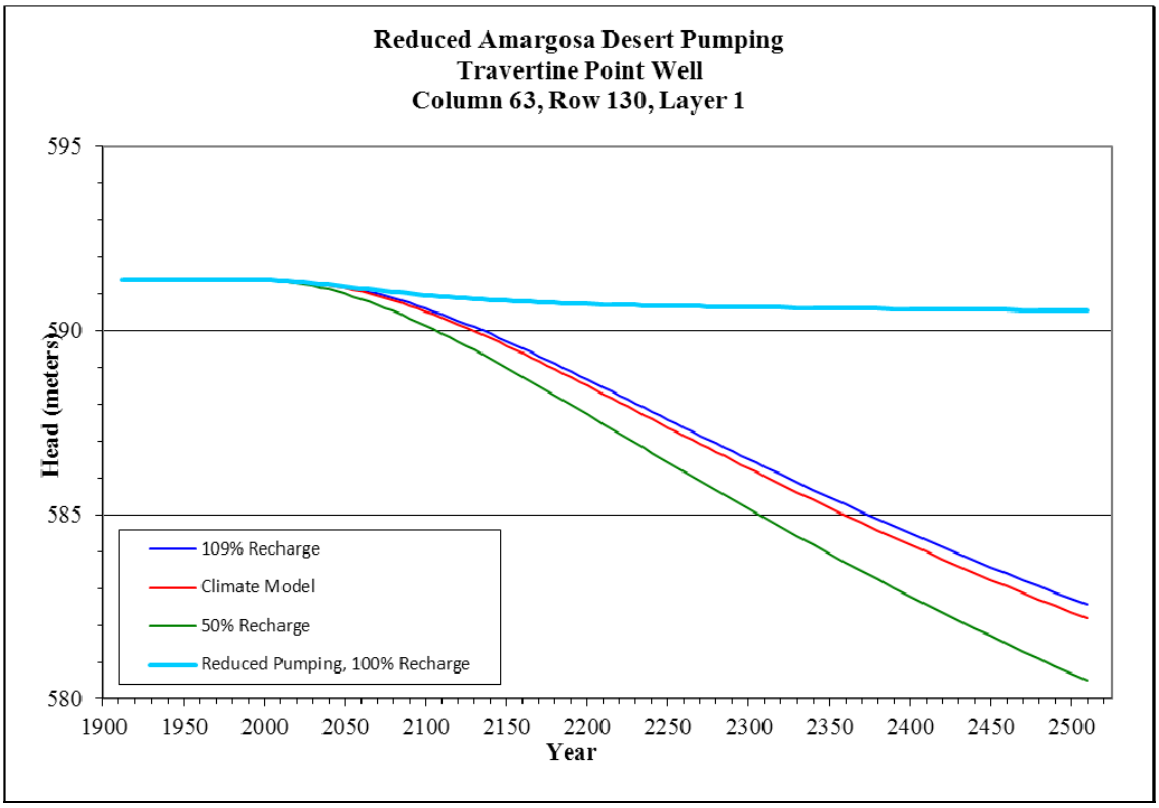

Figure 73. Head Change with Pumping Minimized: Column 63, Row 130, Layer 1

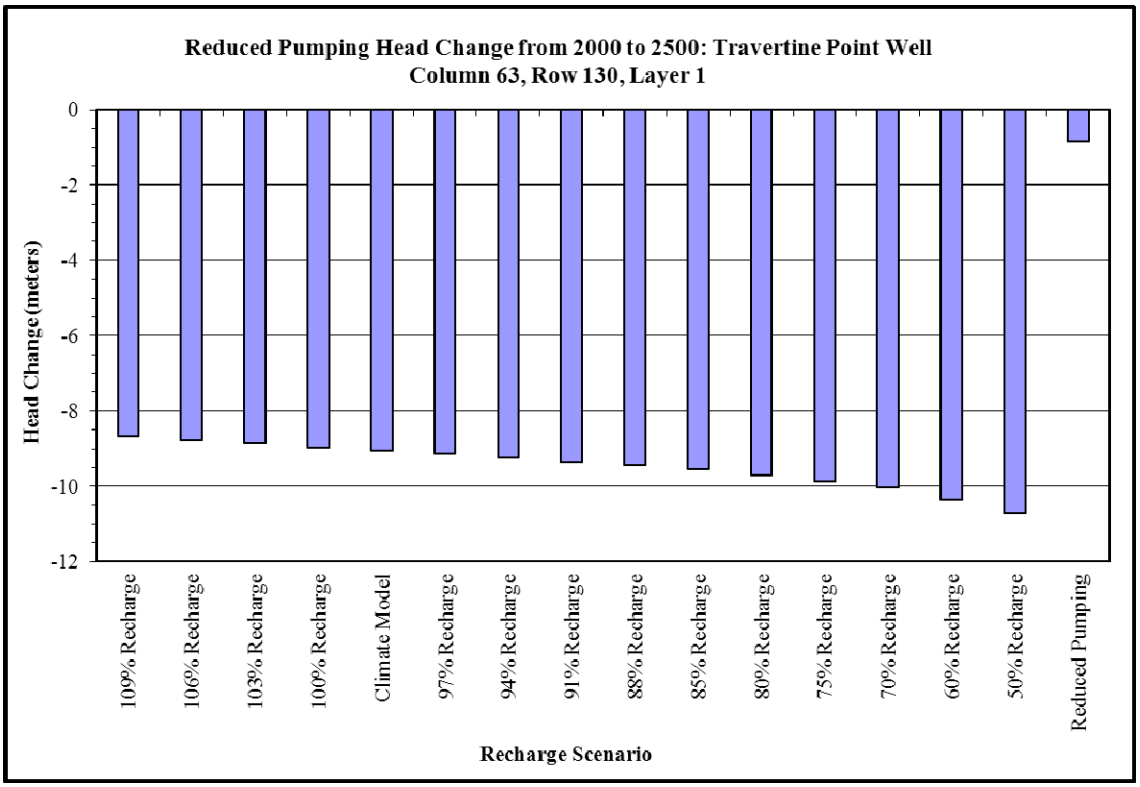

Figure 74. Quantified Head Change: Pumping Minimized: Column 63, Row 130, Layer 1

6.1.4 Groundwater Contours

Contours of simulated head in Layer 1 within the study area suggest no substantive change in overall groundwater flow direction as recharge changes. As expected based on the changes in simulated head, most of the change in contours occurs in the eastern portion of the study area. For example, in comparing contours from 2000 (the same situation for all simulations before recharge is altered) and the Climate Model simulation in 2500, the change in location of the 600 meter contour with respect to cells in which monitoring wells (Travertine Point Well and Caltrans Well) are located is negligible. However, the contours suggest a greater than 25 meter head loss (Wells AD-7, -7a and Well NA-9) in the Amargosa Farms portion of the study area. In addition, the location of the 700 meter contour has migrated to the east and northeast between the years 2000 and 2500. Similar conditions are observed in contours for other simulations. Contour plots for 2000 and the climate change, 109 percent, and 50 percent of 20^{th} Century recharge simulations are shown in Figures 75 through 78. Plots of contours for the remaining simulations are included in Appendix C.

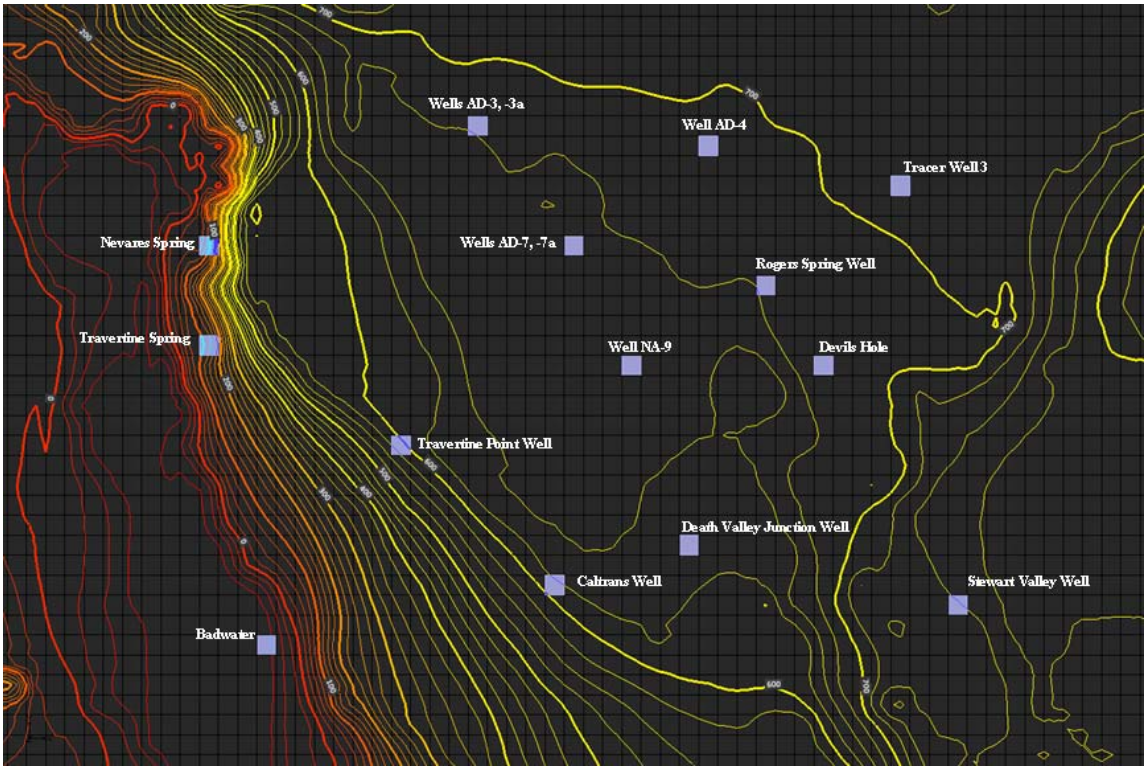

Figure 75. Simulated Contours, Year 2000 Baseline Conditions

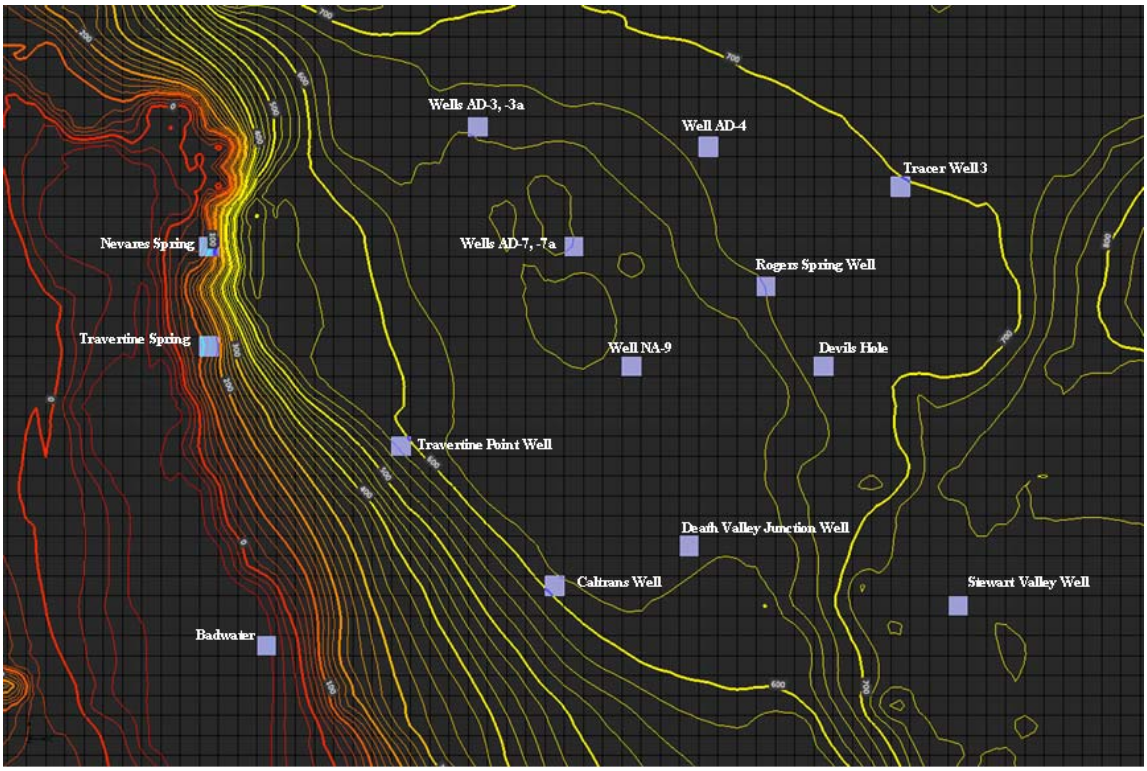

Figure 76. Simulated Contours Year 2500, with 109 % of Baseline Conditions

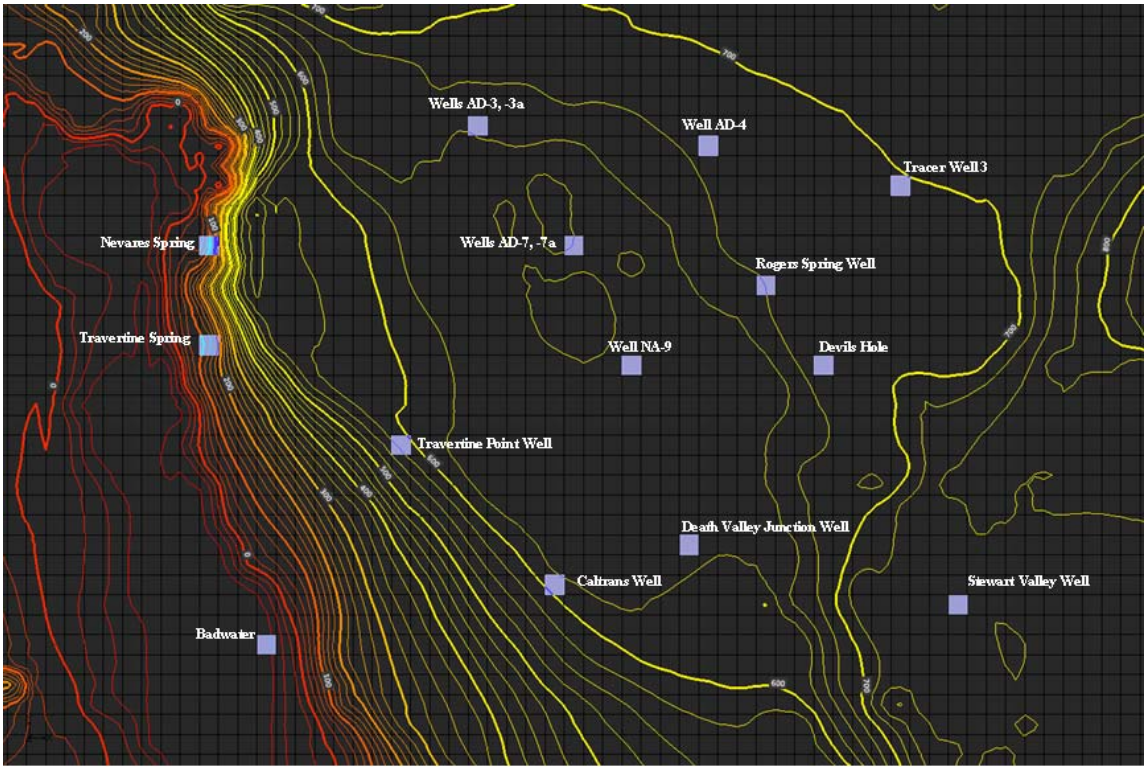

Figure 77. Simulated Contours Year 2500 with Climate Model Recharge

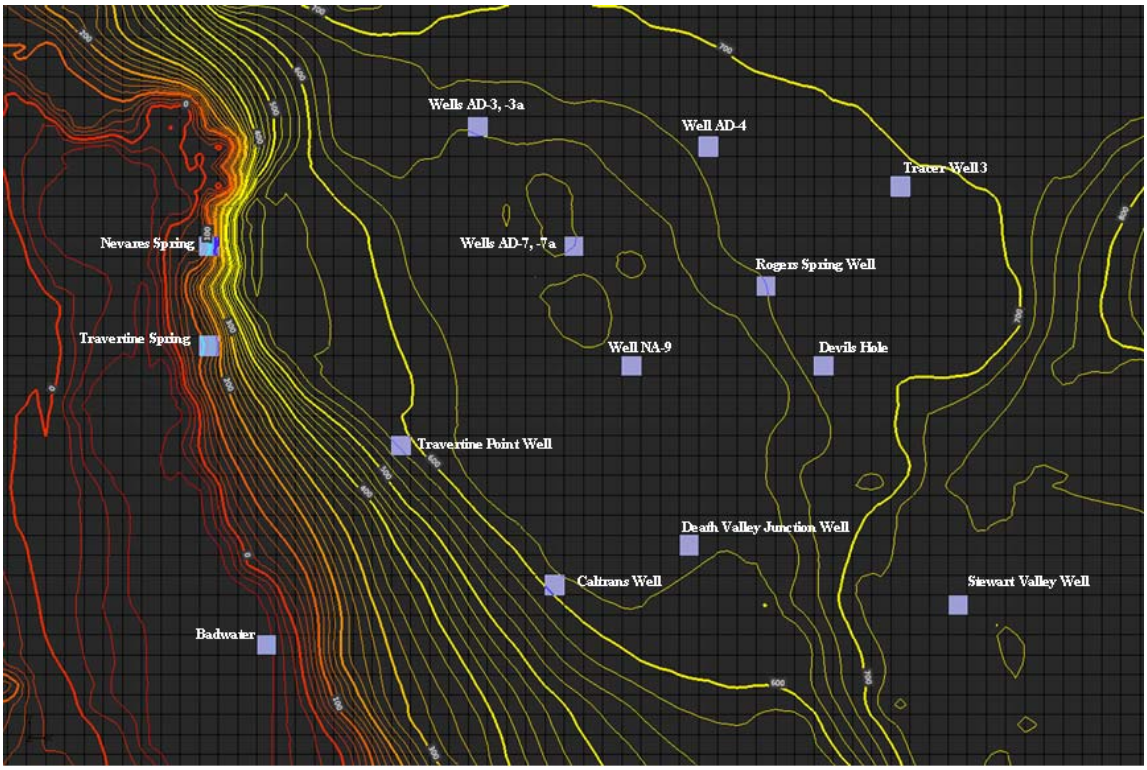

Figure 78. Simulated Contours Year 2500 with 50 % Baseline Conditions

6.2 Simulated Drain Cell Discharge

As with changes to groundwater head, simulated changes in discharge in the study area were evaluated for the approximate 500-year period from 2000 to 2500. Data from the simulations were compared to the baseline condition in which 100 percent of 20th Century recharge was continued throughout entire period from 1912 to 2500.

Discharge in the study area declined over time in all simulations and in all model layers, although the change in discharge at certain cells is negligible in the reduced pumping simulation. The decline began in the mid-20th Century after pumping had occurred in the Amargosa Desert (and other areas of the DVRFS) for several decades. The locations of cells where changes in discharge were examined are shown in Figure 79.

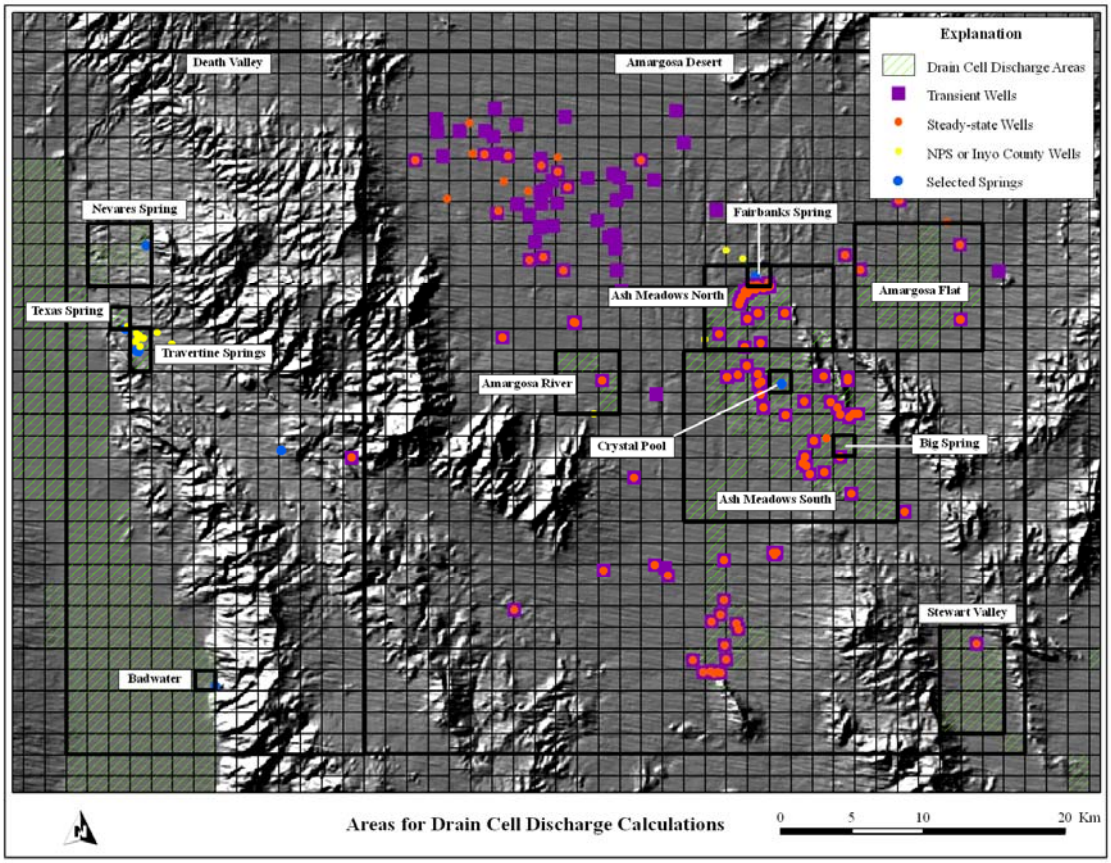

Figure 79. Areas for Drain Cell Discharge Calculations

6.2.1 Comparison of Simulated Drain Cell Discharge by Area Evaluated

The simulated declines in discharge from drain cells or groups of drain cells for the baseline condition of 100 percent of 20th Century recharge ranged from zero in Death Valley to 786 m^3/day in the Amargosa Desert between 1912 and 2000. For the period from 2000 to 2500, the additional decline in discharge ranged from approximately 300 m^3/day in Death Valley to approximately 16,500 m^3/day in the Amargosa Desert.

For the model runs with recharge greater than the baseline scenario, simulations indicate discharge increases relative to baseline. However, simulations also indicate overall decline in discharge even when recharge is increased. For the period from 2000 to 2500, the increase in simulated discharge relative to baseline ranged from zero m^3/day at Texas Spring to approximately 370 m^3/day in the Amargosa Desert.

For the model runs with recharge less than the baseline scenario, simulations indicate discharge declines relative to baseline. For the period from 2000 to 2500, the decline in simulated discharge relative to baseline ranged from zero m^3/day at Texas Spring and Nevares Spring to approximately 2,100 m^3/day in the Amargosa Desert.

Simulated changes in discharge for specific cells and groups of cells within the study area are shown in Figures 80 through 97. Each figure presents the overall change in discharge for the scenarios of 109 percent of baseline recharge, the Climate Model, and 50 percent of baseline recharge. Locations are shown in Figure 79. Additional drain cell discharge graphs are included in Appendix D.

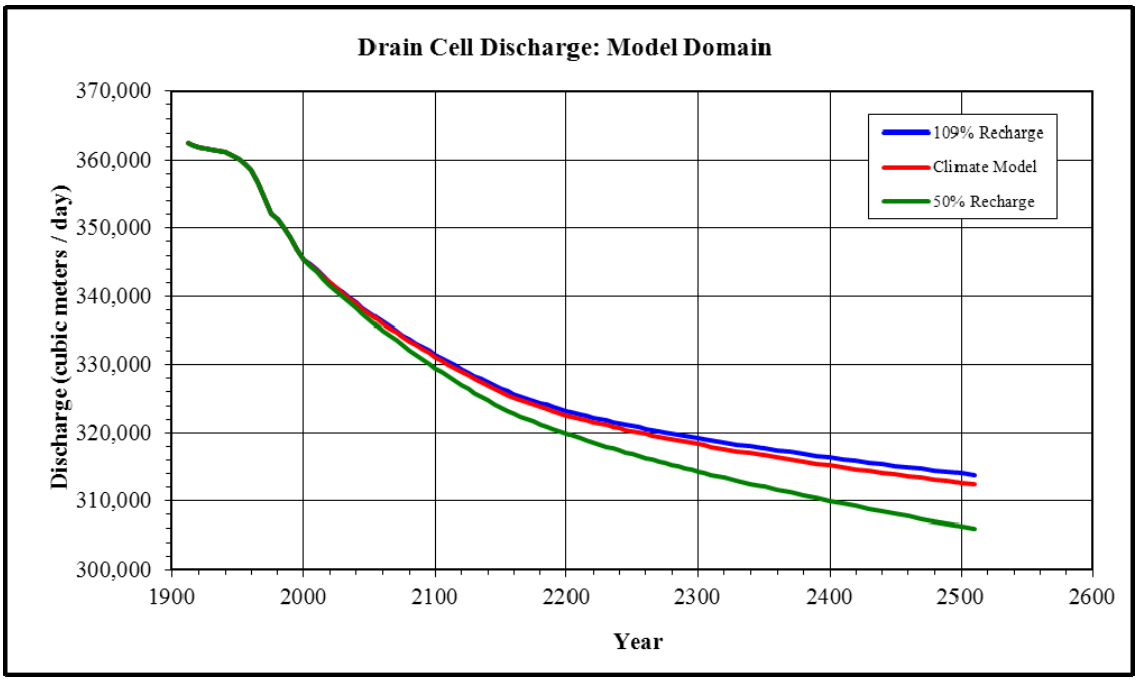

Figure 80. Drain Cell Discharge Comparison, Model Domain

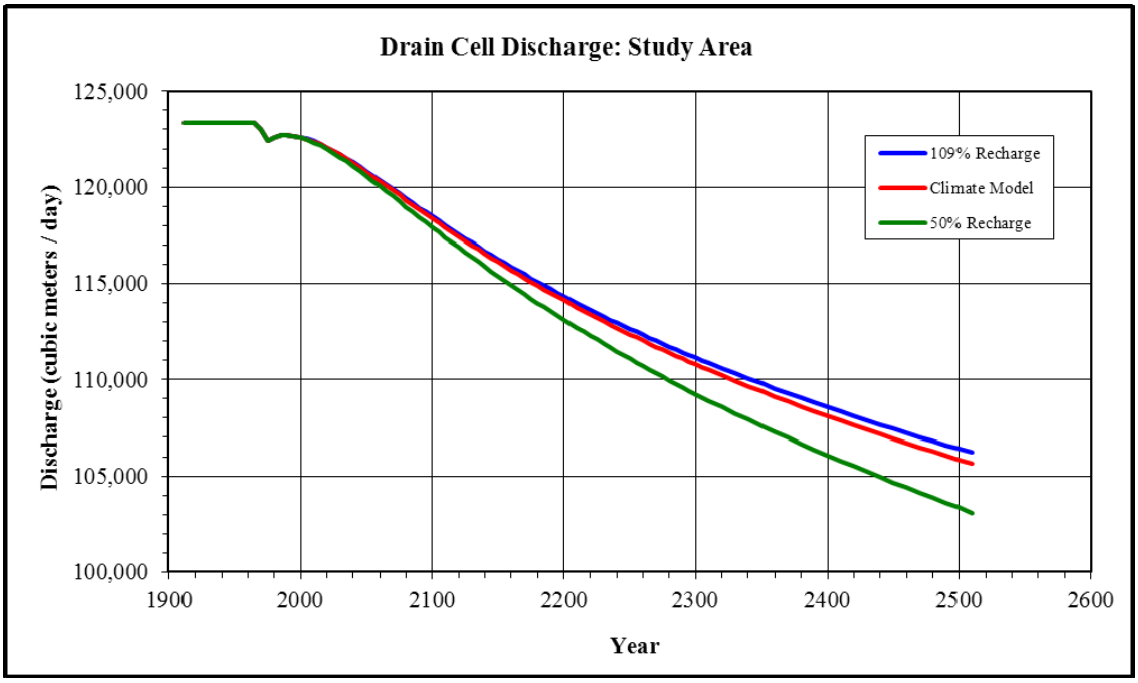

Figure 81. Drain Cell Discharge Comparison, Study Area

The simulation of reduced pumping in comparison with continuation of current pumping rates indicates that discharge is affected substantially by pumping. As shown in Figure 83, discharge increases in the Amargosa Desert when pumping is reduced in the study area.

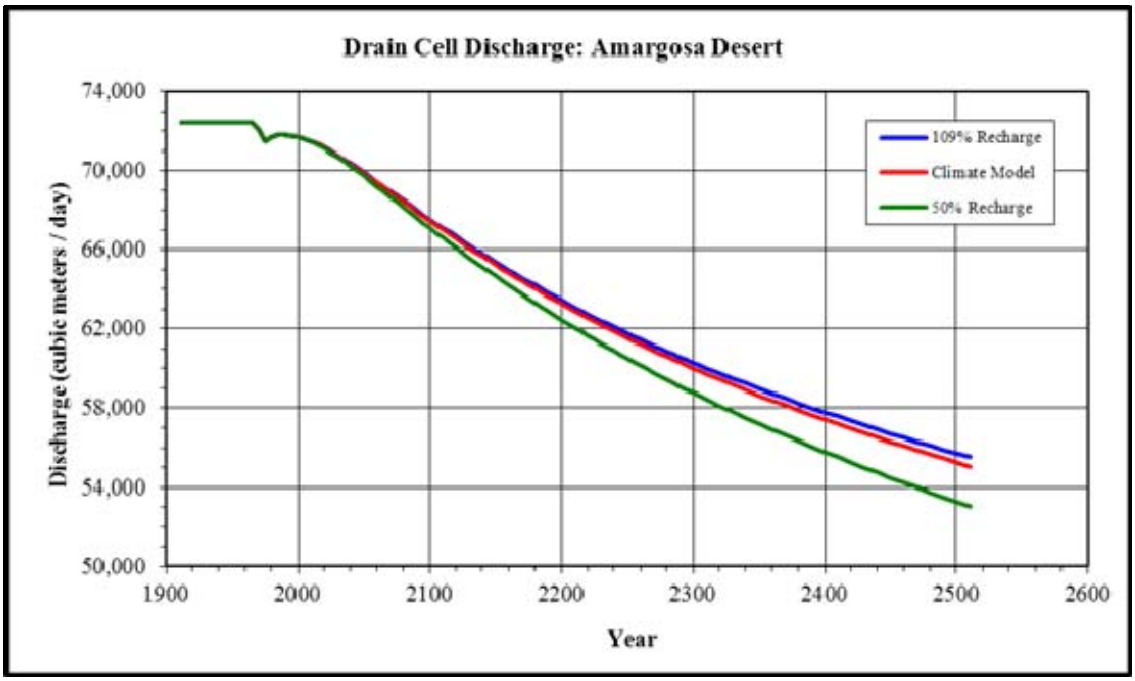

Figure 82. Drain Cell Discharge Comparison, Amargosa Desert

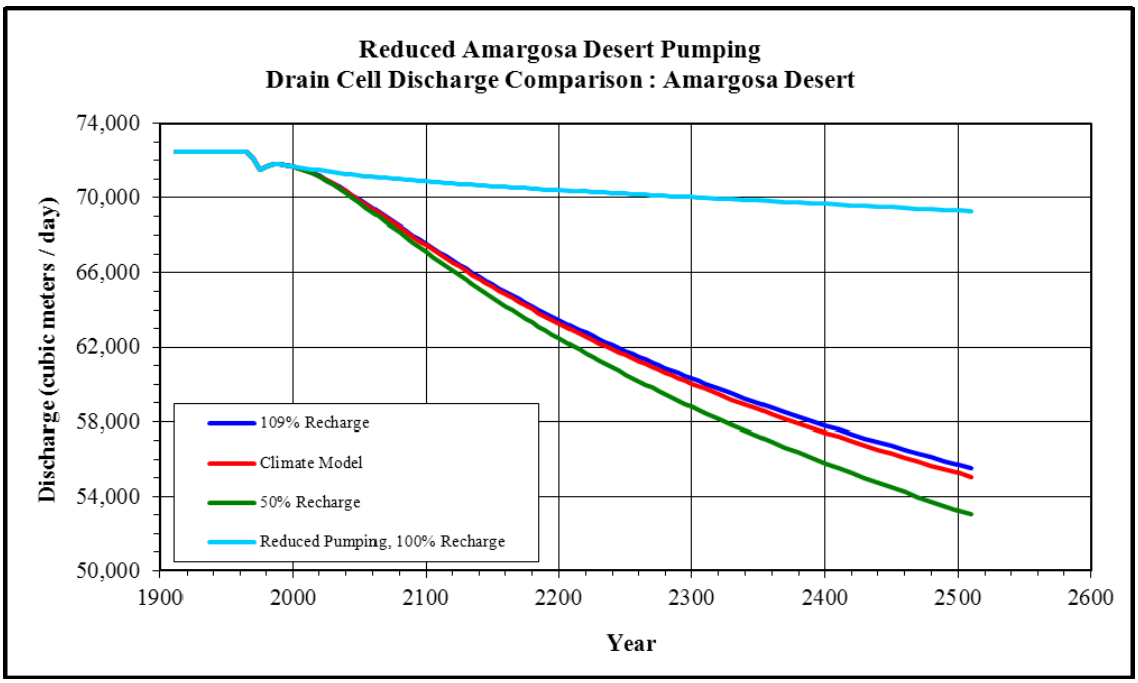

Figure 83. Drain Cell Discharge Comparison with Pumping Minimized, Amargosa Desert

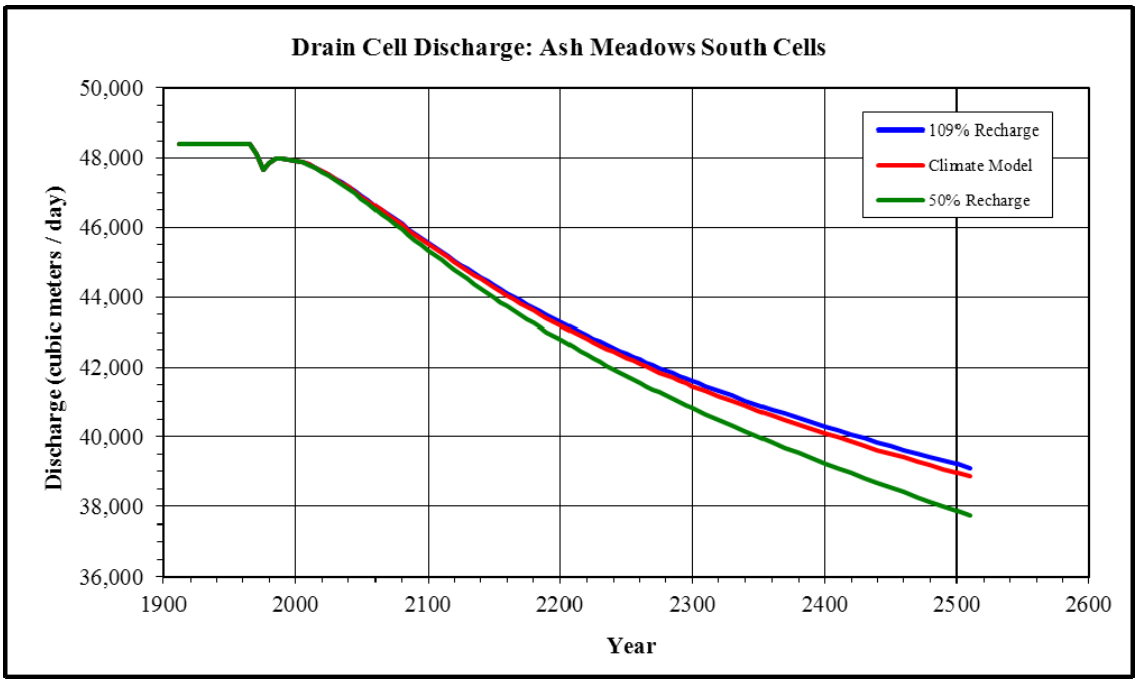

Figure 84. Drain Cell Discharge Comparison, Ash Meadows South

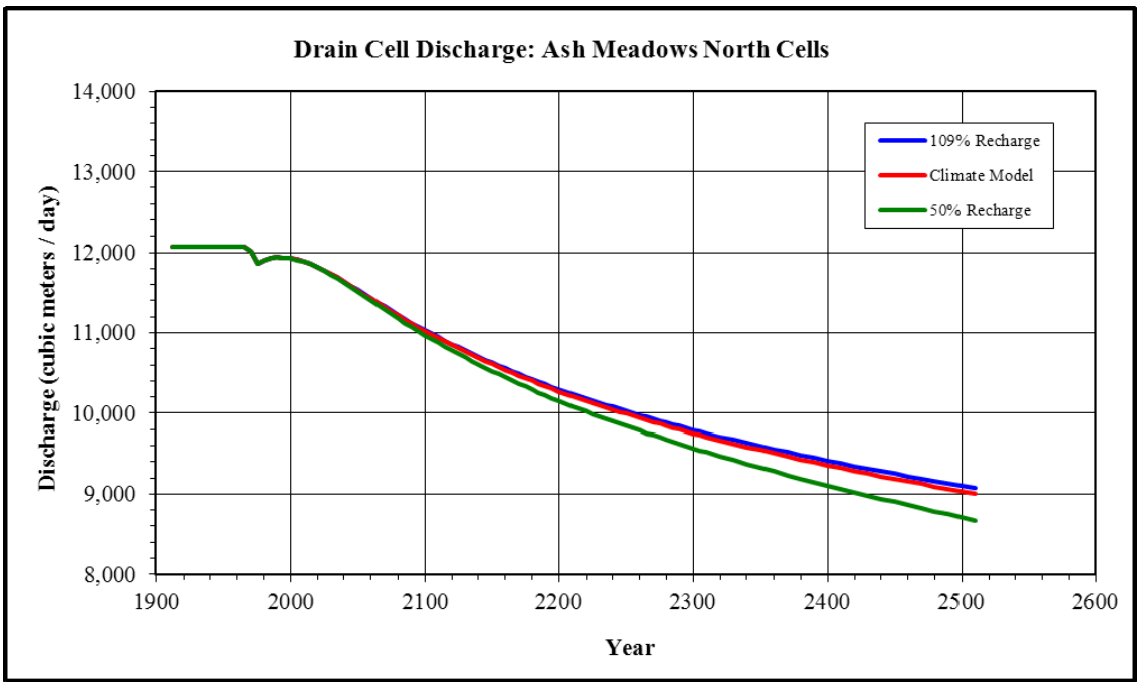

Figure 85. Drain Cell Discharge Comparison, Ash Meadows North

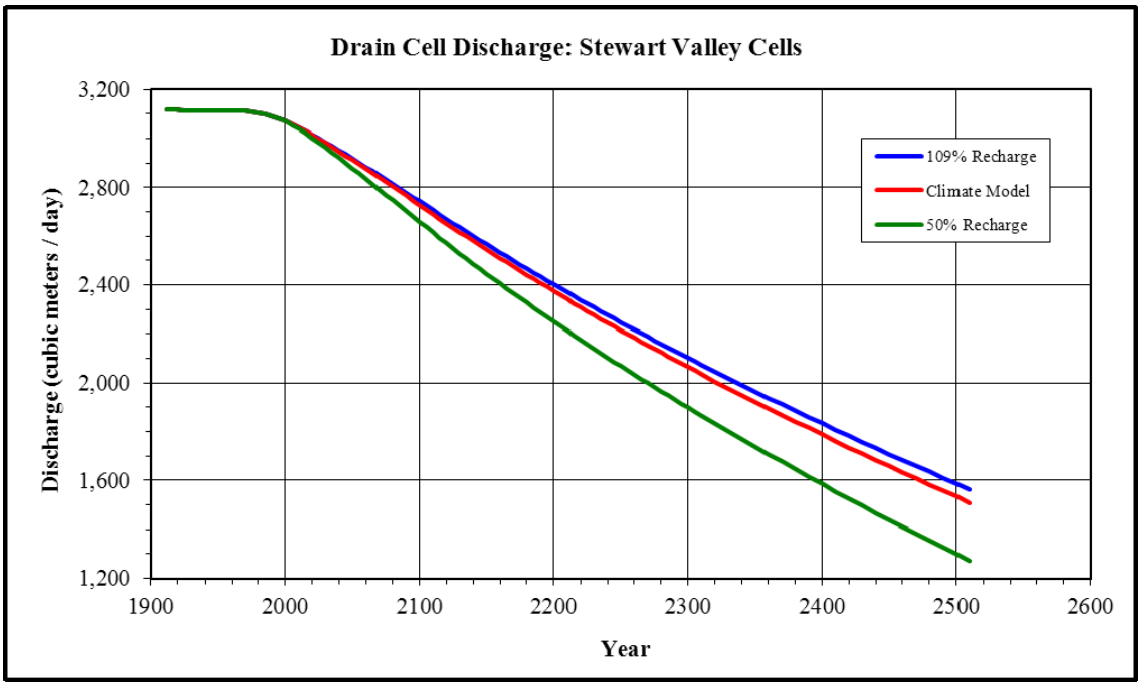

Figure 86. Drain Cell Discharge Comparison, Stewart Valley

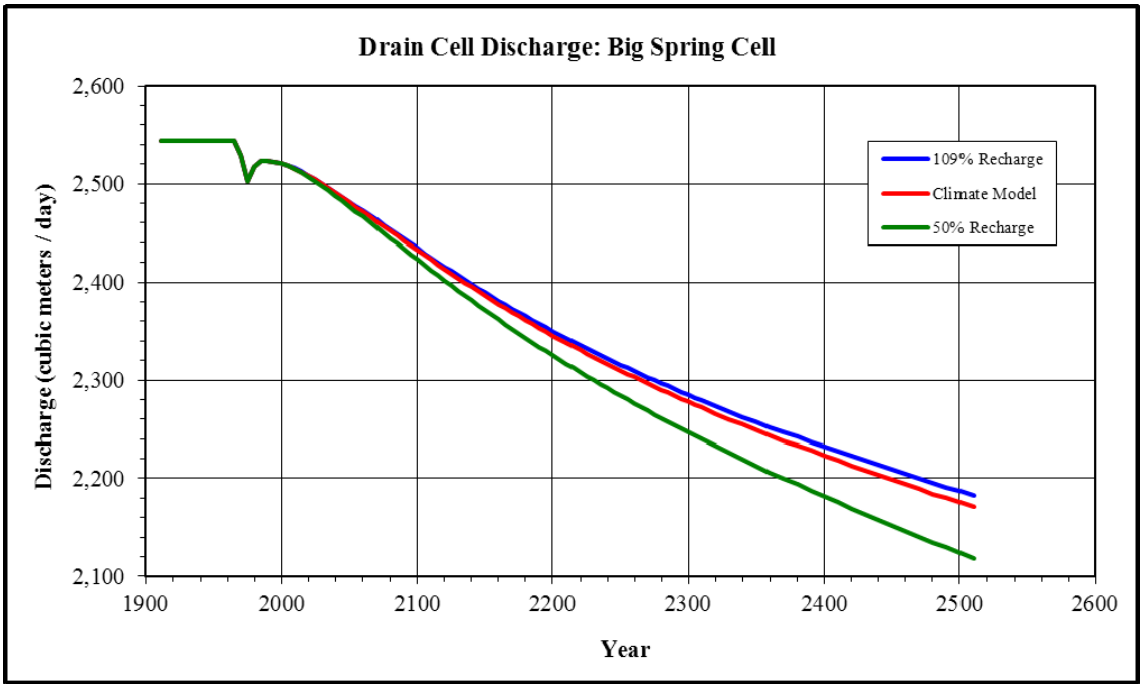

Figure 87. Drain Cell Discharge Comparison, Big Spring

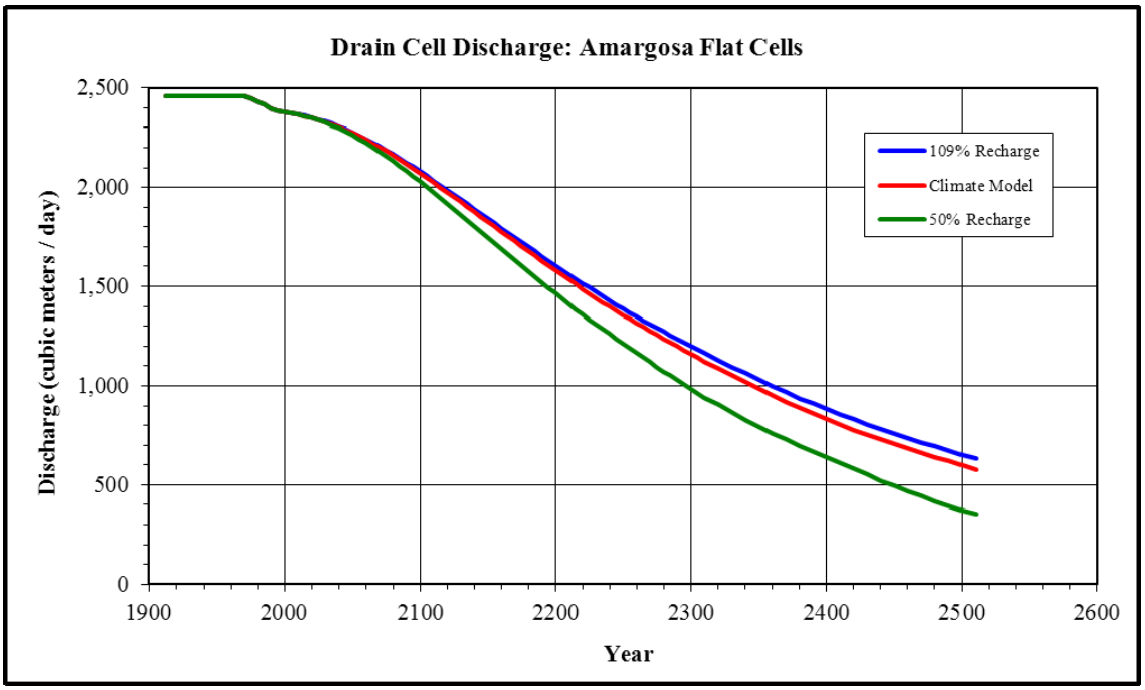

Figure 88. Drain Cell Discharge Comparison, Amargosa Flat

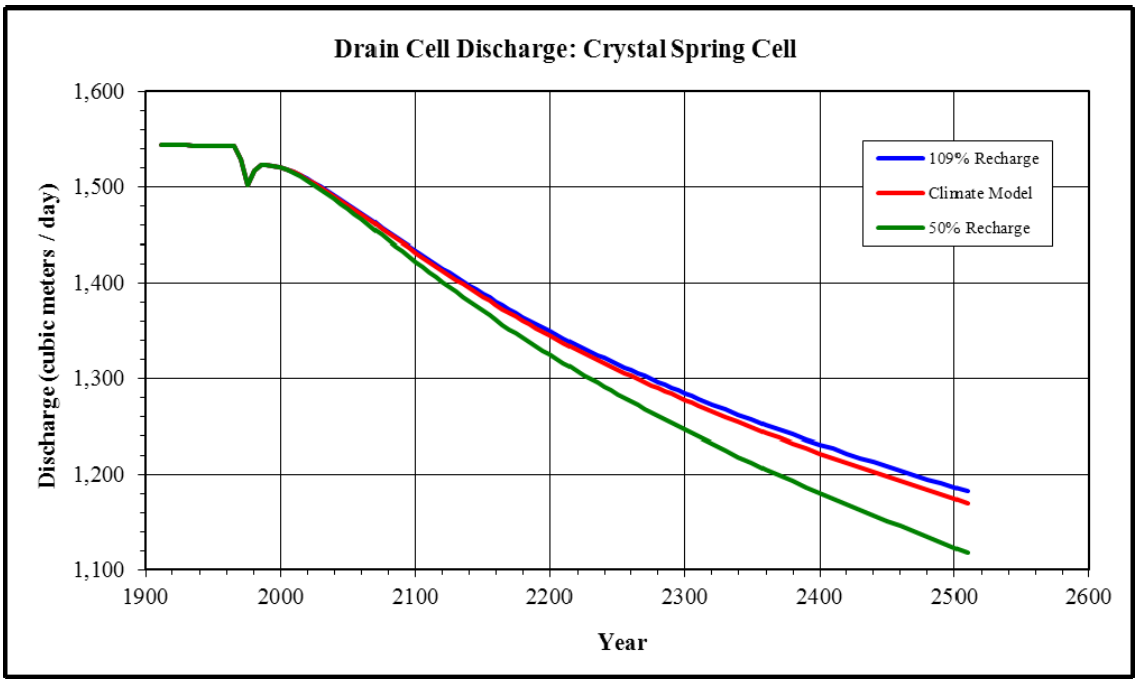

Figure 89. Drain Cell Discharge Comparison, Crystal Spring

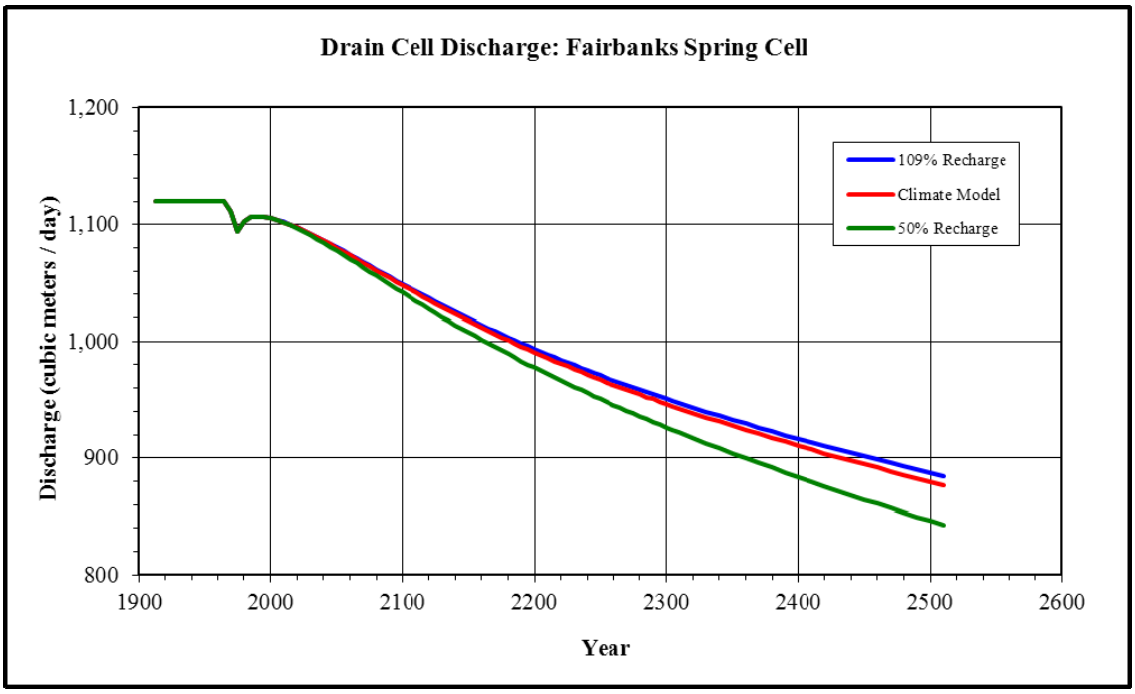

Figure 90. Drain Cell Discharge Comparison, Fairbanks Spring

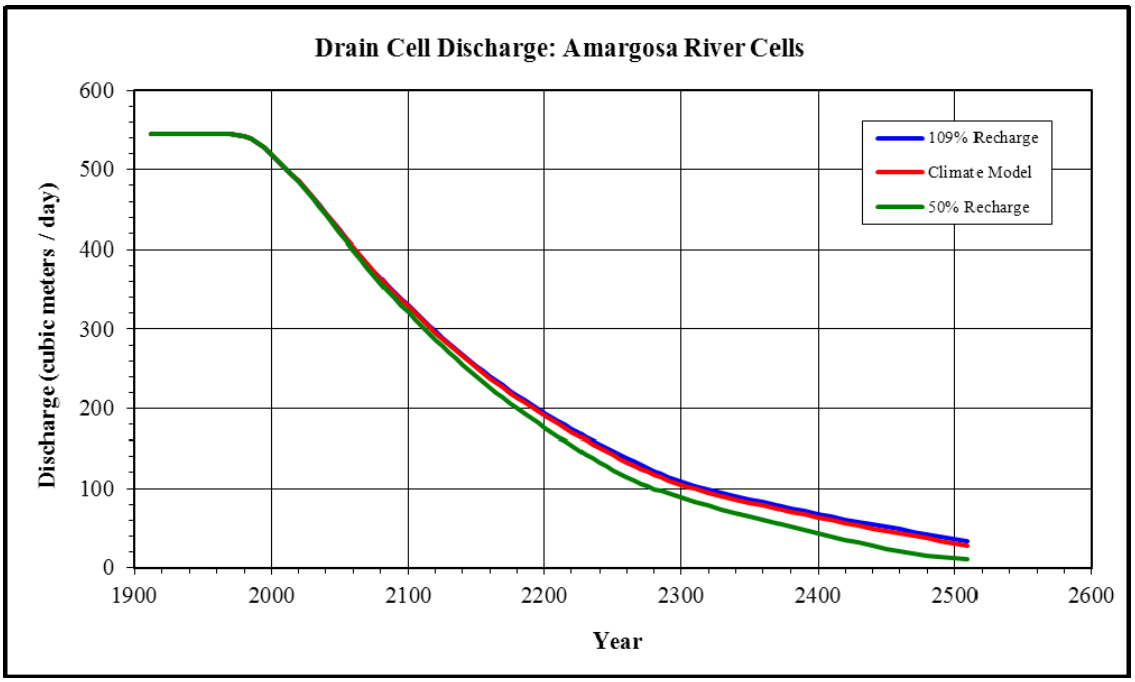

Figure 91. Drain Cell Discharge Comparison, Amargosa River

In the Death Valley portion of the study area, the change in drain discharge for the 50 percent simulation (Figure 92) indicates a downward step at approximately the year 2000. The step is an error and is related to the ZoneBudget program. The error appears to affect only drain discharge values for the cells forming the Death Valley area in its entirety, and does not appear to affect subsets of cells within Death Valley. The cause of the error has not been identified.

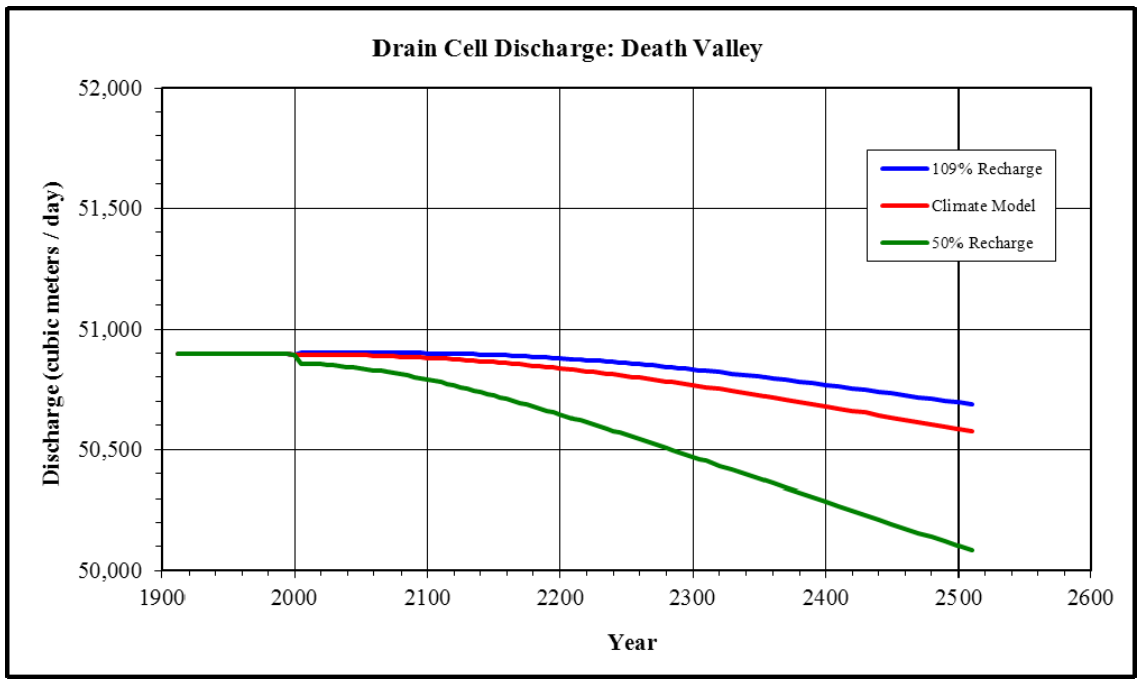

Figure 92. Drain Cell Discharge Comparison, Death Valley

As shown in Figure 93, discharge in Death Valley is greater when pumping is reduced in the study area.

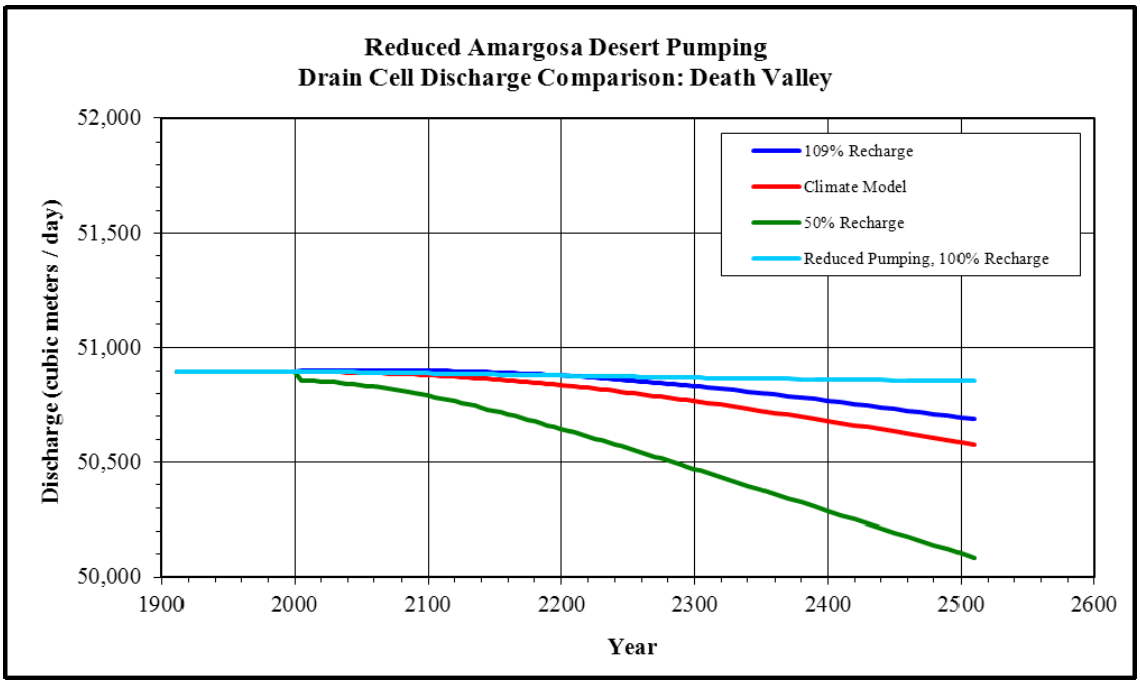

Figure 93. Drain Cell Discharge Comparison with Pumping Minimized, Death Valley

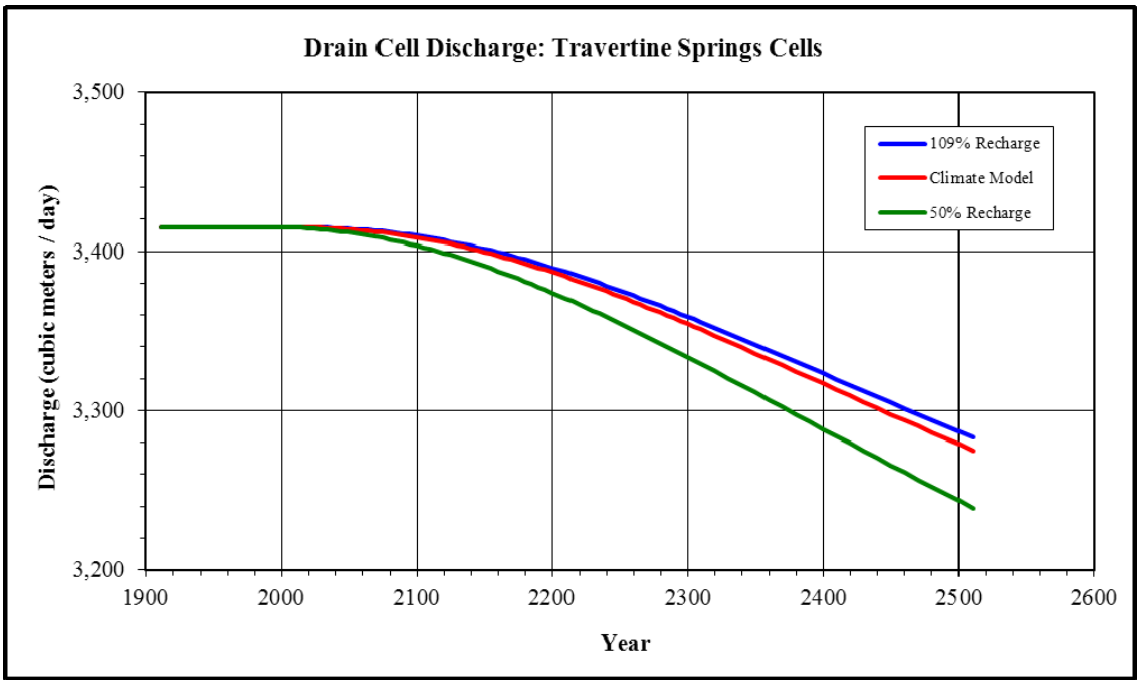

Figure 94. Drain Cell Discharge Comparison, Travertine Springs

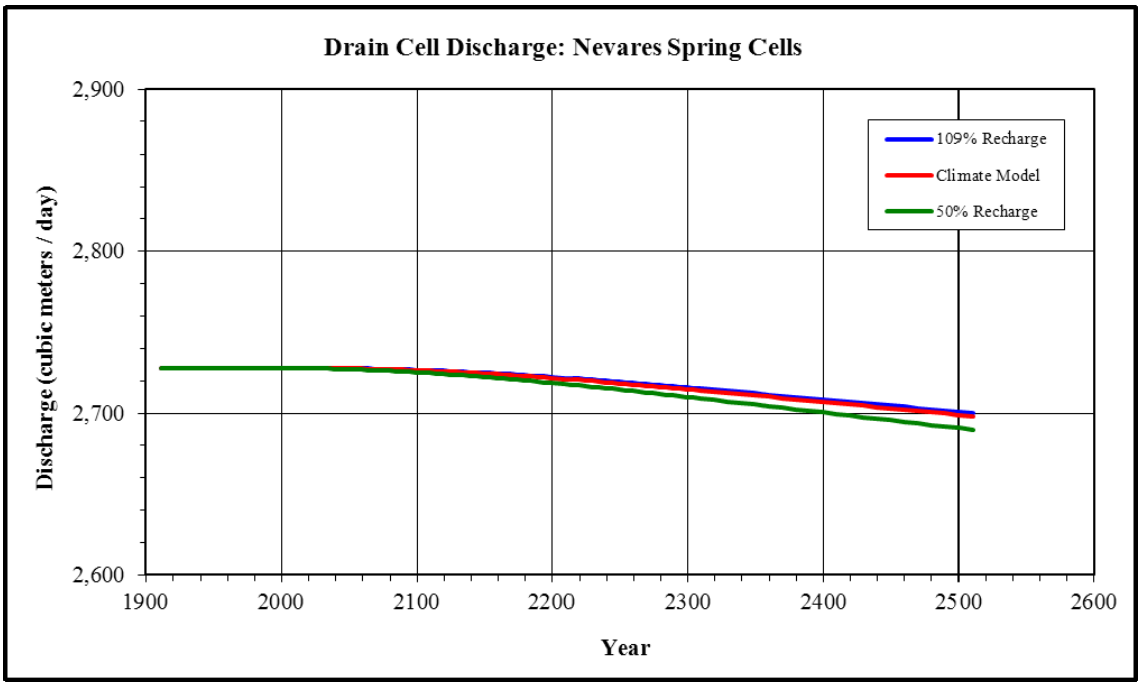

Figure 95. Drain Cell Discharge Comparison, Nevares Spring

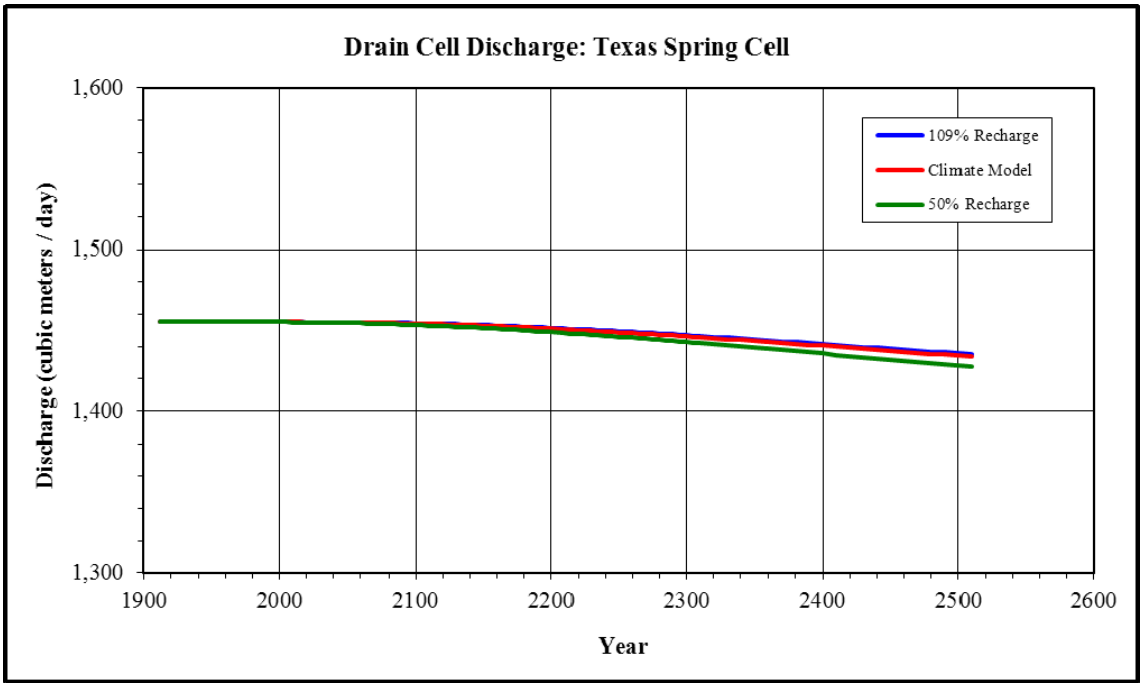

Figure 96. Drain Cell Discharge Comparison, Texas Spring

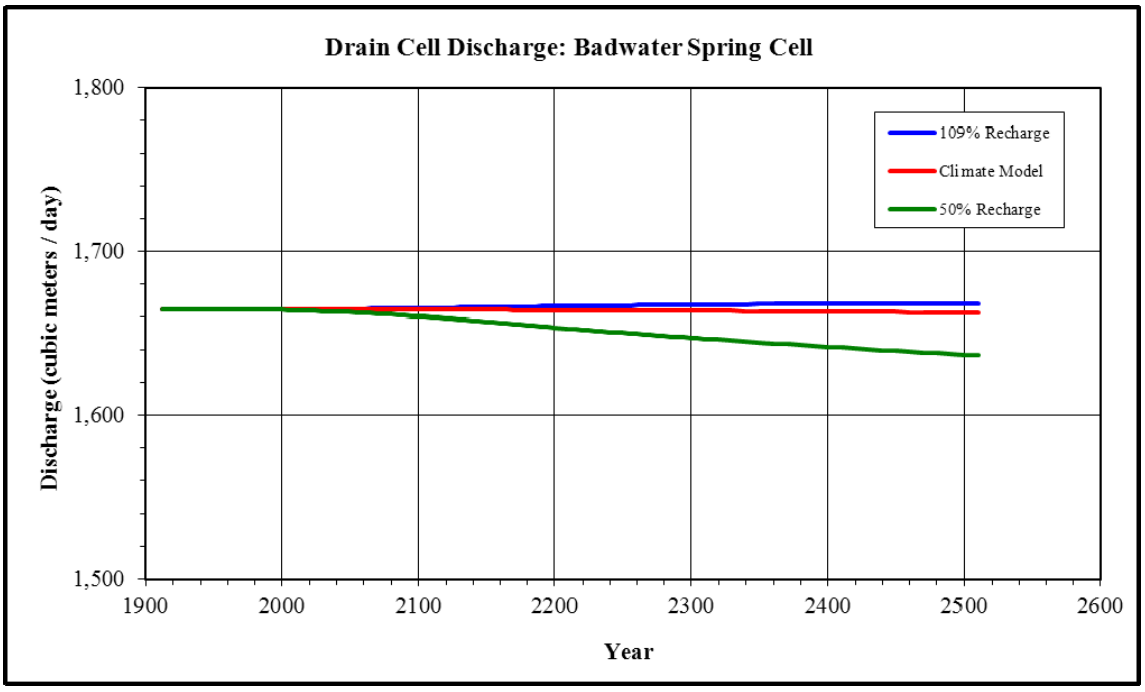

Figure 97. Drain Cell Discharge Comparison, Badwater Spring

6.2.2 Comparison of Simulated Drain Cell Discharge by Recharge Percentage Simulation

In the previous section, changes in simulated discharge were viewed based on the effects in each cell or group of cells. This section presents changes in discharge based on the effects of each recharge scenario across the range of cells examined.

6.2.2.1 Simulation of 100 Percent of 20th Century Recharge

In the baseline simulation with recharge maintained at 100 percent of 20th Century rates, discharge from drain cells declined at all locations in the study area over time. Table 8 presents the discharge data for selected years in the baseline simulation.

Table 8. Drain Cell Discharge, 100 % of 20th Century Recharge (m^3/day)

Year	Model Domain	Study Area	Amargosa Desert	Ash Meadows South	Ash Meadows North	Stewart Valley	Big Spring	Amargosa Flat
1912	362,455	123,370	72,474	48,401	12,076	3,116	2,544	2,459
2000	345,347	122,580	71,688	47,924	11,926	3,070	2,521	2,380
2100	331,197	118,380	67,494	45,528	11,024	2,730	2,432	2,073
2200	322,697	114,160	63,314	43,214	10,276	2,380	2,346	1,587
2300	318,498	110,860	60,078	41,494	9,763	2,073	2,279	1,169
2400	315,438	108,200	57,501	40,143	9,371	1,797	2,225	843
2500	312,908	105,950	55,347	39,011	9,046	1,545	2,178	608
Total Change 2000 to 2500	-32,438	-16,630	-16,341	-8,913	-2,880	-1,525	-343	-1,772
% Change 2000 to 2500	-9.39%	-13.57%	-22.79%	-18.60%	-24.15%	-49.67%	-13.60%	-74.45%

Year	Crystal Pool	Fairbanks Spring	Amargosa River	Death Valley	Travertine Springs	Nevares Spring	Badwater	Texas Spring
1912	1,543	1,120	546	50,896	3,415	2,728	1,665	1,455
2000	1,520	1,105	520	50,895	3,415	2,728	1,665	1,455
2100	1,432	1,048	328	50,884	3,409	2,727	1,665	1,454
2200	1,345	991	192	50,844	3,388	2,722	1,665	1,451
2300	1,279	947	105	50,780	3,355	2,715	1,664	1,446
2400	1,224	912	64	50,698	3,318	2,707	1,664	1,441
2500	1,177	881	32	50,608	3,280	2,699	1,664	1,435
Total Change 2000 to 2500	-343	-224	-488	-287	-135	-29	-1	-21
% Change 2000 to 2500	-22.56%	-20.27%	-93.77%	-0.56%	-3.95%	-1.06%	-0.05%	-1.41%

The comparative change in discharge for each drain cell or group of drain cells evaluated for the 100 percent of 20th Century recharge simulation is shown in Figures 98 through 100.

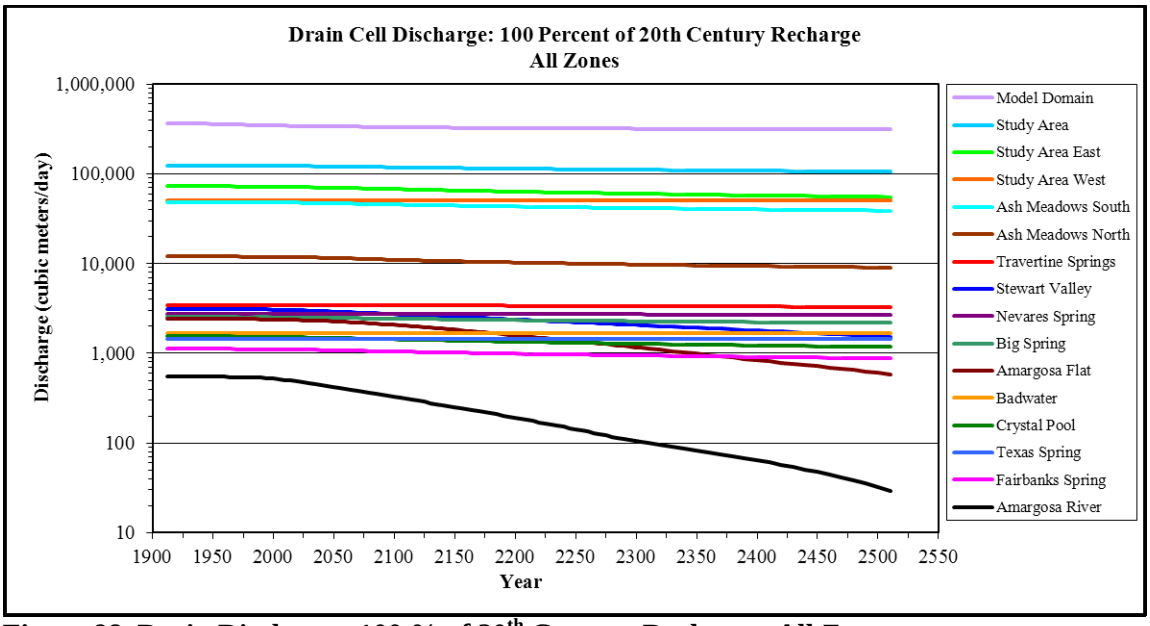

Figure 98. Drain Discharge, 100 % of 20th Century Recharge, All Zones

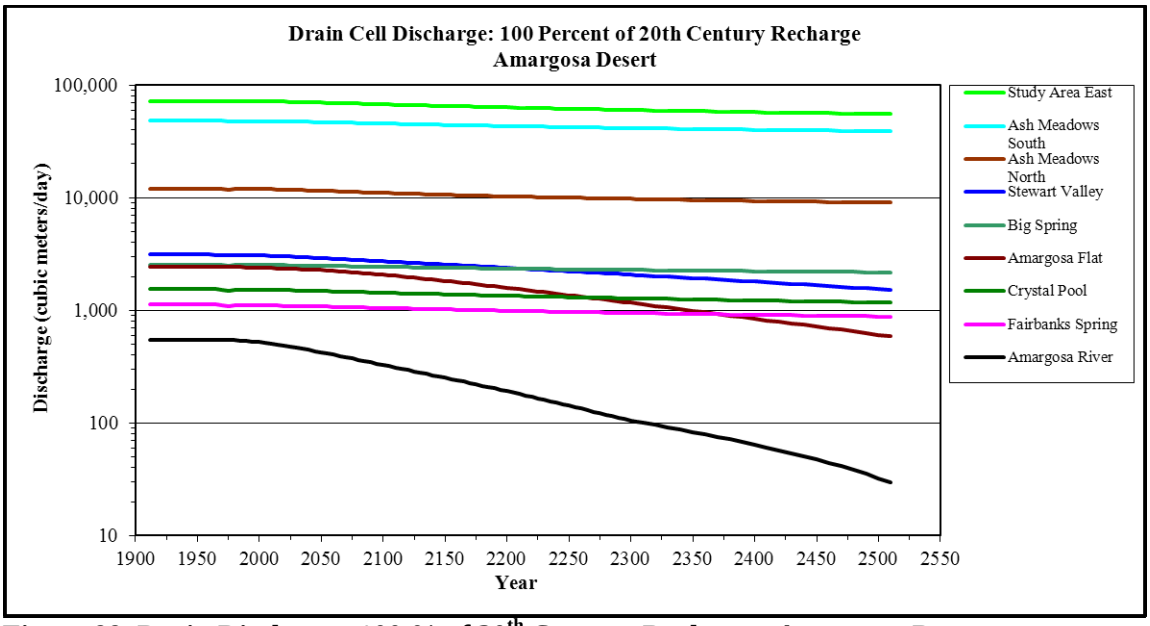

Figure 99. Drain Discharge, 100 % of 20th Century Recharge, Amargosa Desert

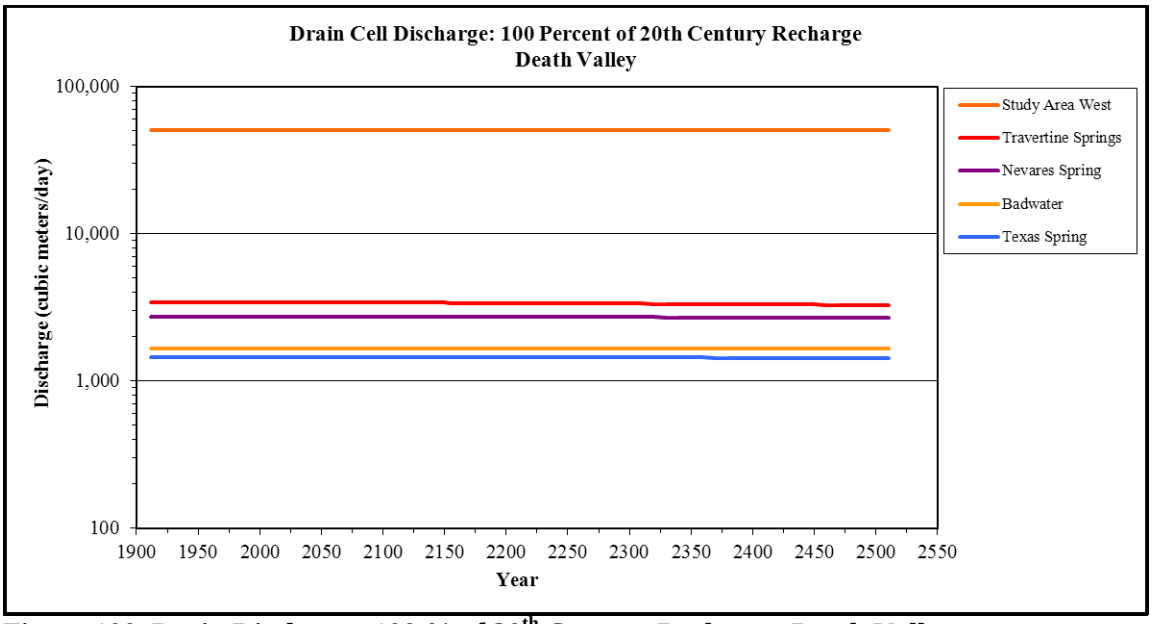

Figure 100. Drain Discharge, 100 % of 20th Century Recharge, Death Valley

6.2.2.2 Simulation of Reduced Pumping and Baseline Recharge

In the simulation in which pumping in the study area is reduced and recharge is continued at 100 percent of 20th Century rates, discharge from drain cells declined from 2000 to 2500 at all locations in the study area, except in the Badwater cell. However, the decline was substantially less than the decline simulated under scenarios in which pumping is continued at current rates. Table 9 presents the discharge data for selected years in the reduced pumping simulation relative to the baseline recharge condition.

Table 9. Drain Cell Discharge, Reduced Pumping with 20th Century Recharge (m^3/day)

Year	Model Domain	Study Area	Amargosa Desert	Ash Meadows South	Ash Meadows North	Stewart Valley	Big Spring	Amargosa Flat
1912	362450	123370	72474	48401	12076	3116	2544	2459
2000	345350	122580	71688	47924	11926	3070	2521	2380
2100	334580	121760	70876	47680	11834	2730	2513	2287
2200	329830	121290	70410	47630	11832	2381	2511	2249
2300	328550	120900	70030	47601	11829	2075	2510	2228
2400	327780	120530	69669	47559	11819	1801	2507	2208
2500	327150	120170	69311	47503	11804	1551	2505	2187
Total Change 2000 to 2500	-18,200	-2,410	-2,377	-421	-122	-1,519	-16	-193
% Change 2000 to 2500	-5.27%	-1.97%	-3.32%	-0.88%	-1.02%	-49.49%	-0.63%	-8.13%
Baseline (100% Recharge) Change	-32,438	-16,630	-16,341	-8,913	-2,880	-1,525	-343	-1,772
Difference Relative to Baseline	14,238	14,220	13,964	8,492	2,758	6	327	1,579

Year	Crystal Pool	Fairbanks Spring	Amargosa River	Death Valley	Travertine Springs	Nevares Spring	Badwater	Texas Spring
1912	1543	1120	546	50896	3415	2728	1665	1455
2000	1520	1105	520	50895	3415	2728	1665	1455
2100	1513	1100	506	50889	3412	2727	1665	1455
2200	1511	1099	509	50879	3407	2726	1665	1454
2300	1509	1098	511	50870	3404	2726	1665	1453
2400	1507	1097	512	50863	3401	2725	1664	1453
2500	1504	1095	511	50856	3400	2725	1664	1453
Total Change 2000 to 2500	-16	-10	-9	-39	-16	-3	0	-3
% Change 2000 to 2500	-1.05%	-0.93%	-1.71%	-0.08%	-0.46%	-0.12%	-0.01%	-0.17%
Baseline (100% Recharge) Change	-343	-224	-488	-287	-135	-29	-1	-21
Difference Relative to Baseline	327	214	479	248	119	25	1	18

The comparative change in discharge for each drain cell or group of drain cells evaluated for the scenario in which recharge is maintained at the baseline condition and pumping is reduced is shown in Figures 101 through 103.

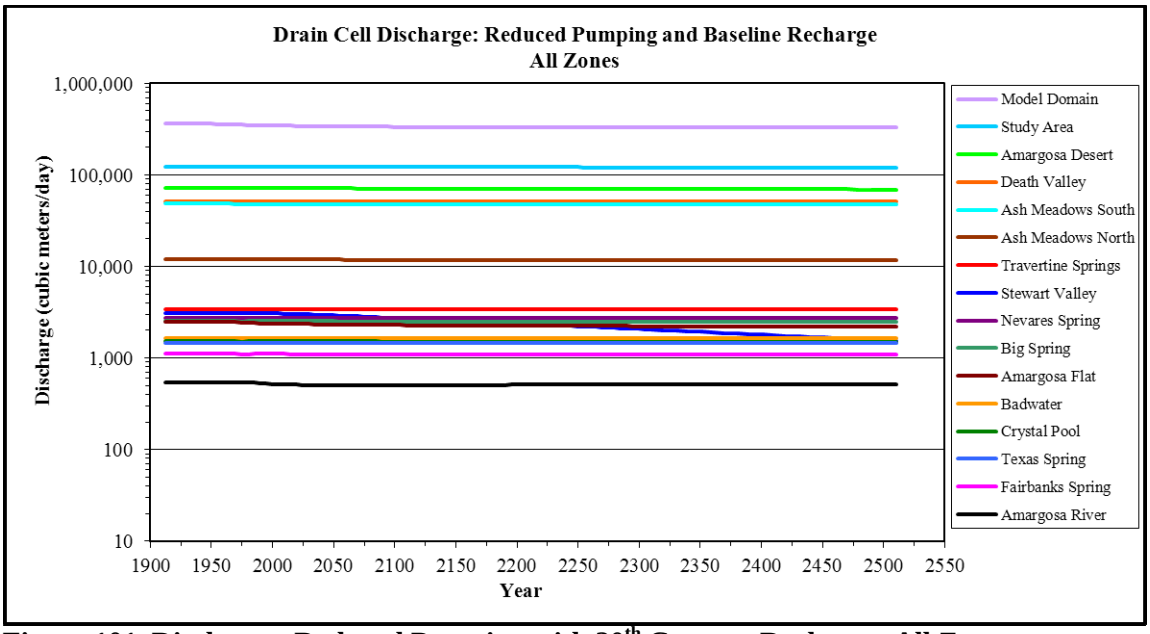

Figure 101. Discharge: Reduced Pumping with 20th Century Recharge, All Zones

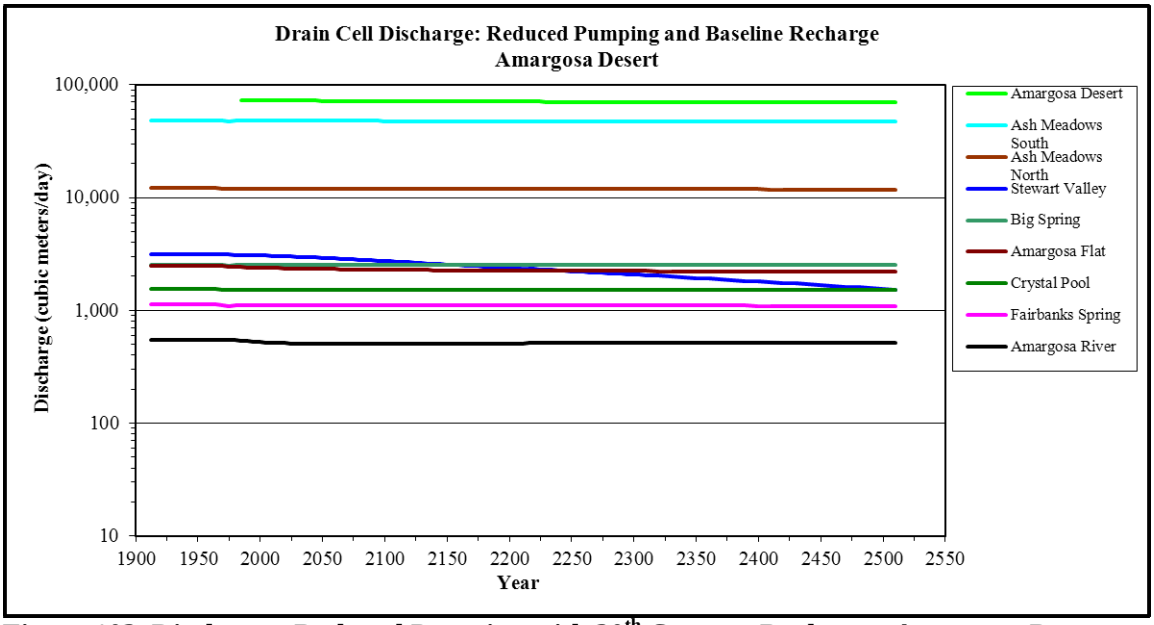

Figure 102. Discharge: Reduced Pumping with 20th Century Recharge, Amargosa Desert

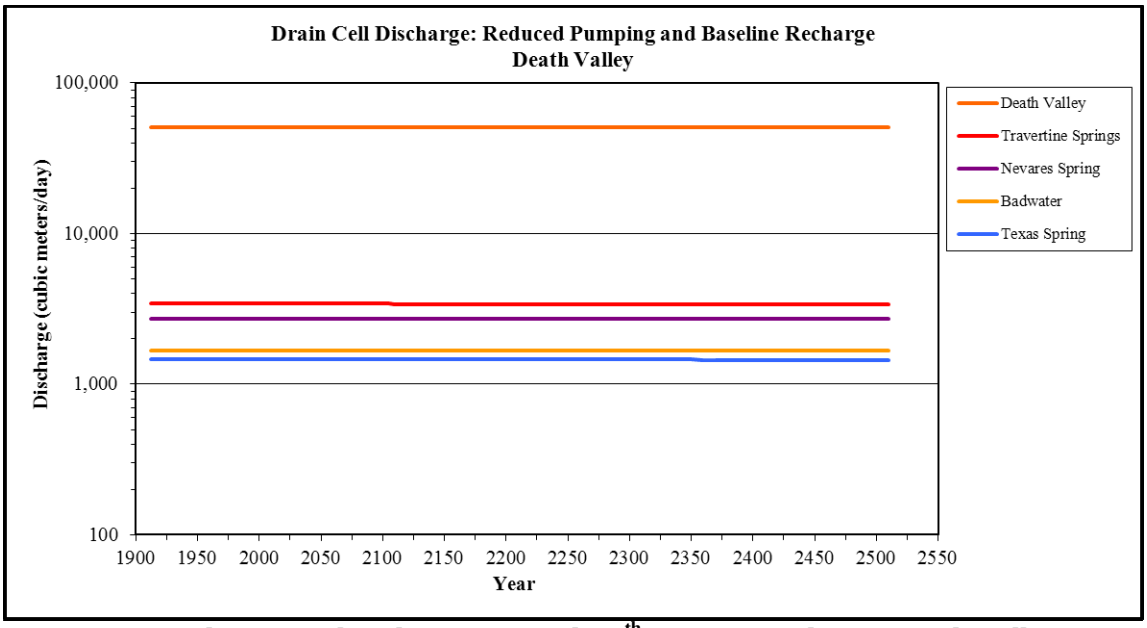

Figure 103. Discharge: Reduced Pumping with 20th Century Recharge, Death Valley

6.2.2.4 Simulation of 109 Percent of 20th Century Recharge

In the simulation with recharge at 109 percent of 20th Century rates, discharge from drain cells declined from 2000 to 2500 at all locations in the study area, except for the Badwater cell. Table 10 presents the discharge data for selected years relative to the baseline recharge condition.

Table 10. Drain Cell Discharge, 109% of 20th Century Recharge (m^3/day)

Year	Model Domain	Study Area	Amargosa Desert	Ash Meadows South	Ash Meadows North	Stewart Valley	Big Spring	Amargosa Flat
1912	362,455	123,370	72,474	48,401	12,076	3,116	2,544	2,459
2000	345,347	122,580	71,688	47,924	11,926	3,070	2,521	2,380
2100	331,488	118,460	67,559	45,560	11,034	2,742	2,434	2,081
2200	323,225	114,340	63,461	43,287	10,298	2,402	2,350	1,608
2300	319,223	111,140	60,302	41,608	9,796	2,103	2,285	1,201
2400	316,369	108,560	57,795	40,297	9,416	1,834	2,232	882
2500	314,041	106,400	55,708	39,205	9,103	1,587	2,187	651
Total Change 2000 to 2500	-31,306	-16,180	-15,980	-8,719	-2,824	-1,483	-334	-1,729
% Change 2000 to 2500	-9.07%	-13.20%	-22.29%	-18.19%	-23.68%	-48.30%	-13.23%	-72.64%
Baseline (100% Recharge) Change	-32,438	-16,630	-16,341	-8,913	-2,880	-1,525	-343	-1,772
Difference Relative to Baseline	1,132	450	361	194	57	42	9	43

Year	Crystal Pool	Fairbanks Spring	Amargosa River	Death Valley	Travertine Springs	Nevares Spring	Badwater	Texas Spring
1912	1,543	1,120	546	50,896	3,415	2,728	1,665	1,455
2000	1,520	1,105	520	50,895	3,415	2,728	1,665	1,455
2100	1,433	1,049	329	50,900	3,410	2,727	1,665	1,454
2200	1,349	993	194	50,879	3,390	2,723	1,666	1,451
2300	1,284	951	108	50,833	3,359	2,716	1,667	1,447
2400	1,231	917	68	50,769	3,323	2,709	1,668	1,441
2500	1,186	887	37	50,695	3,287	2,701	1,668	1,436
Total Change 2000 to 2500	-334	-218	-483	-200	-129	-27	4	-19
% Change 2000 to 2500	-21.97%	-19.74%	-92.92%	-0.39%	-3.76%	-1.00%	0.22%	-1.33%
Baseline (100% Recharge) Change	-343	-224	-488	-287	-135	-29	-1	-21
Difference Relative to Baseline	9	6	4	87	6	2	5	1

The comparative change in discharge for each drain cell or group of drain cells evaluated for the 109 percent of 20th Century recharge simulation is shown in Figures 104 through 106.

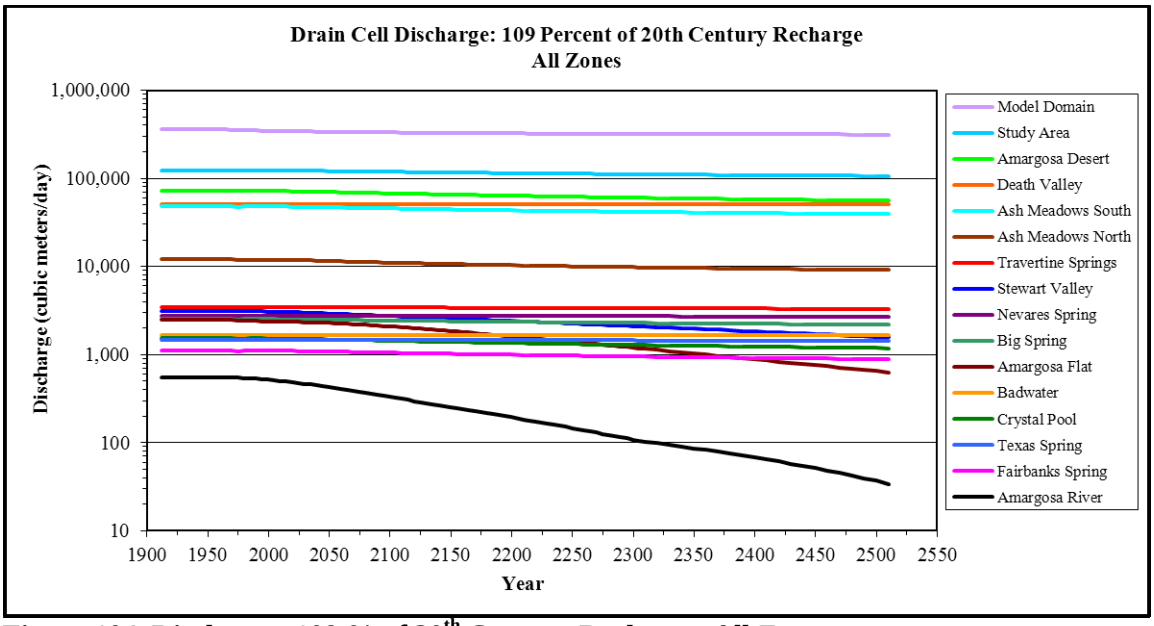

Figure 104. Discharge: 109 % of 20th Century Recharge, All Zones

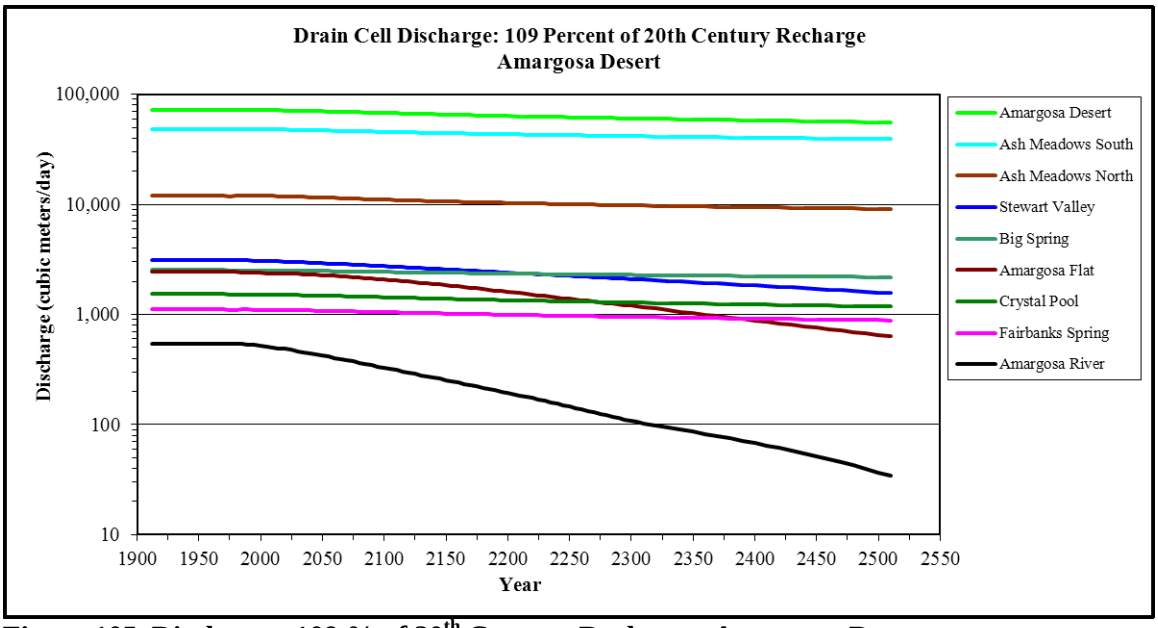

Figure 105. Discharge: 109 % of 20th Century Recharge, Amargosa Desert

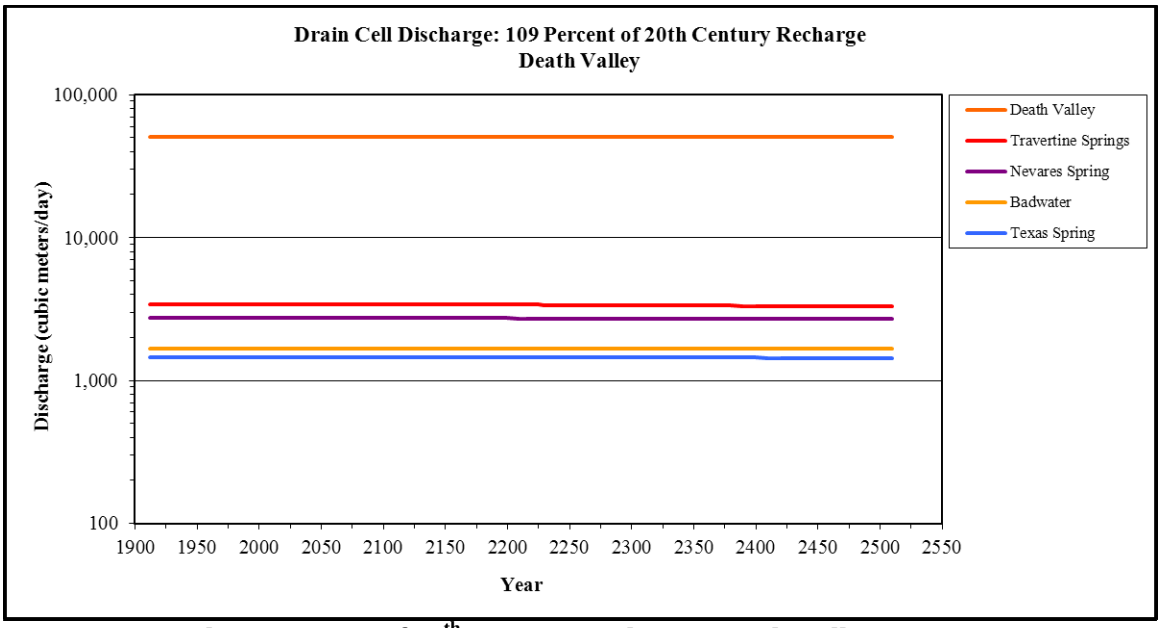

Figure 106. Discharge: 109 % of 20th Century Recharge, Death Valley

6.2.2.3 Simulation of Climate Model Recharge

In the climate model simulation in which recharge is based on the results of the climate models discussed in Section 5.0, discharge from drain cells declined from 2000 to 2500 at all locations in the study area. Table 11 presents the discharge data relative to the baseline condition of 100 percent of 20th Century recharge for selected years in the climate model simulation.

Table 11. Drain Cell Discharge, Climate Model Recharge (m^3/day)

Year	Model Domain	Study Area	Amargosa Desert	Ash Meadows South	Ash Meadows North	Stewart Valley	Big Spring	Amargosa Flat
1912	362,455	123,370	72,474	48,401	12,076	3,116	2,544	2,459
2000	345,347	122,580	71,688	47,924	11,926	3,070	2,521	2,380
2100	331,153	118,370	67,486	45,524	11,023	2,728	2,432	2,072
2200	322,589	114,120	63,283	43,199	10,272	2,375	2,345	1,583
2300	318,321	110,790	60,021	41,464	9,754	2,065	2,278	1,161
2400	315,200	108,100	57,424	40,102	9,359	1,788	2,223	834
2500	312,615	105,840	55,253	38,960	9,031	1,534	2,176	597
Total Change 2000 to 2500	-32,732	-16,740	-16,435	-8,964	-2,895	-1,536	-345	-1,783
% Change 2000 to 2500	-9.48%	-13.66%	-22.93%	-18.70%	-24.27%	-50.04%	-13.69%	-74.91%
Baseline (100% Recharge) Change	-32,438	-16,630	-16,341	-8,913	-2,880	-1,525	-343	-1,772
Difference Relative to Baseline	-294	-110	-94	-51	-15	-11	-2	-11

Year	Crystal Pool	Fairbanks Spring	Amargosa River	Death Valley	Travertine Springs	Nevares Spring	Badwater	Texas Spring
1912	1,543	1,120	546	50,896	3,415	2,728	1,665	1,455
2000	1,520	1,105	520	50,895	3,415	2,728	1,665	1,455
2100	1,431	1,048	328	50,881	3,409	2,727	1,665	1,454
2200	1,345	991	191	50,837	3,387	2,722	1,664	1,451
2300	1,277	946	104	50,767	3,355	2,715	1,664	1,446
2400	1,222	910	63	50,680	3,317	2,707	1,663	1,440
2500	1,175	880	31	50,586	3,279	2,699	1,663	1,434
Total Change 2000 to 2500	-345	-226	-489	-309	-137	-29	-2	-21
% Change 2000 to 2500	-22.72%	-20.42%	-93.99%	-0.61%	-4.00%	-1.07%	-0.13%	-1.43%
Baseline (100% Recharge) Change	-343	-224	-488	-287	-135	-29	-1	-21
Difference Relative to Baseline	-2	-2	-1	-22	-2	0	-1	0

The comparative change in discharge for each drain cell or group of drain cells evaluated for the climate model recharge simulation is shown in Figures 107 through 109.

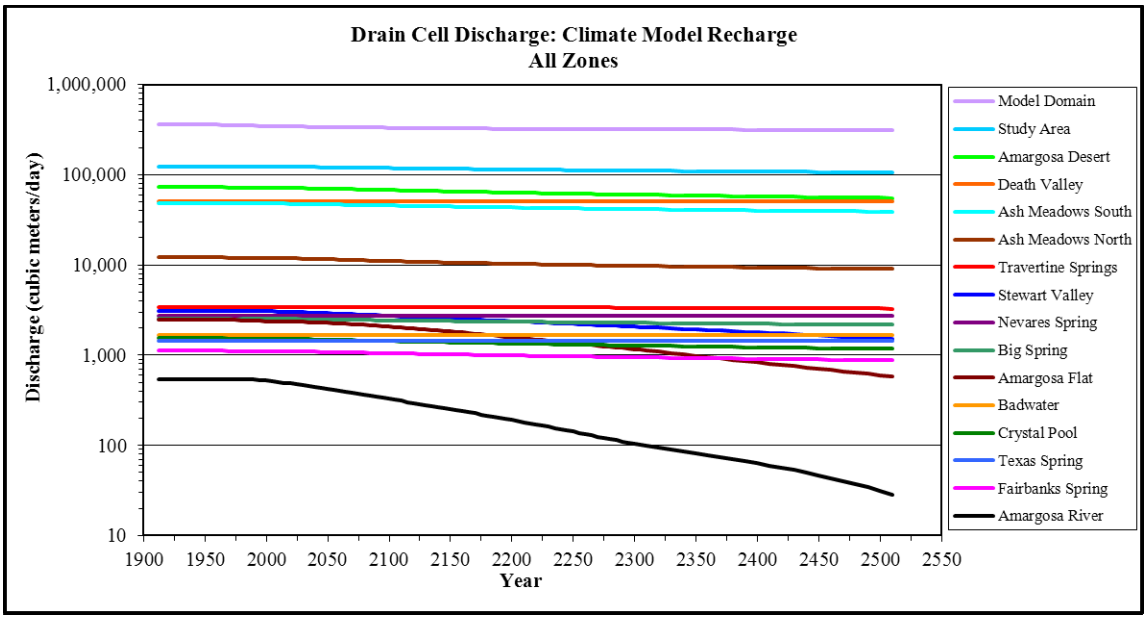

Figure 107. Discharge: Climate Model Recharge, All Zones

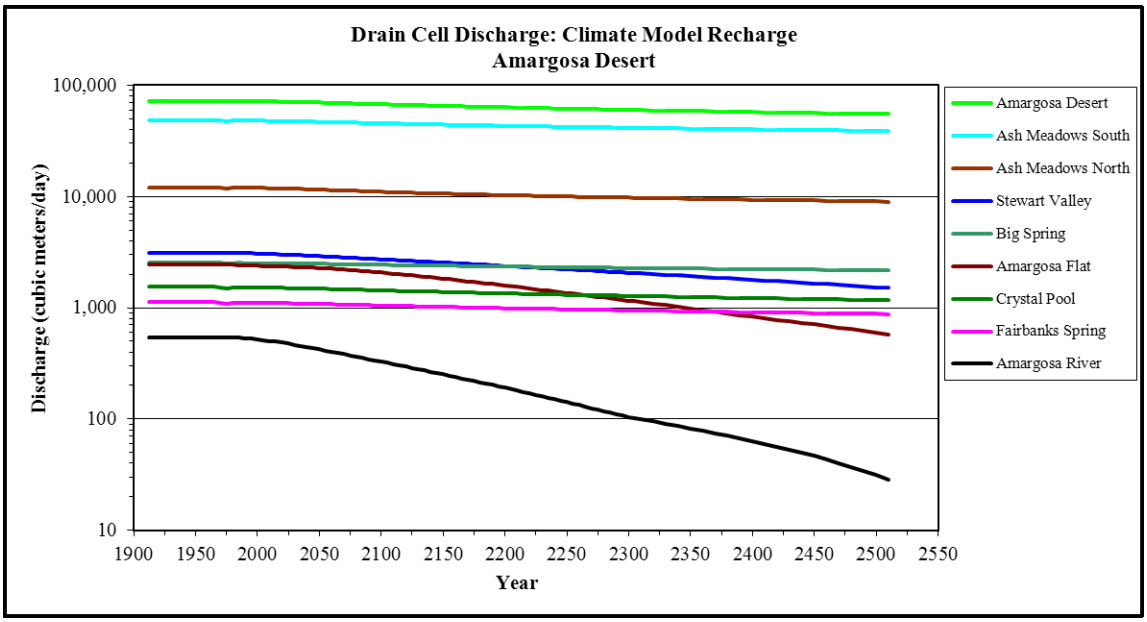

Figure 108. Discharge: Climate Model Recharge, Amargosa Desert

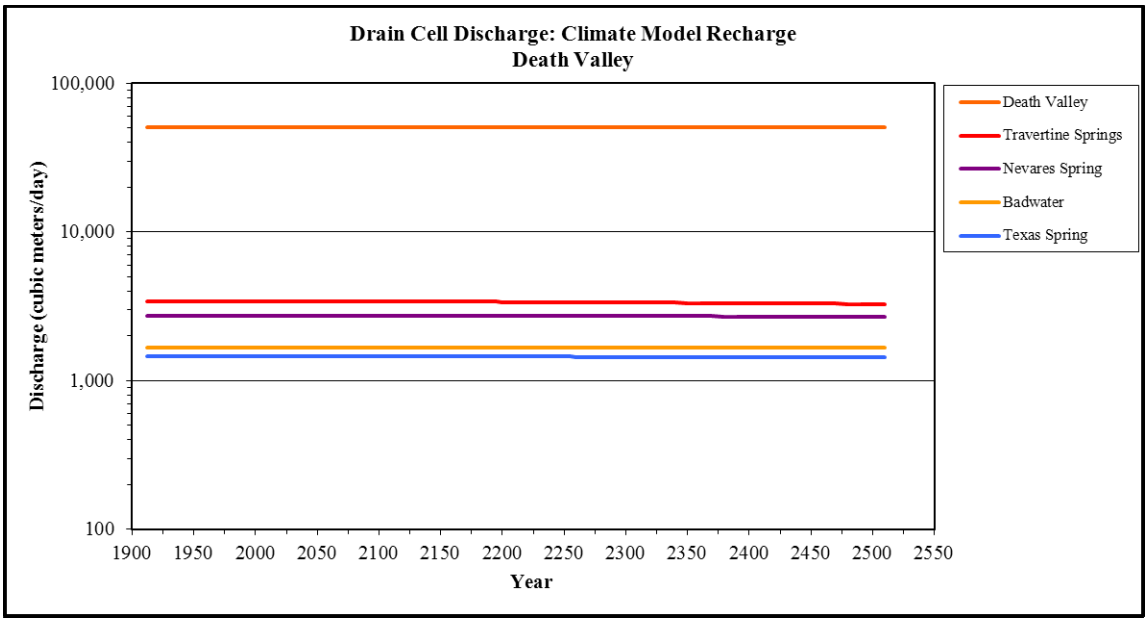

Figure 109. Discharge: Climate Model Recharge, Death Valley

6.2.2.16 Simulation of 50 Percent of 20th Century Recharge

In the simulation with recharge at 50 percent of 20th Century rates, discharge from drain cells declined from 2000 to 2500 at all locations in the study area. Table 12 presents the discharge data for selected years relative to the baseline recharge condition.

Table 12. Drain Cell Discharge, 50 % of 20th Century Recharge (m^3/day)

Year	Model Domain	Study Area	Amargosa Desert	Ash Meadows South	Ash Meadows North	Stewart Valley	Big Spring	Amargosa Flat
1912	362,455	123,370	72,474	48,401	12,076	3,116	2,544	2,459
2000	345,347	122,580	71,688	47,924	11,926	3,070	2,521	2,380
2100	329,538	117,910	67,122	45,347	10,972	2,659	2,423	2,030
2200	319,824	113,110	62,467	42,794	10,154	2,250	2,325	1,467
2300	314,314	109,250	58,775	40,825	9,568	1,899	2,247	984
2400	310,029	106,080	55,795	39,232	9,105	1,586	2,181	638
2500	306,333	103,360	53,252	37,872	8,713	1,299	2,124	370
Total Change 2000 to 2500	-39,013	-19,220	-18,436	-10,052	-3,213	-1,771	-397	-2,010
% Change 2000 to 2500	-11.30%	-15.68%	-25.72%	-20.97%	-26.94%	-57.69%	-15.73%	-84.44%
Baseline (100% Recharge) Change	-32,438	-16,630	-16,341	-8,913	-2,880	-1,525	-343	-1,772
Difference Relative to Baseline	-6,575	-2,590	-2,095	-1,139	-333	-246	-54	-238

Year	Crystal Pool	Fairbanks Spring	Amargosa River	Death Valley	Travertine Springs	Nevares Spring	Badwater	Texas Spring
1912	1,543	1,120	546	50,896	3,415	2,728	1,665	1,455
2000	1,520	1,105	520	50,895	3,415	2,728	1,665	1,455
2100	1,422	1,042	321	50,791	3,404	2,725	1,660	1,453
2200	1,324	978	176	50,646	3,374	2,719	1,654	1,449
2300	1,246	926	89	50,470	3,334	2,710	1,647	1,443
2400	1,180	884	43	50,286	3,289	2,701	1,642	1,436
2500	1,123	846	12	50,103	3,243	2,691	1,637	1,428
Total Change 2000 to 2500	-397	-259	-508	-792	-172	-37	-28	-27
% Change 2000 to 2500	-26.11%	-23.43%	-97.66%	-1.56%	-5.03%	-1.37%	-1.65%	-1.84%
Baseline (100% Recharge) Change	-343	-224	-488	-287	-135	-29	-1	-21
Difference Relative to Baseline	-54	-35	-20	-505	-37	-9	-27	-6

The comparative change in discharge for each drain cell or group of drain cells evaluated for the 50 percent of 20th Century recharge simulation is shown in Figures 110 through 112.

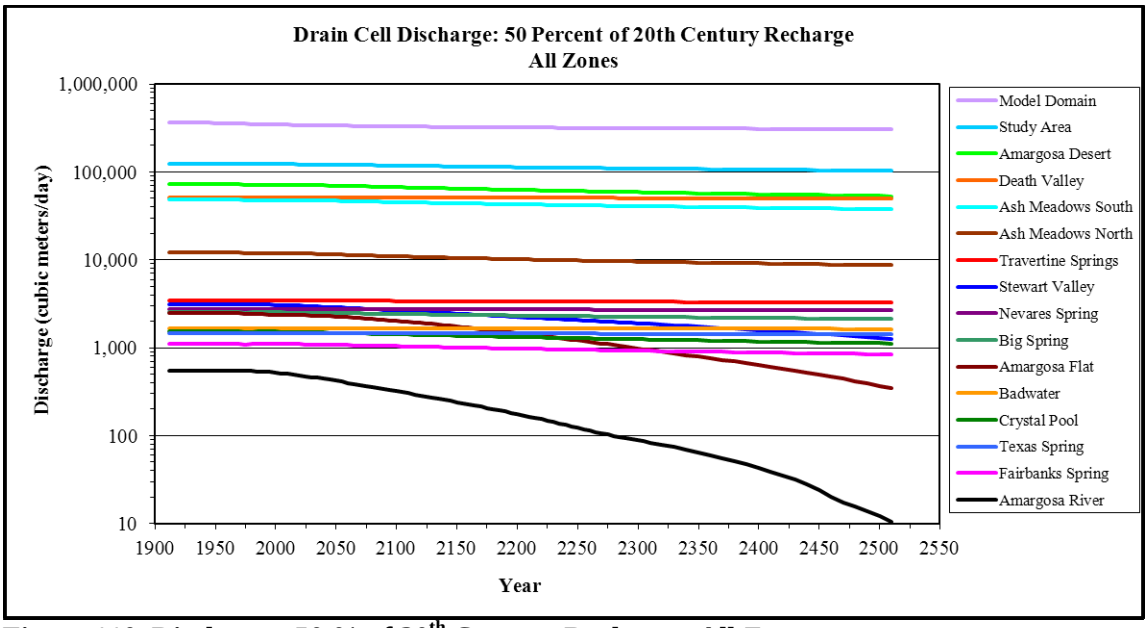

Figure 110. Discharge: 50 % of 20th Century Recharge, All Zones

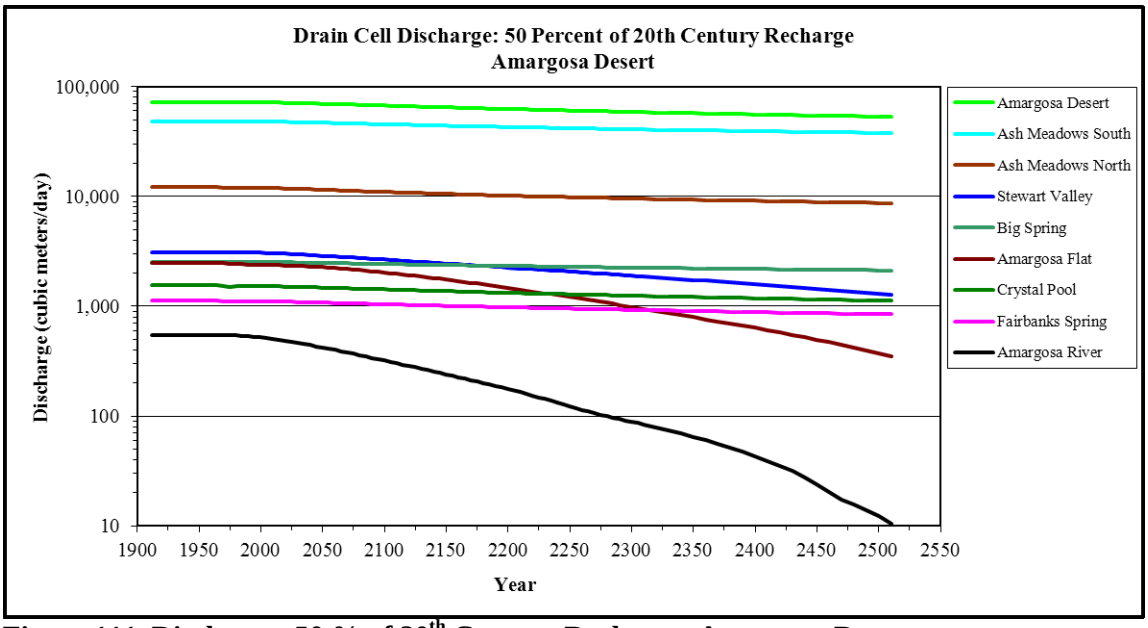

Figure 111. Discharge: 50 % of 20th Century Recharge, Amargosa Desert

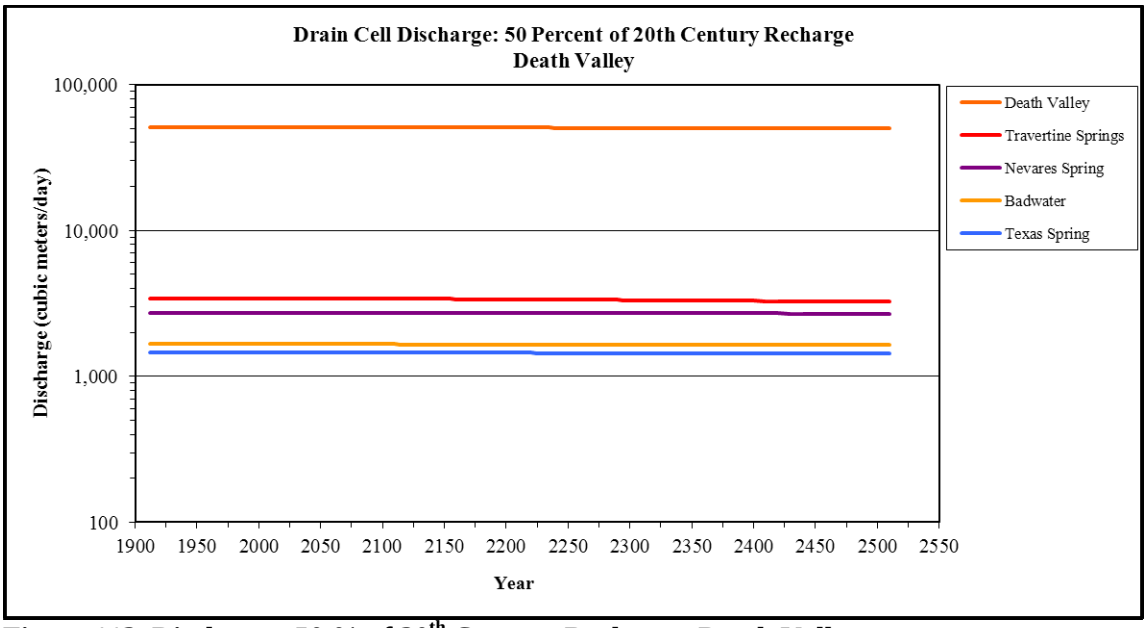

Figure 112. Discharge: 50 % of 20th Century Recharge, Death Valley

7.0 Discussion

7.1 Pumping Influence Compared to Climate Change

The simulations conducted for this project indicate that climate change will affect the Amargosa Desert and Death Valley groundwater system, and the most probable affect will be declines in groundwater head and spring discharge. However, the effects on groundwater head and discharge caused by local and regional groundwater pumping are simulated to be far greater than climate-driven changes. Even if climate change results in increased precipitation and recharge, the simulations suggest groundwater decline will continue as a result of pumping in the study area and throughout the DVRFS.

Reasons for the much greater influence of pumping include (1) the large volume of pumping relative to groundwater discharge from ET and springs, (2) the large size (approximately 45,000 km^2 for the DVRFS) of the groundwater reservoir with recharge areas often distant from discharge zones, and (3) the relative proximity of pumping centers to groundwater discharge zones compared to recharge areas.

The volume of pumping relative to the volume of groundwater discharged from springs and as ET is considered the most important factor. For example, the USGS reports (Belcher and Sweetkind 2010) that by 1998 pumping in the entire DVRFS was close to 75 percent of the natural discharge from the regional flow system before groundwater development.

The estimated groundwater withdrawal in the portion of the Amargosa Desert roughly corresponding to the study area was approximately 9,800 ac-ft/yr (32,000 m^3/day) between 1966 and 2000, based on USGS data (Fenelon and Moreo 2002). Between 1991 and 2000, groundwater withdrawal in the Amargosa Desert was approximately 12,400 ac-ft/yr (42,000 m^3/day) (Fenelon and Moreo 2002). Walker and Eakin (1963) estimated 24,000 ac-ft/yr as the total discharge from the Amargosa Desert Basin 230 with 7,000 ac-ft/yr available for groundwater pumping.

Therefore, pumping from the portion of the Amargosa Desert in the near vicinity of the study area between 1966 and 2000 exceeded the estimated perennial yield available for pumping by approximately 43 percent. For the entire Amargosa Desert Basin 230, the percentage is undoubtedly higher.

Simulations conducted for this project confirm the high proportion of groundwater pumping relative to spring discharge and ET. In the study area, the average discharge from all drain cells evaluated was 71,525 m^3/day between 2000 and 2010, based on the simulations. In contrast, the reduced pumping scenario resulted in an average reduction of pumping in the study area of 52,670 m^3/day in 2001, 2002, and 2003. Reduced return flow in 2008, 2009, and 2010 averaged 10,630 m^3/day. In effect, between 2011 and 2510 a net average of 42,040 m^3/day less groundwater was pumped from the study area. This is approximately 60 percent of the average drain cell discharge in the study area between 2000 and 2010.

7.2 Amargosa Desert

For the years between 2000 and 2500, simulated groundwater decline in the Amargosa Desert under 20th Century recharge and current pumping scenarios ranges from approximately 2 to 41 meters in specific model cells. The model cells with the greatest declines are in the Amargosa Farms pumping area. Cells with the least declines are in the southern and southwestern portion of the Amargosa Desert, distant from pumping.

As described in Section 6.1.3, pumping has a substantial impact on groundwater head. Therefore, the effects of various recharge scenarios were evaluated relative to the baseline condition of 100 percent of 20th Century recharge and current pumping. This essentially normalized the head change data with respect to pumping. Climate change-related effects on groundwater head in the Amargosa Desert relative to the baseline condition are shown in Table 13. For simulations in which recharge was increased, groundwater head increased by 0.02 to 0.26

meters relative to baseline. For simulations in which recharge was reduced, groundwater head declined by 0.01 to 1.54 meters relative to baseline.

Table 13. Range of Amargosa Desert Head Changes from 2000 to 2500 Relative to Baseline (values in meters)

Percent of 20th Century Recharge						
109 %	106 %	103 %	Climate Model	97 %	94 %	91 %
+0.05 to +0.26 m	+0.04 to +0.18 m	+0.02 to +0.09 m	-0.01 to -0.07 m	-0.03 to -0.16 m	-0.05 to -0.25 m	-0.07 to -0.33 m
88 %	85 %	80 %	75 %	70 %	60 %	50 %
-0.09 to -0.42 m	-0.10 to -0.51 m	-0.13 to -0.66 m	-0.17 to -0.81 m	-0.20 to -0.95 m	-0.26 to -1.25 m	-0.32 to -1.54 m

Although not strictly a part of the analysis for this project, it is interesting to note that many of the hydrographs of simulated head change in the Amargosa Desert, and particularly Ash Meadows (for example, Figures 26 and 30, and Appendix B), show evidence of a brief sharp decline and subsequent rise in groundwater levels between 1960 and about 1980. This dip is from initiation and then cessation of irrigation pumping within Ash Meadows in the 1960s and 1970s, before the area became a National Wildlife Refuge. It was this pumping and subsequent challenges by the U.S. Department of Interior that led to the Supreme Court decision, Cappaert v. United States, providing Devils Hole in 1976 with a federal reserved water right to prevent extinction of the endangered Devils Hole Pupfish.

The federal reserved water right established for Devils Hole is Elevation 718.505 meters (2,357.3 feet), determined as the minimum water level needed to fulfill the purposes for the reservation of Devils Hole. During 2010, the water level elevation in Devils Hole ranged between approximately 0.15 meters and 0.33 meters above the court-mandated minimum elevation (Death Valley National Park, personal communication). Simulations conducted for this project suggest

the water level in the Devils Hole model cell could decline by approximately 1 meter by 2050 and 2 meters by 2100, as a result of climate change and groundwater pumping.

The declines in simulated drain cell discharge in the Amargosa Desert between 2000 and 2500 under 20th Century recharge and current pumping scenarios range from approximately -490 to -16,540 m^3/day in specific drain cells or groups of drain cells.

Climate change-related effects on groundwater discharge in Amargosa Desert drain cells relative to the baseline condition are shown in Table 14. For scenarios in which recharge increased, groundwater discharge increased by 2 to 369 m^3/day relative to baseline. For scenarios in which recharge was reduced, groundwater discharge declined by 1 to 2,130 m^3/day relative to baseline.

Table 14. Range of Amargosa Desert Discharge Changes from 2000 to 2500 Relative to Baseline (m^3/day)

Percent of 20th Century Recharge						
109 %	106 %	103 %	Climate Model	97 %	94 %	91 %
+5 to +369 m^3/d	+3 to +244 m^3/d	+2 to +124 m^3/d	-1 to -100 m^3/d	-3 to -223 m^3/d	-4 to -343 m^3/d	-6 to -470 m^3/d
88 %	85 %	80 %	75 %	70 %	60 %	50 %
-7 to -586 m^3/d	-9 to -714 m^3/d	-11 to -917 m^3/d	-12 to -1,121 m^3/d	-14 to -1,318 m^3/d	-16 to -1,729 m^3/d	-19 to -2,130 m^3/d

The simulations indicate the most affected drain cell discharge environments in the Amargosa Desert are those areas where groundwater is several meters below land surface, there is no spring discharge, and phreatophytic vegetation and evaporation dominate groundwater discharge processes. These areas include Amargosa Flat, Amargosa River, and Stewart Valley (Figure 79). The decline in discharge from these areas, particularly the Amargosa River, in comparison with other discharge areas is evident on Figures 113 and 114.

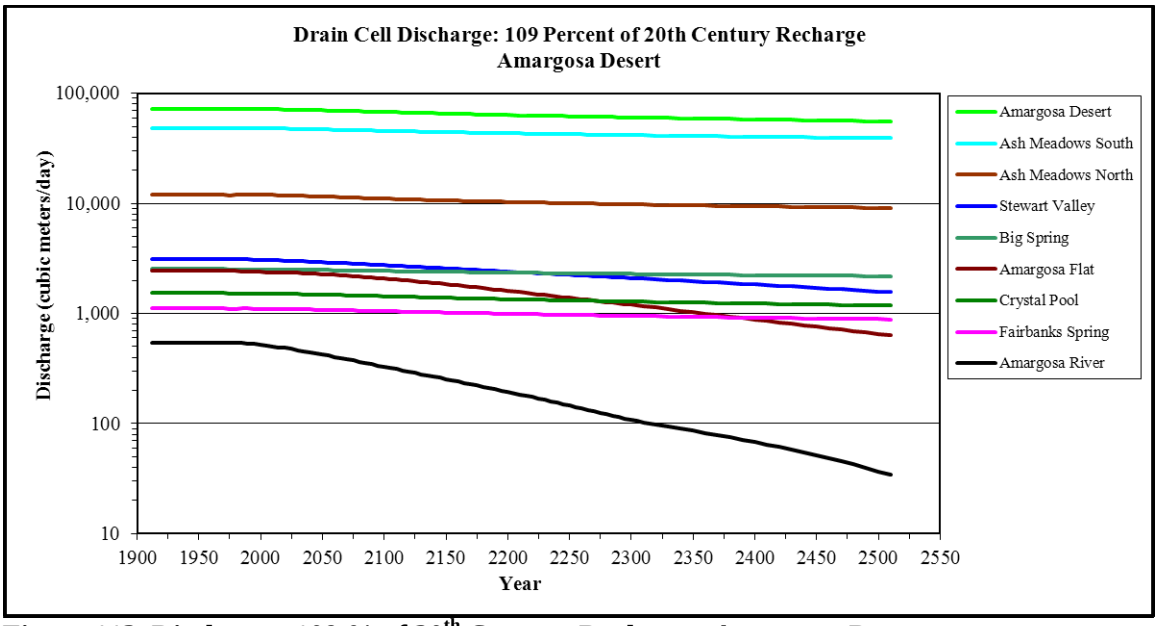

Figure 113. Discharge: 109 % of 20th Century Recharge, Amargosa Desert

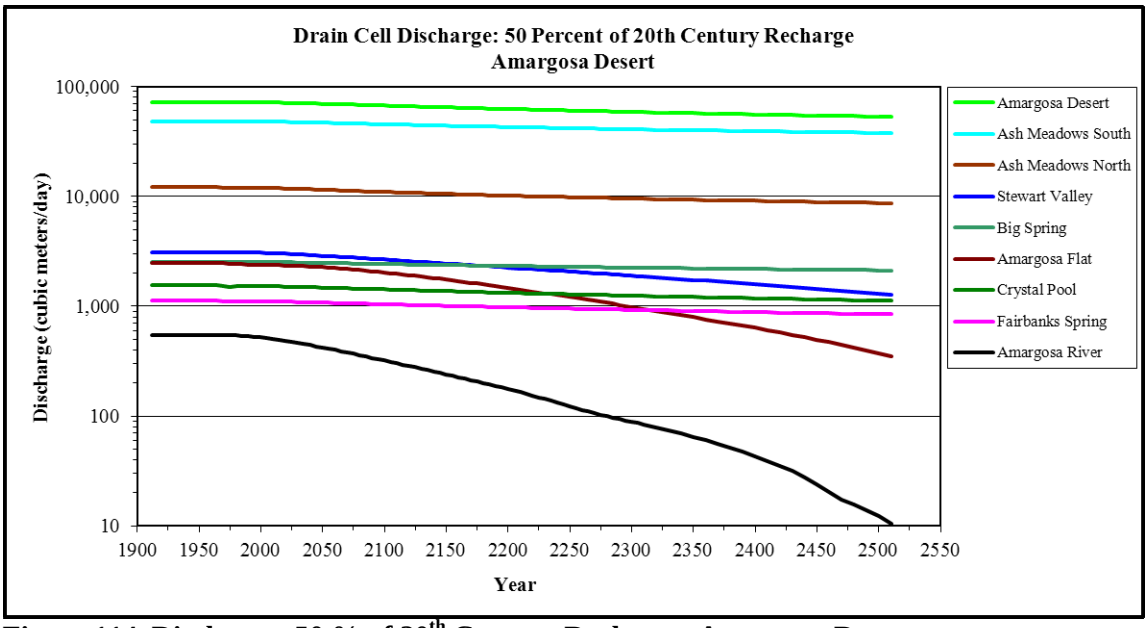

Figure 114. Discharge: 50 % of 20th Century Recharge, Amargosa Desert

In contrast, spring discharge areas in Ash Meadows (Ash Meadows North and South, Big Spring, Crystal Pool, and Fairbanks Spring) have an overall lower and steadier rate of decline (Figures 113 and 114). Ash Meadows is one of the major groundwater discharge zones from the Lower Carbonate Aquifer within the DVRFS because structural processes juxtapose lower

permeability basin fill rocks and sediments against higher permeability rocks of the carbonate aquifer. Therefore, it is reasonable to expect that discharge and groundwater head in Ash Meadows would be less directly affected by stresses than other portions of the Amargosa Desert. The simulations support this concept, and even though discharge declines in Ash Meadows, the rate of decline is less than in drain cells not associated with the discharge area.

The reduced pumping scenario indicates that groundwater head in two cells analyzed in the southeastern portion of the Amargosa Desert responds differently to minimization of pumping than groundwater head at other locations in the Amargosa Desert. Head in these cells, observed in column 89, row 132 (Well USGS GS-01) and column 92, row 138 (BLM Stewart Valley Well), continued to decline even in the reduced pumping scenario. In the Stewart Valley Well, the reduction in pumping had almost no effect on groundwater head. Hydrographs for these wells are shown in Figures 115 and 116. In contrast, head in the next nearest well analyzed (column 86, row 130, Big Spring Well) did not decline appreciably in the reduced pumping scenario (Figure 117). The critical difference appears to be proximity to Pahrump Valley, in which groundwater pumping was not reduced for any simulations. As shown in Figure 52, the Stewart Valley Well is closest to Pahrump Valley, the USGS GS-01 Well is next nearest to Pahrump Valley, and the Big Spring Well is the furthest of the three. The interpretation of these hydrographs is that groundwater in the southeast portion of the Amargosa Desert responds to pumping from the nearby Pahrump Valley rather than (or much more than) responding to pumping in the Amargosa Farms area. This is further evidence that pumping has a greater effect on head and discharge in the groundwater flow system than effects expected to result from climate change.

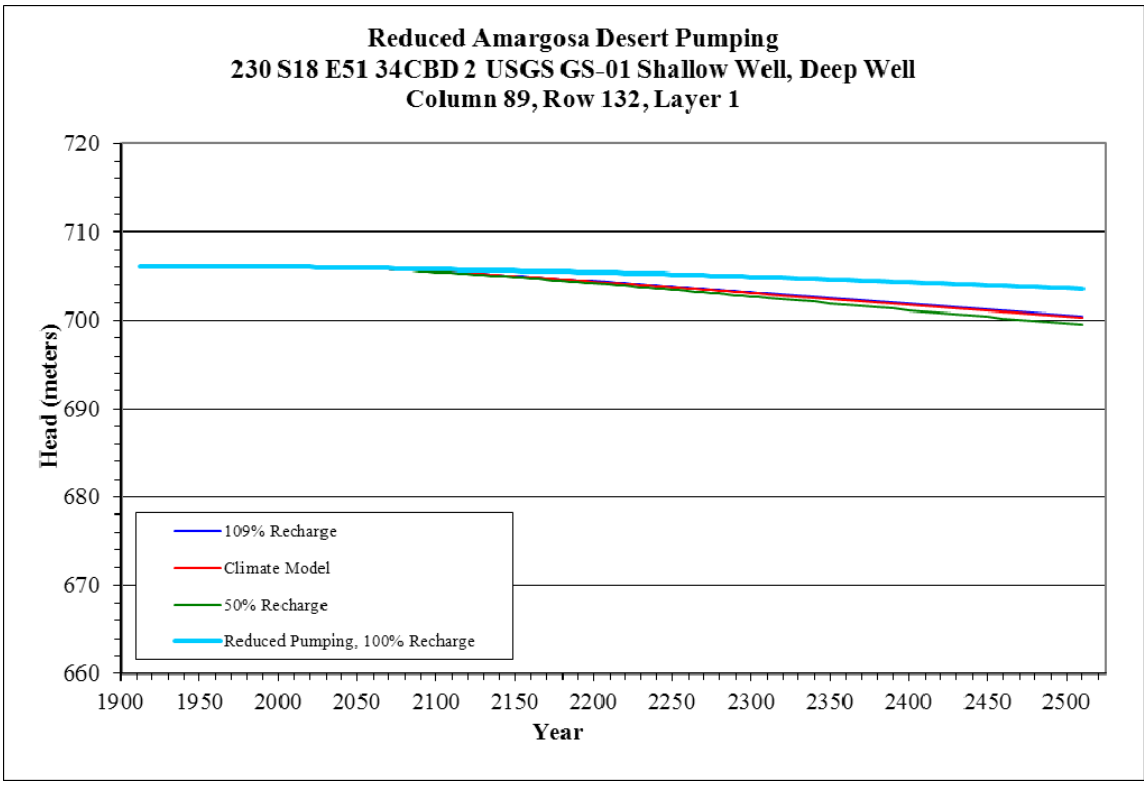

Figure 115. Head Change with Pumping Minimized: Column 89, Row 132, Layer 1

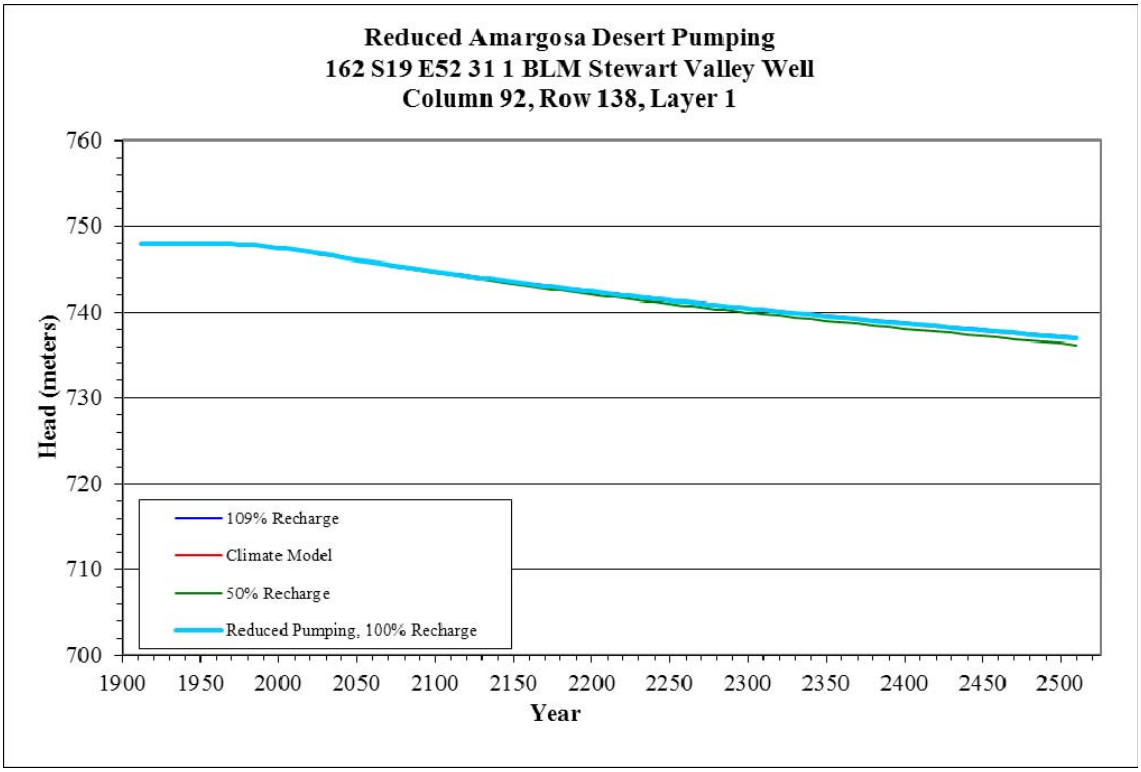

Figure 116. Head Change with Pumping Minimized: Column 92, Row 138, Layer 1

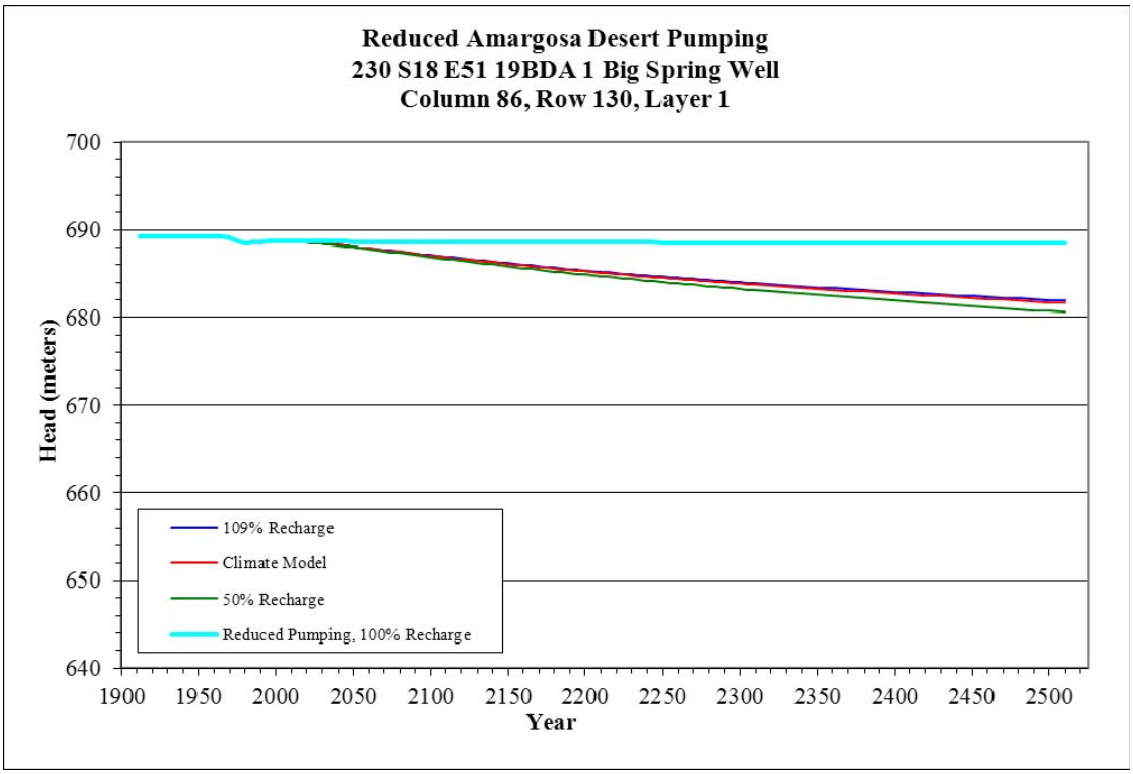

Figure 117. Head Change with Pumping Minimized: Column 86, Row 130, Layer 1

7.3 Death Valley

Simulations completed for this project indicate spring discharge areas and groundwater elevations in Death Valley should be much less effected by overall groundwater head and discharge changes than the Amargosa Desert when pumping influences are considered. However, the data also suggest that when pumping effects are factored out Death Valley is slightly more susceptible to the effects of climate change than the Amargosa Desert, within the next 500 years. The results also suggest that locations in the eastern portion of Death Valley nearer to the Amargosa Desert, such as the cell in which Travertine Point well is located, are affected by pumping stresses in the Amargosa and will continue to be affected by those stresses.

For the years between 2000 and 2500, simulated groundwater head decline in Death Valley under 20th Century recharge and current pumping scenarios ranges from zero to

approximately 9 meters in specific model cells. The model cells with the greatest declines are at Travertine Point Well, Navel Spring, and Texas Spring Syncline (Figure 19). These locations are upgradient from the Furnace Creek spring discharge areas. Cells with the least declines are at Badwater, Travertine Springs, Texas Spring, and Nevares Spring (Figure 19).

Climate change-related effects on groundwater head in Death Valley relative to the baseline condition are shown in Table 15. For scenarios in which recharge increased, groundwater head increased by zero to 0.34 meters relative to baseline. For scenarios in which recharge was reduced, groundwater head declined by zero to 2 meters relative to baseline.

Table 15. Range of Death Valley Head Changes from 2000 to 2500 Relative to Baseline (meters)

Percent of 20th Century Recharge						
109 %	106 %	103 %	Climate Model	97 %	94 %	91 %
zero to +0.34 m	zero to +0.23 m	zero to +0.12 m	zero to -0.09 m	zero to -0.21 m	zero to -0.32 m	zero to -0.44 m
88 %	85 %	80 %	75 %	70 %	60 %	50 %
zero to -0.55 m	zero to -0.67 m	zero to -0.86 m	zero to -1.05 m	zero to -1.24 m	zero to -1.62 m	zero to -2.00 m

In comparison to the Amargosa Desert (Table 13), the relative head changes in Death Valley are consistently very slightly greater than those in the Amargosa Desert for each recharge scenario. For example, in the 109 % of recharge scenario, the range of head changes in Death Valley is zero to 0.34 meters, while in the Amargosa Desert the range is 0.50 to 0.26 meters. In the 50 % of recharge scenario, the range of head changes in Death Valley is zero to -2.00 meters, while in the Amargosa Desert the range is -0.32 to -1.54 meters.

The declines in simulated drain cell discharge in Death Valley between 2000 and 2500 under 20th Century recharge and current pumping scenarios range from approximately -1 to -300 m^3/day in specific drain cells or groups of drain cells.

Climate change-related effects on groundwater discharge in Death Valley drain cells relative to the baseline condition are shown in Table 16. For scenarios in which recharge increased, groundwater discharge increased by 1 to 88 m^3/day relative to baseline. For scenarios in which recharge was reduced, groundwater discharge declined by 1 to 513 m^3/day relative to baseline.

Table 16. Range of Death Valley Discharge Changes from 2000 to 2500 Relative to Baseline (m^3/day)

Percent of 20th Century Recharge						
109 %	106 %	103 %	Climate Model	97 %	94 %	91 %
+1 to +88 m^3/d	+1 to +59 m^3/d	zero to +29 m^3/d	zero to -23 m^3/d	-1 to -53 m^3/d	-1 to -82 m^3/d	-1 to -111 m^3/d
88 %	85 %	80 %	75 %	70 %	60 %	50 %
-2 to -141 m^3/d	-2 to -170 m^3/d	-3 to -219 m^3/d	-3 to -268 m^3/d	-4 to -317 m^3/d	-5 to -415 m^3/d	-7 to -513 m^3/d

Unlike head change, the discharge data presented in Tables 14 and 16 cannot be compared directly to evaluate differences between Death Valley and the Amargosa Desert because the number of cells in respective drain zones varies. However, for drains consisting of single cells (Badwater and Texas Spring in Death Valley and Fairbanks Spring, Crystal Pool, and Big Spring in the Amargosa Desert), comparison of percentage changes in discharge may be made as shown in Table 17.

Table 17. Percent Change in Discharge from 2000 to 2500 Relative to Baseline for Single Cell Drains (m^3/day)

Percent of 20th Century Recharge						
	109 %	Climate Model	91 %	85 %	70 %	50 %
Death Valley Drain Cells						
Badwater Spring	+0.28 %	-0.07 %	-0.35 %	-0.53 %	-1.00 %	-1.62 %
Texas Spring	+0.08 %	-0.02 %	-0.10 %	-0.14 %	-0.27 %	-0.45 %
Amargosa Desert Drain Cells						
Fairbanks Spring	+0.56 %	-0.33 %	-0.71 %	-1.07 %	-1.98 %	-3.23 %
Crystal Pool	+0.62 %	-0.17 %	-0.79 %	-1.19 %	-2.22 %	-3.63 %
Big Spring	+0.37 %	-0.11 %	-0.48 %	-0.73 %	-1.34 %	-2.19 %

The data in Table 17 indicate that, as opposed to groundwater head, Death Valley is slightly less susceptible than the Amargosa Desert to changes in discharge. The percent change in discharge for individual drain cells in Death Valley is consistently slightly less than those in the Amargosa Desert for each recharge scenario.

It is not immediately apparent why the simulations suggests that Death Valley may experience slightly greater decline in head and slightly less decline in discharge than the Amargosa Desert. It is reasonable to hypothesize that groundwater resources in Death Valley should be somewhat more susceptible to climate change than in the Amargosa Desert because (1) Death Valley is a greater distance from recharge zones for the regional aquifer, and (2) the aquifer thicknesses in Death Valley are substantially less (hundreds to thousands of meters) than in the Amargosa Desert, therefore, less groundwater storage is available, and (3) Death Valley is the terminus of the regional groundwater flow system and stresses are magnified at the margin of the regional system. However, Death Valley may be simulated as having less change in discharge than the Amargosa Desert because of groundwater response time within the aquifer system.

Hydrographs of head change, particularly hydrographs from Death Valley, indicate the system is not near equilibrium after the 500 year simulation period. It is likely that if simulations were carried out for a longer period of time, until the system reached something approaching at least quasi-equilibrium that Death Valley would be shown to be more susceptible than the Amargosa Desert.

Badwater Spring appears more susceptible to changes in discharge than Texas Spring because Badwater Spring is associated with a moderate to low elevation (approximately 1,500 meters to -84 meters) local groundwater flow system in the adjacent Black Mountains and does not discharge from a regional flow system. Climate change can be expected to have an overall greater impact on local systems without the benefit of high elevation recharge areas.

7.3.1 Death Valley Springs

One aspect of this project is to incorporate anticipated changes in the groundwater flow regime into a current examination by Drs. Don Sada and Mark Stone of how changes in the aquatic environment of springs effect benthic macroinvertebrate abundance and community structure. Travertine Springs is the primary Death Valley research location for Drs. Sada and Stone, however, the results of their research and this project are expected to be applicable to other spring ecosystems in the desert Southwest. Attributes of particular importance to aquatic invertebrates include volume, depth, and velocity of springbrook flow, and water chemistry.

In 2009, the National Park Service changed the Furnace Creek water system so that direct diversion from Travertine Springs will be phased out gradually. Instead, potable water is pumped from new production wells upgradient from the springs. Previously diverted spring flow will be returned to the riparian system, even as water is pumped from the upgradient production wells. Changes to the aquatic ecosystem caused by restoration of some surface flow and Death Valley pumping may provide a proxy to evaluate how aquifer dynamics, spring discharge, and aquatic ecosystems could be affected by climate change. In addition, Death Valley National Park is

interested in gauging the timing and magnitude of potential response to climate change, in comparison with changes caused by pumping within the park and upgradient from the park.

The simulated changes in groundwater head and drain discharge data compared to baseline for the years 2000 to 2500 are presented in Table 18. Groundwater head changes were simulated for multiple cells and layers at each spring except Badwater. Therefore, the head data shown in Table 18 reflect the maximum simulated head change for each group of cells associated with a spring. Discharge data are aggregated from all cells associated with a spring.

Table 18. Head Changes and Percent Change in Discharge from 2000 to 2500 Relative to Baseline for Death Valley Springs

Percent of 20th Century Recharge						
	109 %	Climate Model	94 %	88 %	75 %	50 %
Groundwater Head Change (meters)						
Travertine Springs	+0.036	-0.009	-0.032	-0.056	-0.108	-0.206
Texas Spring	+0.034	-0.009	-0.032	-0.054	-0.104	-0.199
Nevares Spring	+0.002	zero	-0.001	-0.002	-0.005	-0.009
Badwater Spring	zero	zero	-0.001	-0.001	-0.002	-0.003
Percent Change in Discharge (m^3/day)						
Badwater Springs	+0.28 %	-0.07 %	-0.26 %	-0.44 %	-0.84 %	-1.62 %
Texas Spring	+0.08 %	-0.02 %	-0.07 %	-0.12 %	-0.23 %	-0.45 %
Nevares Spring	+0.06 %	-0.01 %	-0.05 %	-0.08 %	-0.16 %	-0.32 %
Travertine Spring	+0.19 %	-0.05 %	-0.17 %	-0.30 %	-0.58 %	-1.10 %

It is the opinion of the author that the differences in head and discharge should be considered negligible, and may result more from structure and processes built into the model, and the scale of the model cells, rather than any real difference among the springs. It is conceptually

valid that simulated head change at Badwater Spring is essentially zero while discharge is more responsive to climate change. As stated previously, Badwater Spring discharges from a local basin in the adjacent Black Mountains. However, Badwater Spring is within 1 meter of the lowest elevation of the Death Valley playa, therefore head will not change substantially as long as water is available. Discharge, however, will change depending on the volume of water recharged to the local groundwater flow system.

Death Valley National Park has been monitoring spring discharge and groundwater levels at several locations in the Furnace Creek area for approximately 20 years. Beginning in the mid-2000s, several monitoring wells were constructed in the Furnace Creek area in anticipation of future monitoring needs, particularly production wells in the Texas Spring Syncline upgradient from Texas and Travertine springs. Furnace Creek area spring and well locations are shown in Figure 118. Hydrographs for two wells and Travertine, Texas, and Nevares springs are shown in Figures 119 through 123. The wells (Texas Spring Syncline Well No. 1 and Water Rights Protection Well MW-2) are located between the production wells and Travertine and Texas springs.

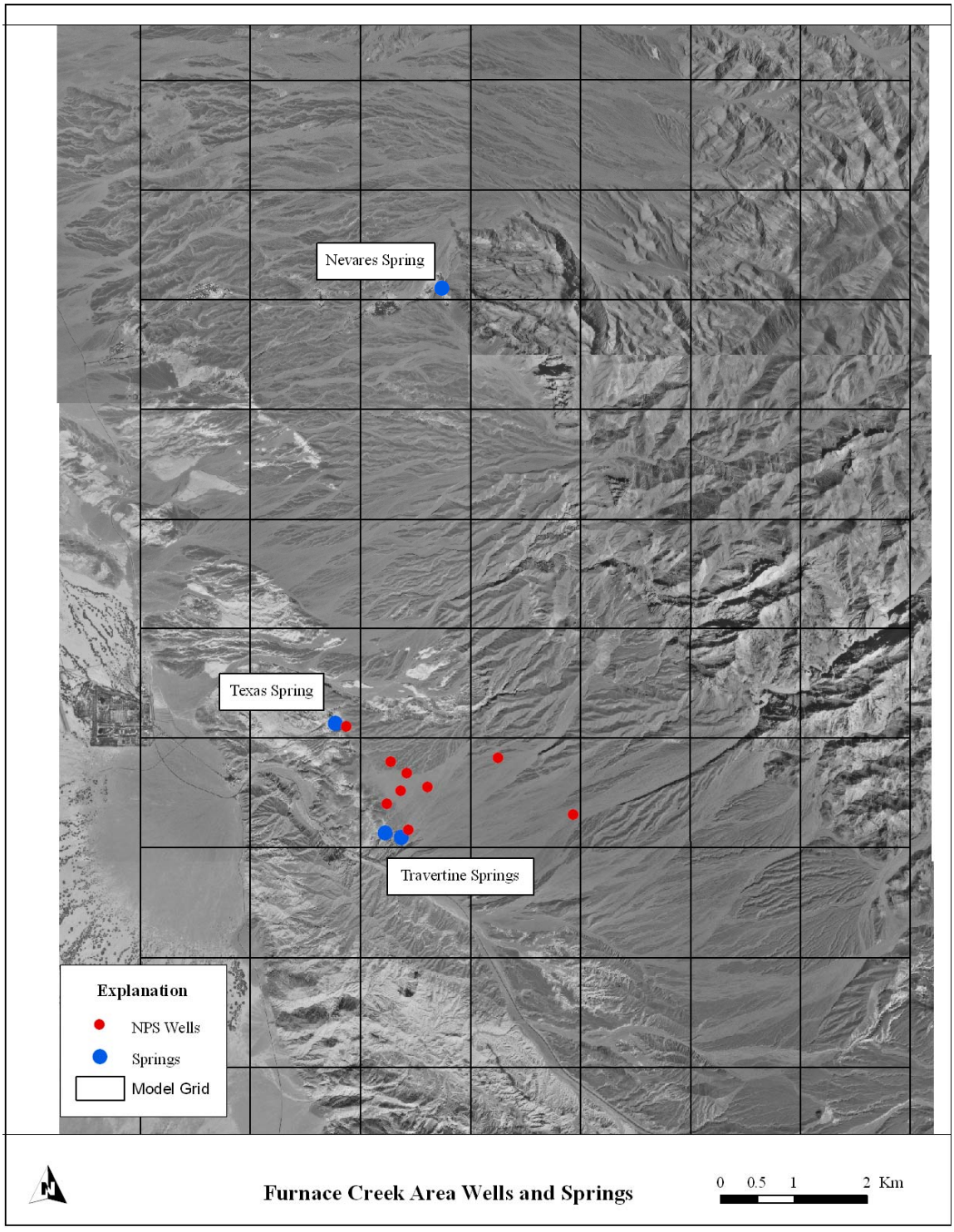

Figure 118. Furnace Creek Springs and Wells

Texas Spring Syncline Well No. 1

Texas Spring Syncline Well No. 1 water levels between 1991 and 2011 are shown in Figure 119. This well was drilled in 1958 to evaluate the water supply potential of the syncline. It is located approximately 60 m from the nearest production well. The water level responds to earthquakes and has been equilibrating slowly since the Landers – Little Skull Mountain earthquake in June 1992, with a slight downward trend. The water level declined abruptly when the NPS production wells went online. Groundwater head has varied since pumping began, but appears to be recovering from initial pumping stresses as the system was tested and brought online, storage tanks filled, and demand evaluated, and is within approximately 1 meter of the pre-pumping elevation.

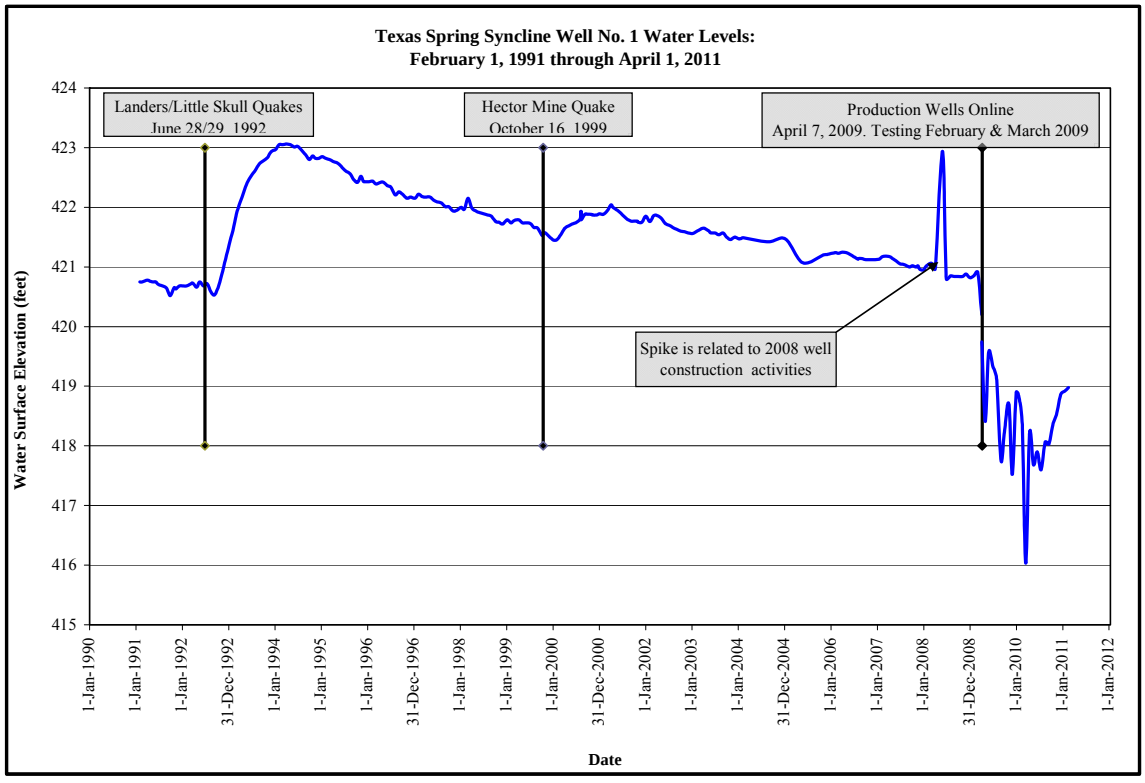

Figure 119. Texas Spring Syncline Well TSS-1 Hydrograph (data courtesy Death Valley National Park)

Water Rights Protection MW – 2

Water Rights Protection MW-2 water levels between 2008 and 2011 are shown in Figure 120. This monitoring well was drilled in 2008 to evaluate the effects of the NPS production wells. It is located approximately 500 meters from the nearest production well, and between the production wells and Travertine Springs. The April and May 2008 data were likely affected by water level equilibration after drilling and development. The water level shows a decline before the production wells went online because of production well testing in February and March 2009. Groundwater head in the well has declined less than 1 meter since the NPS production wells went online, and shows possible recovery in recent months.

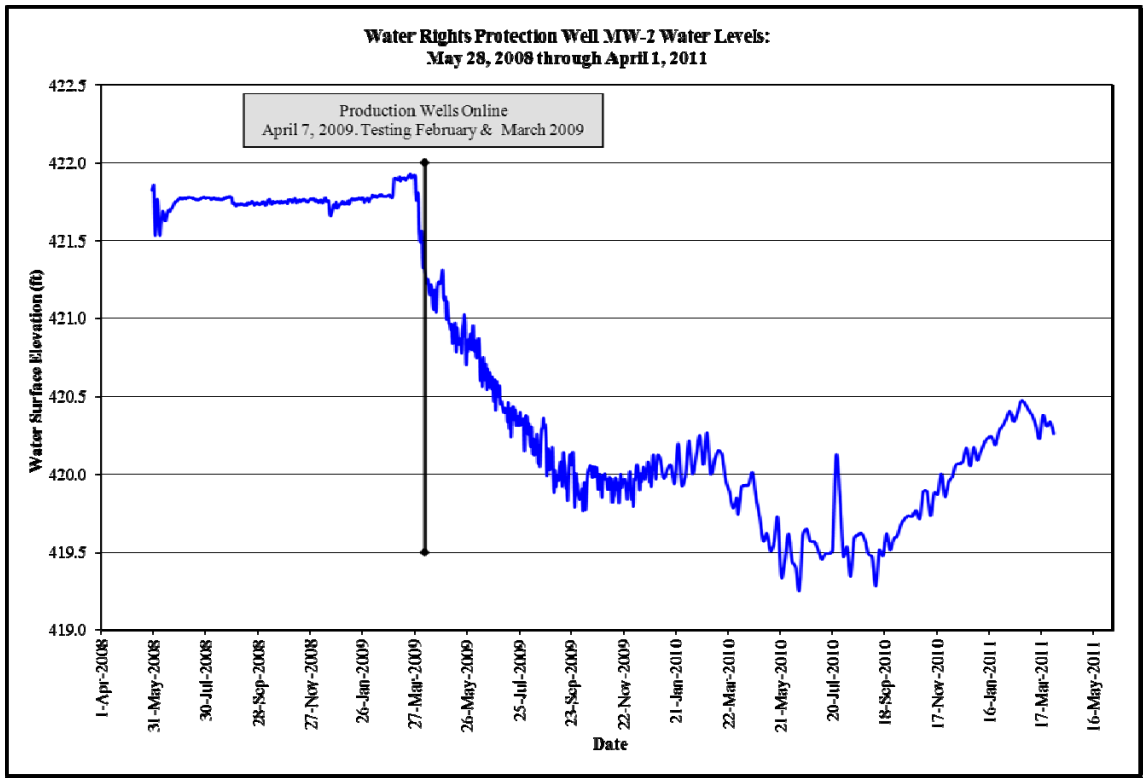

Figure 120. Water Rights Protection Well MW-2 Hydrograph (data courtesy Death Valley National Park)

Travertine, Texas, and Nevares Springs

Discharge from Travertine and Texas springs appears to have declined slightly as a result of pumping from Death Valley's production wells, as shown in Figures 121 and 122. Data for 2011 indicate discharge from Travertine Spring has increased relative to 2010. Discharge from Texas Spring appear similar in 2010 and 2011. Nevares Spring (Figure 123) is not affected by the production wells. Missing data are equipment malfunction or maintenance actions that invalidated discharge measurements.

Travertine Spring discharge has been equilibrating since the Landers – Little Skull Mountain earthquake in June 1992, with a slight downward overall trend. Discharge has declined since the NPS began pumping, although recent data show in increase in discharge.

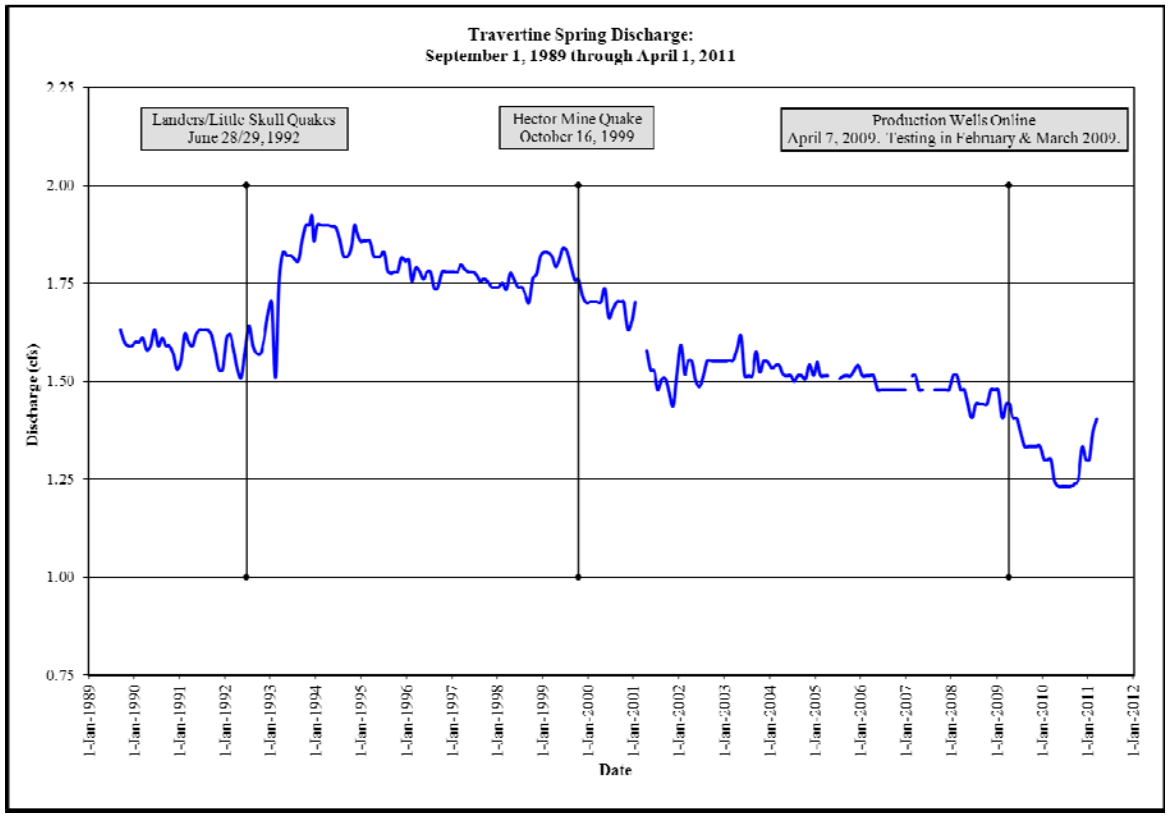

Figure 121. Travertine Springs Hydrograph (data courtesy Death Valley National Park)

Texas Spring discharge indicates a very slight upward trend for the period of record. Discharge has declined a small amount since the NPS began pumping.

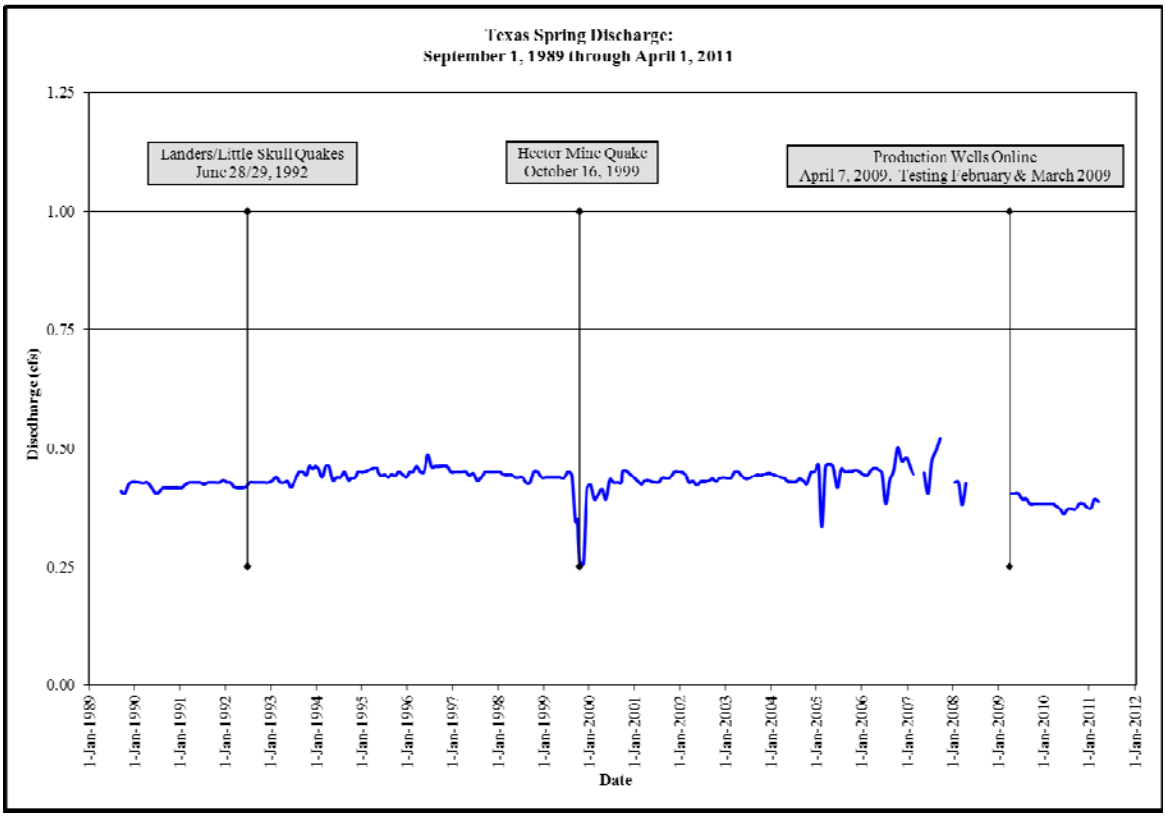

Figure 122. Texas Spring Hydrograph (data courtesy Death Valley National Park)

Nevares Spring discharge has been equilibrating since the Landers – Little Skull Mountain earthquake in June 1992, with a downward overall trend until 2007, followed by an upward trend. Discharge is not effected by the NPS production wells.

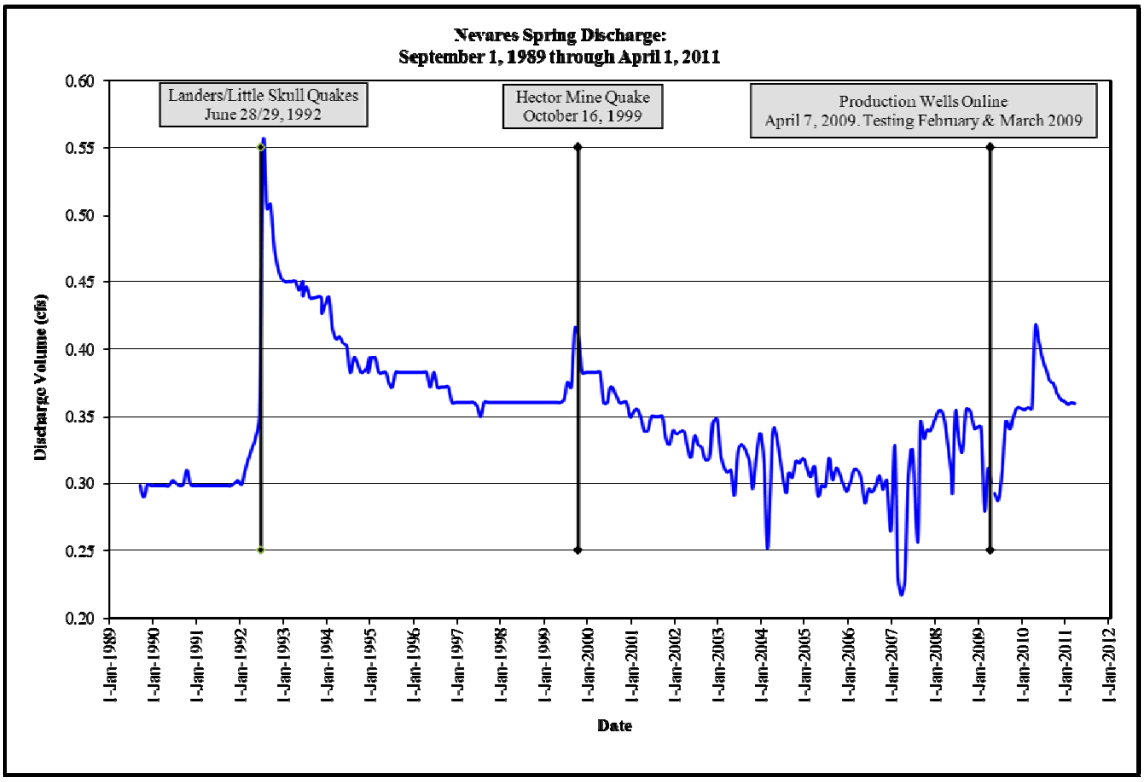

Figure 123. Nevares Spring Hydrograph (data courtesy Death Valley National Park)

7.3.1.1 Timing of Changes at Death Valley Springs

Simulations conducted for this project suggest that groundwater head and discharge will decline in the future in model cells that include Travertine, Texas, and Nevares springs. However, as described above, the climate change-related decline in head loss and discharge are expected to be minor. Simulated changes in head and discharge for Travertine, Texas, and Nevares springs during only the 21st Century are shown in Figures 124 through 129. These data are not relative to baseline, therefore, the effects of pumping in the Amargosa Desert are incorporated in the graphs.

At Travertine and Texas springs, groundwater head change is simulated to be approximately 0.01 meters during the 21st Century. No change in head is simulated at Nevares Spring. Travertine Springs is simulated to have the greatest decline in discharge during the 21st Century: between 5 and 10 m^3/day. The decline in discharge at Texas and Nevares springs is simulated to be approximately 2 m^3/day.

Figures 124 through 129 suggest simulated head change at Travertine and Texas spring could begin in the 2030s, while simulated declines in discharge could be occurring at present.

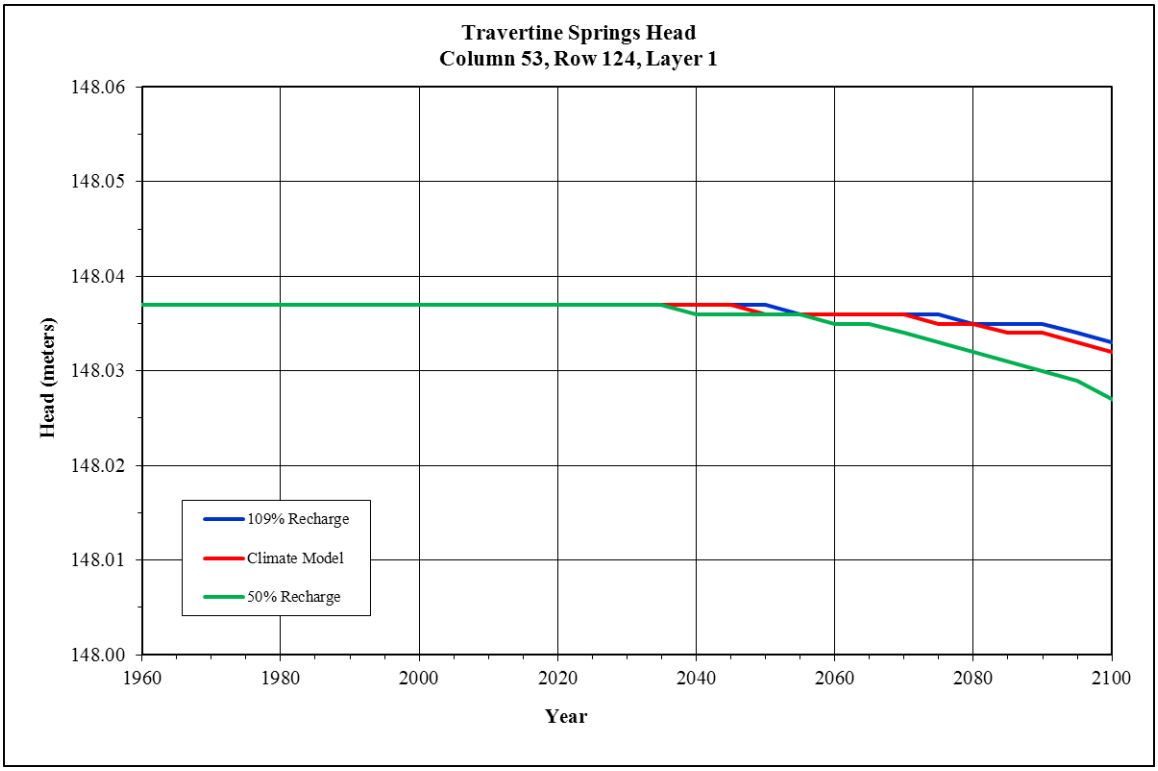

Figure 124. Travertine Springs Cell Column 53, Row 124, Layer 1 Head: 1960 to 2100

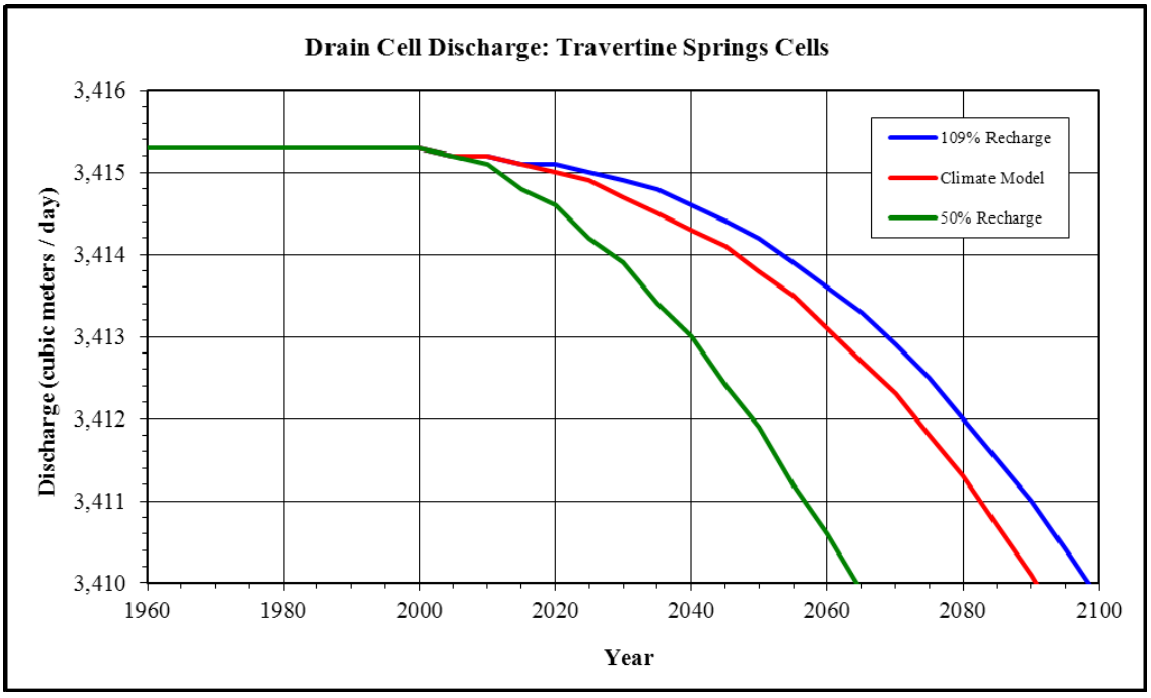

Figure 125. Travertine Springs Cells Drain Discharge: 1960 to 2100

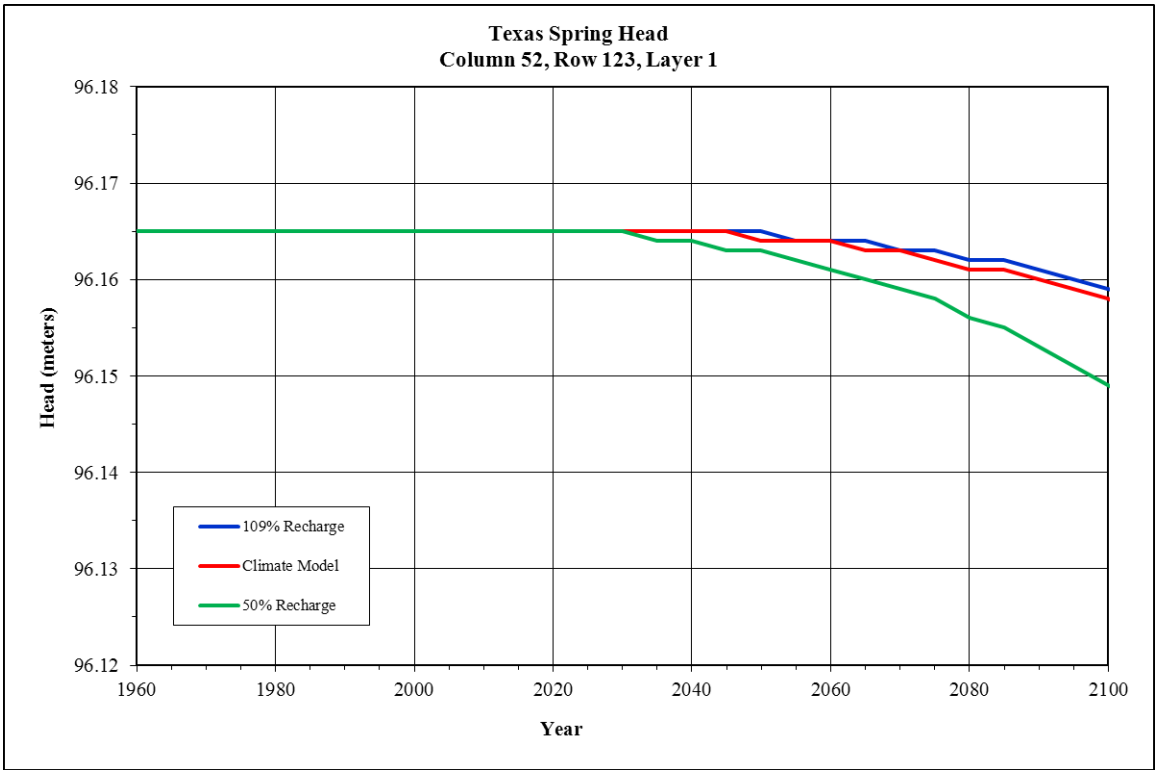

Figure 126. Texas Spring Cell Column 52, Row 123, Layer 1 Head: 1960 to 2100

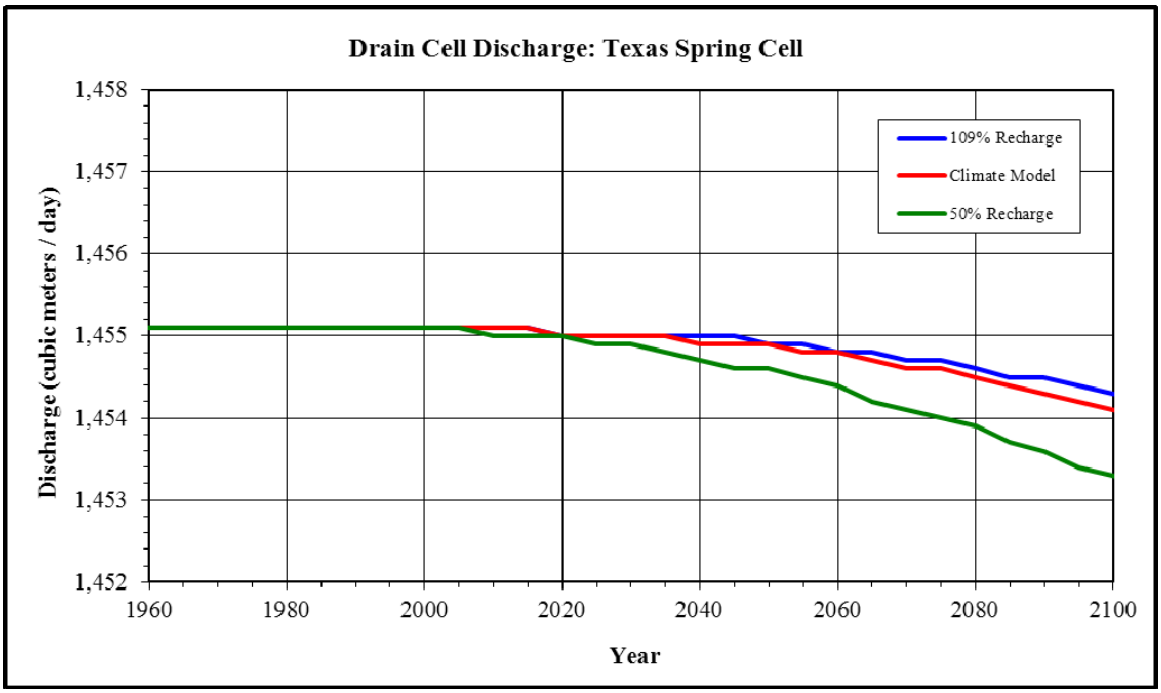

Figure 127. Texas Spring Cell Drain Discharge: 1960 to 2100

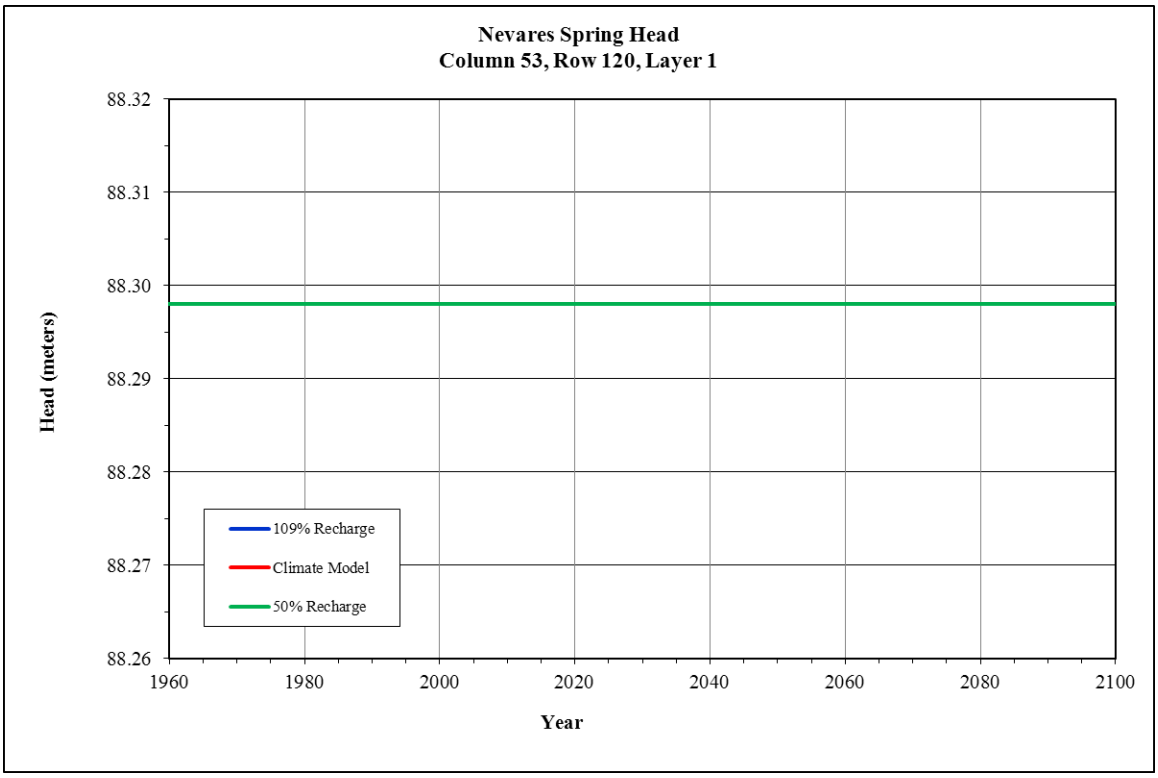

Figure 128. Nevares Spring Cell Column 53, Row 120, Layer 1 Head: 1960 to 2100

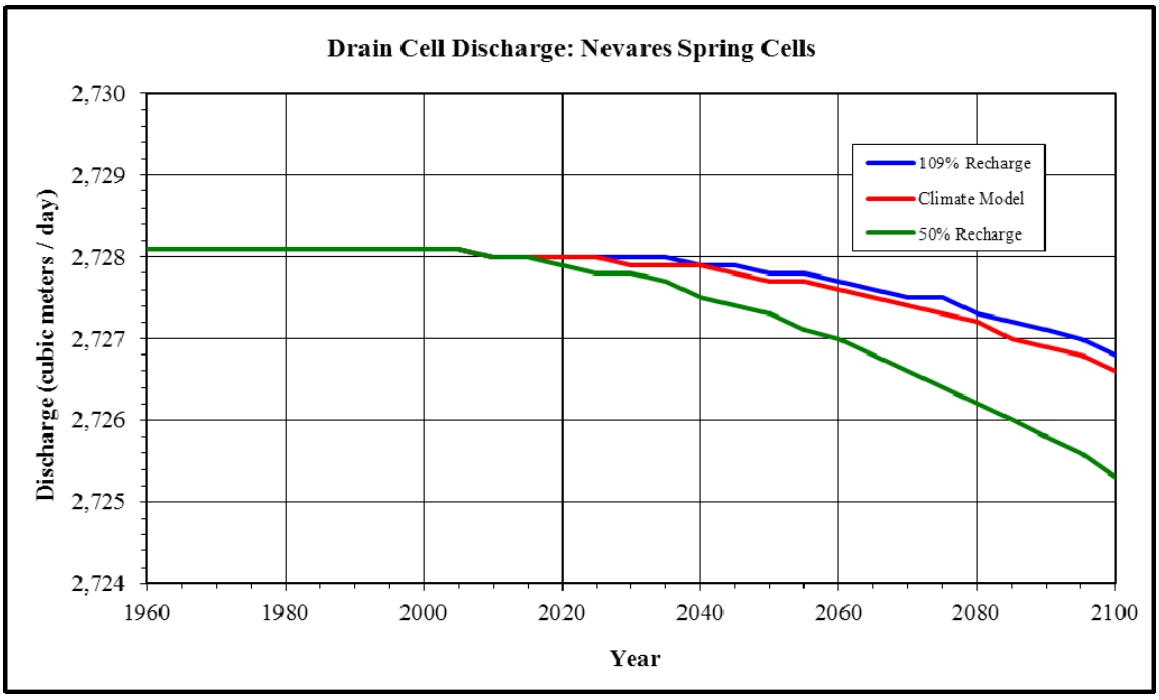

Figure 129. Nevares Spring Cells Drain Discharge: 1960 to 2100

8.0 Conclusions

- The overriding conclusion of this project is that climate change will affect the Amargosa Desert and Death Valley groundwater system. However, the effects on groundwater head and discharge from local and regional groundwater pumping are far greater than simulated climate-driven changes. This is not to suggest the potential effects of climate change are unimportant. It means that in a region where competition for water has been fierce for decades and current pumping has been shown to affect head and discharge, climate change will likely exacerbate conditions of limited water supply. Even if climate change results in increasing precipitation and recharge, groundwater decline will continue as a result of pumping in the study area and throughout the DVRFS.
- In the Amargosa Desert, simulated groundwater head changes relative to baseline 20th Century conditions ranged from an increase of 0.26 meters to a decline of 1.54 meters, depending on the climate scenario. Simulated groundwater discharge changes relative to baseline conditions ranged from an increase of 369 m^3/day to a decline of 2,130 m^3/day.
- The water level in Devils Hole is likely to decline below the elevation of the federal reserved water right within the next several decades.
- The most affected drain cell discharge environments in the Amargosa Desert are those areas where transpiration by phreatophytic vegetation and evaporation dominate groundwater discharge processes instead of direct spring discharge.
- Groundwater in the southeast portion of the Amargosa Desert responds to pumping from nearby Pahrump Valley rather than responding to pumping in the Amargosa Farms area.
- In Death Valley, simulated groundwater head changes relative to baseline 20th Century conditions ranged from an increase of 0.34 meters to a decline of 2.00 meters, depending on

the climate scenario. Simulated groundwater discharge changes relative to baseline 20th Century conditions ranged from an increase of 88 m^3/day to a decline of 513 m^3/day.

- Within the 500 year simulation period, groundwater head in Death Valley is slightly more susceptible to the effects of climate change than the Amargosa Desert when pumping effects are factored out. Reasons for the difference are related to the distance between Death Valley and recharge zones, aquifer thicknesses, and Death Valley as the terminus of the regional groundwater flow system.
- Within the 500 year simulation period, discharge in Death Valley is slightly less susceptible to the effects of climate change than the Amargosa Desert when pumping effects are factored out. This difference is hypothesized to be related to travel time of groundwater within the regional aquifer. Within Death Valley, Badwater Spring appears more susceptible to changes in discharge than Travertine, Texas, and Nevares springs.
- Head declines related to Amargosa Desert pumping are very likely occurring or will occur at locations in Death Valley upgradient (generally east-southeast to east-northeast) from Travertine and Texas springs. Locations include cells in Texas Spring Syncline, at Navel Spring, and at Travertine Point well. These locations should be considered as warning points reflecting migration of pumping stresses from the Amargosa Desert into Death Valley.
- Observed declines in discharge from Travertine and Texas springs since April 2009 appear to result from pumping of Death Valley National Park production wells. It is uncertain at this time if any decline in discharge from Travertine or Texas spring may be attributed to groundwater pumping in the Amargosa Desert. Observed data do not support such an interpretation. However, simulations suggest very minor declines in discharge could occur at present. Simulations suggest minimal head changes at Travertine and Texas spring could begin in the 2030s.

- Simulated differences in head and discharge data between springs in Death Valley are negligible and should not be considered to represent significant differences among Travertine, Texas, and Nevares Springs in response to climate change.
- The simulated changes in discharge at Travertine and Texas springs resulting from climate change, and the observed changes in discharge resulting from National Park Service wells provide an excellent platform for understanding spring dynamics and the possible effects of climate change and other stresses. It is expected this information also can be extrapolated to other areas of the desert southwest.

9.0 Limitations

The results described herein are based on model simulations. Within the limitations of the Regional Model structure, input data, and calibration, and the changes made to the model code for this project, the results are useful for comparing across a range of possible future scenarios. Indeed, one of the primary benefits of modeling is the ability to hold many factors constant while changing variables of interest and evaluating simulated changes. However, the possible future scenarios evaluated for this project may never occur, and there are an infinite number of futures that may occur. The results of this project should not be considered as conditions that will happen within the physical aquifer system of the Amargosa Desert and Death Valley.

The most critical assumption for this project is that percentage changes in future precipitation will be matched by an equal percentage change in recharge to the groundwater system. Because recharge in the Death Valley groundwater flow system, and much of the desert Southwest in general, is such a small percentage of an already low precipitation volume, it is difficult to gauge how recharge will respond to changes in climate and precipitation. It is possible that current research conducted in the desert Southwest will lead to answers regarding this question.

The evaluation of reduced pumping described for this project is not a realistic scenario of possible future pumping rates in the study area. However the simulation demonstrated the significant effects of pumping as compared to climate change.

Not all possible responses to climate change have been evaluated. For example, ET could increase with an increase in temperature. The DVRFS model simulates ET using the drain cell package, therefore, changes in ET cannot be simulated directly as the model currently exists. In addition, this project did not attempt to evaluate possible changes to plant communities that may occur with climate change.

10.0 References

Bates, B.C., Z.W. Kundzewicz, S. Wu, and J.P. Palutikof, Eds., 2008. Climate Change and Water. Technical Paper of the Intergovernmental Panel on Climate Change, IPPC Secretariat, Geneva, 210 p.

Barnett, T.P., D.W. Pierce, H.G. Hidalgo, C. Bonfils, B.D. Santer, T. Das, G. Bala, A.W. Wood, T. Nozawa, A.A. Mirin, D.R. Cayan, and M.D. Dettinger. 2008. Human induced changes in the hydrology of the western United States. Science 309:10801-1083.

Bedinger, M.S. and J.R. Harrill. 2008. Ground-water hydrogeology of Death Valley National Park, Nevada and California. Unpublished report to the U.S. National Park Service, Death Valley National Park.

Belcher, W.R. and D.S. Sweetkind (ed.). 2010. Death Valley regional groundwater flow system, Nevada and California – Hydrogeologic framework and transient ground-water flow model: U.S. Geological Survey Professional Paper 1711, 398 p.

Belcher, Wayne R., ed. 2004. Death Valley regional ground-water flow system, Nevada and California – Hydrogeologic framework and transient ground-water flow model: U.S. Geological Survey Scientific Investigations Report 2004-5205, 408 p

Blainey, J.B., C.C. Faunt, and M.C. Hill. 2006. A guide for using the transient ground-water flow model of the Death Valley Regional Ground-Water Flow System, Nevada and California. U.S. Geological Survey Open-File Report 2006-1104. 26 p.

Blakely, R.J., V.E. Langenheim, D.A. Ponce, and G L. Dixon. 2000. Aeromagnetic survey of the Amargosa Desert, Nevada and California: a tool for understanding near-surface geology and hydrology. U.S. Geological Survey Open-File Report 00-188. 32 p.

Blakely, R.J., J.W. Hillhouse, and R.L. Morin. 2005. Ground-magnetic studies of the Amargosa Desert region, California and Nevada. U.S. Geological Survey Open-File Report 2005-1132. 23 p.

Bredehoeft, J.D., C. Fridrich, J. Jansen, and M. King. 2005. Death Valley lower carbonate aquifer monitoring program – Wells down gradient of the proposed Yucca Mountain nuclear waste repository. Inyo County Yucca Mountain Repository Assessment Office, for U.S. Department of Energy. Cooperative Agreement DE-FC08-02RW12162. Final Project Report.

Carr, W.J. 1988. Geology of the Devils Hole area, Nevada. U.S. Geological Survey Open-File Report 87-560. 32 p.

Christiansen, N.S. and D.P. Lettenmaier. 2007. A multimodal ensemble approach to assessment of climate change impacts on the hydrology and water resources of the Colorado River Basin. Hydrology and Earth System Sciences 11:1417-1434.

Christiansen, N.S., A.W. Wood, N. Voisin, D.P. Lettenmaier, and R.N. Palmer. 2004. The effects of climate change on the hydrology and water resources of the Colorado River Basin. Climate Change 62:337-363.

Dudley, W.W. Jr., and J.D. Larson. 1976. Effect of irrigation pumping on desert pupfish habitats in Ash Meadows, Nye County, Nevada. U.S. Geological Survey Professional Paper 927. 52 p.

Fenelon, J.M., and M.T. Moreo. 2002. Trend analysis of ground-water levels and spring discharge in the Yucca Mountain region, Nevada and California, 1960-2000. U.S. Geological Survey Water-Resources Investigations Report 02-4178. 97 p.

Fridrich, C.J., R.A. Thompson, J.L. Slate, M.E. Berry, and M.N. Machette. 2008. Preliminary Geologic Map of the Southern Funeral Mountains and Adjacent Ground-Water Discharge Sites, Inyo County, California, and Nye County, Nevada. U.S. Geological Survey Open-File Report 2008-1366. 16 p.

Harbaugh, A.W., E.R. Banta, M.C. Hill, and M.G. McDonald. 2000. MODFLOW-2000, the U.S. Geological Survey modular ground-water model user guide to modularization concepts and the ground-water flow process. U.S. Geological Survey Open-File Report 00-92. 121 p.

Hevesi, J.A., A.L. Flint, and L.E. Flint. 2003. Simulation of Net Infiltration and Potential Recharge Using a Distributed-Parameter Watershed Model of the Death Valley Region, Nevada and California. U.S. Geological Survey Open-File Report 03-4090. 171 p.

IPCC. 2000. IPCC Special Report, Emissions Scenarios. Summary for Policy Makers. A Special Report of the IPCC Working Group III. 27 pp.

IPCC. 2007. Climate Change 2007: Synthesis Report. Contribution of Working Groups I, II and III to the Fourth Assessment Report of the Intergovernmental Panel on Climate Change [Core Writing Team, Pachauri, R.K and Reisinger, A. (eds.)]. IPCC, Geneva, Switzerland. 104 pp.

Lenert, Melanie. 2004. Global warming could affect groundwater recharge, in M. Lenert (ed) *Global Warming in the Southwest, Projections, Observations and Impacts.* 2007. Climate Assessment for the Southwest, University of Arizona, Institute for Study of Planet Earth. Tucson, Arizona.

Maurer, E. P., L. Brekke, T. Pruitt, and P. B. Duffy. 2007. Fine-resolution climate projections enhance regional climate change impact studies. Eos Transactions. AGU 88 (47), 504.

Moreo, M.T. and L. Justet. 2008. Update to the ground-water withdrawals database for the Death Valley regional ground-water flow system, Nevada and California, 1913-2003: U.S. Geological Survey Data Series 340, 10 p.

Pavelko, M.T. 2010. Water-level database update for the Death Valley regional groundwater flow system, Nevada and California, 1907-2007: U.S. Geological Survey Data Series 519, 14 p.

Sada, D.W. and D.B. Herbst. 2006. Ecology of aquatic macroinvertebrates in Travertine and Nevares Springs, Death Valley National Park, California, with an examination of water diversion effects on their abundance and community structure. Unpublished report to U.S. National Park Service, Death Valley National Park.

Sada, D.W., E. Fleishman, and D.D. Murphy. 2005. Associations among spring-dependent aquatic assemblages and environmental and land use gradients in a Mojave Desert mountain range. Diversity and Distributions 11:91-99.

Seager, R., M. Ting, I. Held, Y. Kushnir, J. Lu, G. Vecchi, H-P. Huang, N. Harnik, A. Leetmaa, N-C. Lau, C. Li, J. Velez, and N. Naik. 2007. Model Projections of an Imminent Transition to a More Arid Climate in Southwestern North America. Science 316:1181-1184.

Sweetkind, D.S., and J.B. Workman. 2006. Memorandum: Questions about the gravity fault, Personal Communication. 11 p.

Sweetkind, D.S., R.P. Dickerson, R.J. Blakely, and P.D. Denning. 2001. Interpretive geologic cross-sections for the Death Valley Regional flow system and surrounding areas, Nevada and California. U.S. Geological Survey Miscellaneous Field Studies Map MF-2370. 3 sheets and accompanying pamphlet.

Thomas, J.M., A.H. Welch, and M.D. Dettinger. 1996. Geochemistry and isotope hydrology of representative aquifers in the Great Basin region of Nevada, Utah, and adjacent states. U.S. Geological Survey Professional Paper 1409-C.

Walker, G.E. and T.E. Eakin. 1963. Geology and ground water of Amargosa Desert, Nevada-California. State of Nevada Department of Conservation and Natural Resources. Ground-Water Resources – Reconnaissance Series Report 14. 45 p.

Winograd, I. J., and W. Thordarson. 1975. Hydrogeologic and hydrochemical framework, south-central Great Basin, Nevada-California, with special reference to Nevada Test Site. U.S. Geological Survey Professional Paper 712-C. 123 p.

Appendix A Climate Model Graphs

Climate Model bccr_bcm2_0.1 (page 1 of 3)

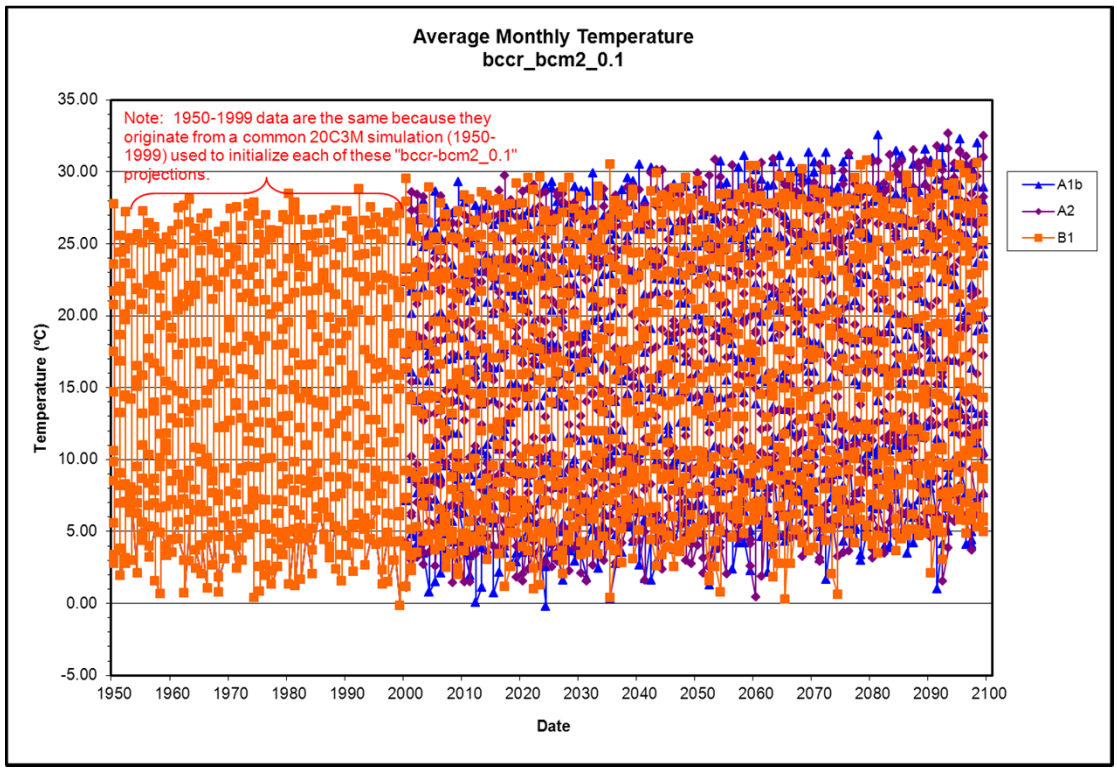

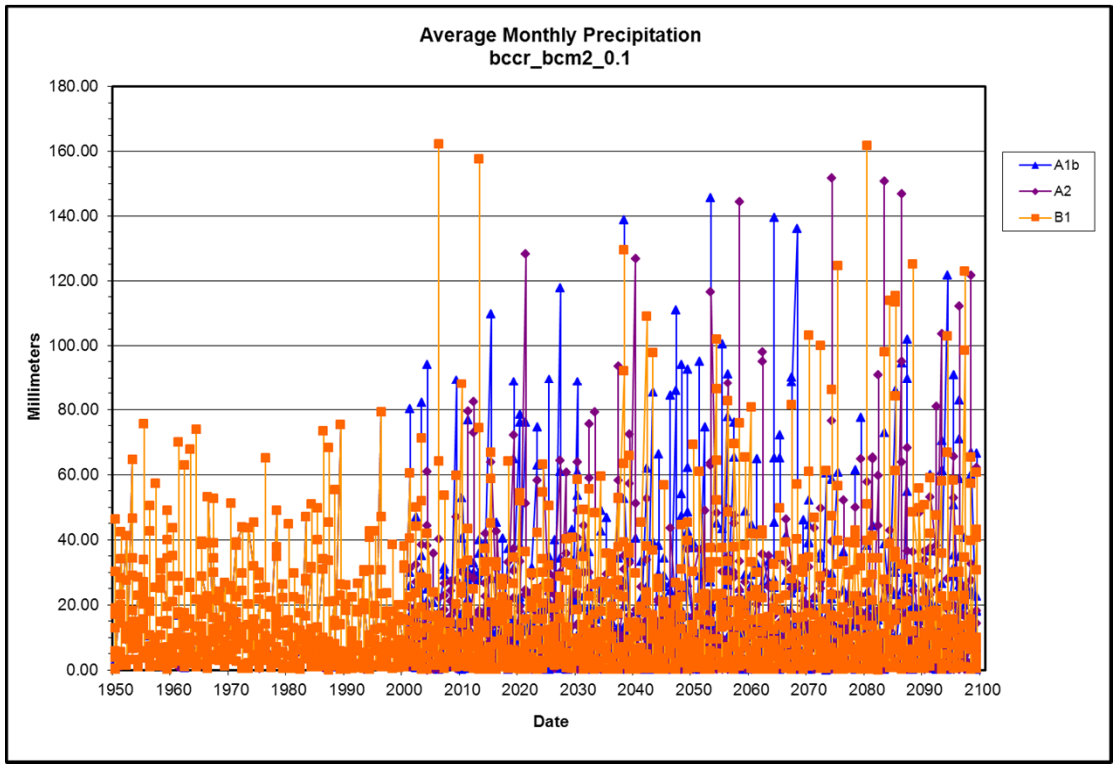

Climate Model bccr_bcm2_0.1 (page 2 of 3)

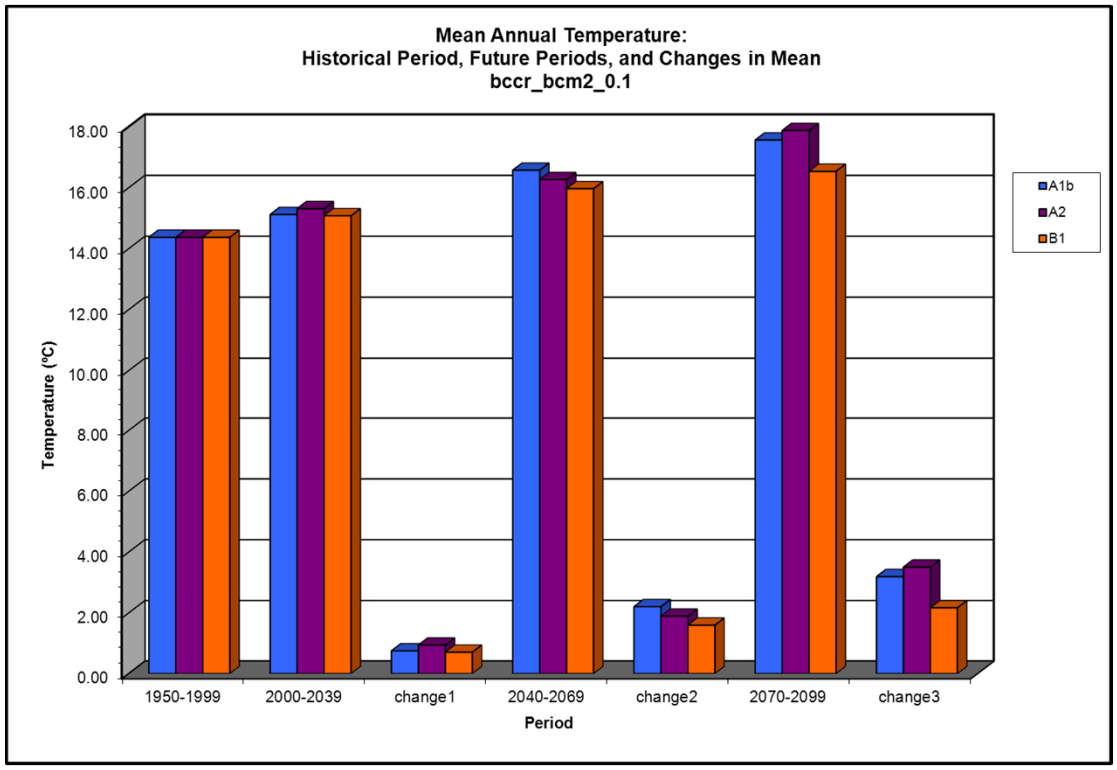

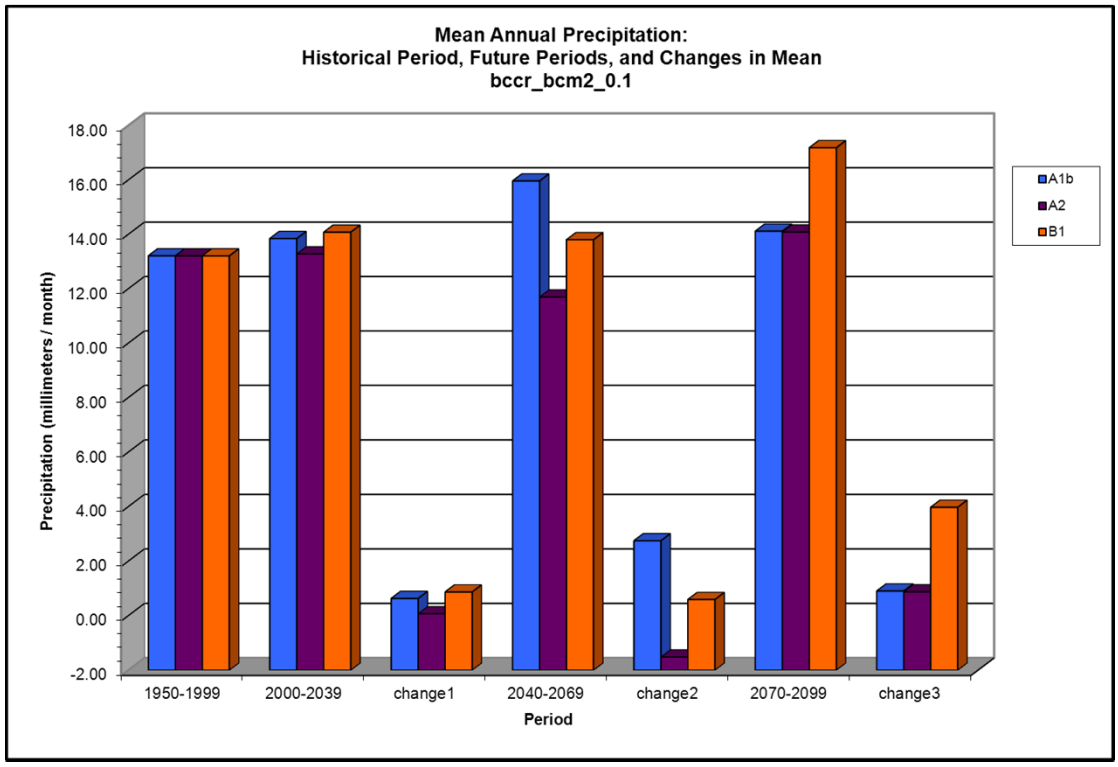

Climate Model bccr_bcm2_0.1 (page 3 of 3)

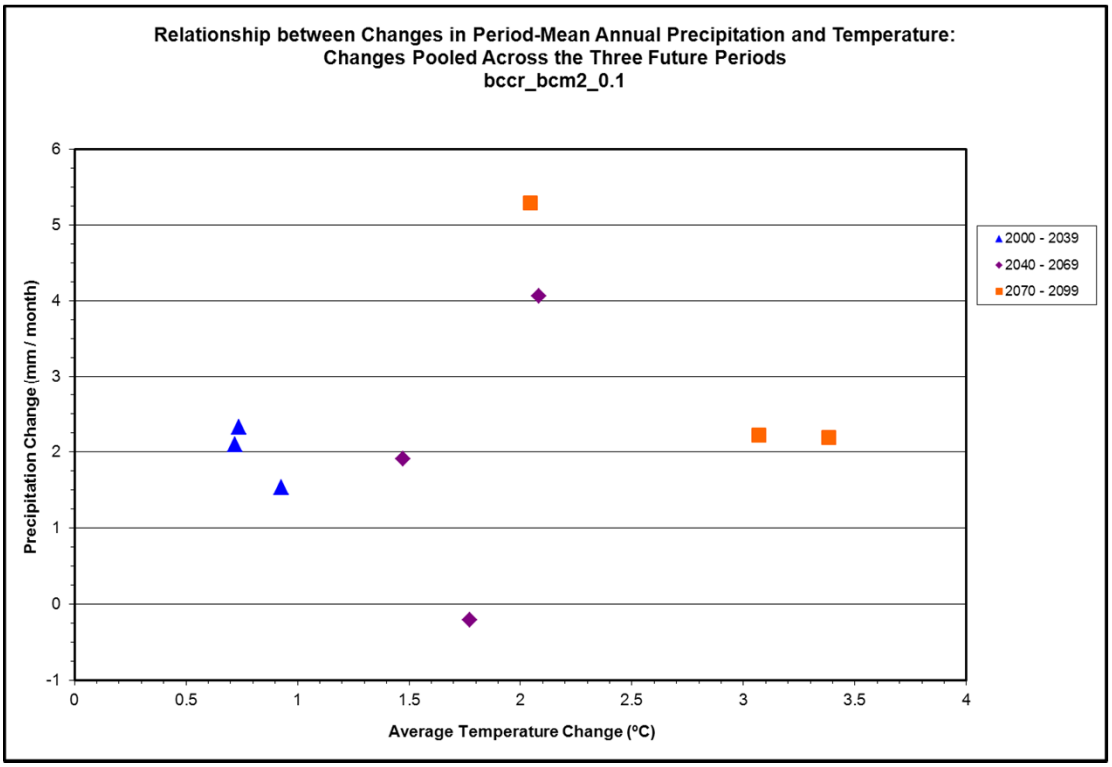

Climate Model cccma_cgcm3_1.1 (page 1 of 3)

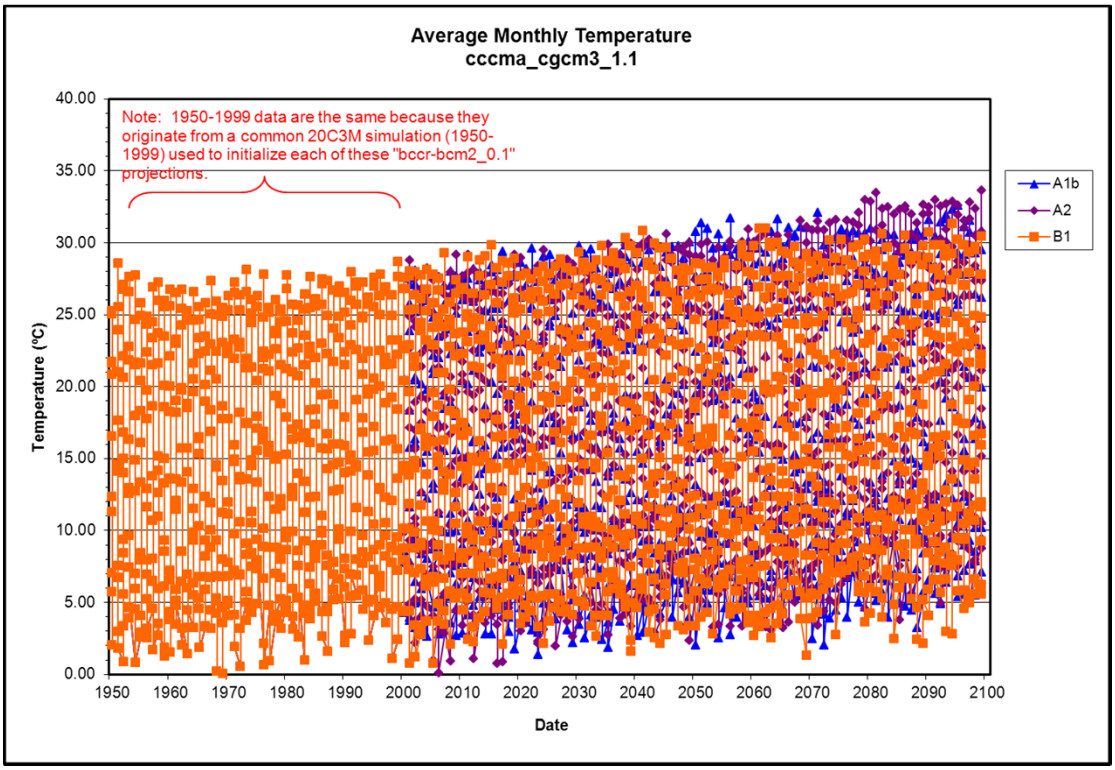

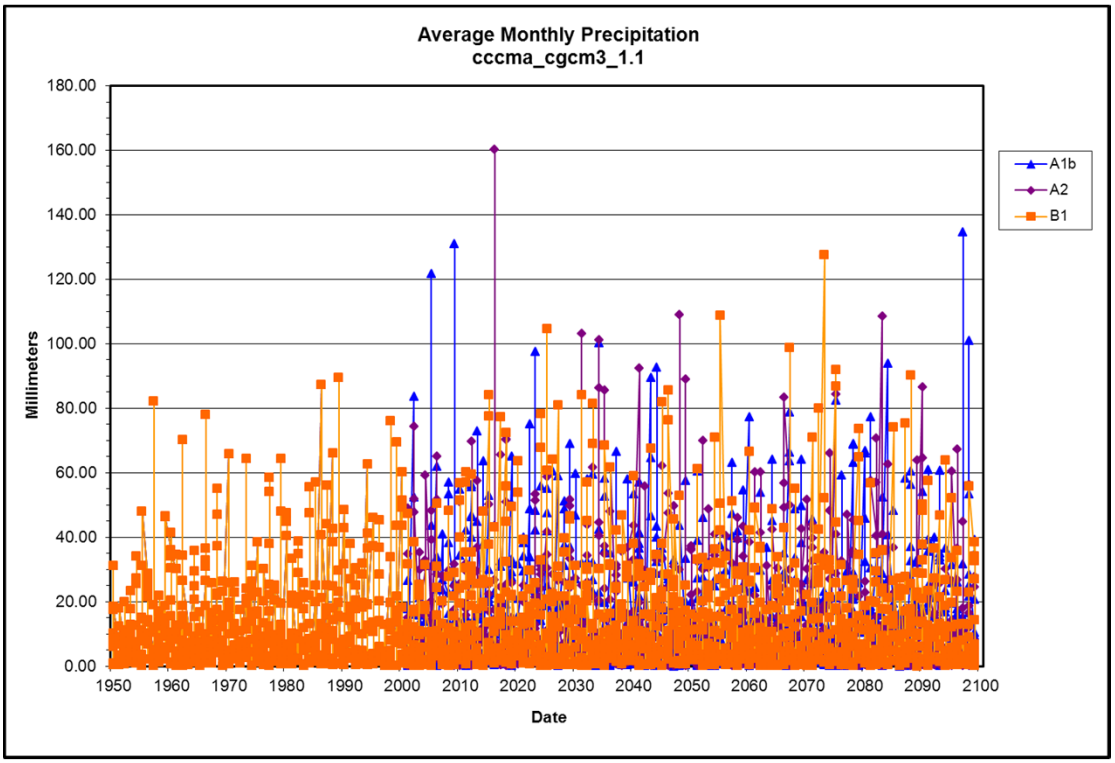

Climate Model cccma_cgcm3_1.1 (page 2 of 3)

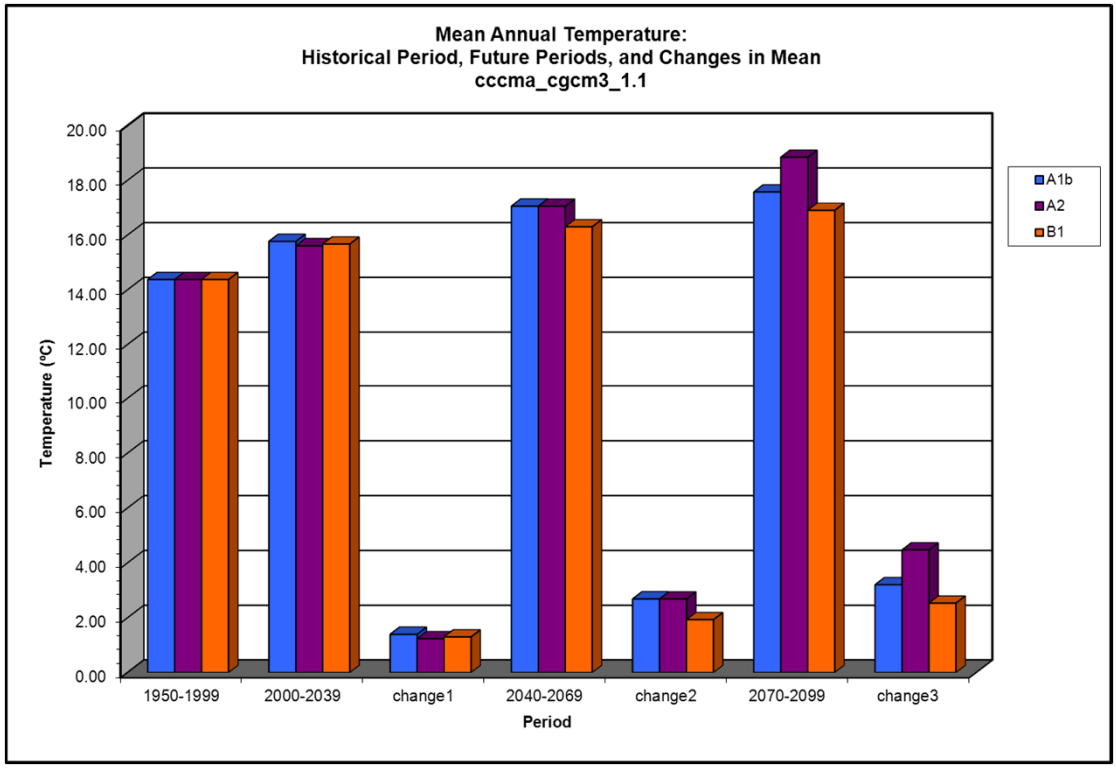

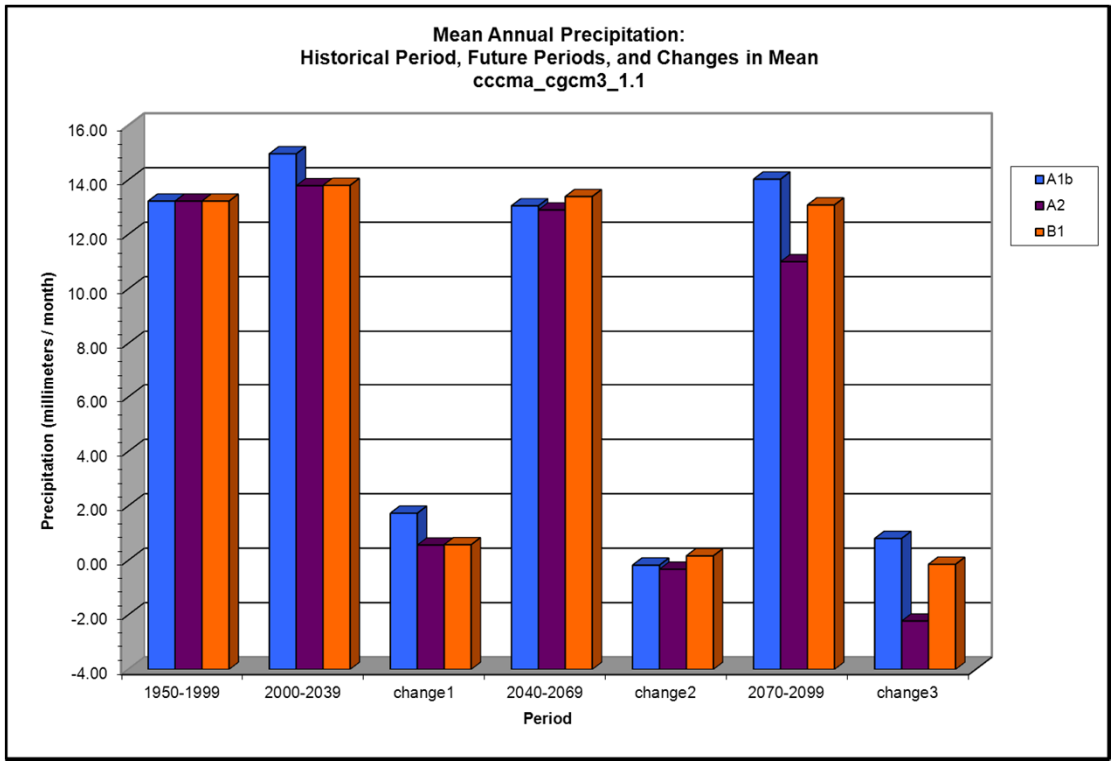

Climate Model cccma_cgcm3_1.1 (page 3 of 3)

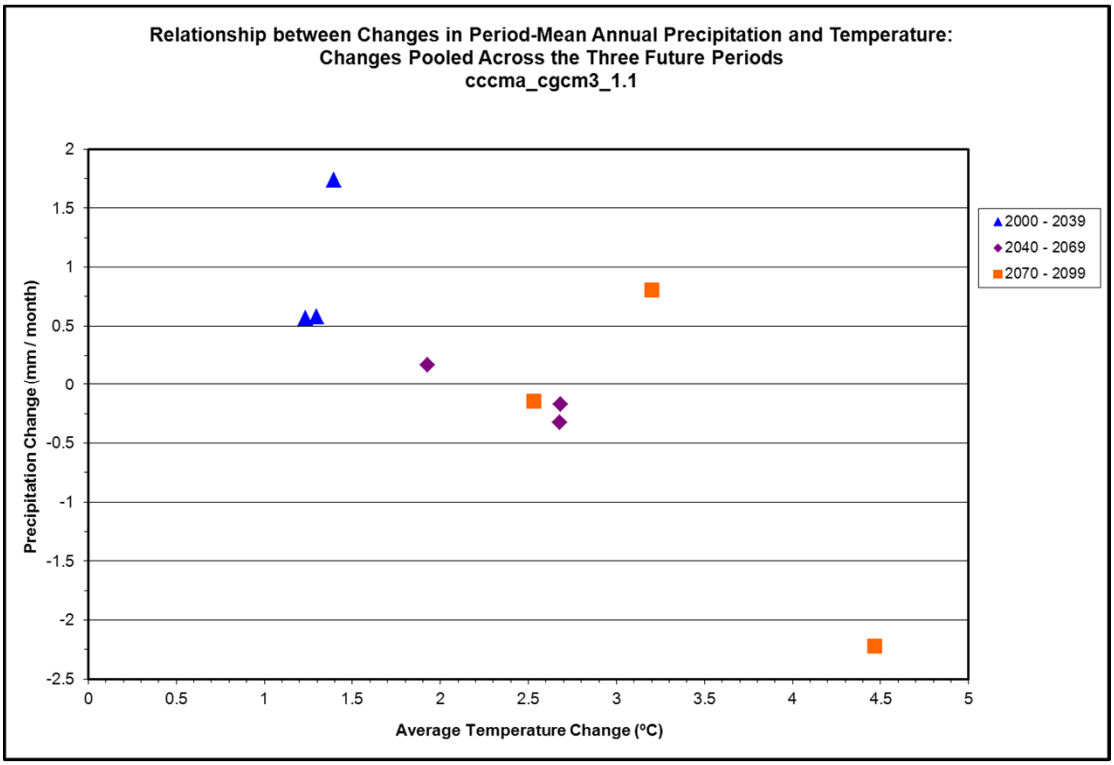

Climate Model cccma_cgcm3_1.2 (page 1 of 3)

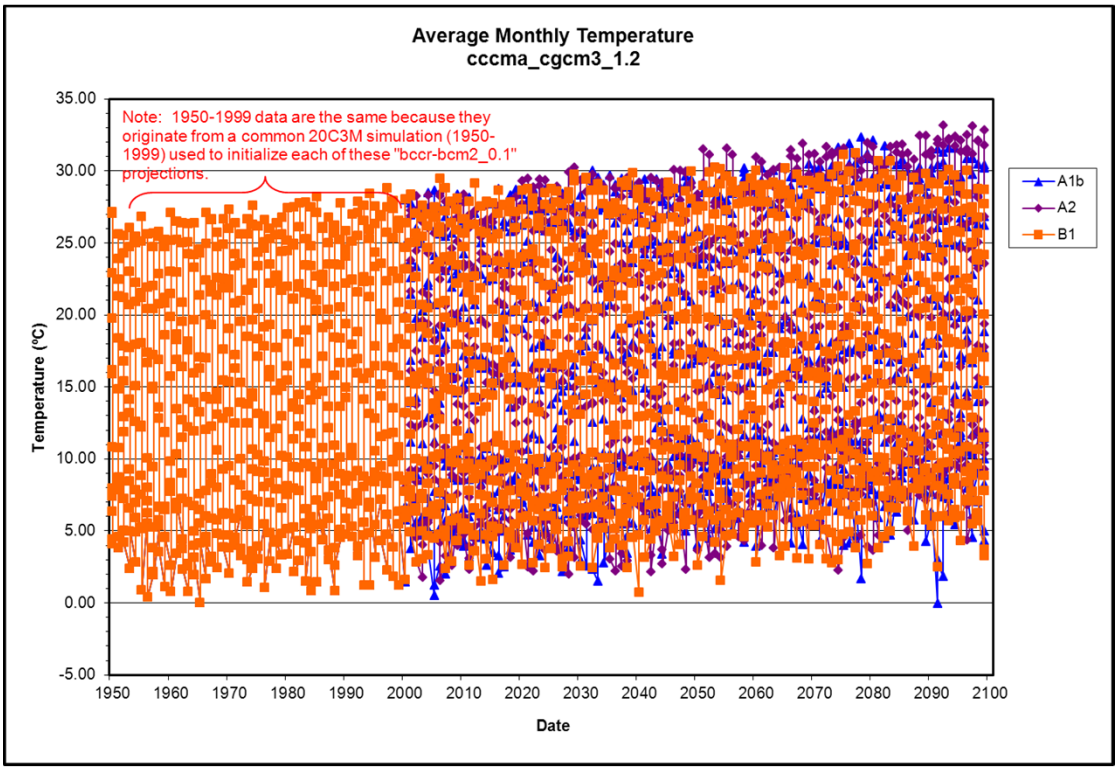

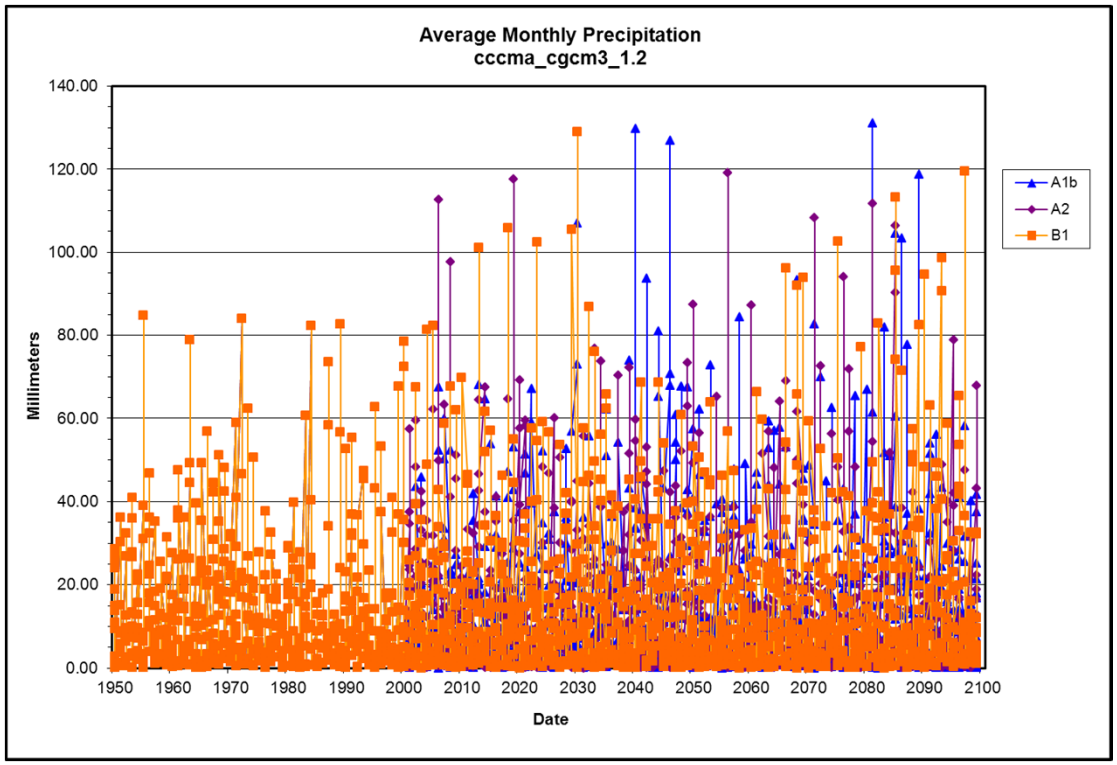

Climate Model cccma_cgcm3_1.2 (page 2 of 3)

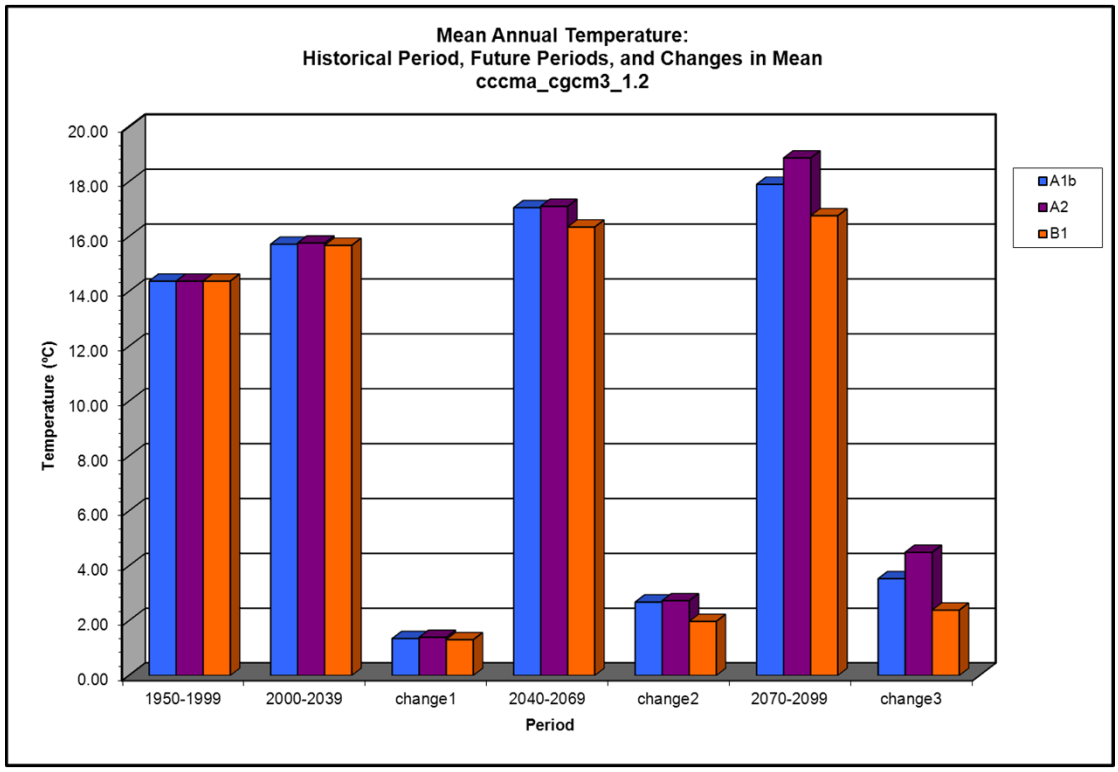

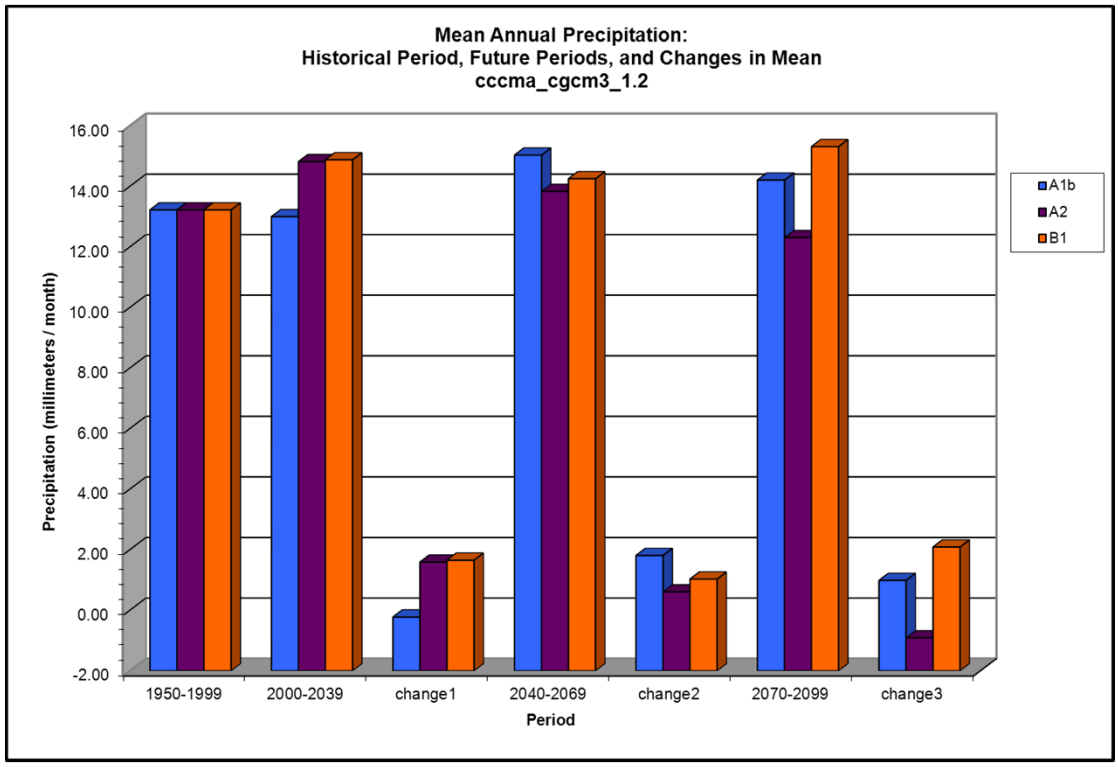

Climate Model cccma_cgcm3_1.2 (page 3 of 3)

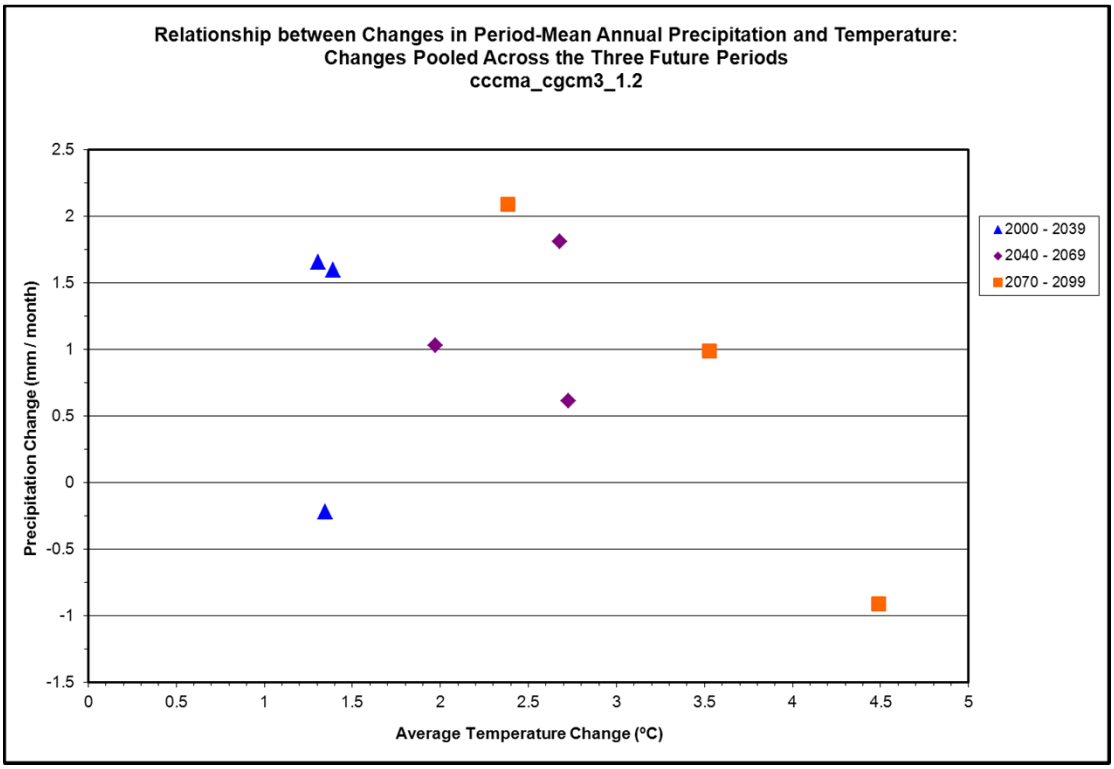

Climate Model cccma_cgcm3_1.3 (page 1 of 3)

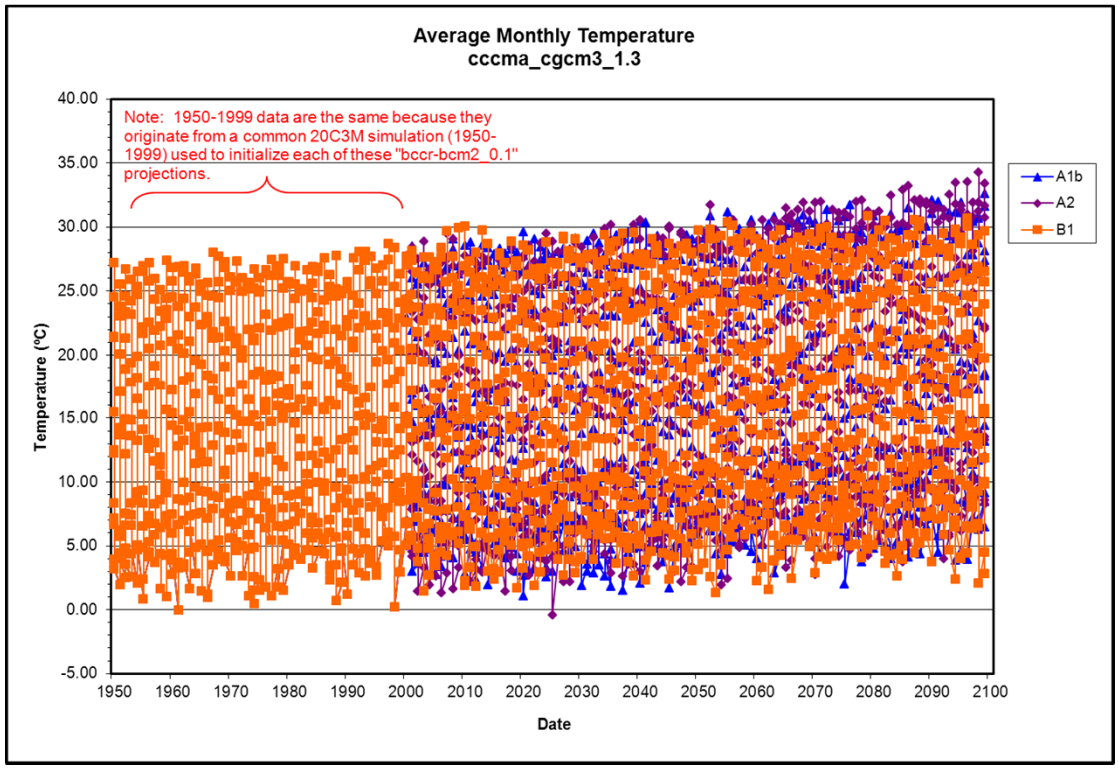

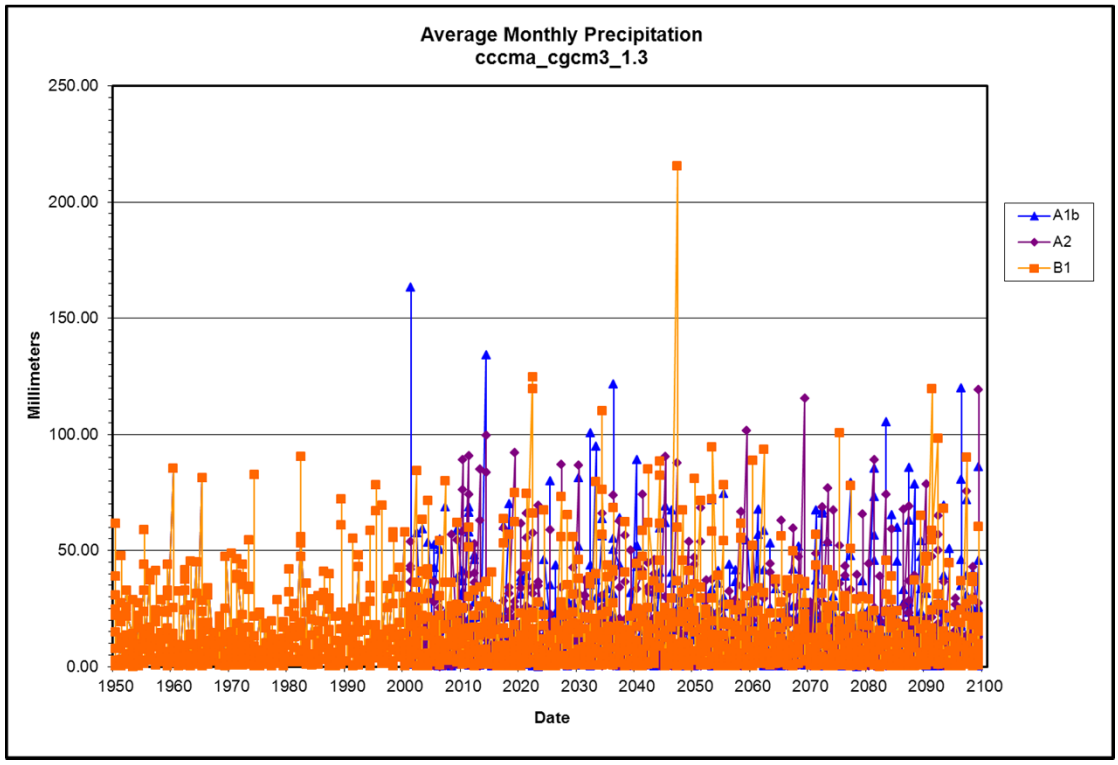

Climate Model cccma_cgcm3_1.3 (page 2 of 3)

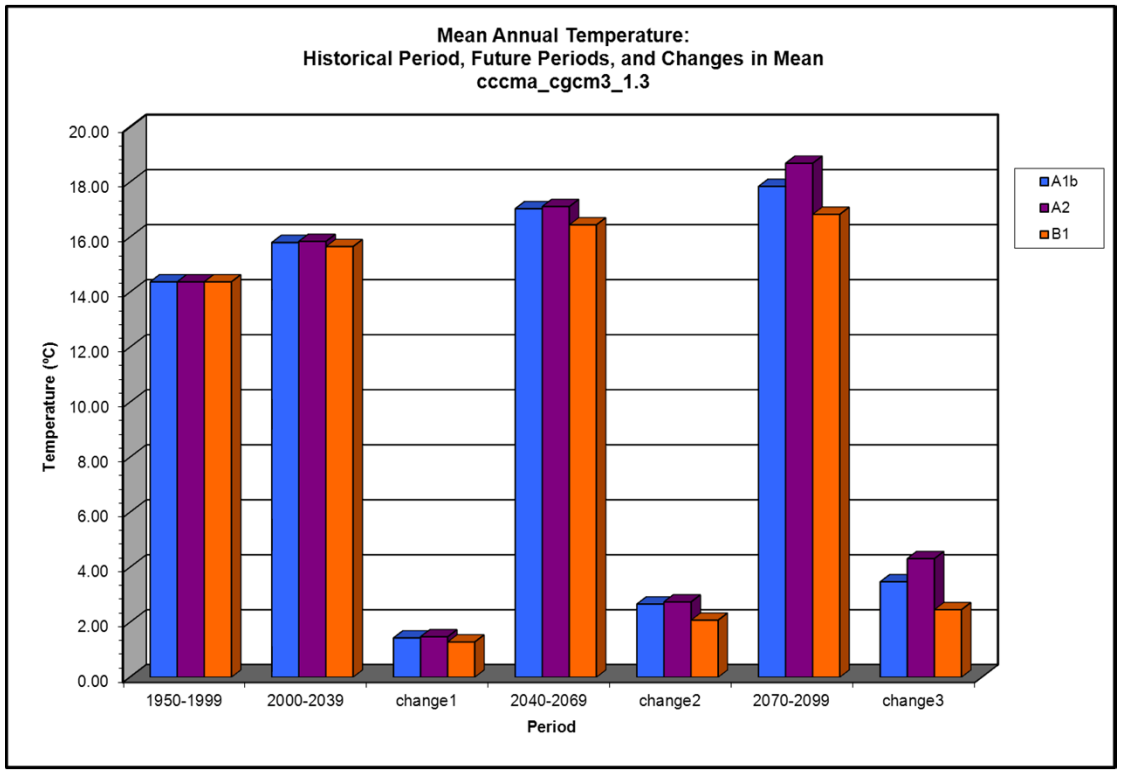

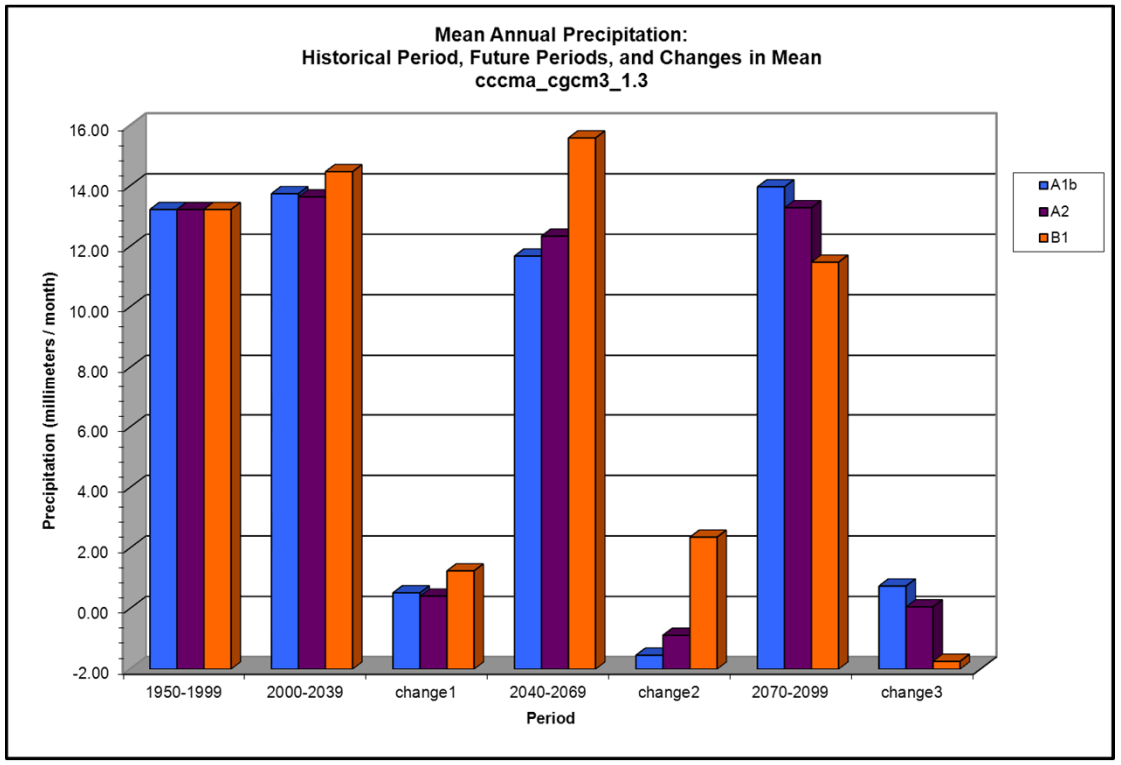

Climate Model cccma_cgcm3_1.3 (page 3 of 3)

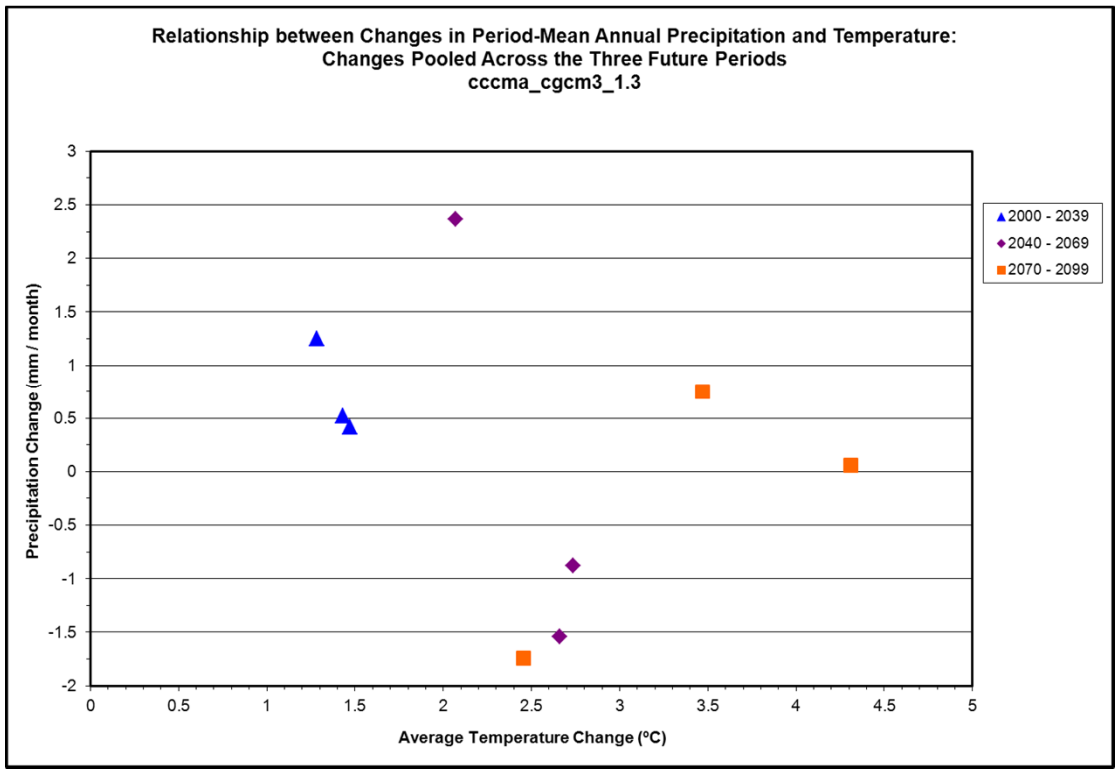

Climate Model cccma_cgcm3_1.4 (page 1 of 3)

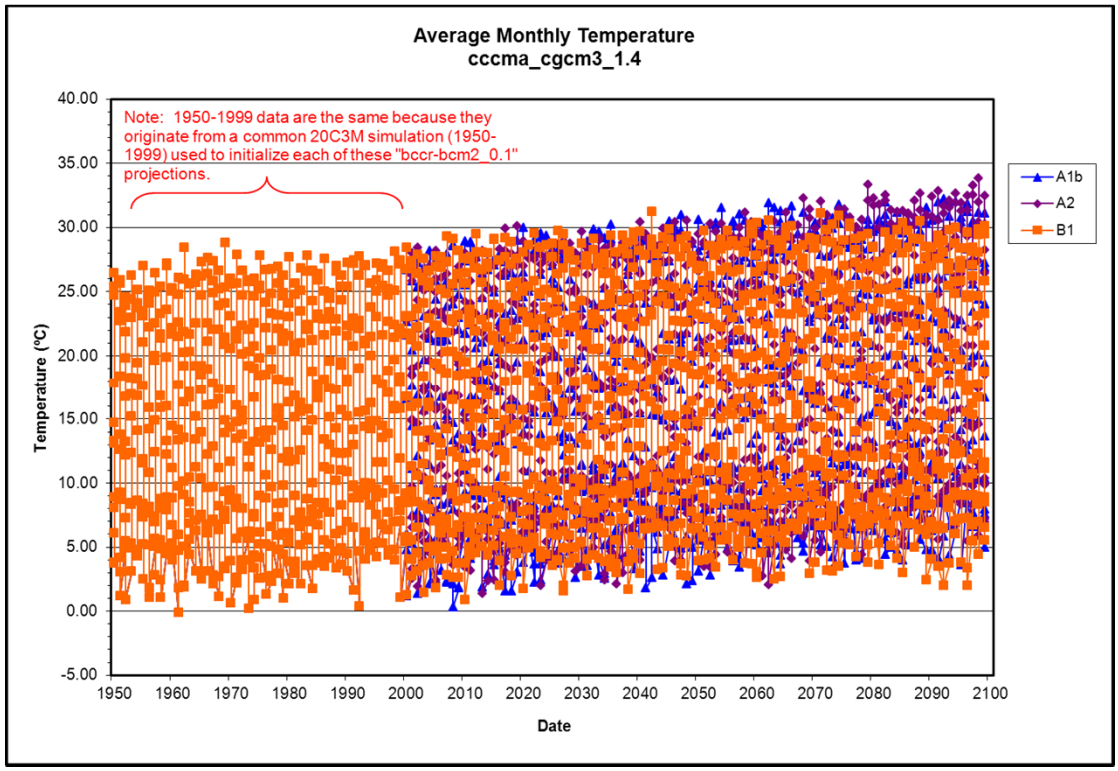

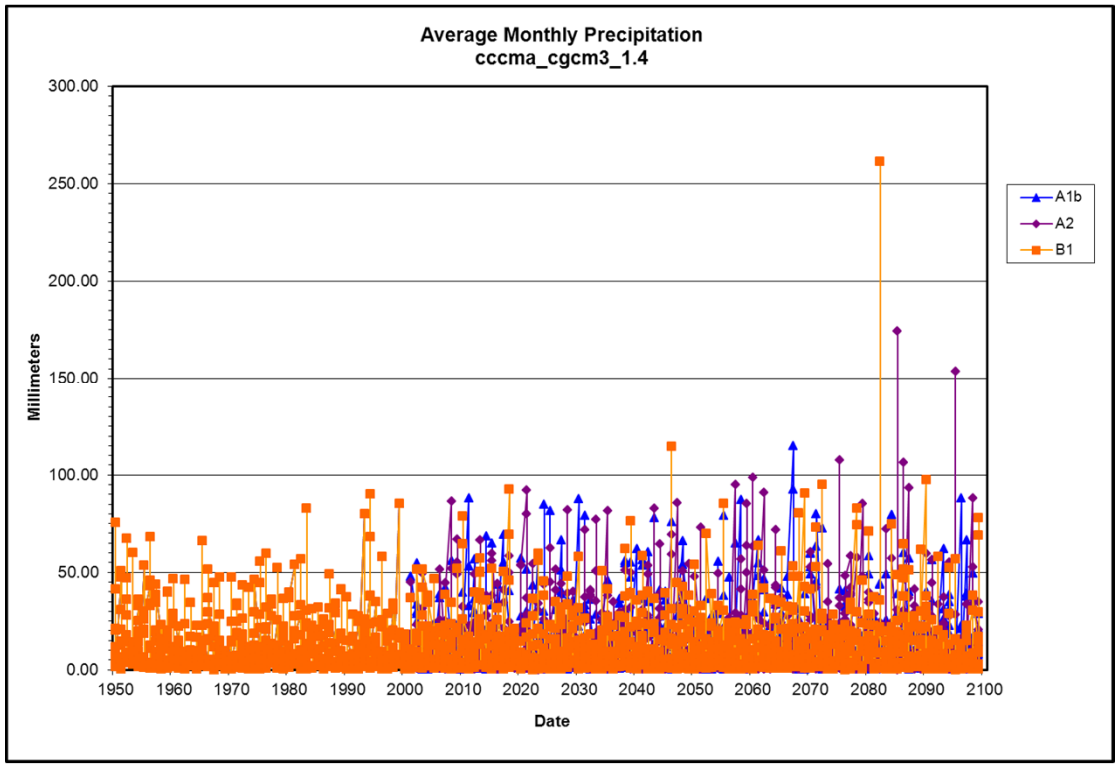

Climate Model cccma_cgcm3_1.4 (page 1 of 3)

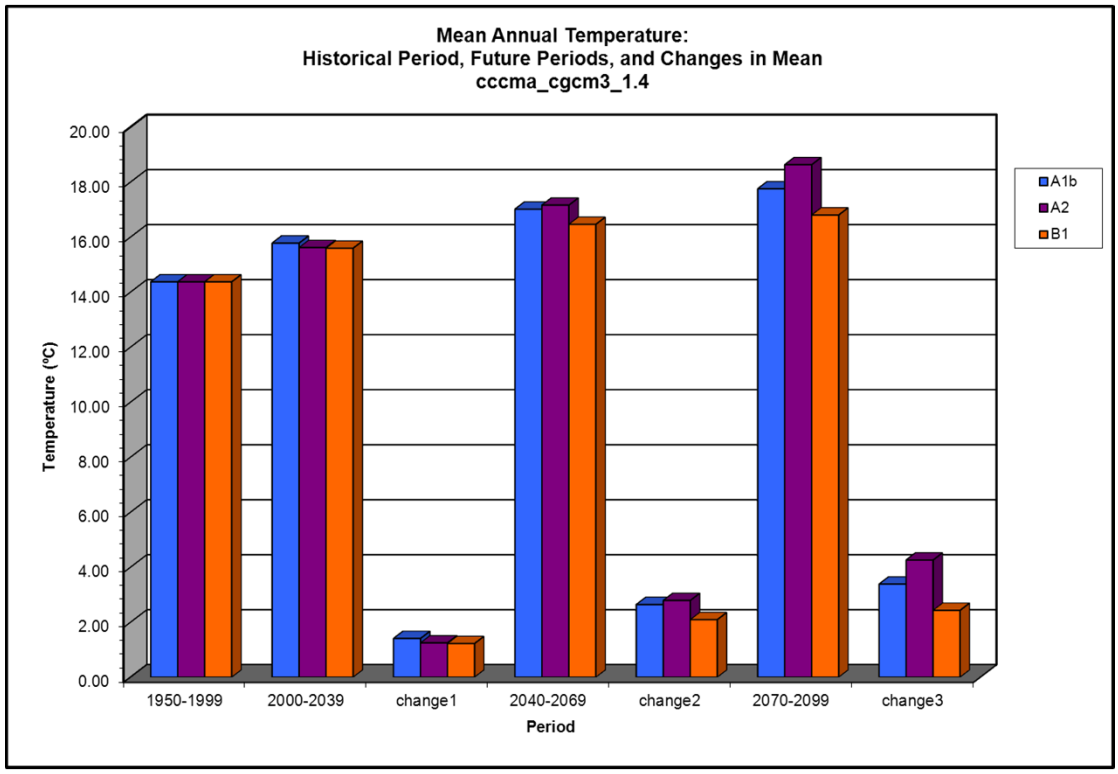

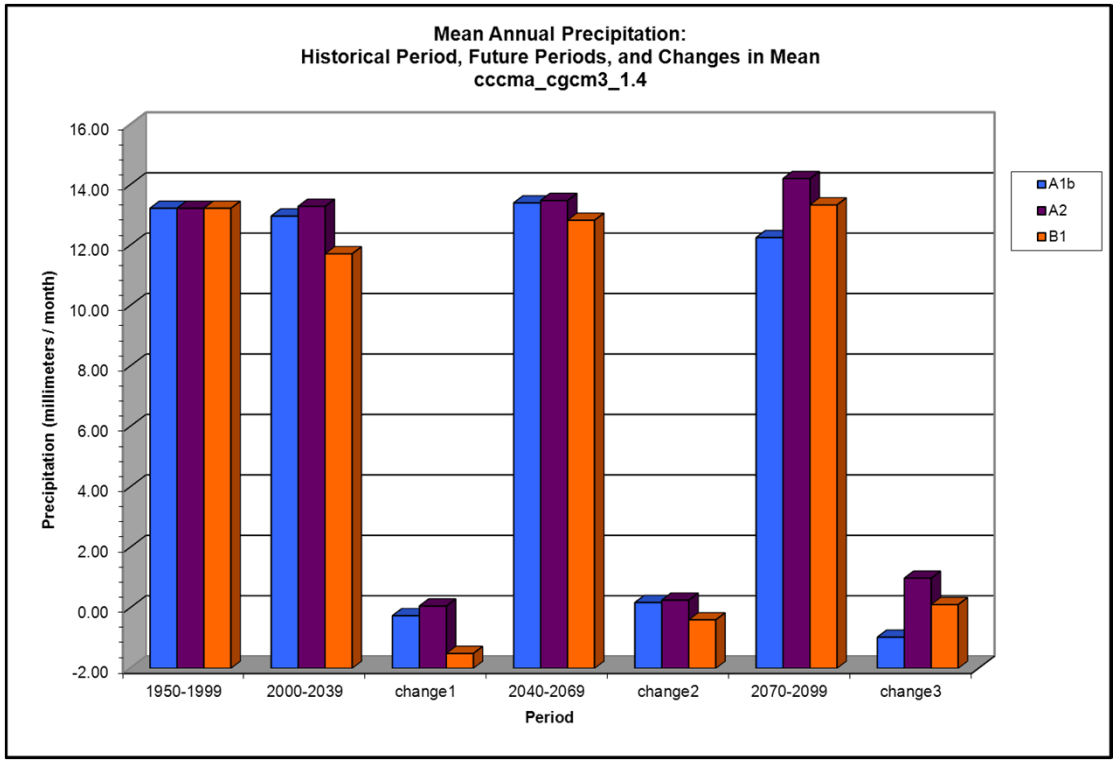

Climate Model cccma_cgcm3_1.4 (page 1 of 3)

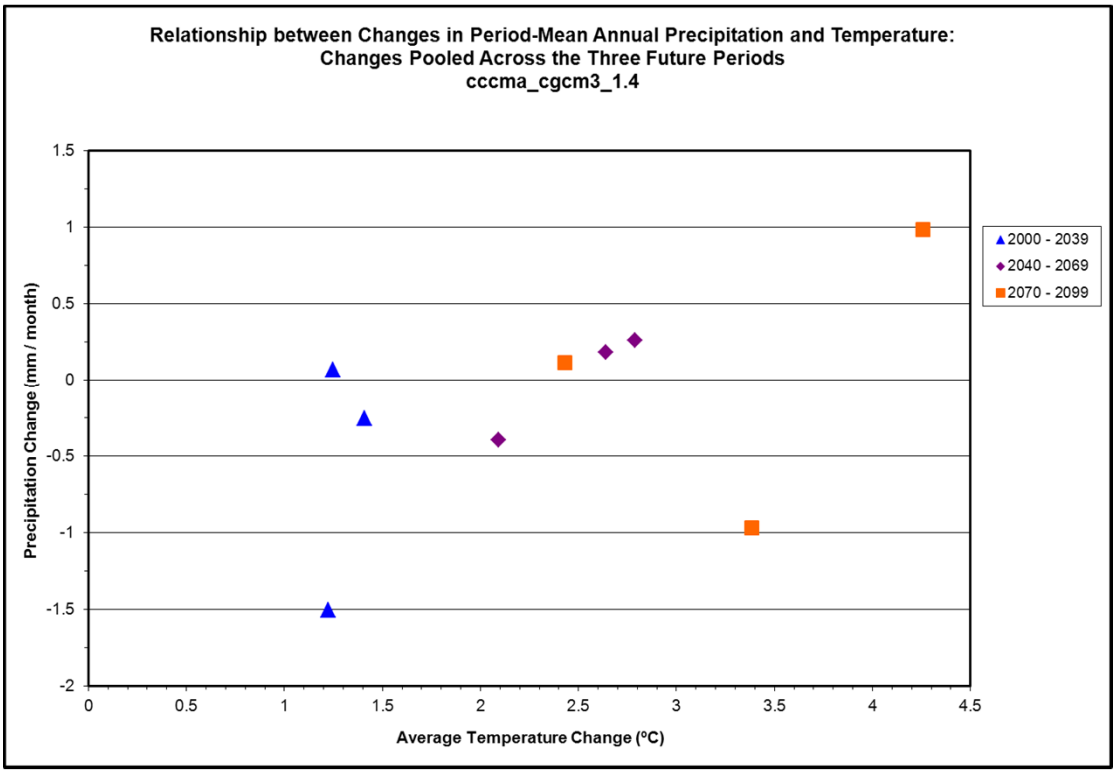

Climate Model cccma_cgcm3_1.5 (page 1 of 3)

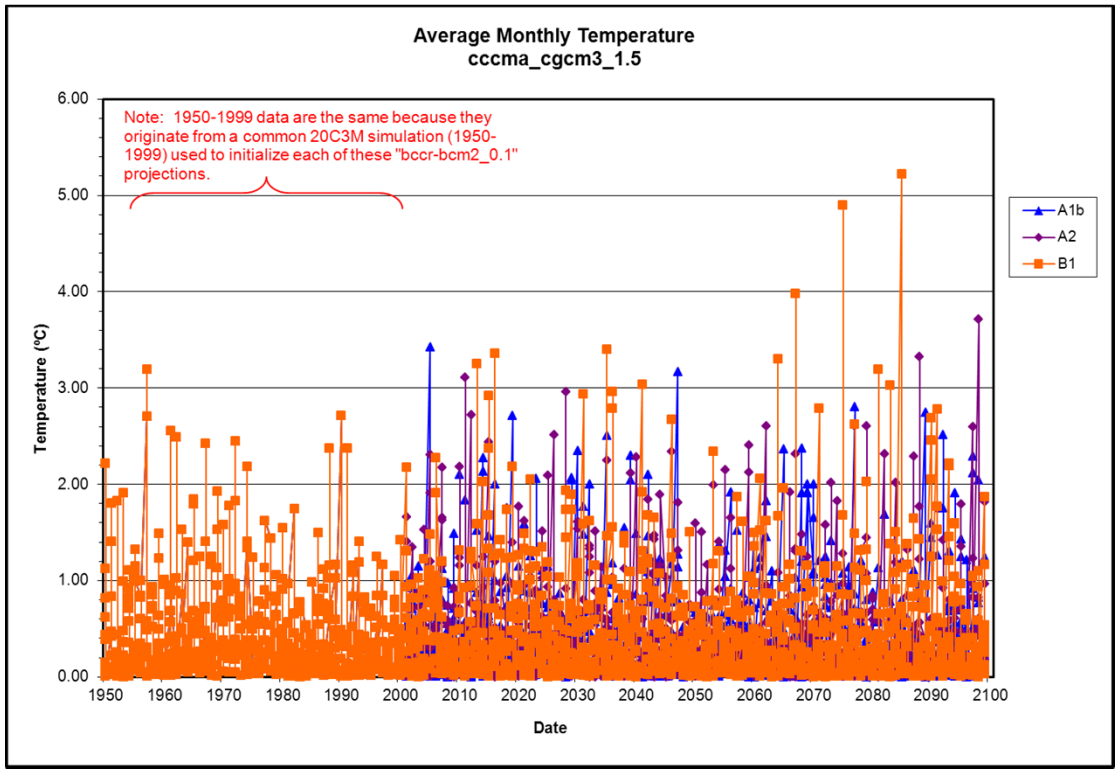

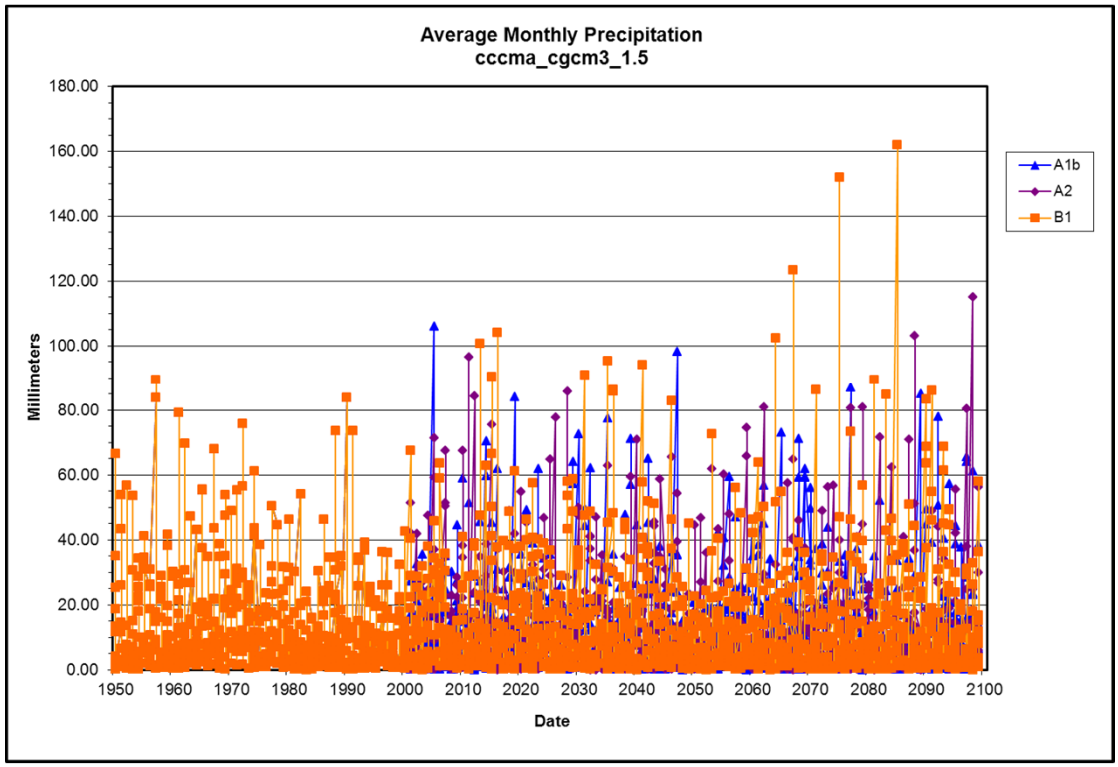

Climate Model cccma_cgcm3_1.5 (page 2 of 3)

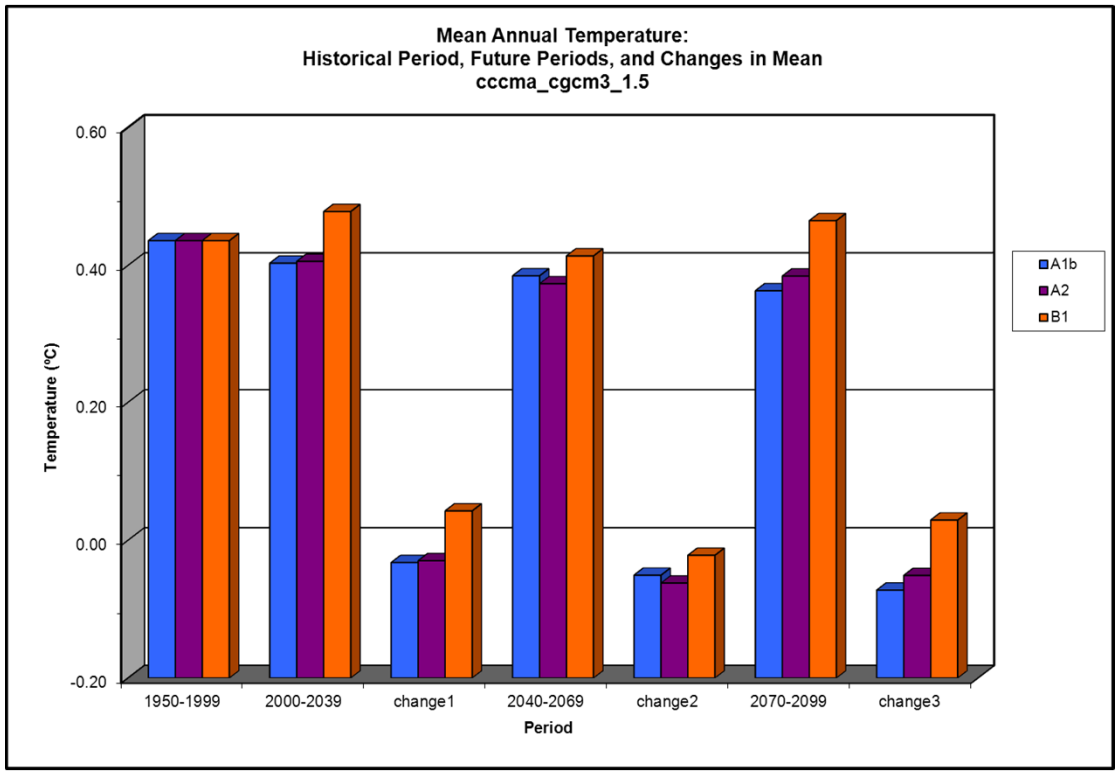

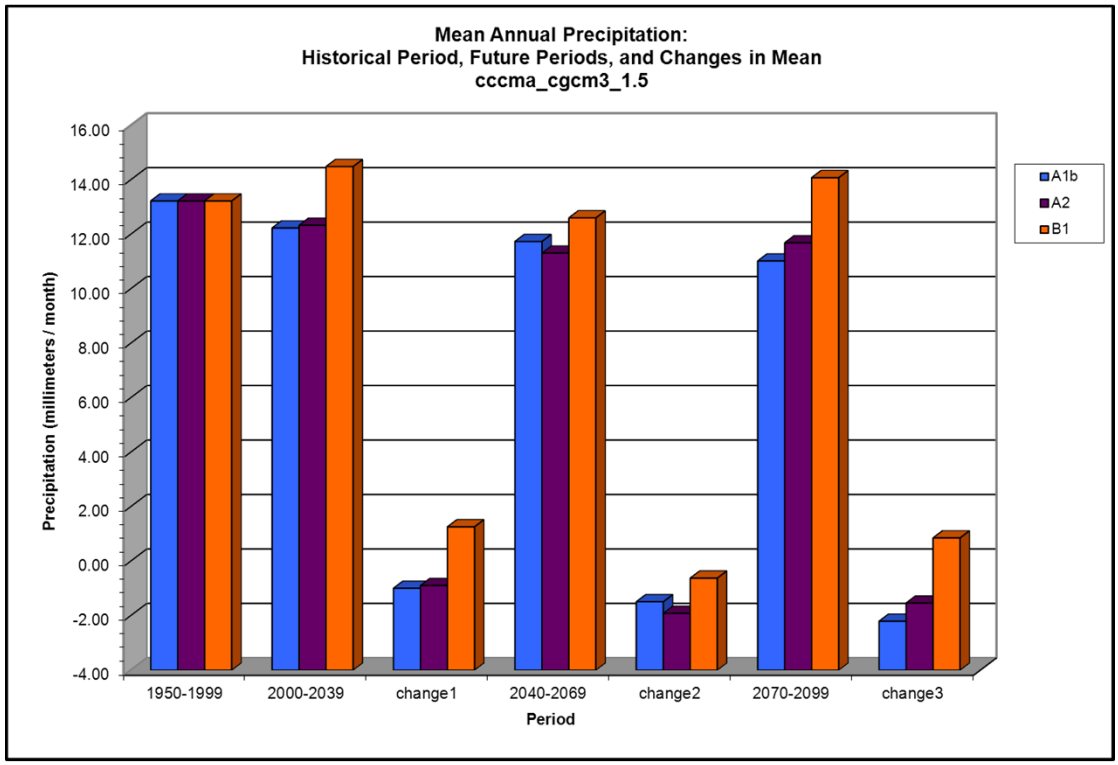

Climate Model cccma_cgcm3_1.5 (page 3 of 3)

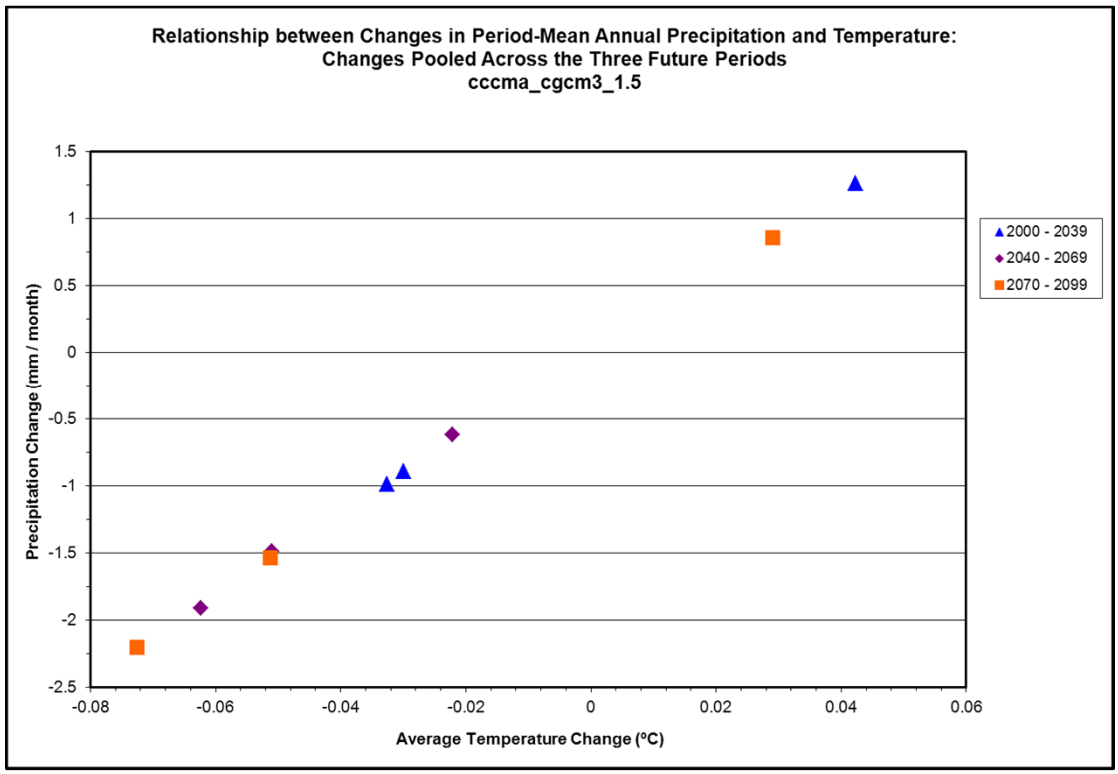

Climate Model cnrm_cm3.1 (page 1 of 3)

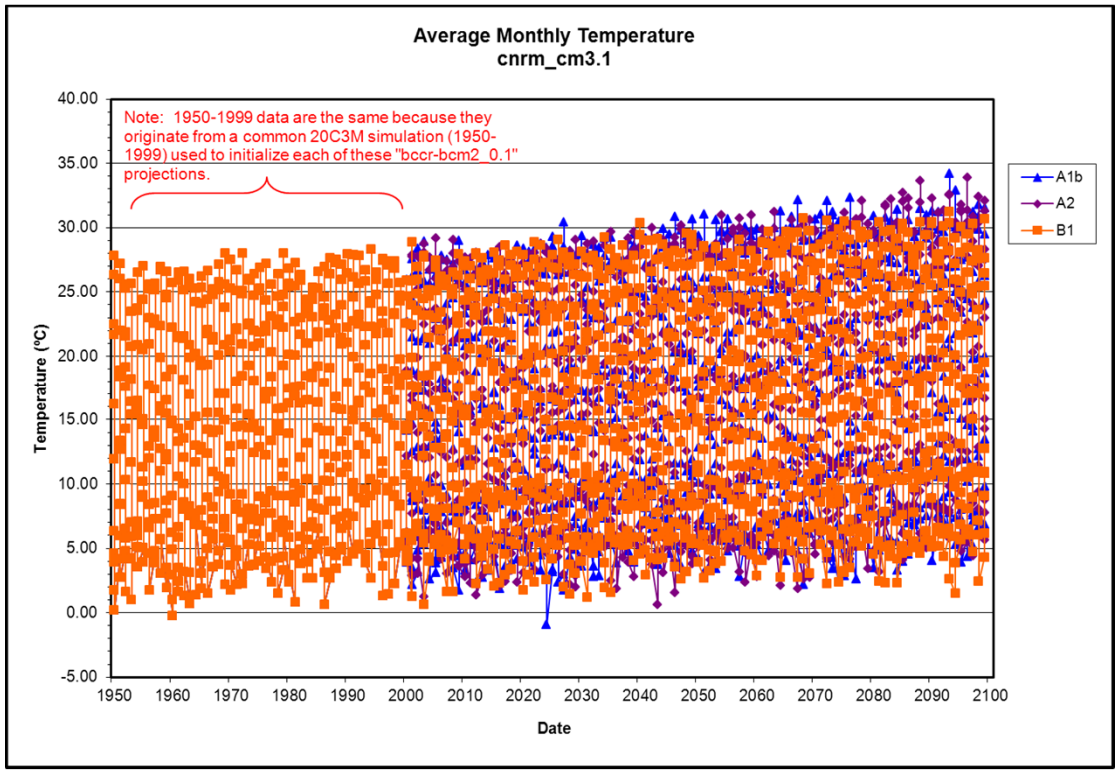

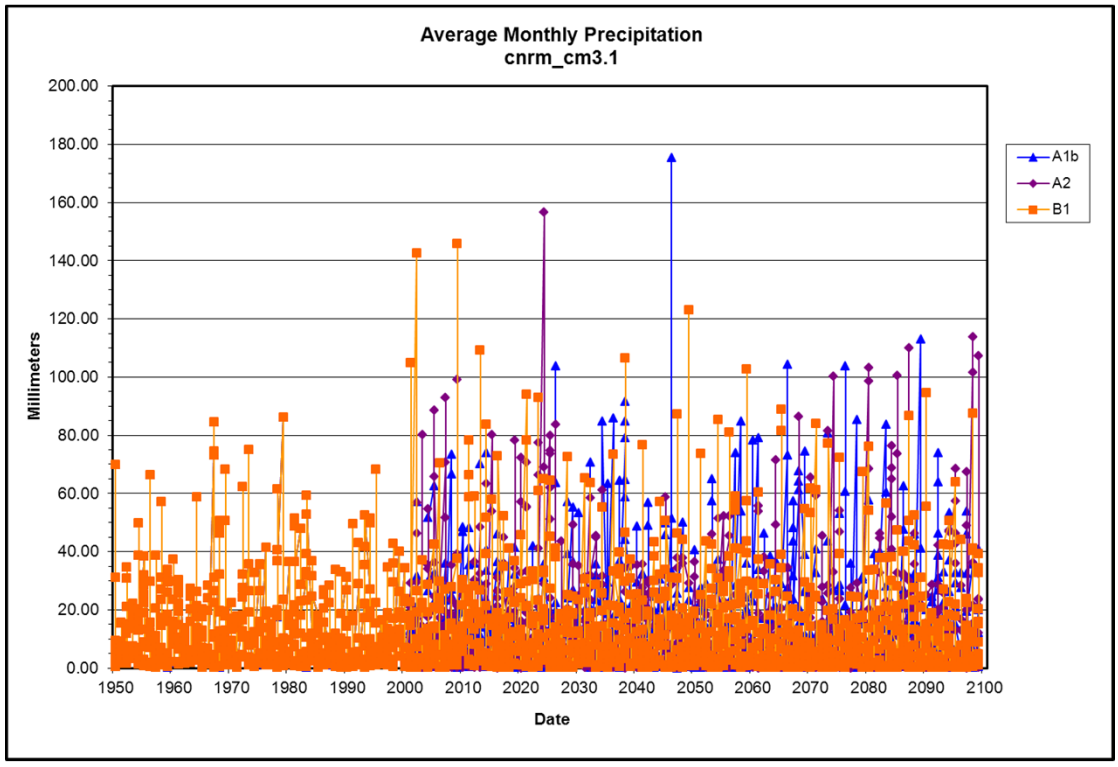

Climate Model cnrm_cm3.1 (page 2 of 3)

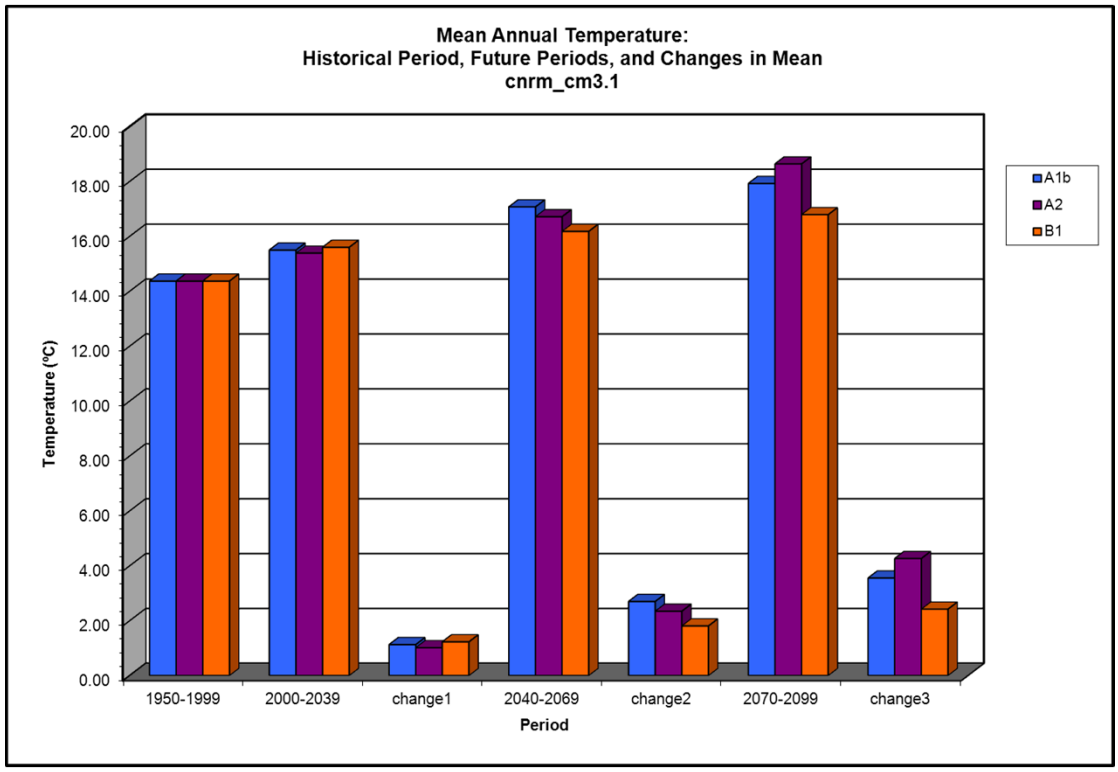

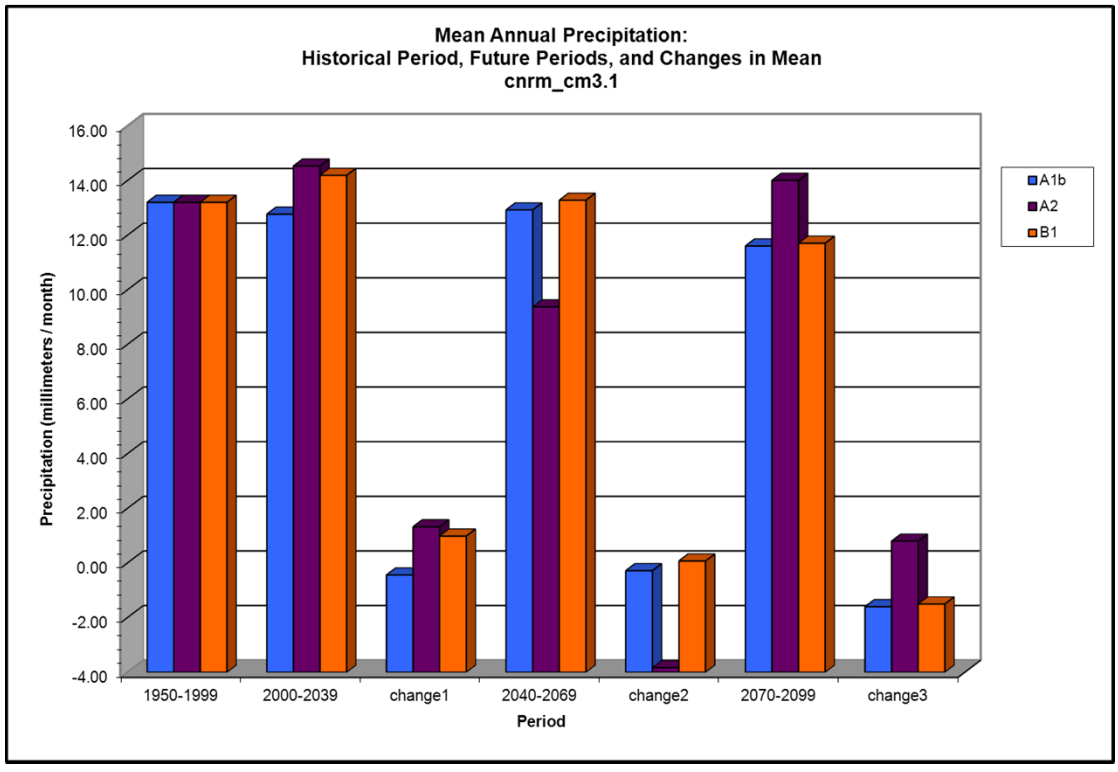

Climate Model cnrm_cm3.1 (page 3 of 3)

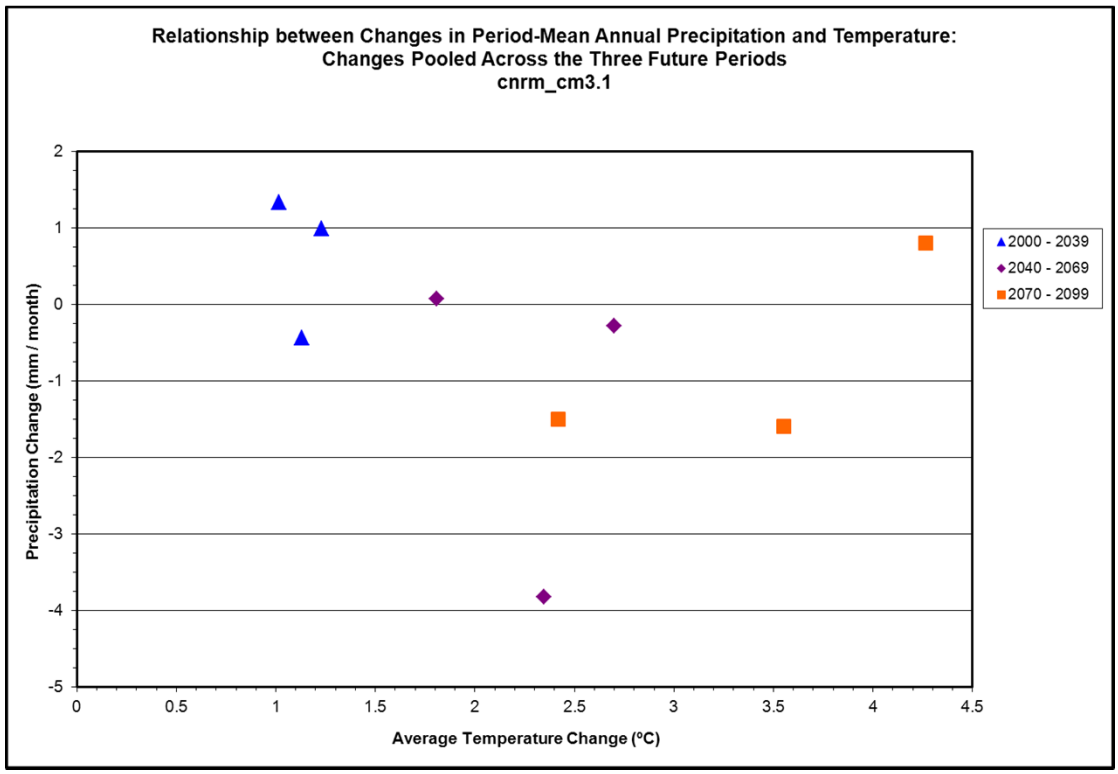

Climate Model csiro_mk3_0.1 (page 1 of 3)

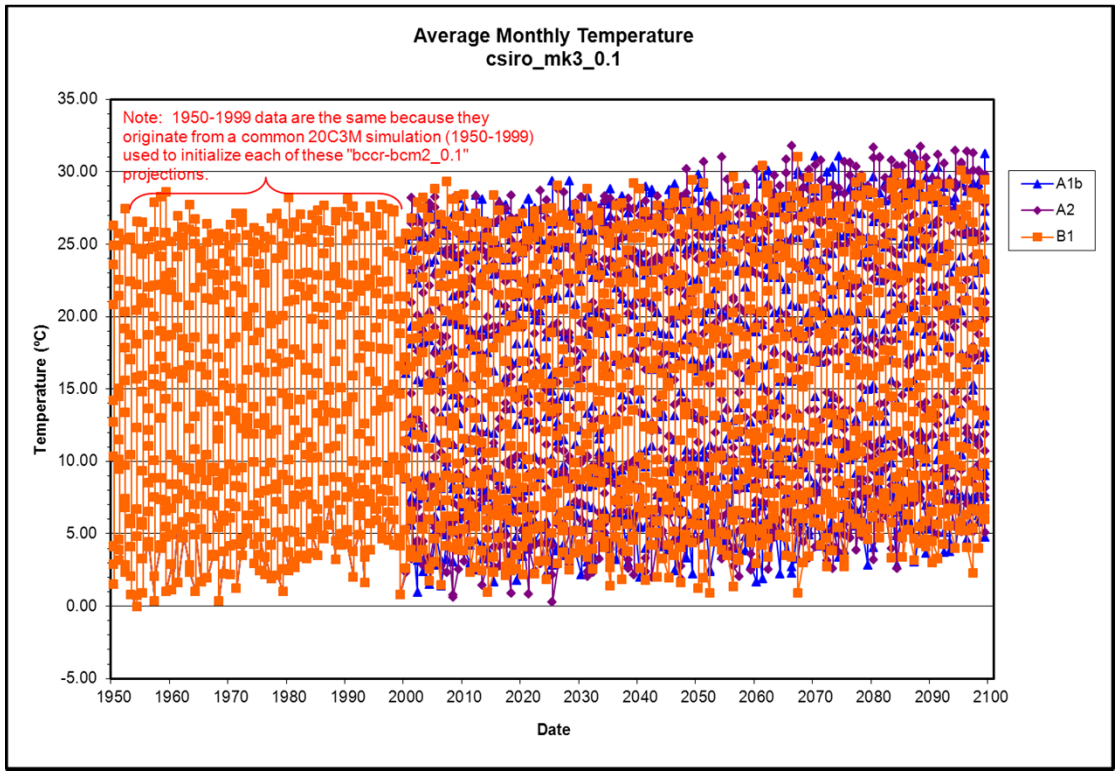

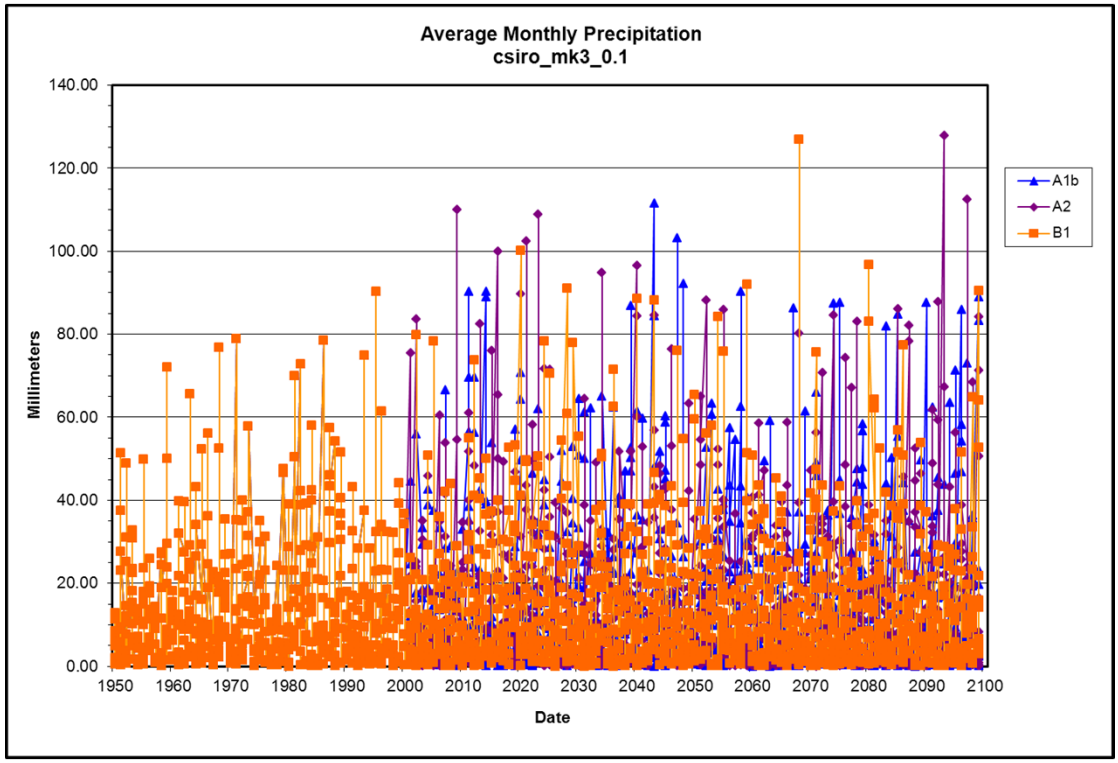

Climate Model csiro_mk3_0.1 (page 2 of 3)

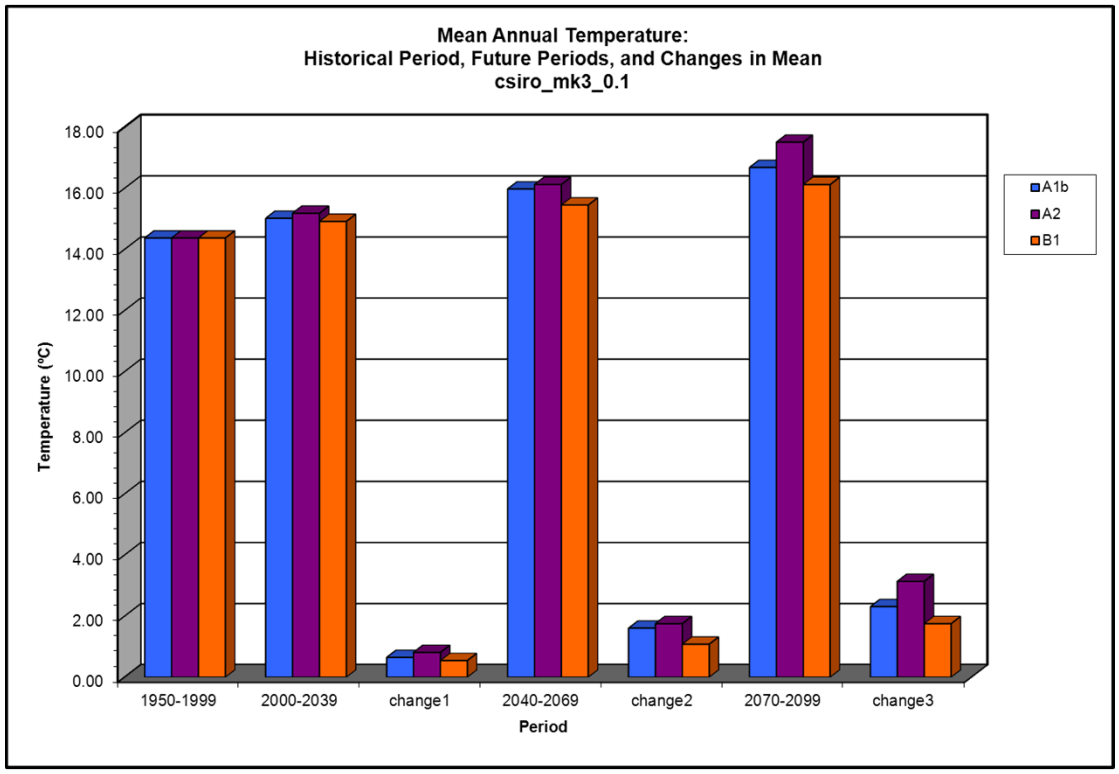

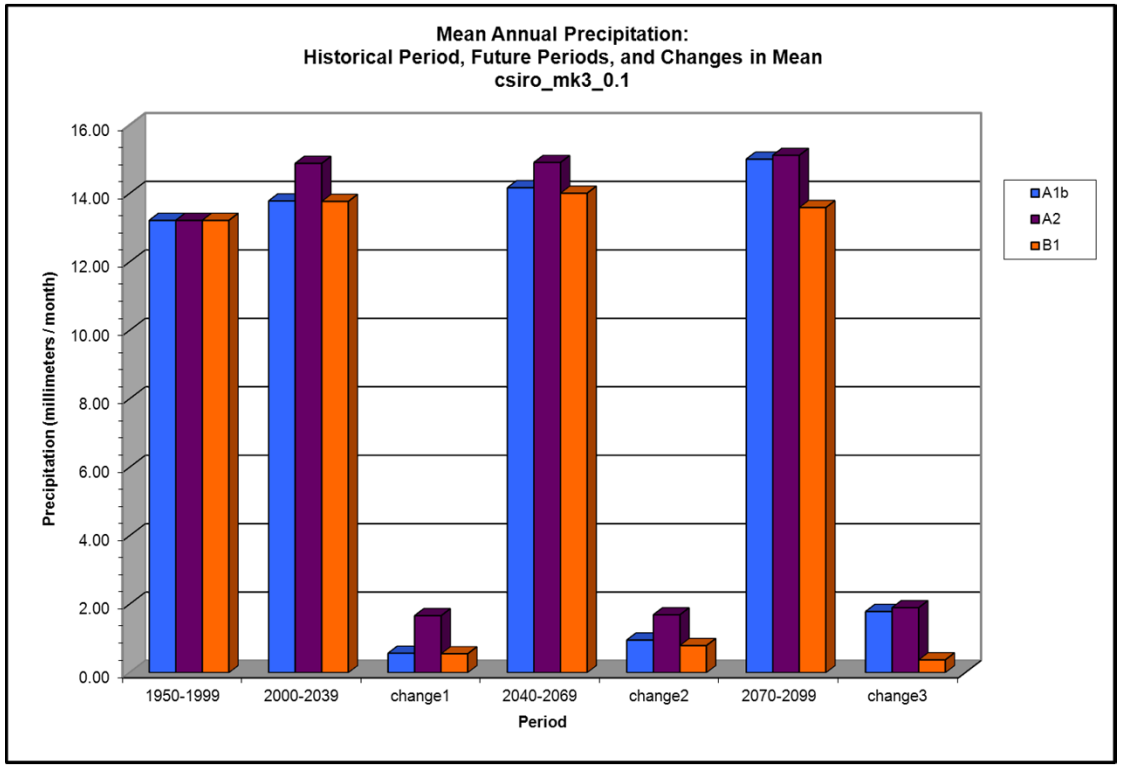

Climate Model csiro_mk3_0.1 (page 3 of 3)

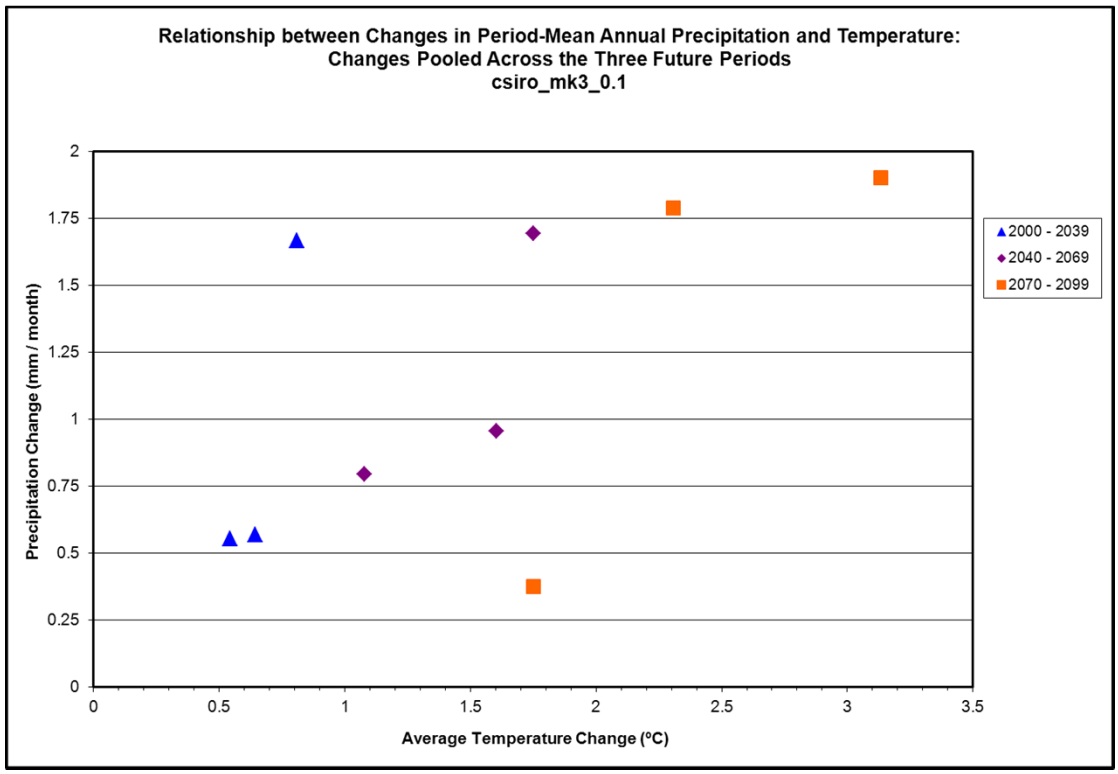

Climate Model gfdl_cm2_0.1 (page 1 of 3)

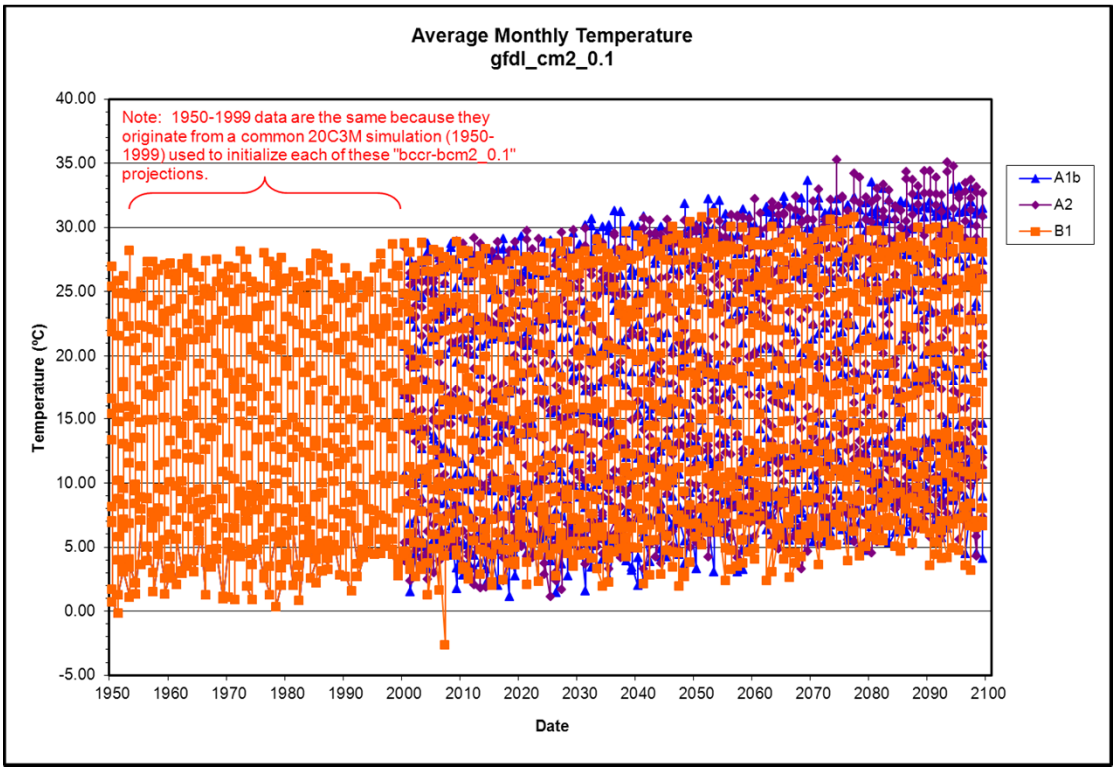

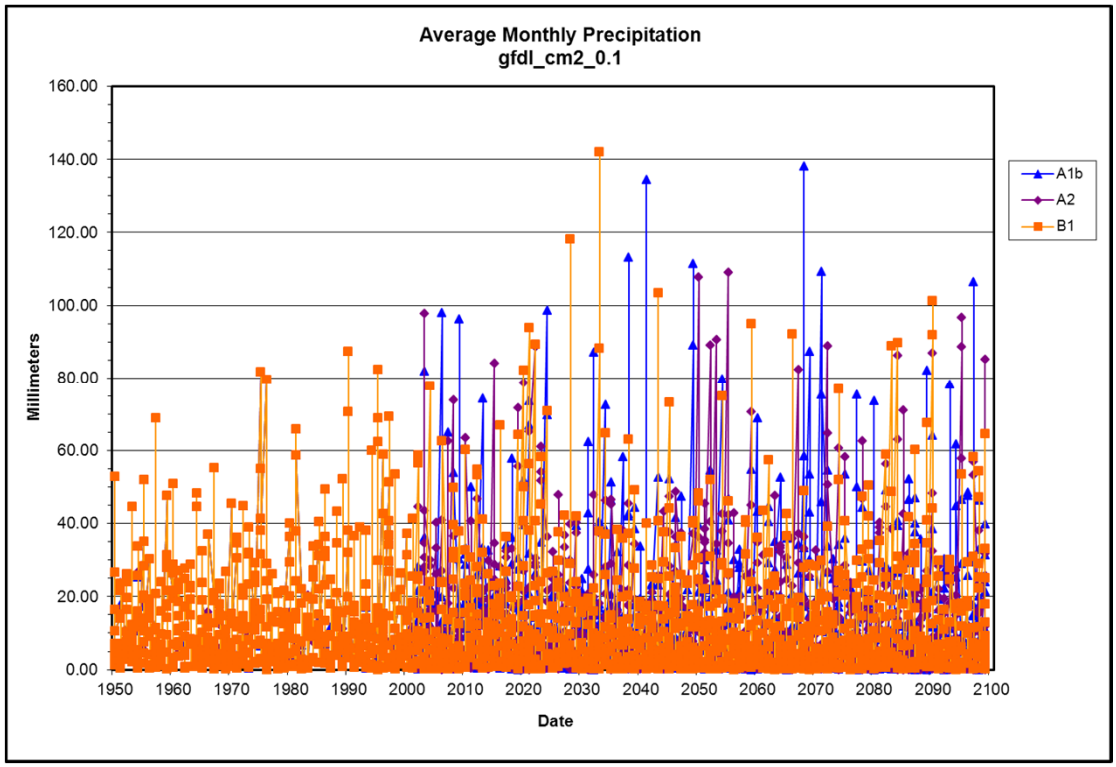

Climate Model gfdl_cm2_0.1 (page 2 of 3)

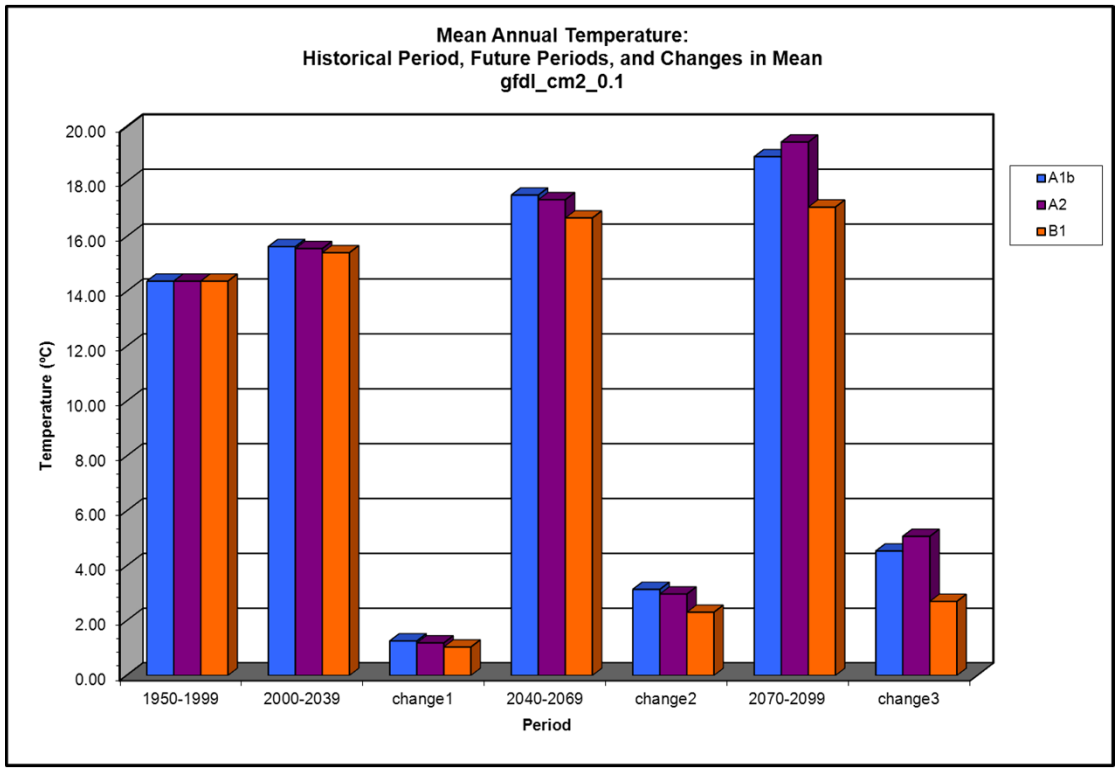

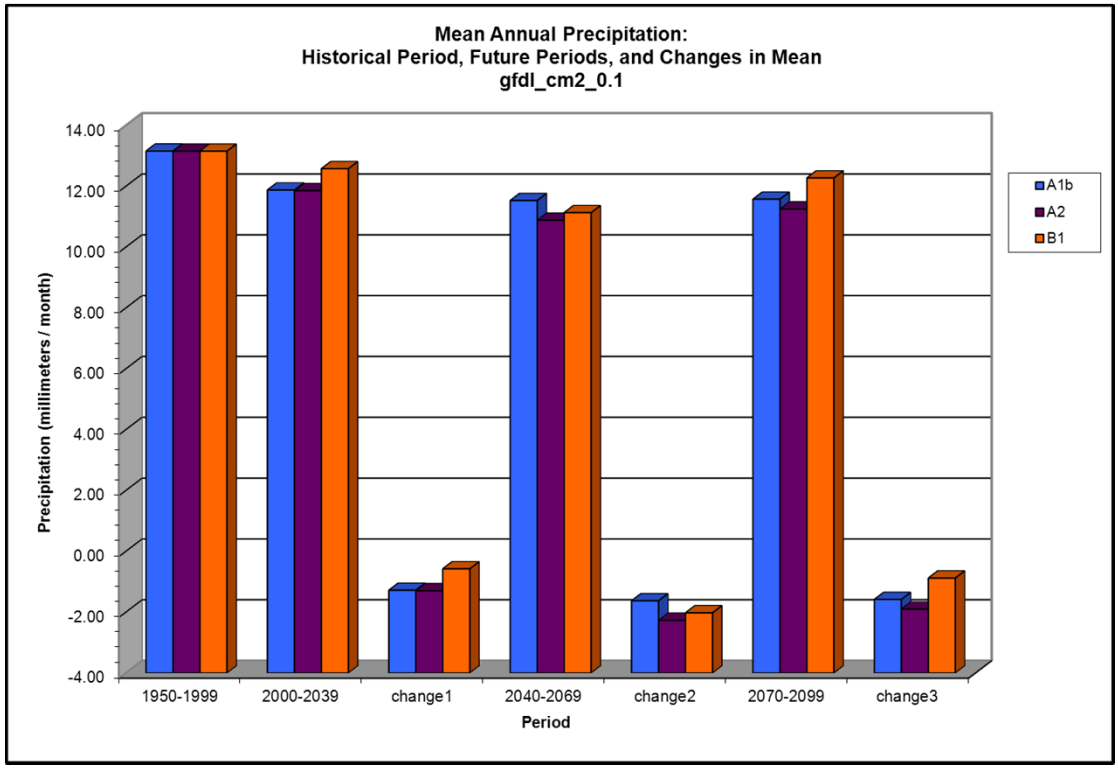

Climate Model gfdl_cm2_0.1 (page 3 of 3)

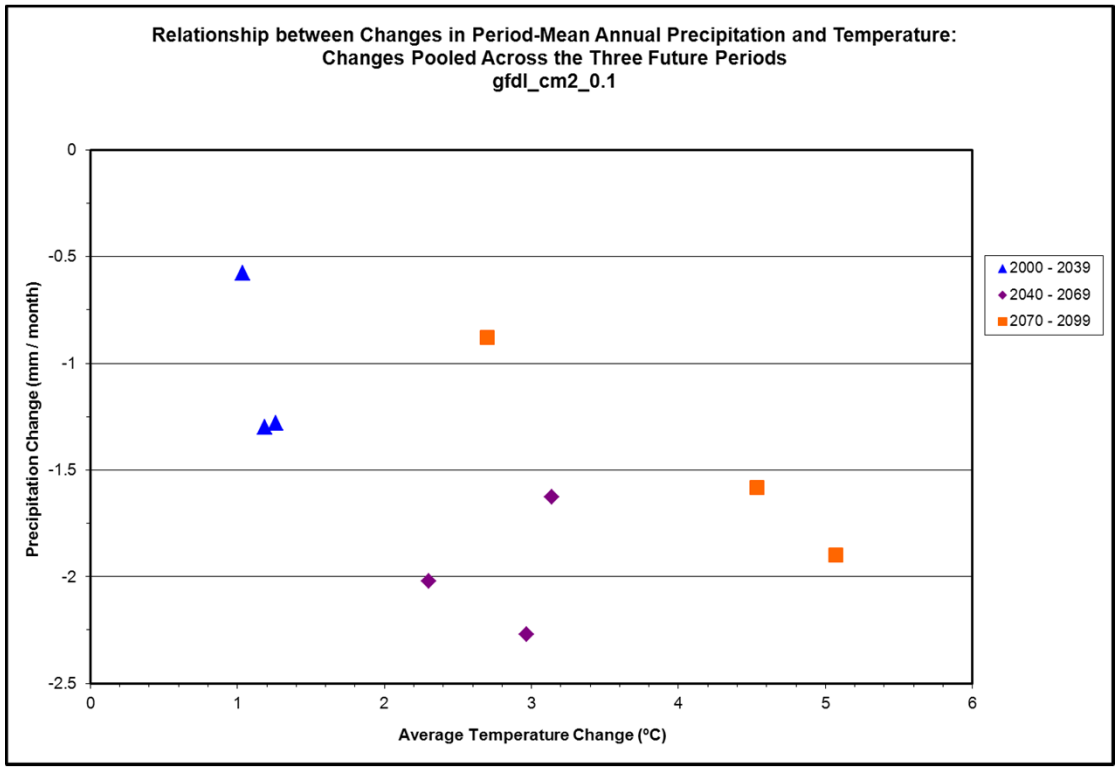

Climate Model gfdl_cm2_1.1 (page 1 of 3)

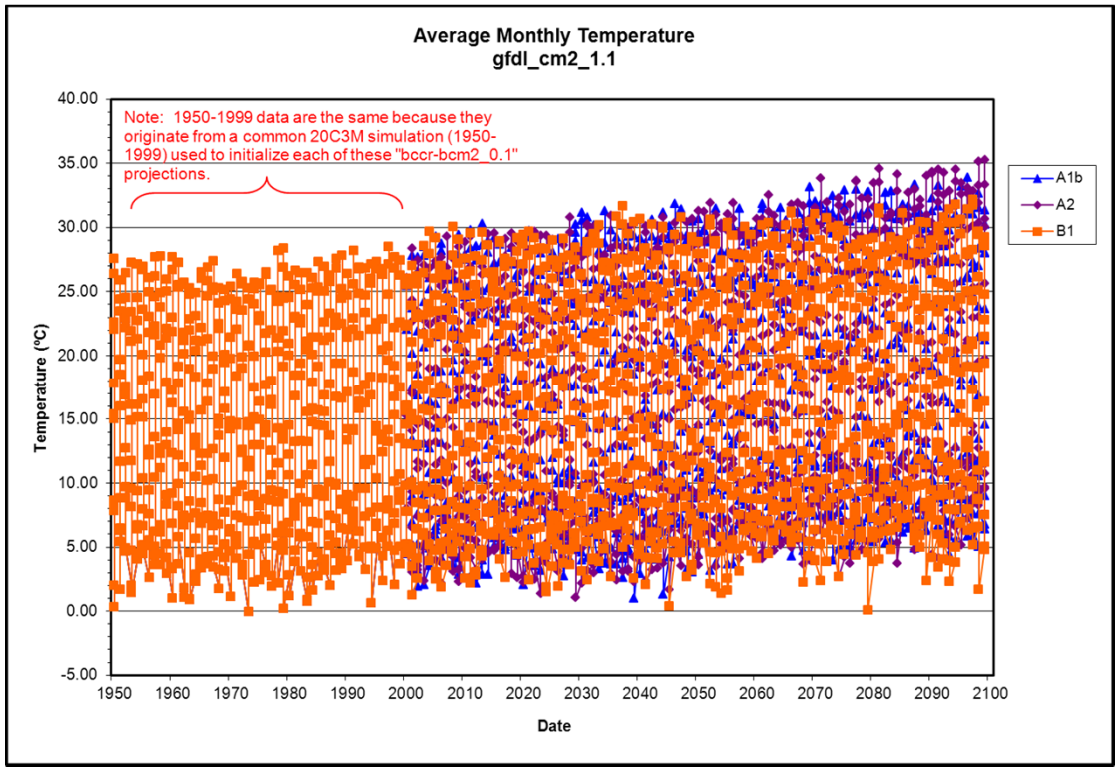

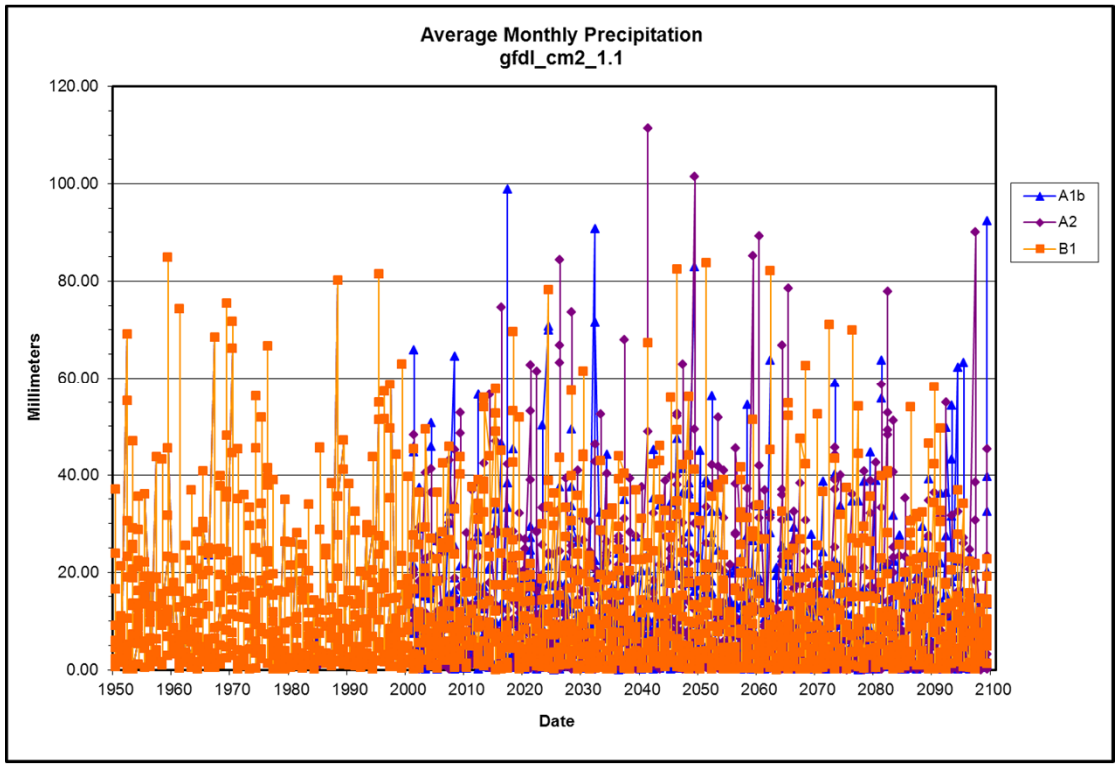

Climate Model gfdl_cm2_1.1 (page 2 of 3)

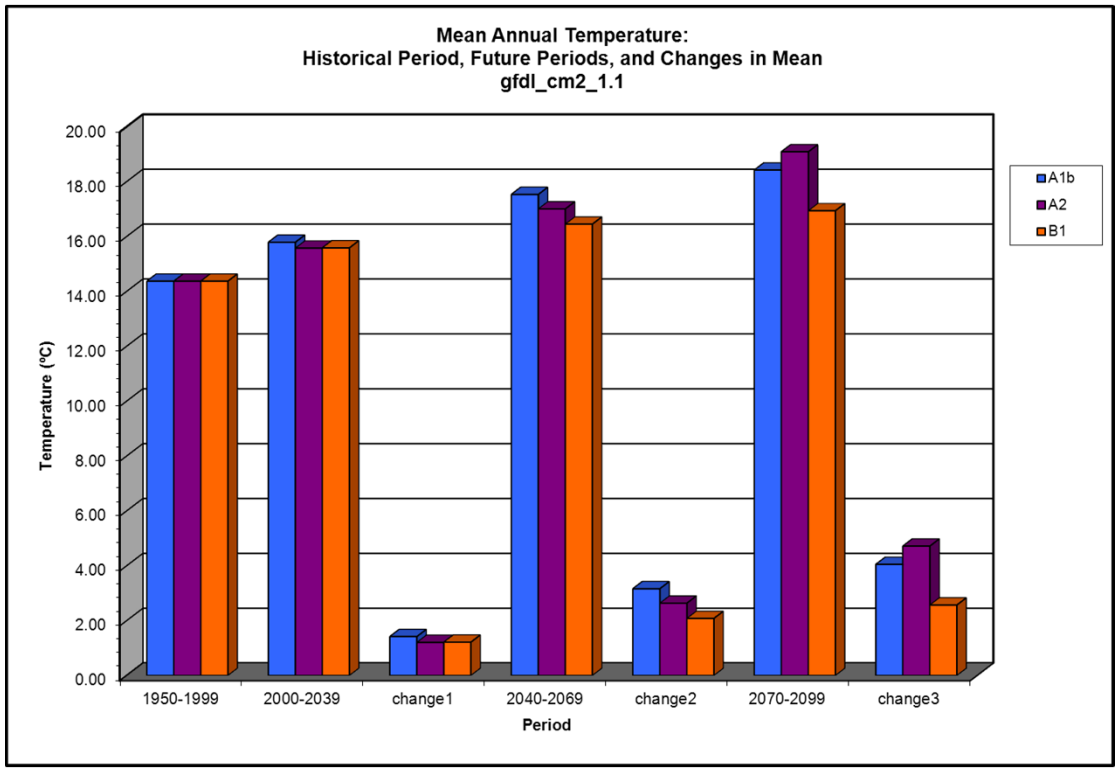

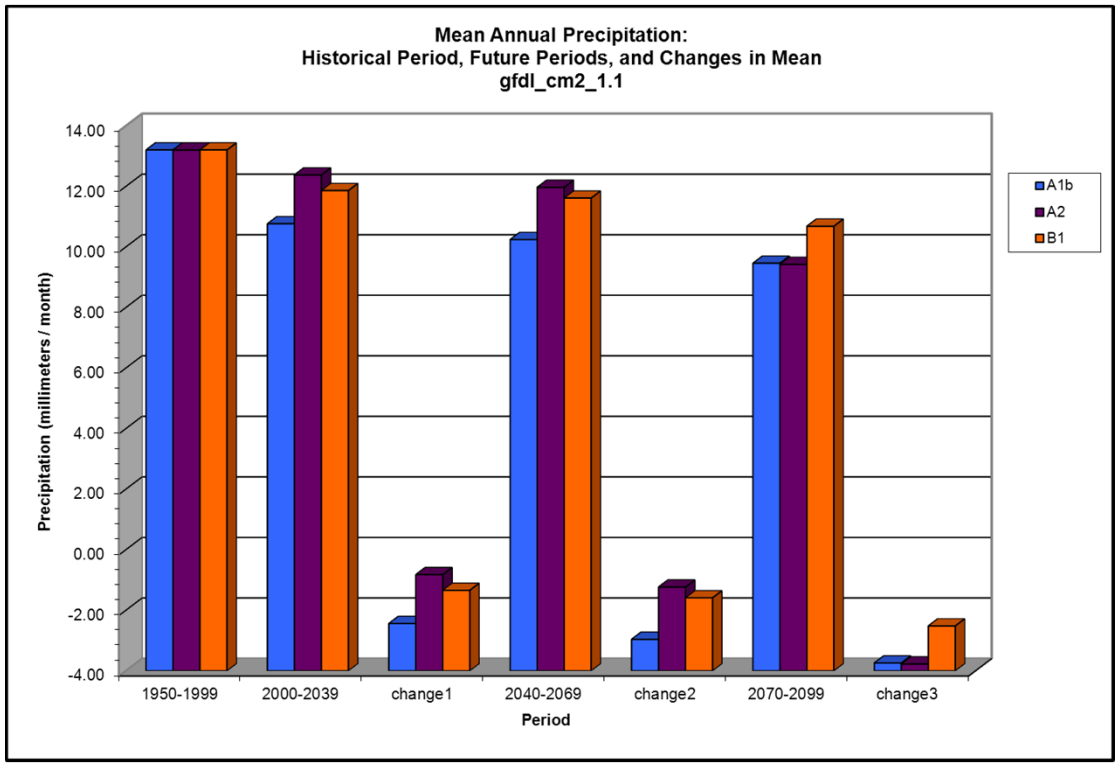

Climate Model gfdl_cm2_1.1 (page 3 of 3)

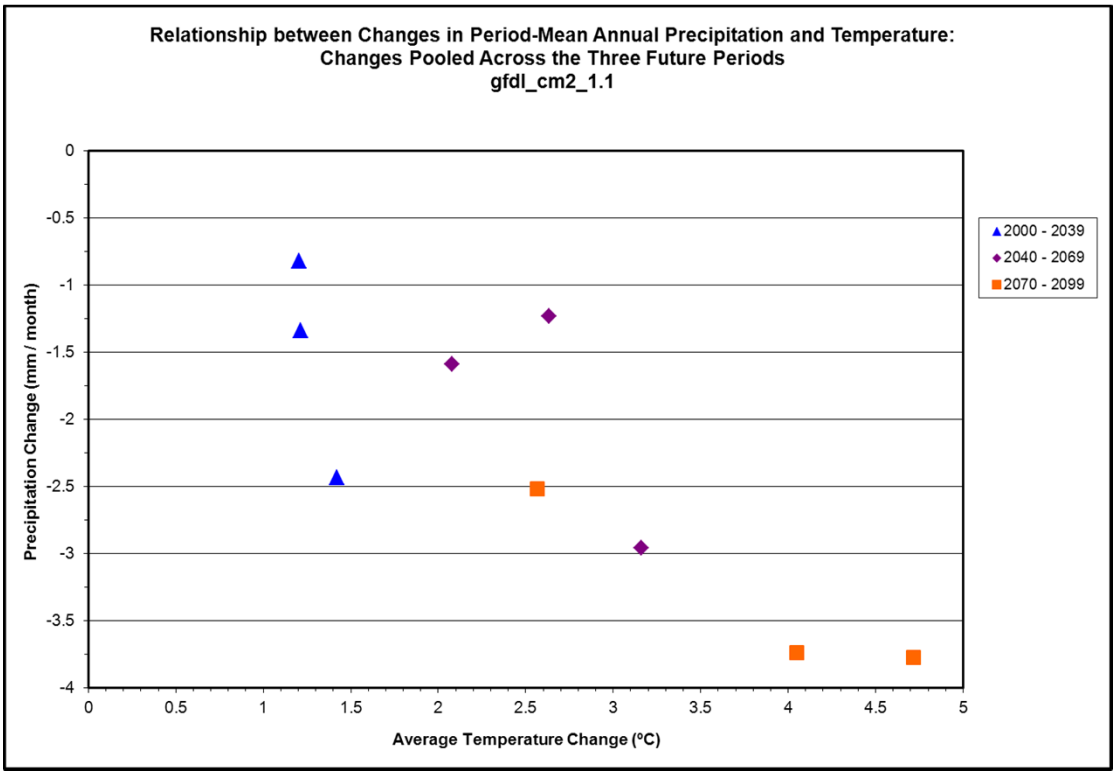

Climate Model giss_model_e_r.1 and r.2 (page 1 of 3)

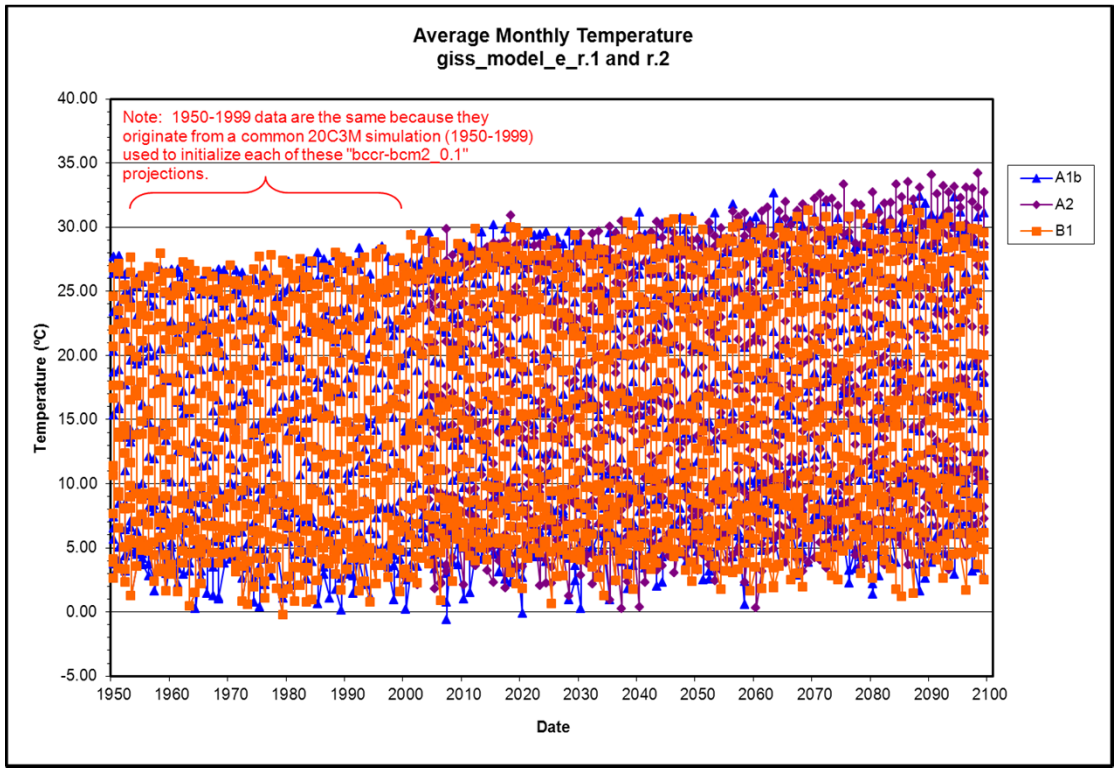

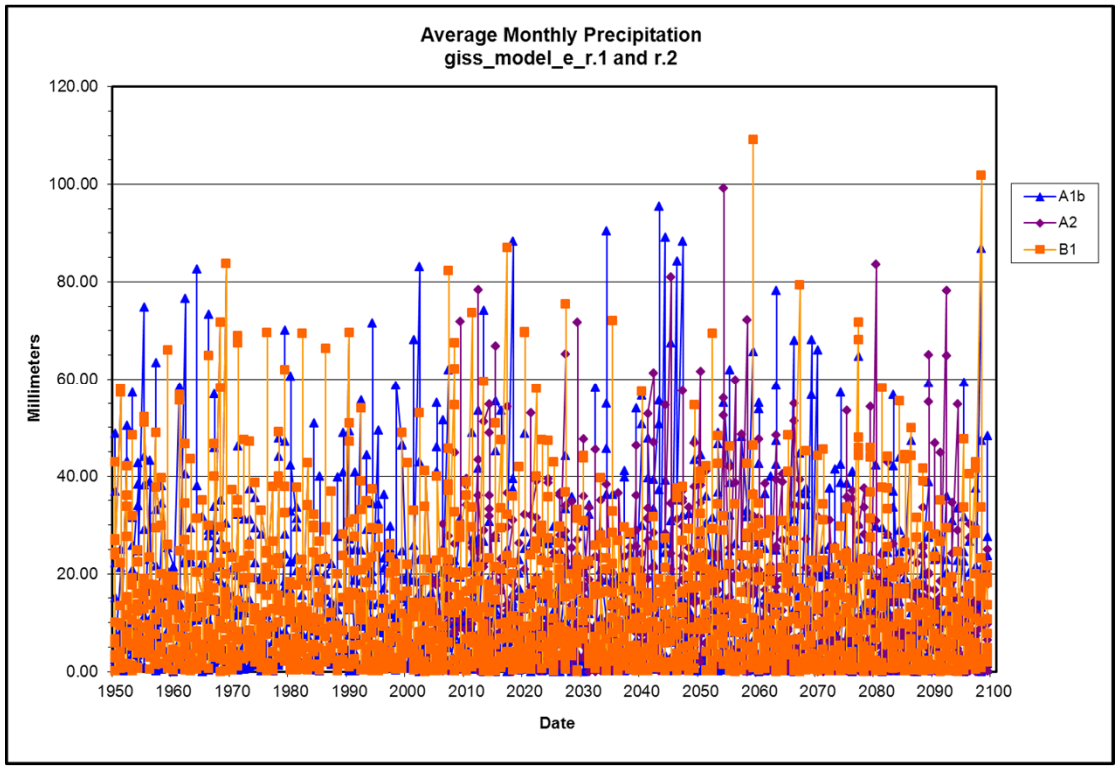

Climate Model giss_model_e_r.1 and r.2 (page 2 of 3)

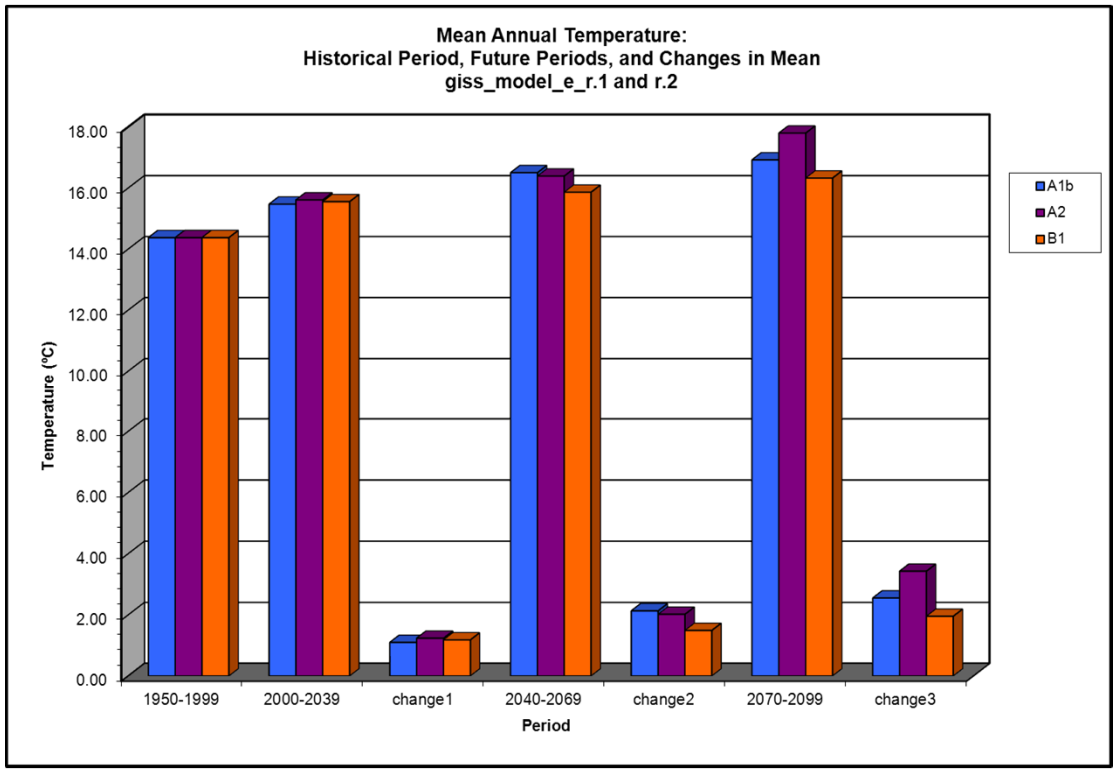

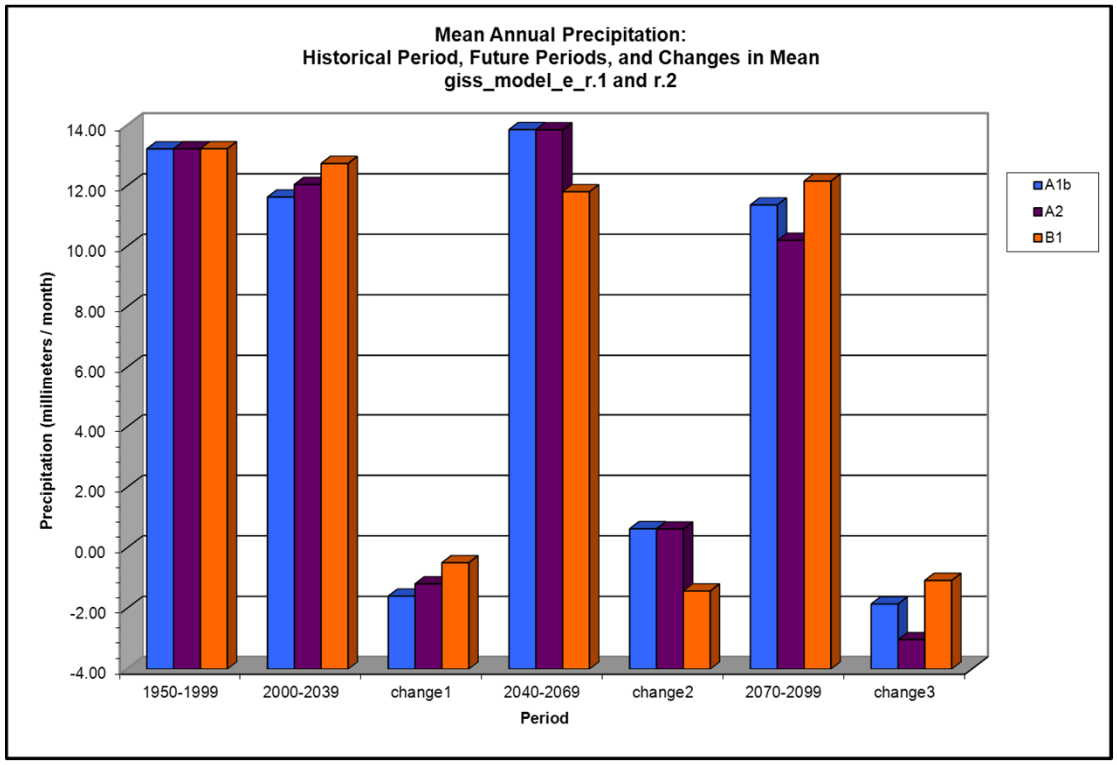

Climate Model giss_model_e_r.1 and r.2 (page 3 of 3)

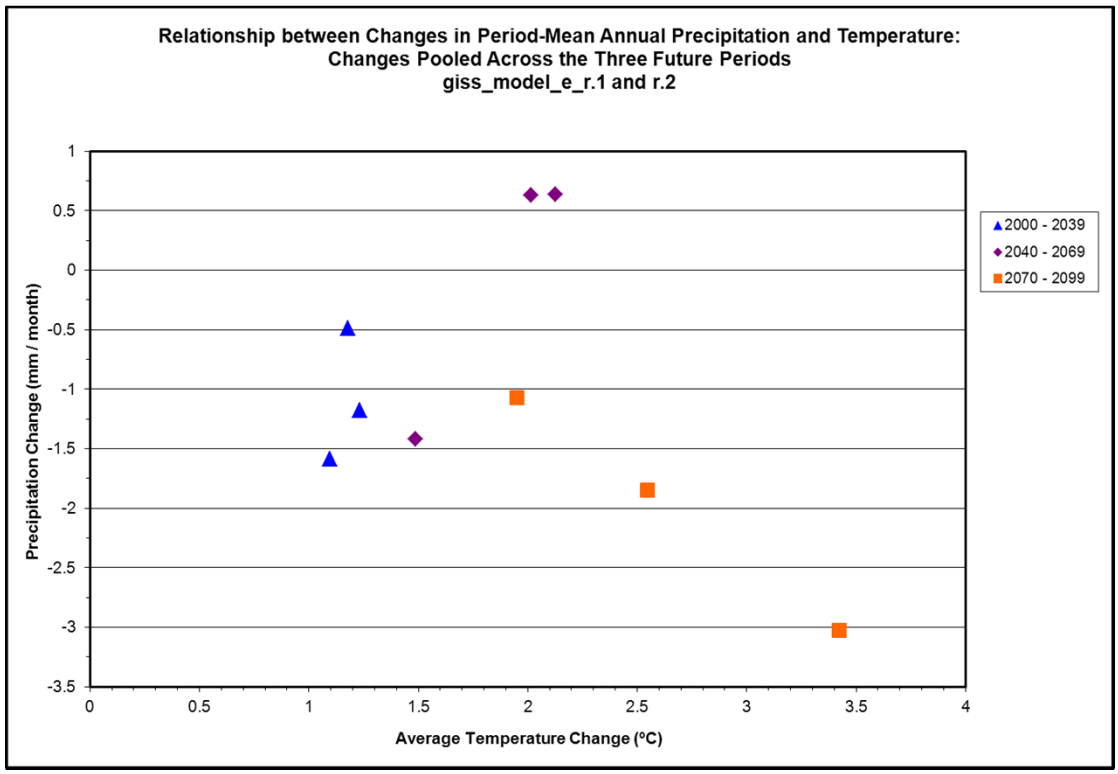

Climate Model giss_model_e_r.1 and r.4 (page 1 of 3)

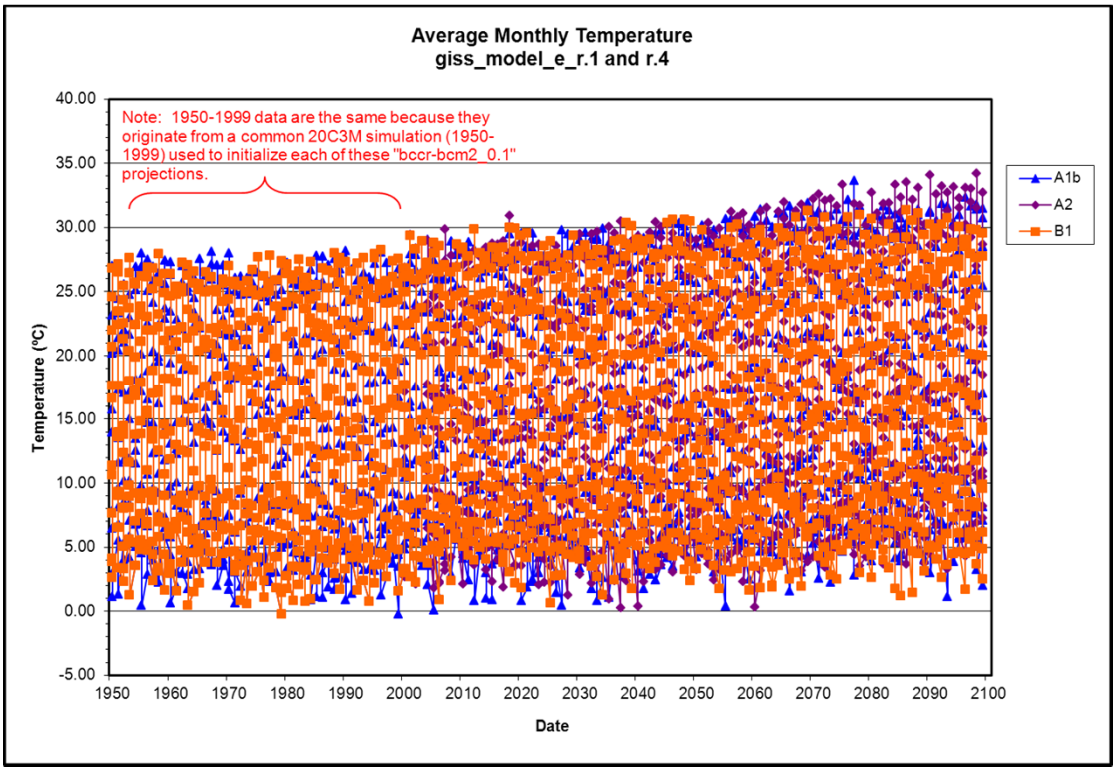

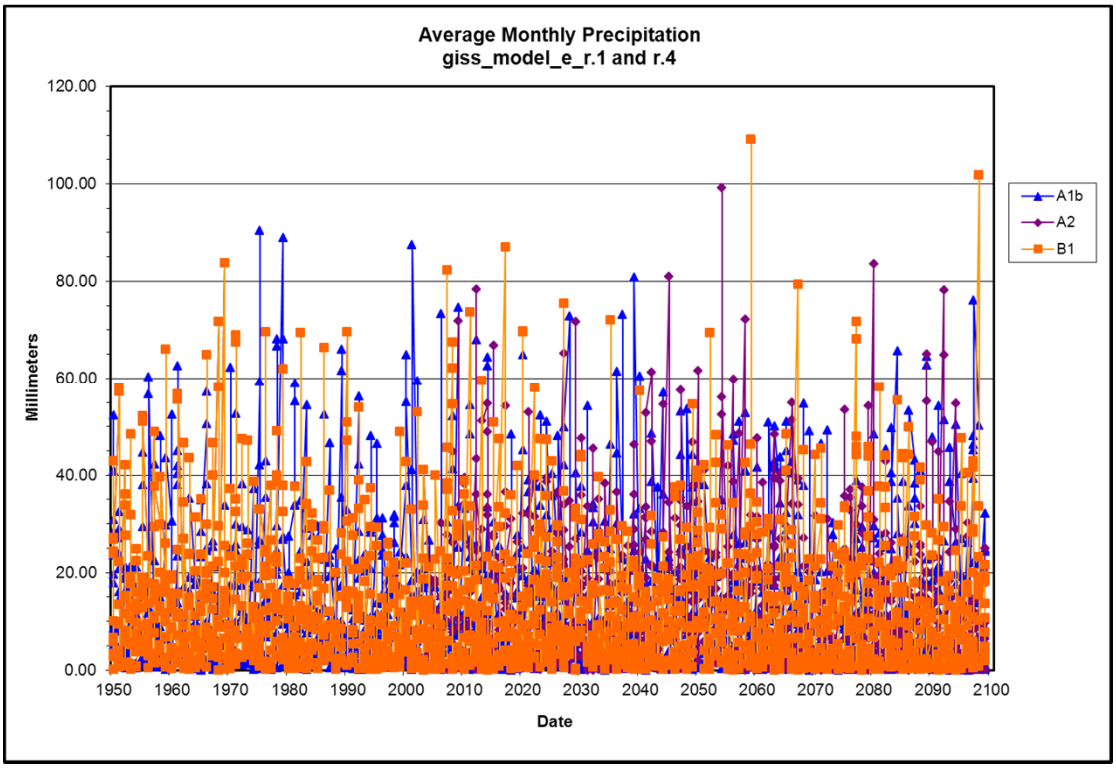

Climate Model giss_model_e_r.1 and r.4 (page 2 of 3)

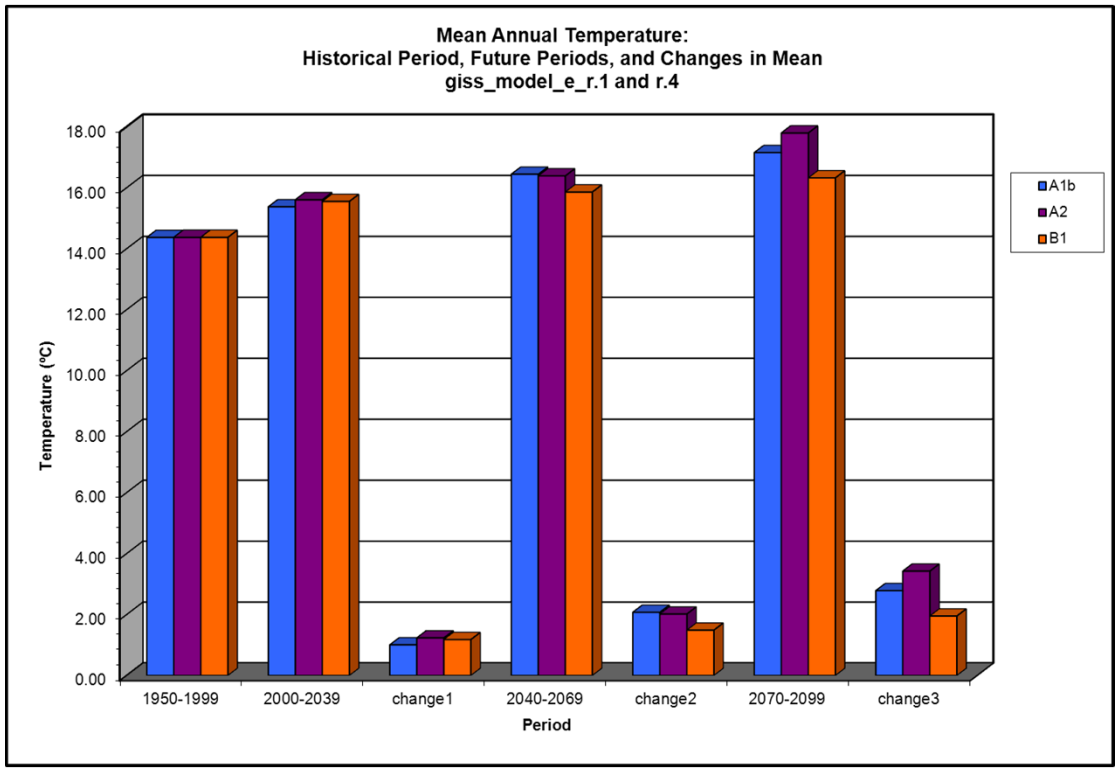

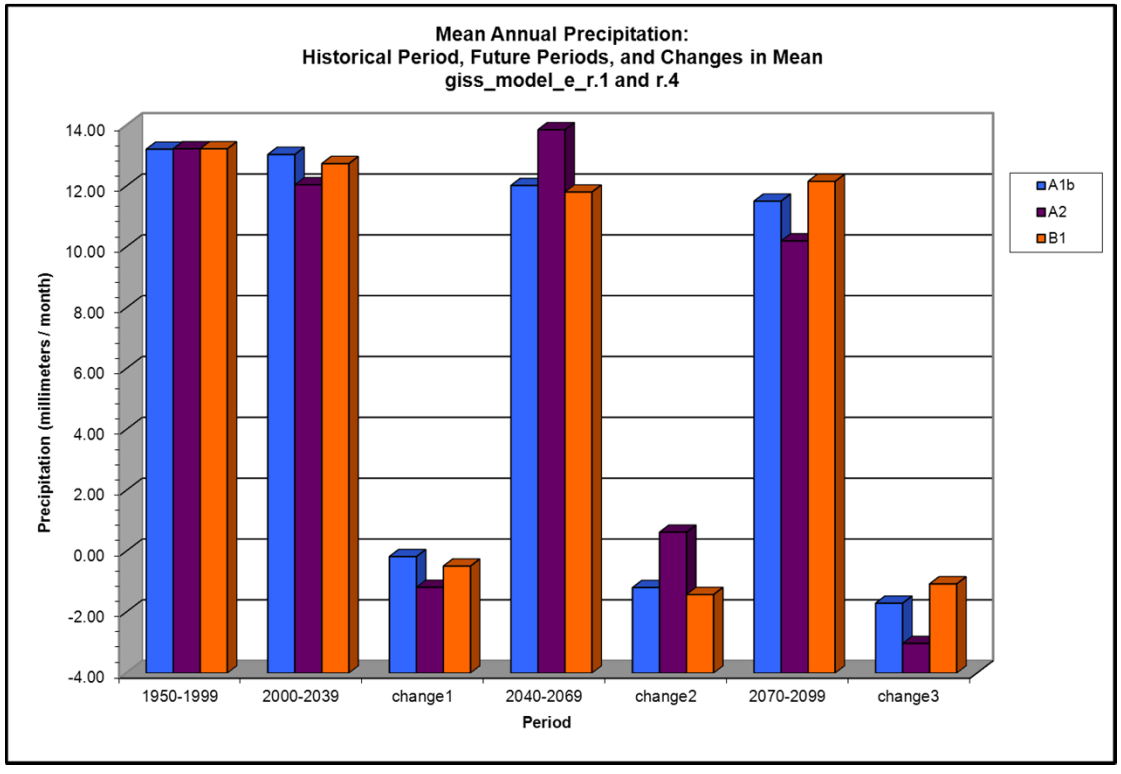

Climate Model giss_model_e_r.1 and r.4 (page 3 of 3)

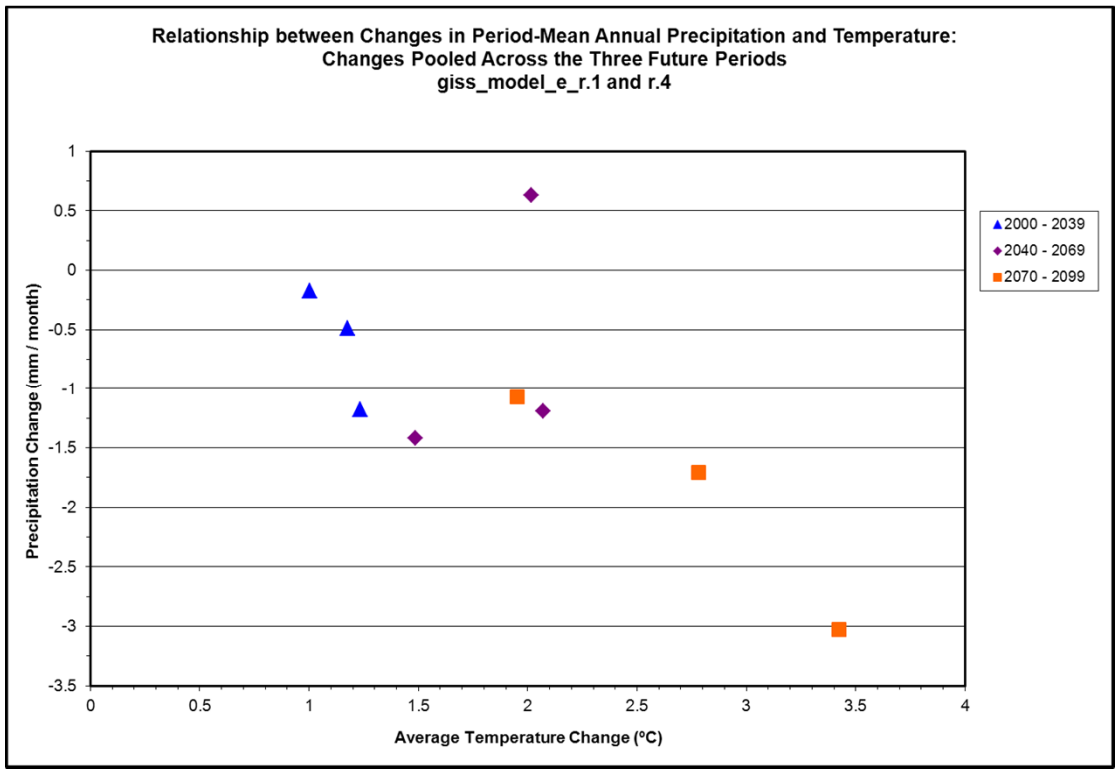

Climate Model inmcm3_0.1 (page 1 of 3)

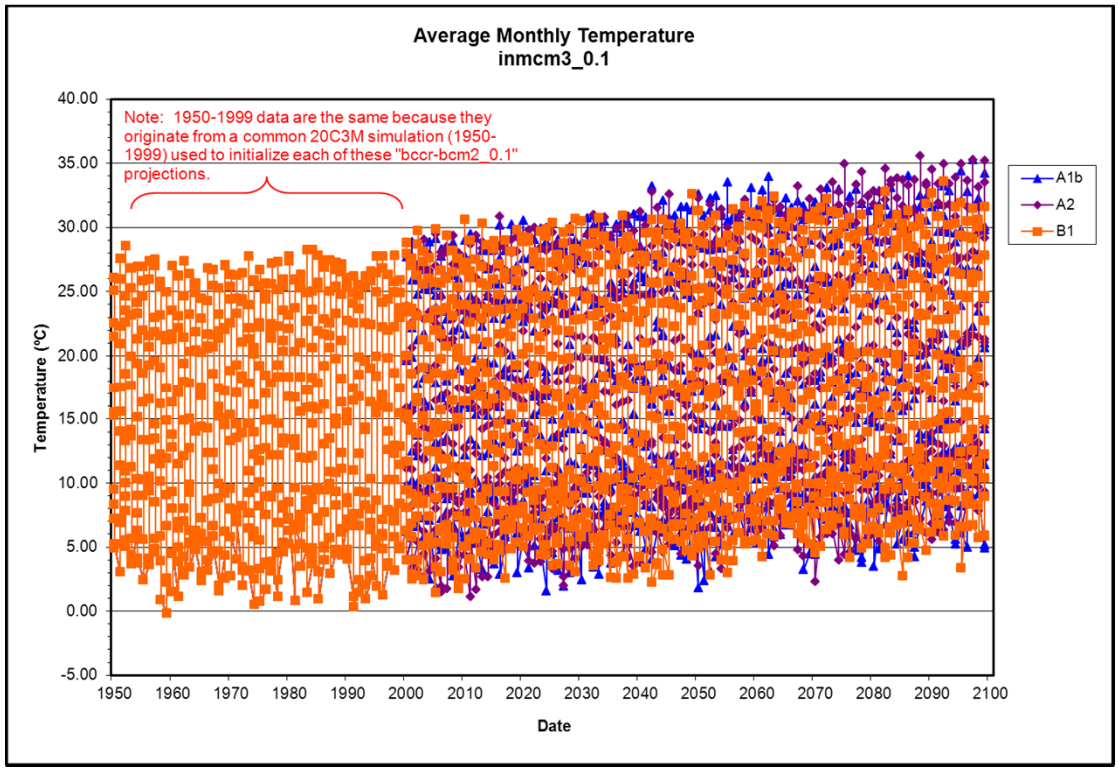

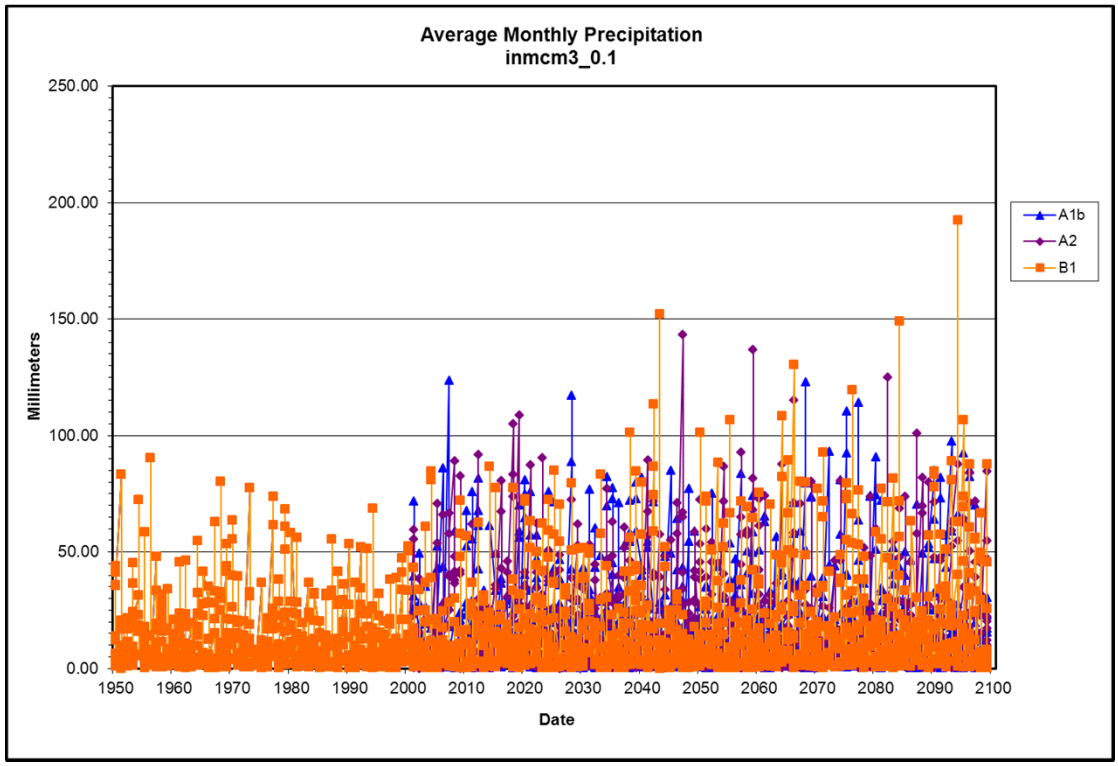

Climate Model inmcm3_0.1 (page 2 of 3)

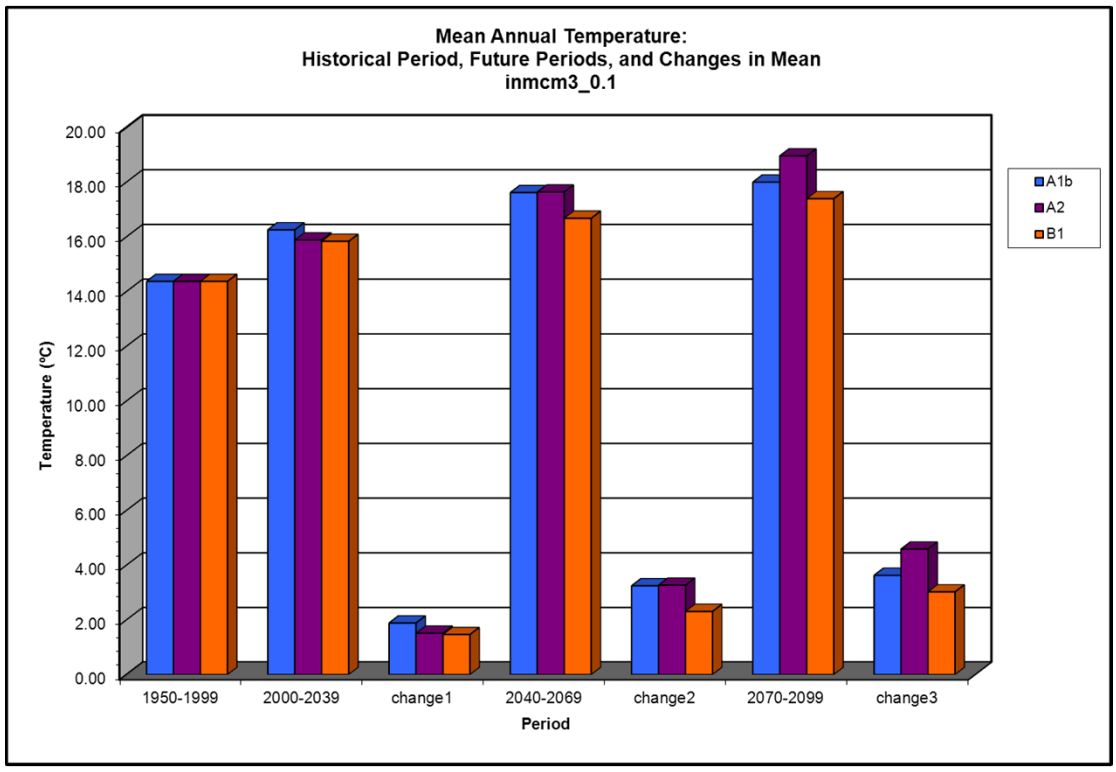

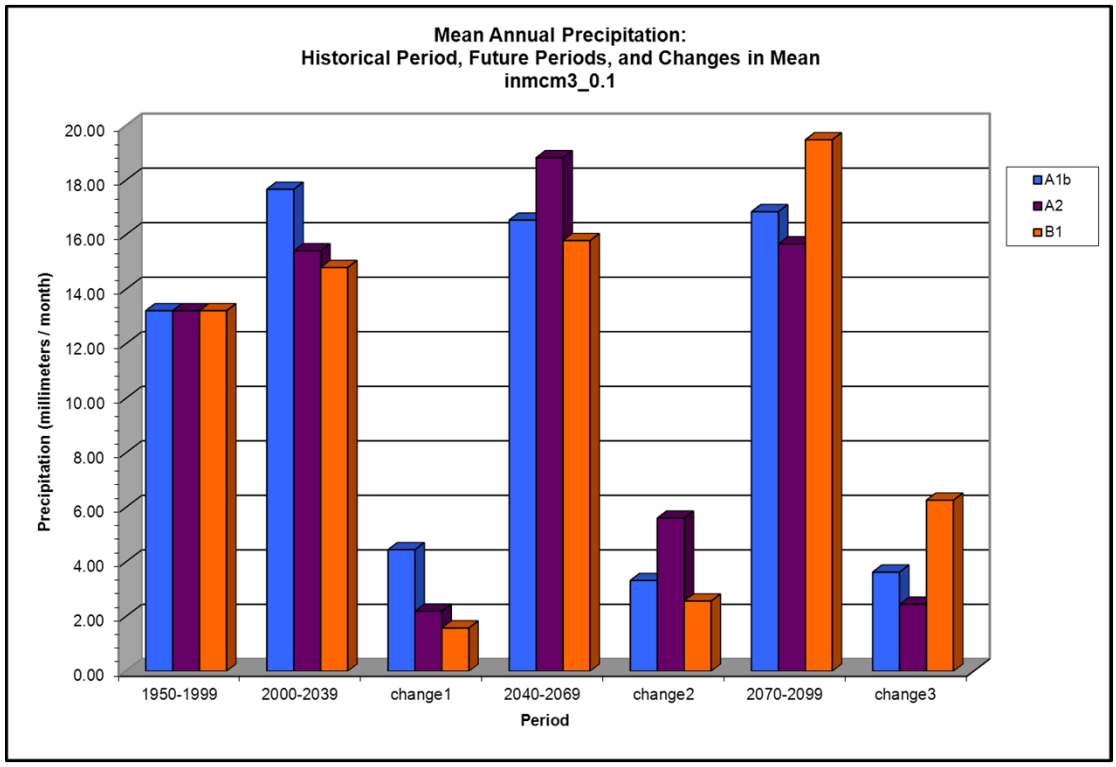

Climate Model inmcm3_0.1 (page 3 of 3)

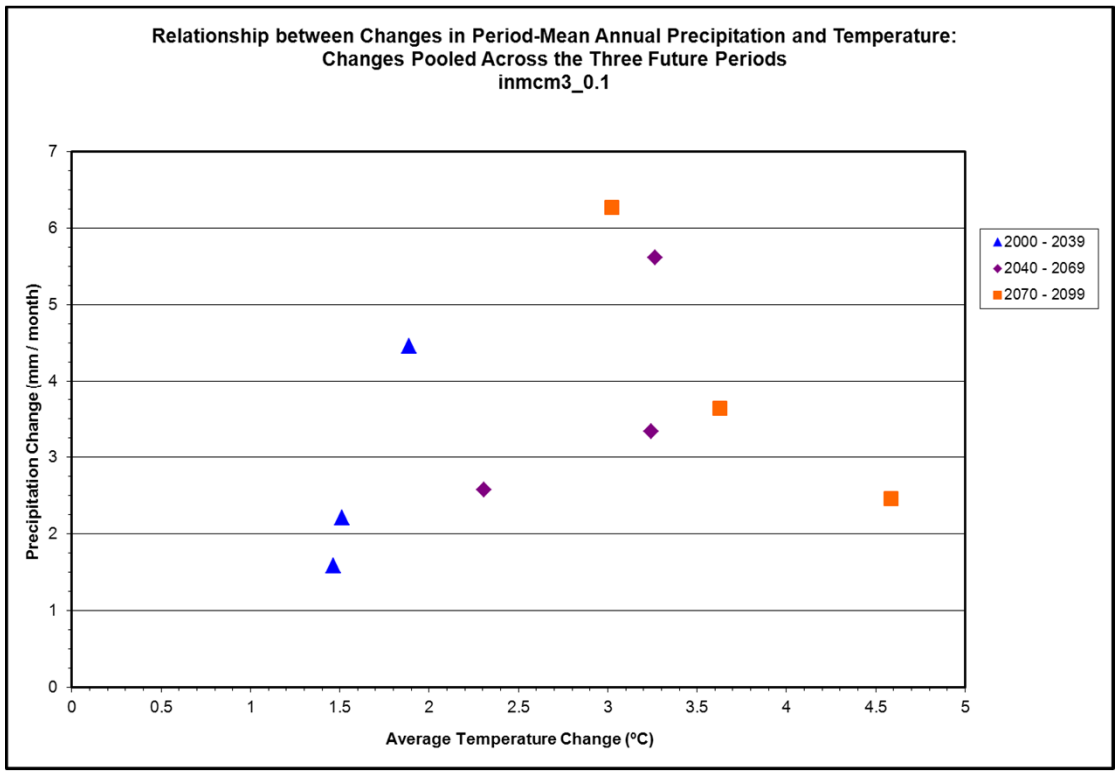

Climate Model ipsl_cm4.1 (page 1 of 3)

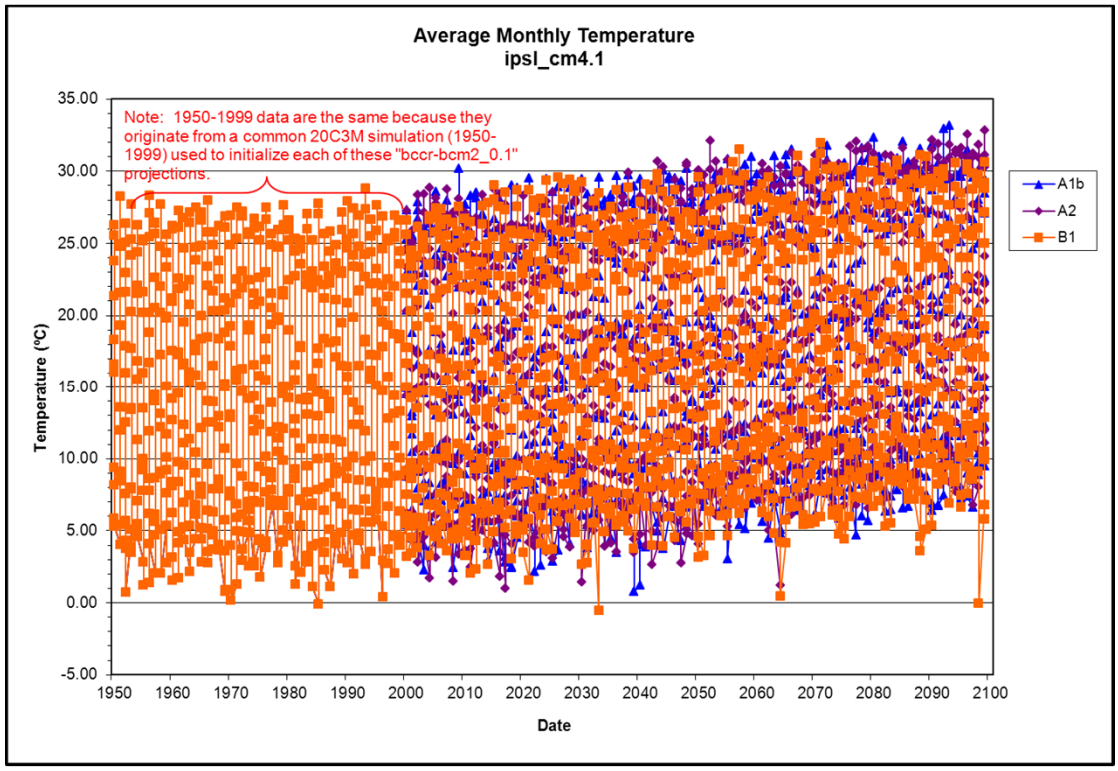

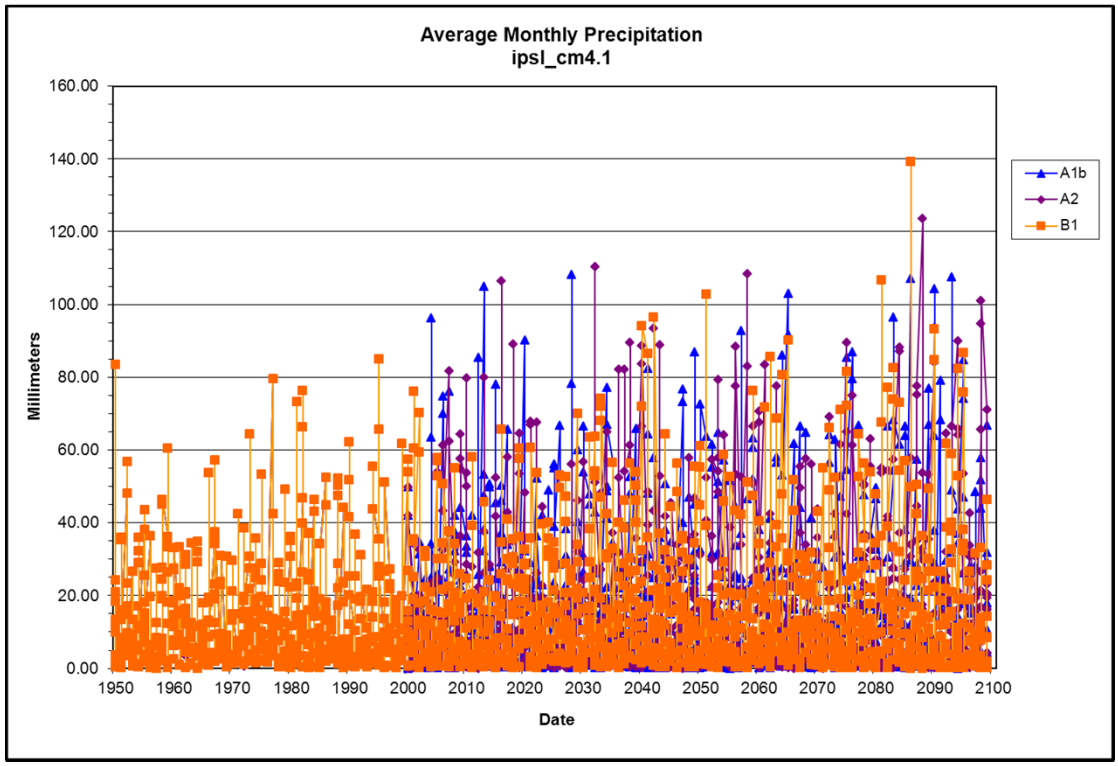

Climate Model ipsl_cm4.1 (page 2 of 3)

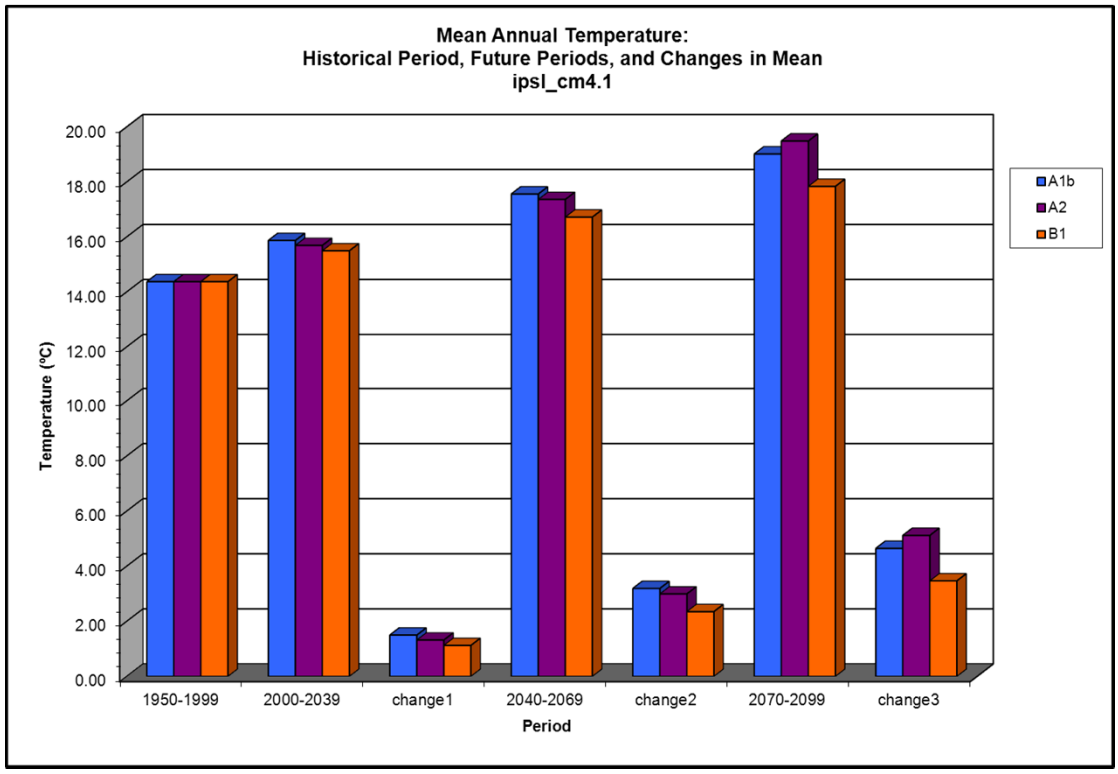

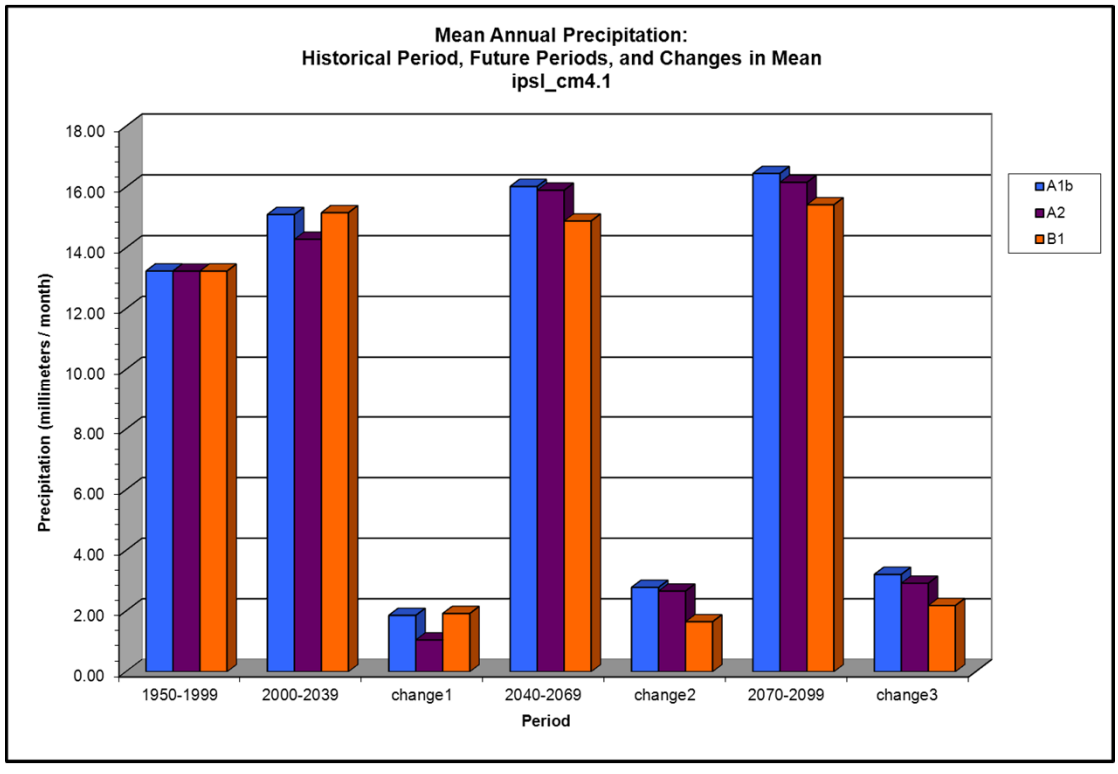

Climate Model ipsl_cm4.1 (page 3 of 3)

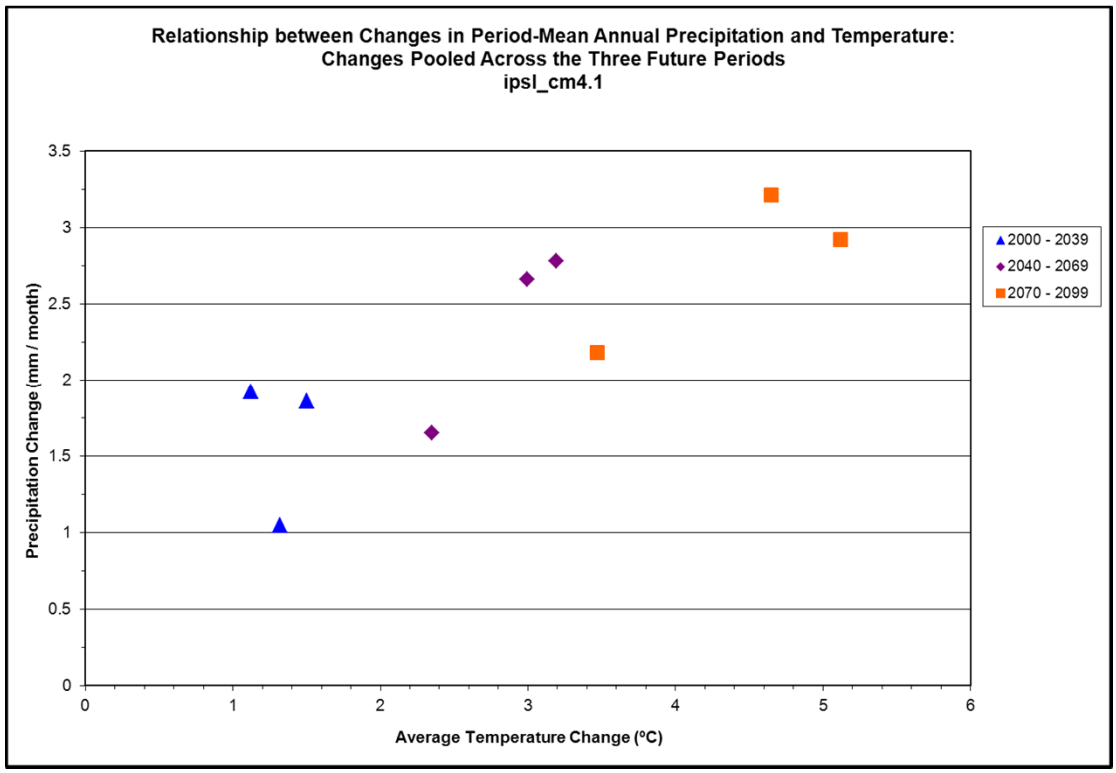

Climate Model miroc3_2_medres.1 (page 1 of 3)

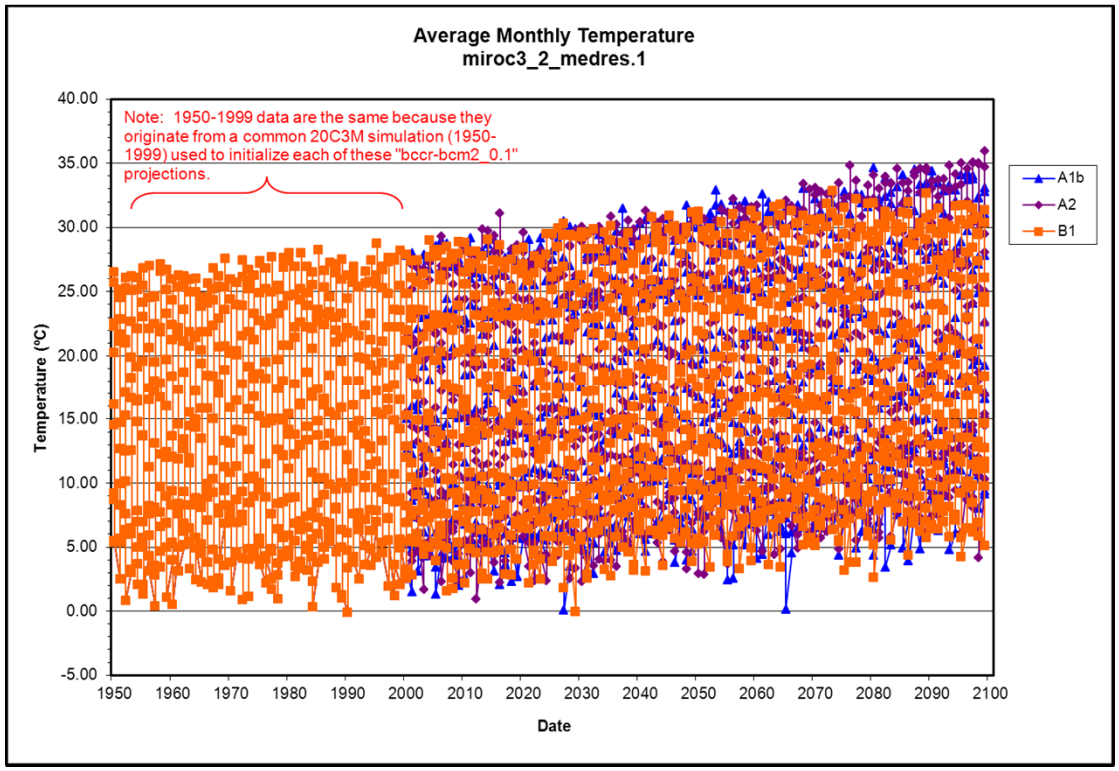

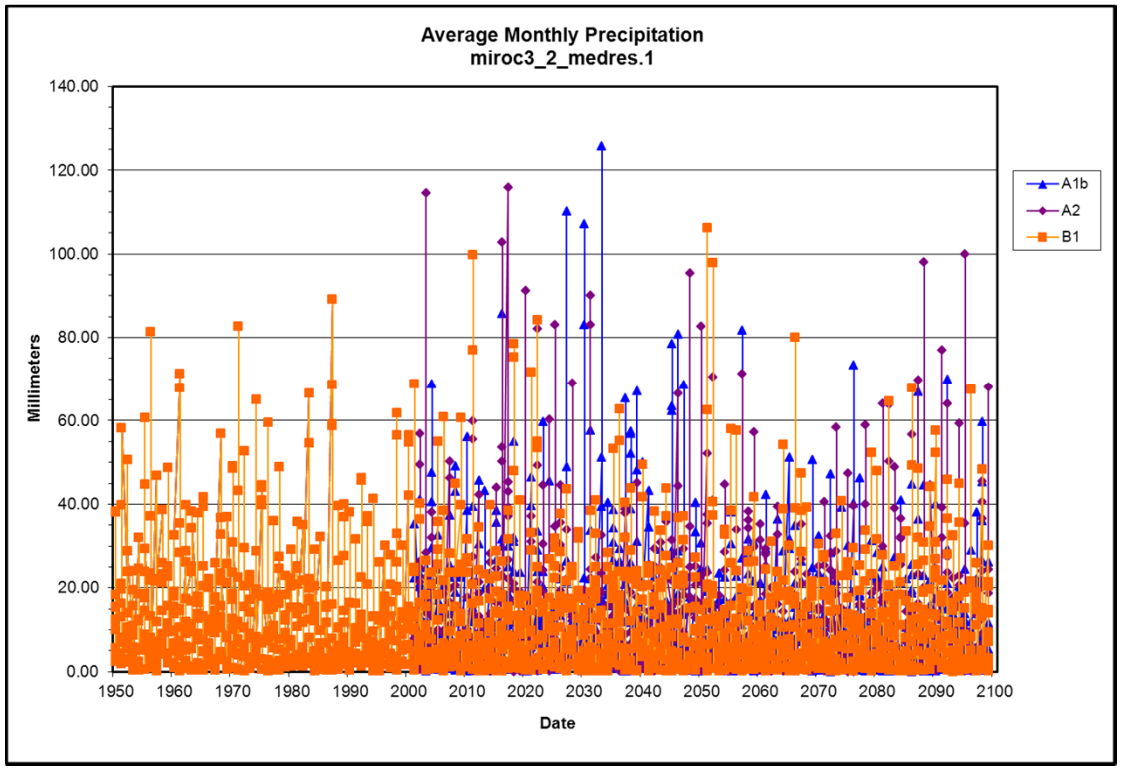

Climate Model miroc3_2_medres.1 (page 2 of 3)

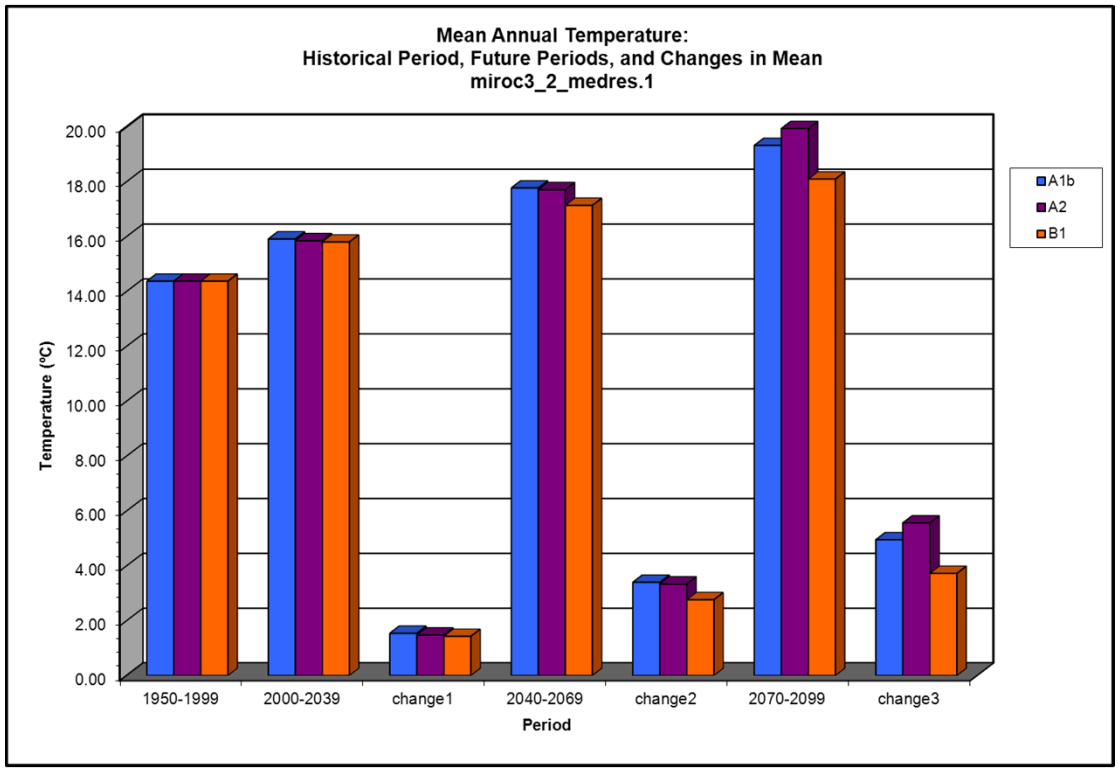

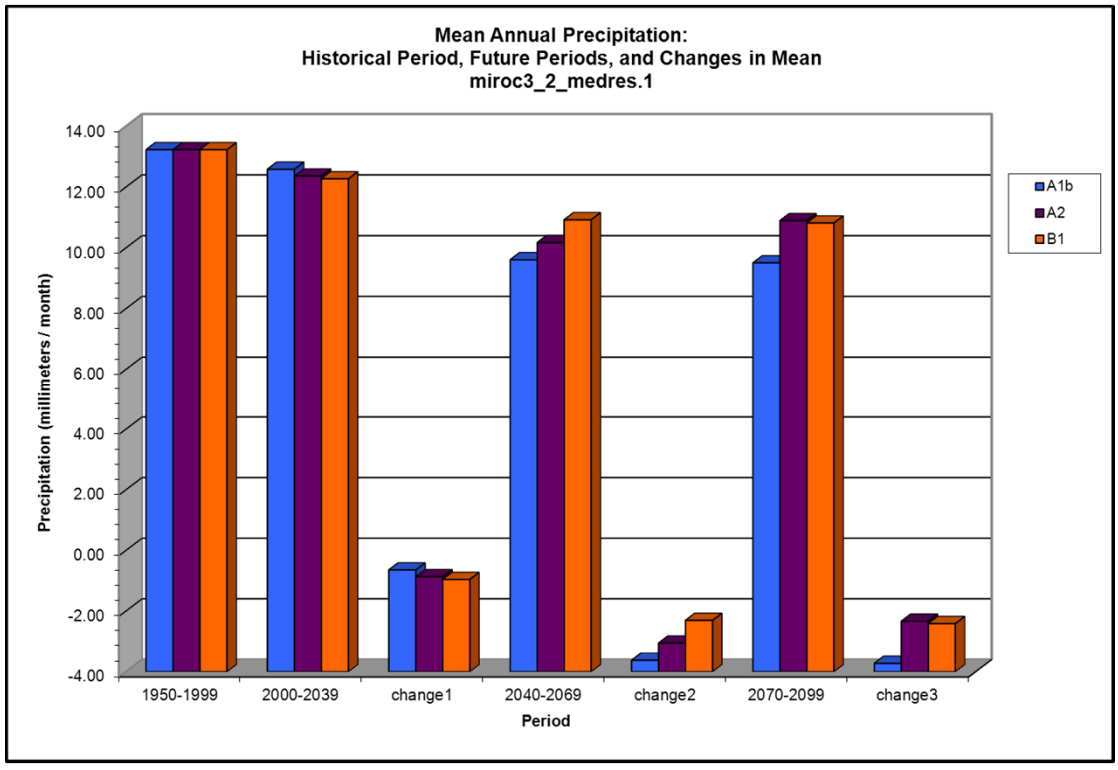

Climate Model miroc3_2_medres.1 (page 3 of 3)

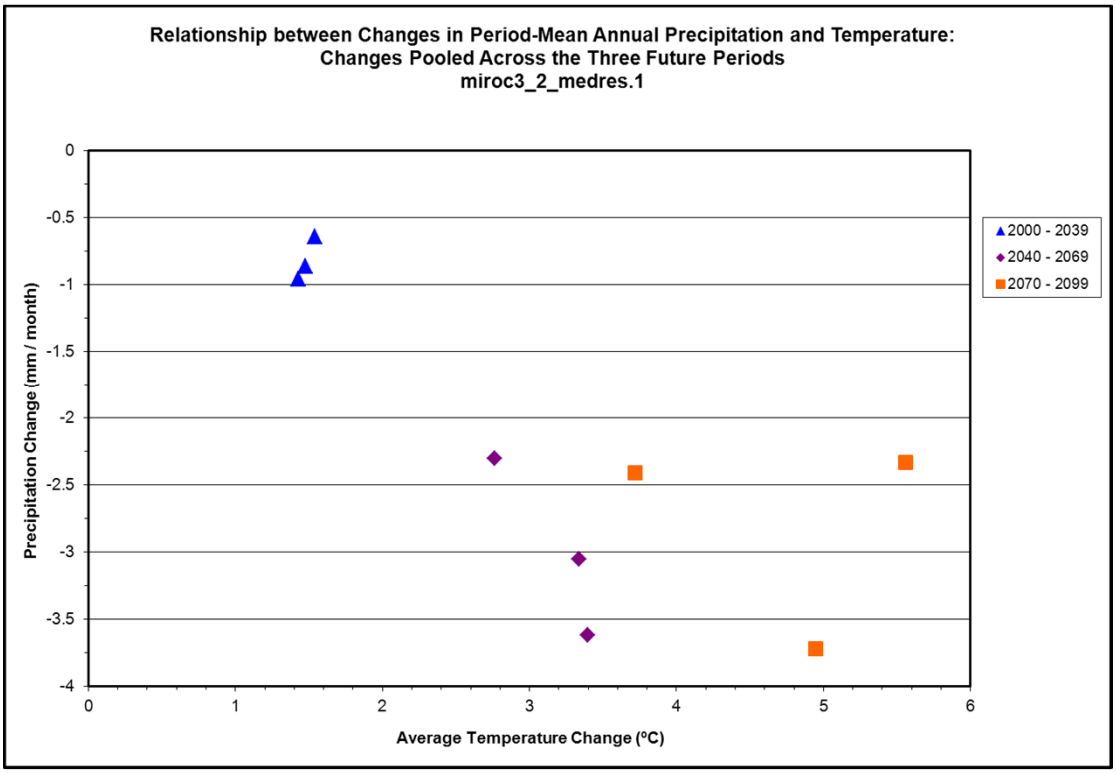

Climate Model miroc3_2_medres.2 (page 1 of 3)

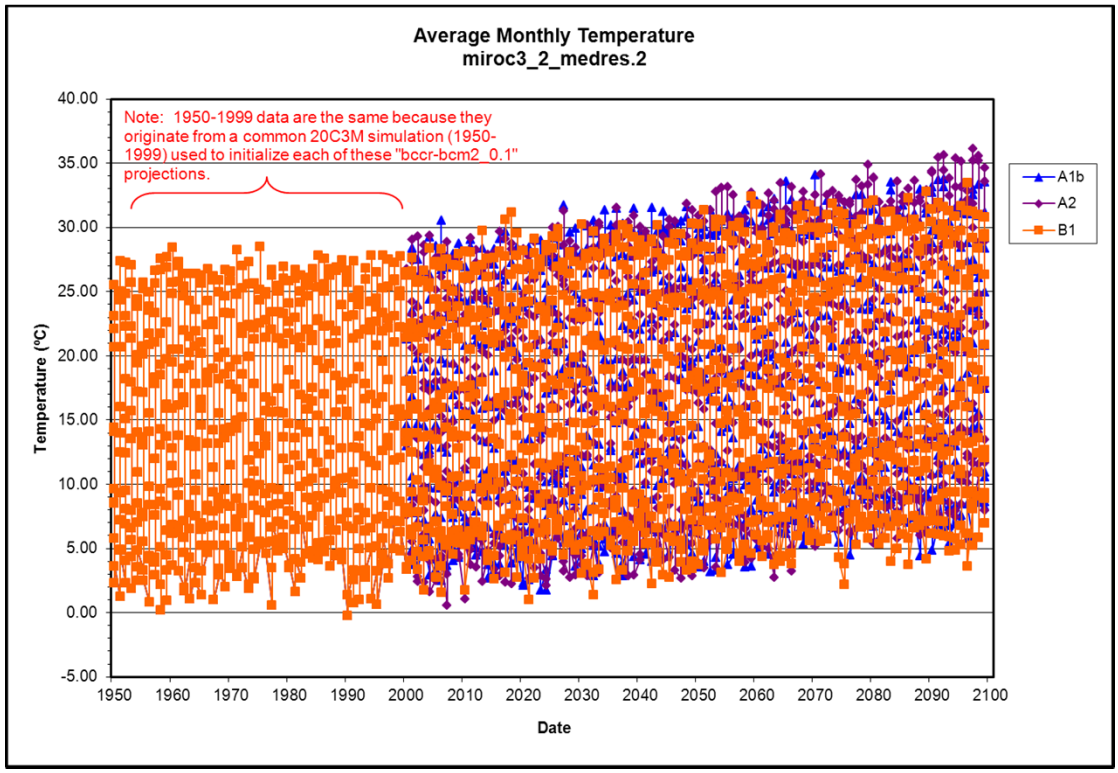

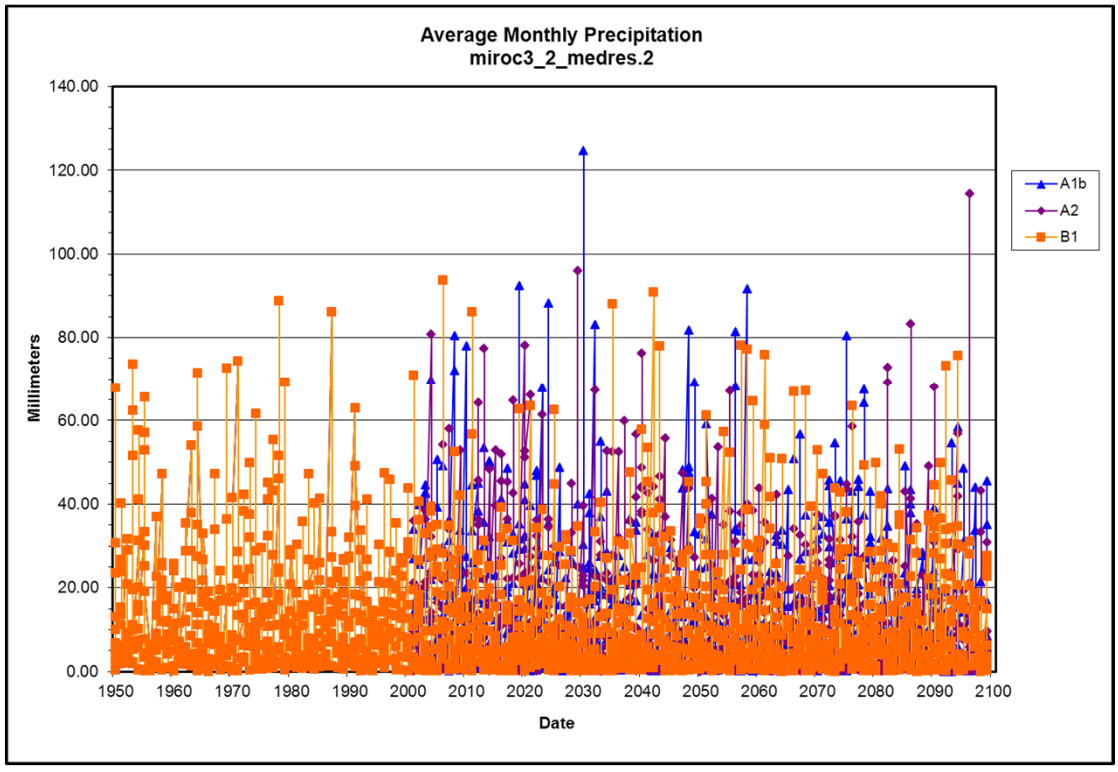

Climate Model miroc3_2_medres.2 (page 2 of 3)

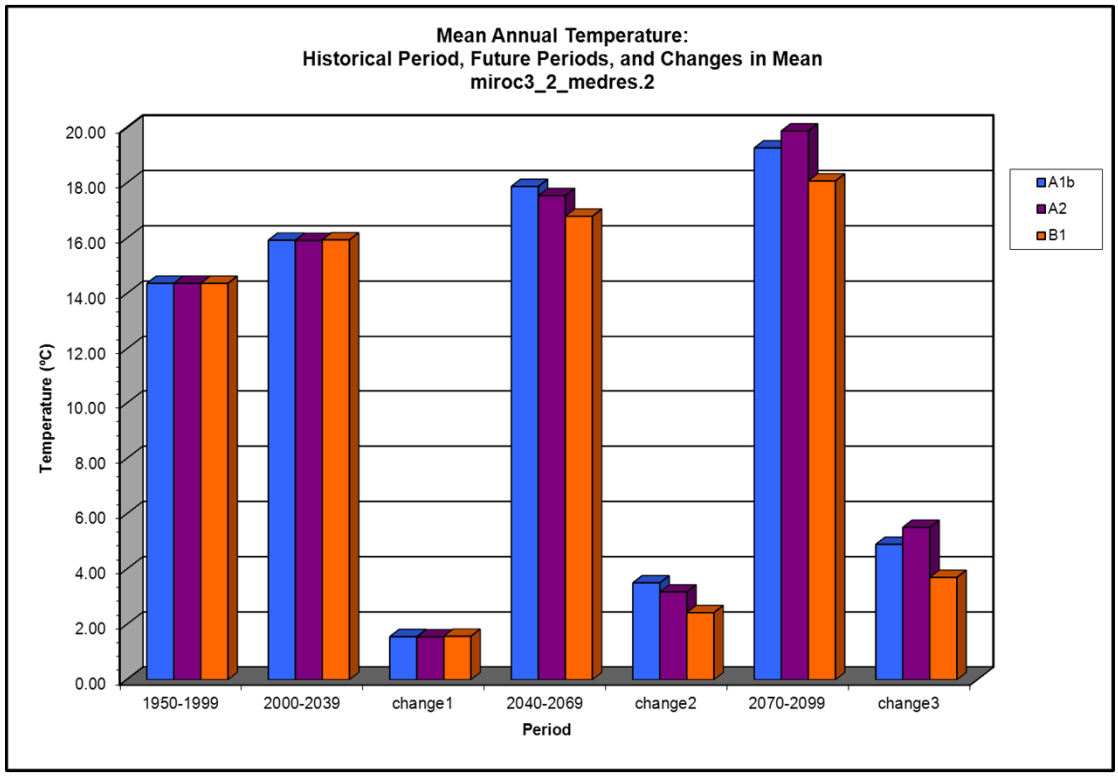

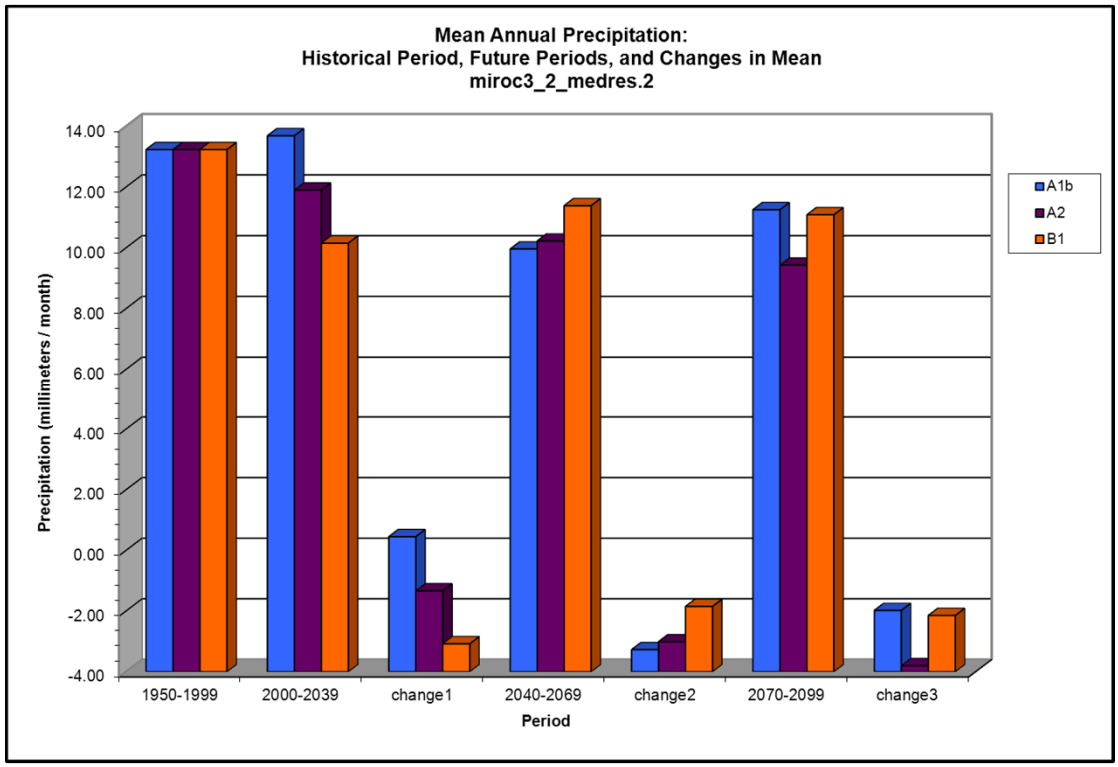

Climate Model miroc3_2_medres.2 (page 3 of 3)

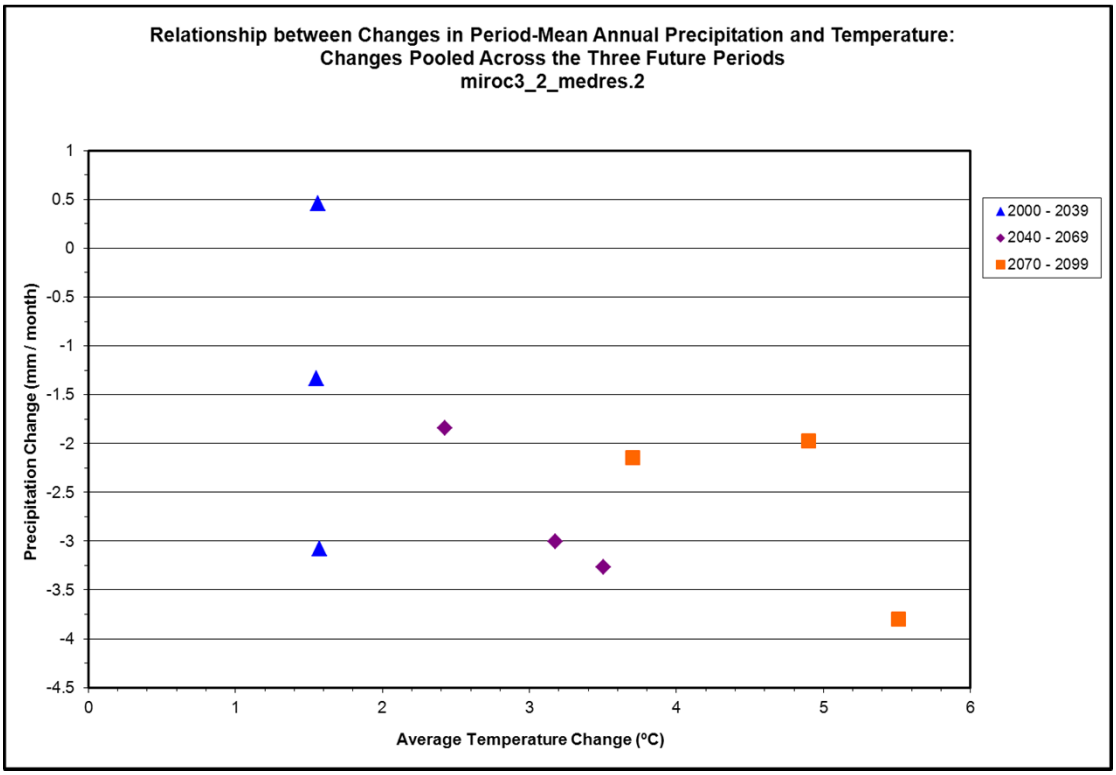

Climate Model miroc3_2_medres.3 (page 1 of 3)

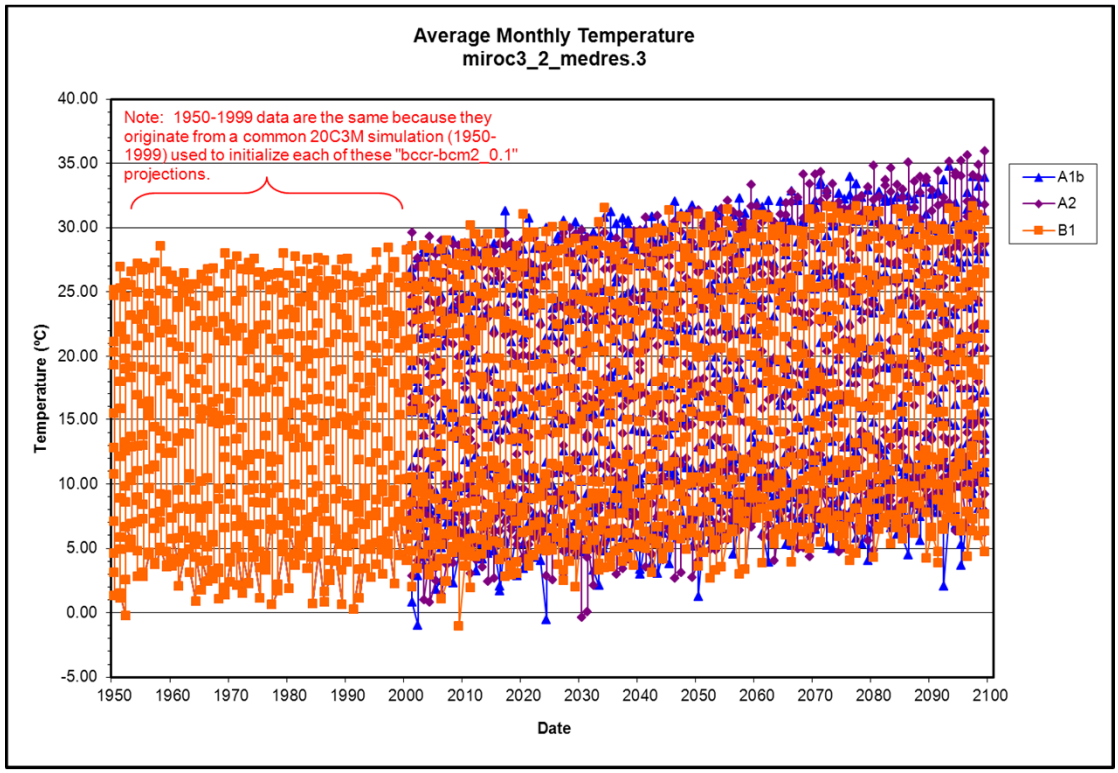

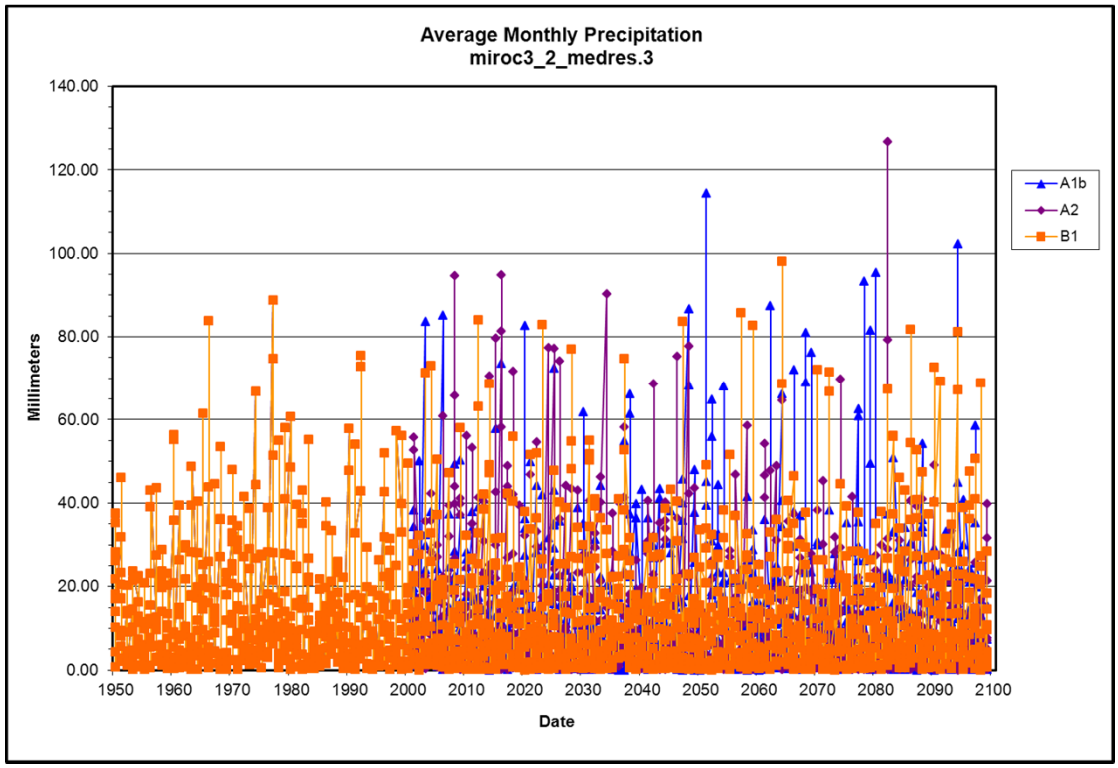

Climate Model miroc3_2_medres.3 (page 2 of 3)

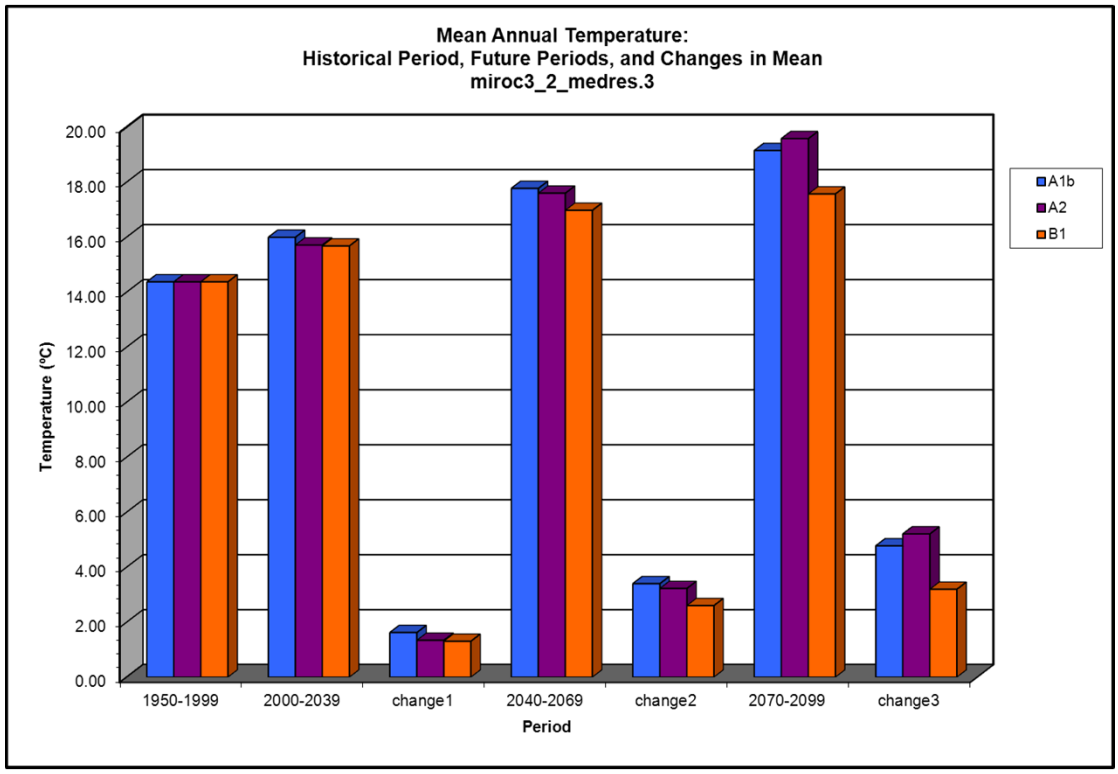

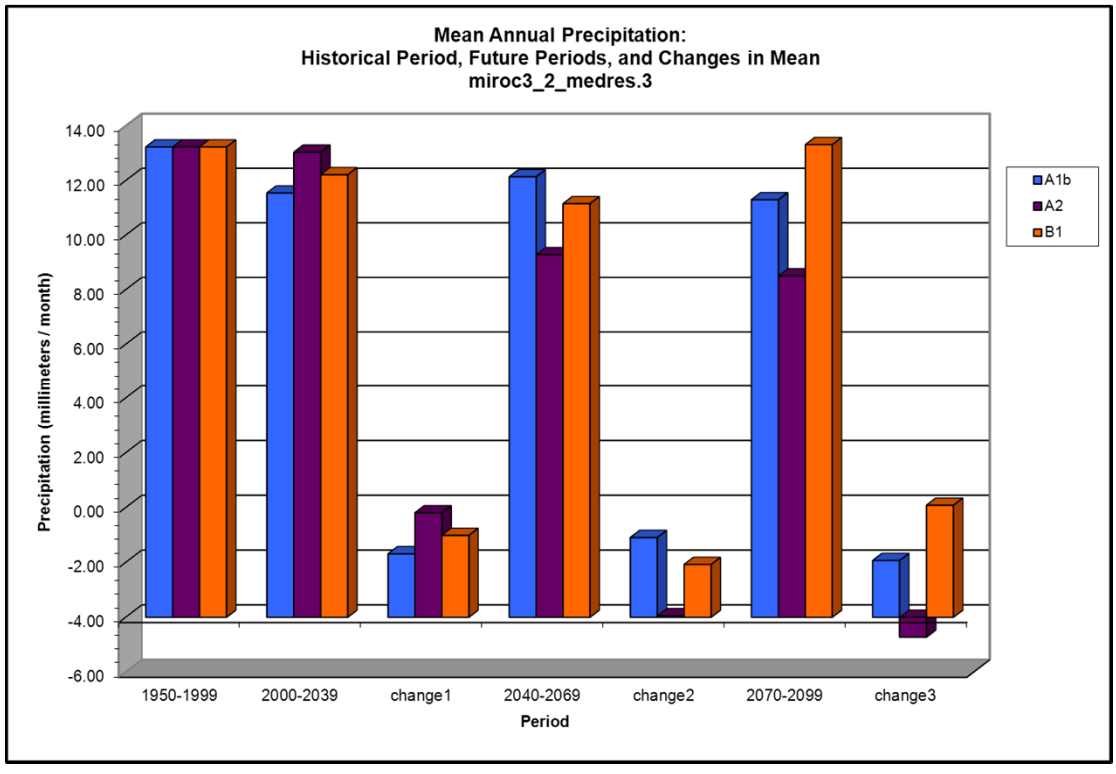

Climate Model miroc3_2_medres.3 (page 3 of 3)

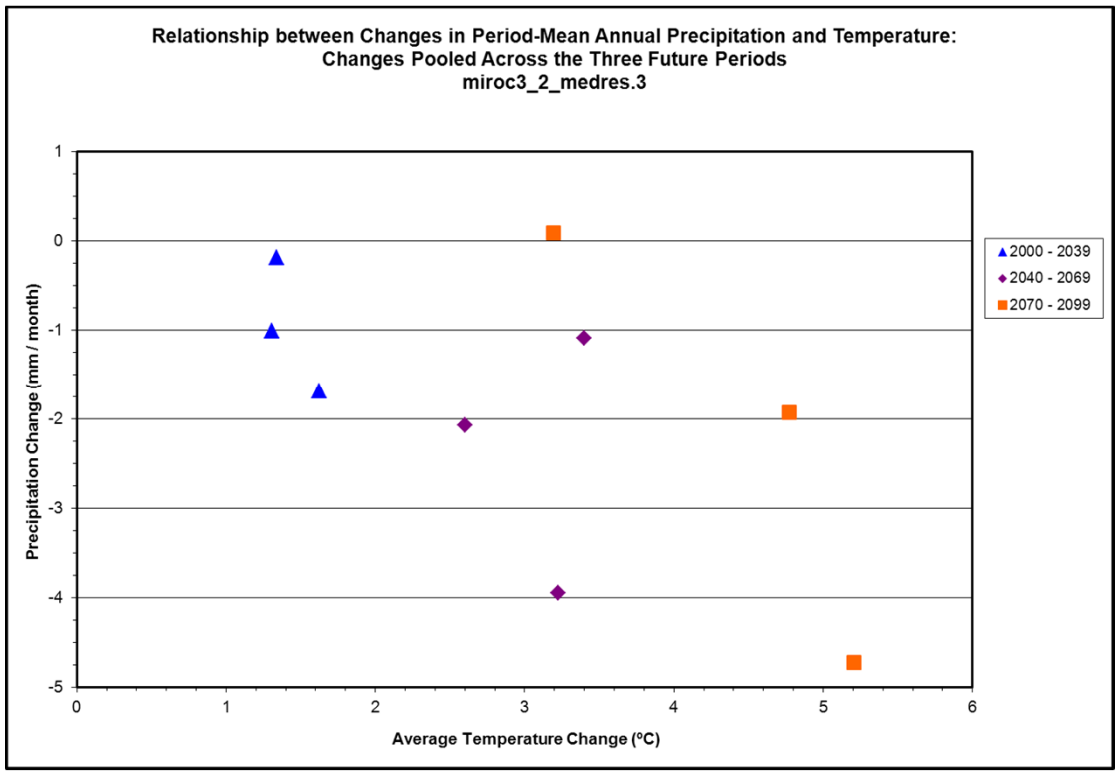

Climate Model miub_echo_g.1 (page 1 of 3)

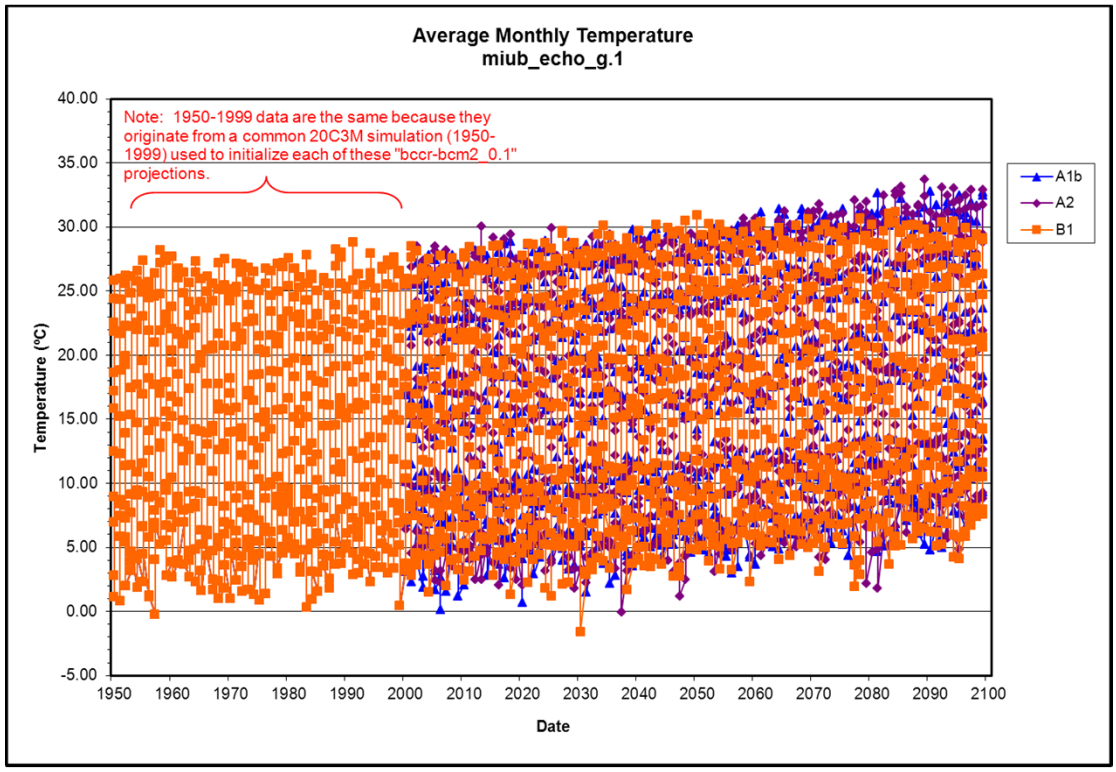

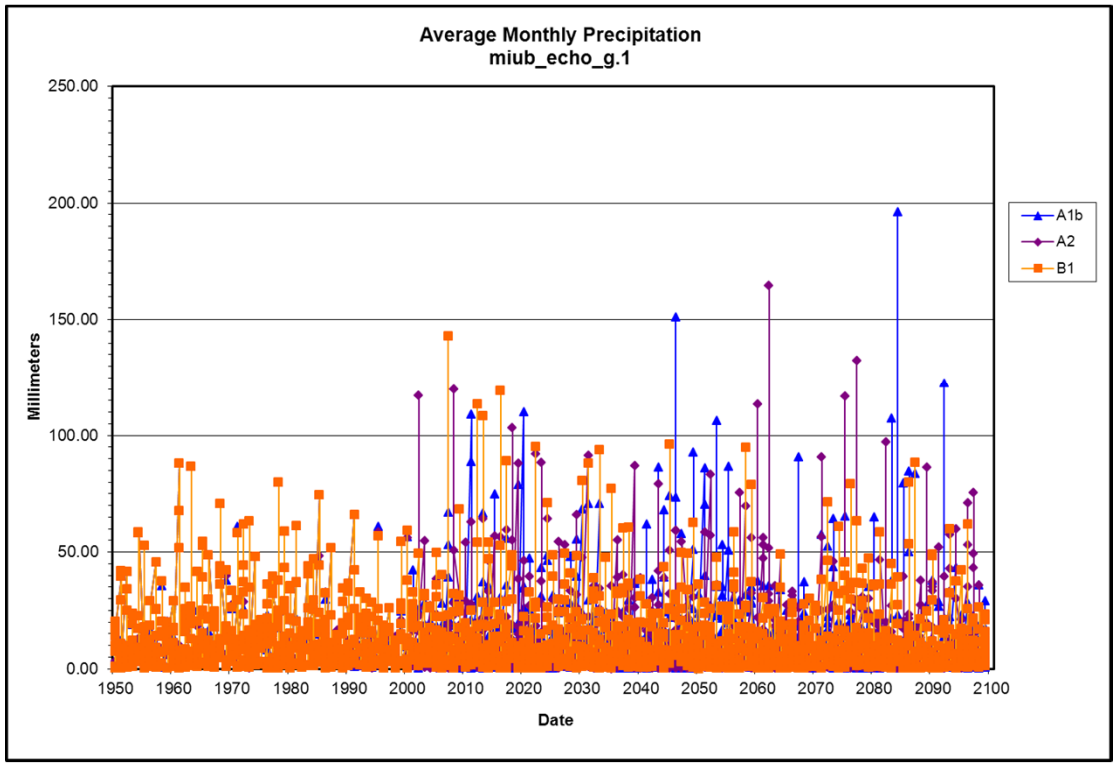

Climate Model miub_echo_g.1 (page 2 of 3)

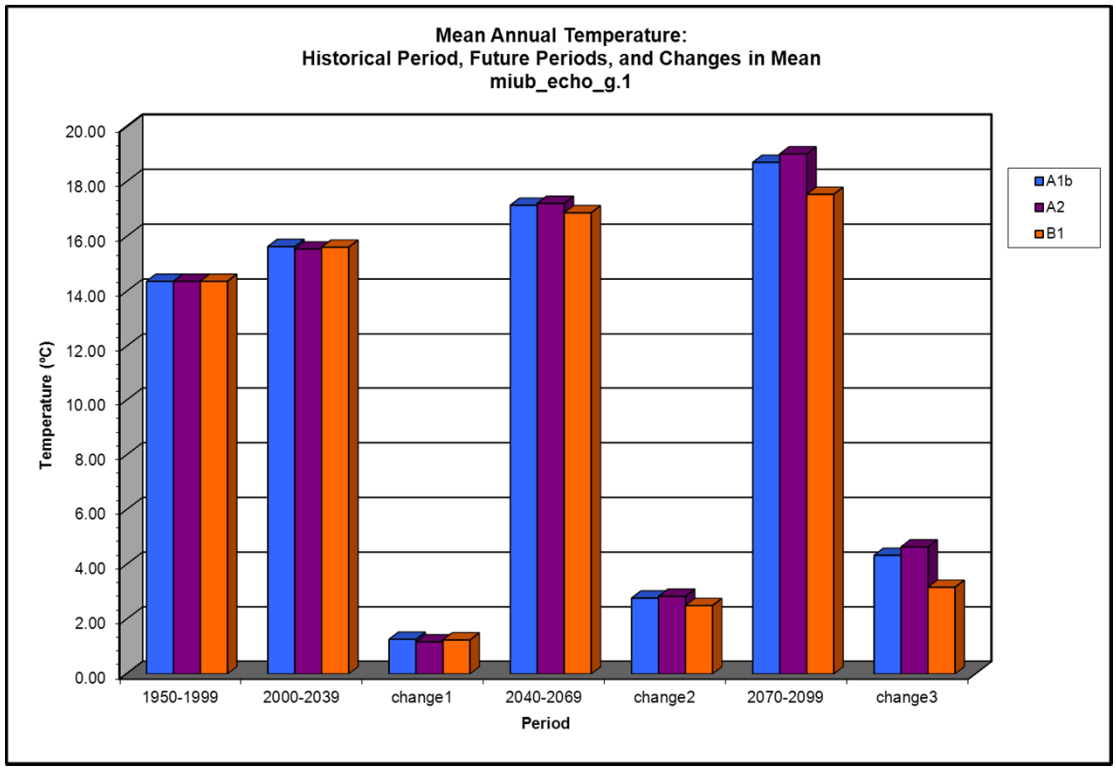

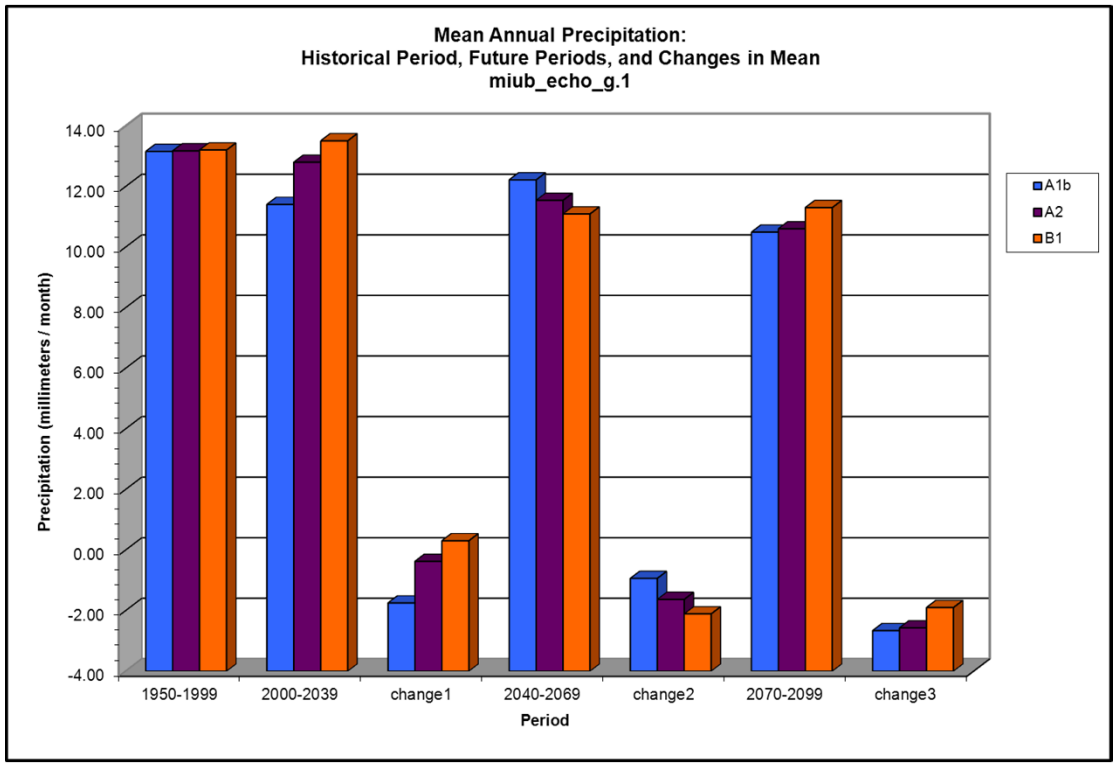

Climate Model miub_echo_g.1 (page 3 of 3)

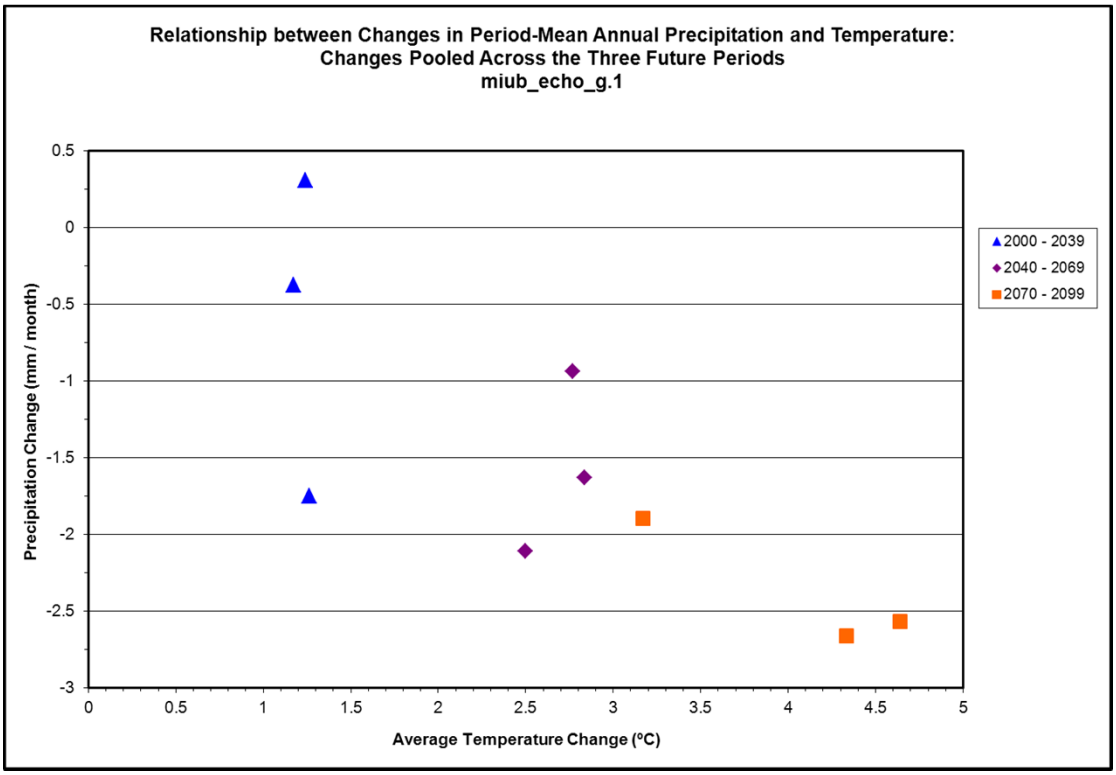

Climate Model miub_echo_g.2 (page 1 of 3)

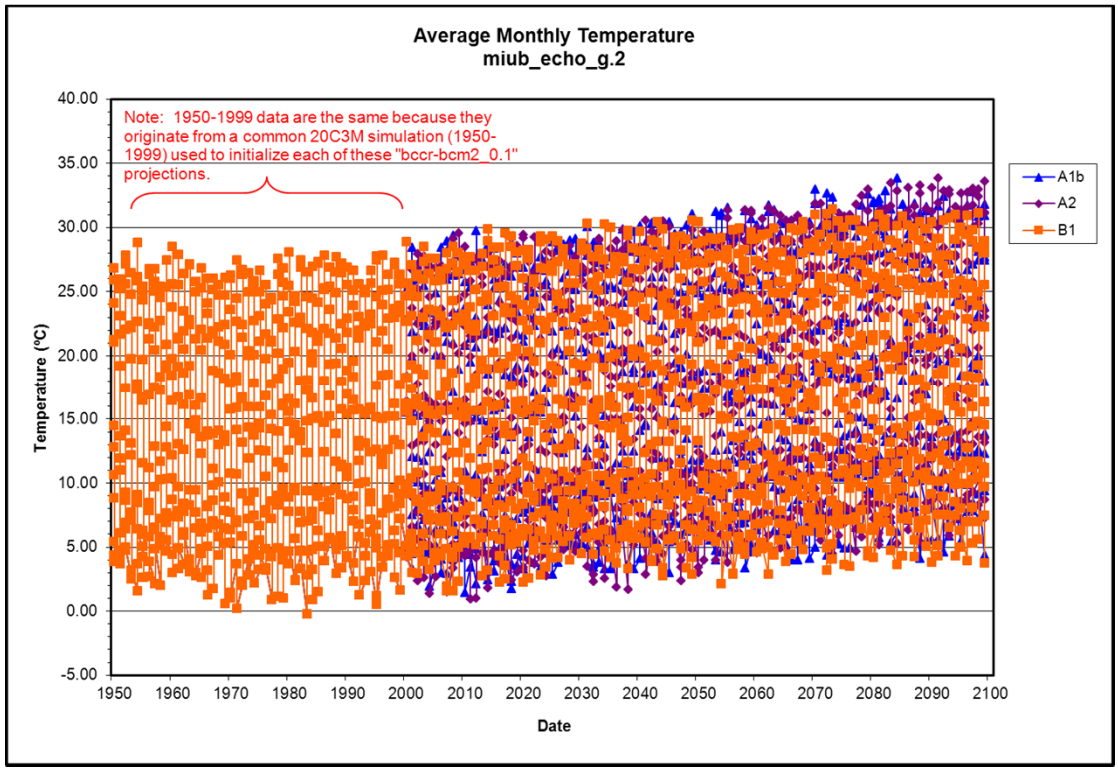

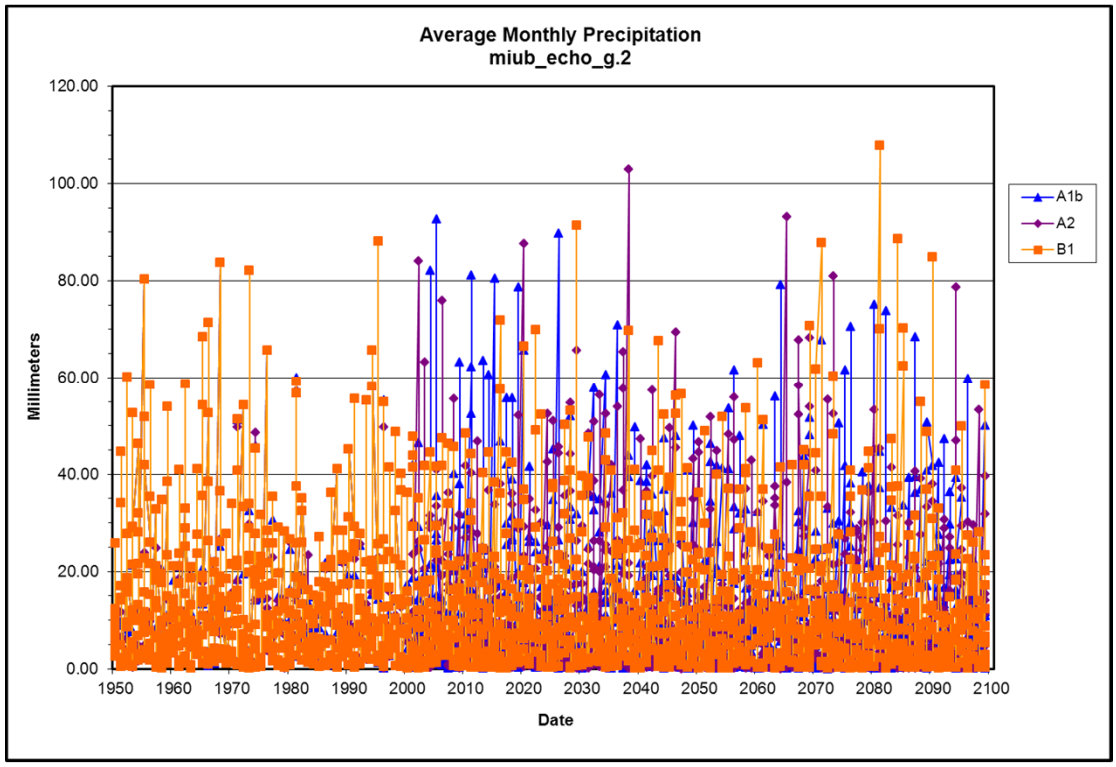

Climate Model miub_echo_g.2 (page 2 of 3)

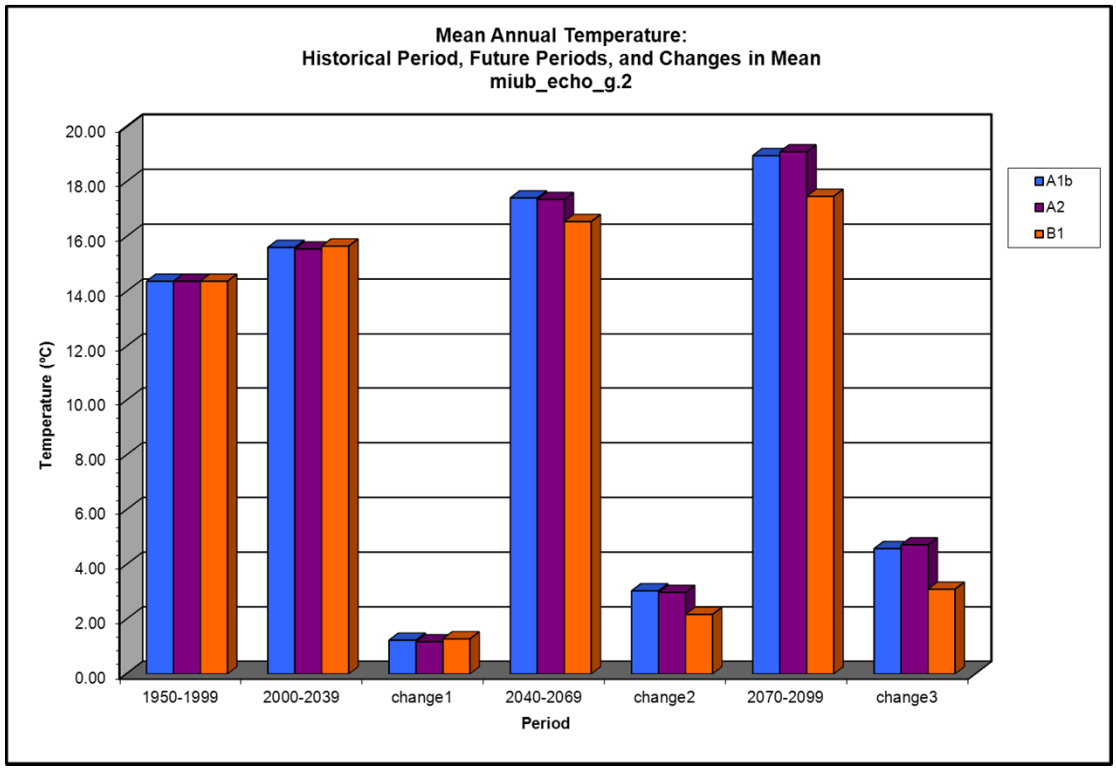

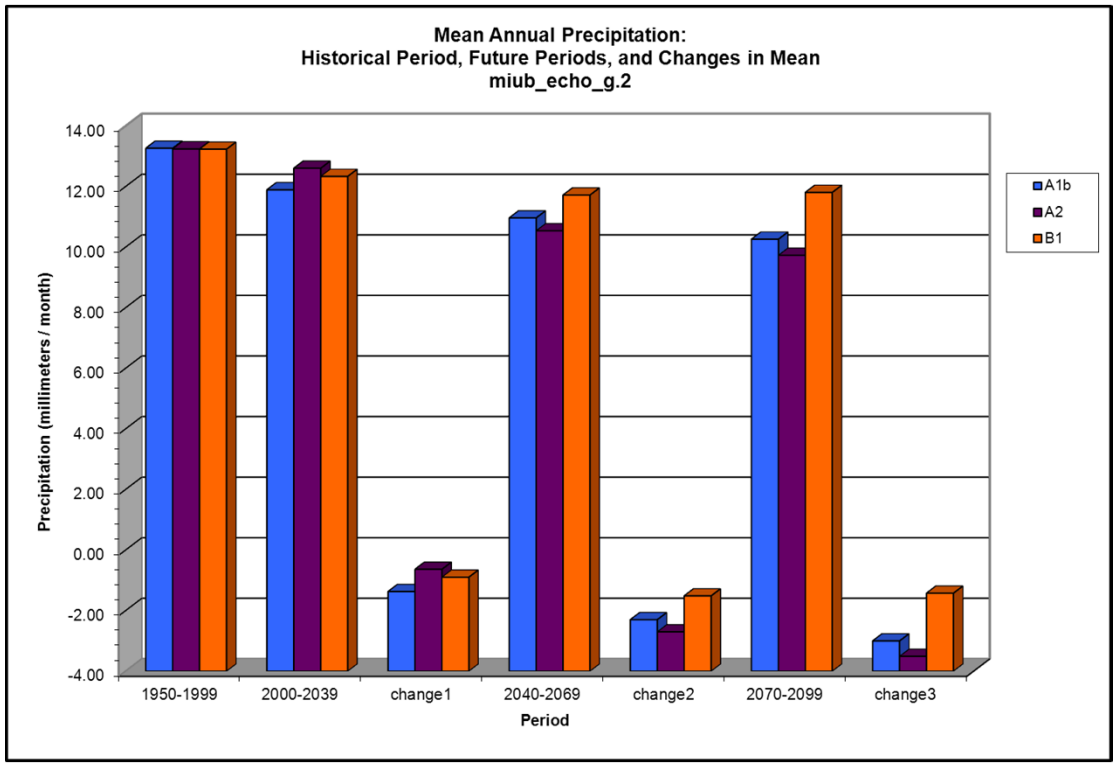

Climate Model miub_echo_g.2 (page 3 of 3)

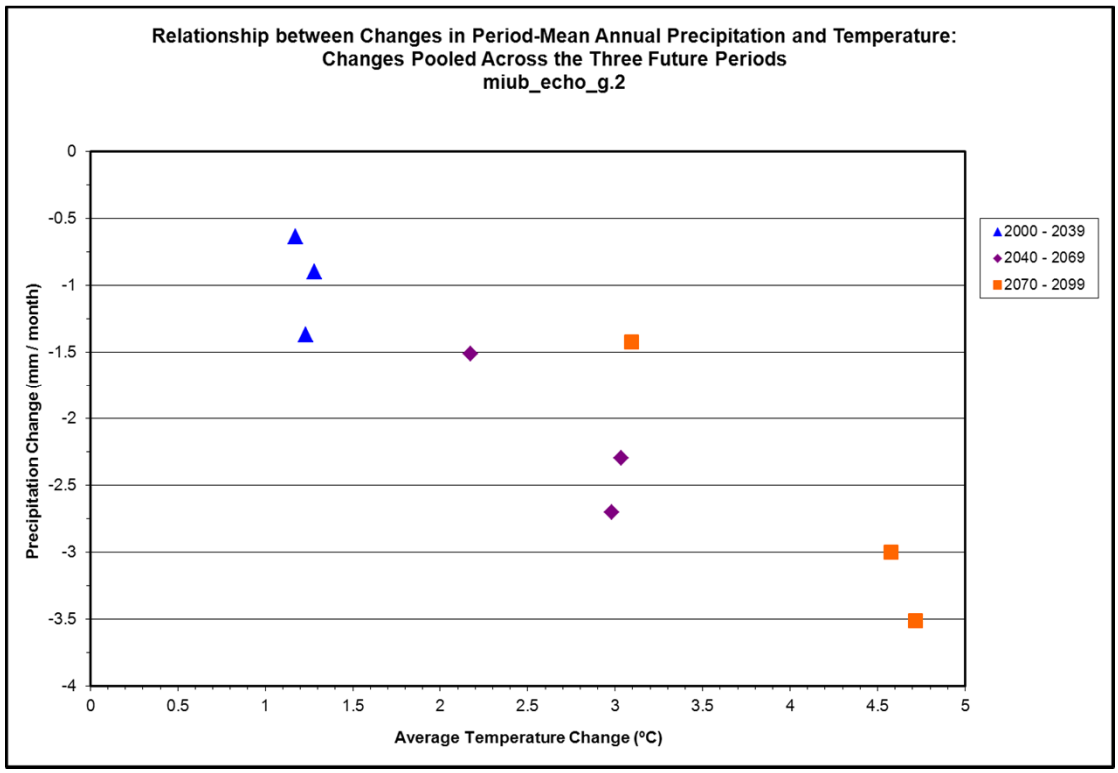

Climate Model miub_echo_g.3 (page 1 of 3)

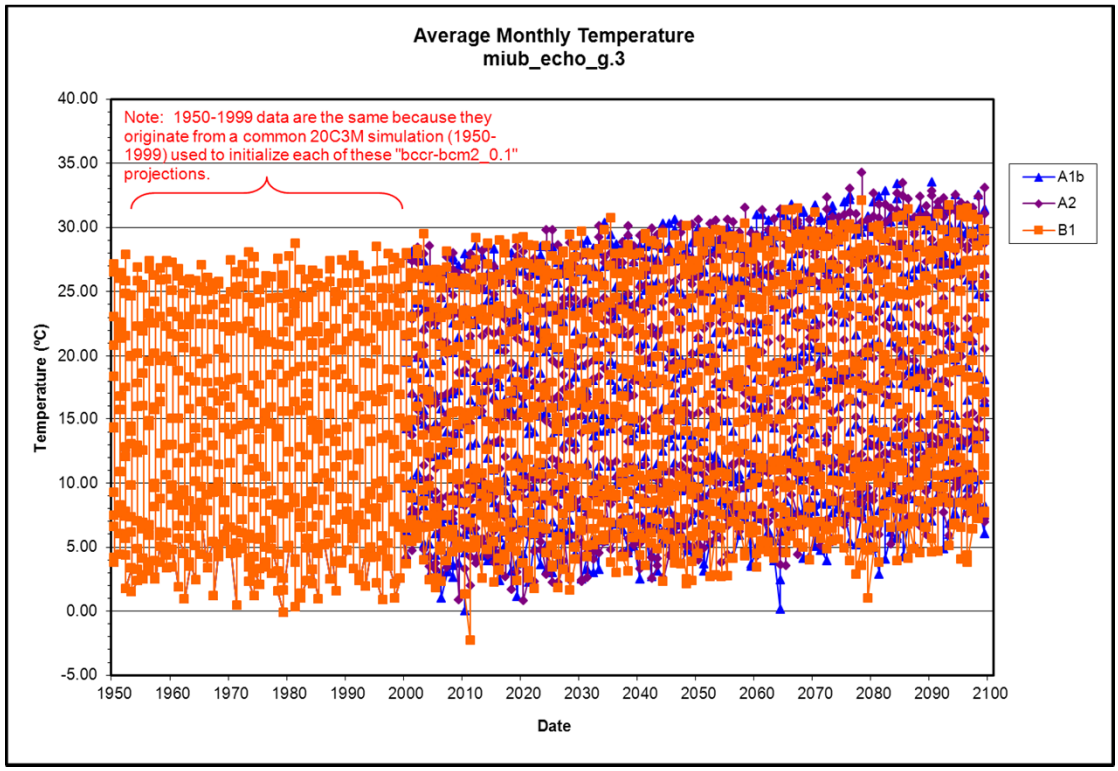

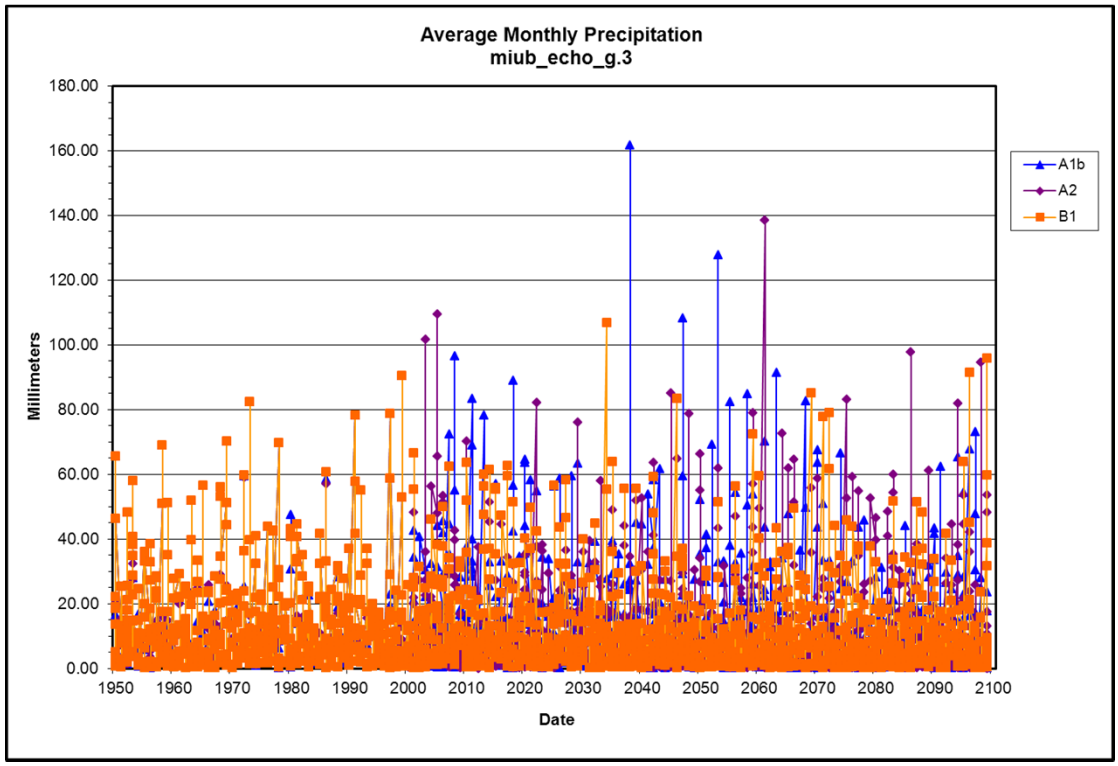

Climate Model miub_echo_g.3 (page 2 of 3)

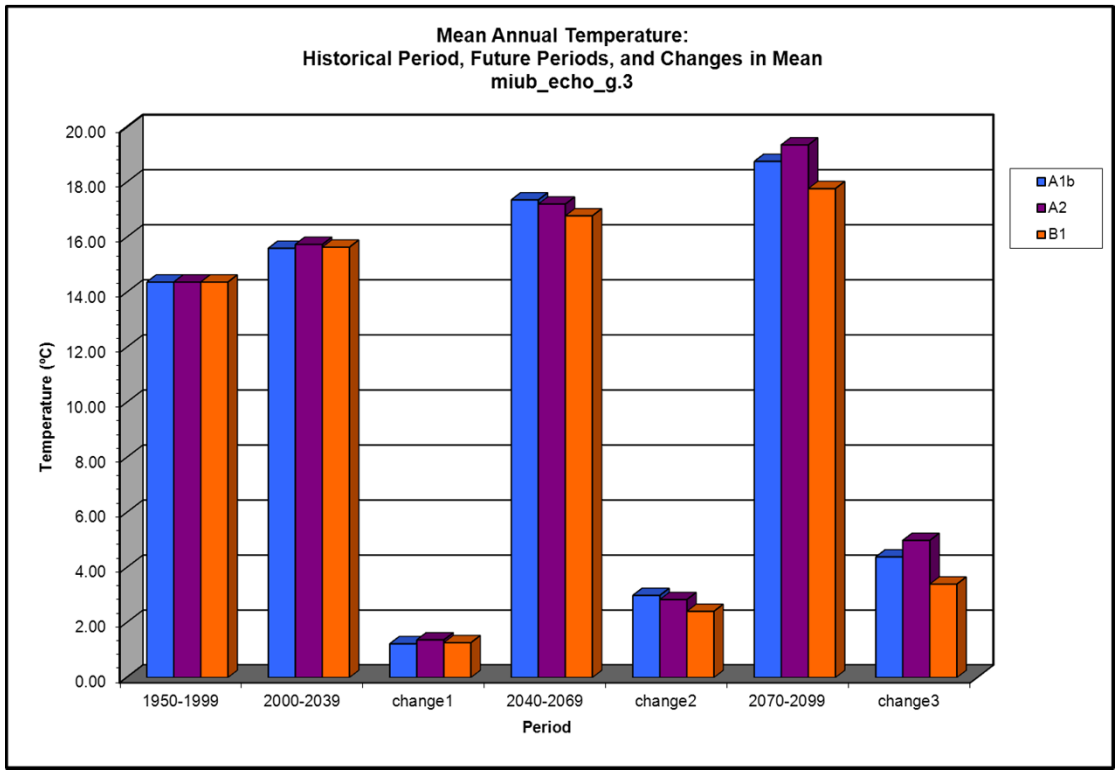

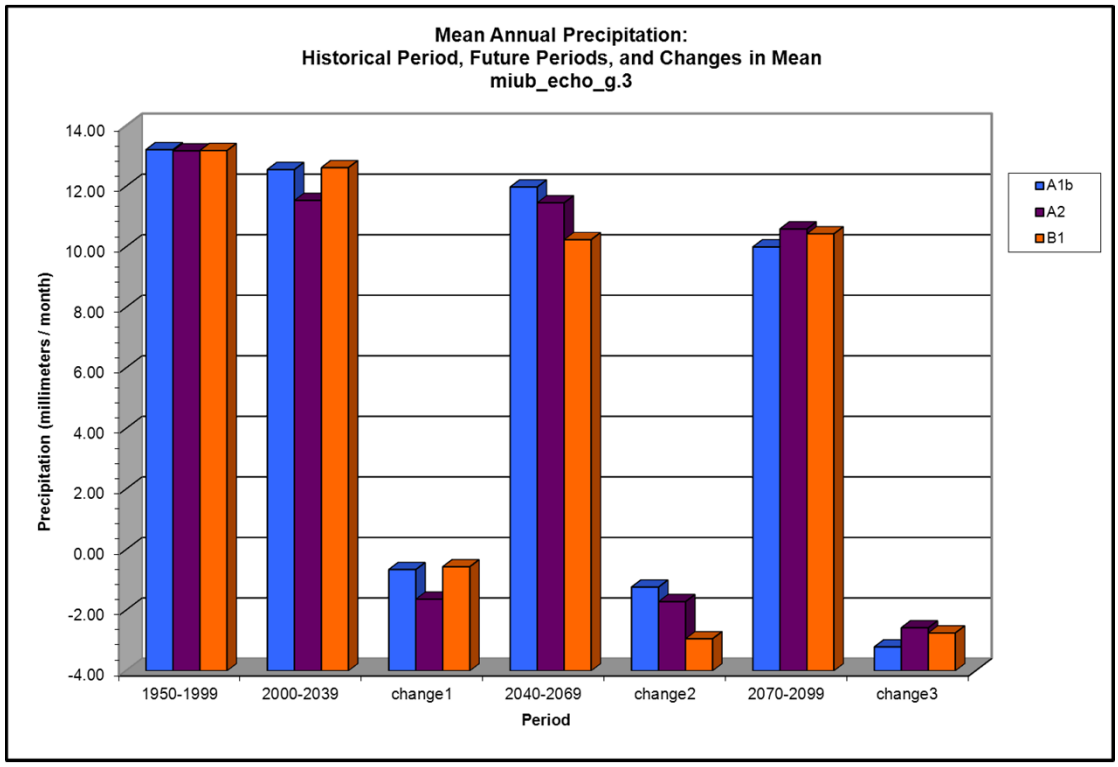

Climate Model miub_echo_g.3 (page 3 of 3)

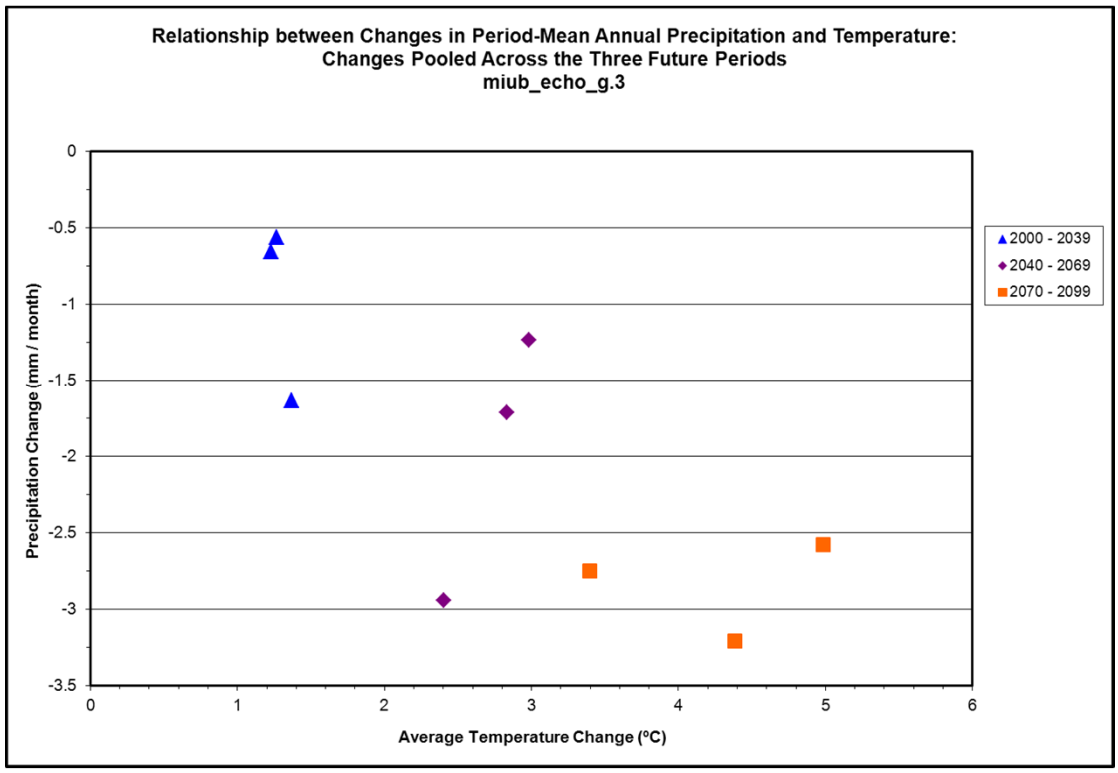

Climate Model mpi_echam5.1 (page 1 of 3)

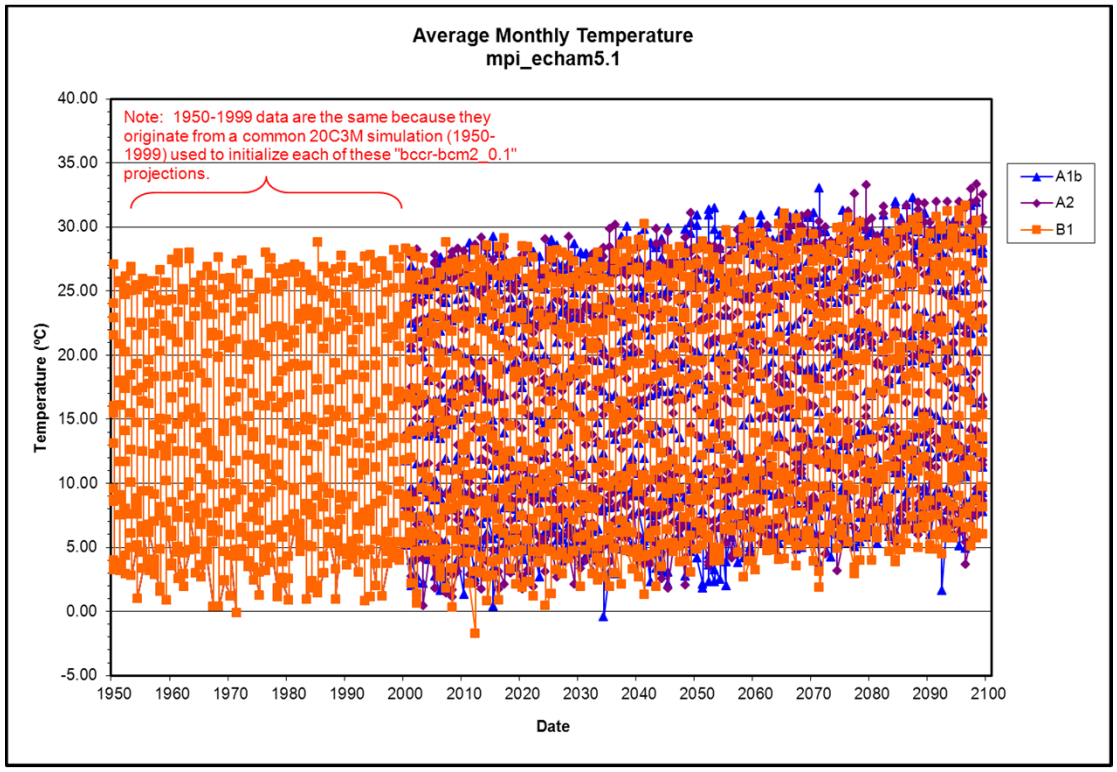

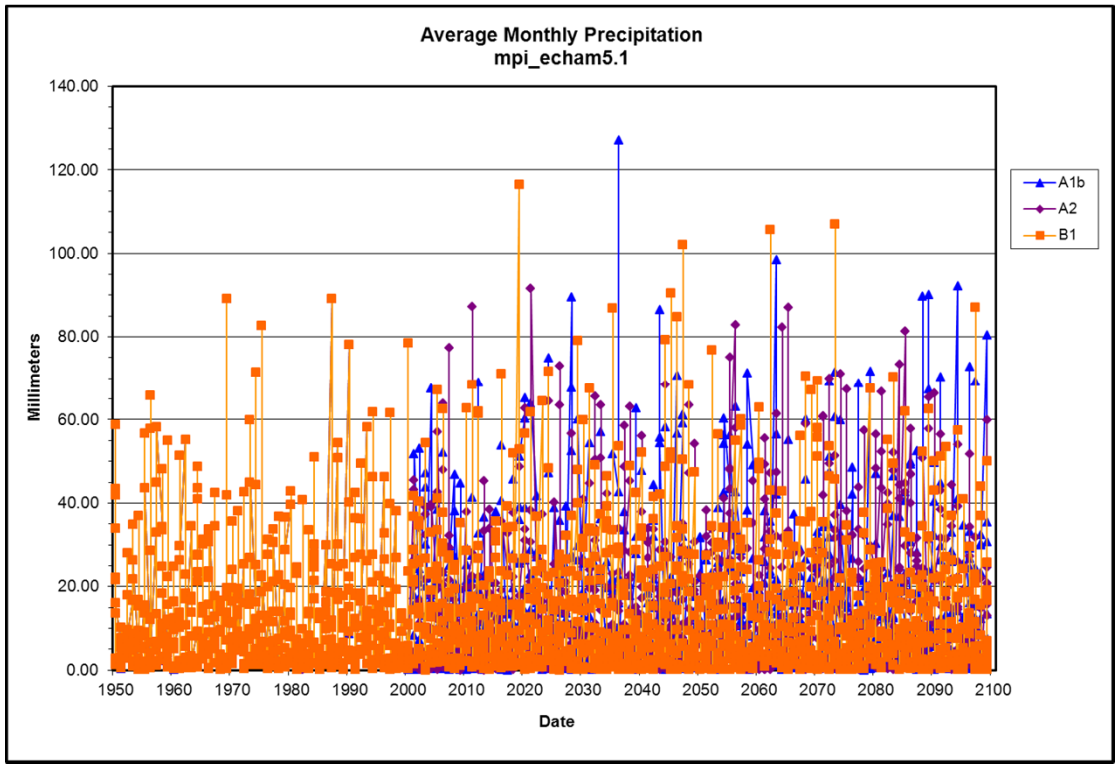

Climate Model mpi_echam5.1 (page 2 of 3)

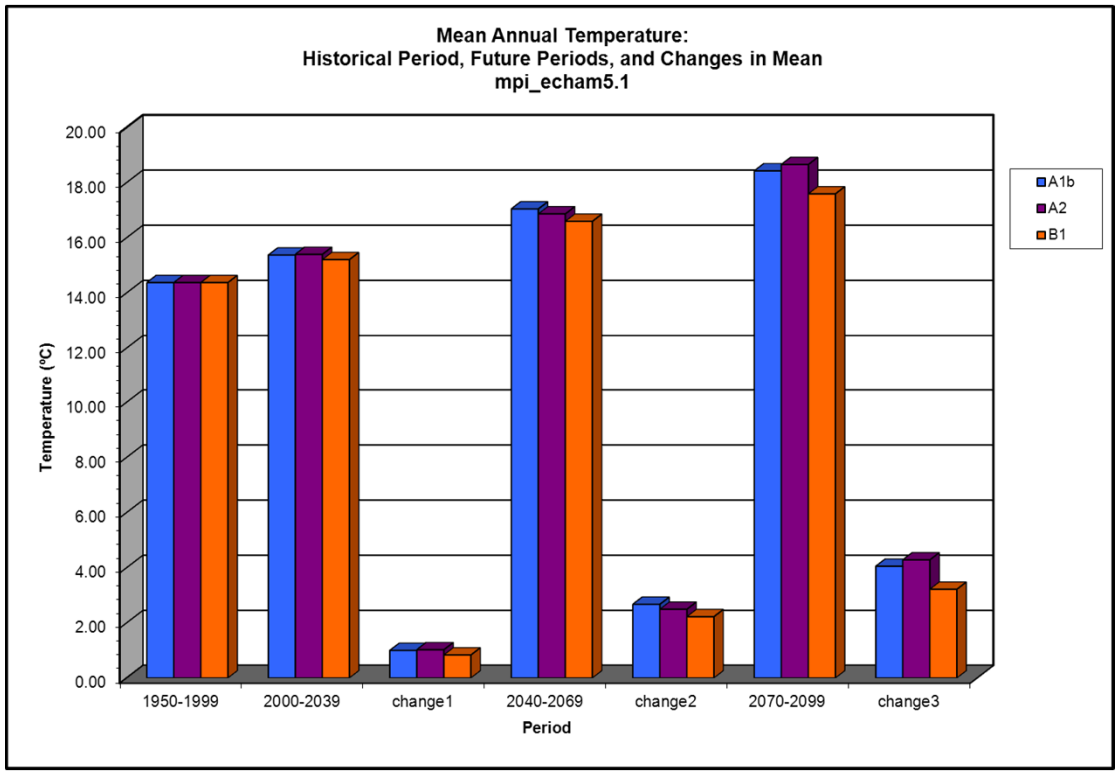

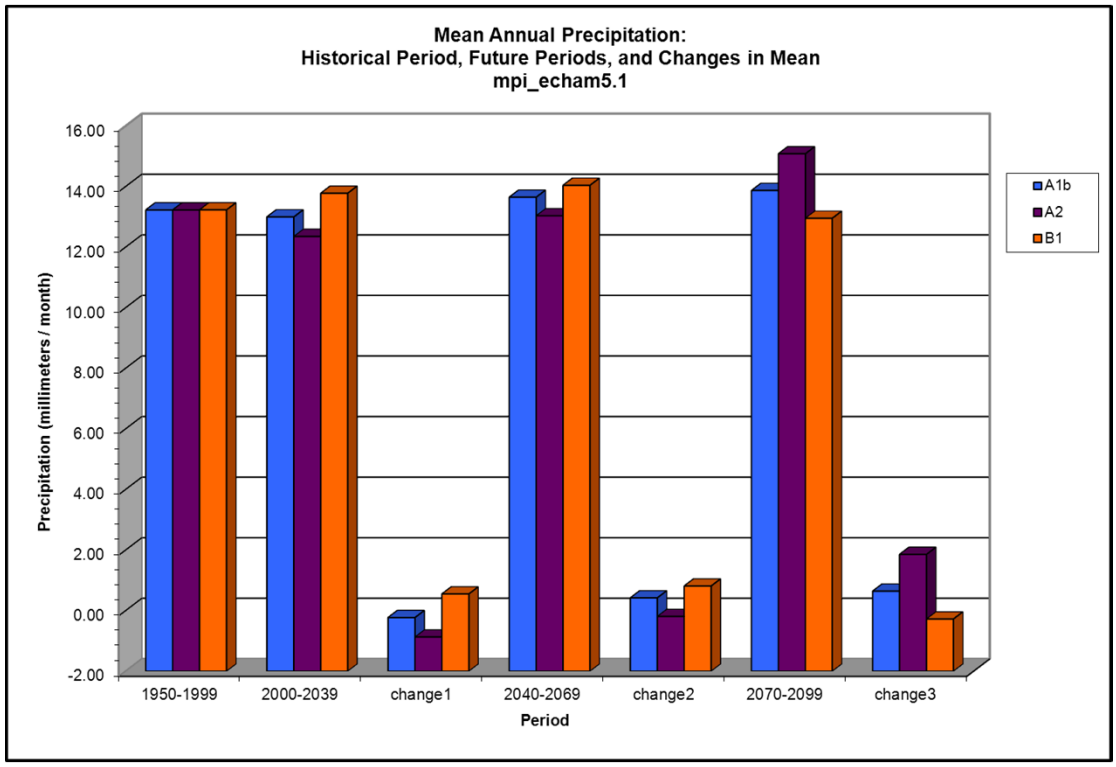

Climate Model mpi_echam5.1 (page 3 of 3)

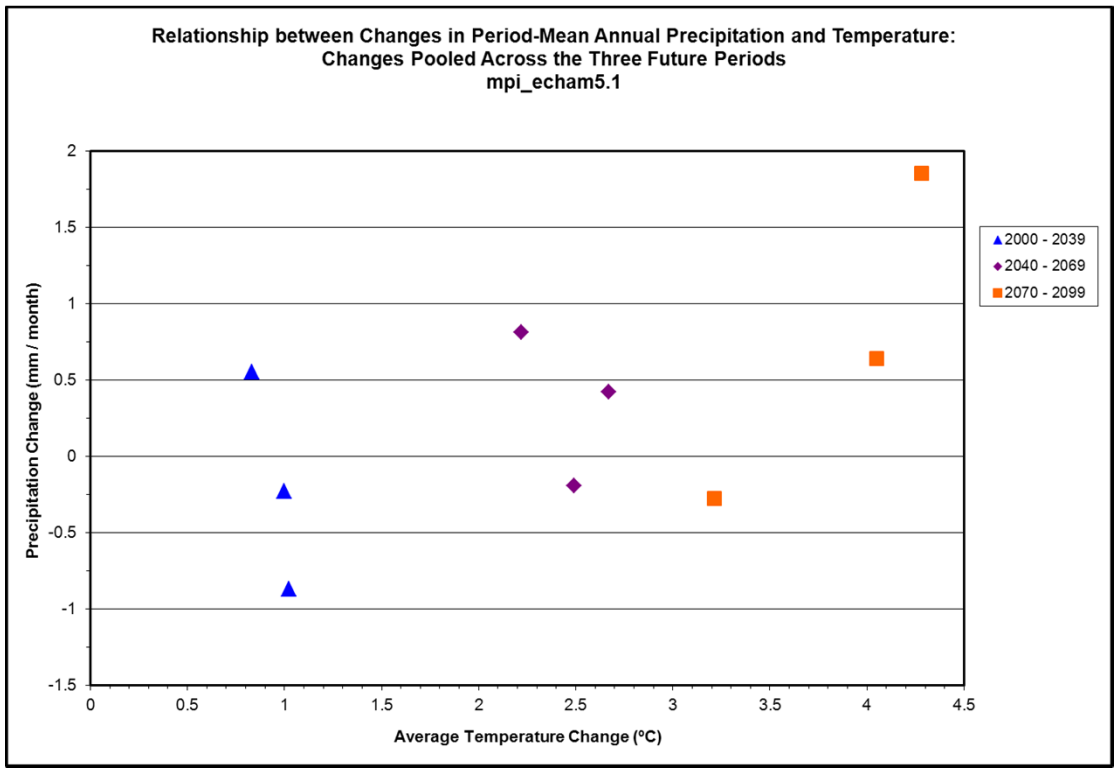

Climate Model mpi_echam5.2 (page 1 of 3)

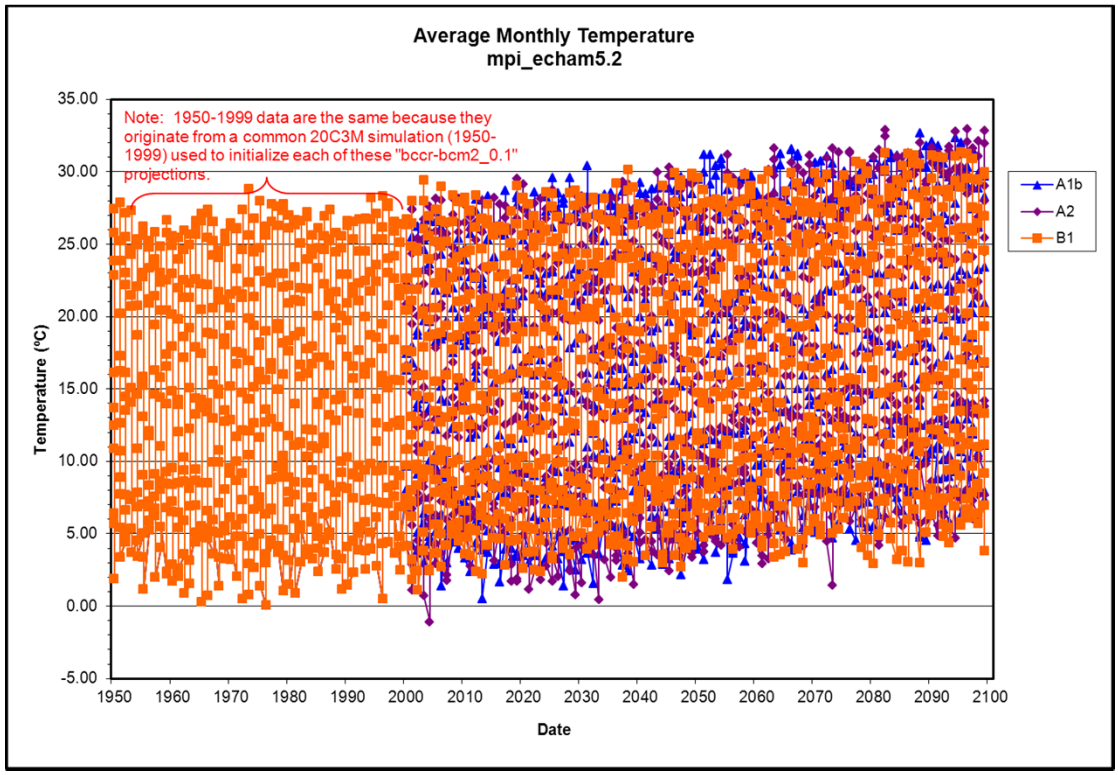

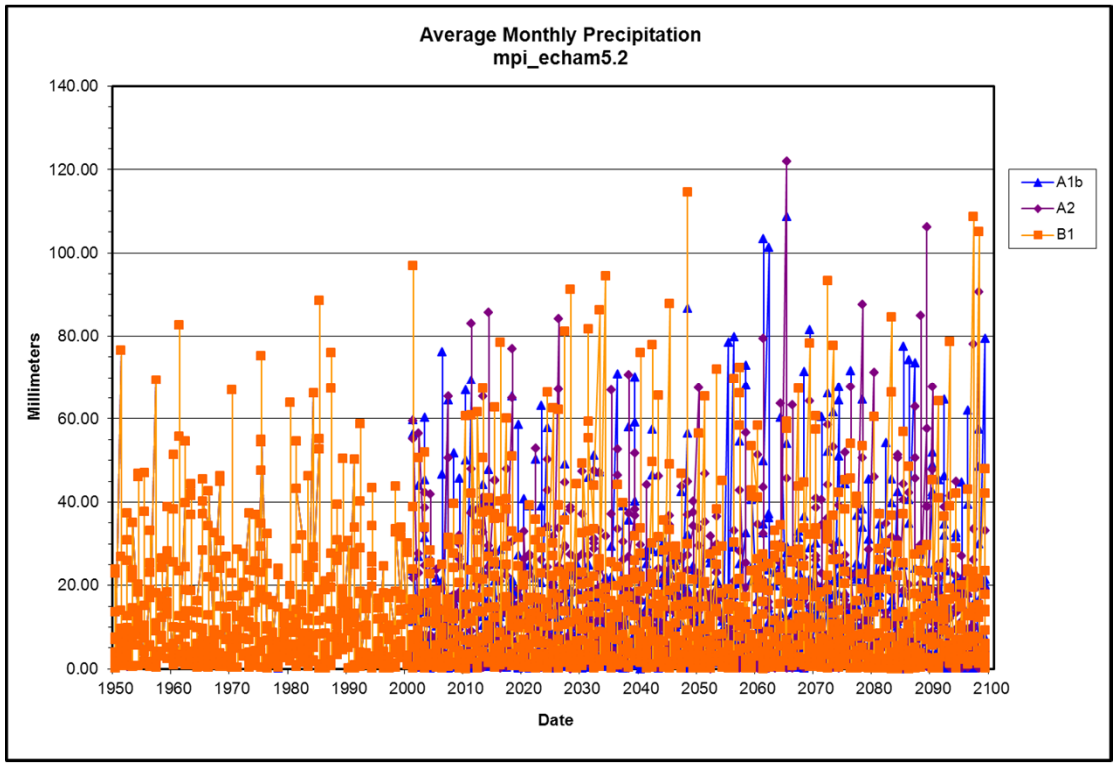

Climate Model mpi_echam5.2 (page 2 of 3)

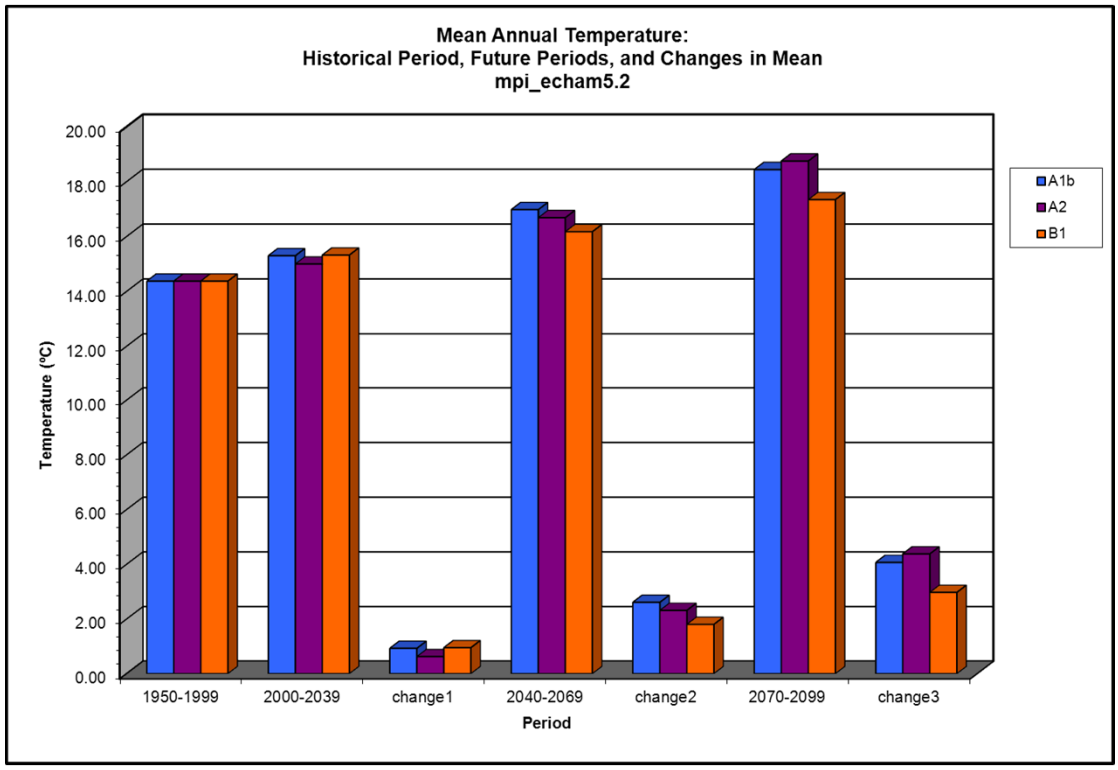

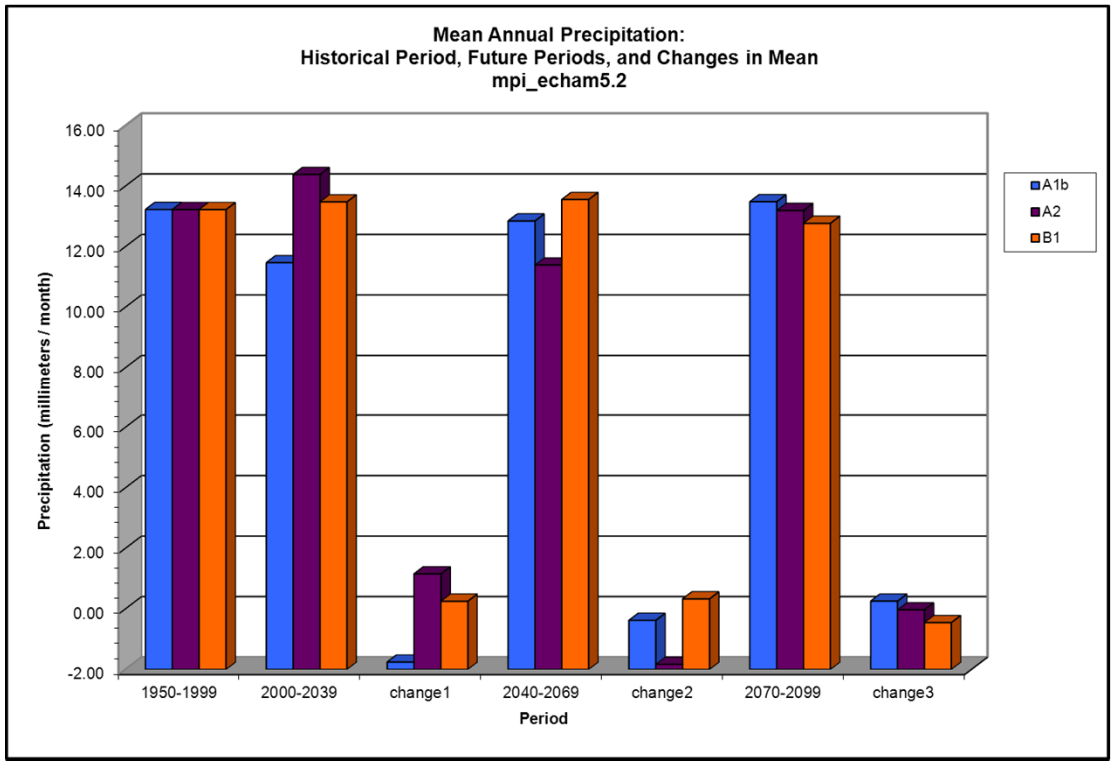

Climate Model mpi_echam5.2 (page 3 of 3)

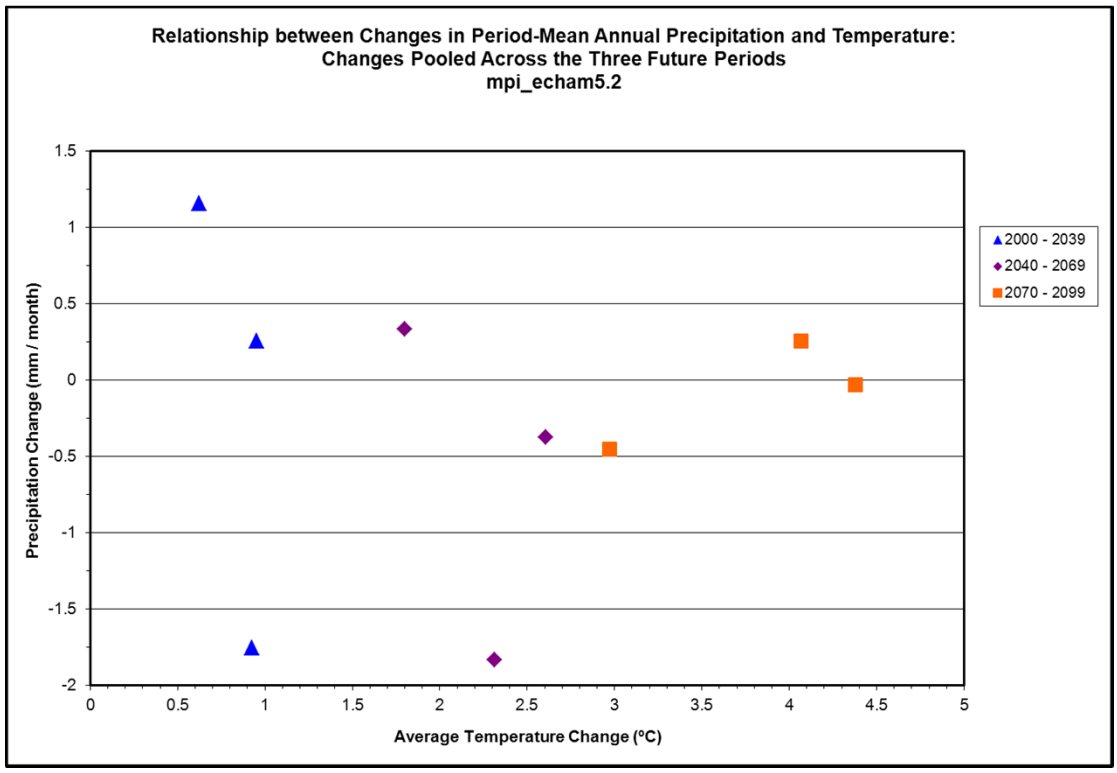

Climate Model mpi_echam5.3 (page 1 of 3)

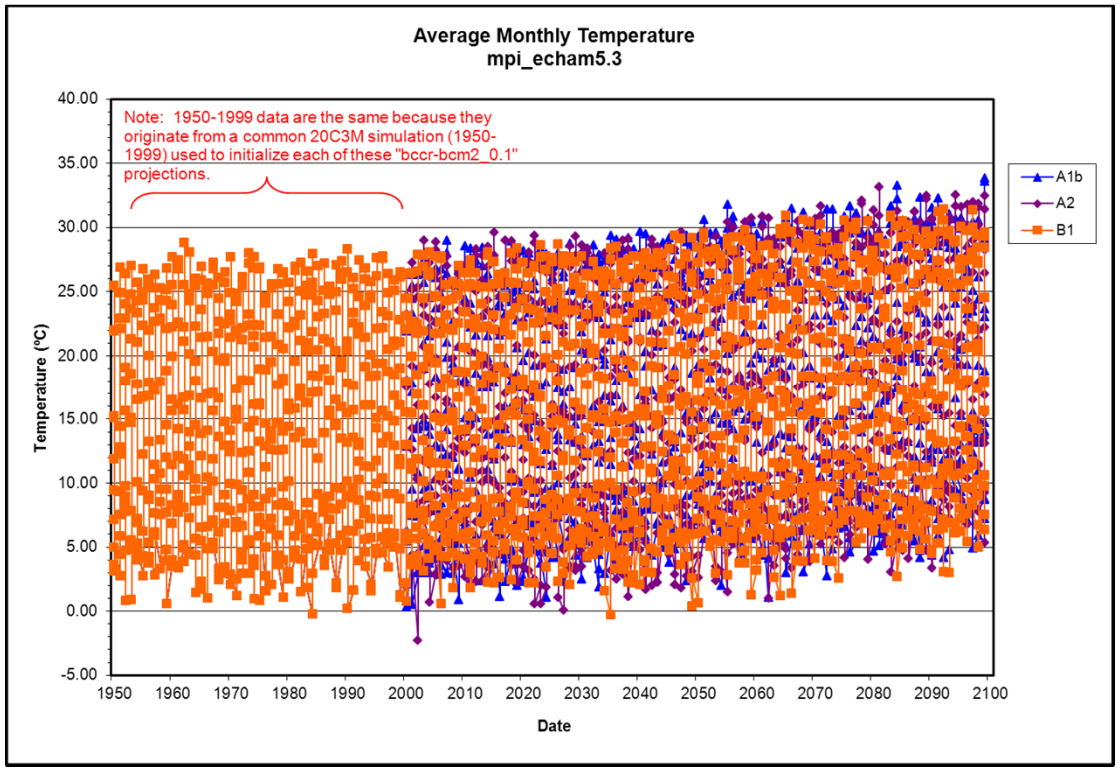

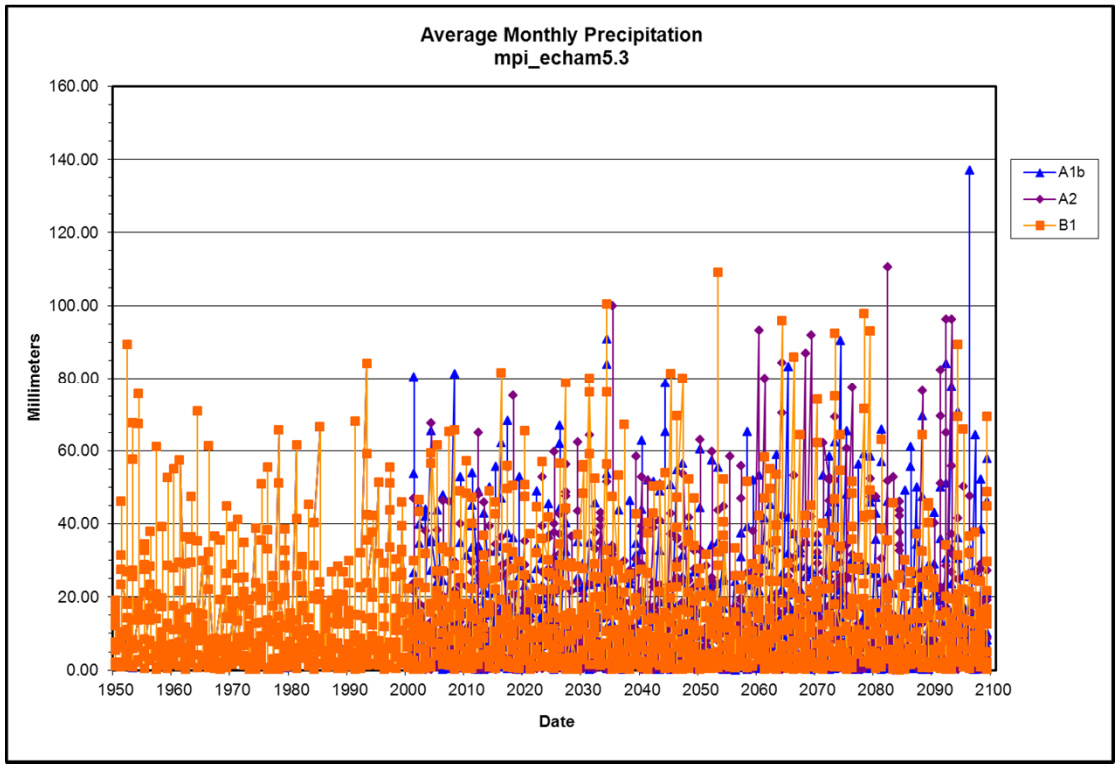

Climate Model mpi_echam5.3 (page 2 of 3)

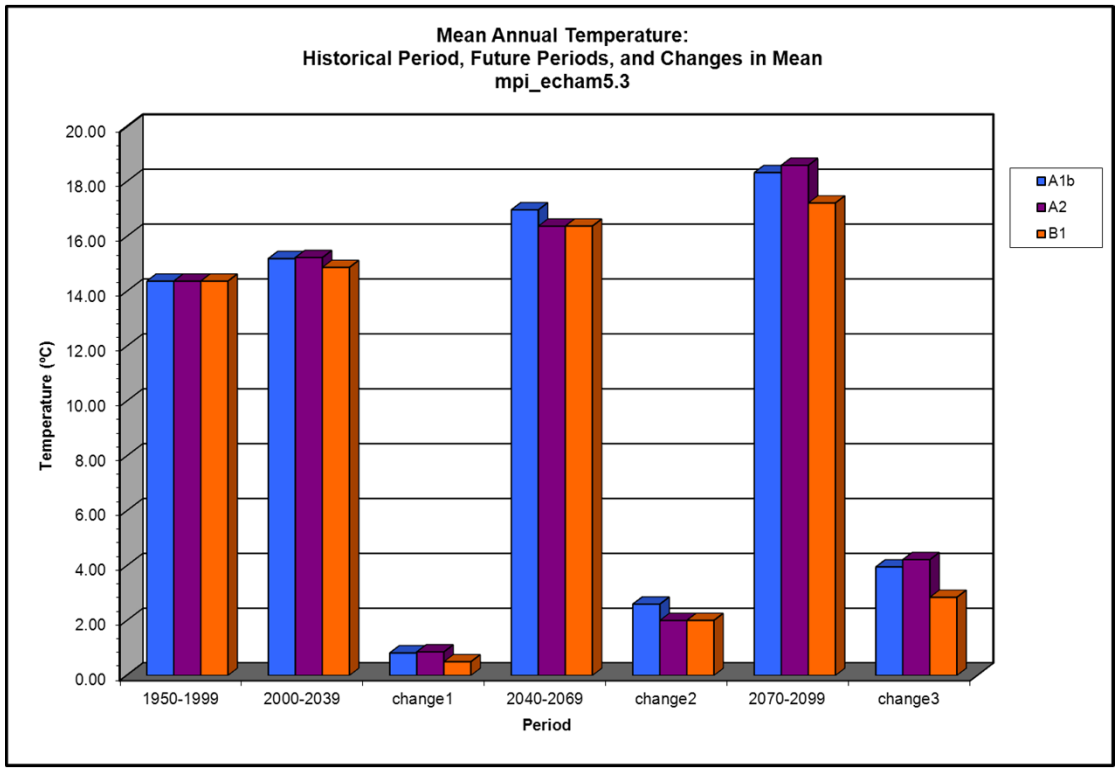

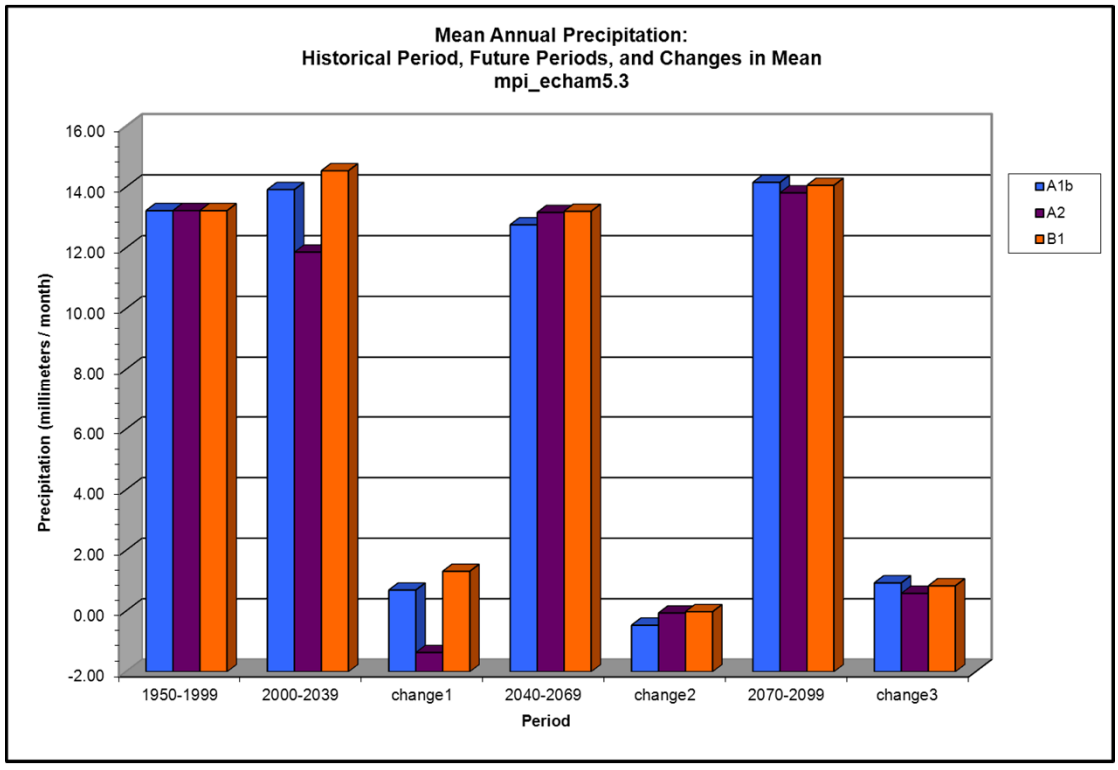

Climate Model mpi_echam5.3 (page 3 of 3)

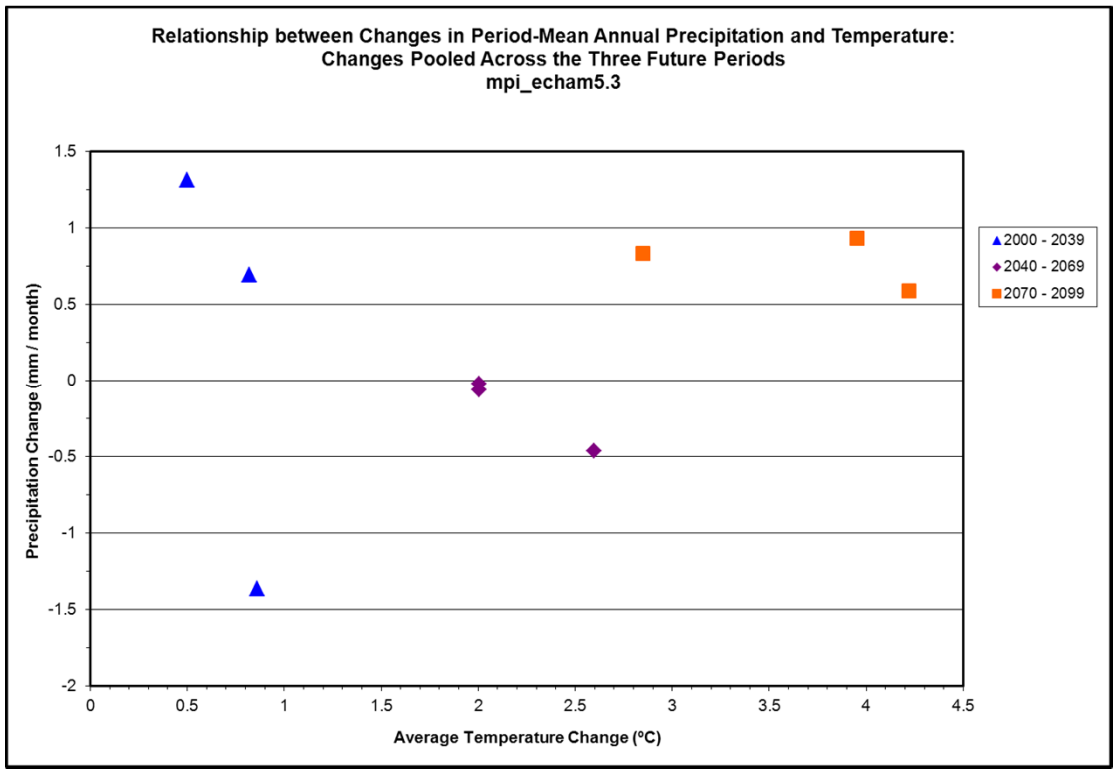

Climate Model mri_cgcm2_2_2a.1 (page 1 of 3)

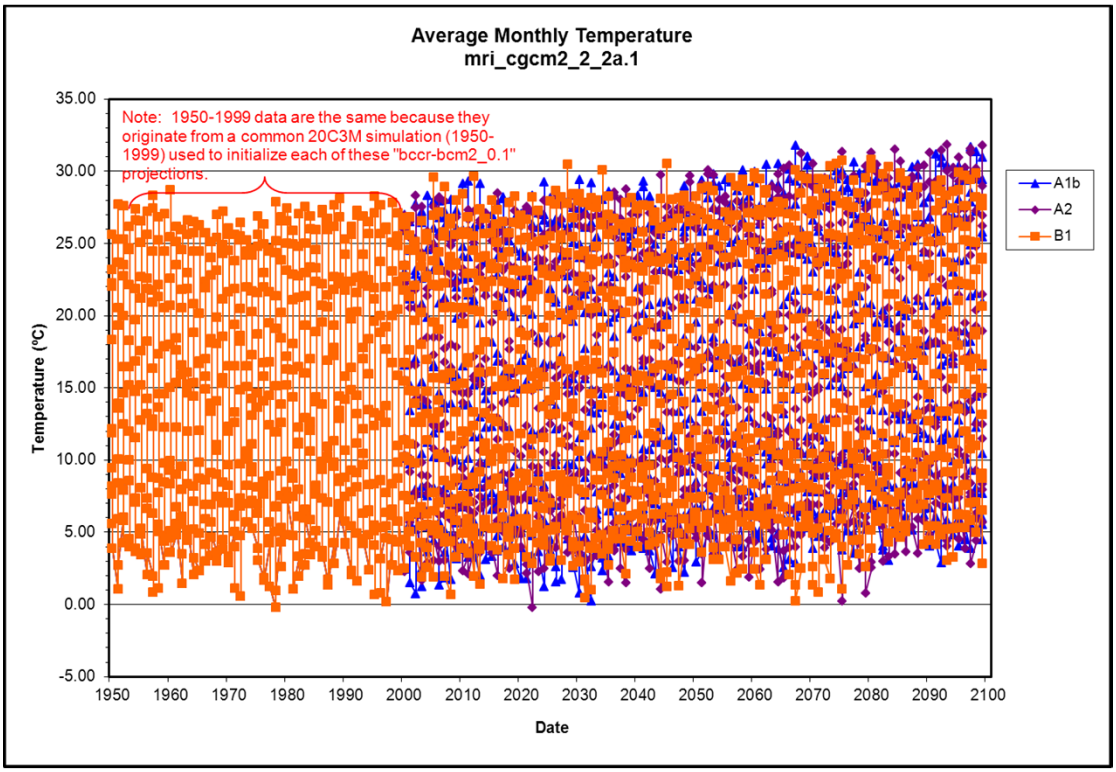

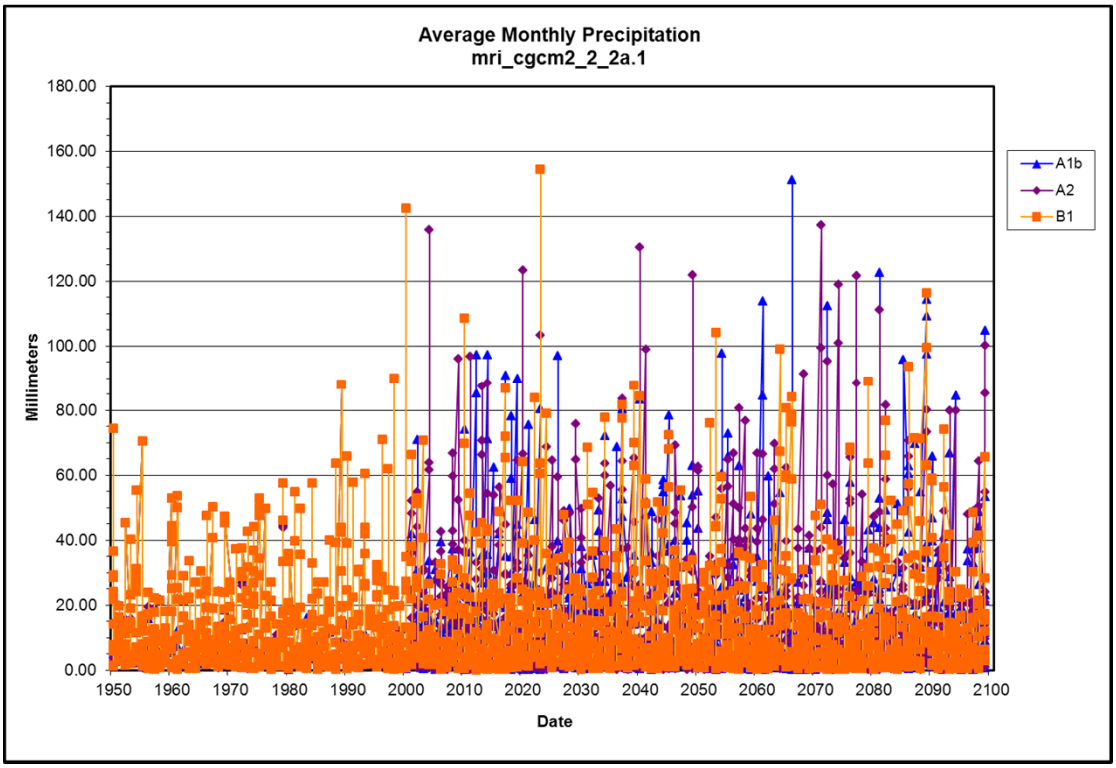

Climate Model mri_cgcm2_2_2a.1 (page 2 of 3)

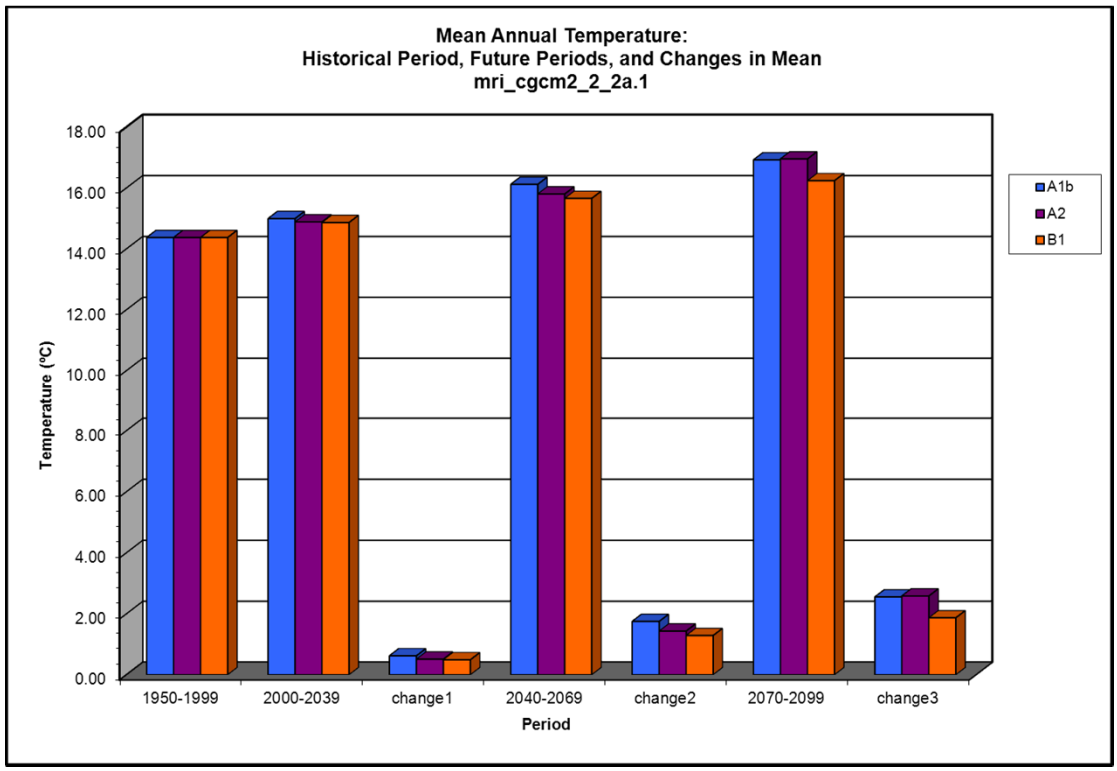

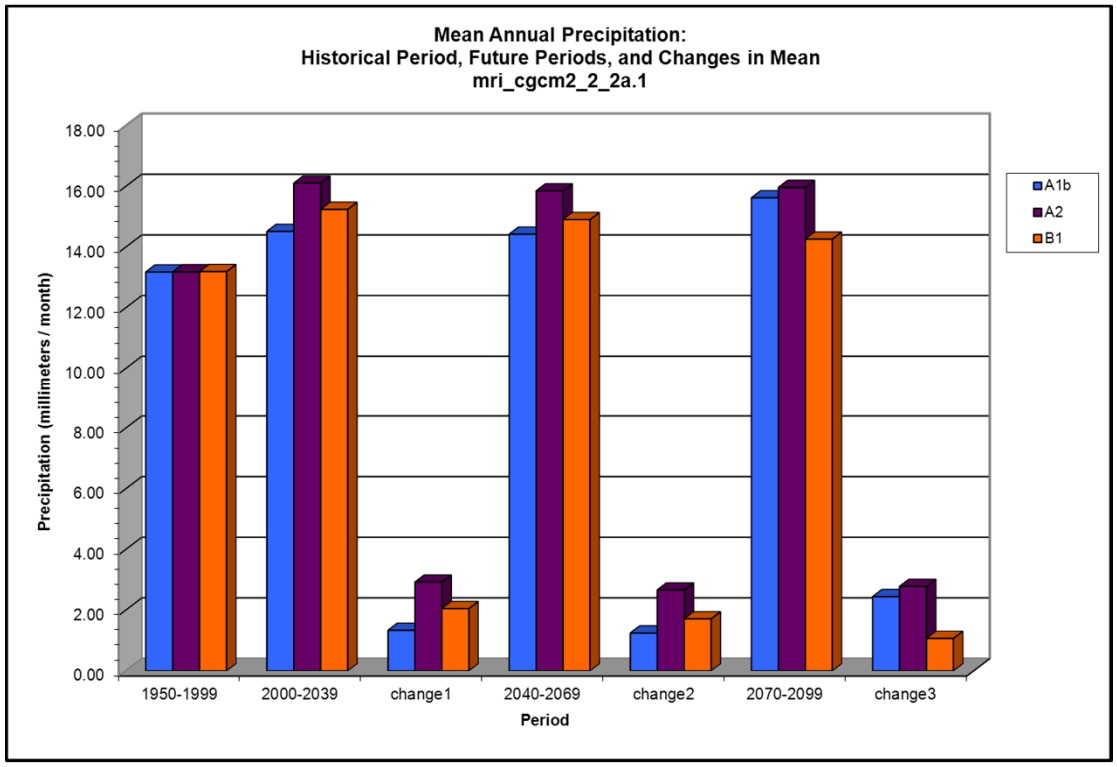

Climate Model mri_cgcm2_2_2a.1 (page 3 of 3)

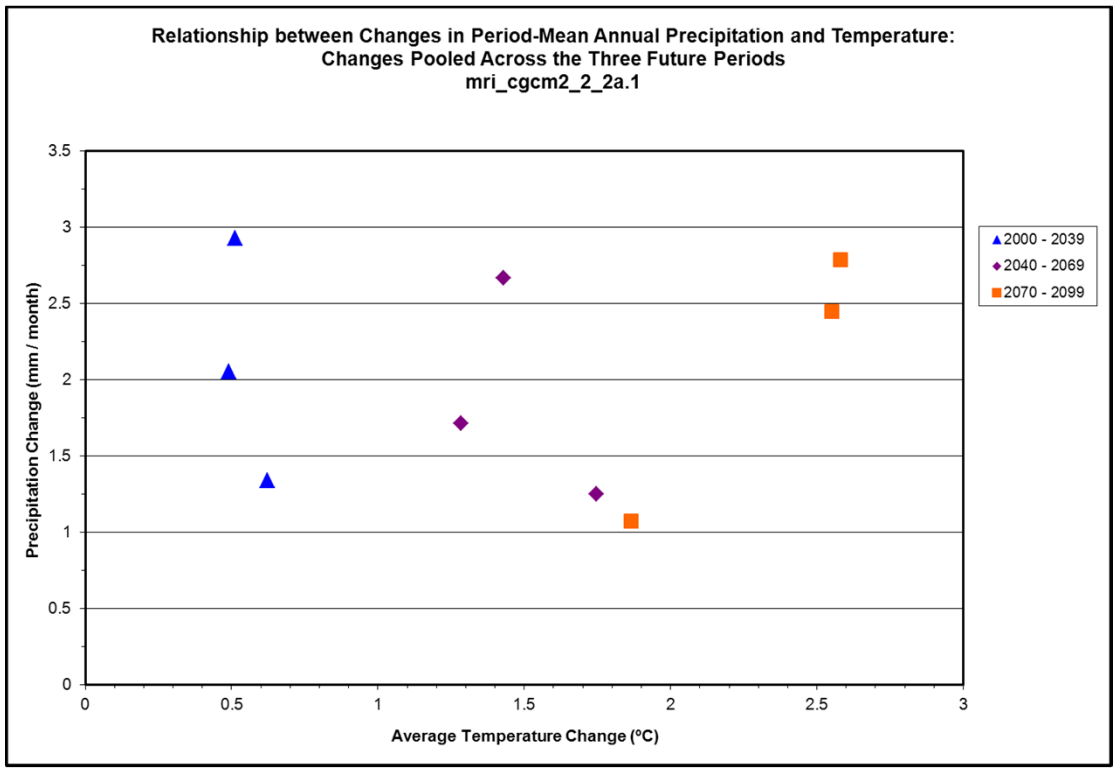

Climate Model mri_cgcm2_2_2a.2 (page 1 of 3)

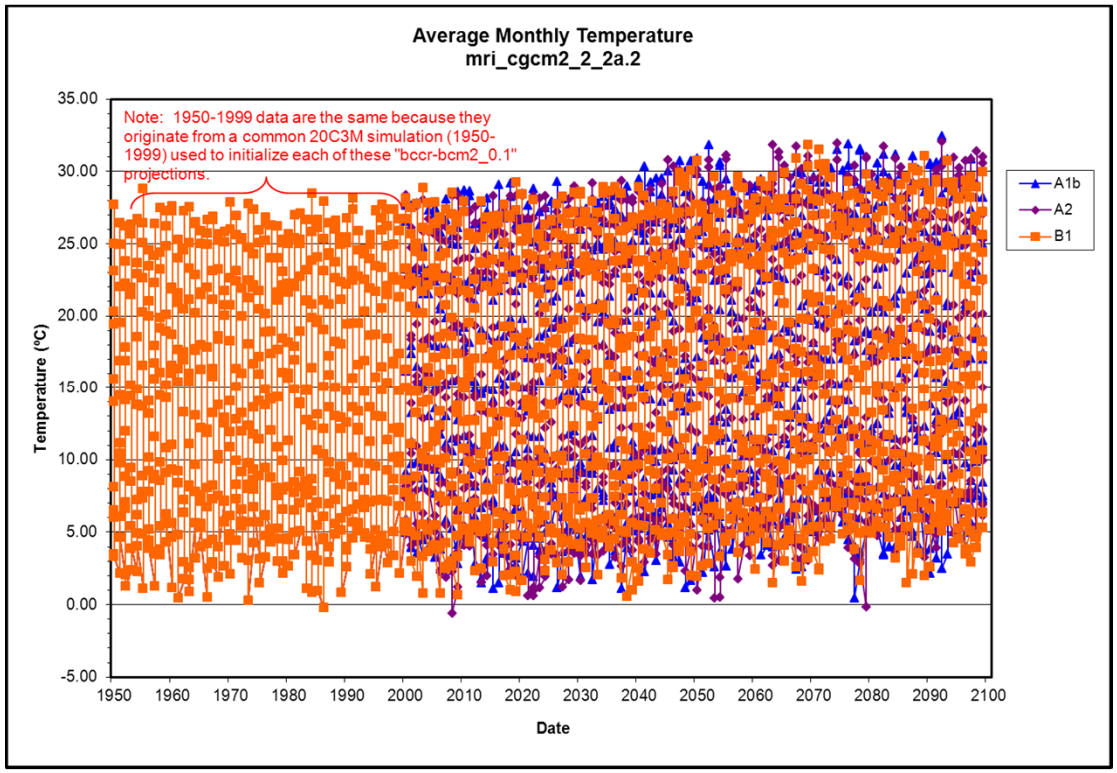

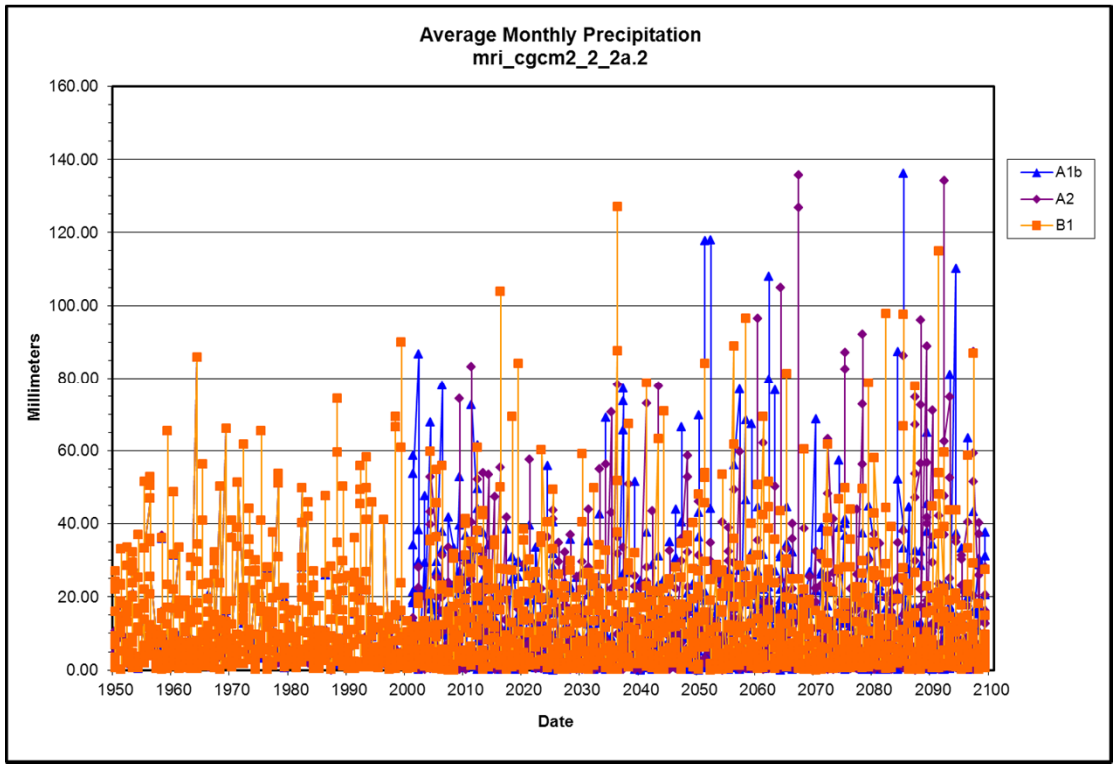

Climate Model mri_cgcm2_2_2a.2 (page 2 of 3)

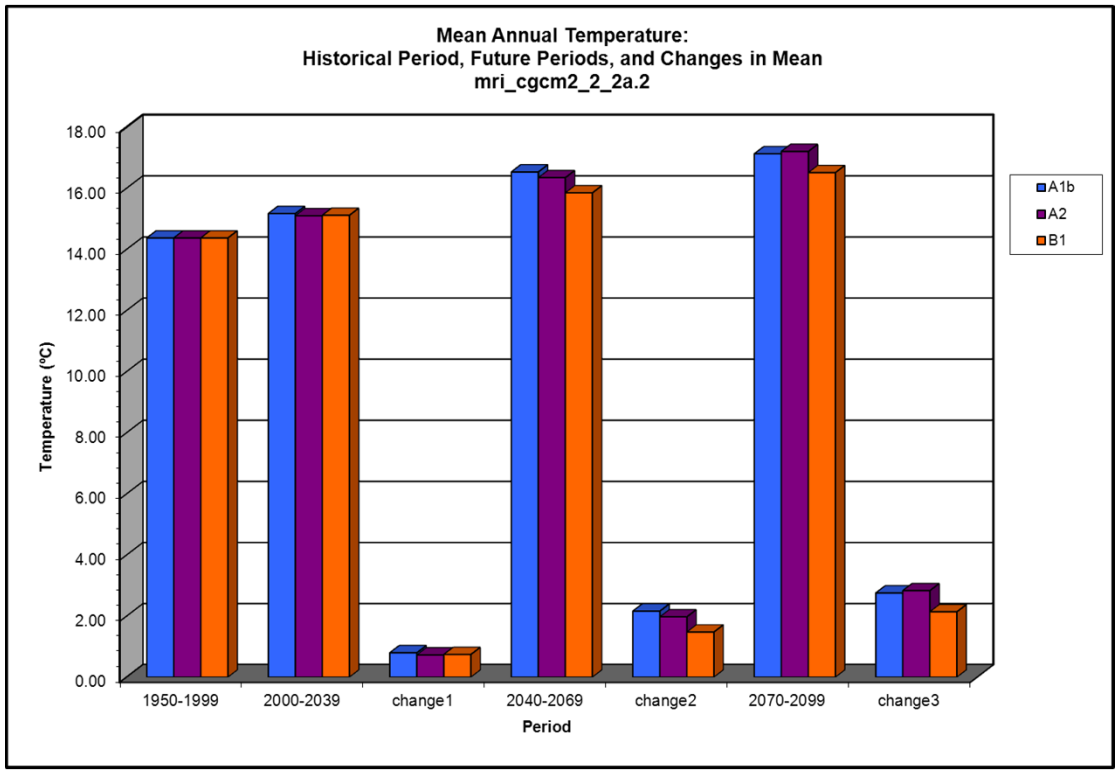

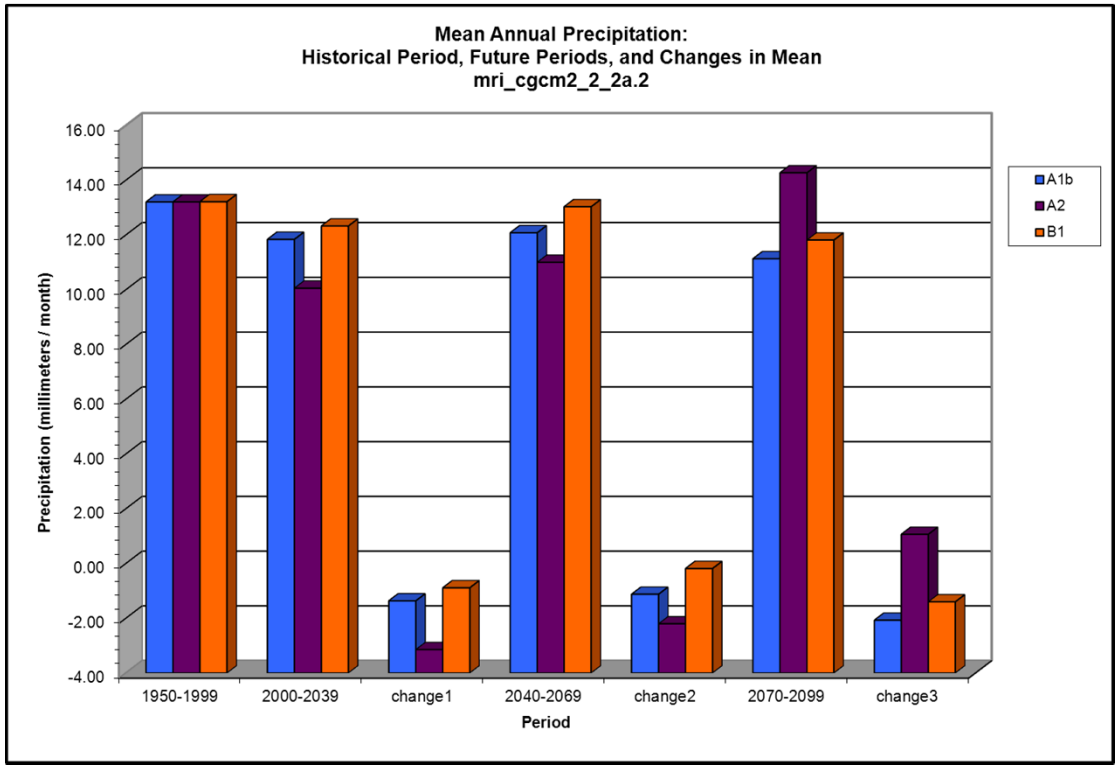

Climate Model mri_cgcm2_2_2a.2 (page 3 of 3)

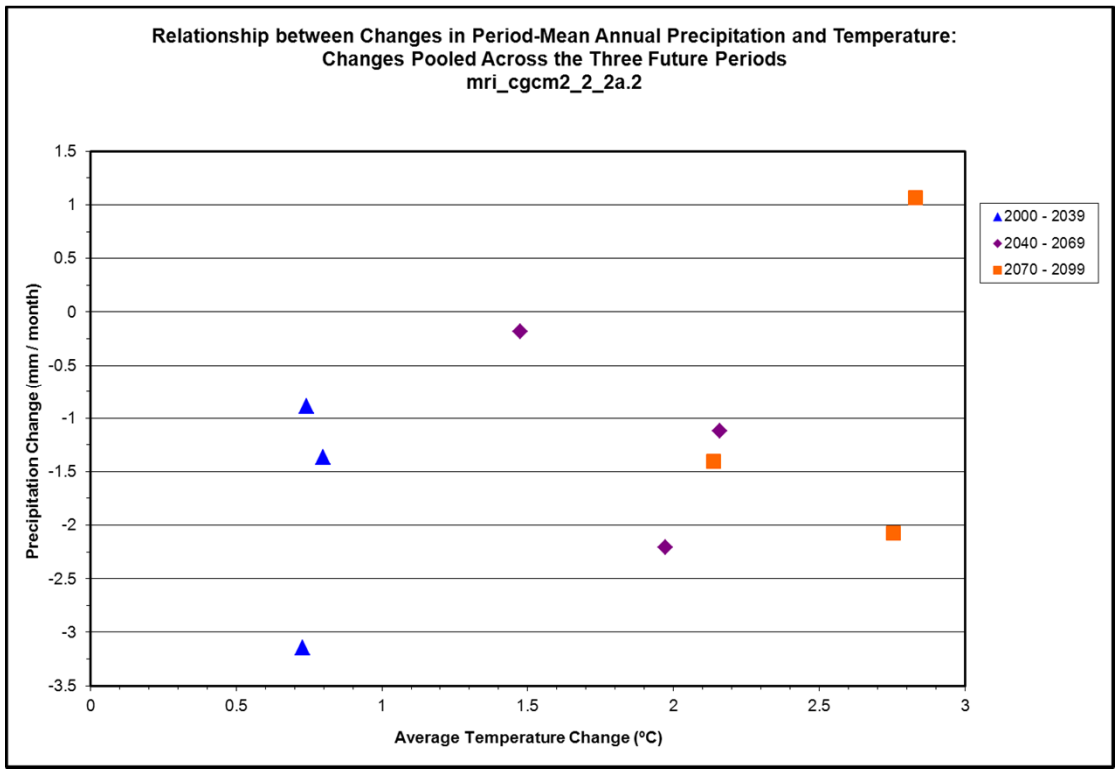

Climate Model mri_cgcm2_2_2a.3 (page 1 of 3)

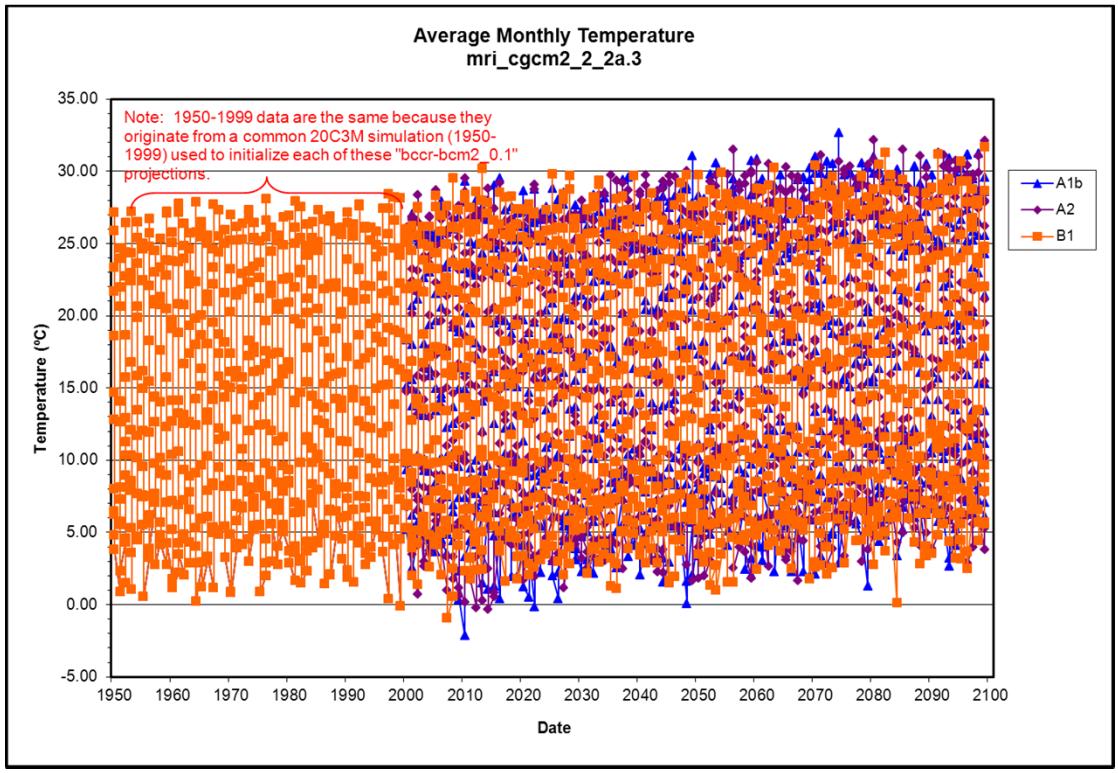

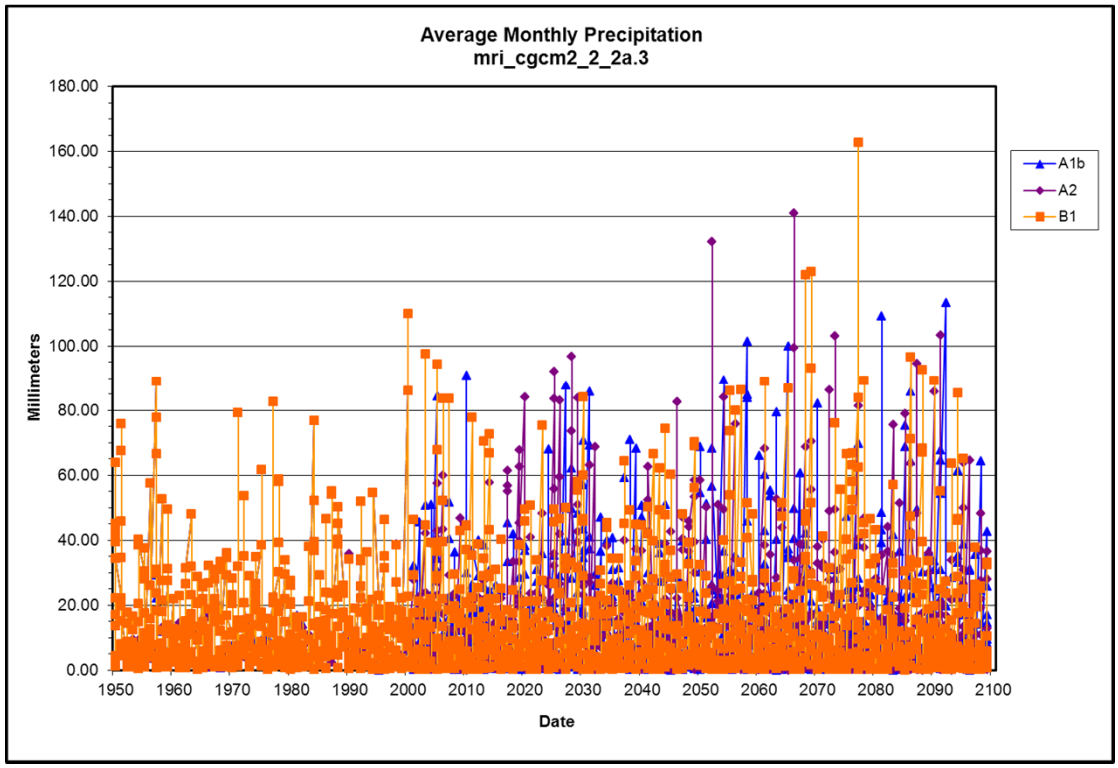

Climate Model mri_cgcm2_2_2a.3 (page 2 of 3)

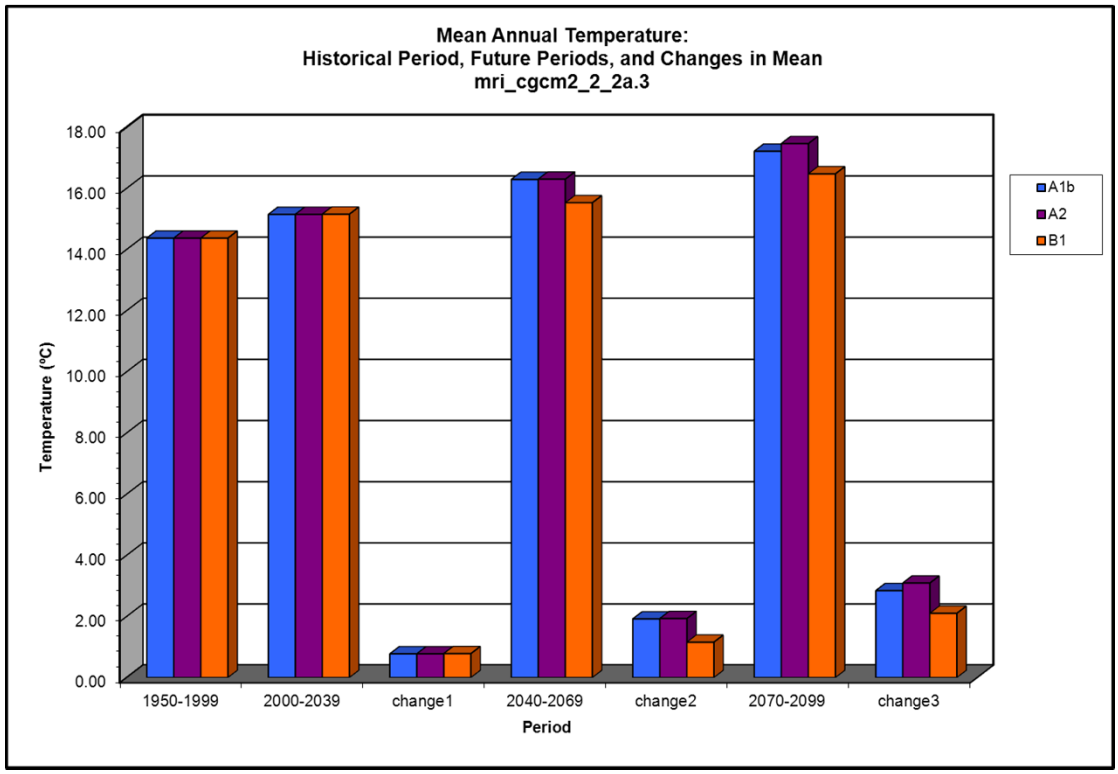

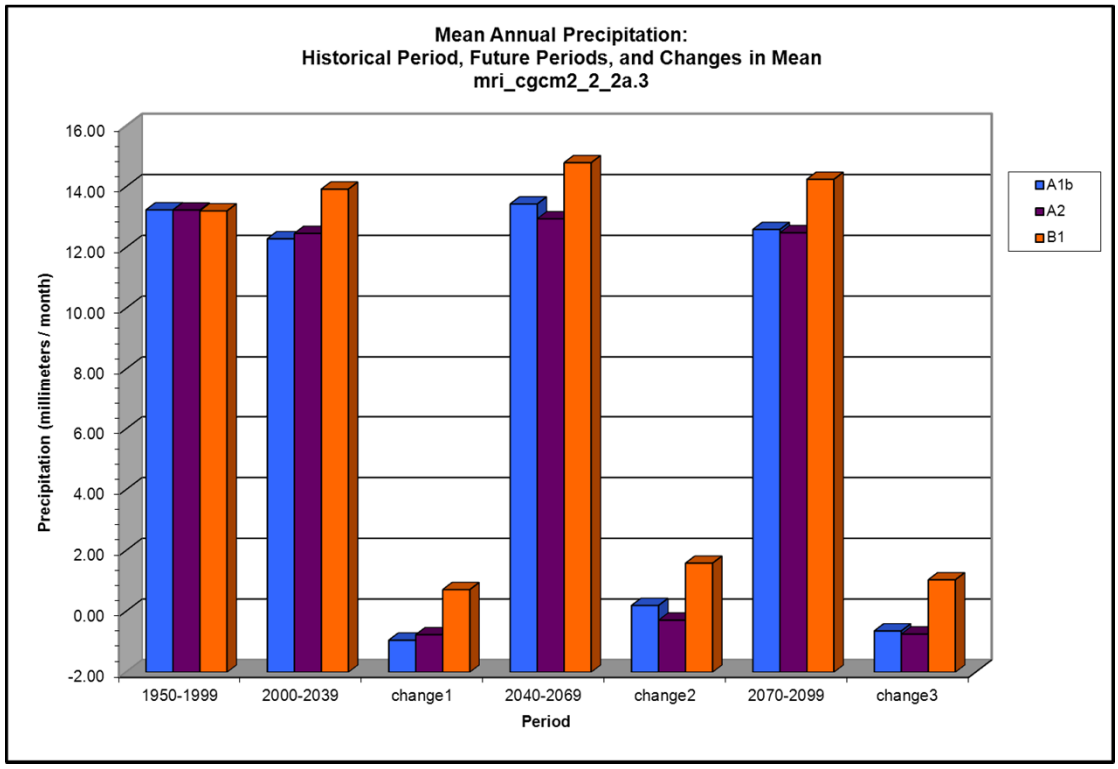

Climate Model mri_cgcm2_2_2a.3 (page 3 of 3)

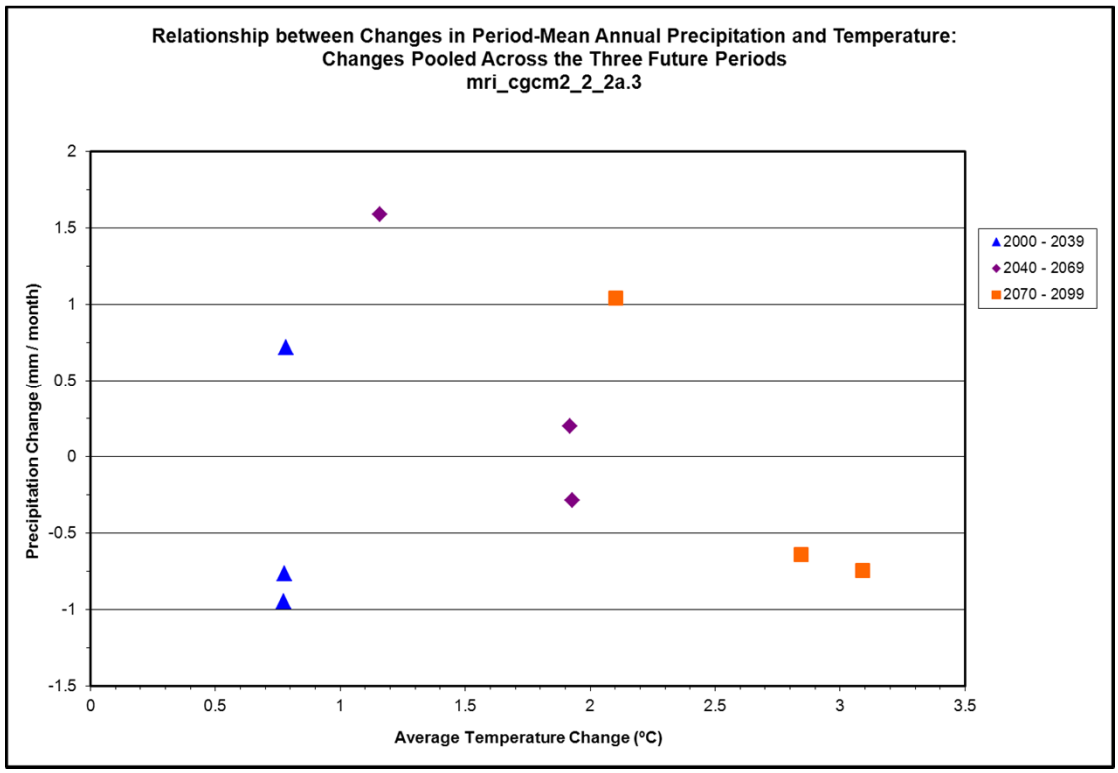

Climate Model mri_cgcm2_2_2a.4 (page 1 of 3)

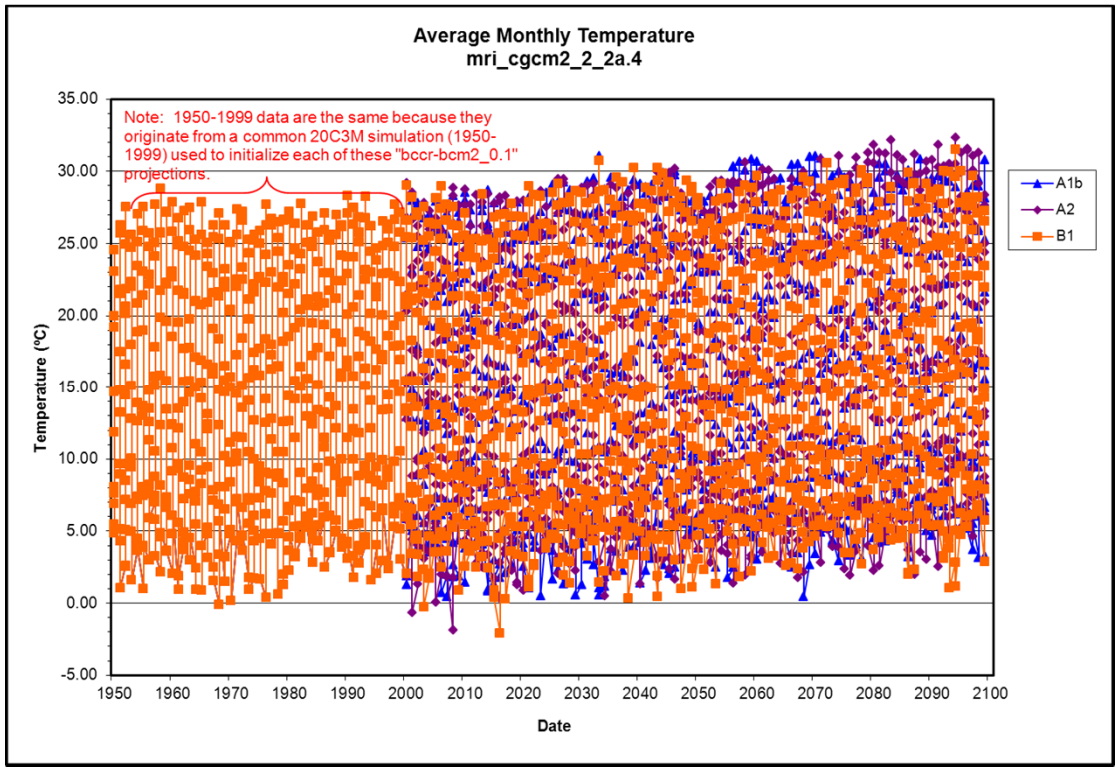

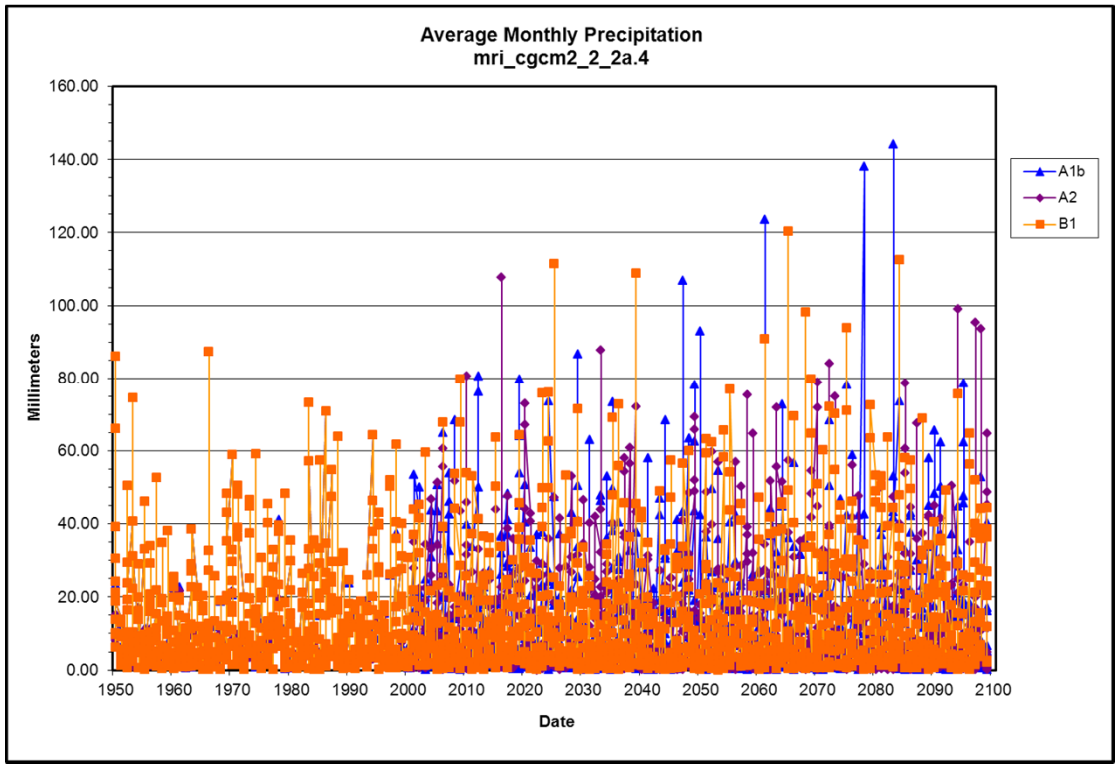

Climate Model mri_cgcm2_2_2a.4 (page 2 of 3)

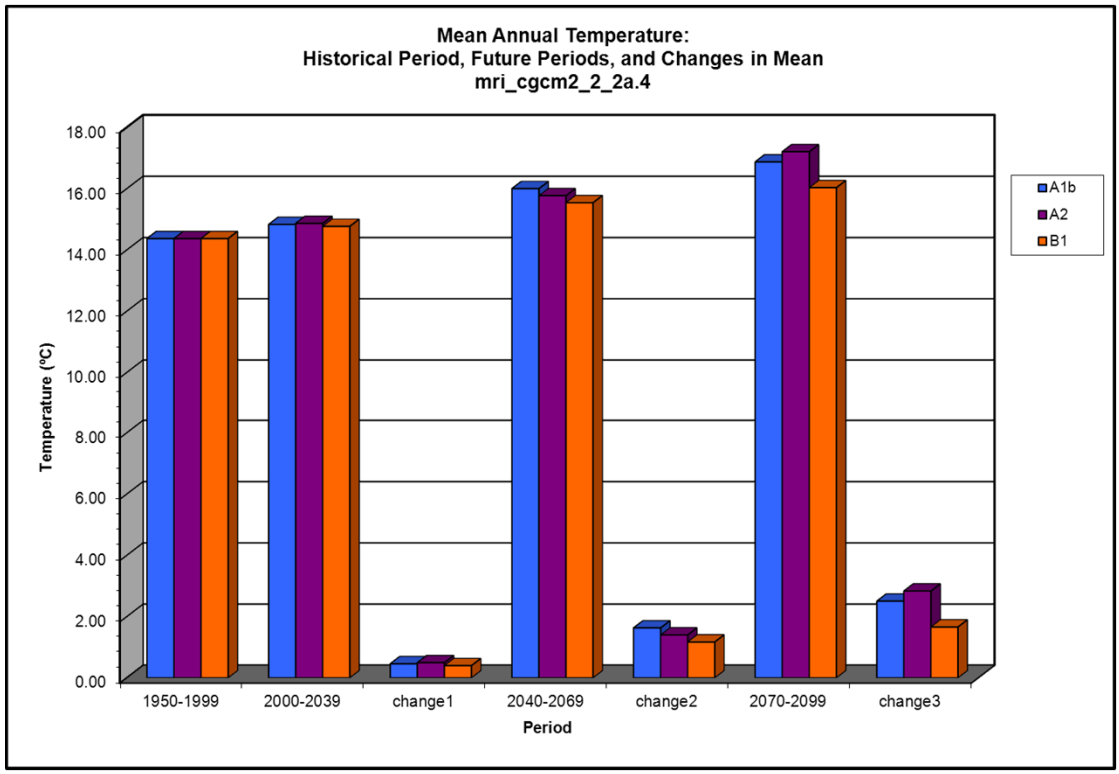

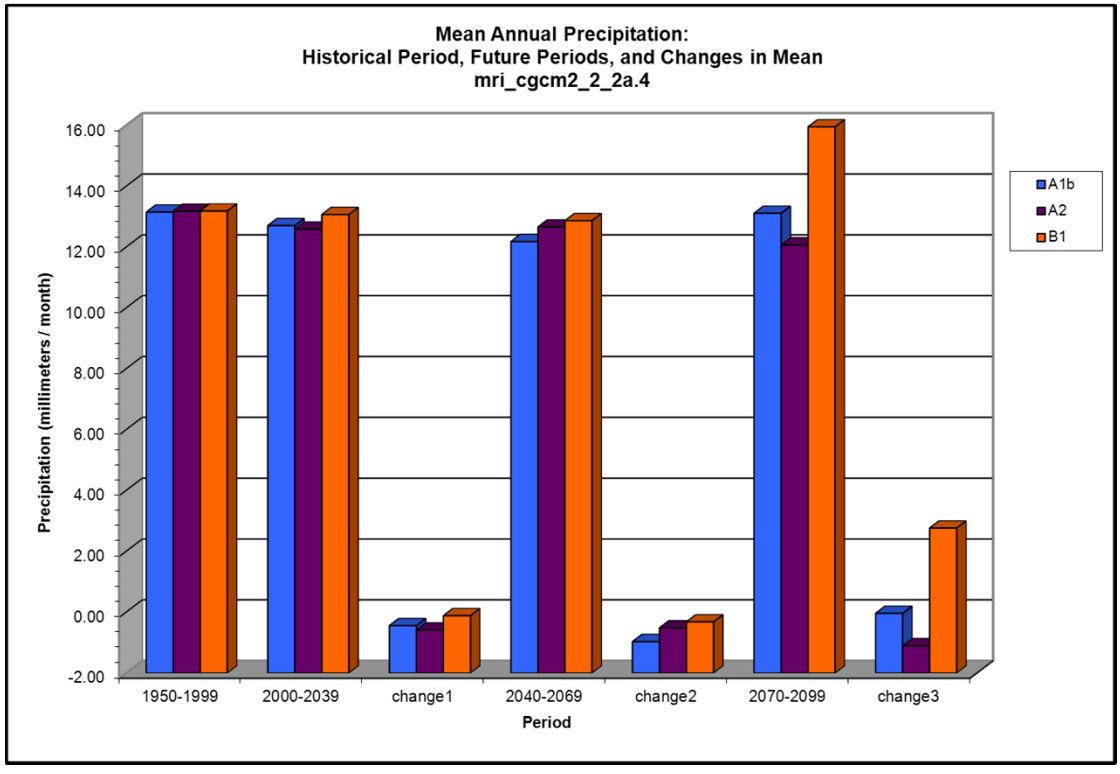

Climate Model mri_cgcm2_2_2a.4 (page 3 of 3)

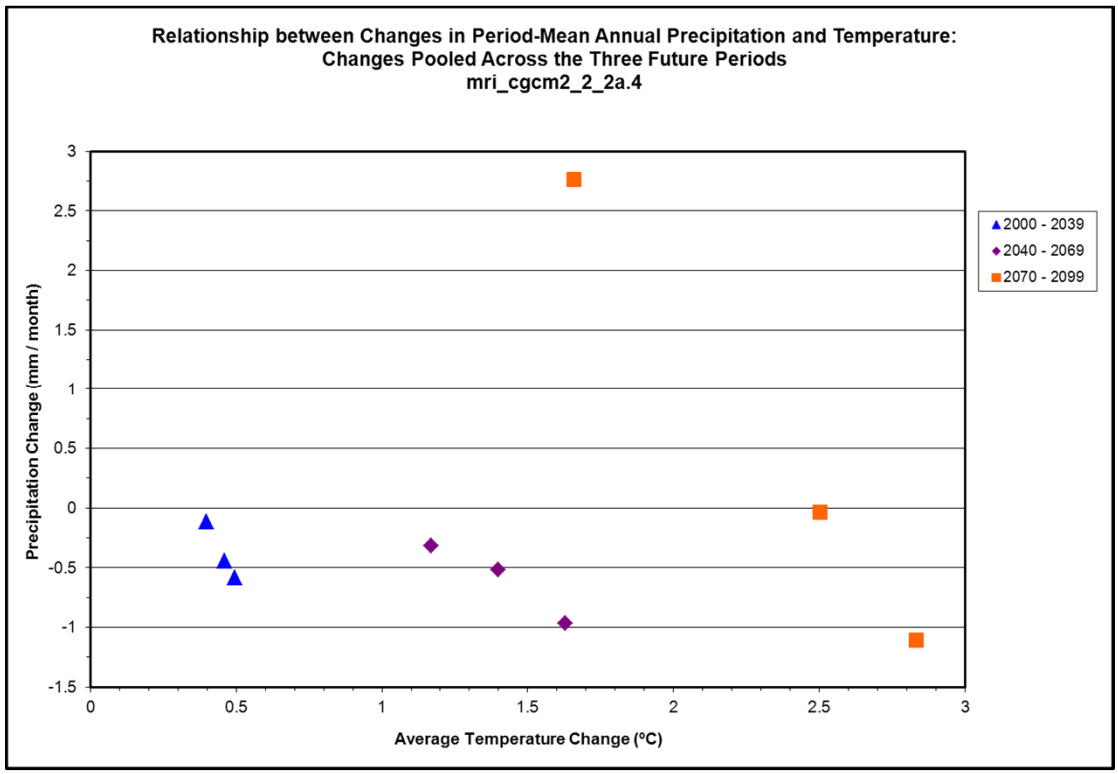

Climate Model mri_cgcm2_2_2a.5 (page 1 of 3)

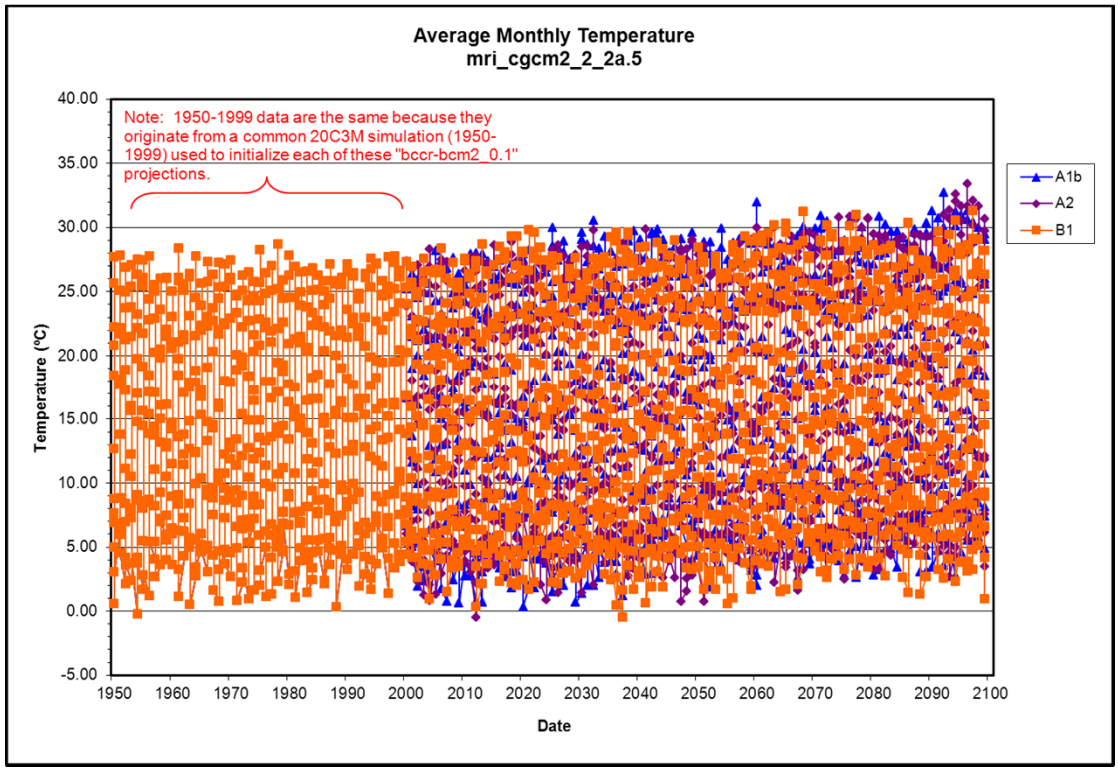

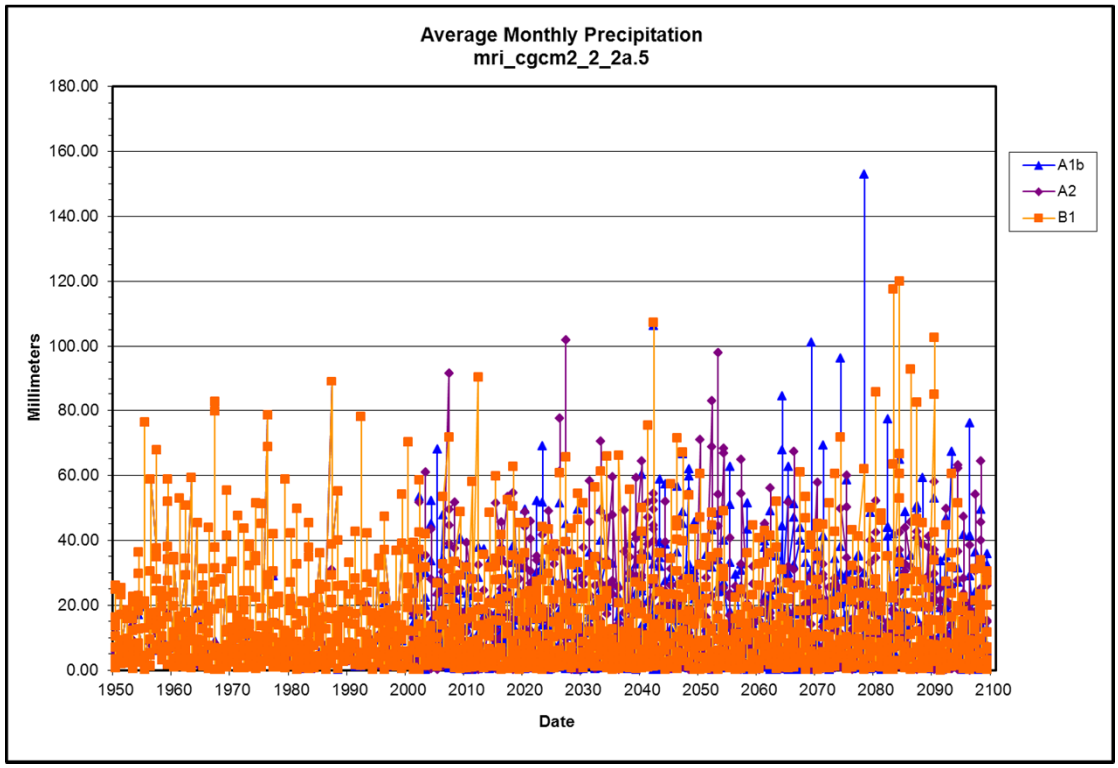

Climate Model mri_cgcm2_2_2a.5 (page 2 of 3)

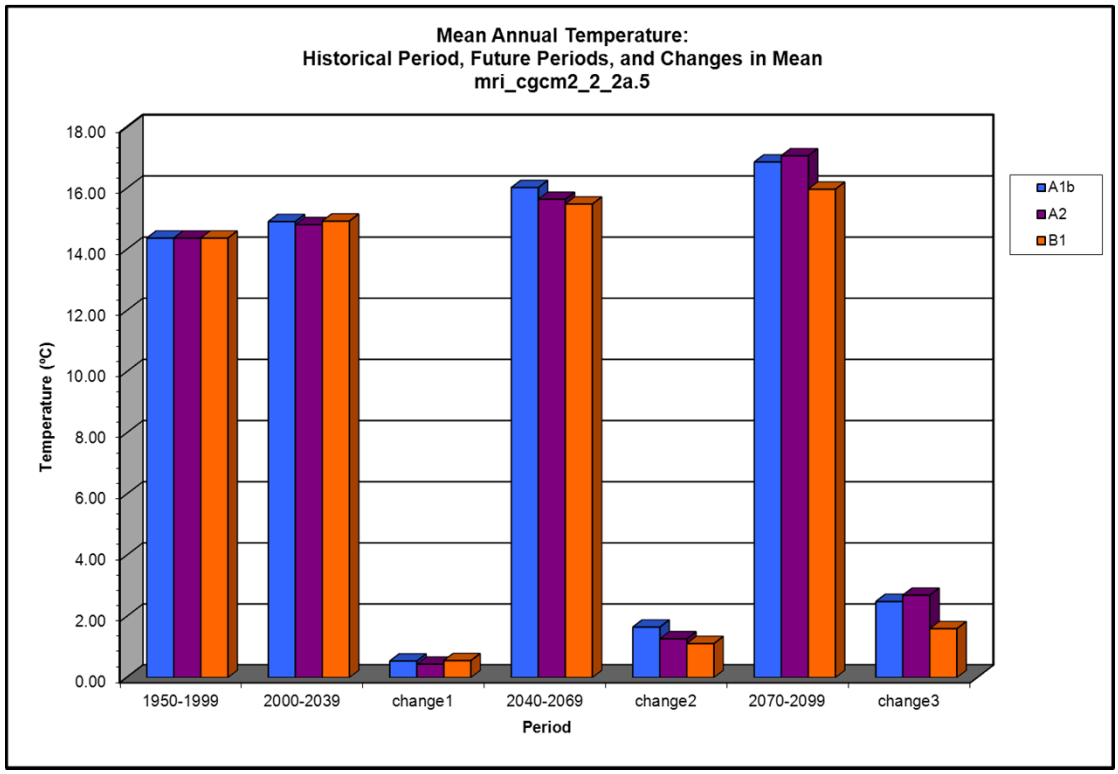

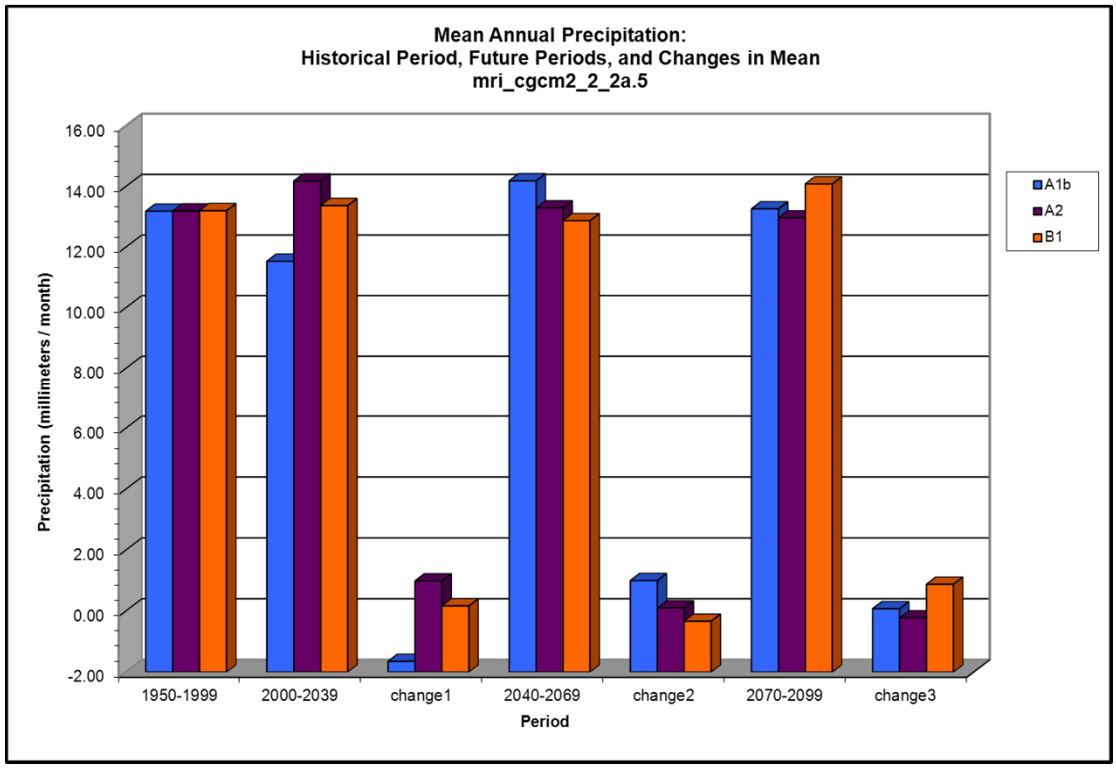

Climate Model mri_cgcm2_2_2a.5 (page 3 of 3)

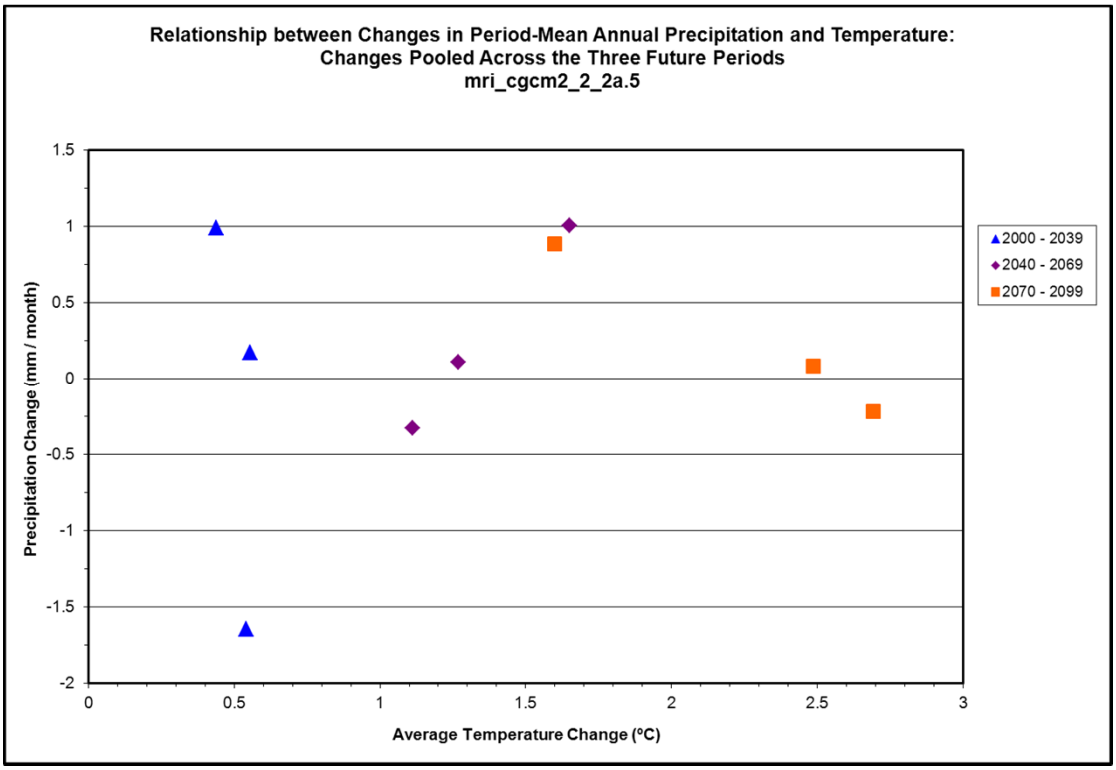

Climate Model ncar_ccsm3_0.1 (page 1 of 3)

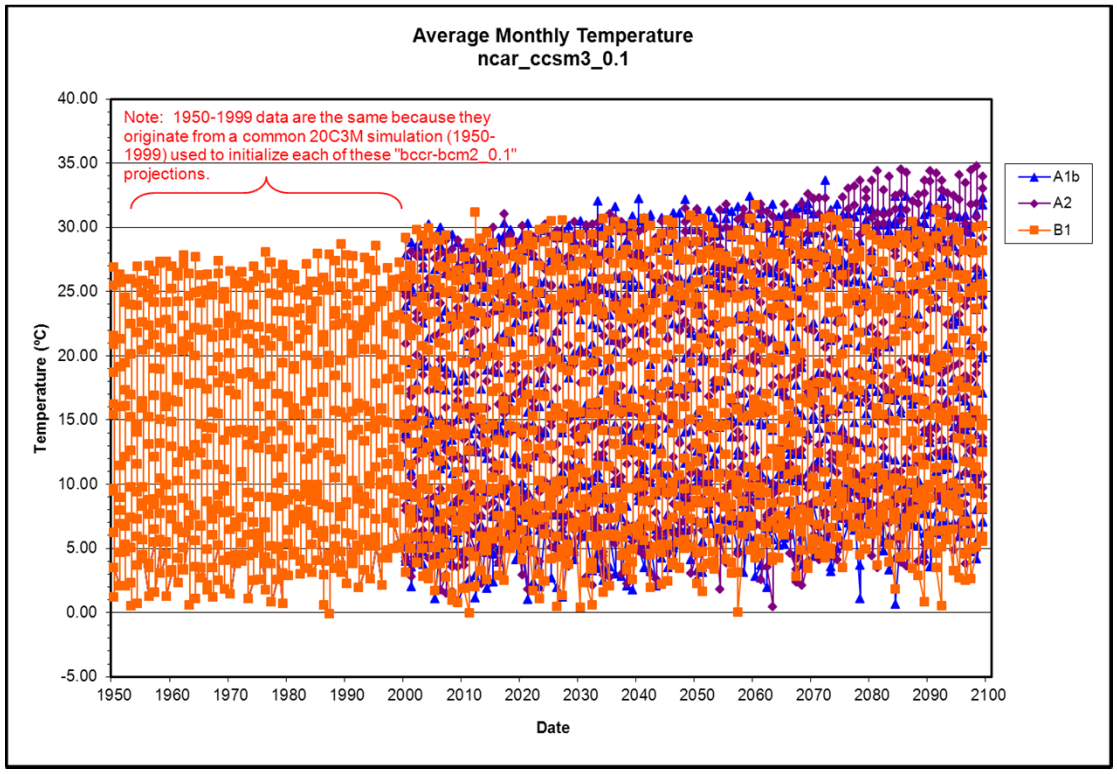

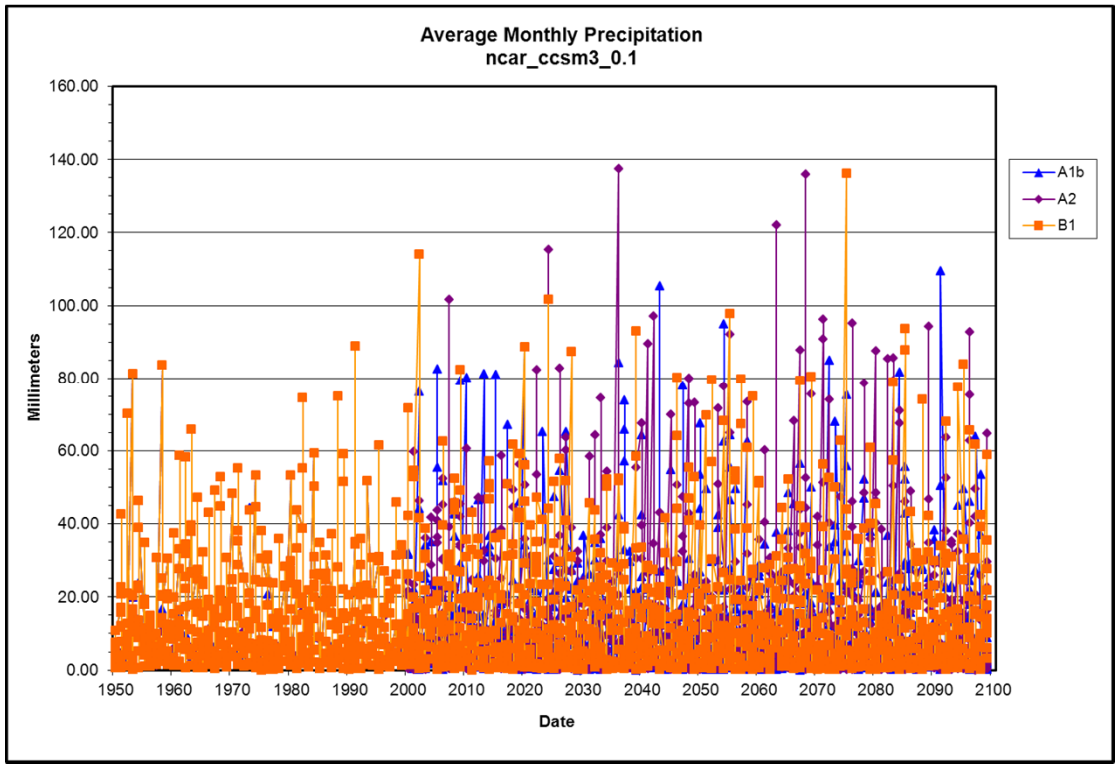

Climate Model ncar_ccsm3_0.1 (page 2 of 3)

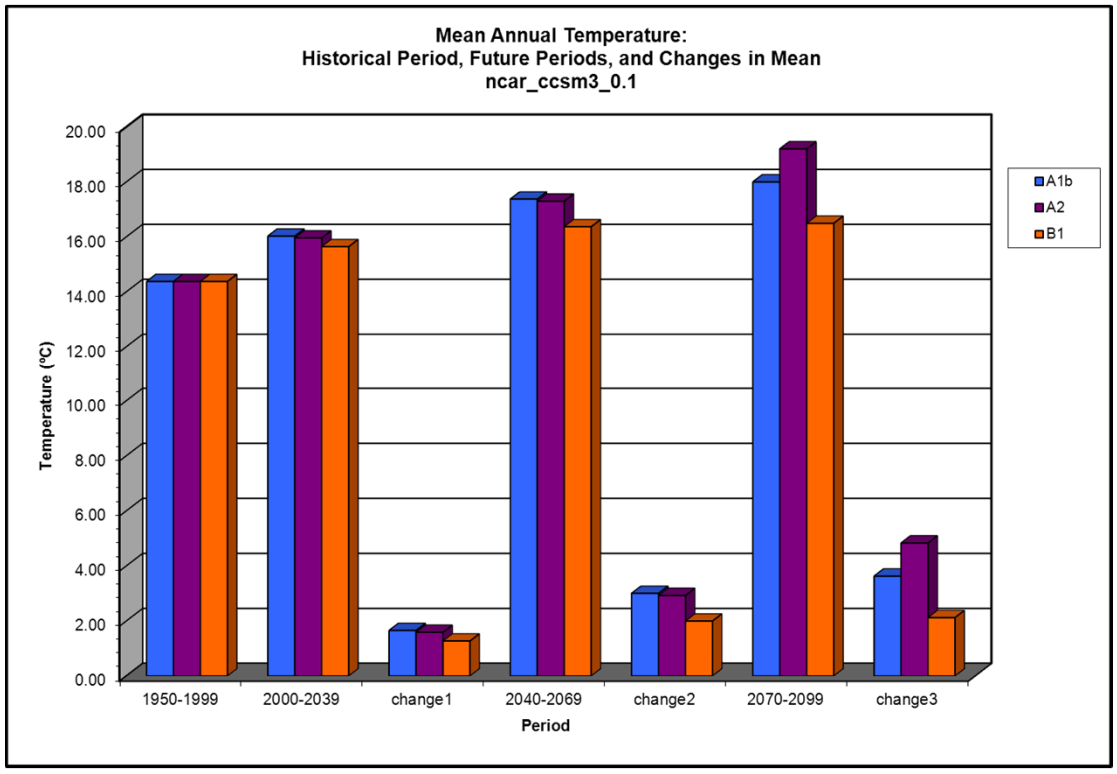

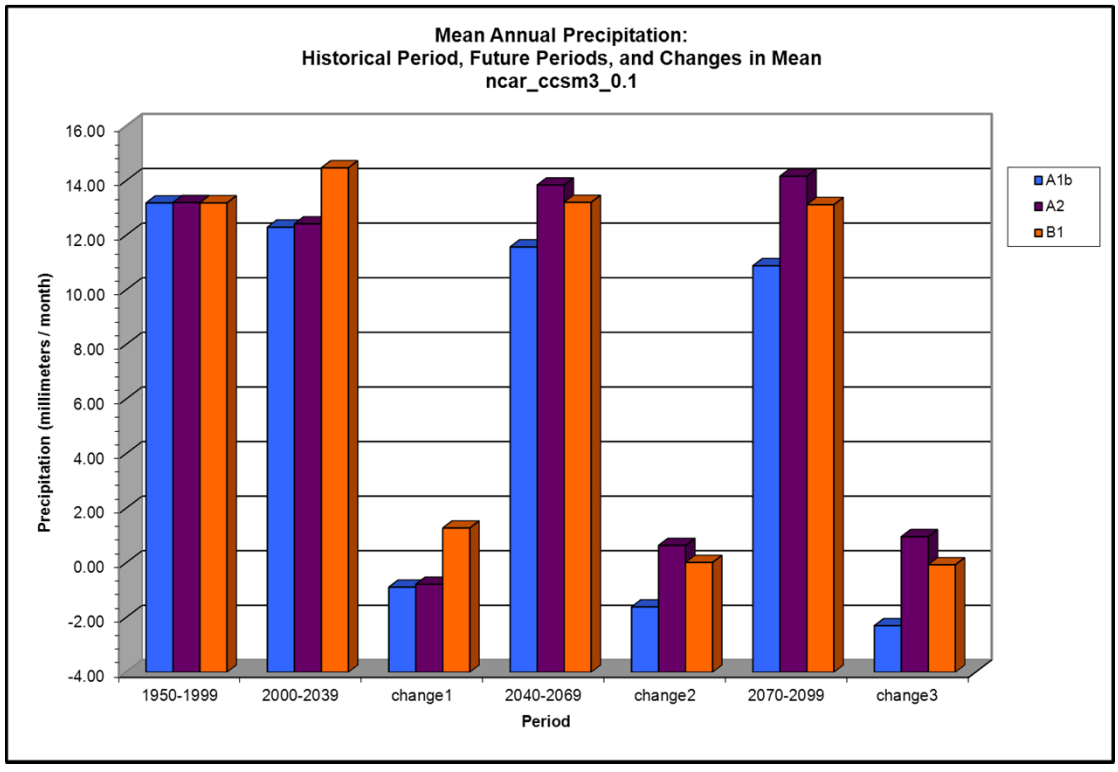

Climate Model ncar_ccsm3_0.1 (page 3 of 3)

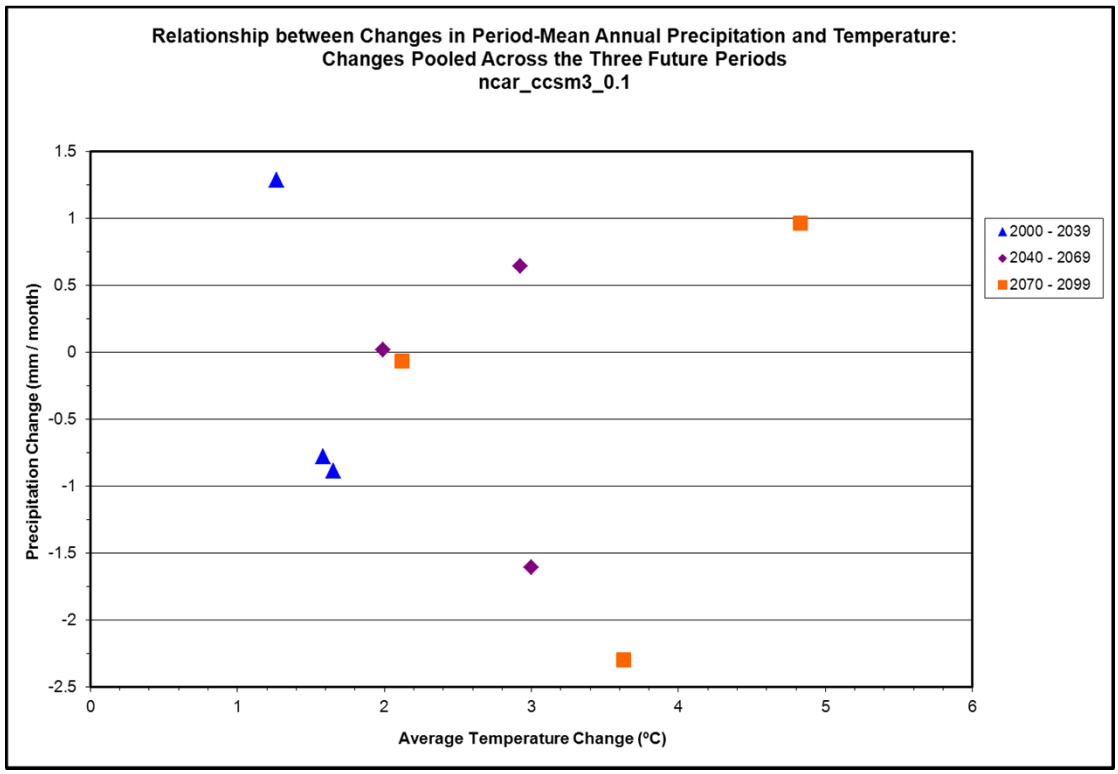

Climate Model ncar_ccsm3_0.2 (page 1 of 3)

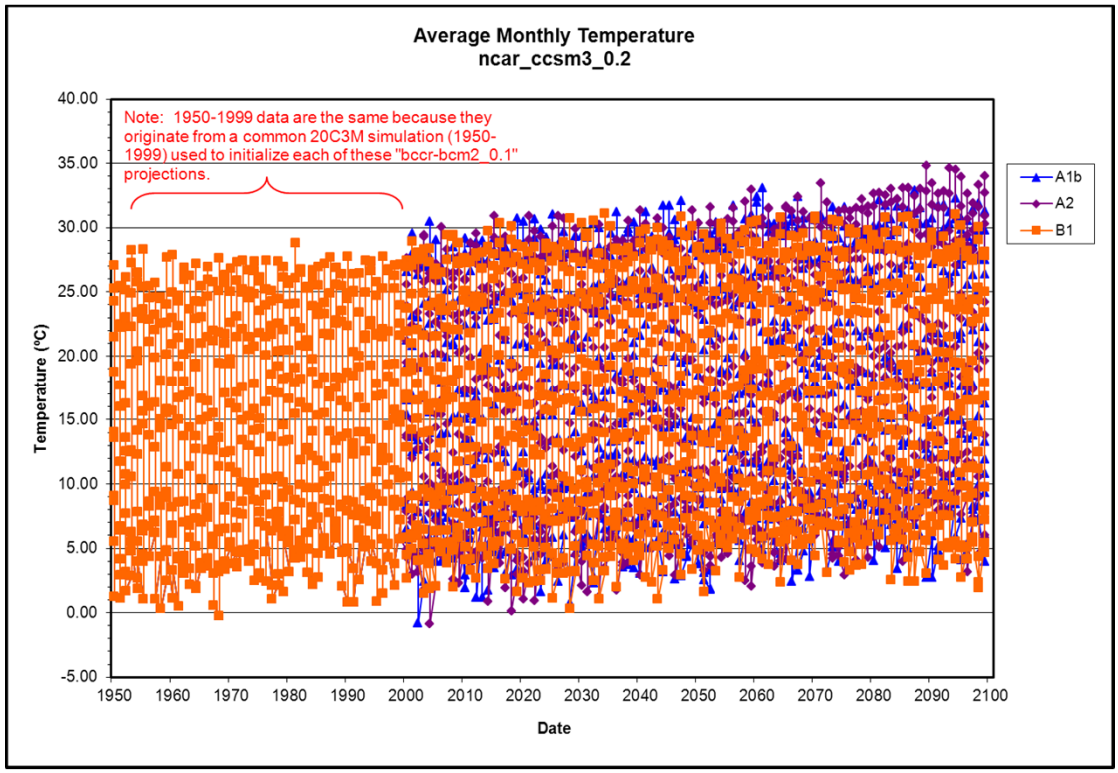

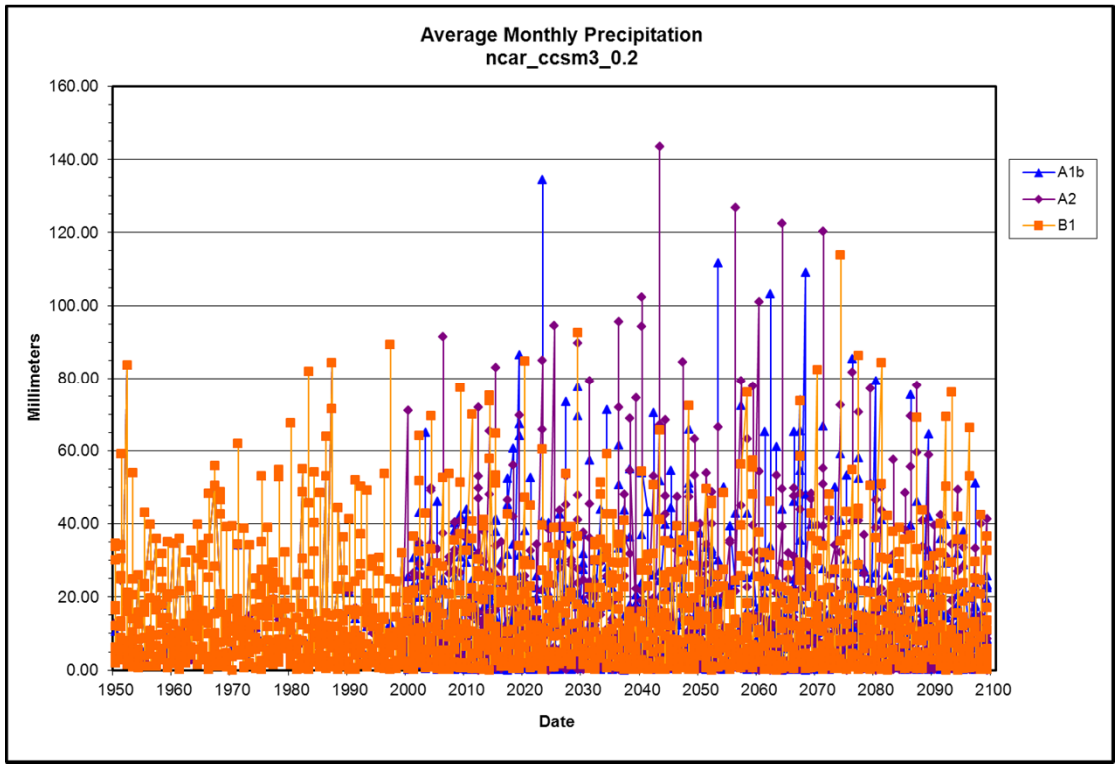

Climate Model ncar_ccsm3_0.2 (page 2 of 3)

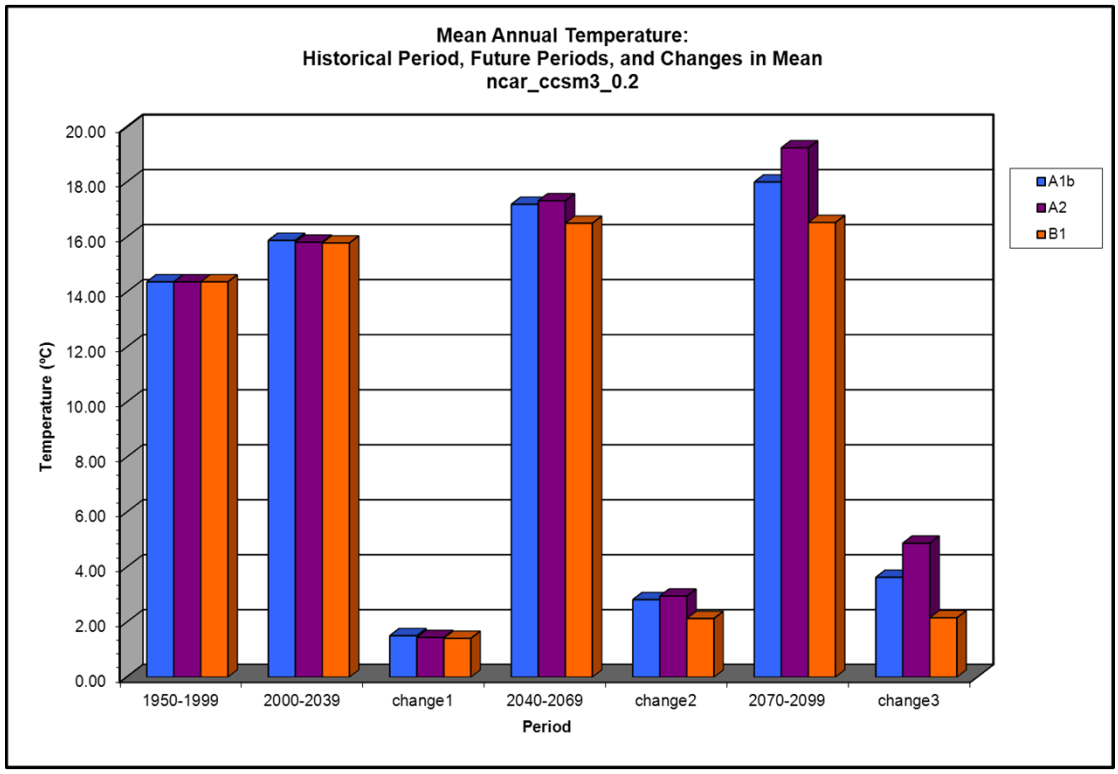

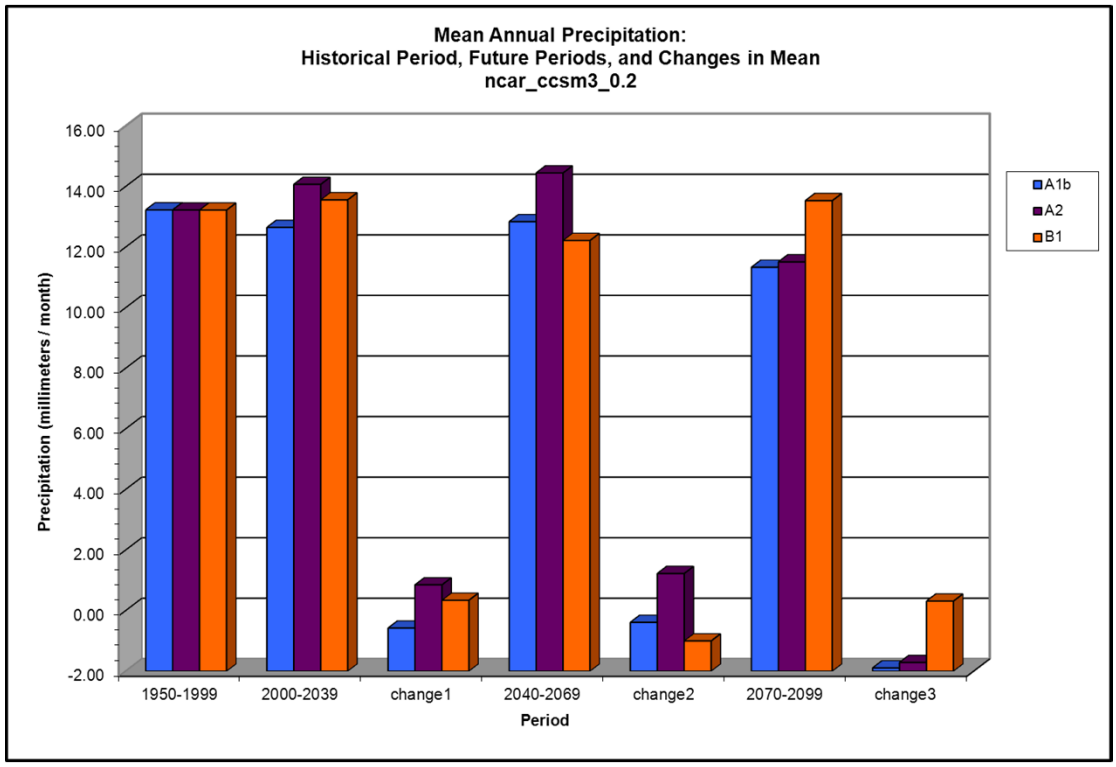

Climate Model ncar_ccsm3_0.2 (page 3 of 3)

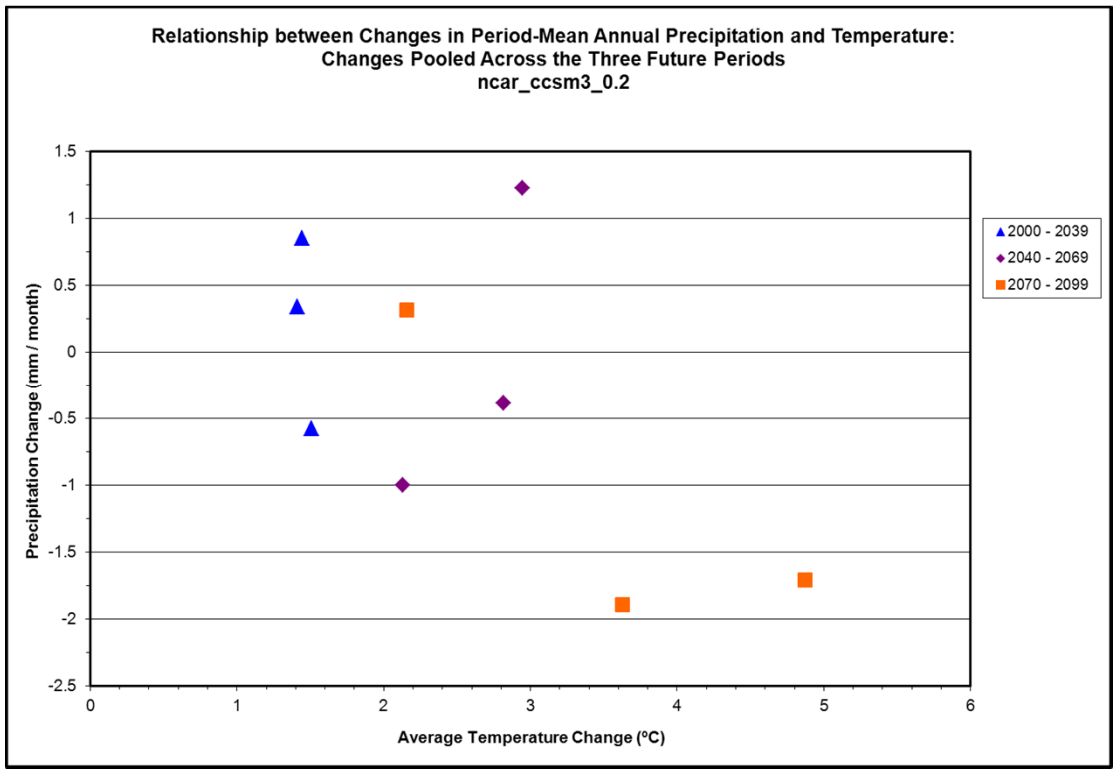

Climate Model ncar_ccsm3_0.3 (page 1 of 3)

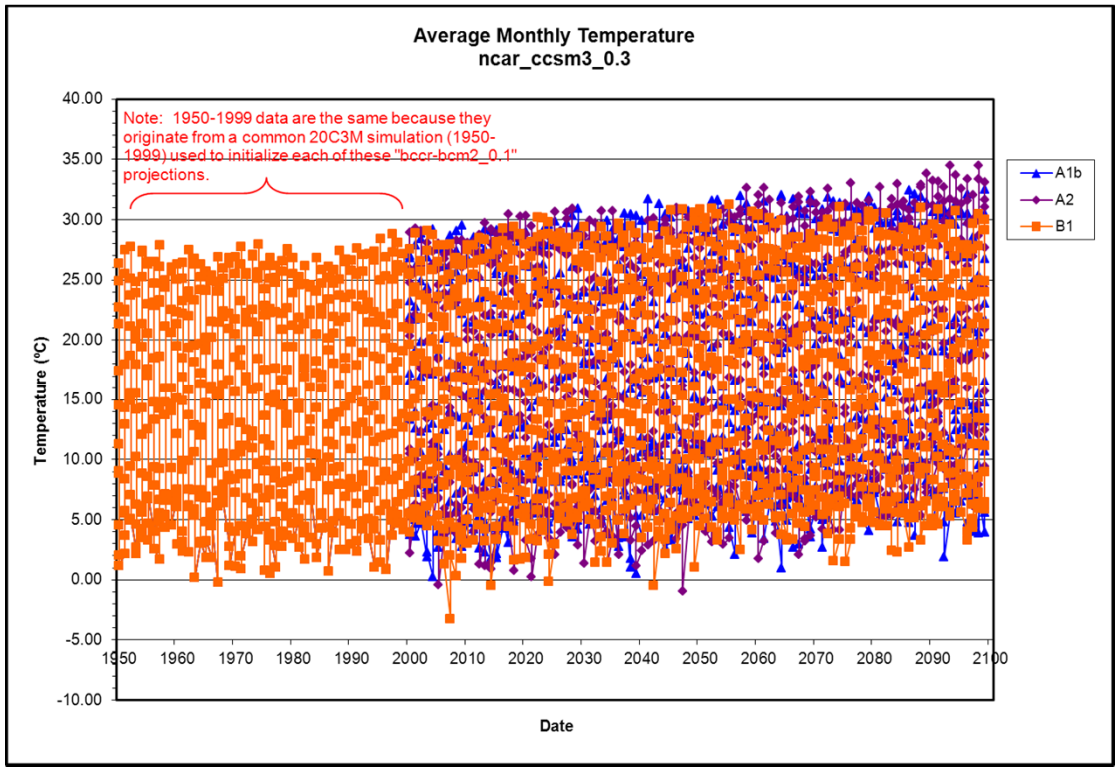

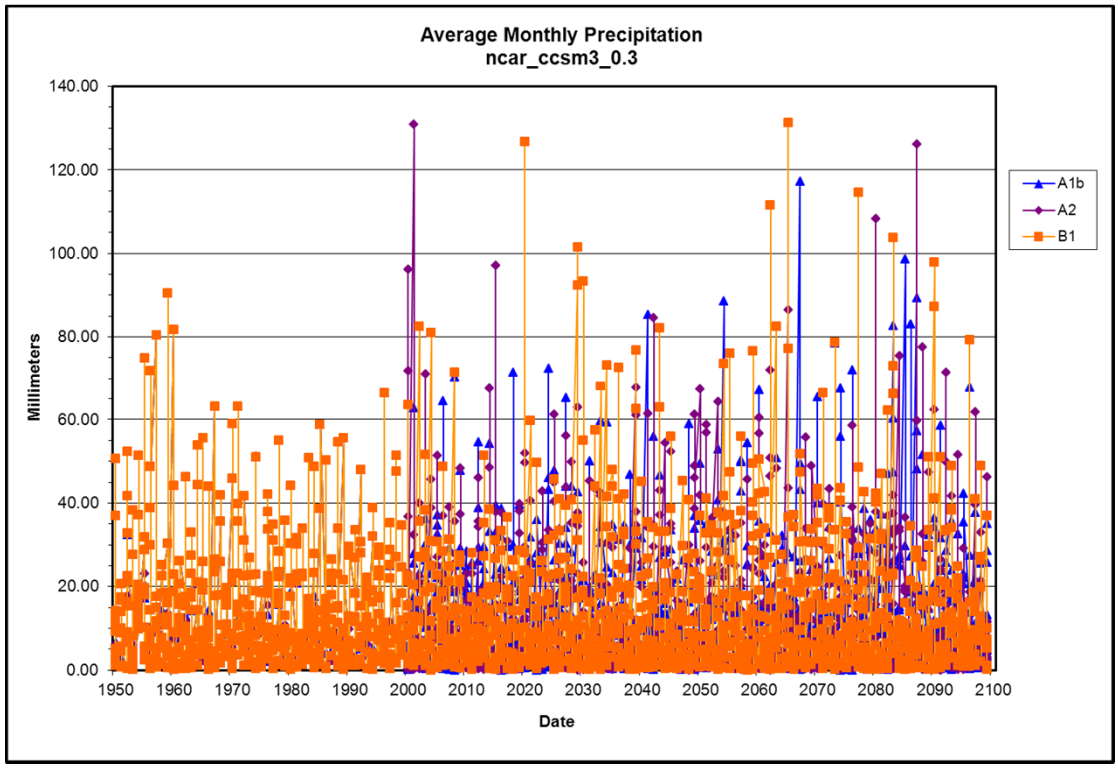

Climate Model ncar_ccsm3_0.3 (page 2 of 3)

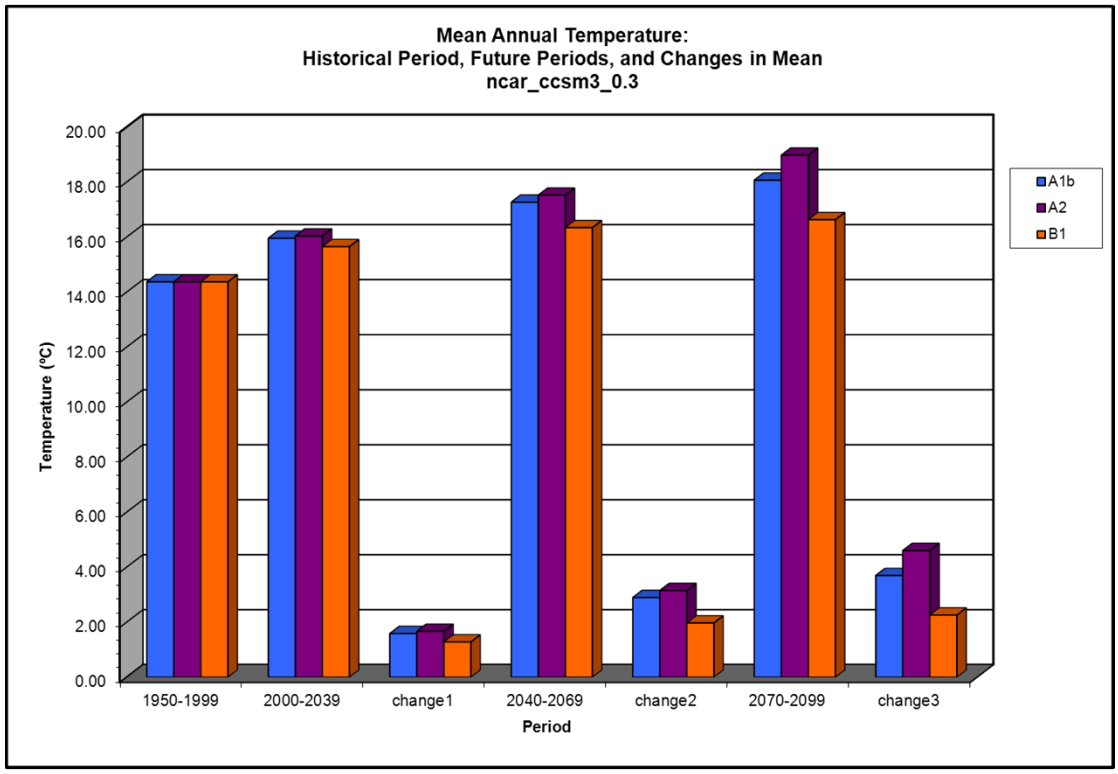

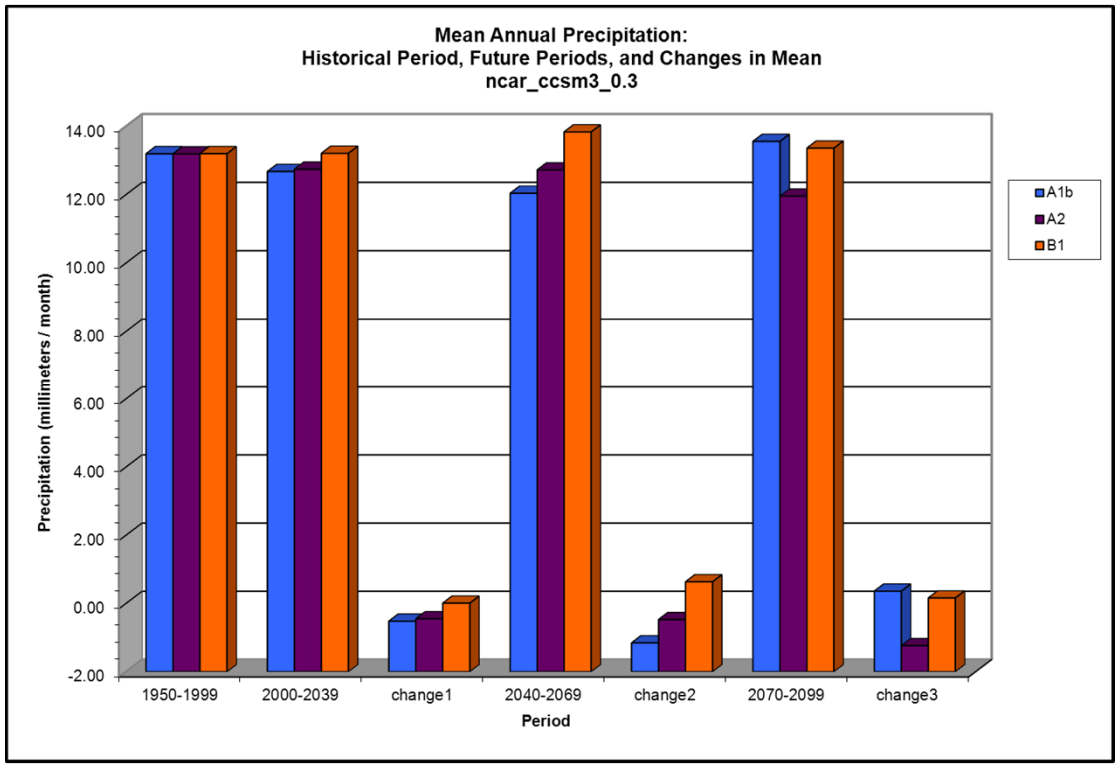

Climate Model ncar_ccsm3_0.3 (page 3 of 3)

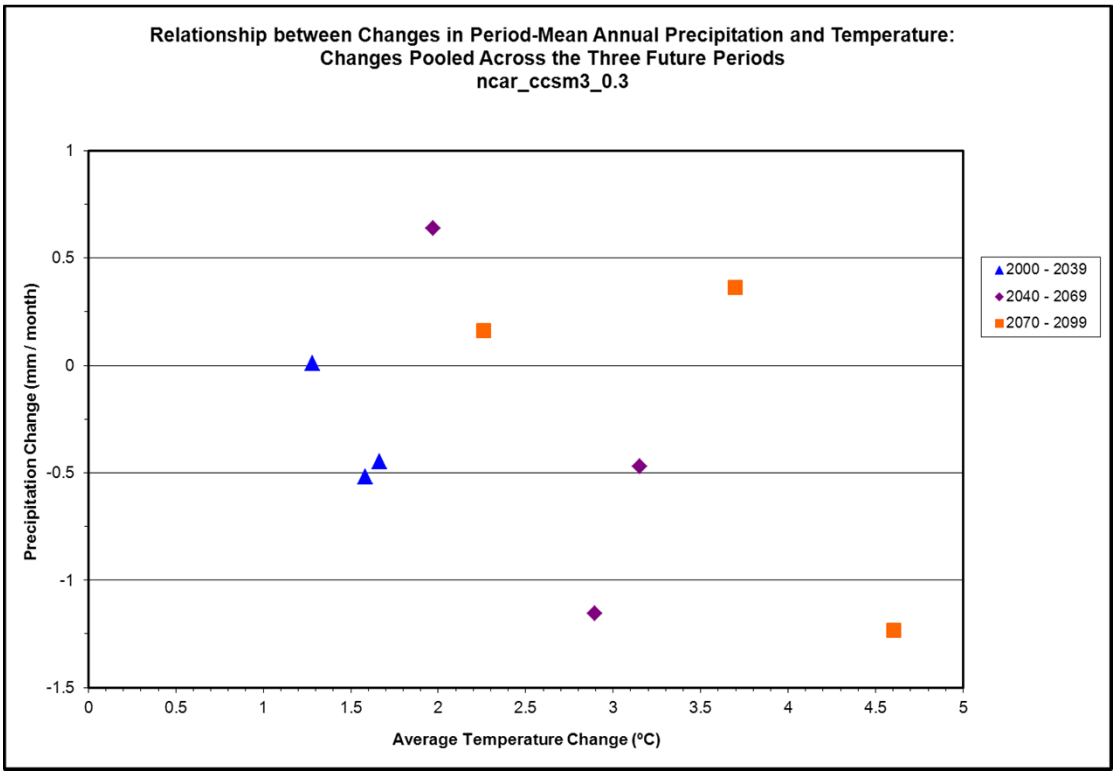

Climate Model ncar_ccsm3_0.4 (page 1 of 3)

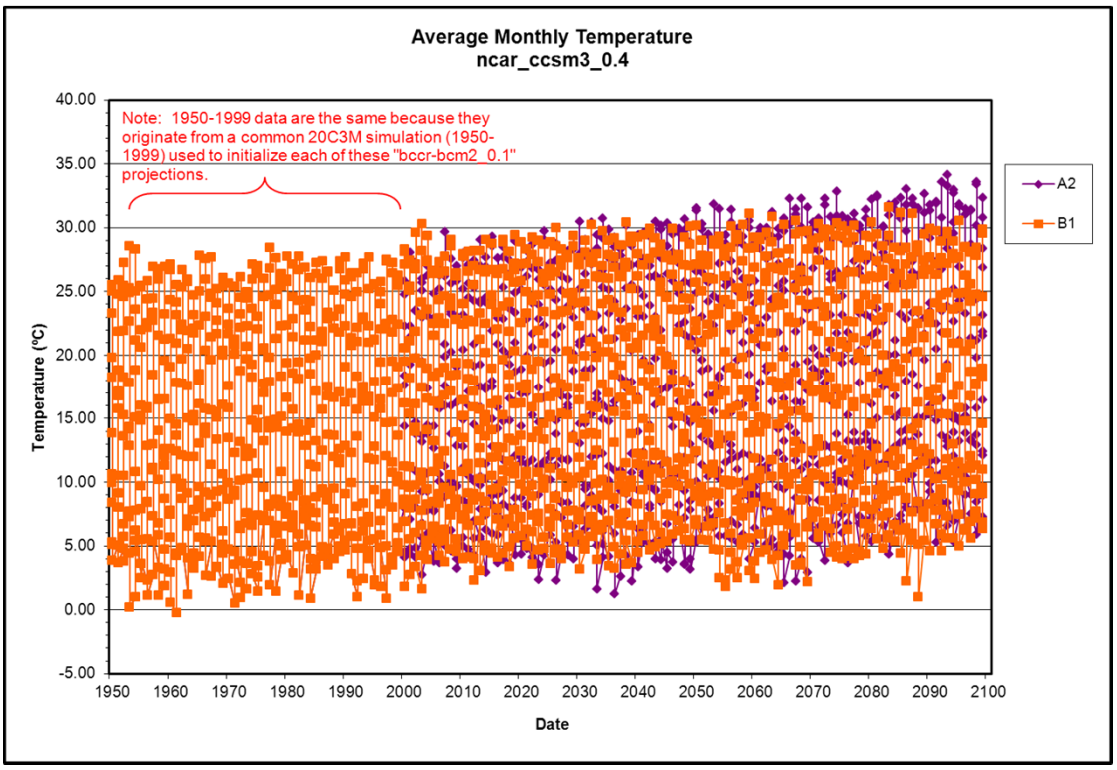

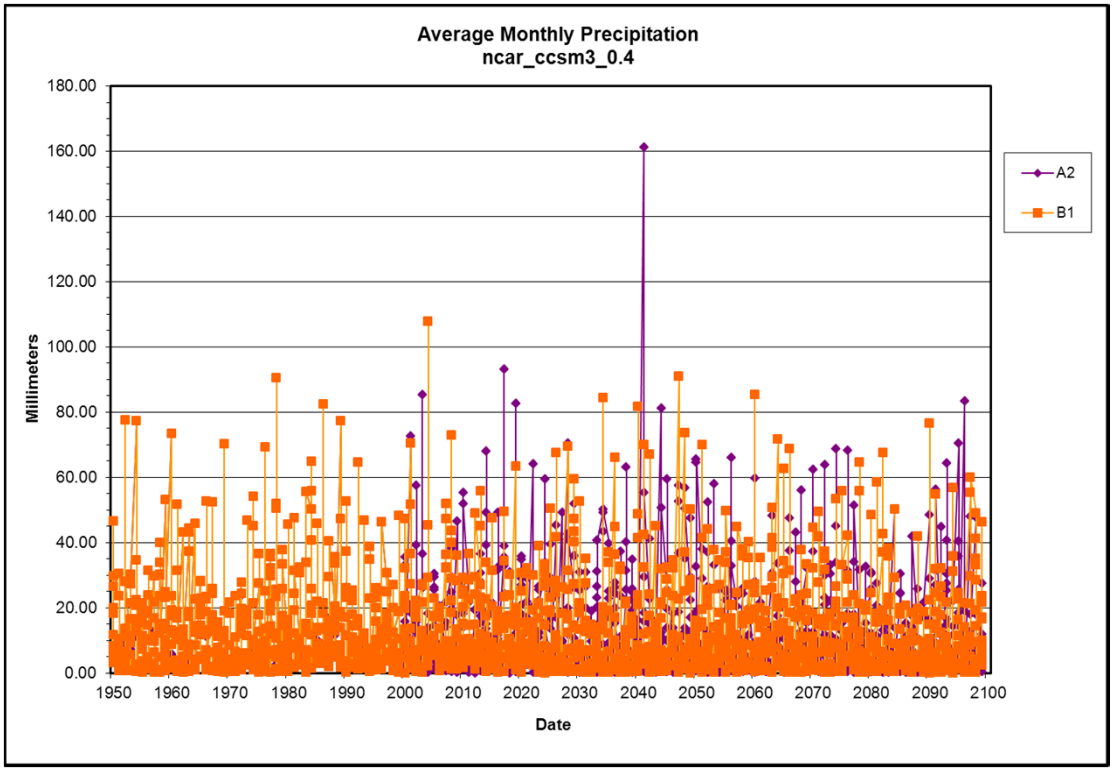

Climate Model ncar_ccsm3_0.4 (page 2 of 3)

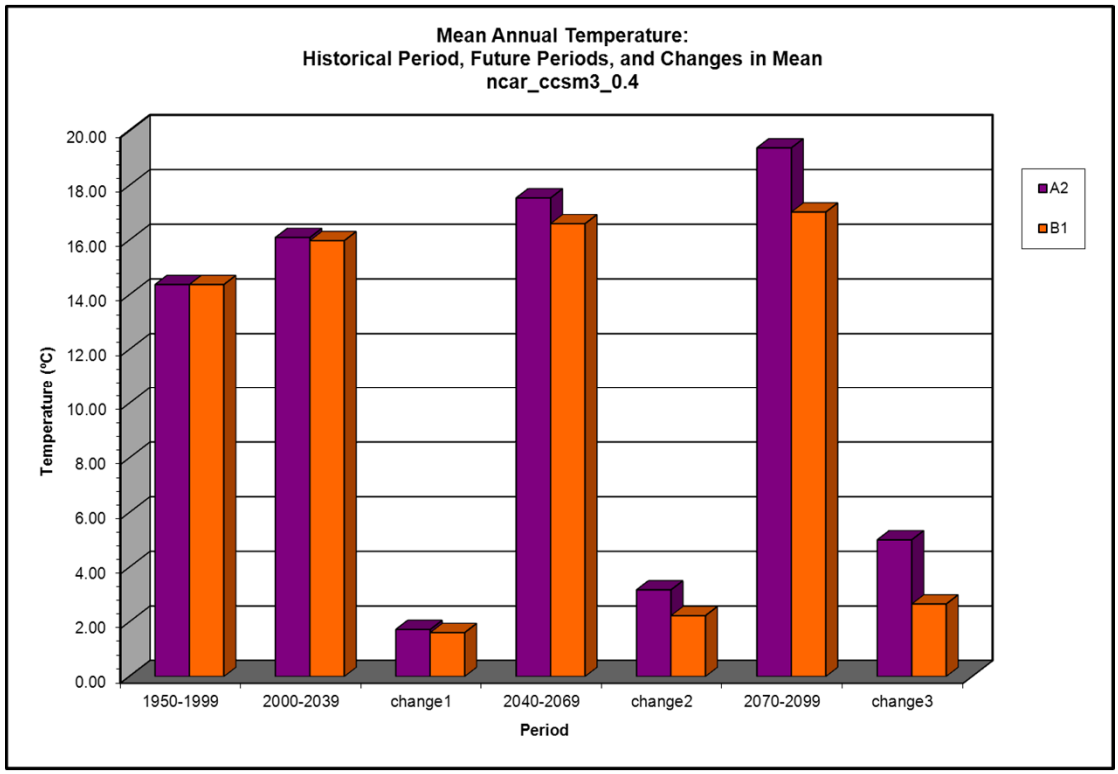

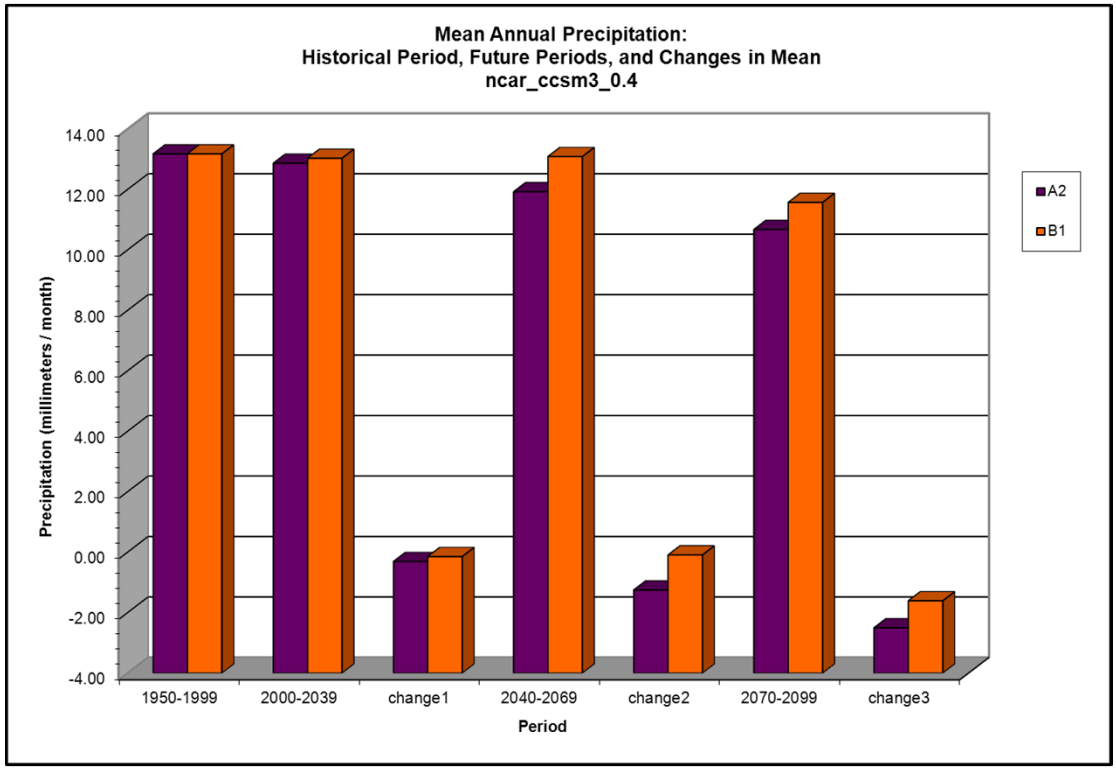

Climate Model ncar_ccsm3_0.4 (page 3 of 3)

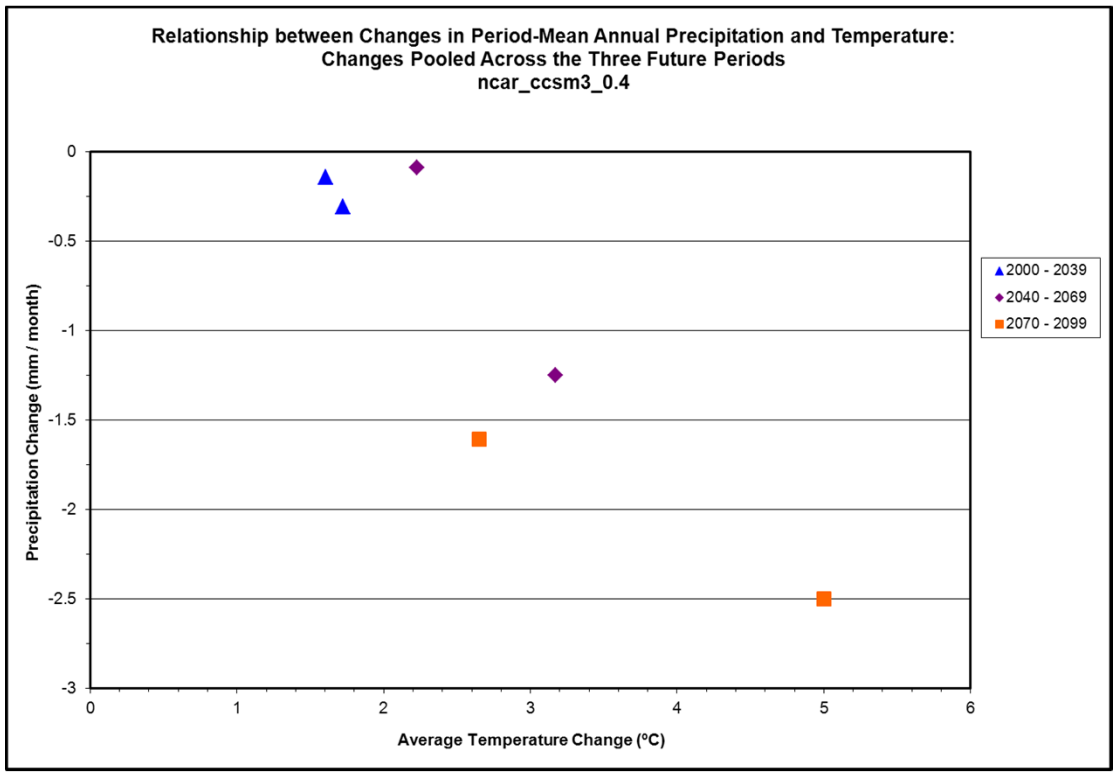

Climate Model ncar_ccsm3_0.5 (page 1 of 3)

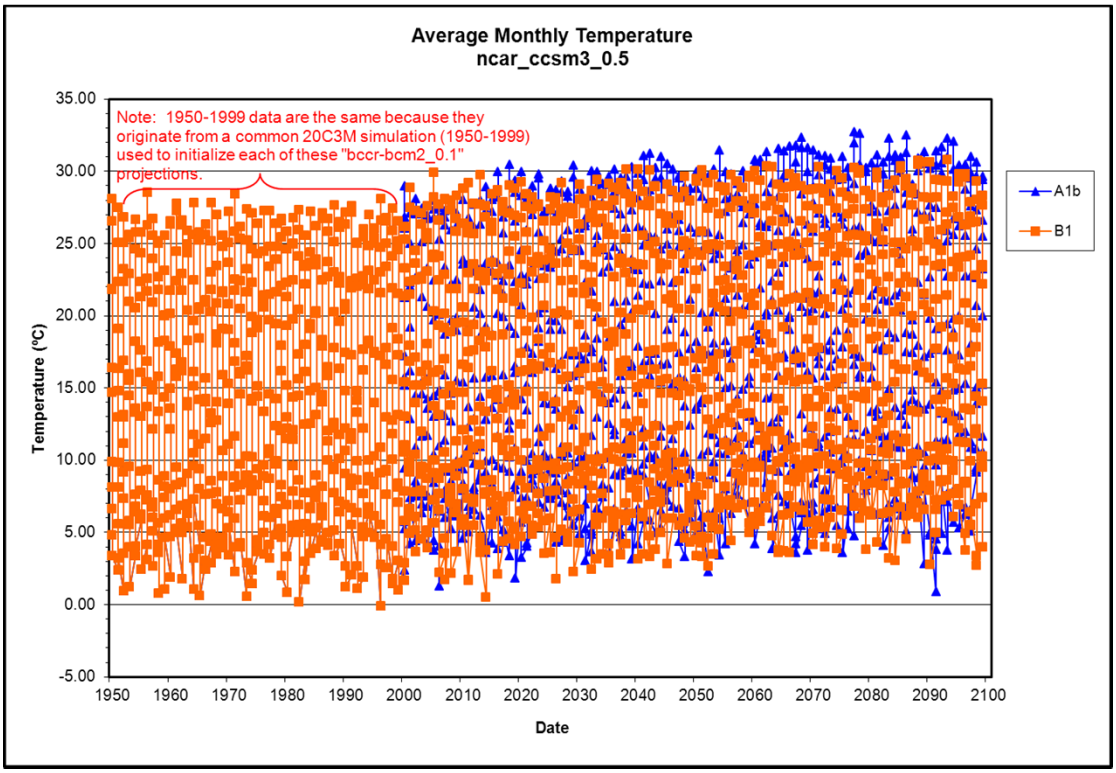

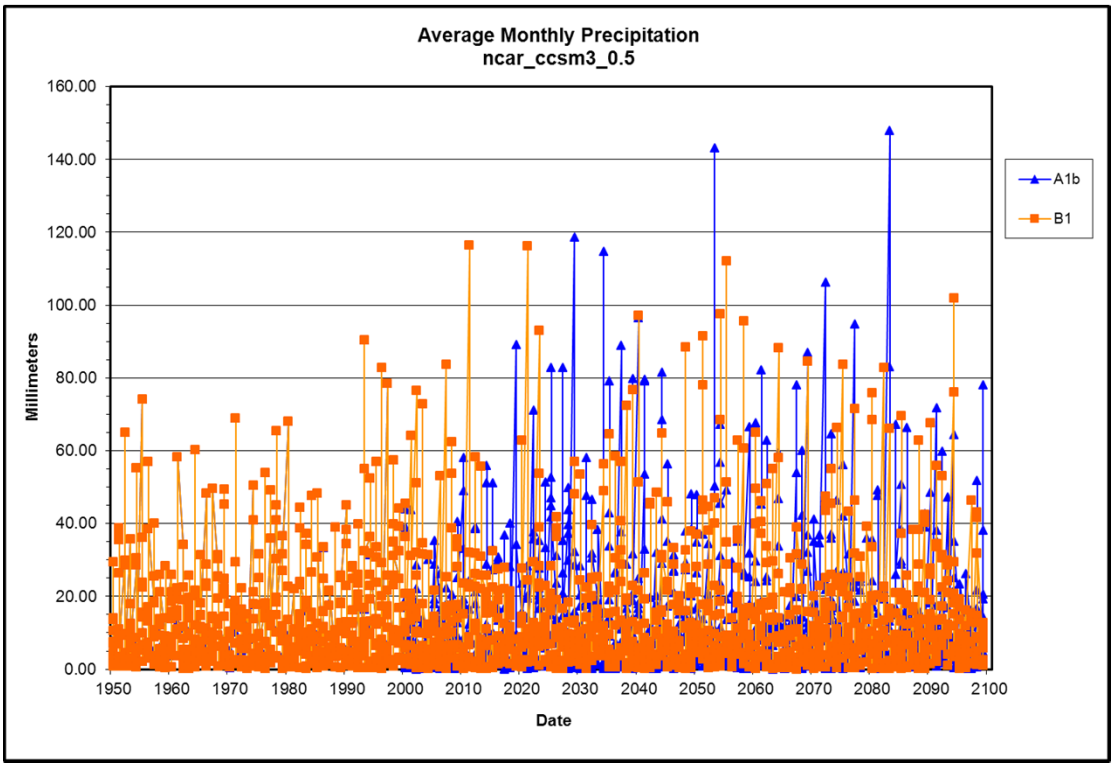

Climate Model ncar_ccsm3_0.5 (page 2 of 3)

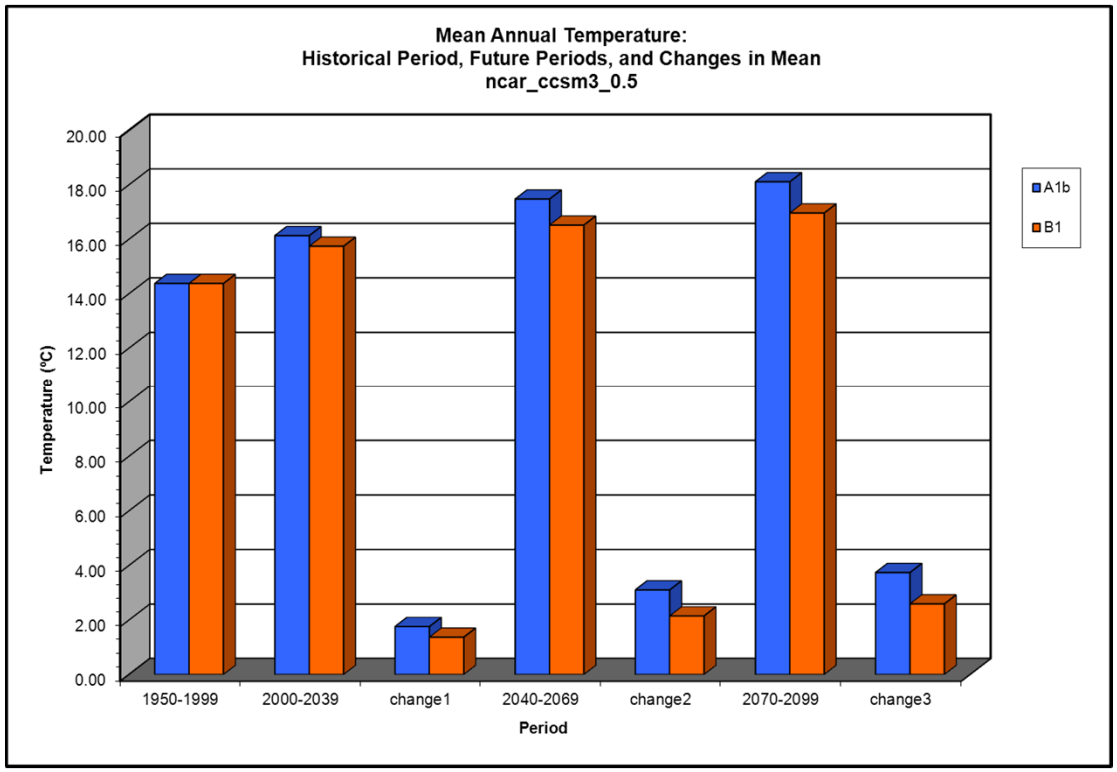

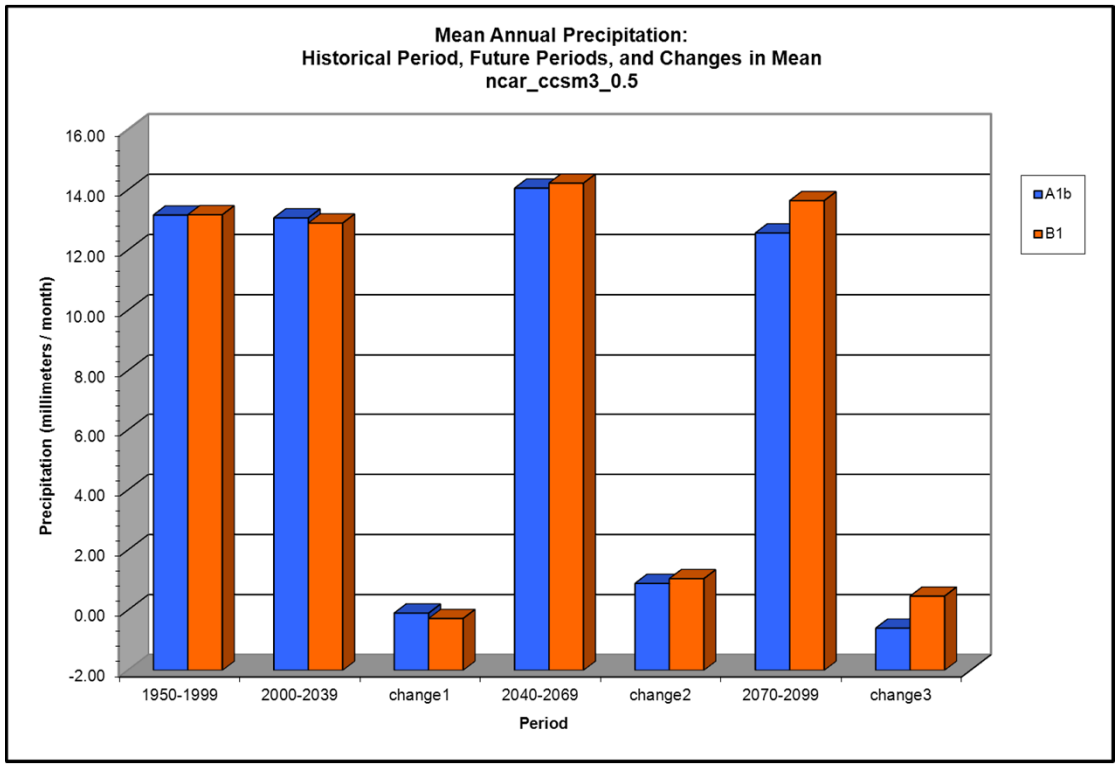

Climate Model ncar_ccsm3_0.5 (page 3 of 3)

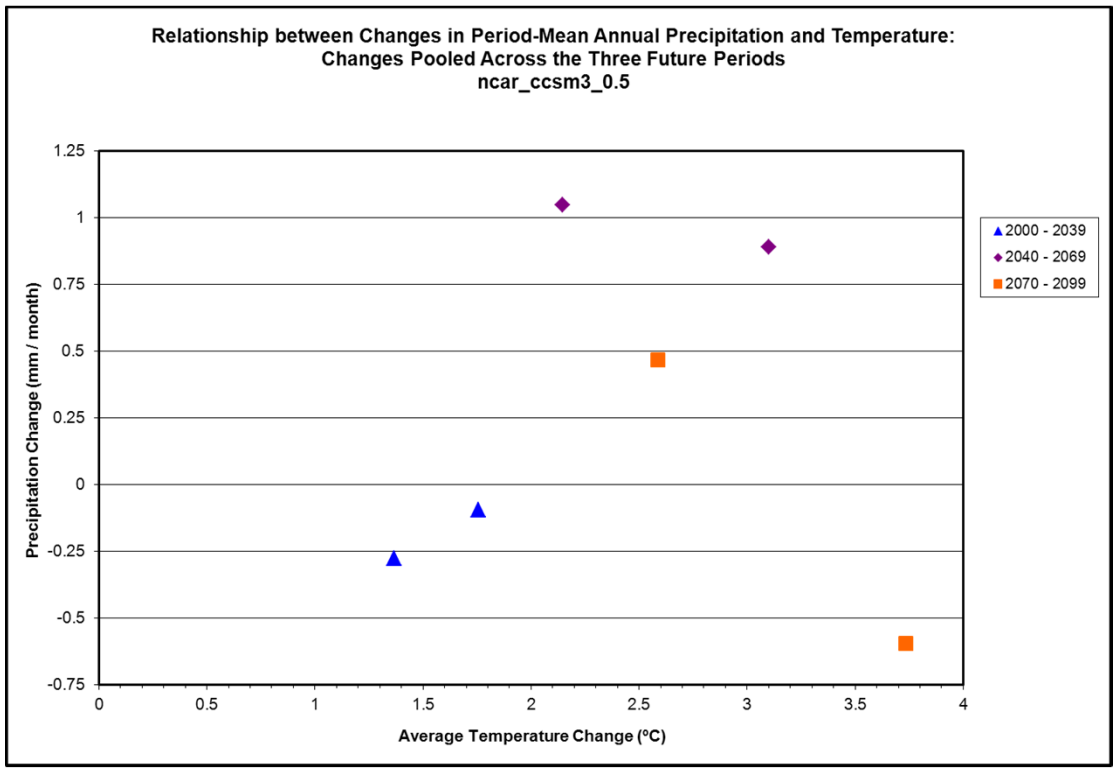

Climate Model ncar_ccsm3_0.6 (page 1 of 3)

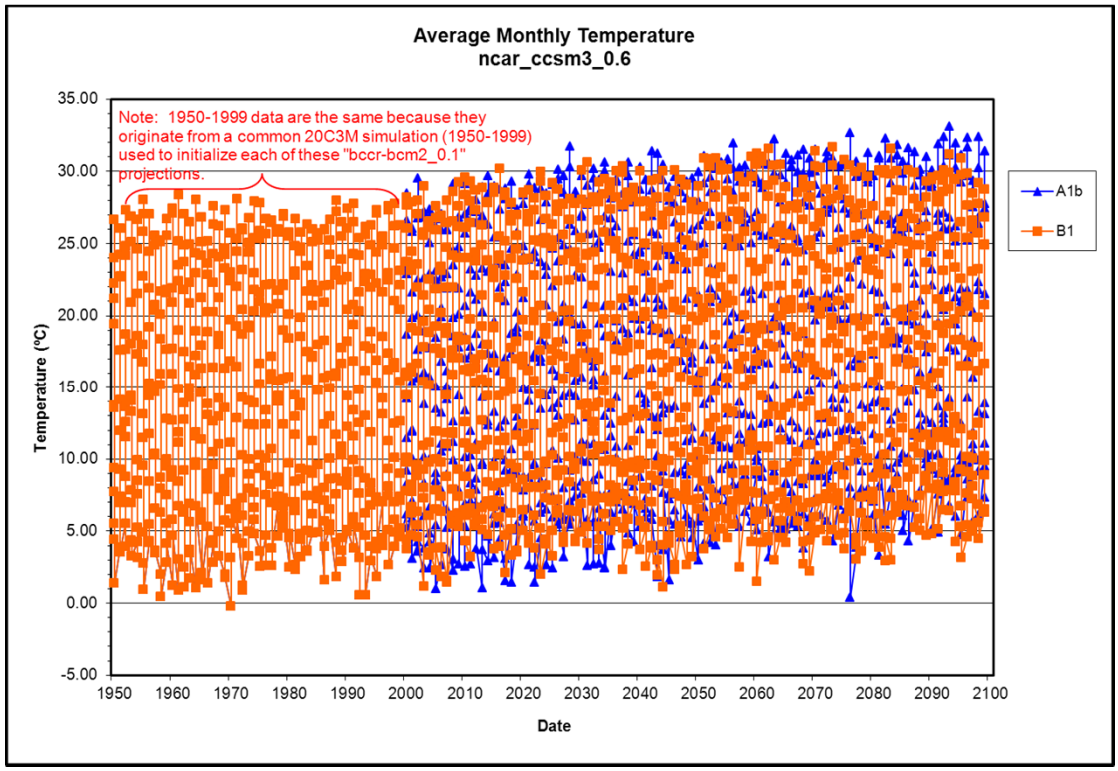

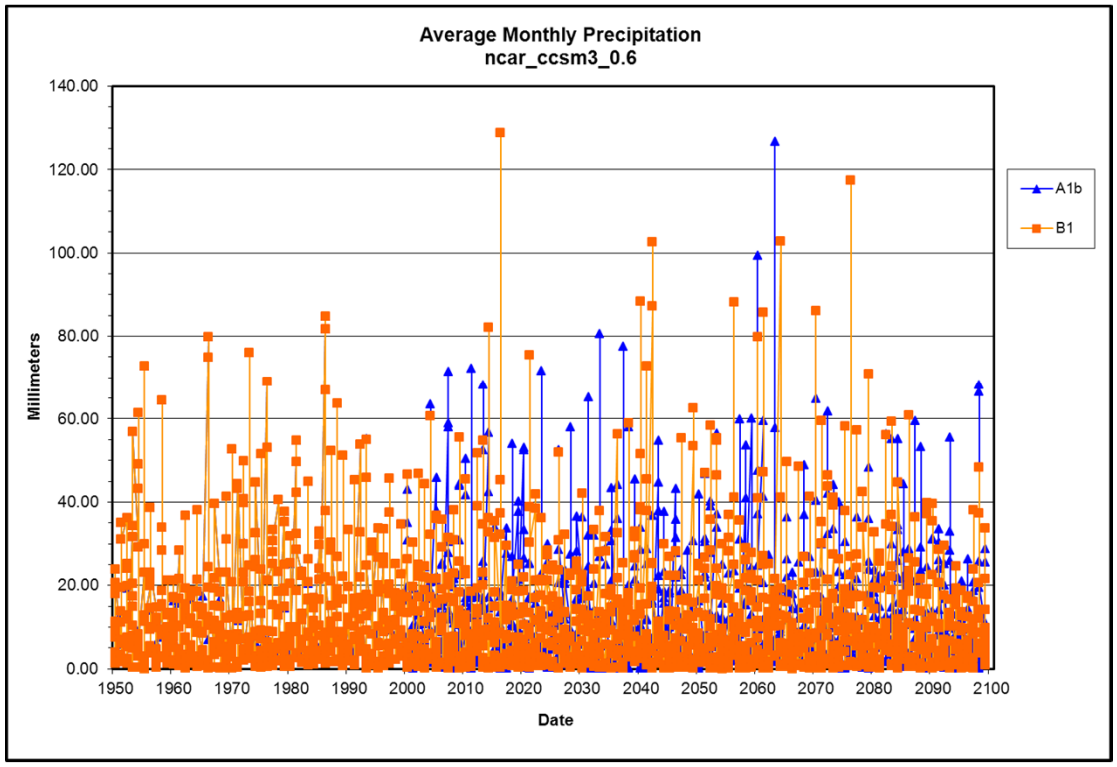

Climate Model ncar_ccsm3_0.6 (page 2 of 3)

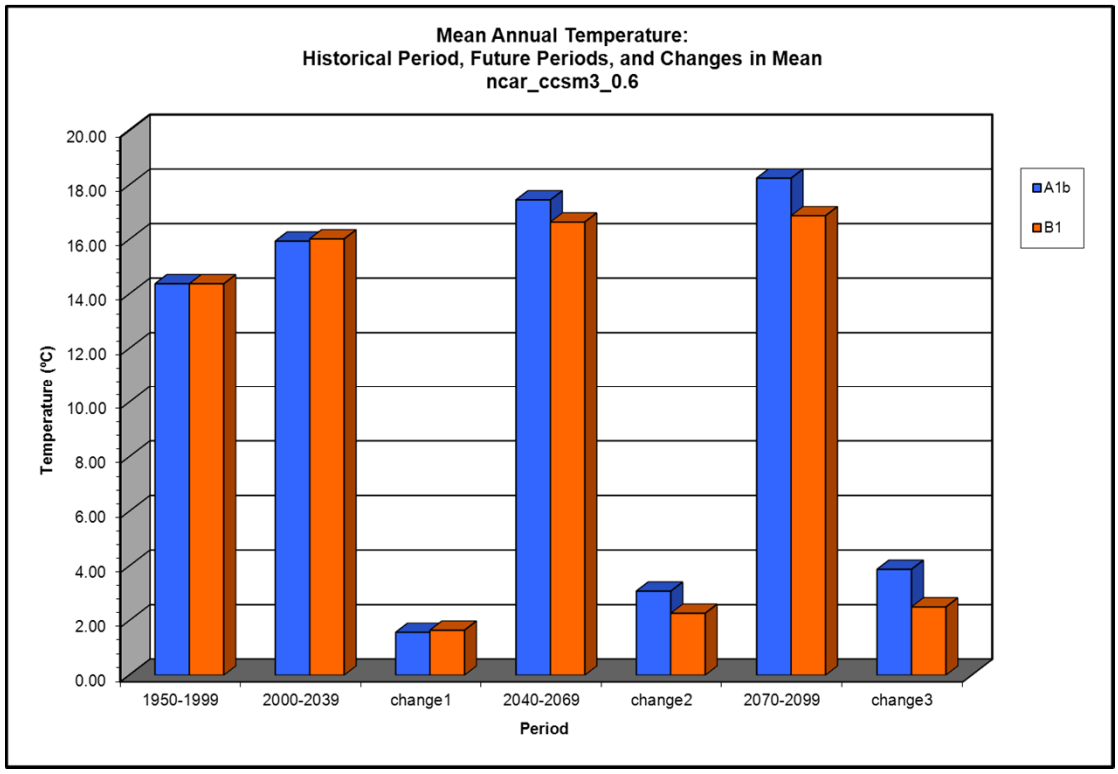

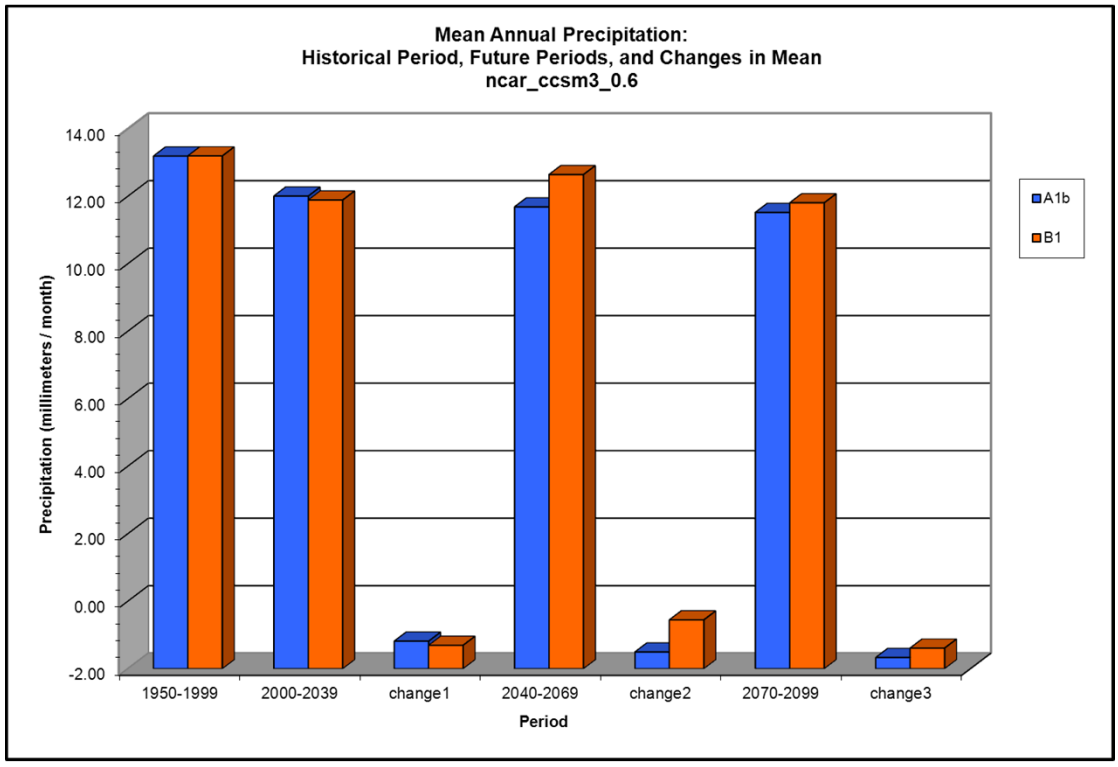

Climate Model ncar_ccsm3_0.6 (page 3 of 3)

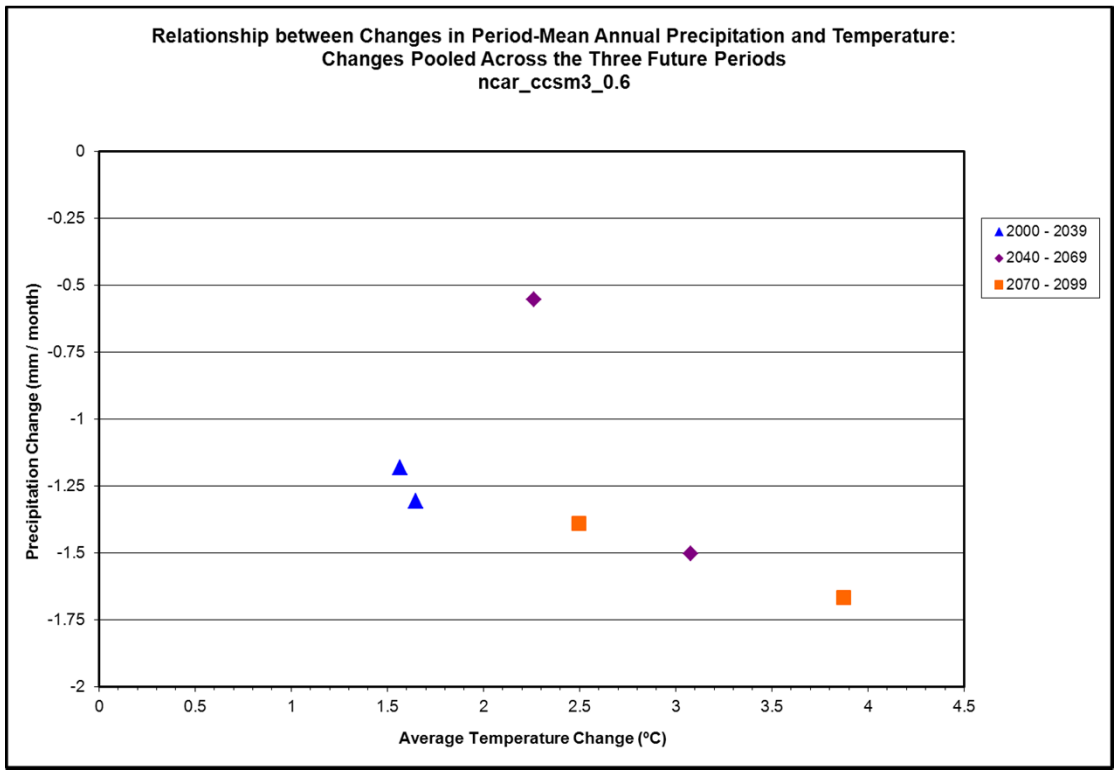

Climate Model ncar_ccsm3_0.7 (page 1 of 3)

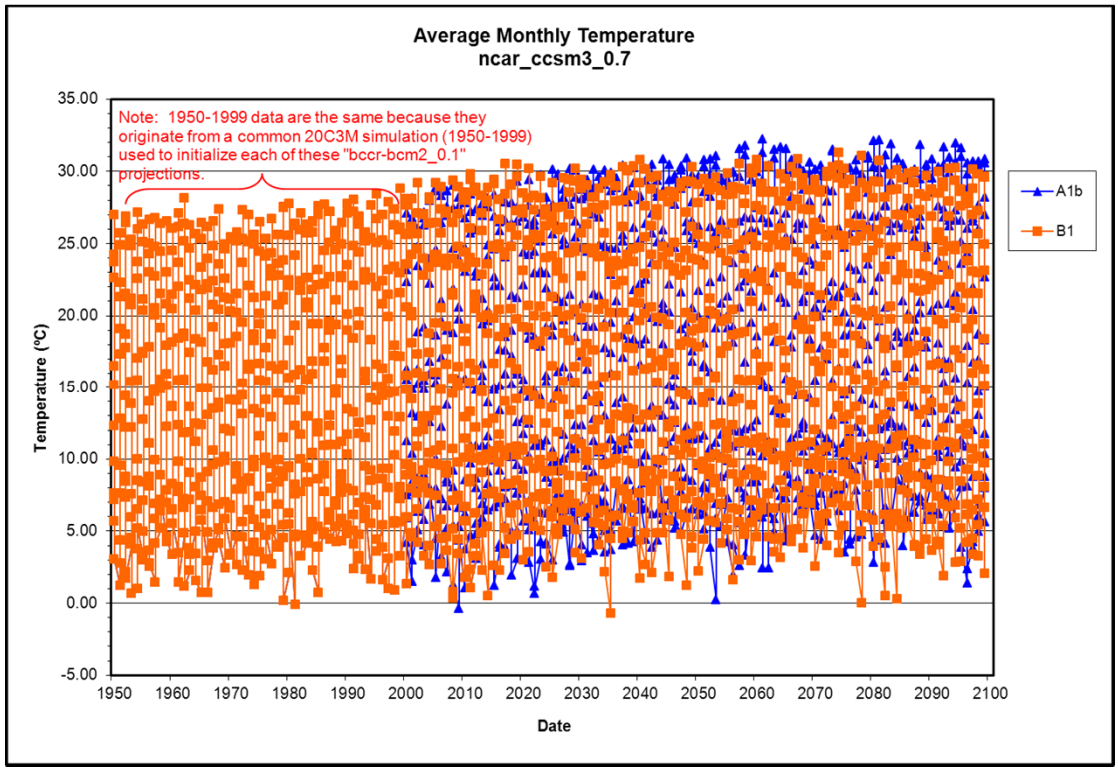

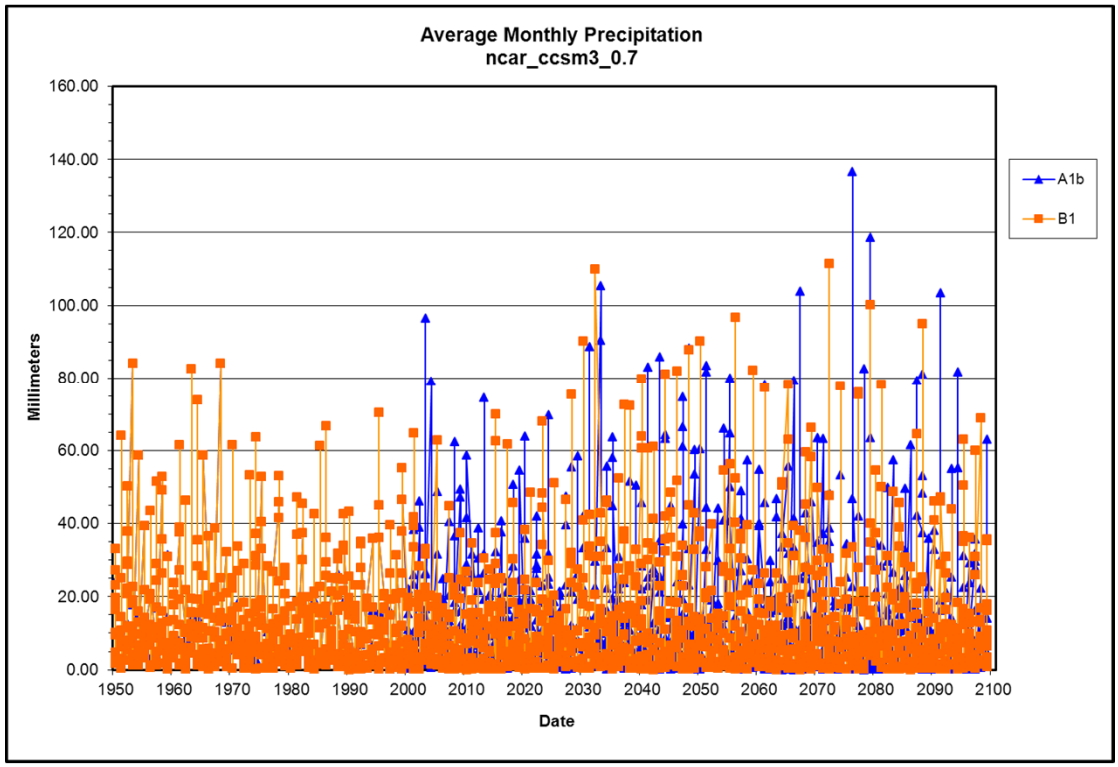

Climate Model ncar_ccsm3_0.7 (page 2 of 3)

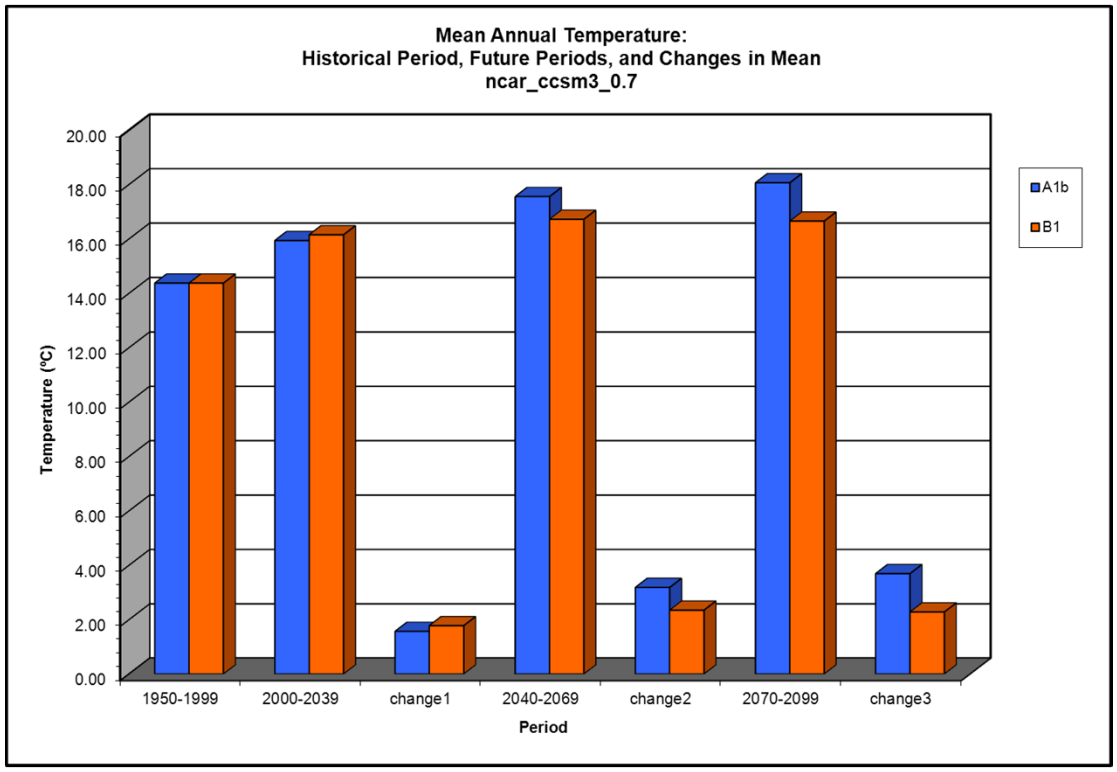

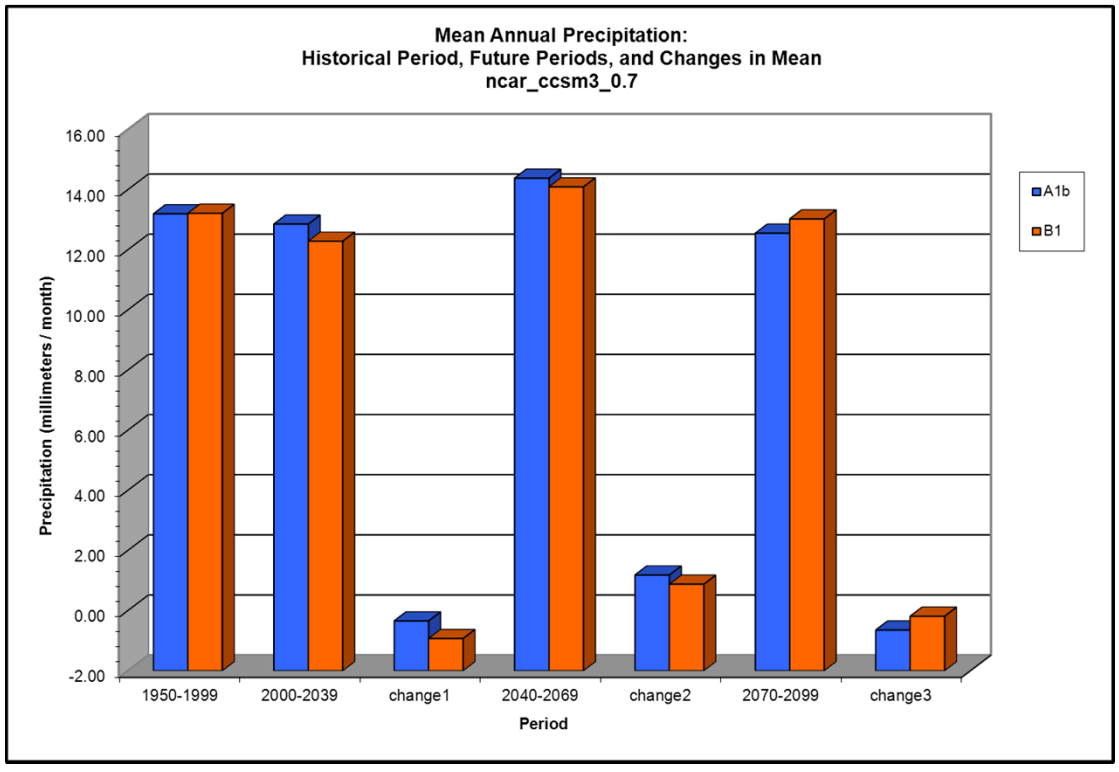

Climate Model ncar_ccsm3_0.7 (page 3 of 3)

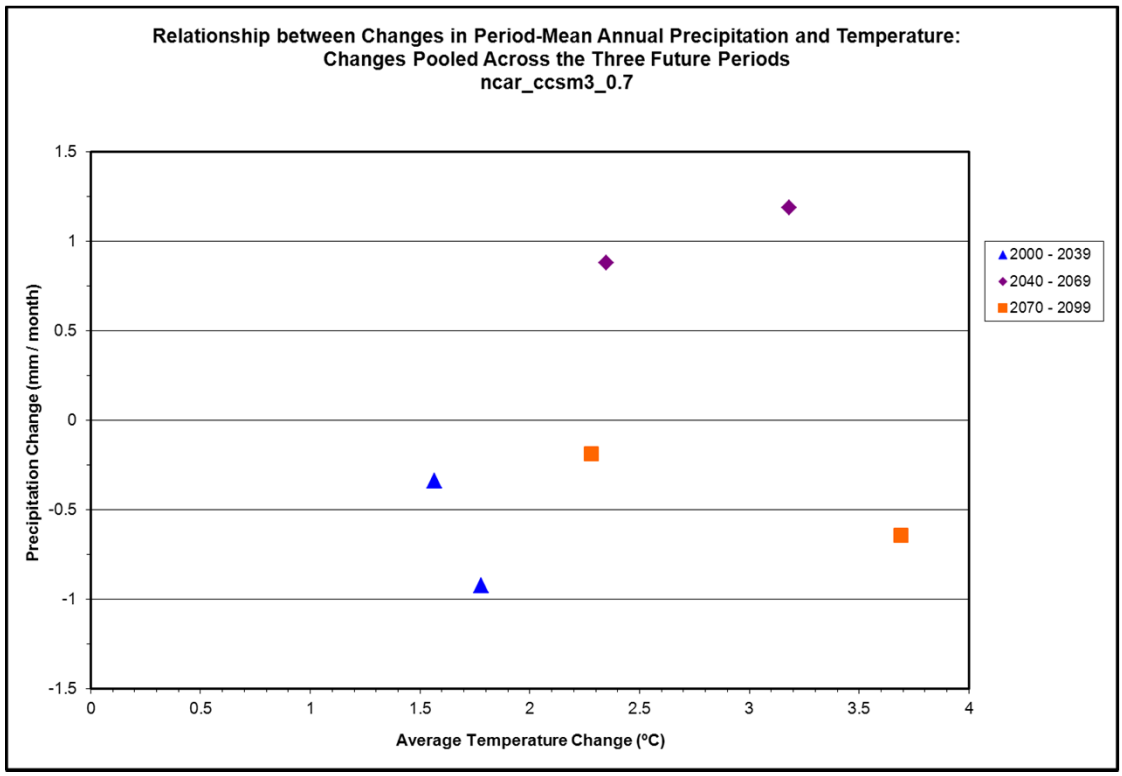

Climate Model ncar_pcm1.1 (page 1 of 3)

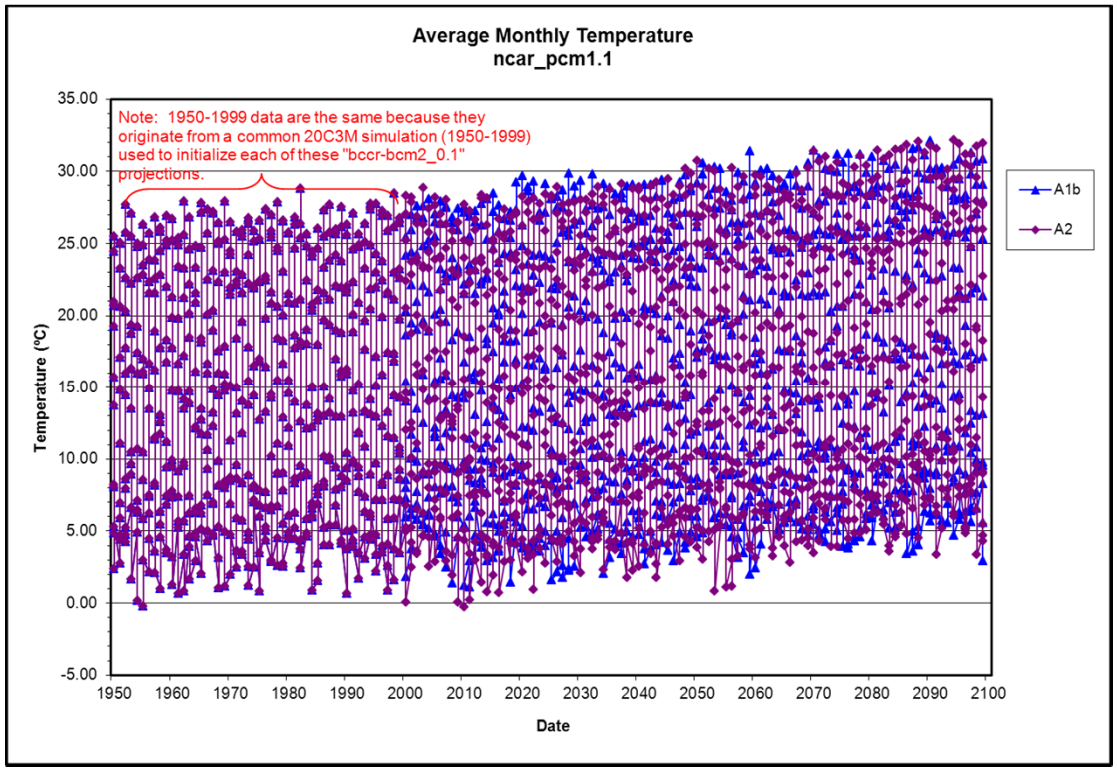

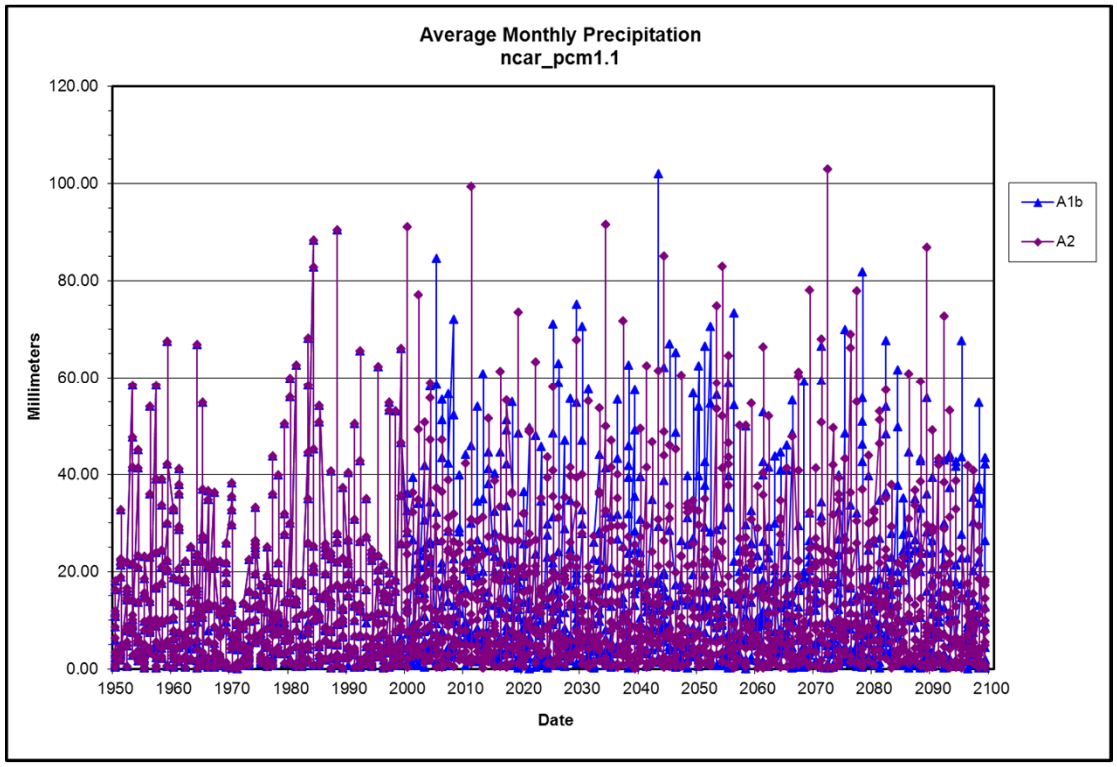

Climate Model ncar_pcm1.1 (page 2 of 3)

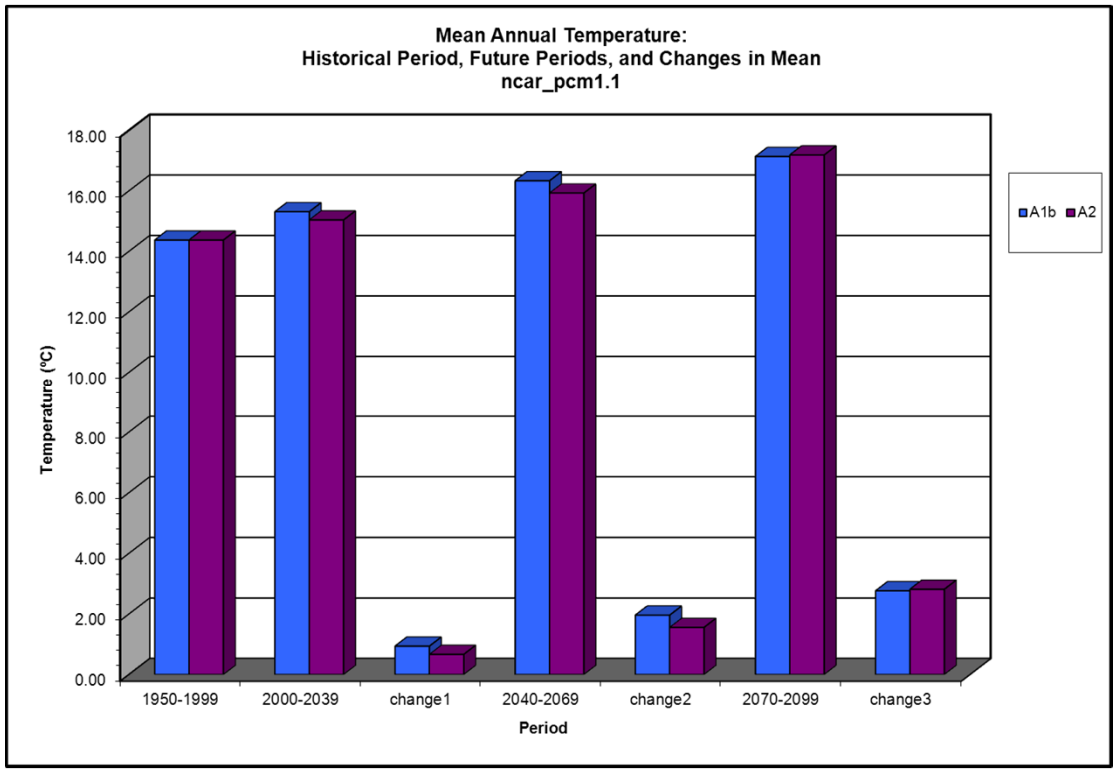

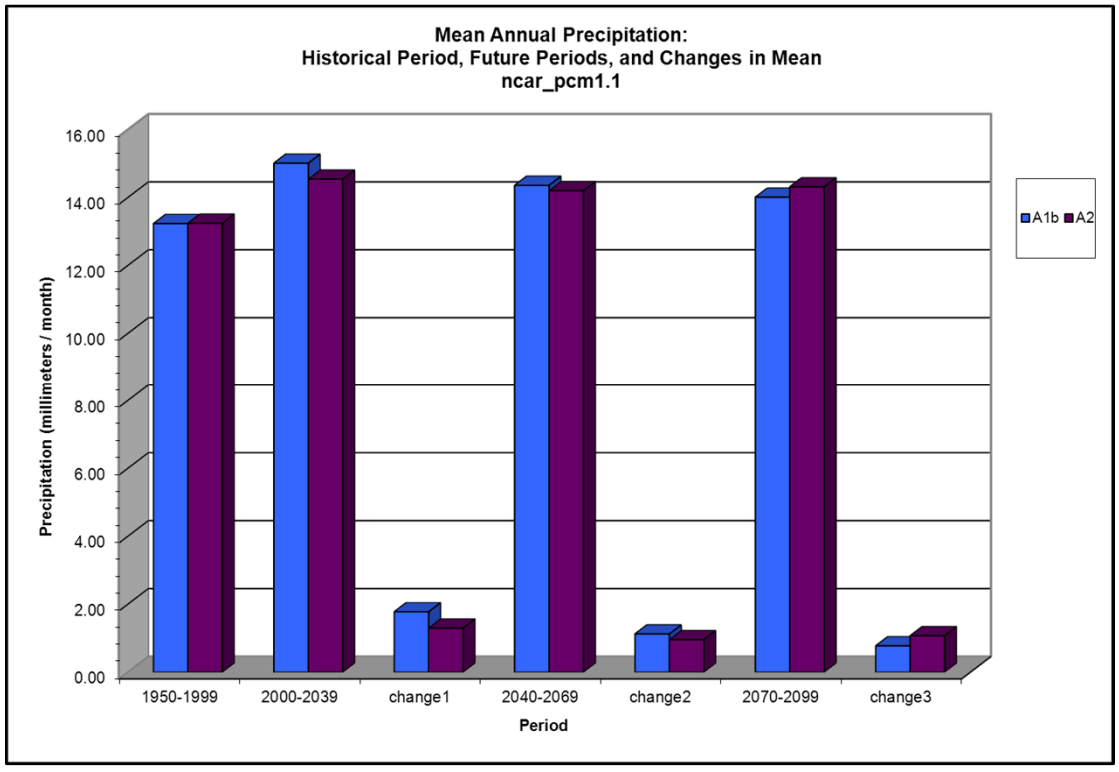

Climate Model ncar_pcm1.1 (page 3 of 3)

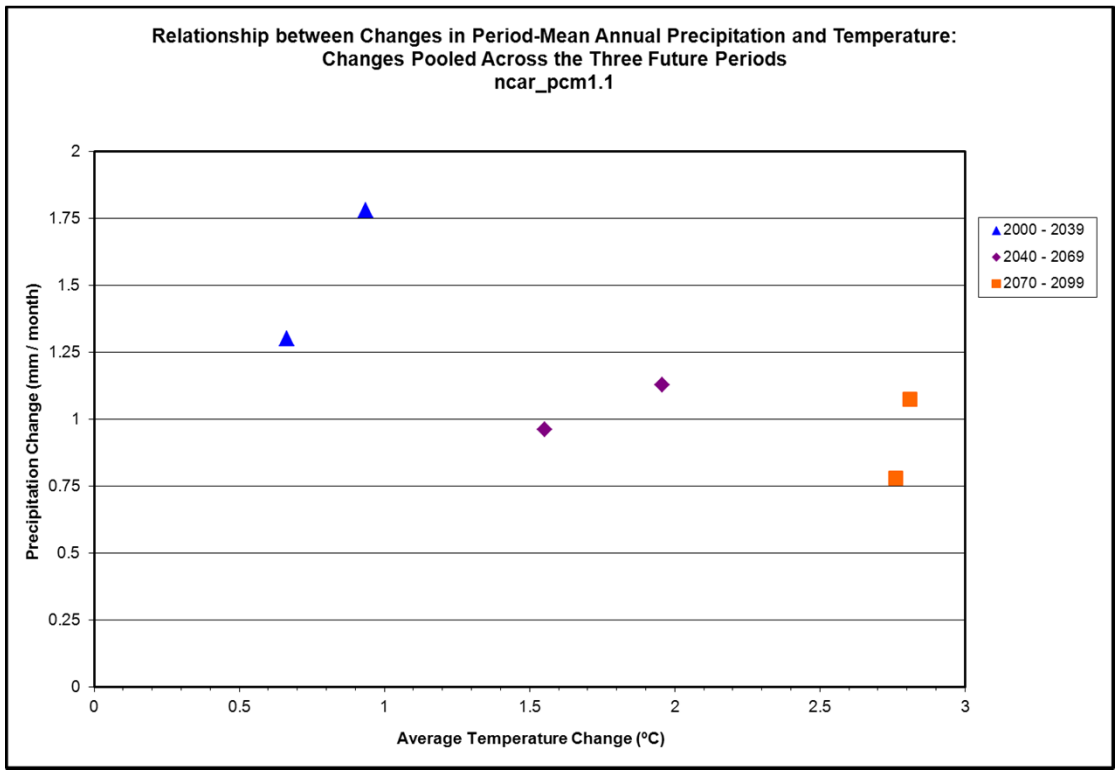

Climate Model ncar_pcm1.2 (page 1 of 3)

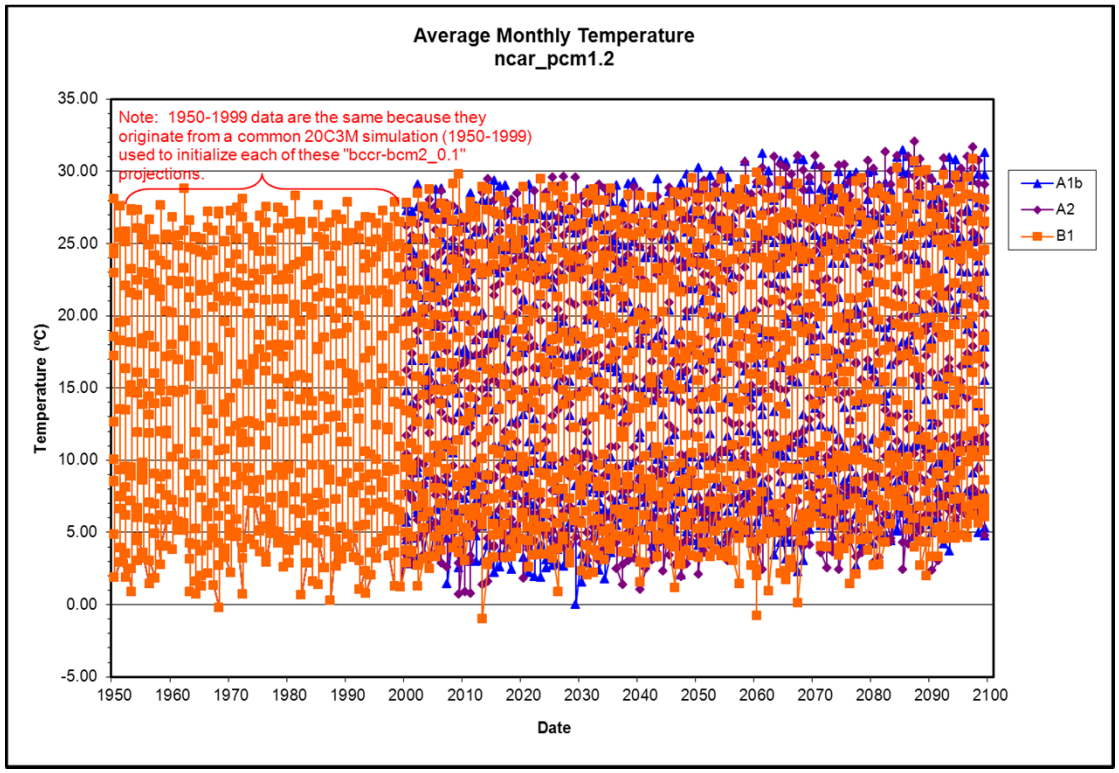

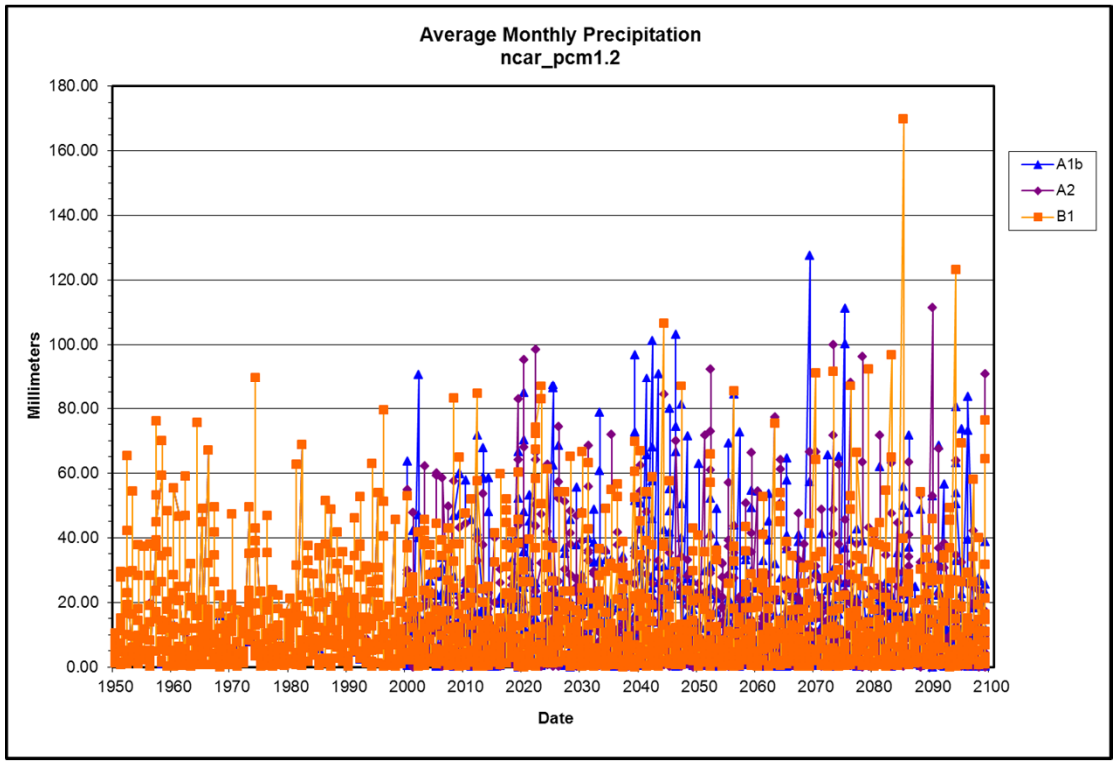

Climate Model ncar_pcm1.2 (page 2 of 3)

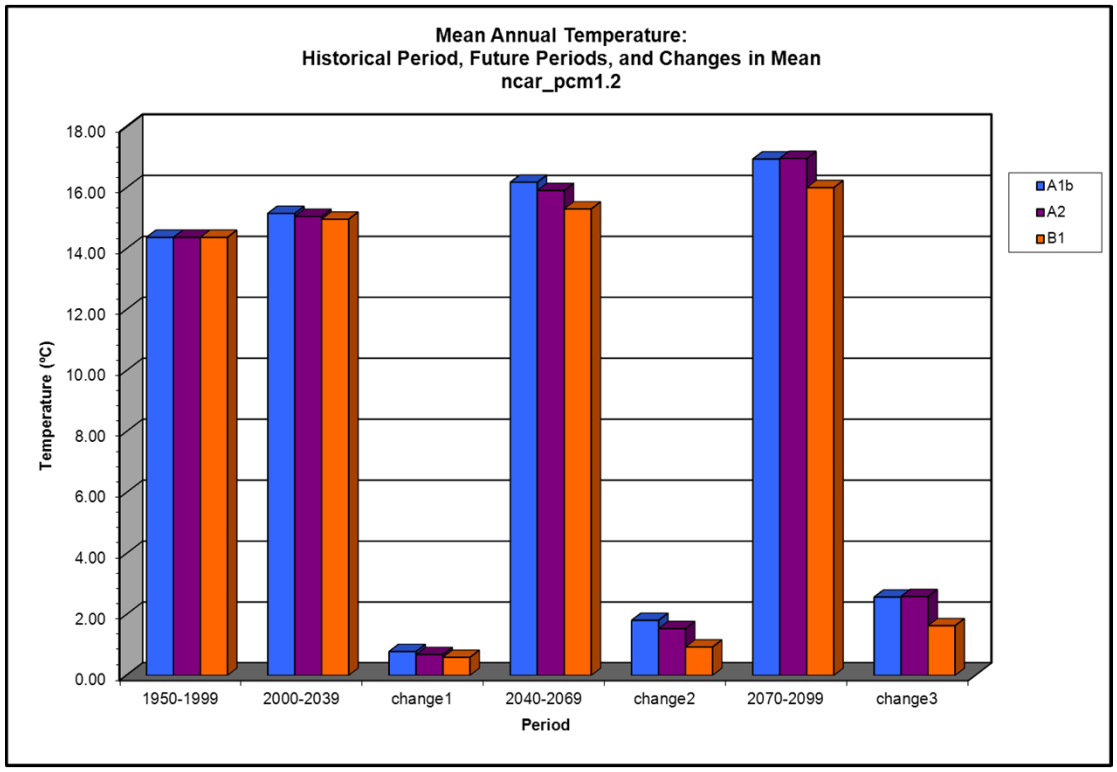

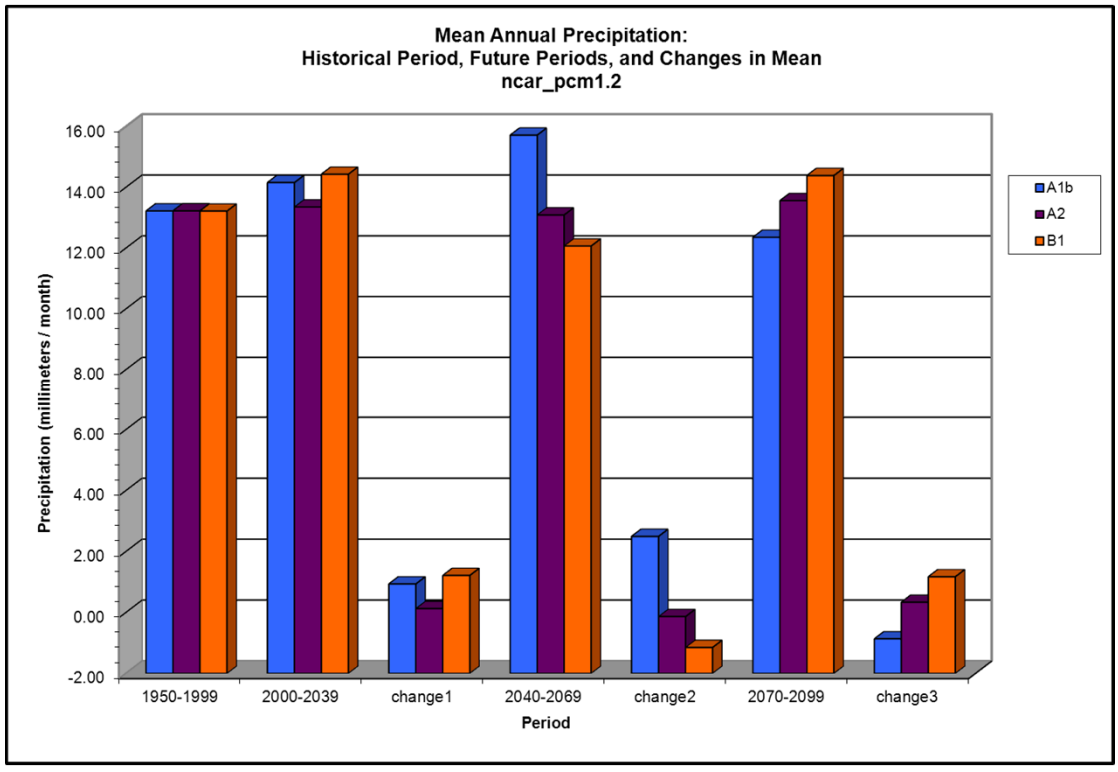

Climate Model ncar_pcm1.2 (page 3 of 3)

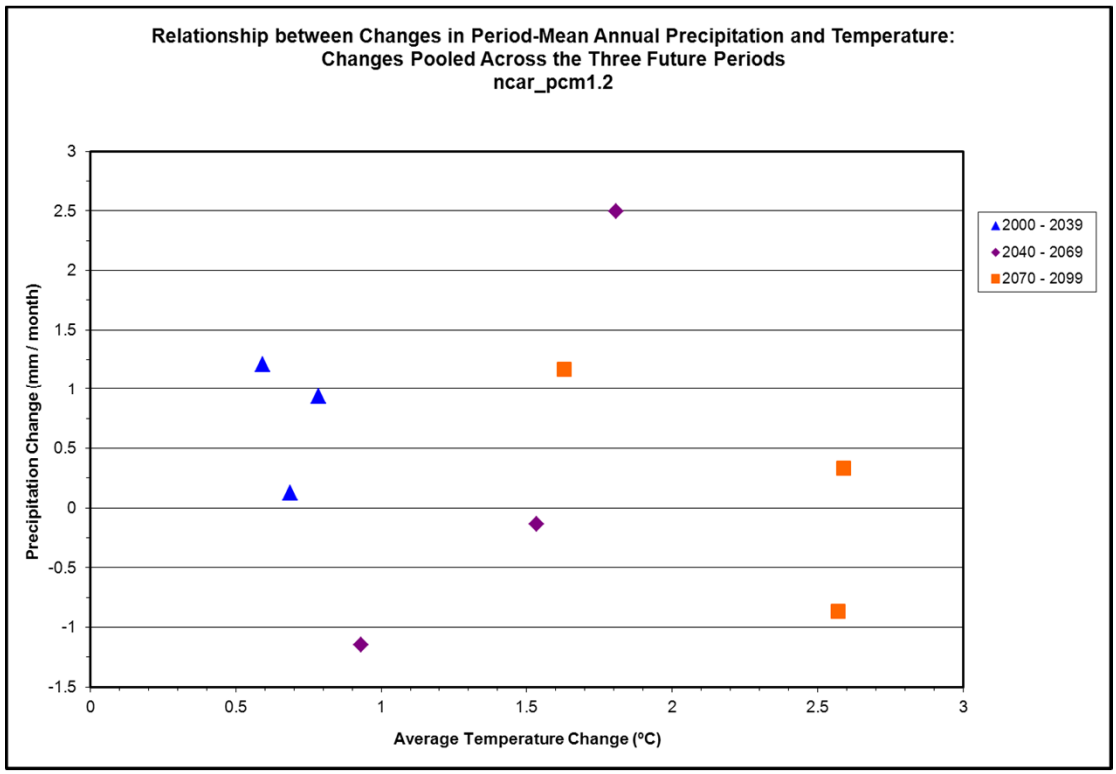

Climate Model ncar_pcm1.3 (page 1 of 3)

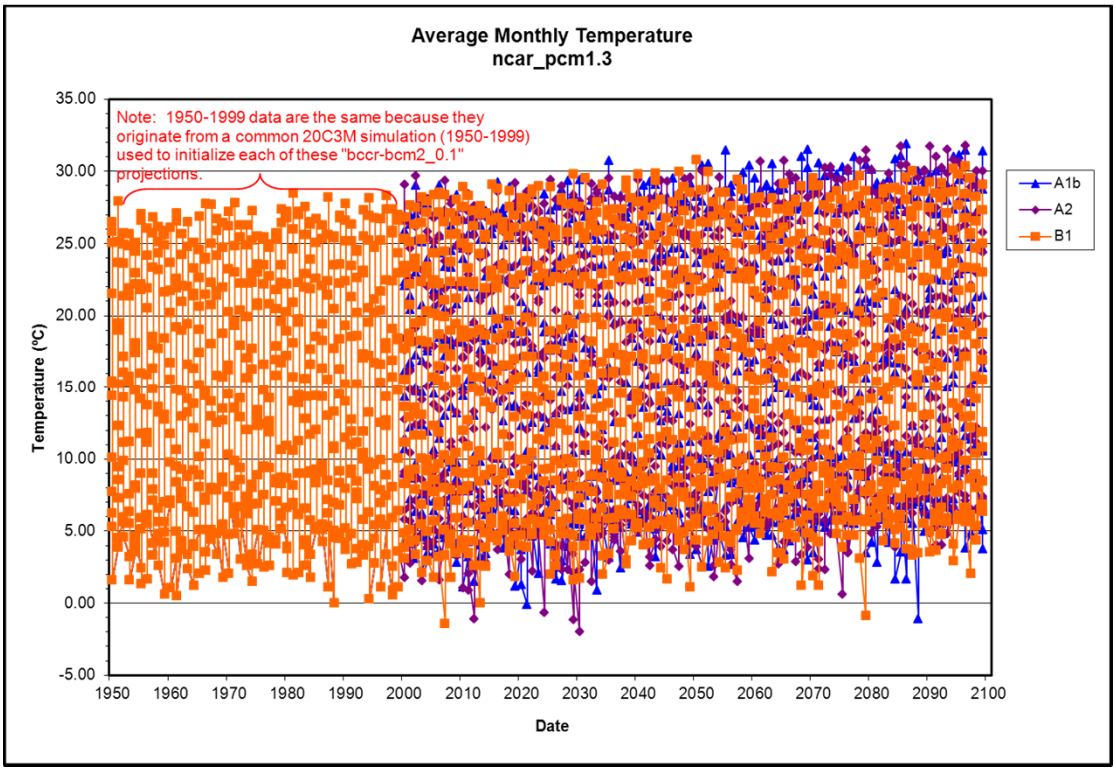

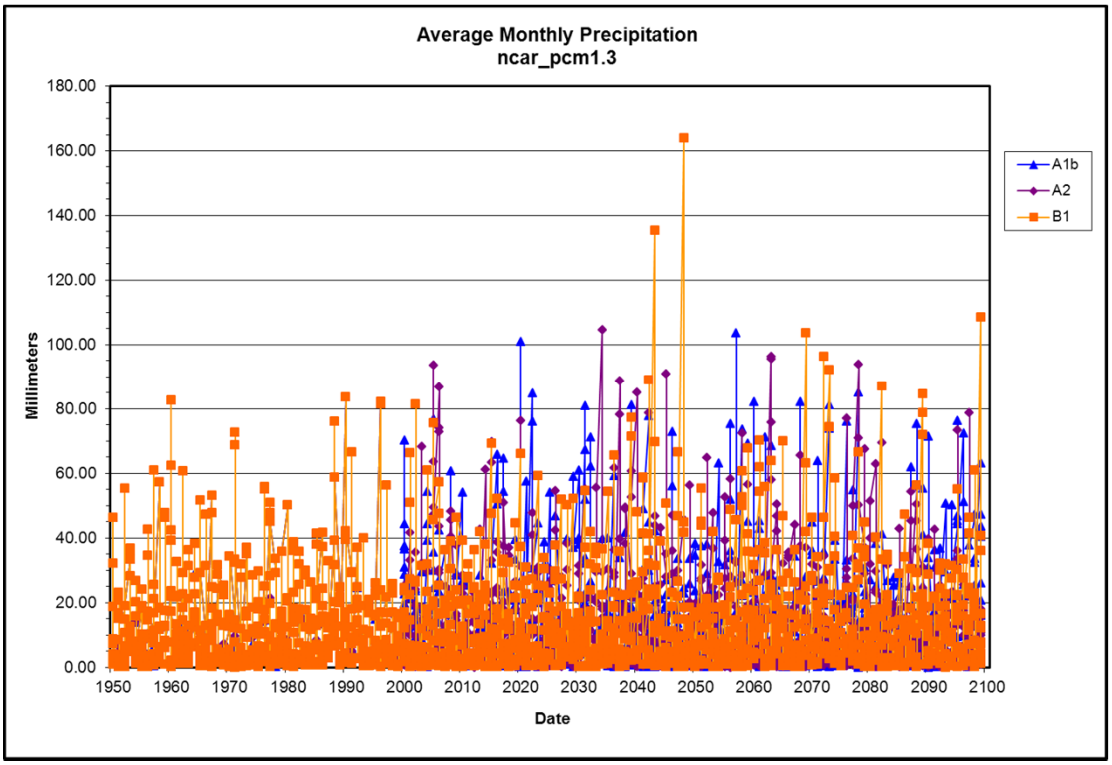

Climate Model ncar_pcm1.3 (page 2 of 3)

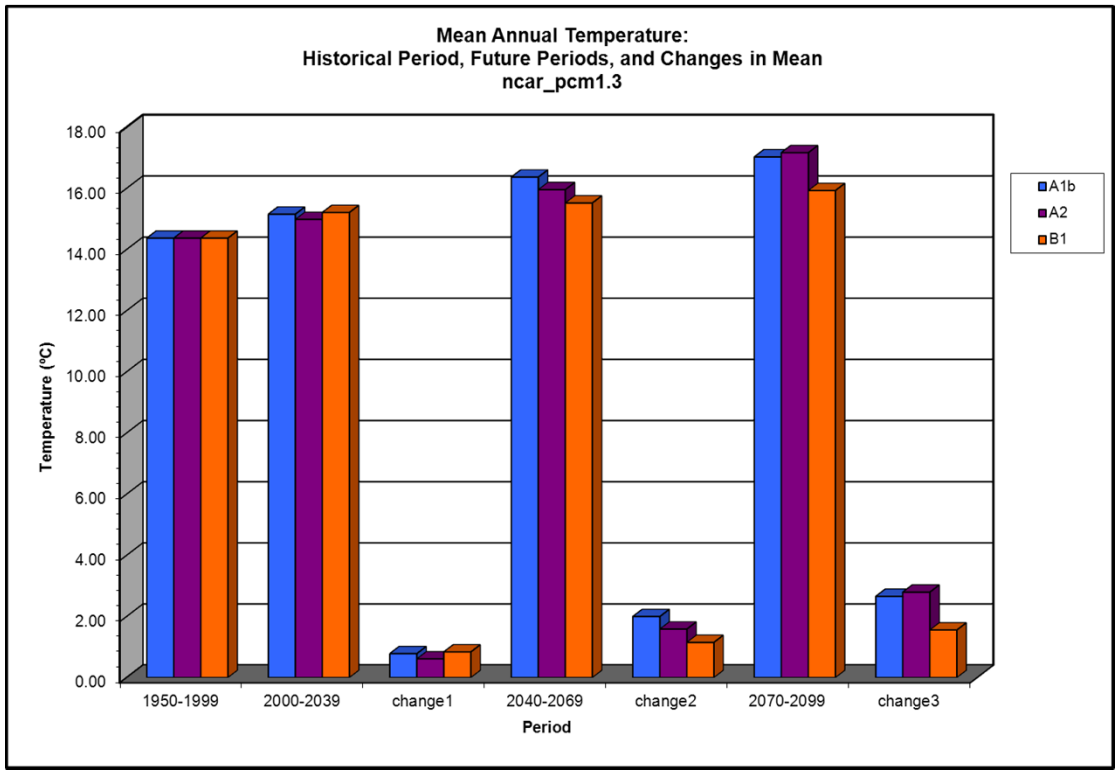

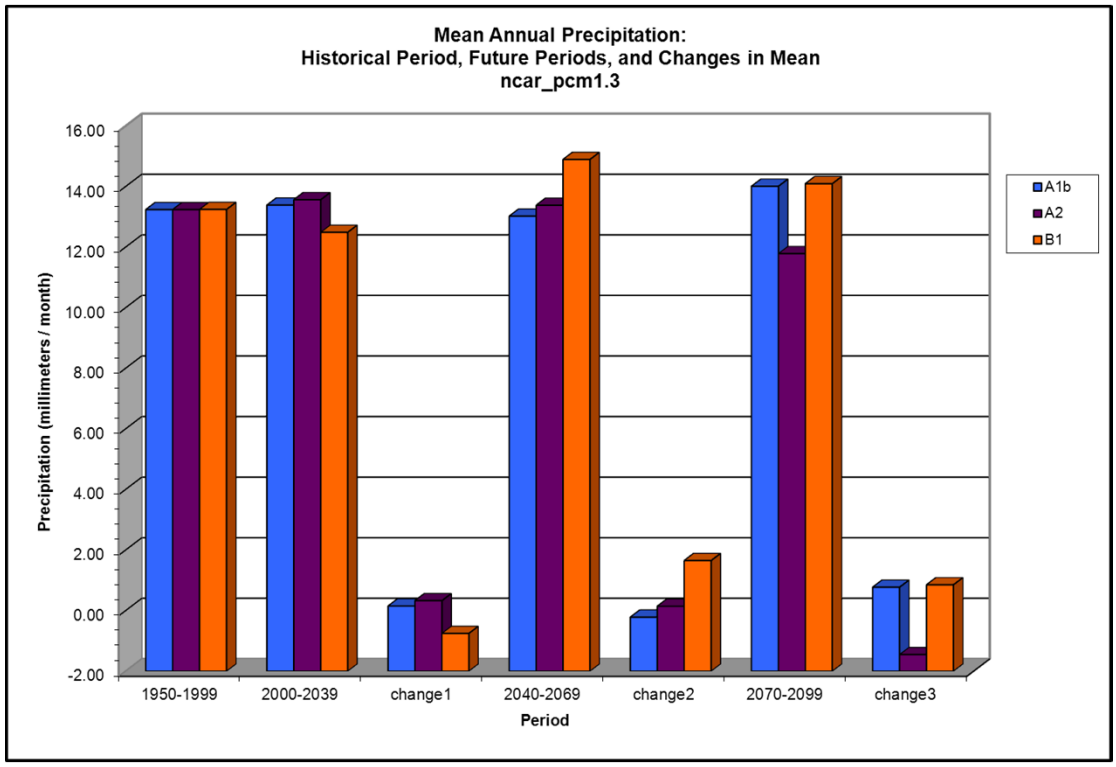

Climate Model ncar_pcm1.3 (page 3 of 3)

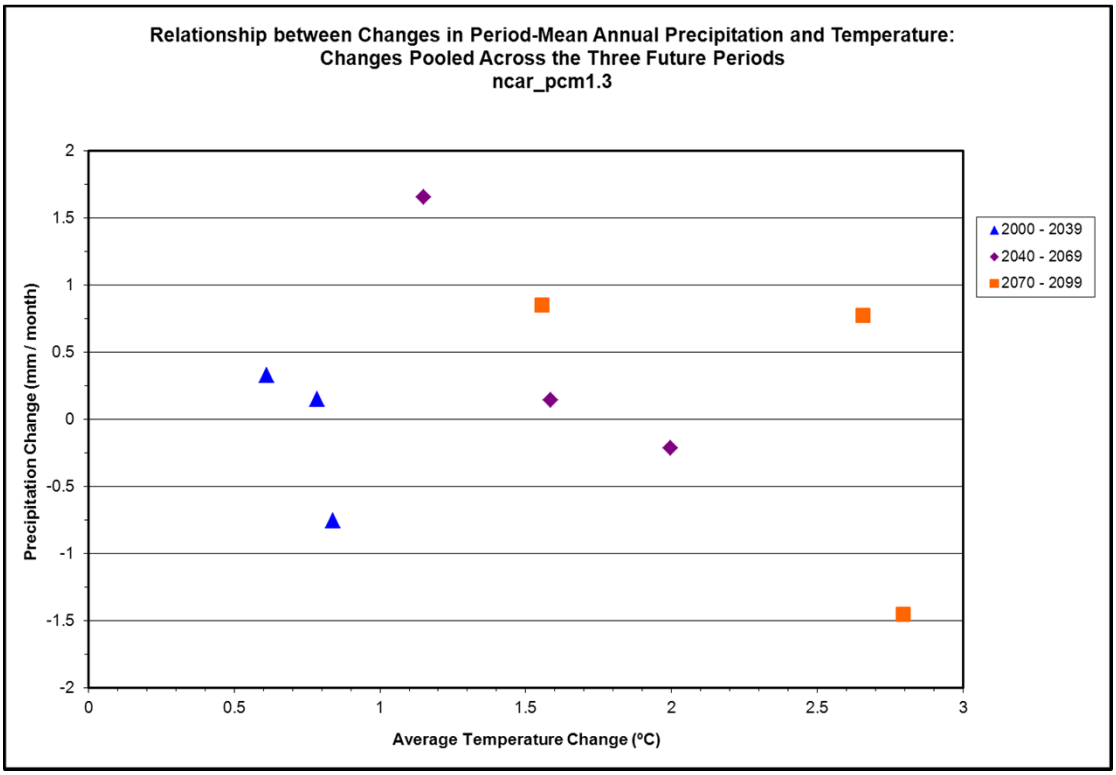

Climate Model ncar_pcm1.4 (page 1 of 3)

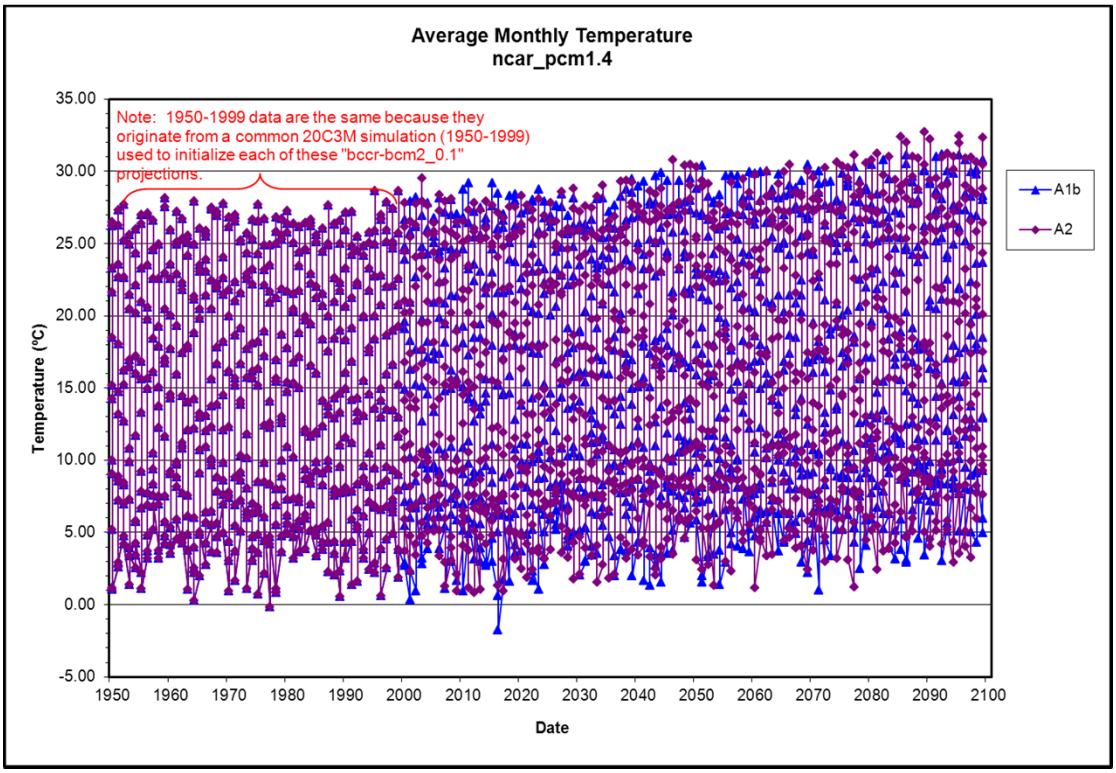

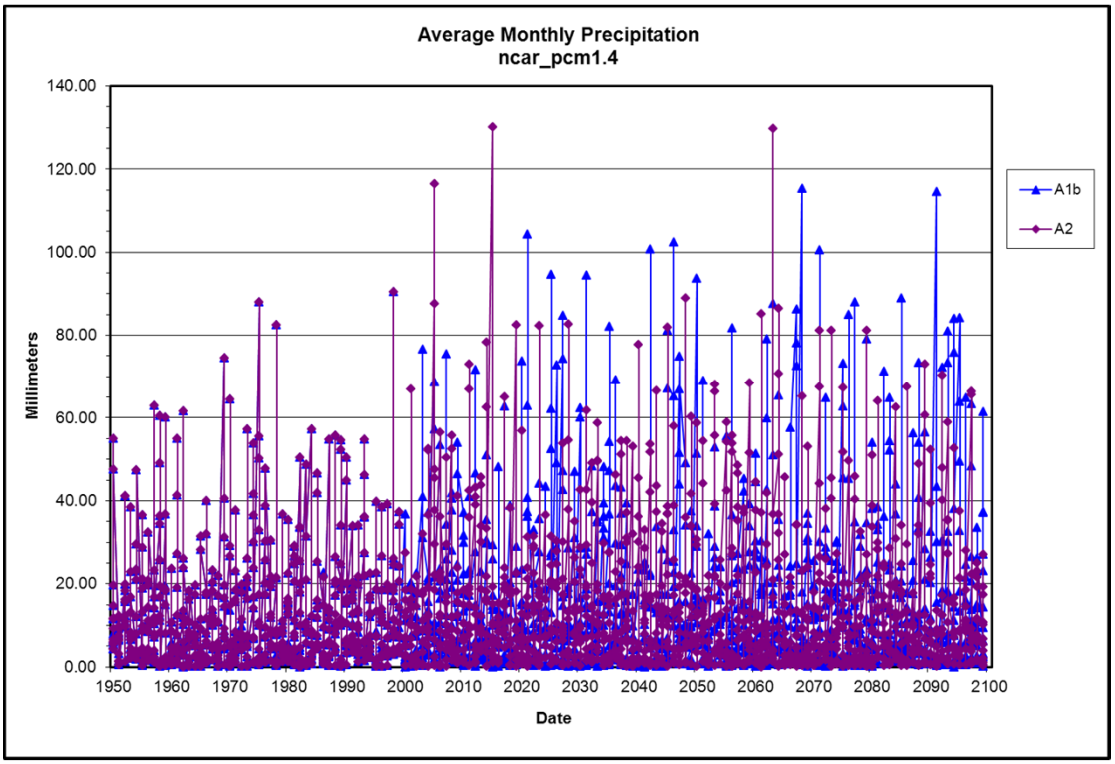

Climate Model ncar_pcm1.4 (page 2 of 3)

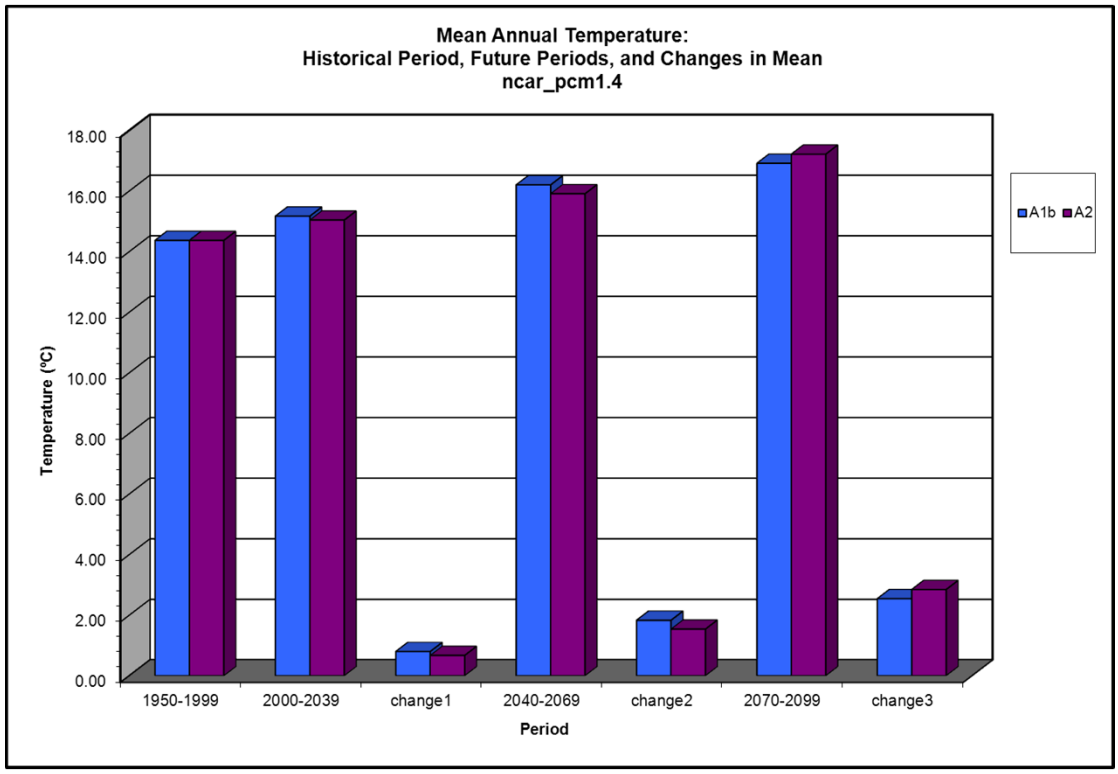

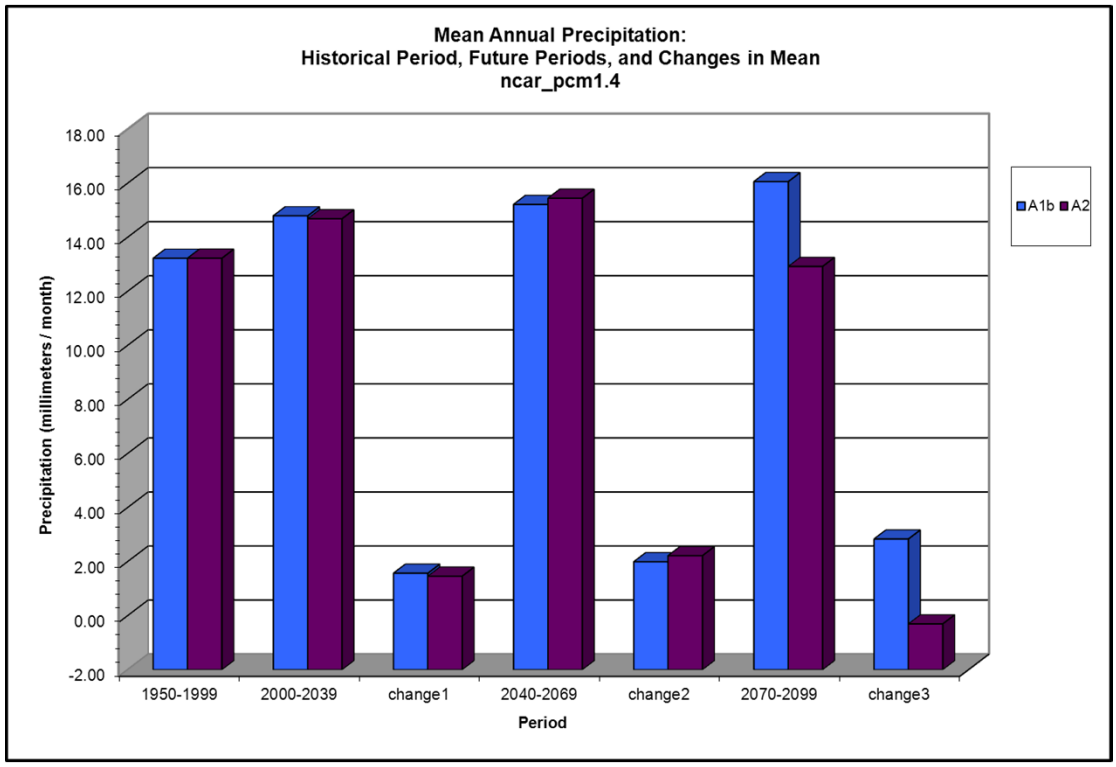

Climate Model ncar_pcm1.4 (page 3 of 3)

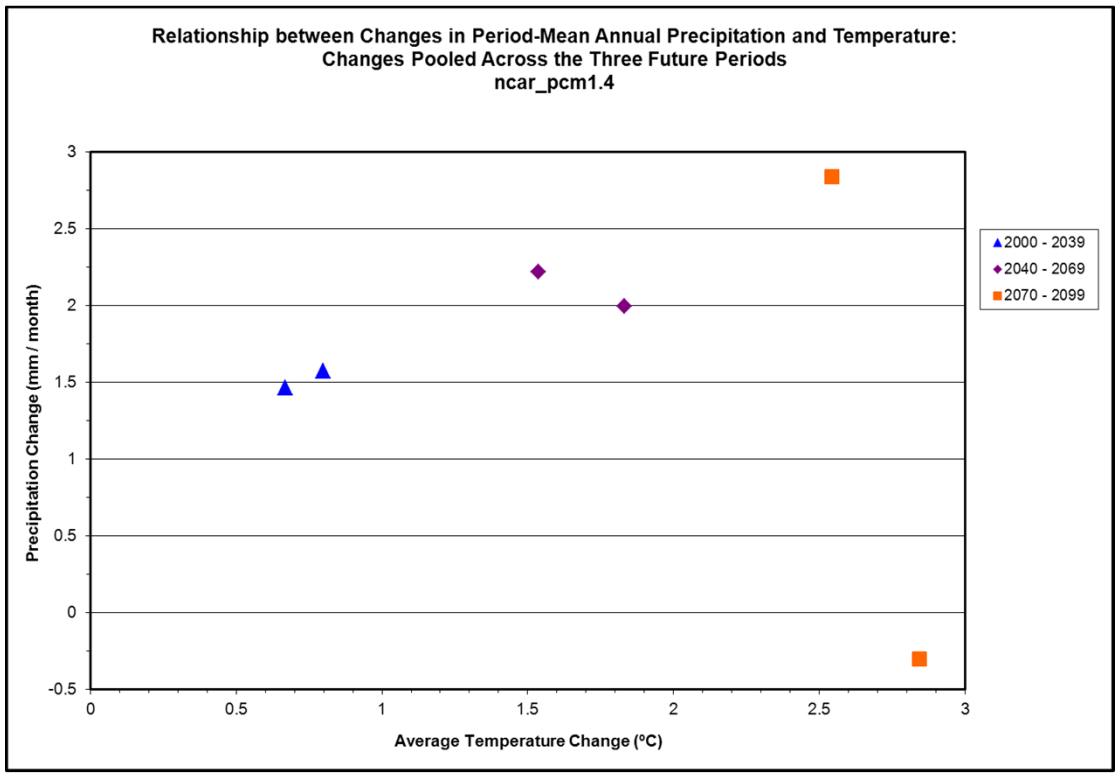

Climate Model ukmo_hadcm3.1 (page 1 of 3)

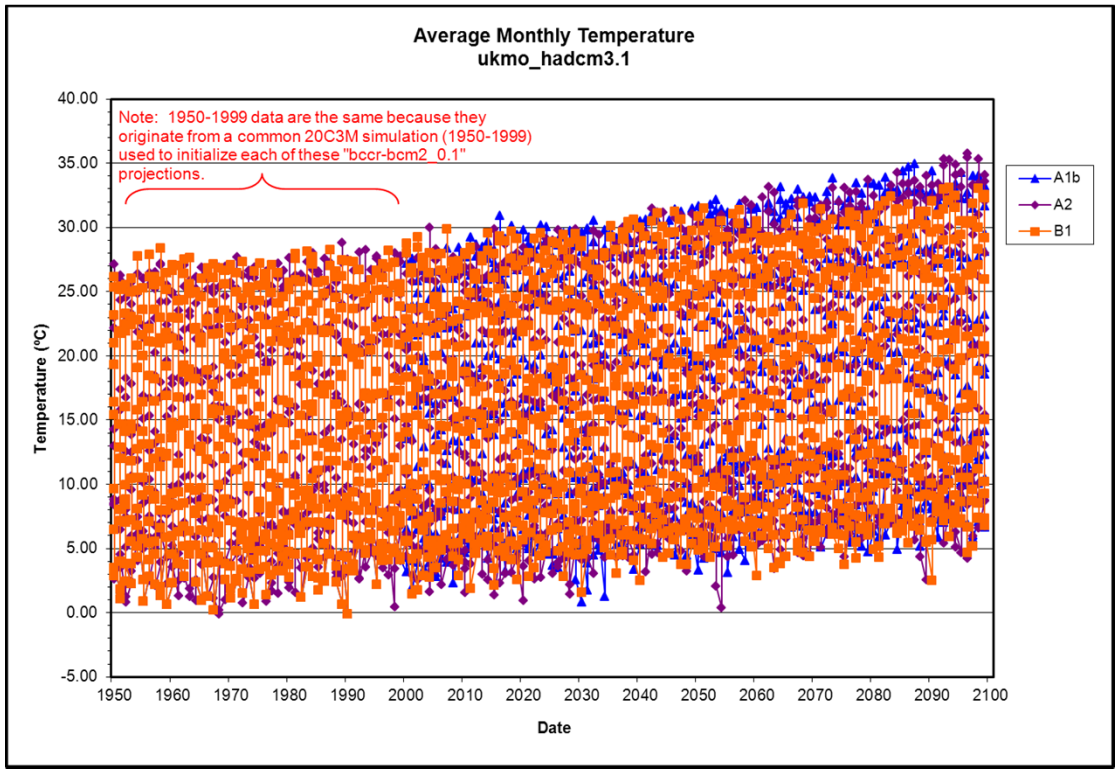

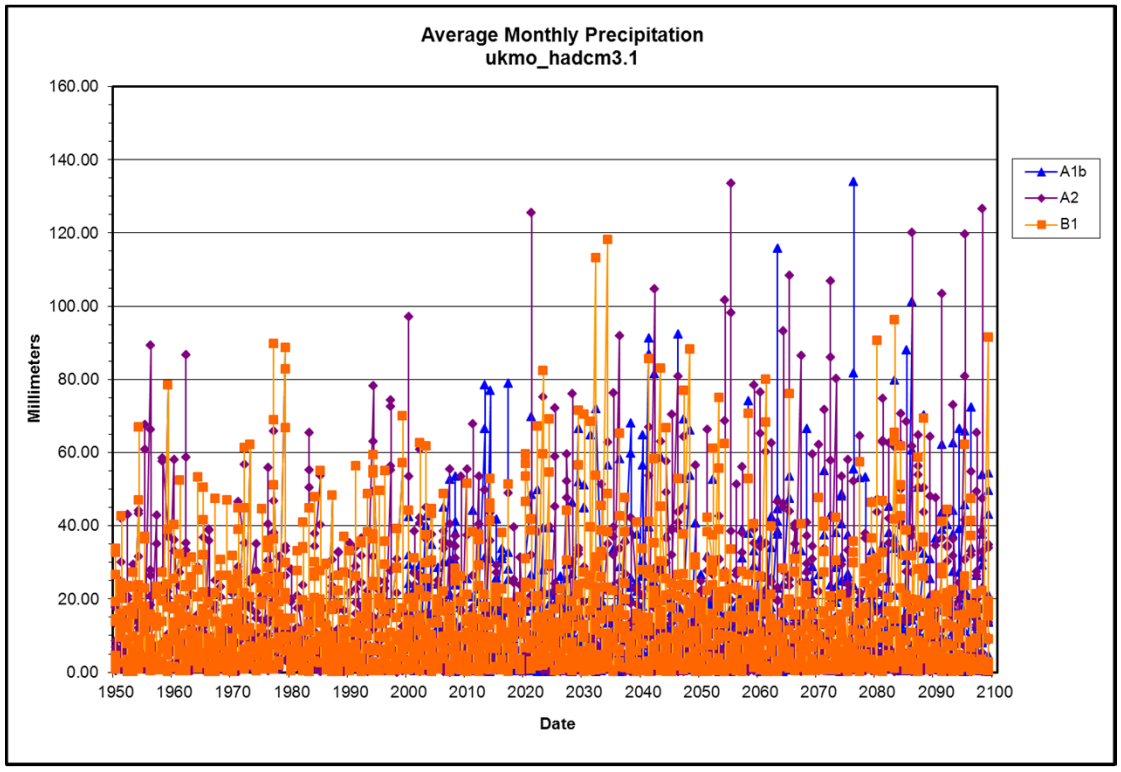

Climate Model ukmo_hadcm3.1 (page 2 of 3)

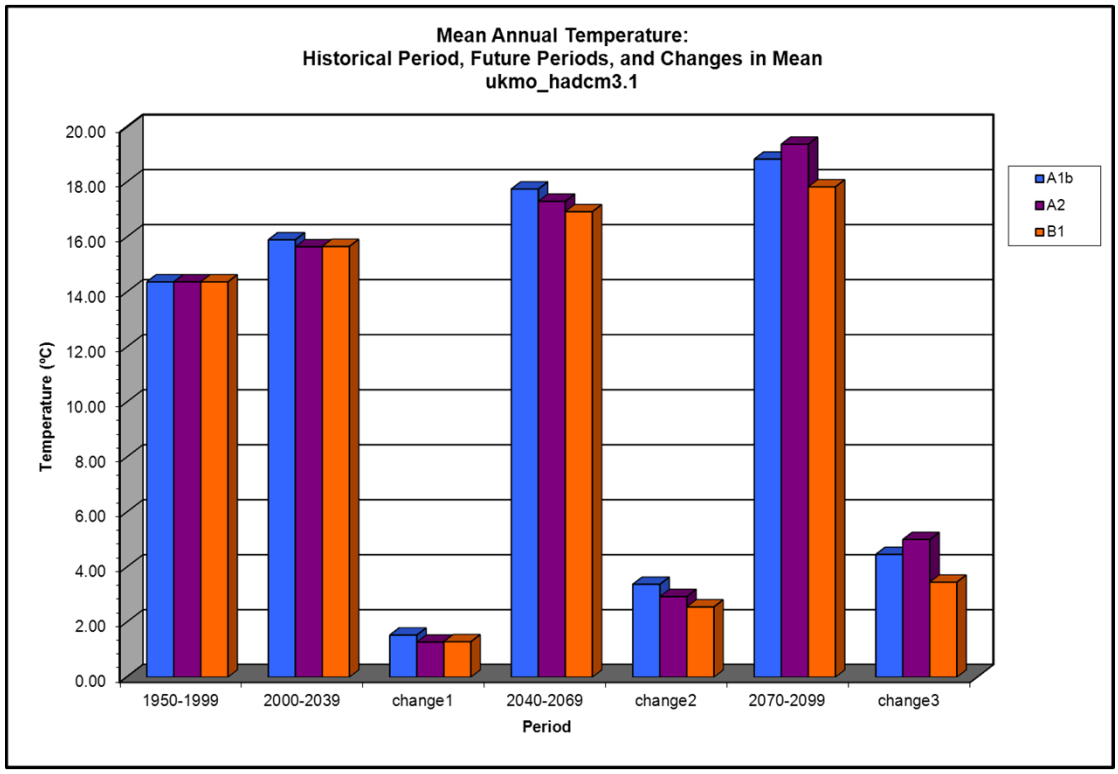

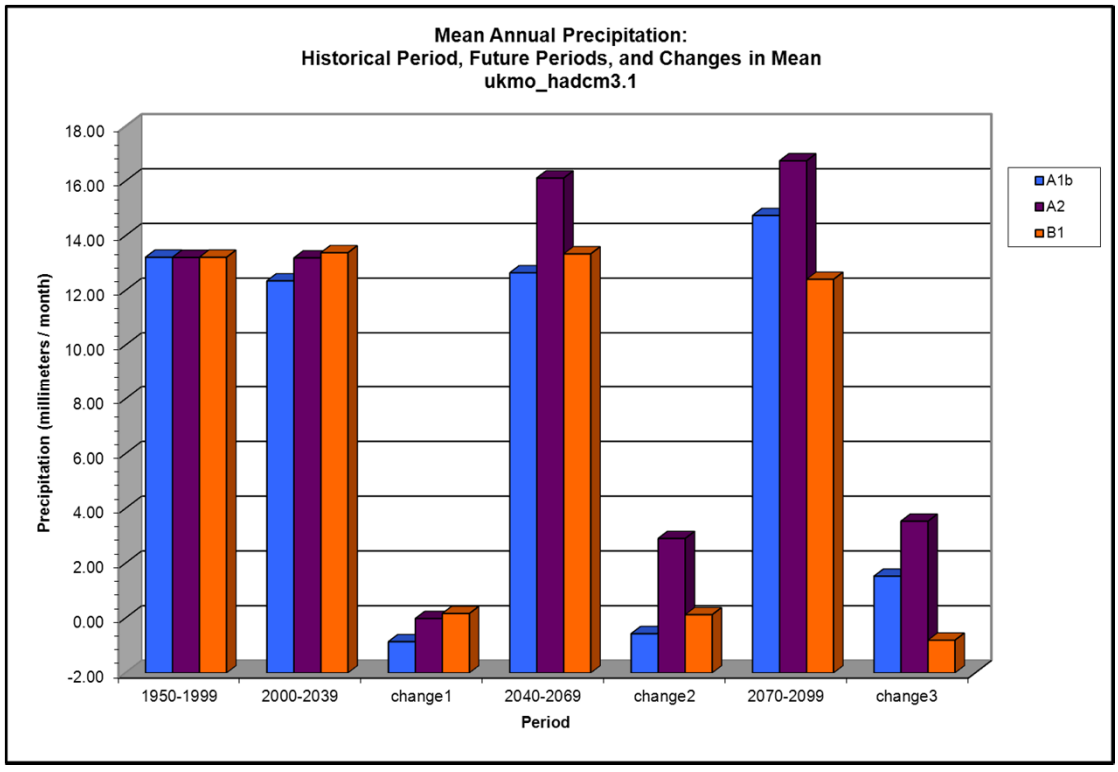

Climate Model ukmo_hadcm3.1 (page 3 of 3)

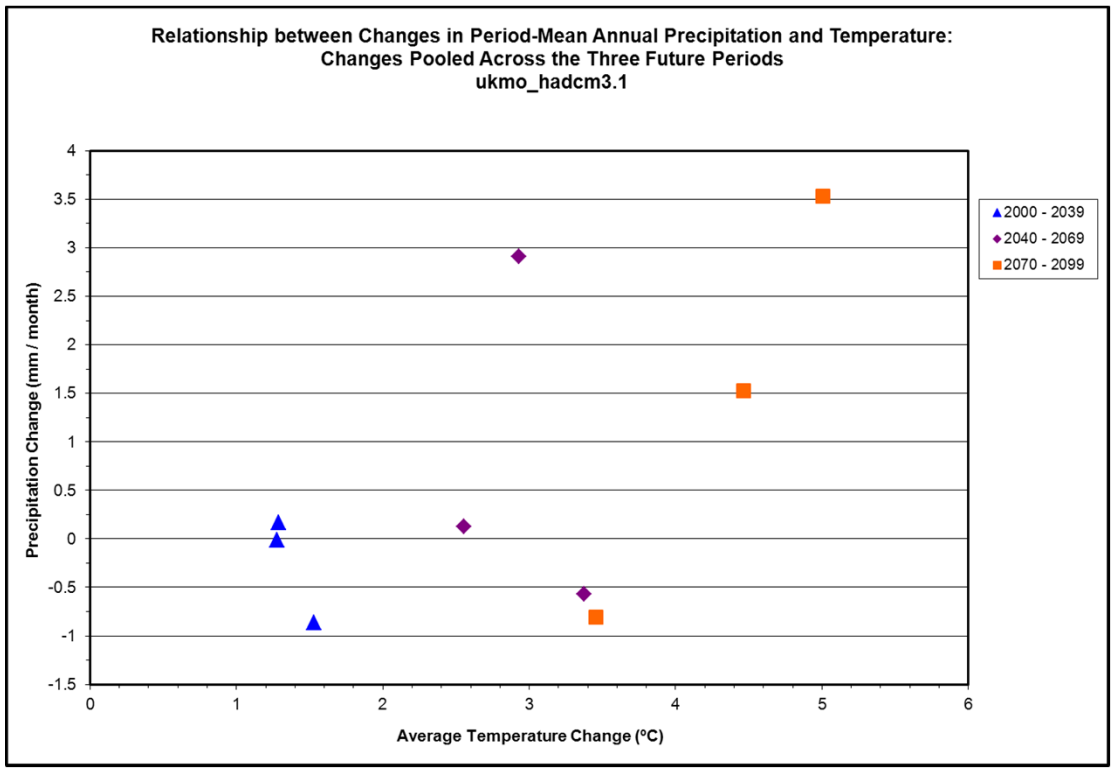

Appendix B Groundwater Head Graphs

Amargosa Pumping Area

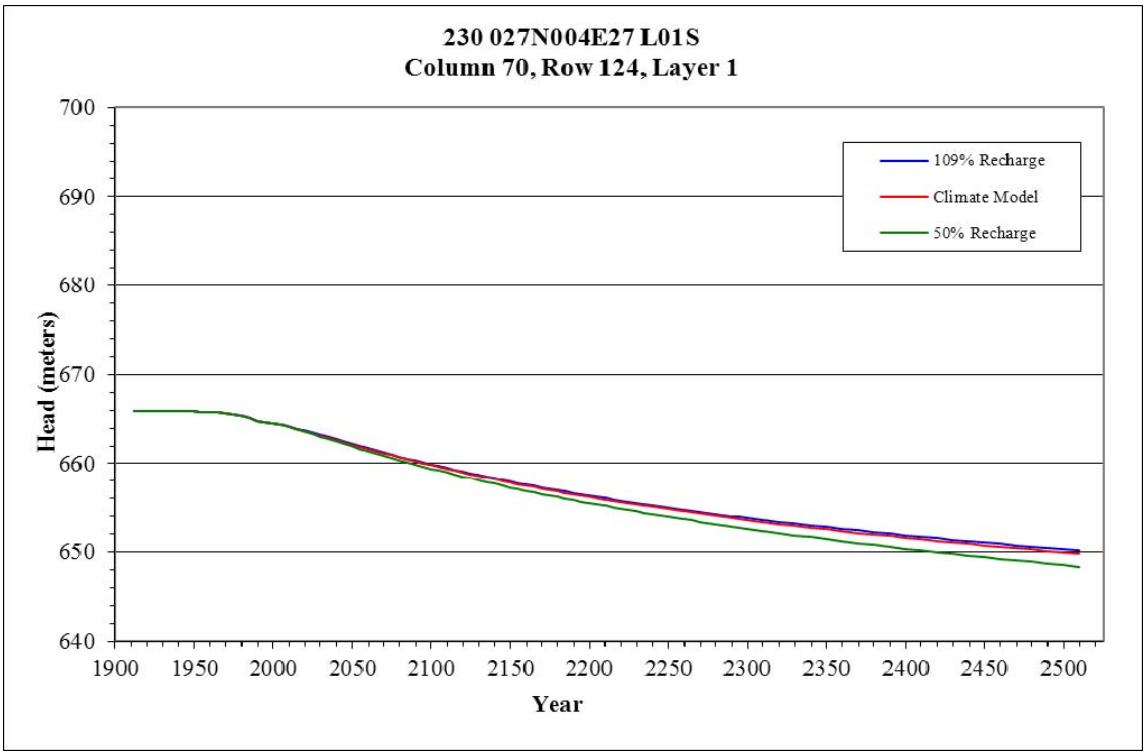

Figure B-1. Head Change in Column 70, Row 124, Layer 1

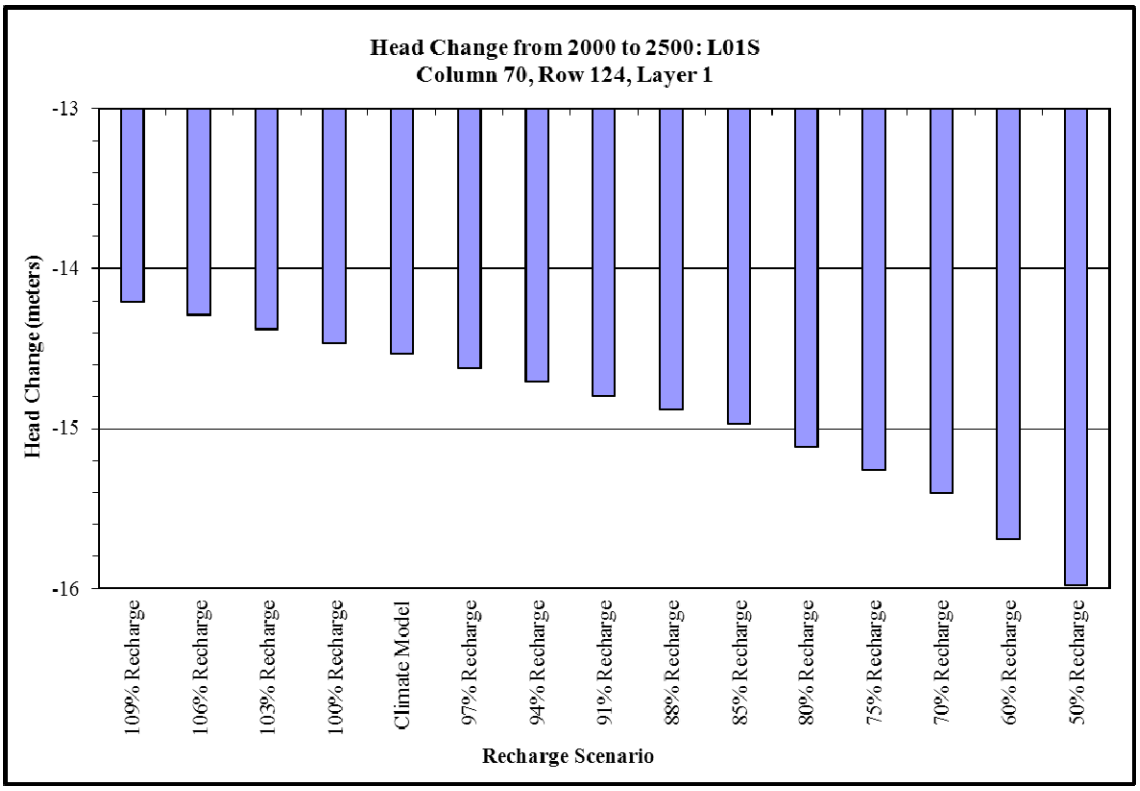

Figure B-2. Quantified Head Change in Column 70, Row 124, Layer 1

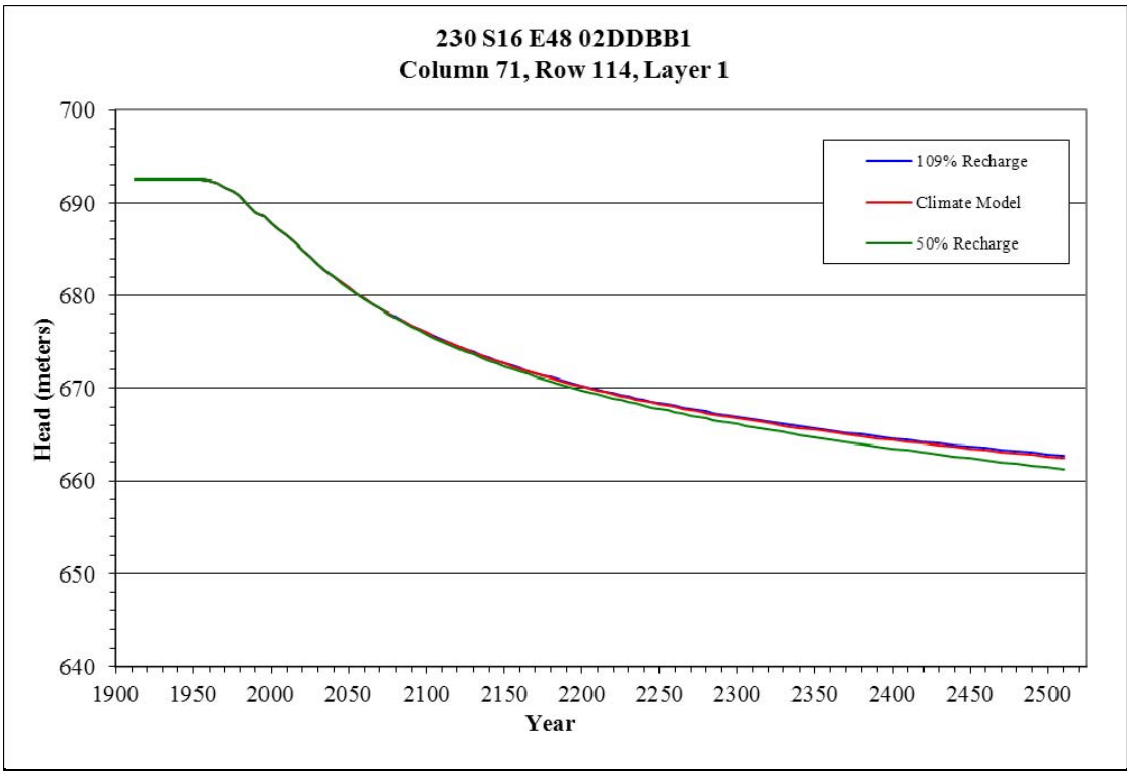

Figure B-3. Head Change in Column 71, Row 114, Layer 1

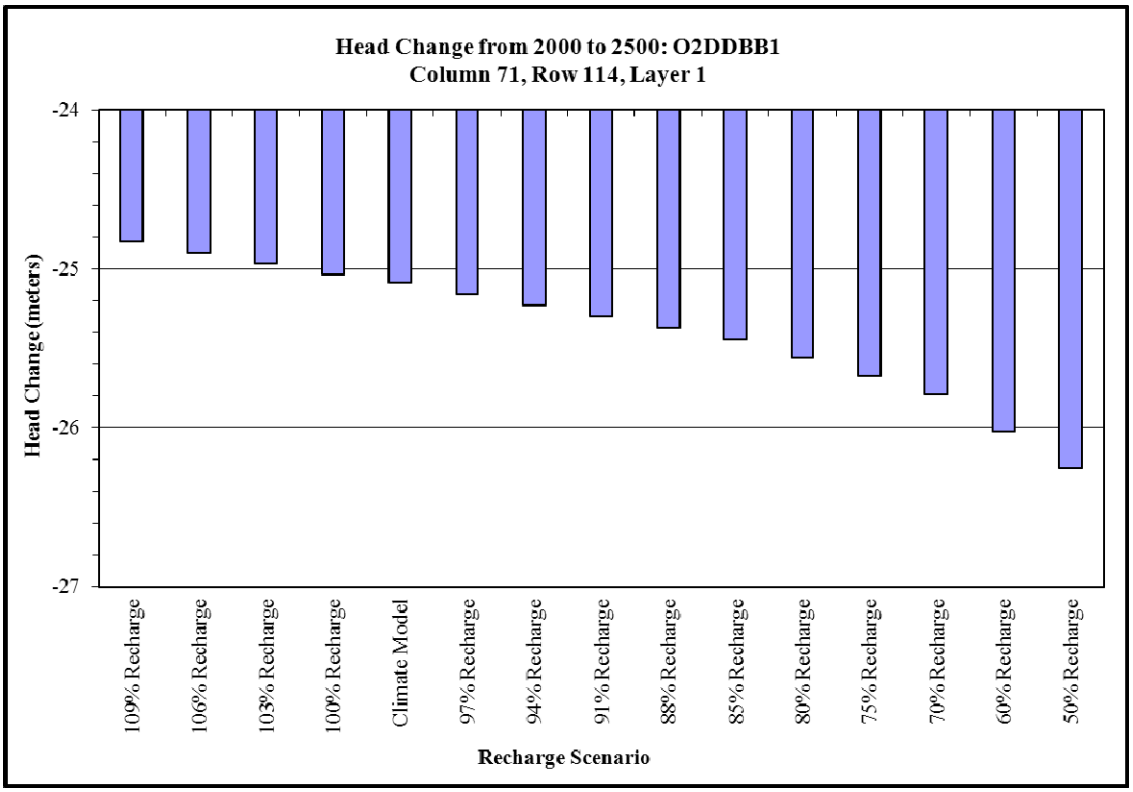

Figure B-4. Quantified Head Change in Column 71, Row 114, Layer 1

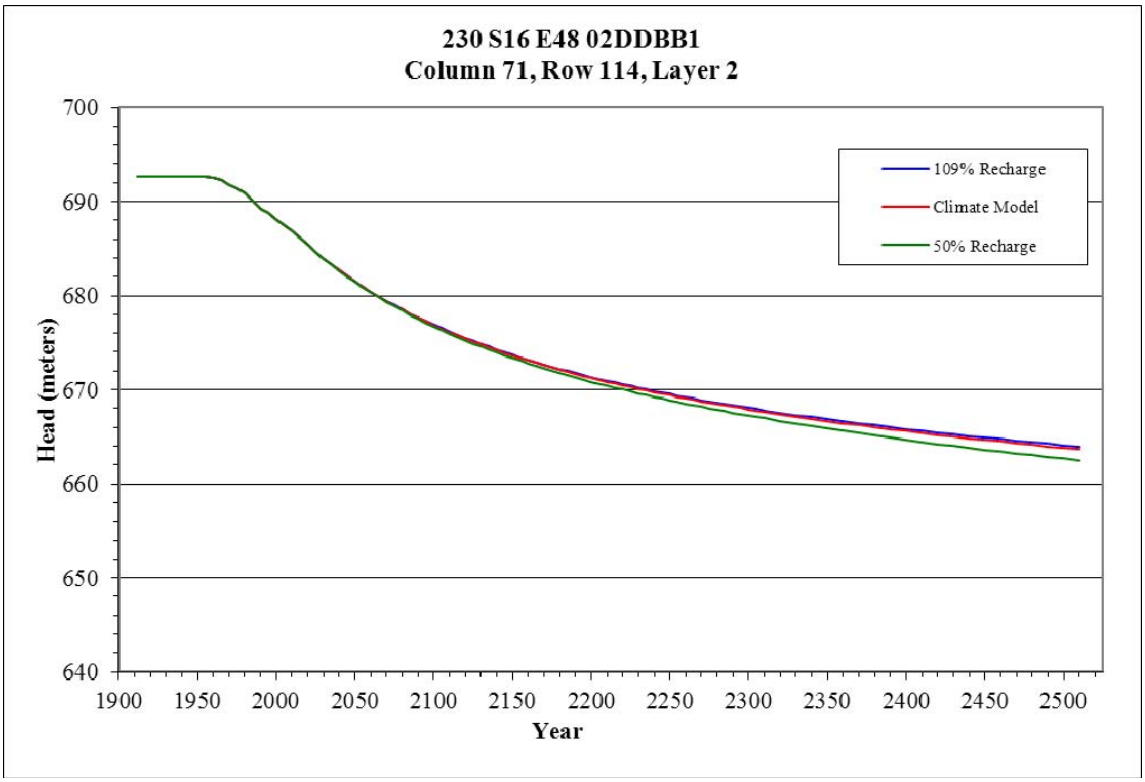

Figure B-5. Head Change in Column 71, Row 114, Layer 2

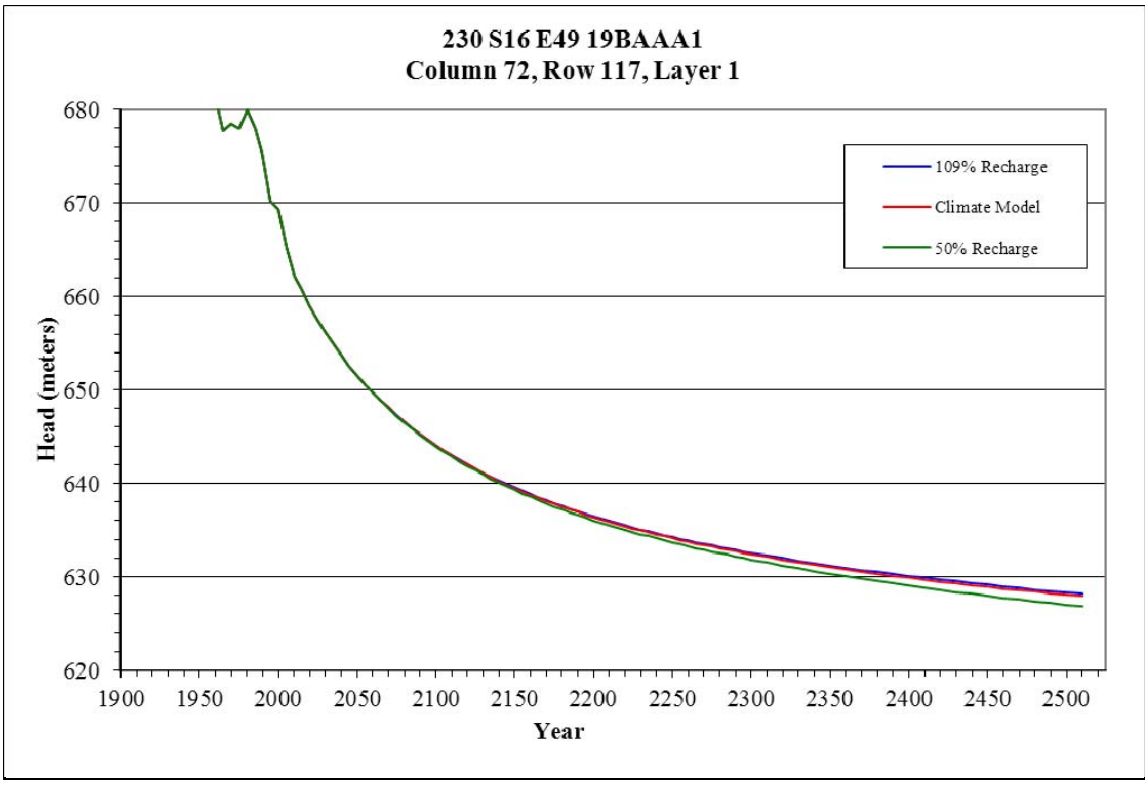

Figure B-6. Head Change in Column 72, Row 117, Layer 1

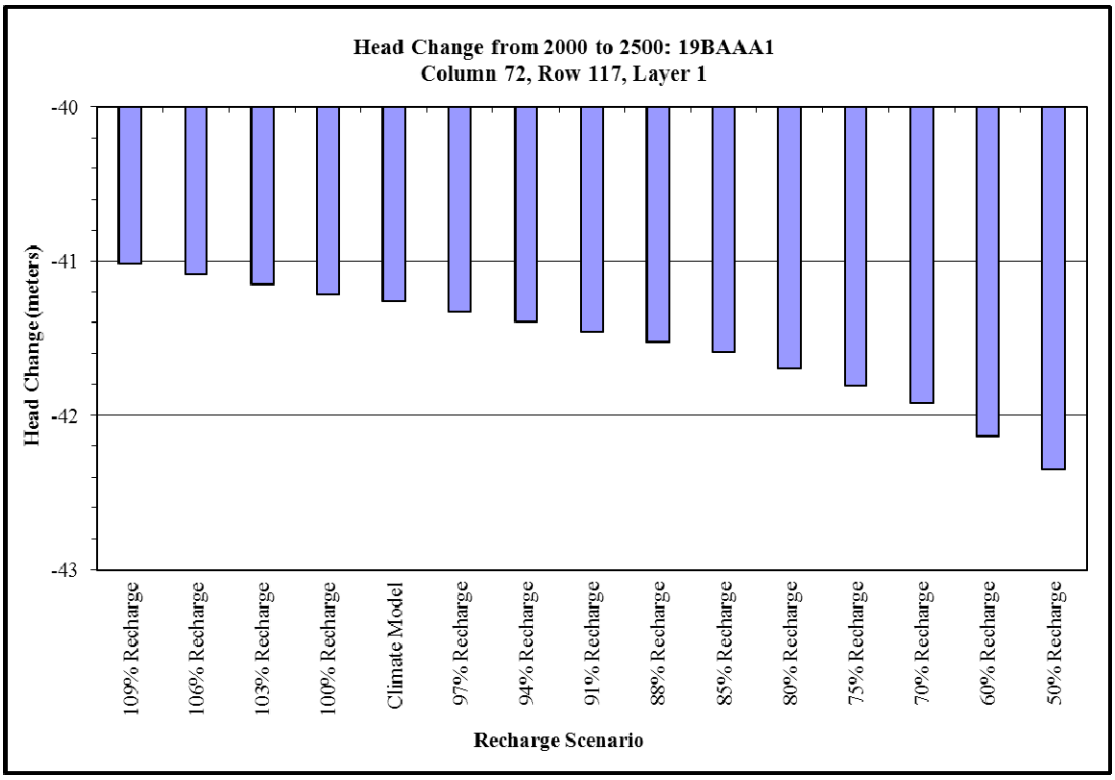

Figure B-7. Quantified Head Change: Column 72, Row 117, Layer 1

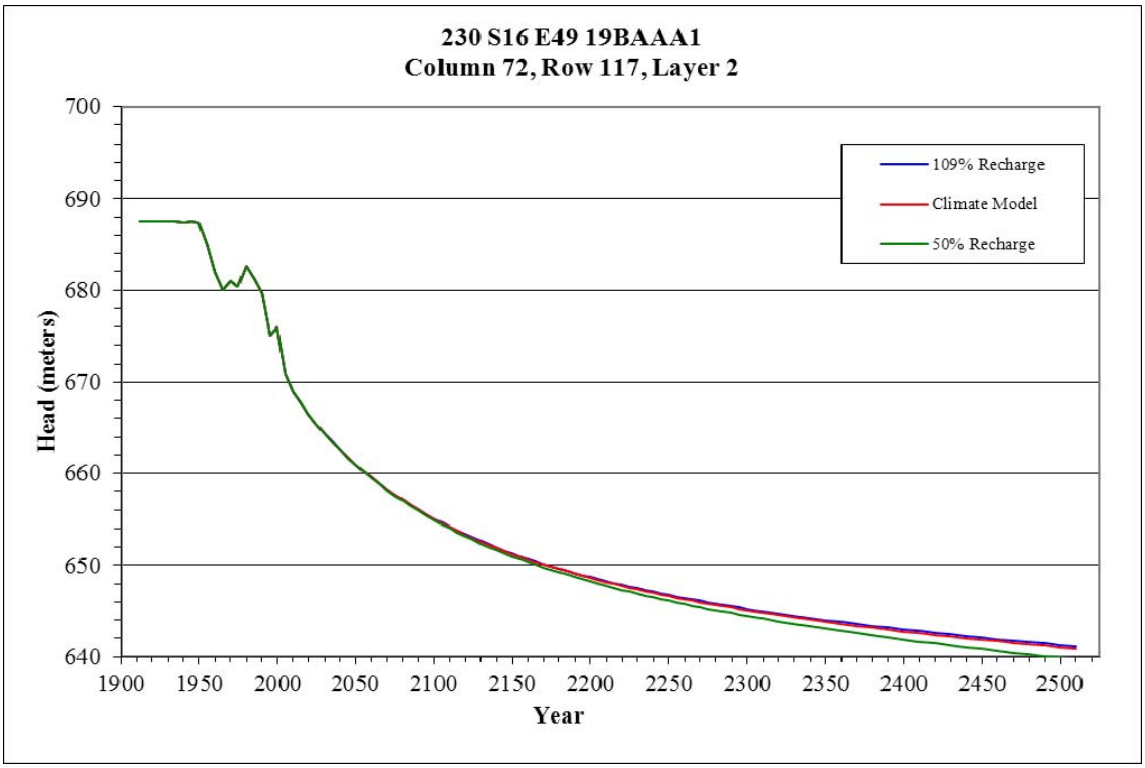

Figure B-8. Head Change in Column 72, Row 117, Layer 2

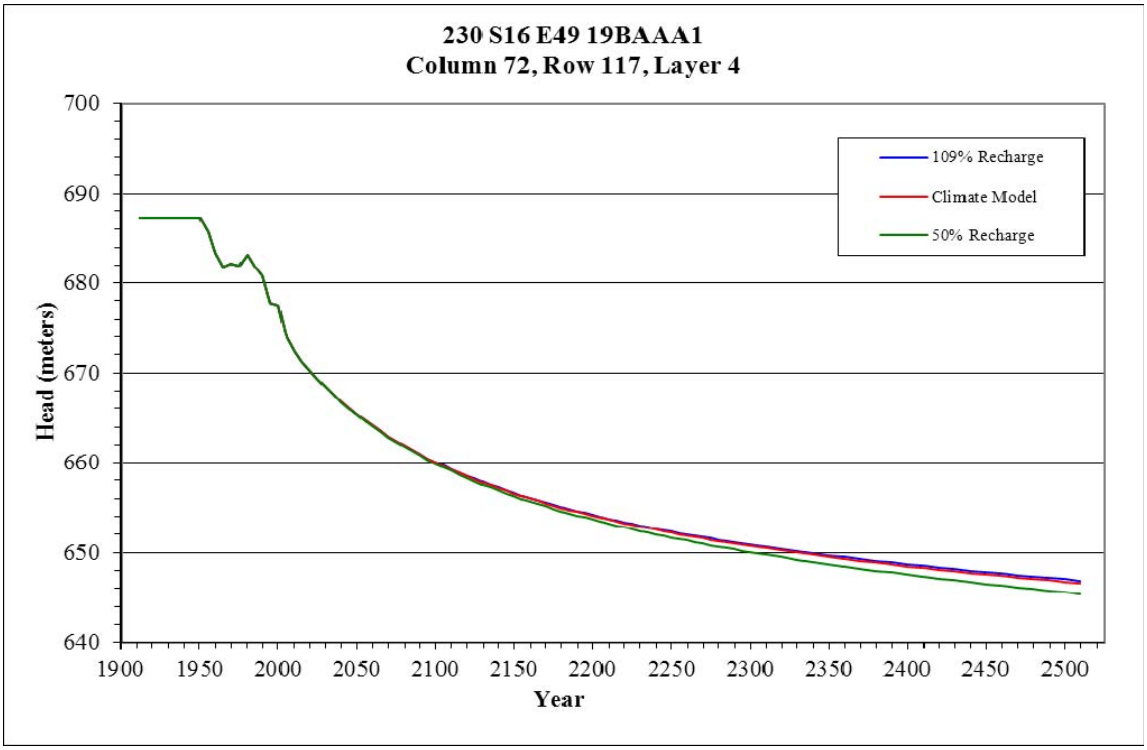

Figure B-9. Head Change in Column 72, Row 117, Layer 4

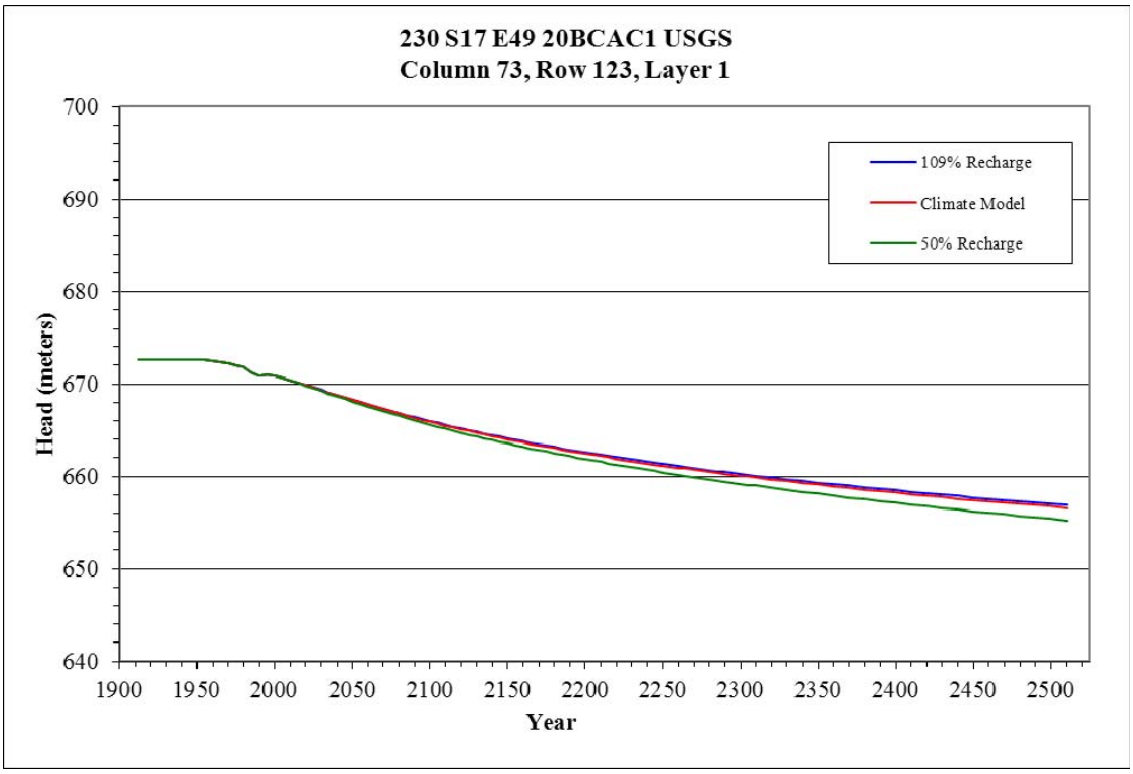

Figure B-10. Head Changes in Column 73, Row 123, Layer 1

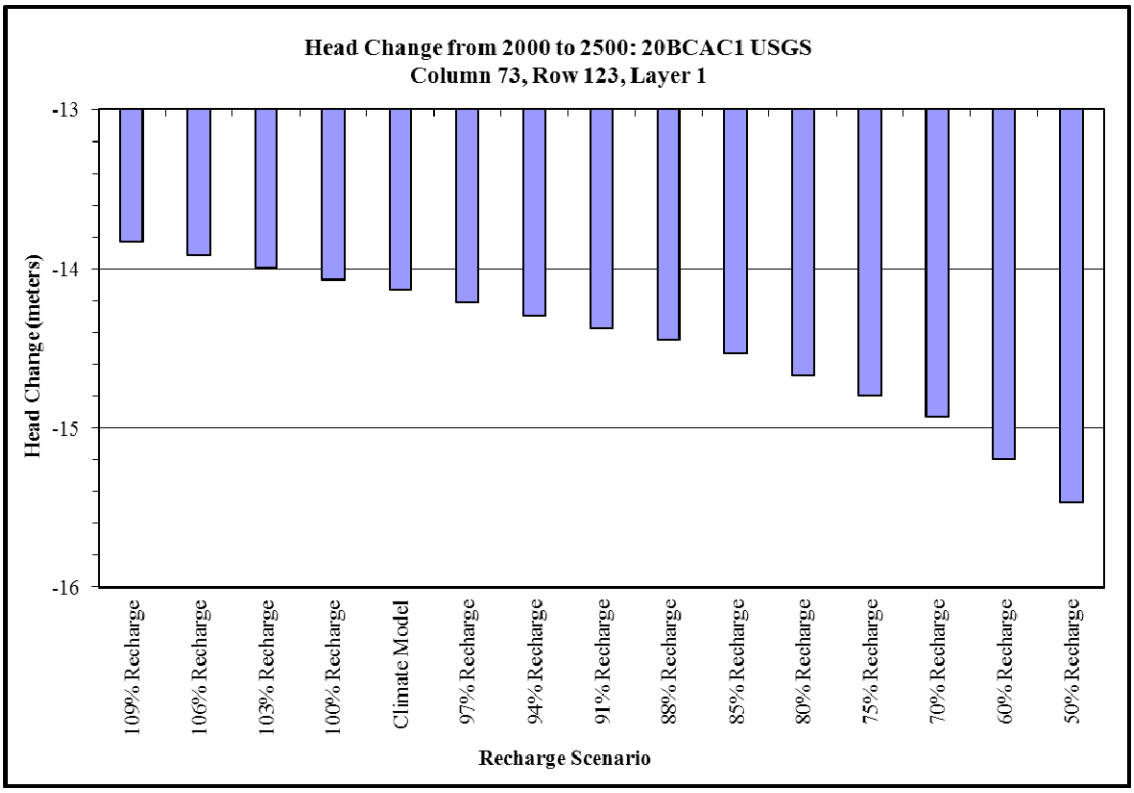

Figure B-11. Quantified Head Change in Column 73, Row 123, Layer 1

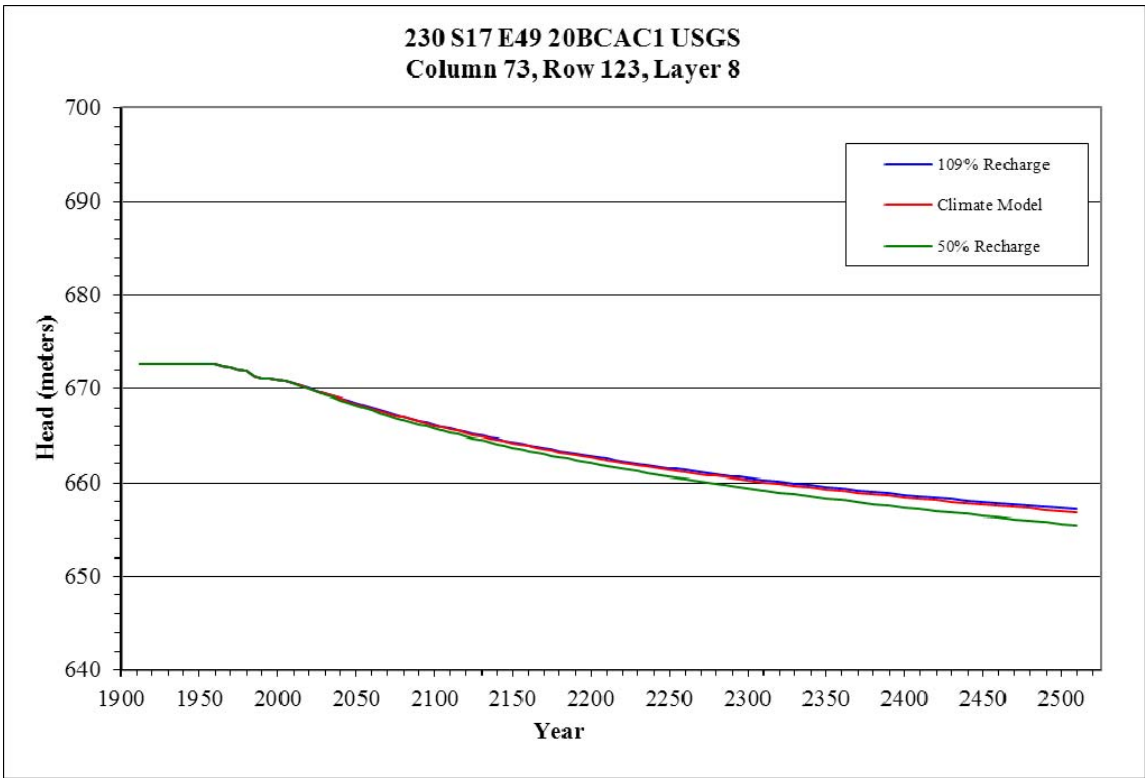

Figure B-12. Head Change in Column 73, Row 123, Layer 8

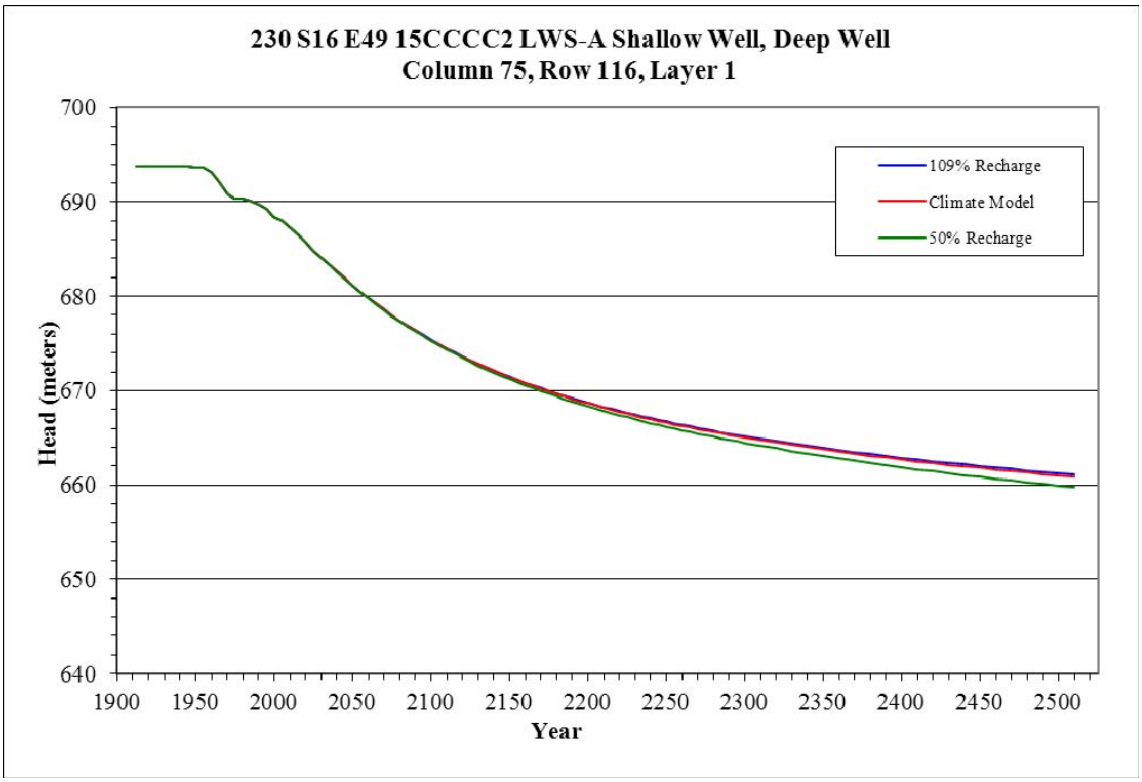

Figure B-13. Head Change in Column 75, Row 116, Layer 1

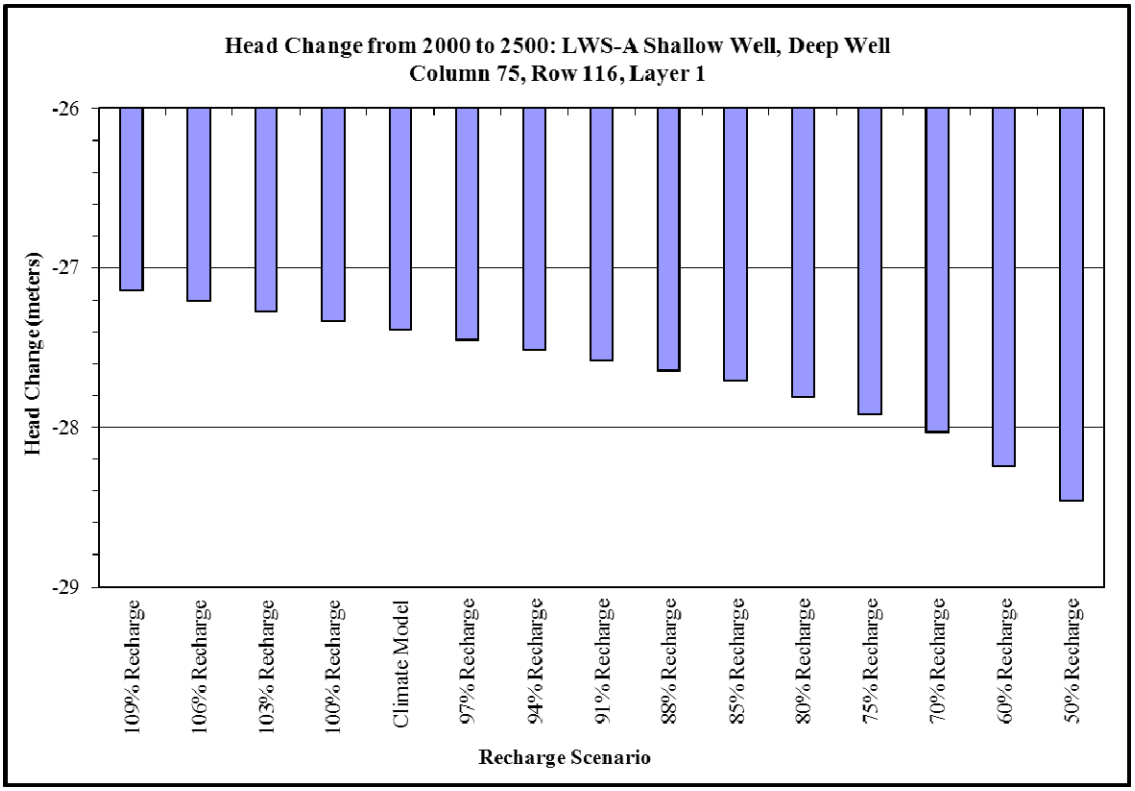

Figure B-14. Quantified Head Change in Column 75, Row 116, Layer 1

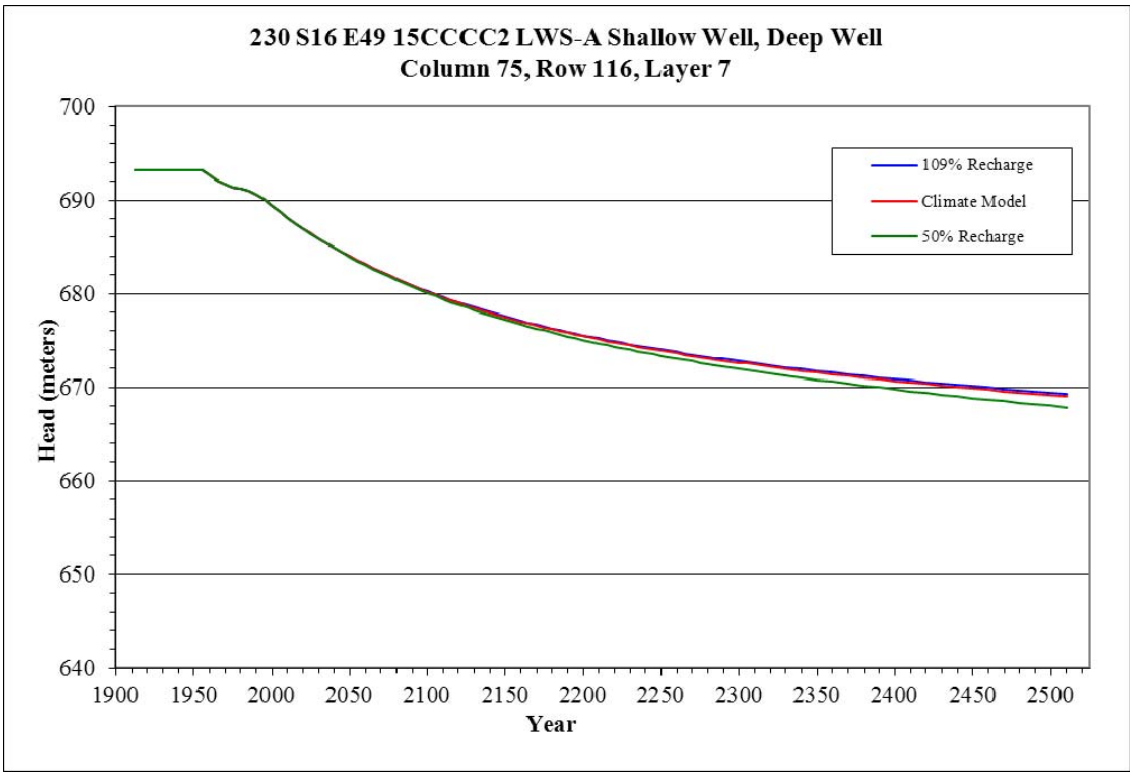

Figure B-15. Head Change in Column 75, Row 116, Layer 7

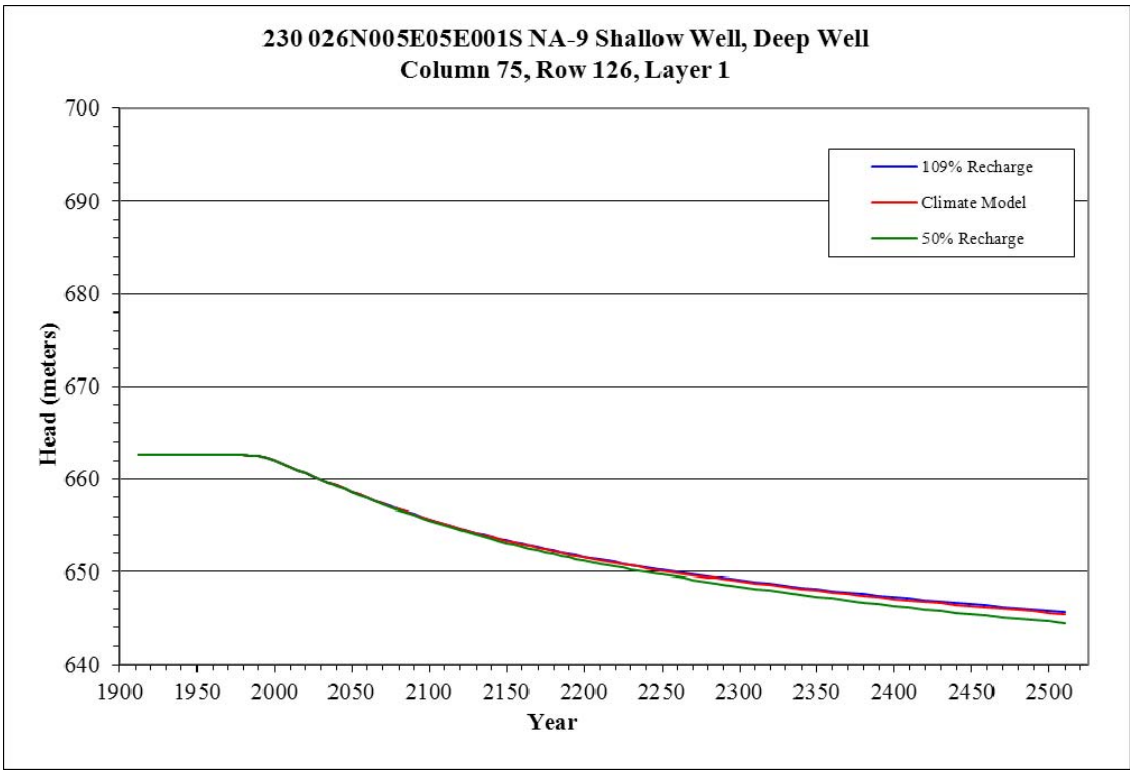

Figure B-16. Head Change in Column 75, Row 126, Layer 1

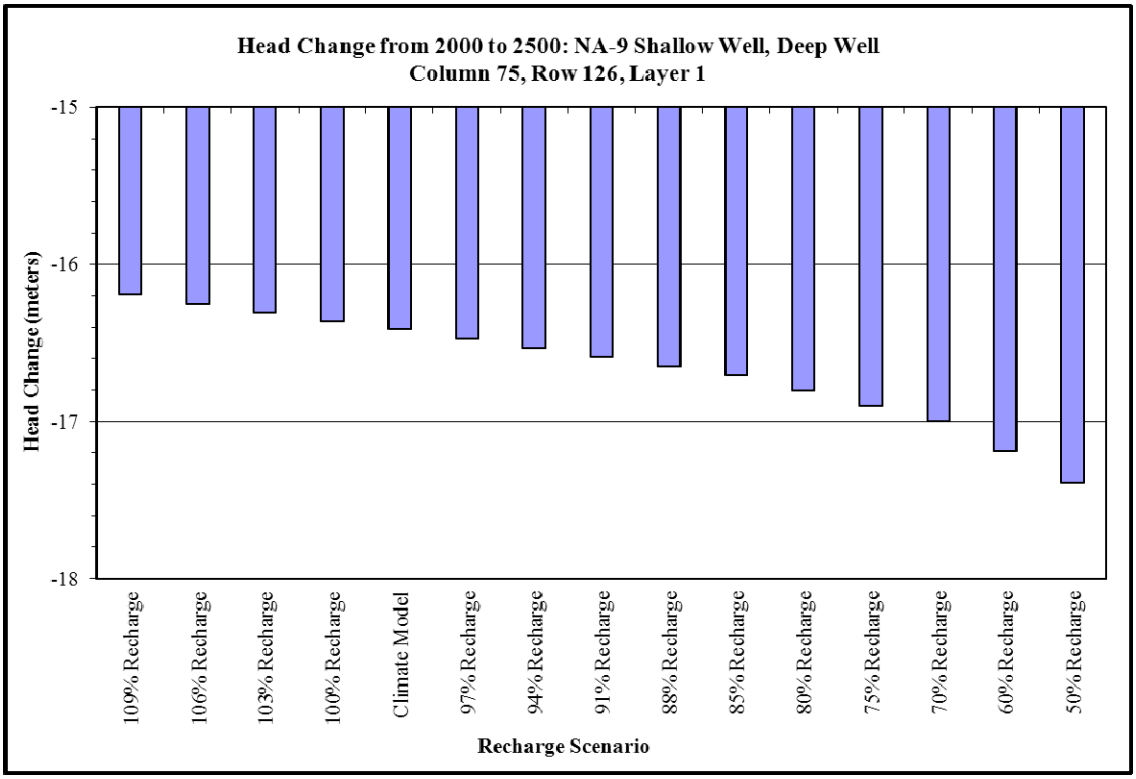

Figure B-17. Quantified Head Change in Column 75, Row 126, Layer 1

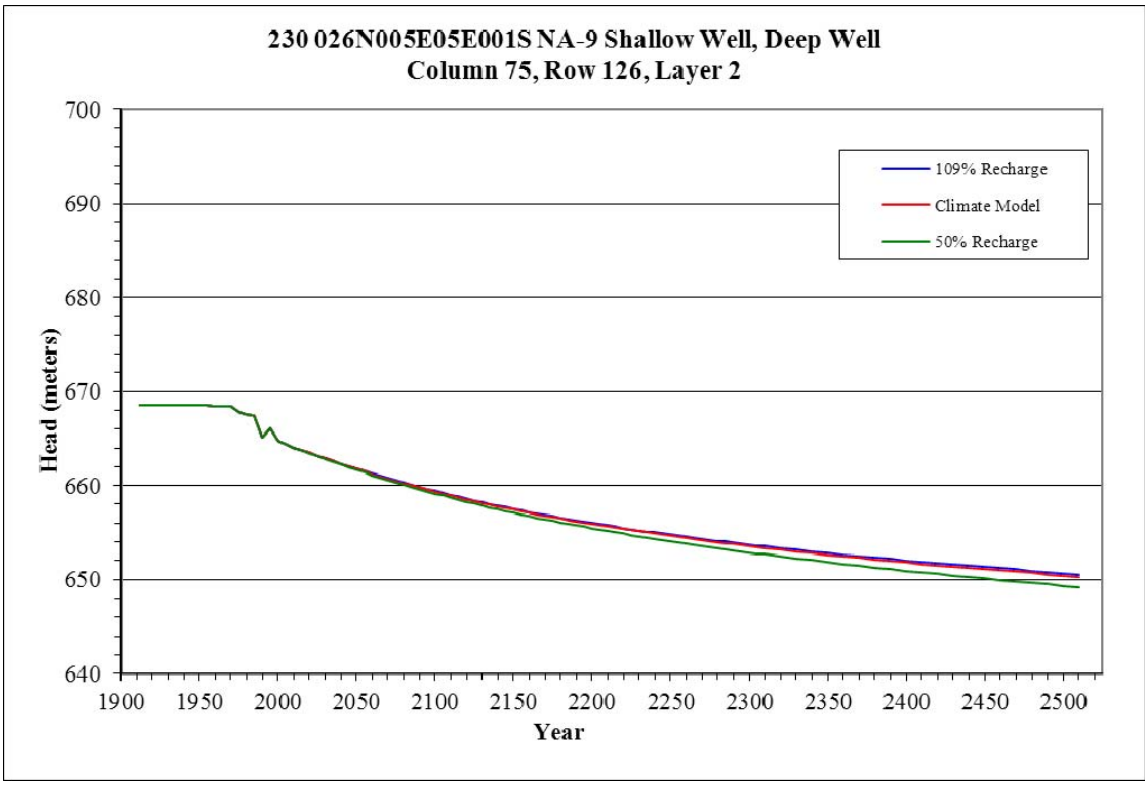

Figure B-18. Head Change in Column 75, Row 126, Layer 2

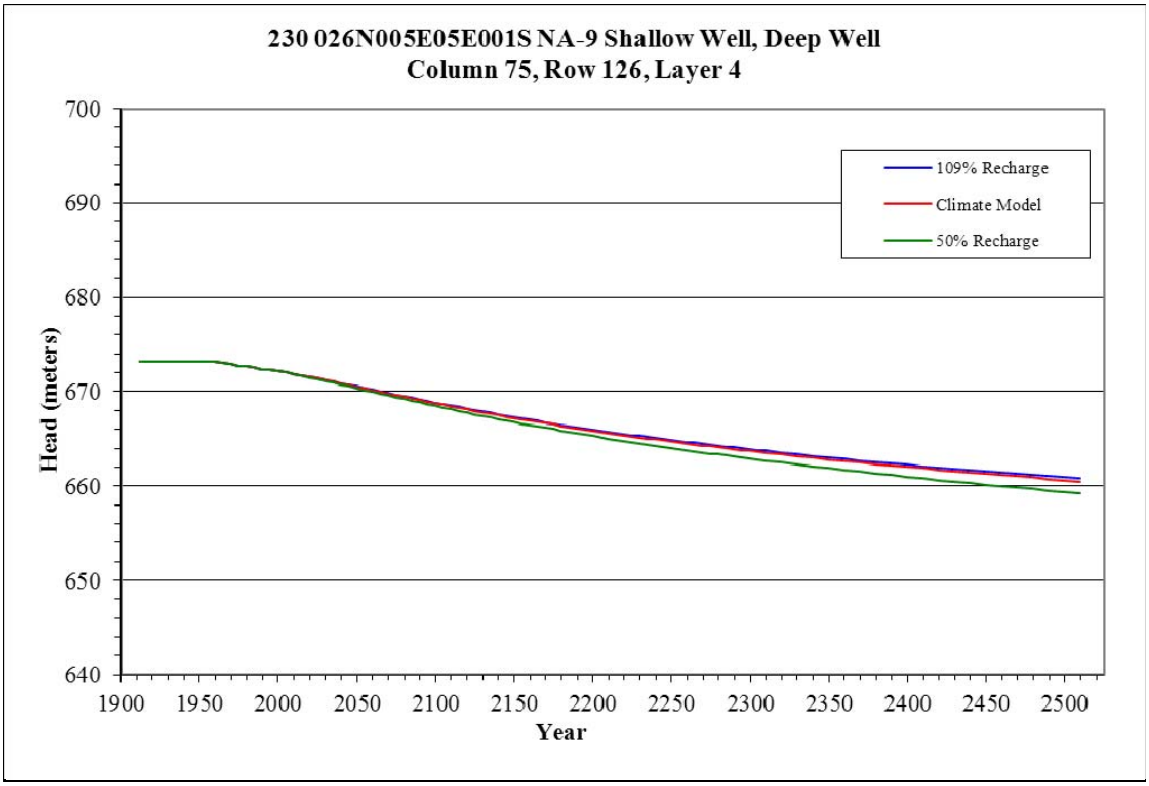

Figure B-19. Head Change in Column 75, Row 126, Layer 4

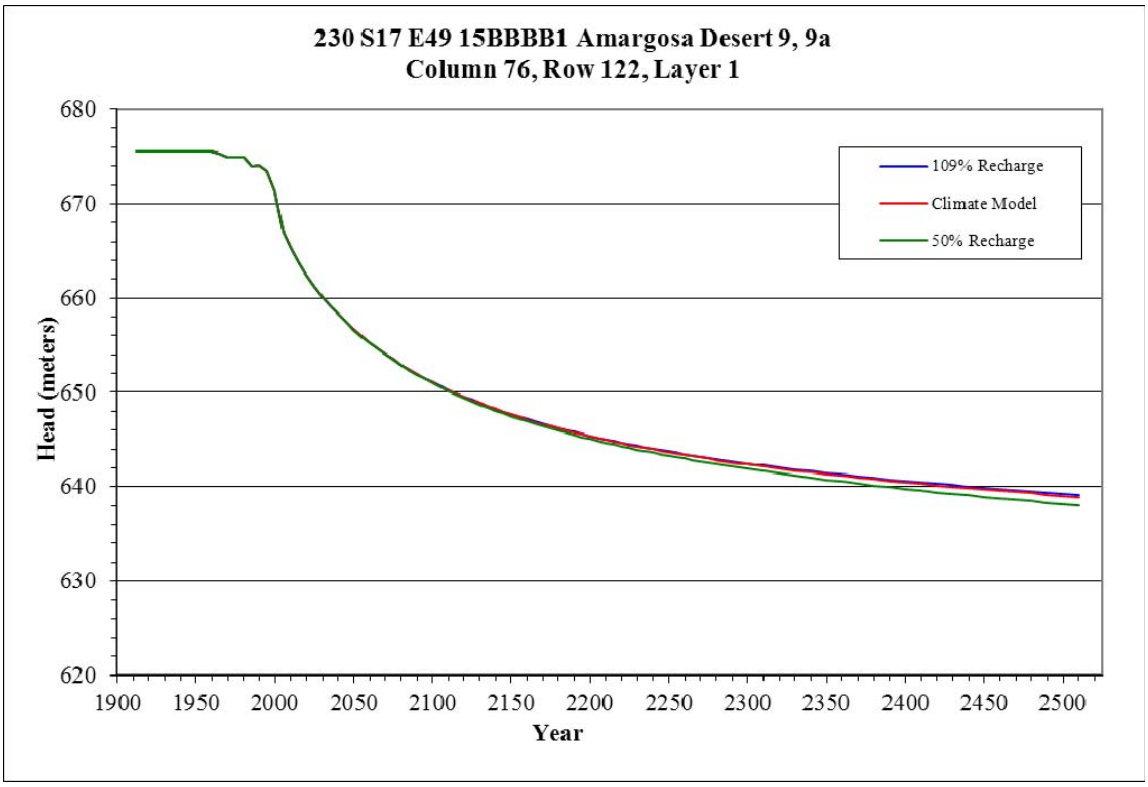

Figure B-20. Head Change in Column 76, Row 122, Layer 1

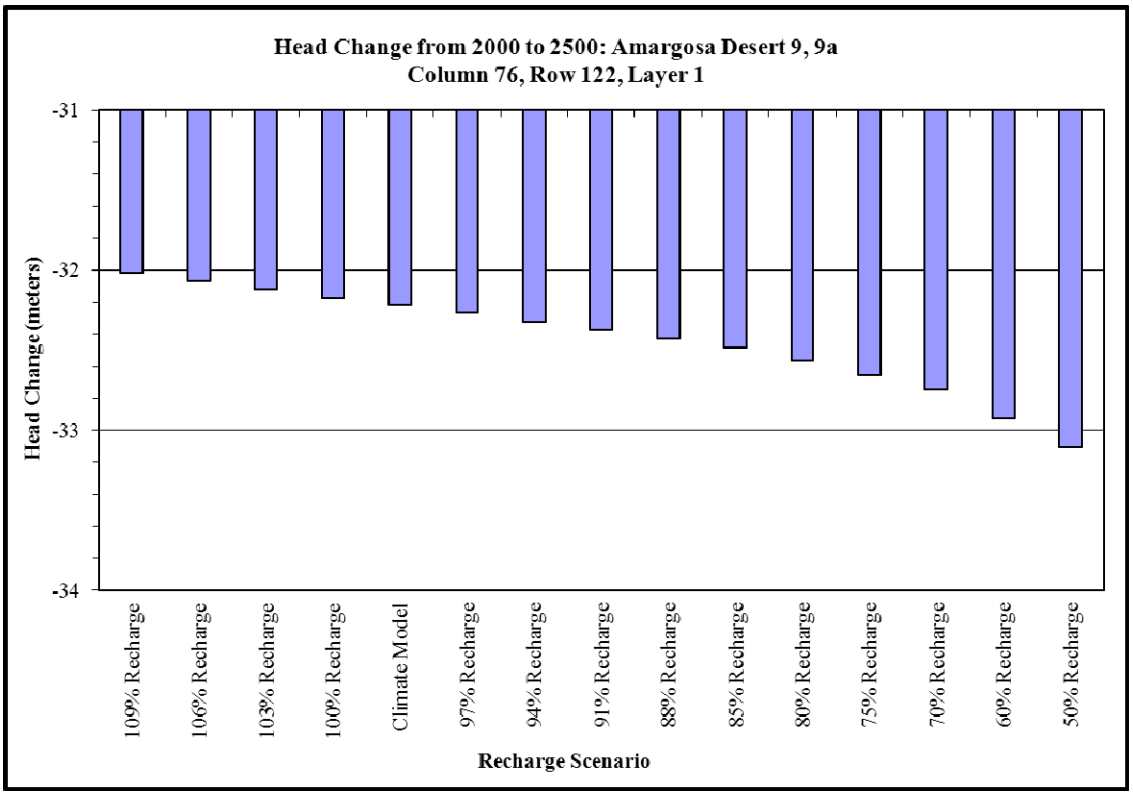

Figure B-21. Quantified Head Change in Column 76, Row 122, Layer 1

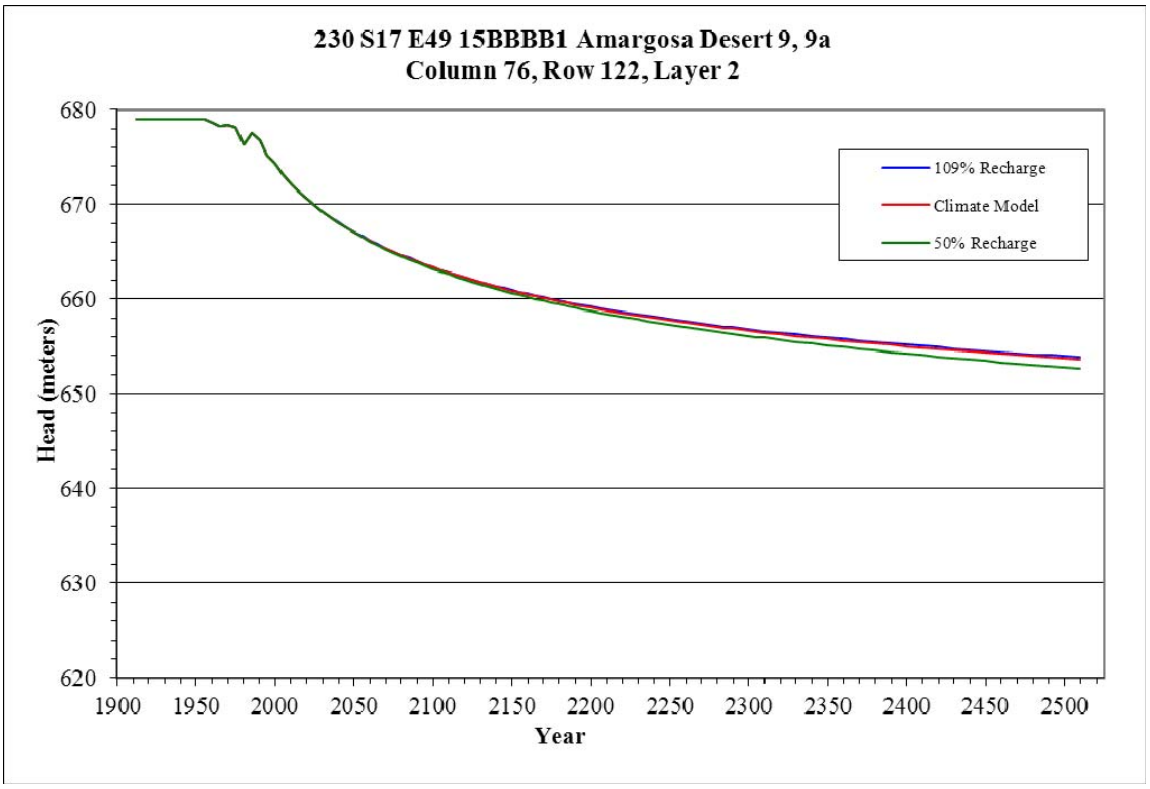

Figure B-22. Head Change in Column 76, Row 122, Layer 2

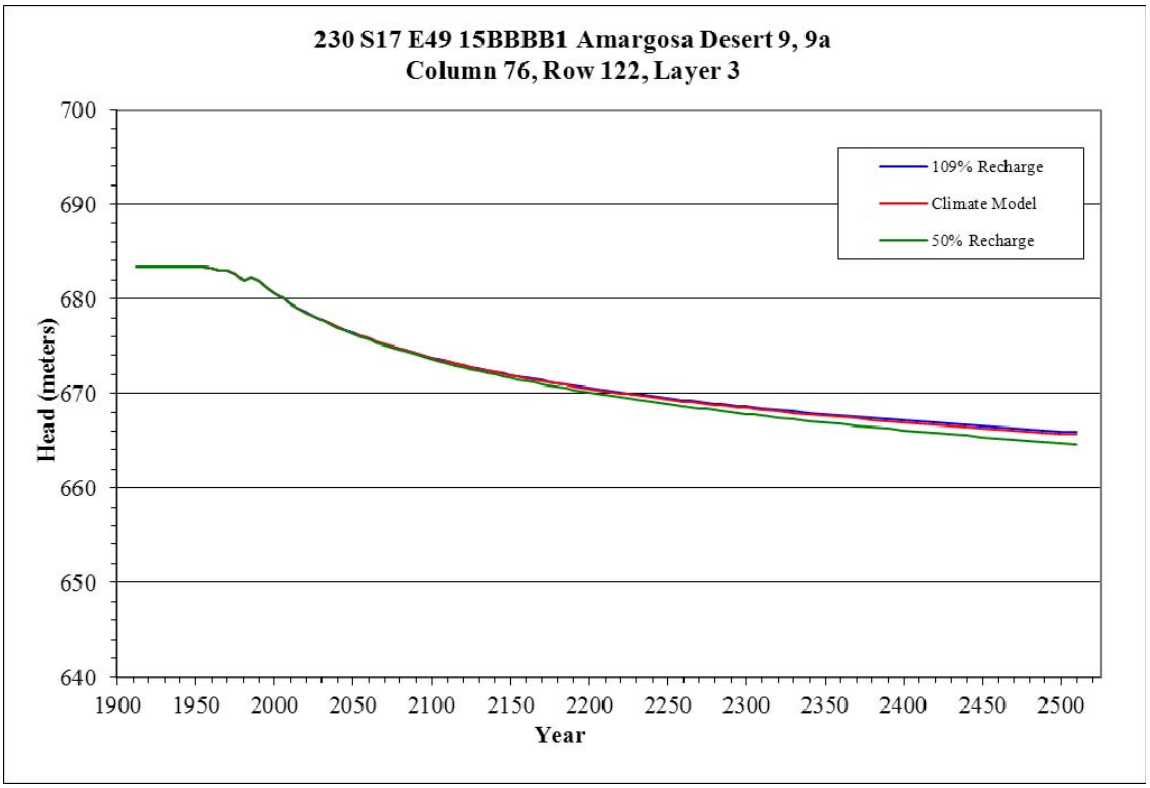

Figure B-23. Head Change in Column 76, Row 122, Layer 3

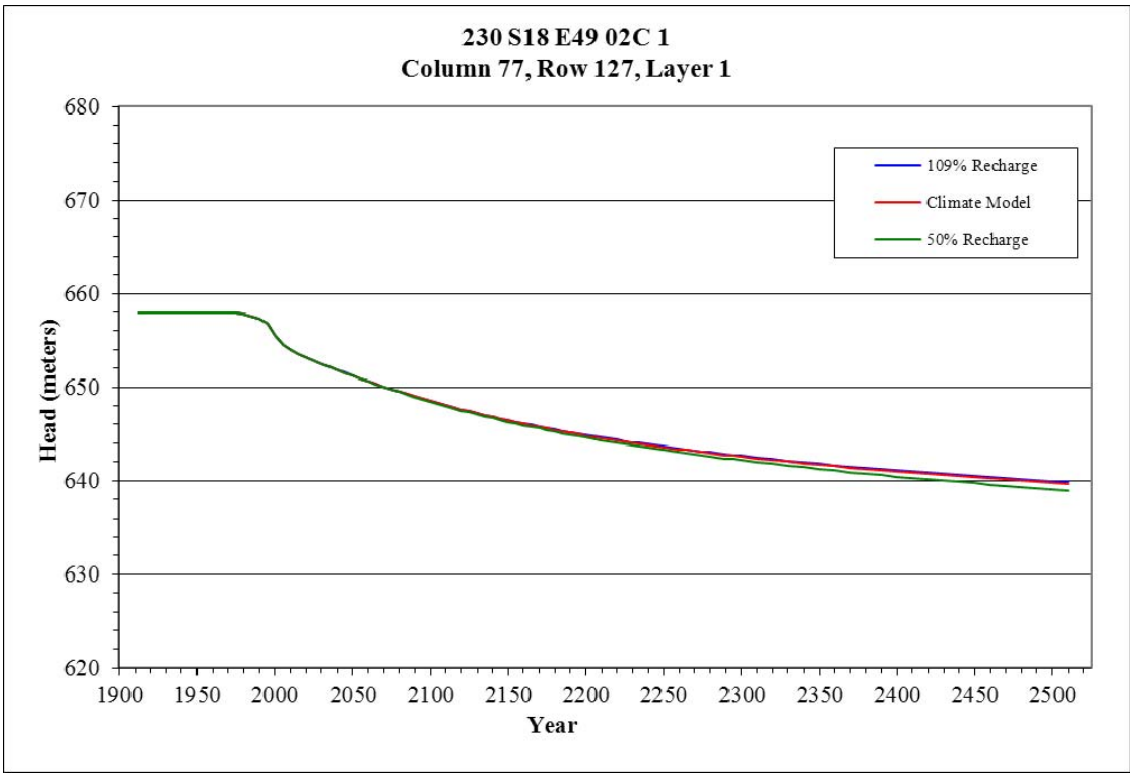

Figure B-24. Head Change in Column 77, Row 127, Layer 1

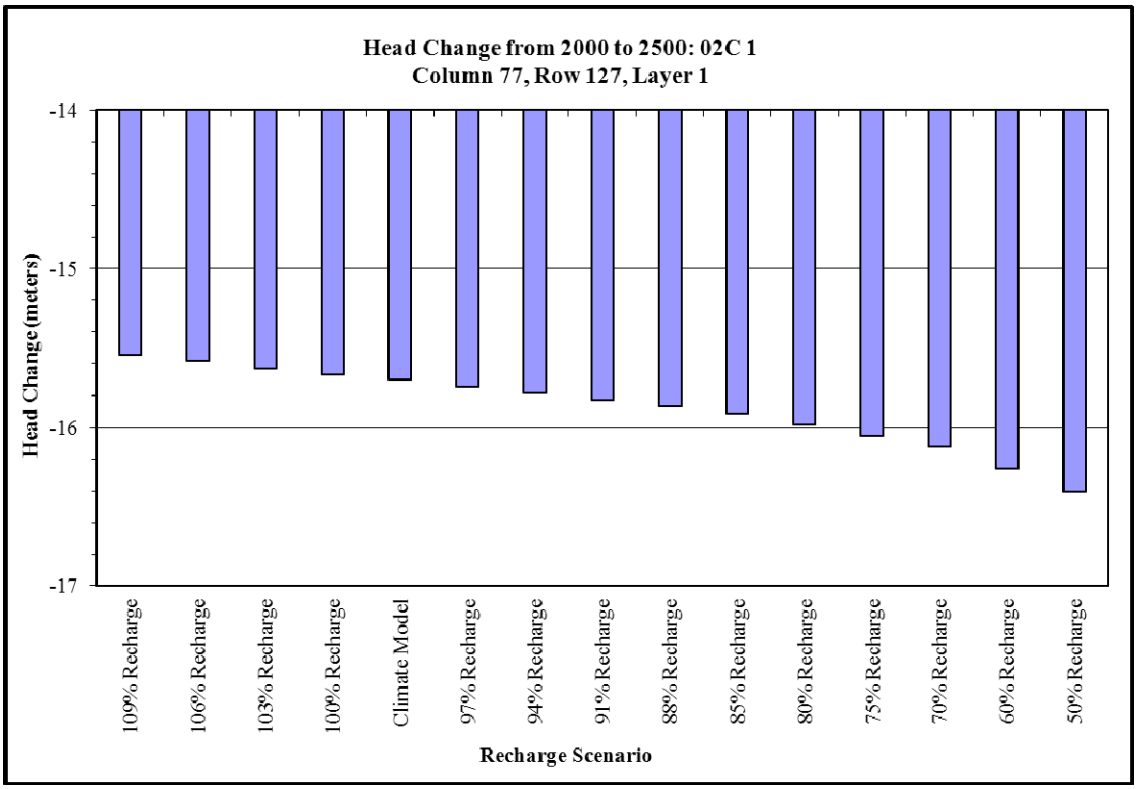

Figure B-25. Quantified Head Change in Column 77, Row 127, Layer 1

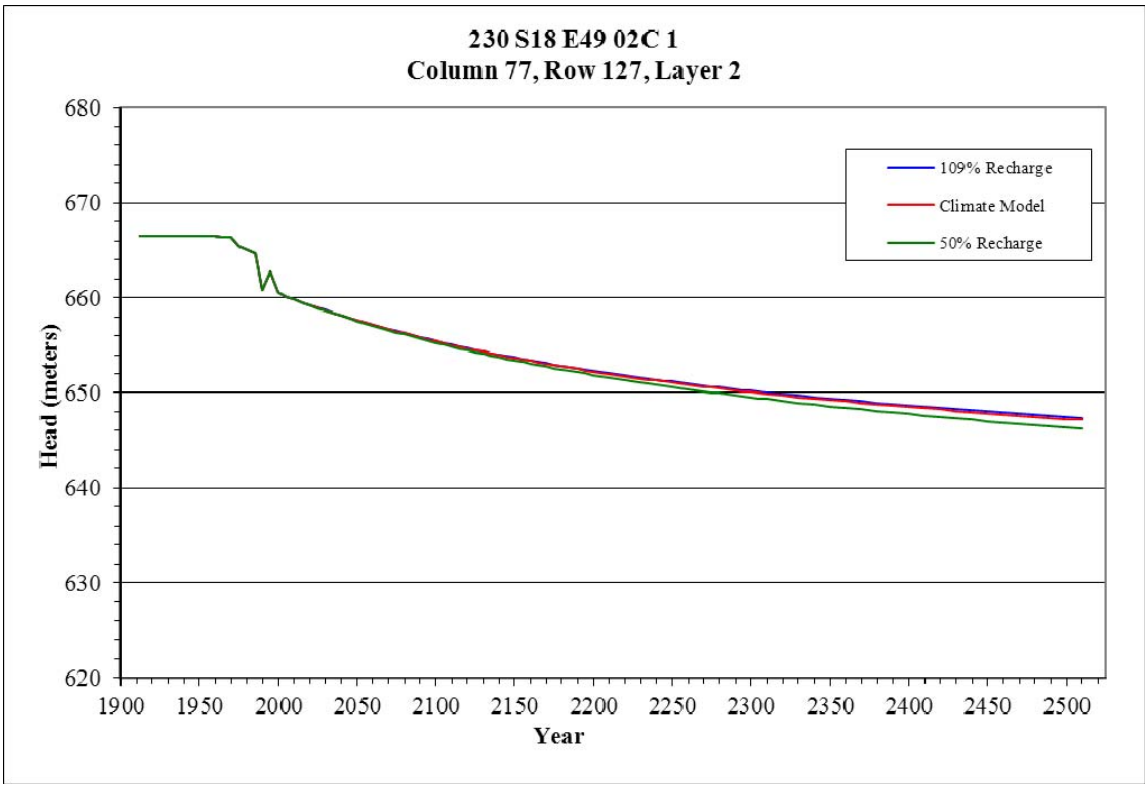

Figure B-26. Head Change in Column 77, Row 127, Layer 2

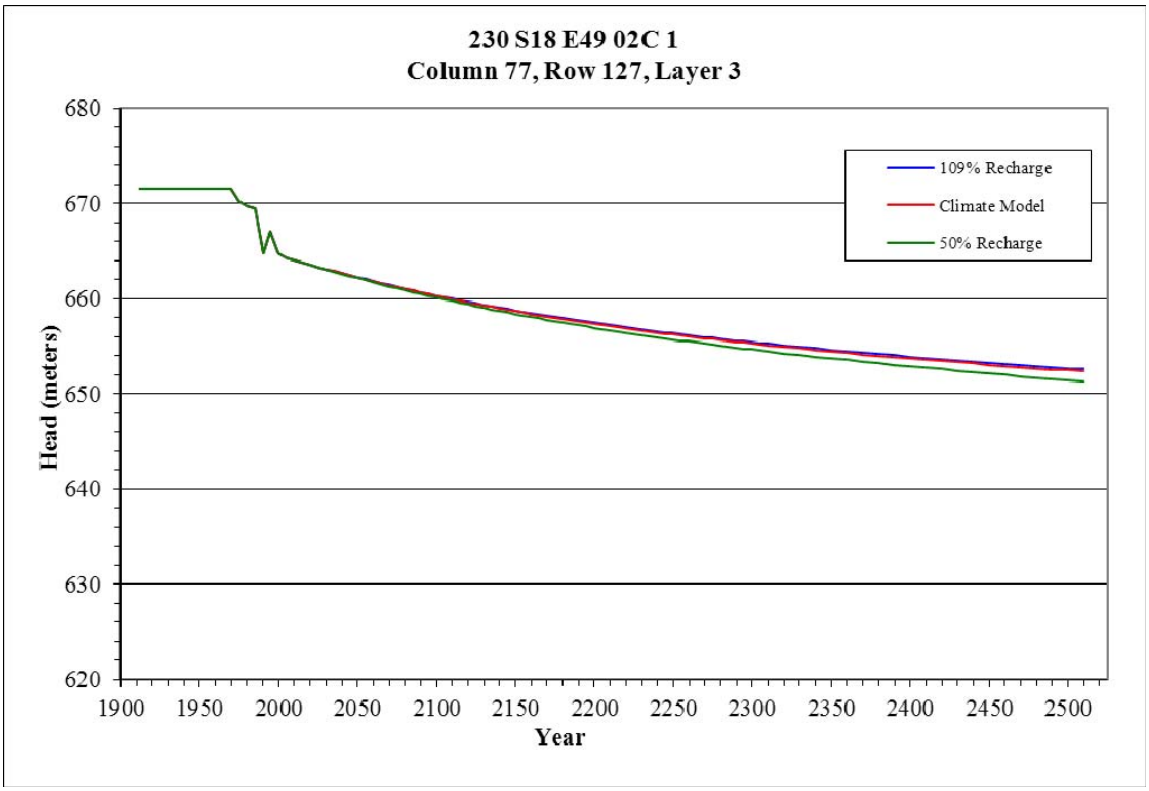

Figure B-27. Head Change in Column 77, Row 127, Layer 3

Ash Meadows Area

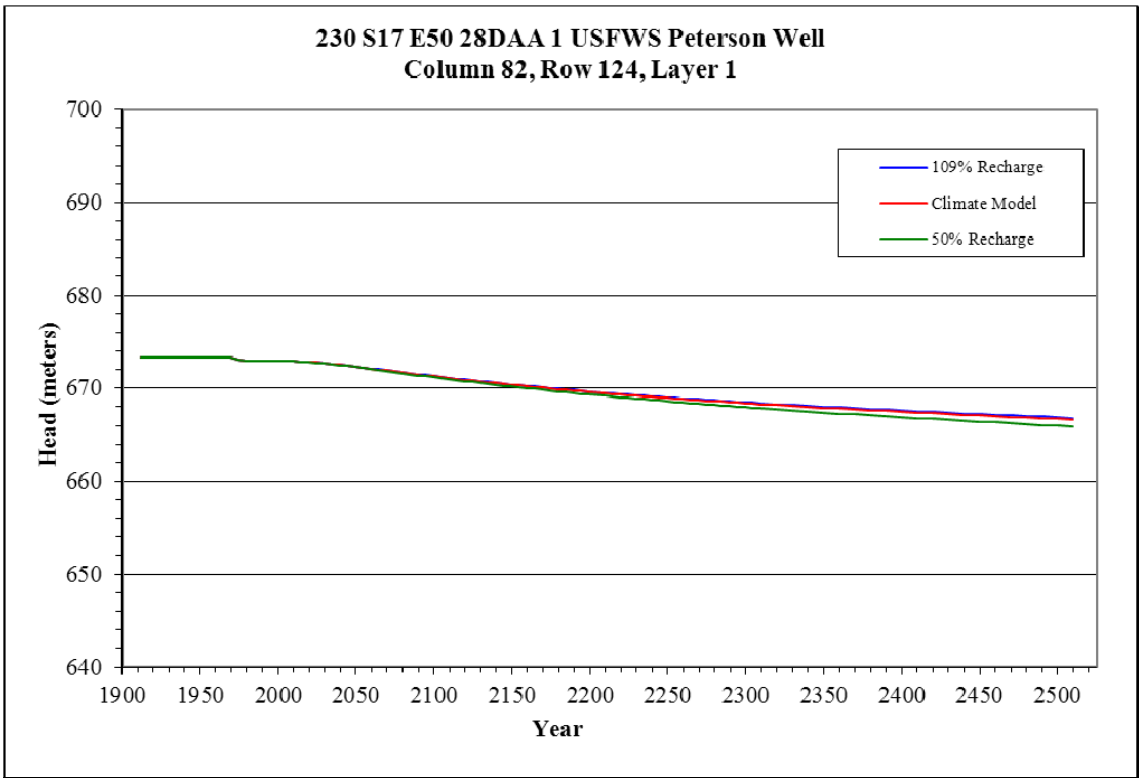

Figure B-28. Head Change in Column 82, Row 124, Layer 1

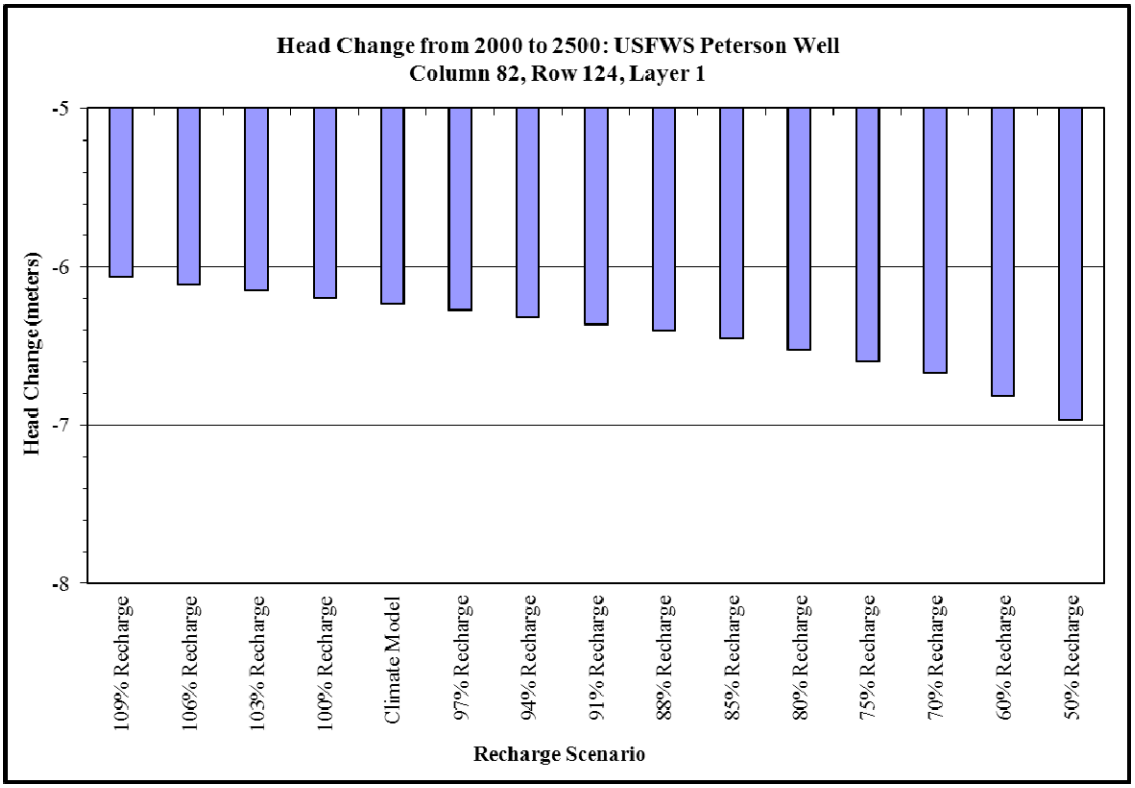

Figure B-29. Quantified Head Change in Column 82, Row 124, Layer 1

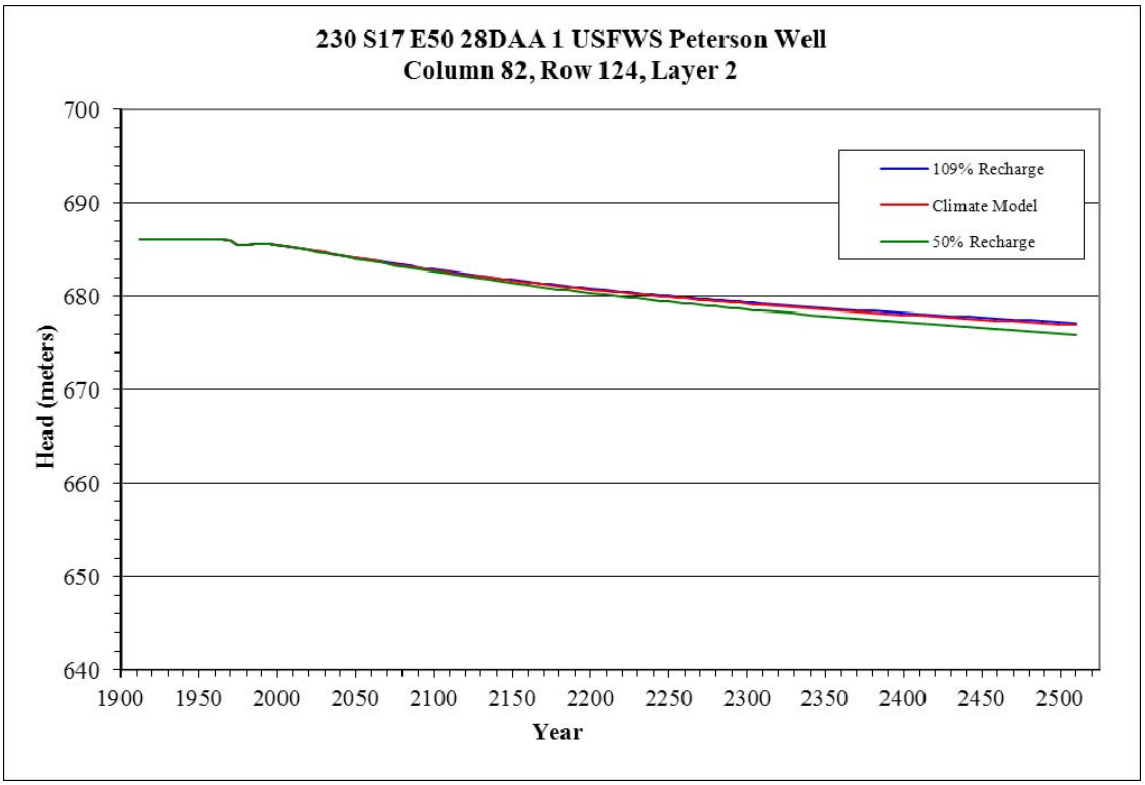

Figure B-30. Head Change in Column 82, Row 124, Layer 2

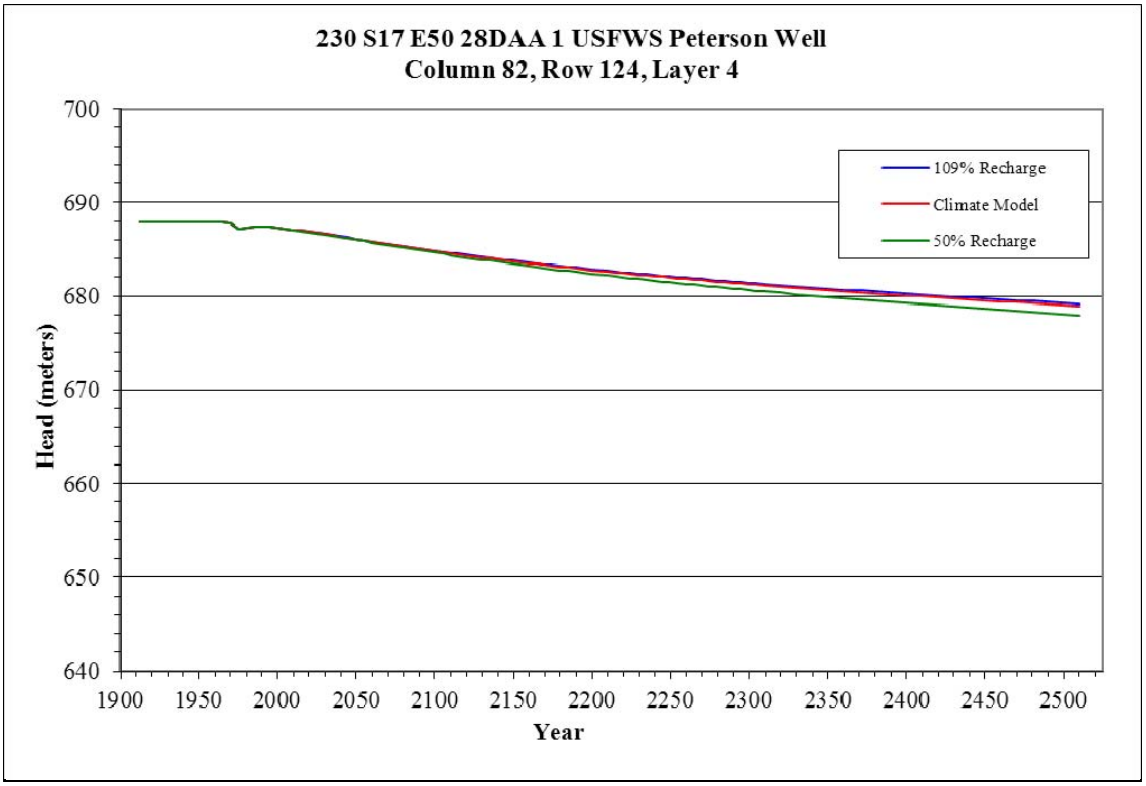

Figure B-31. Head Change in Column 82, Row 124, Layer 4

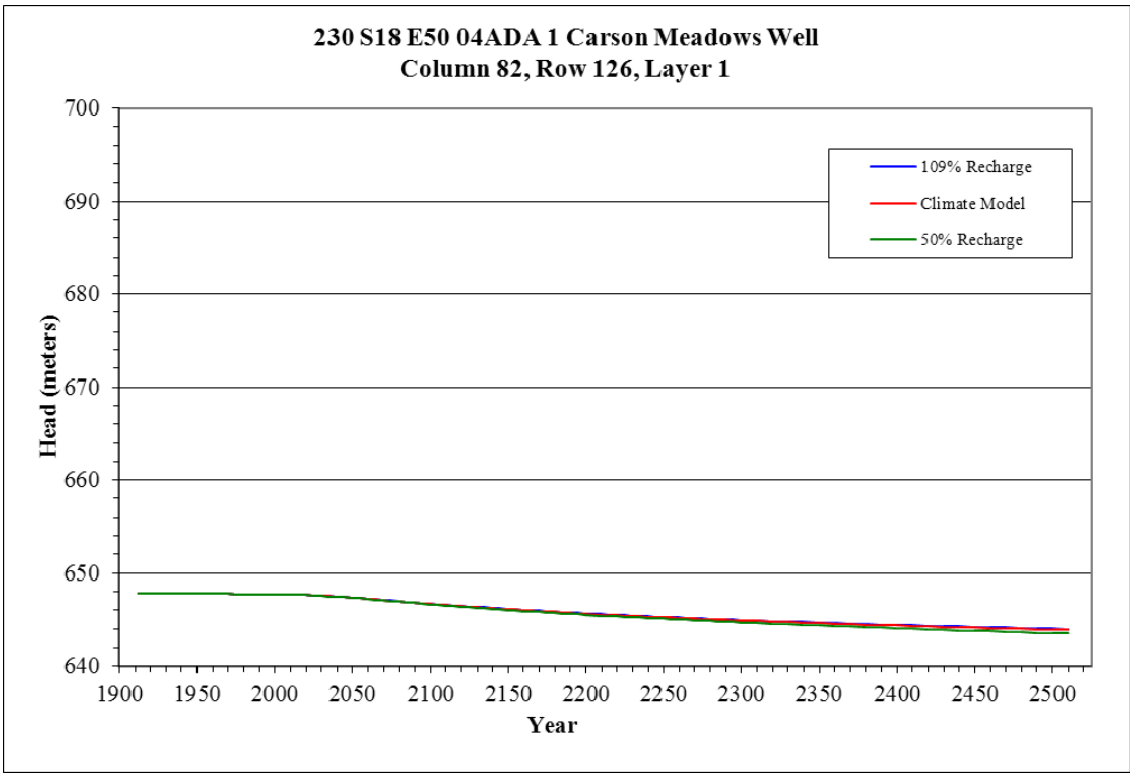

Figure B-32. Head Change in Column 82, Row 126, Layer 1

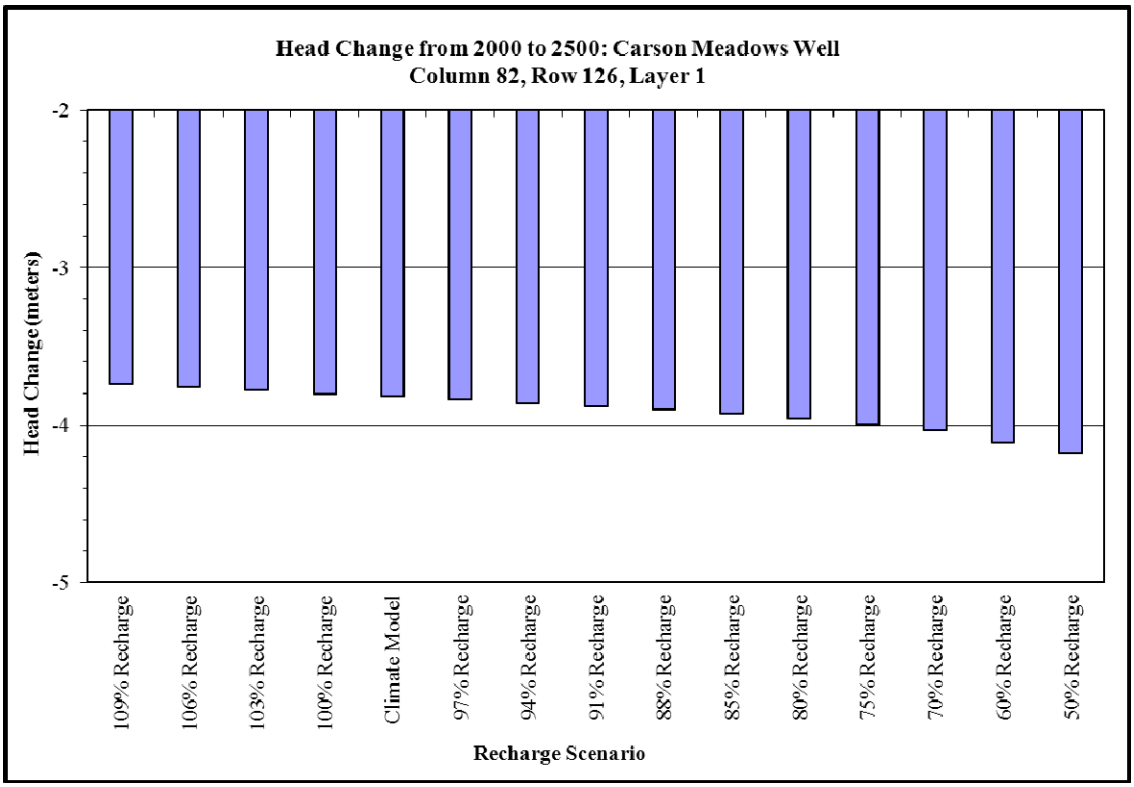

Figure B-33. Quantified Head Change in Column 82, Row 126, Layer 1

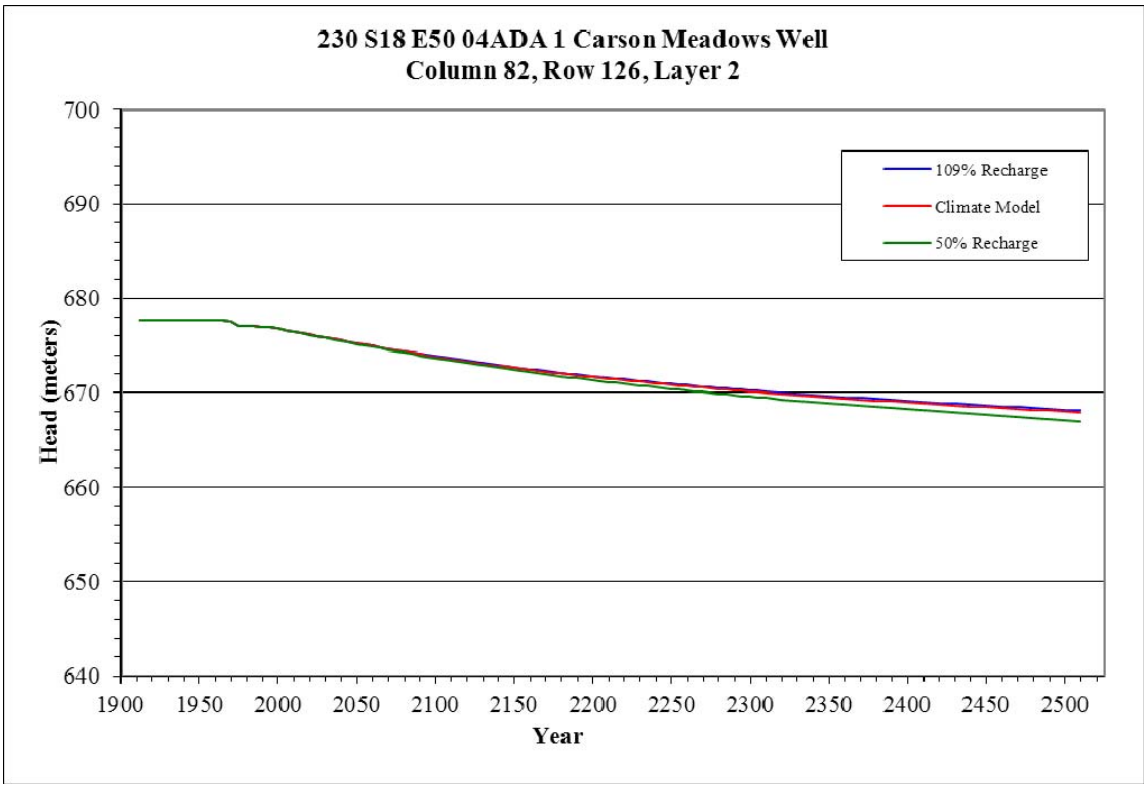

Figure B-34. Head Change in Column 82, Row 126, Layer 2

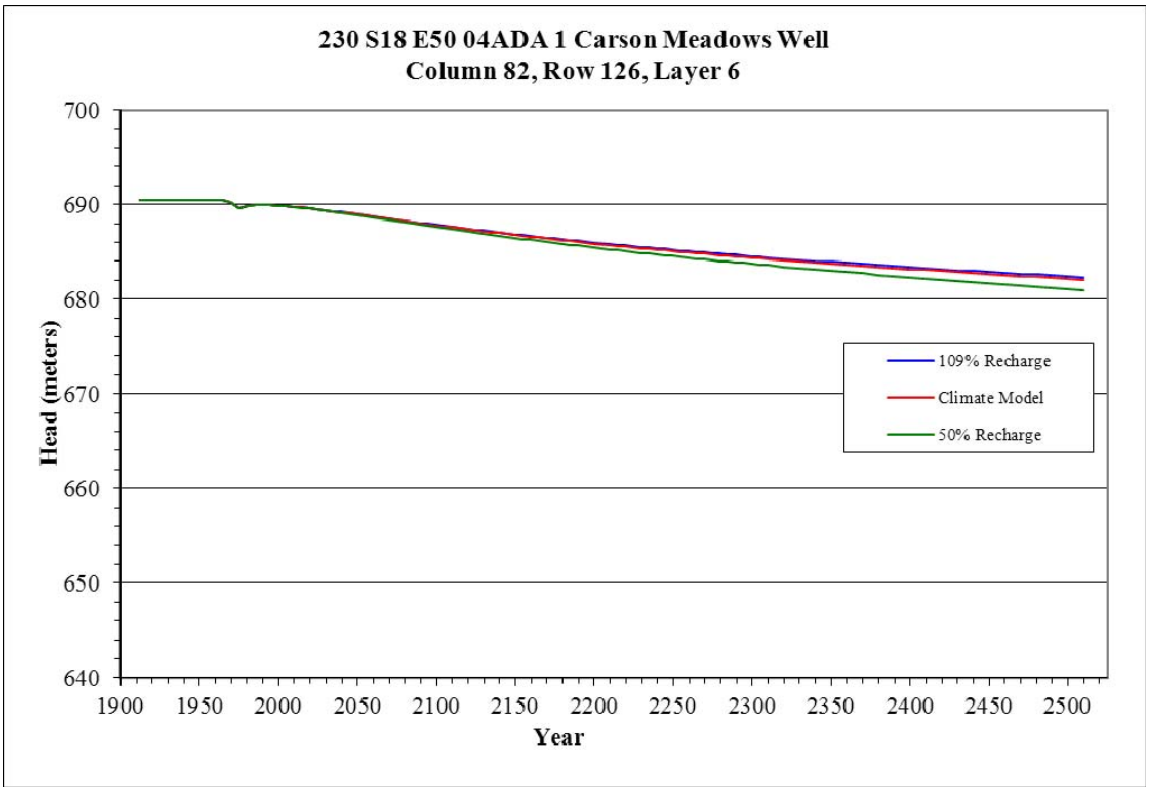

Figure B-35. Head Change in Column 82, Row 126, Layer 6

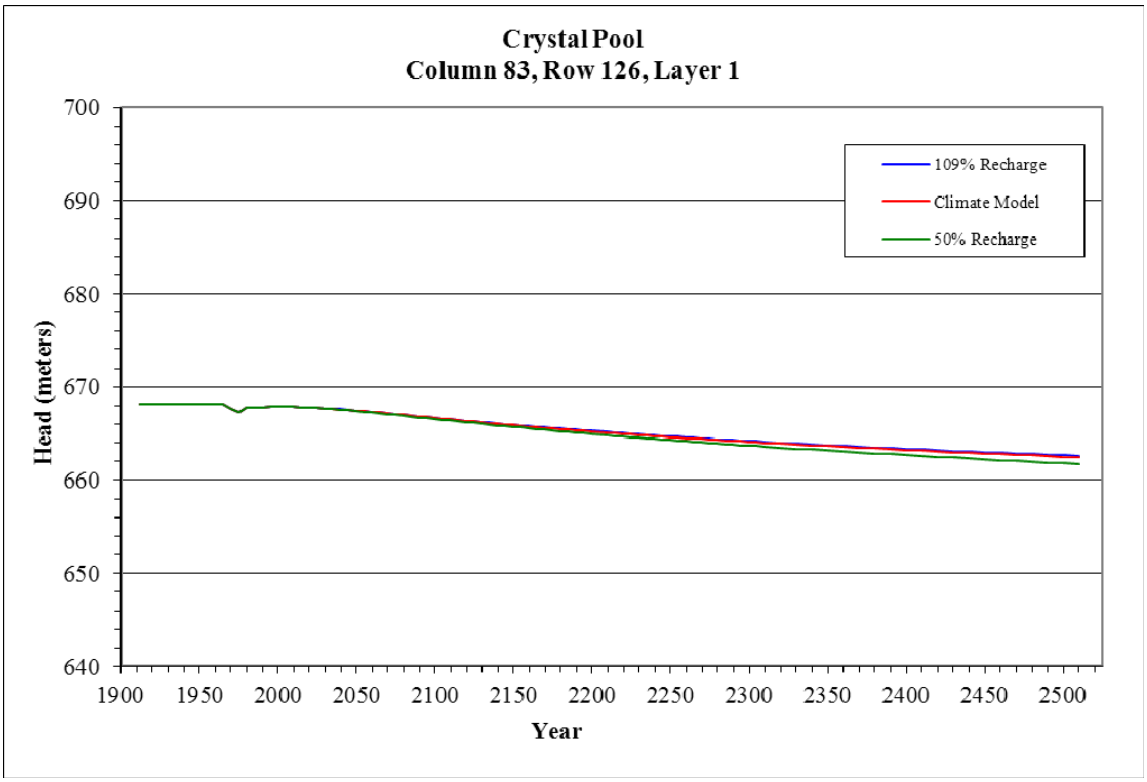

Figure B-36. Head Change in Column 83, Row 126, Layer 1

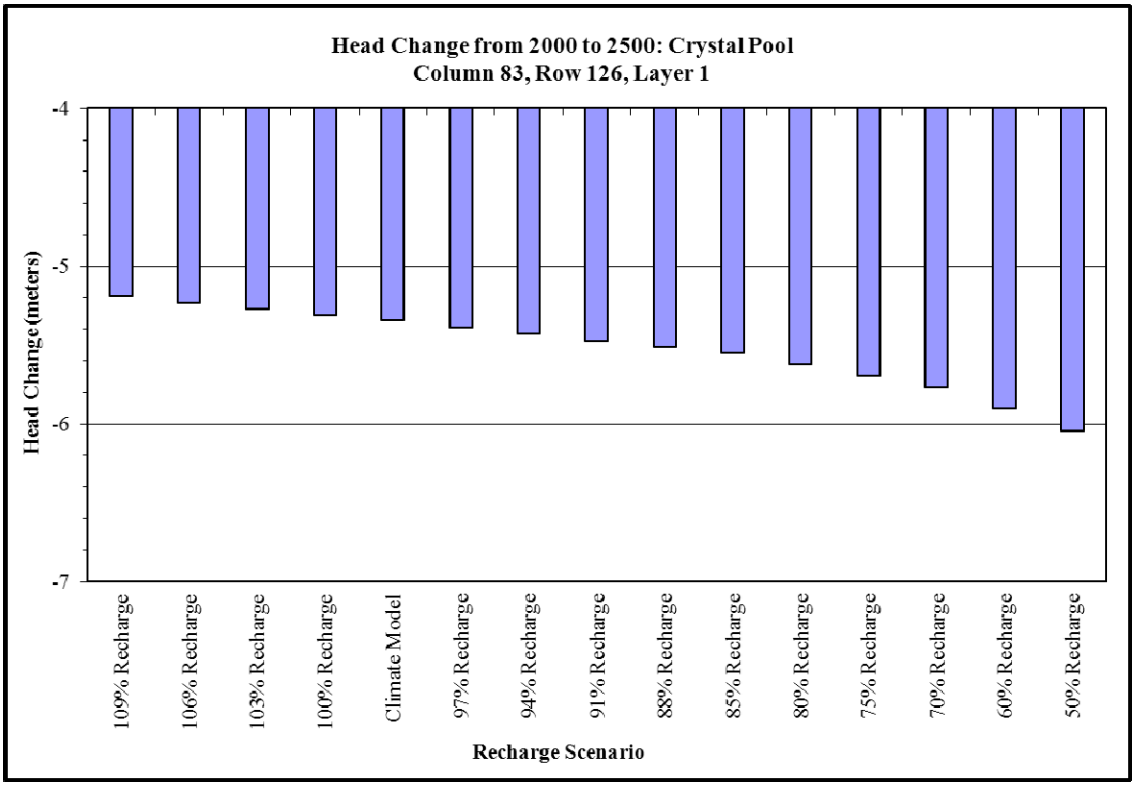

Figure B-37. Quantified Head Change in Column 83, Row 126, Layer 1

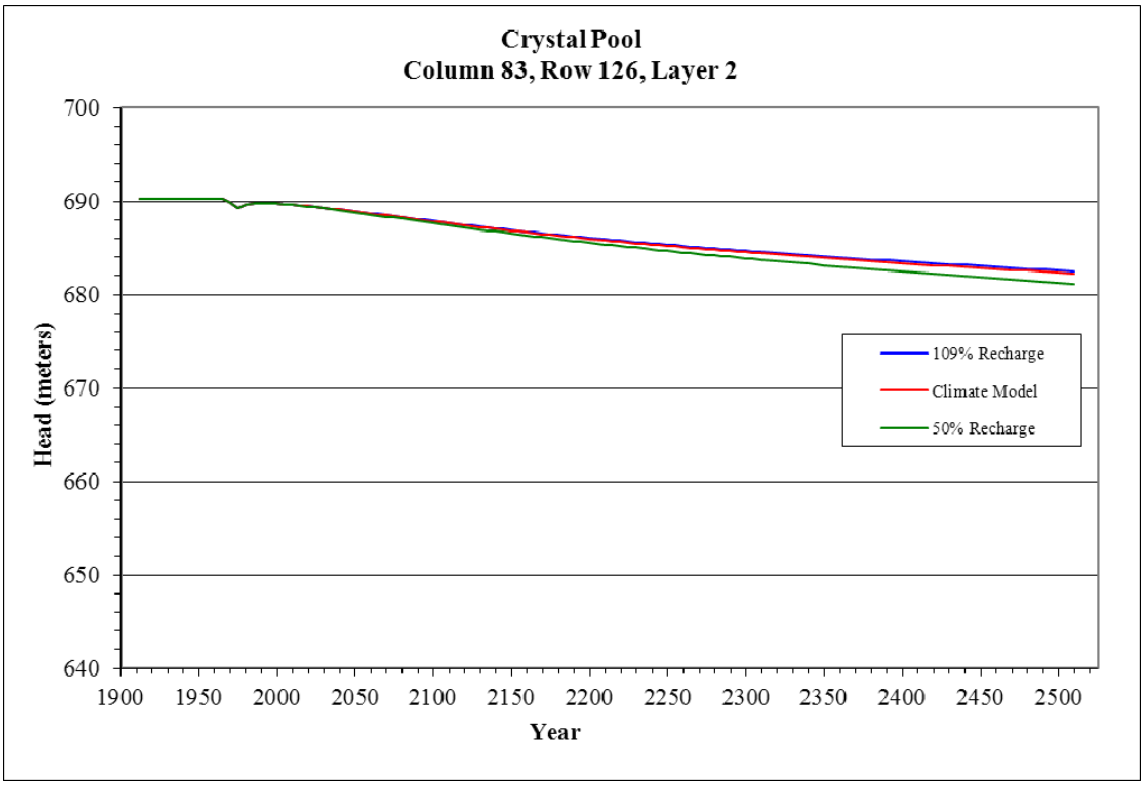

Figure B-38. Head Change in Column 83, Row 126, Layer 2

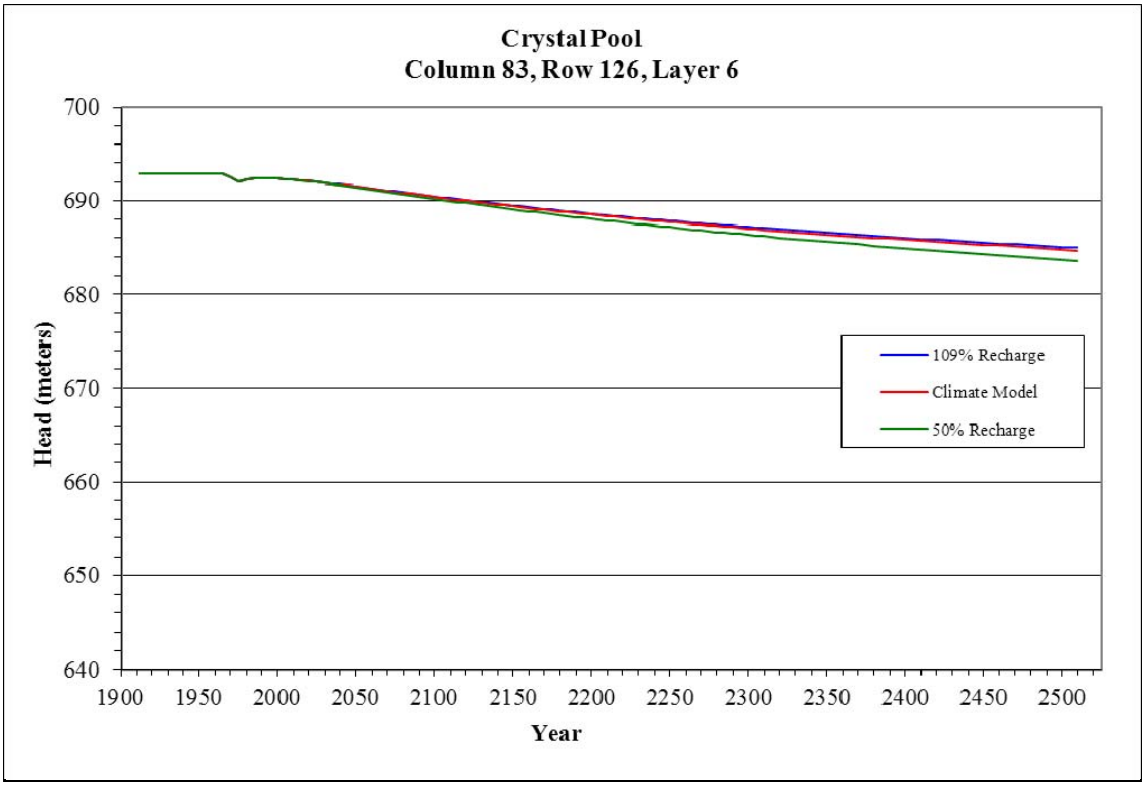

Figure B-39. Head Change in Column 83, Row 126, Layer 6

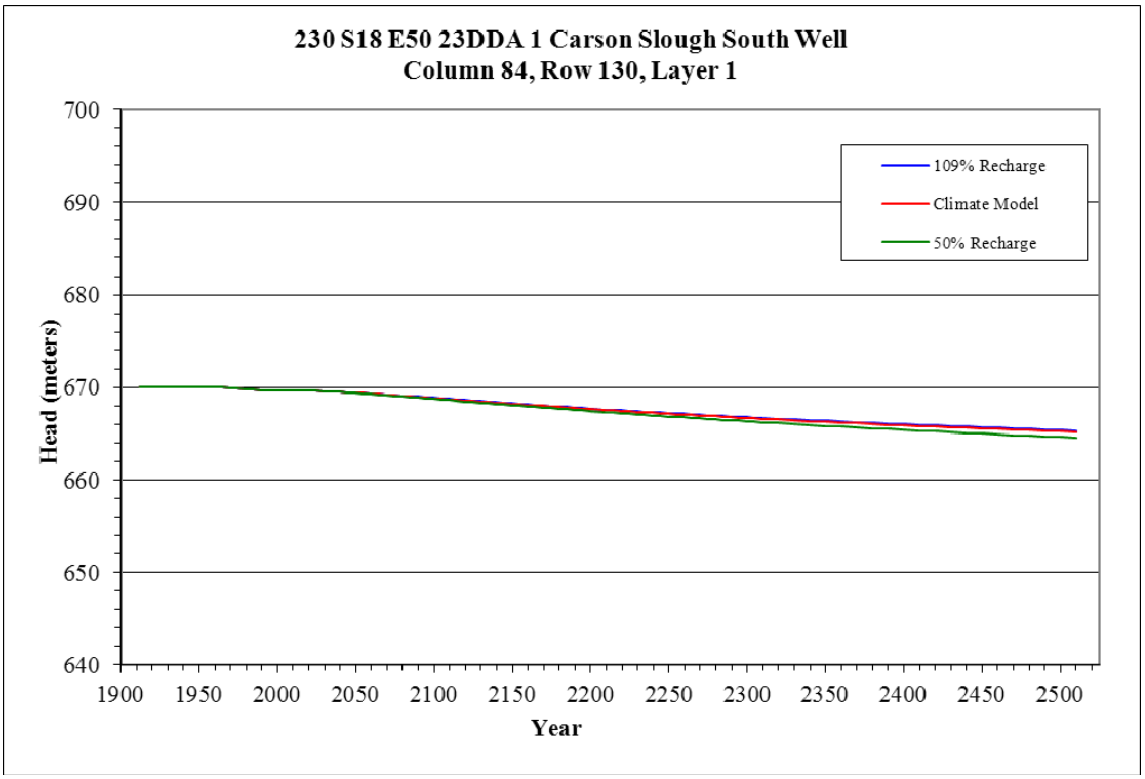

Figure B-40. Head Change in Column 84, Row 130, Layer 1

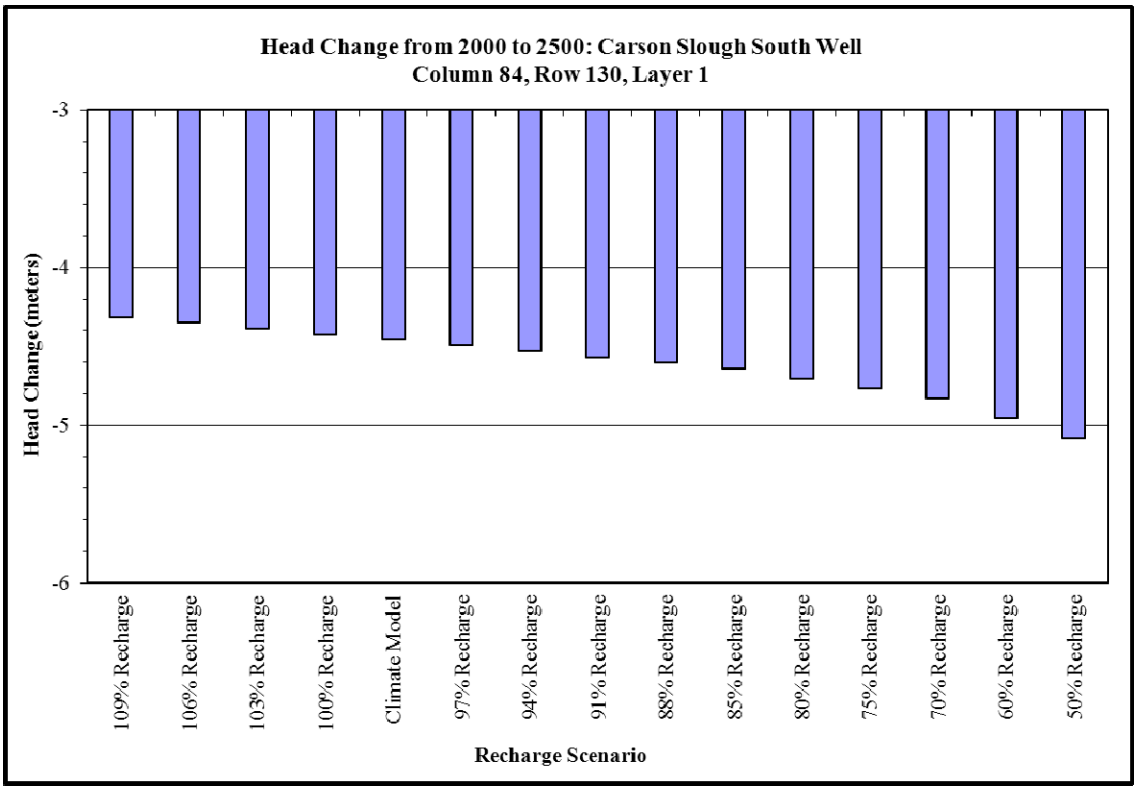

Figure B-41. Quantified Head Change in Column 84, Row 130, Layer 1

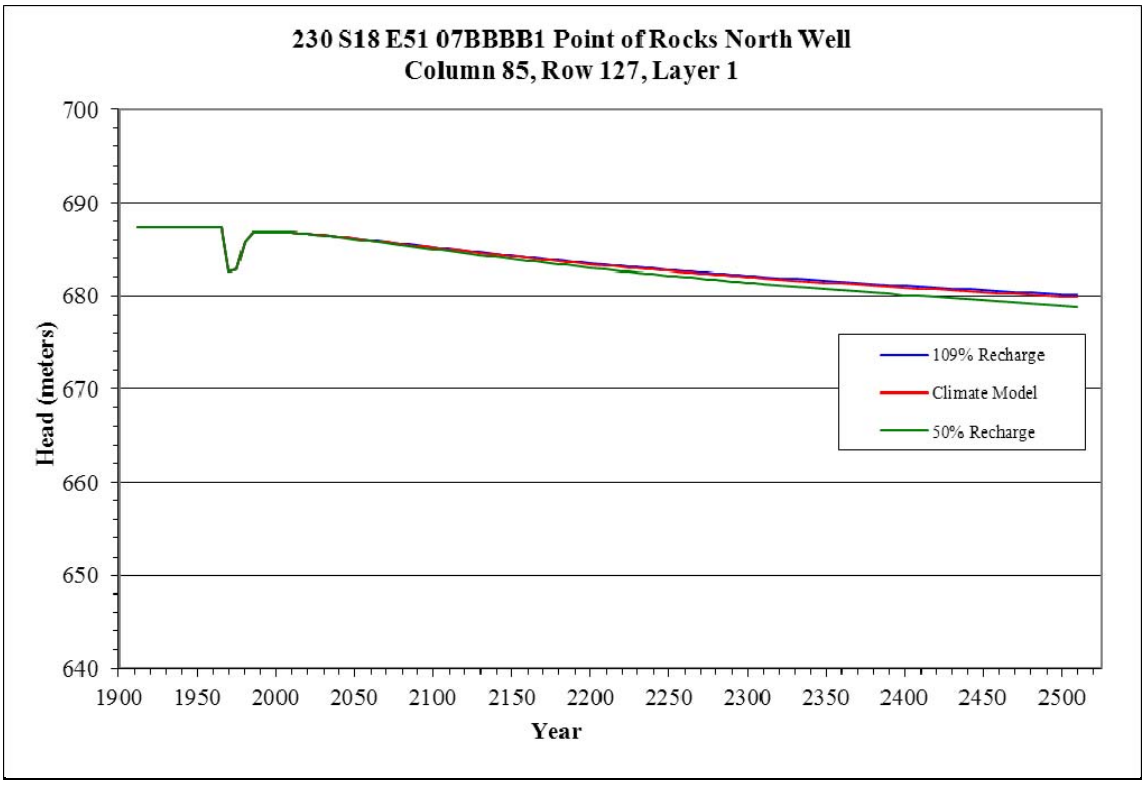

Figure B-42. Head Change in Column 85, Row 127, Layer 1

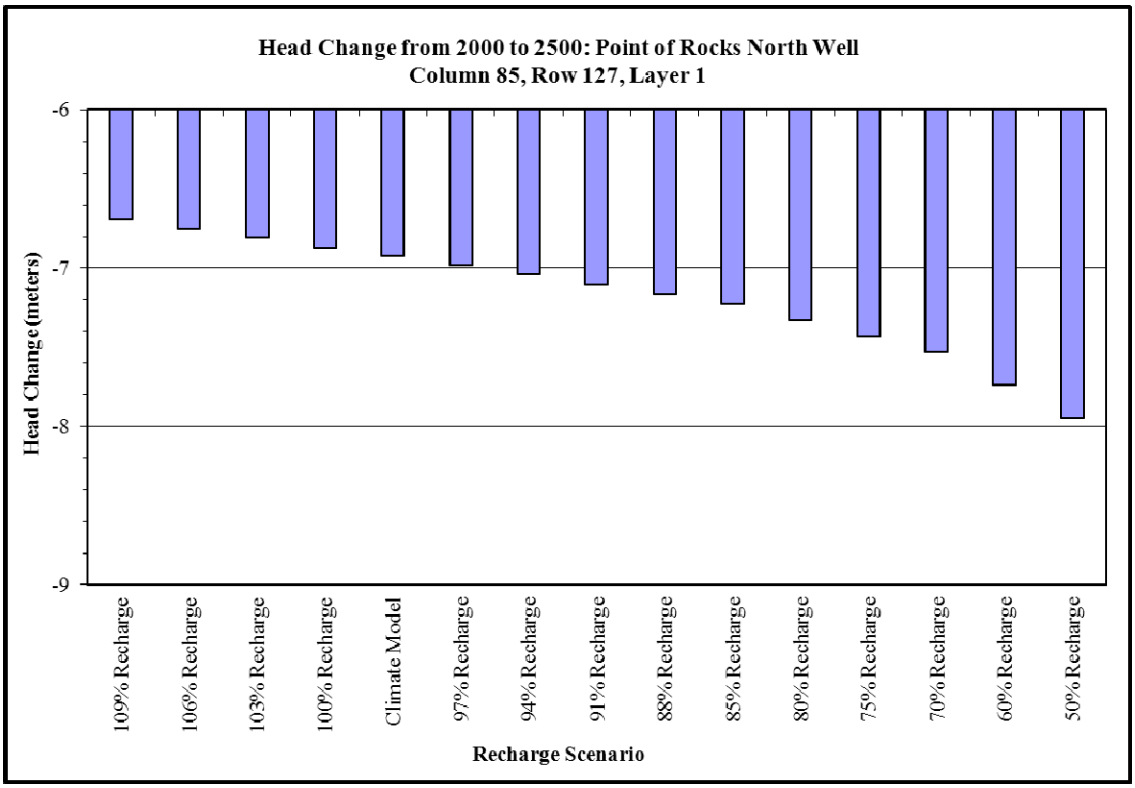

Figure B-43. Quantified Head Change in Column 85, Row 127, Layer 1

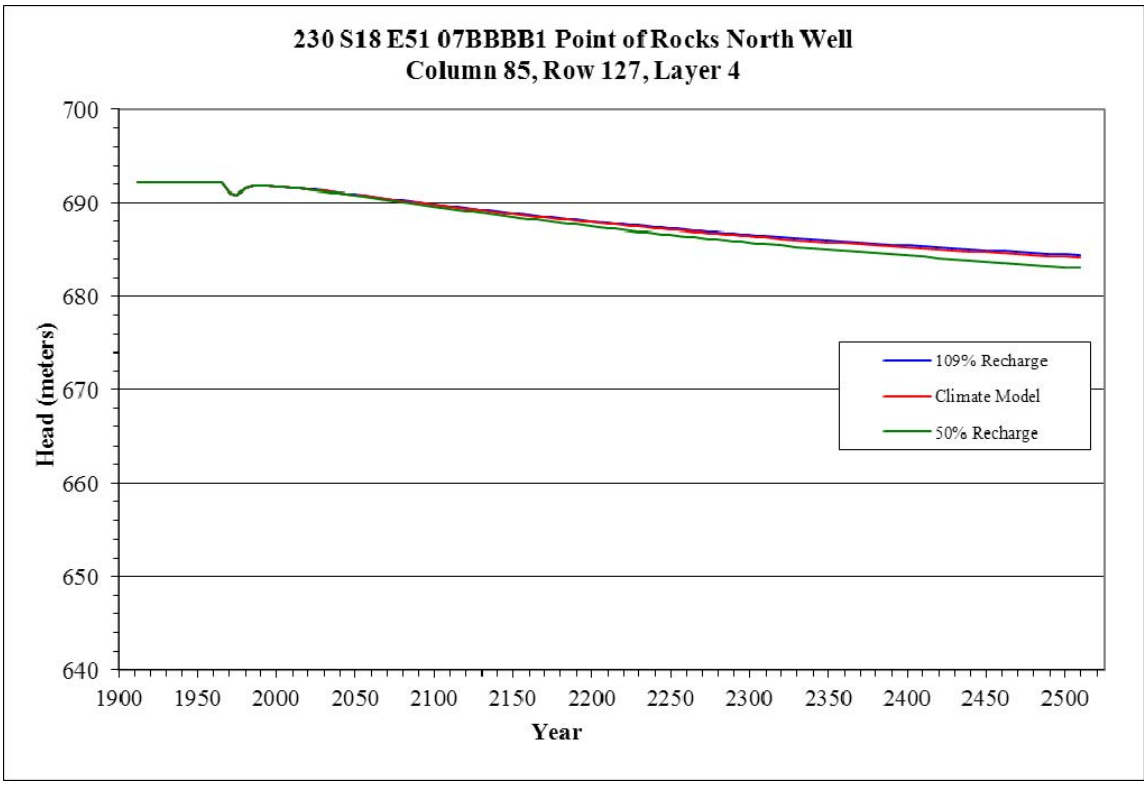

Figure B-44. Head Change in Column 85, Row 127, Layer 4

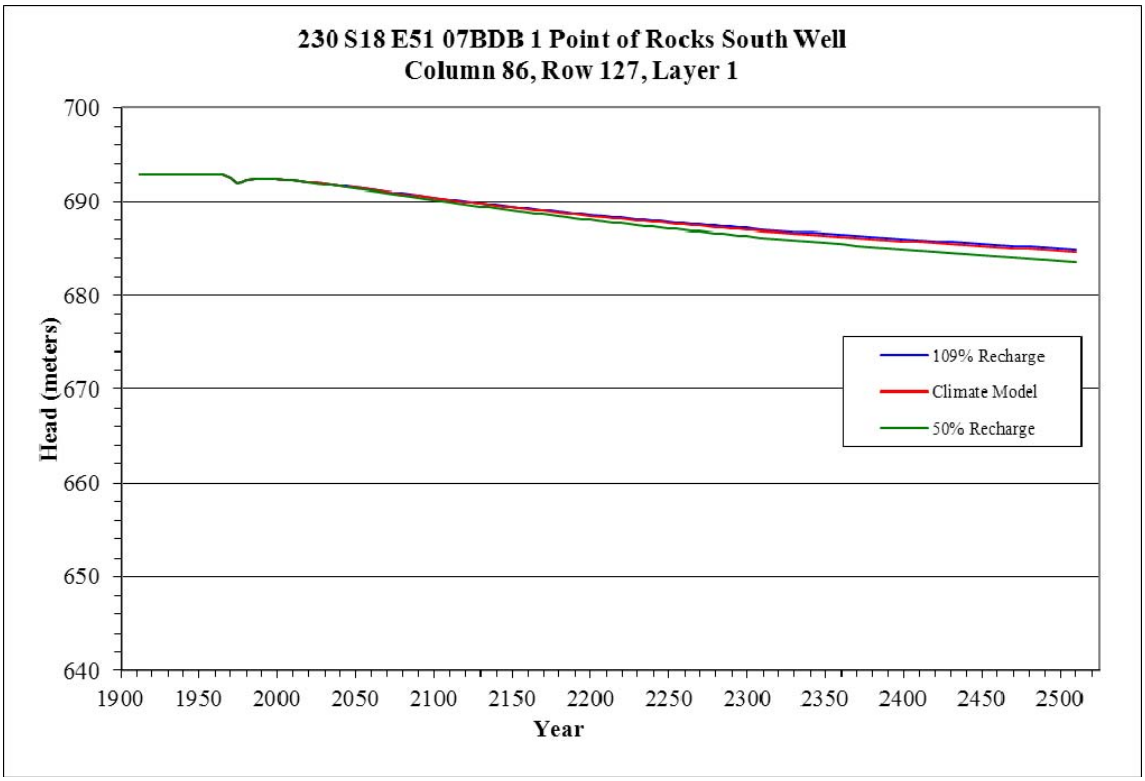

Figure B-45. Head Change in Column 86, Row 127, Layer 1

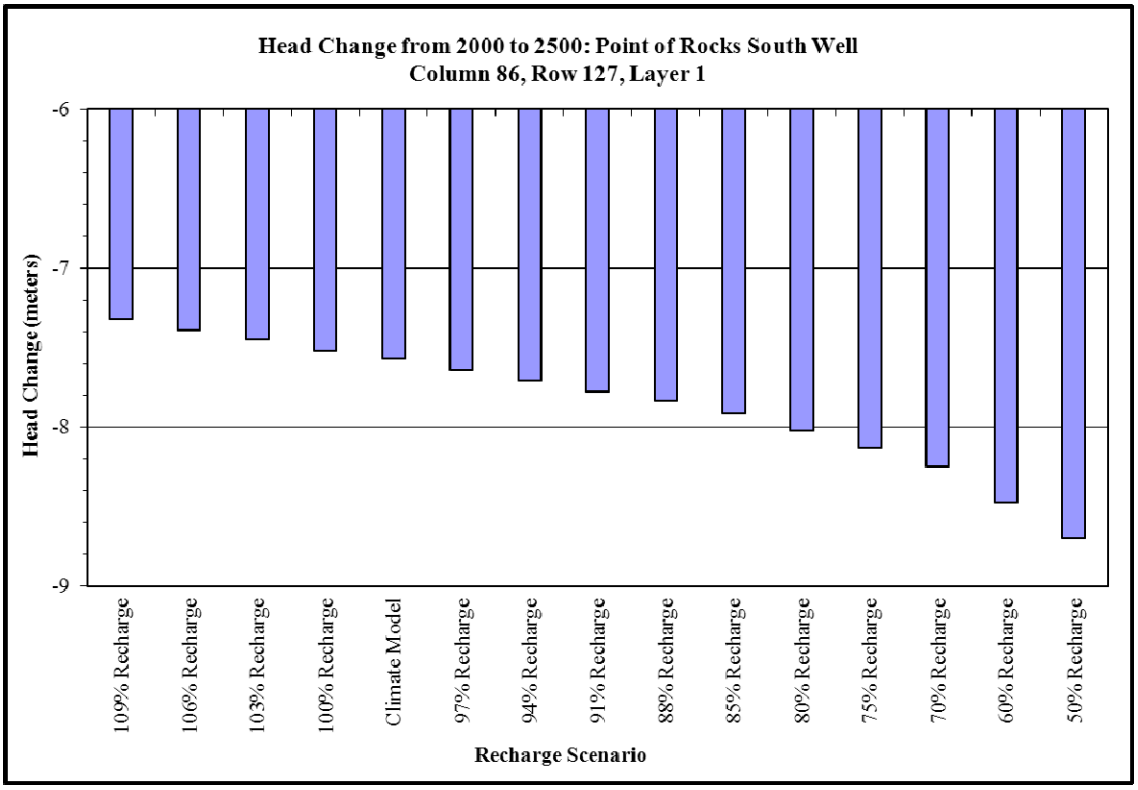

Figure B-46. Quantified Head Change in Column 86, Row 127, Layer 1

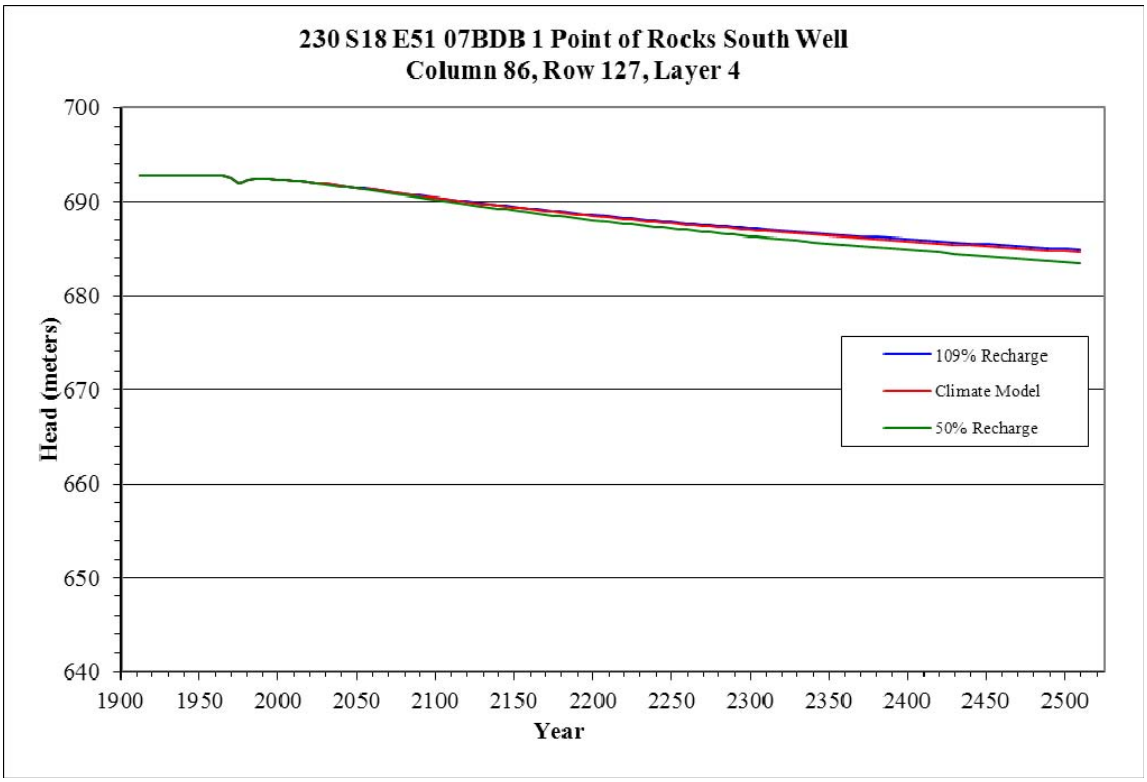

Figure B-47. Head Change in Column 86, Row 127, Layer 4

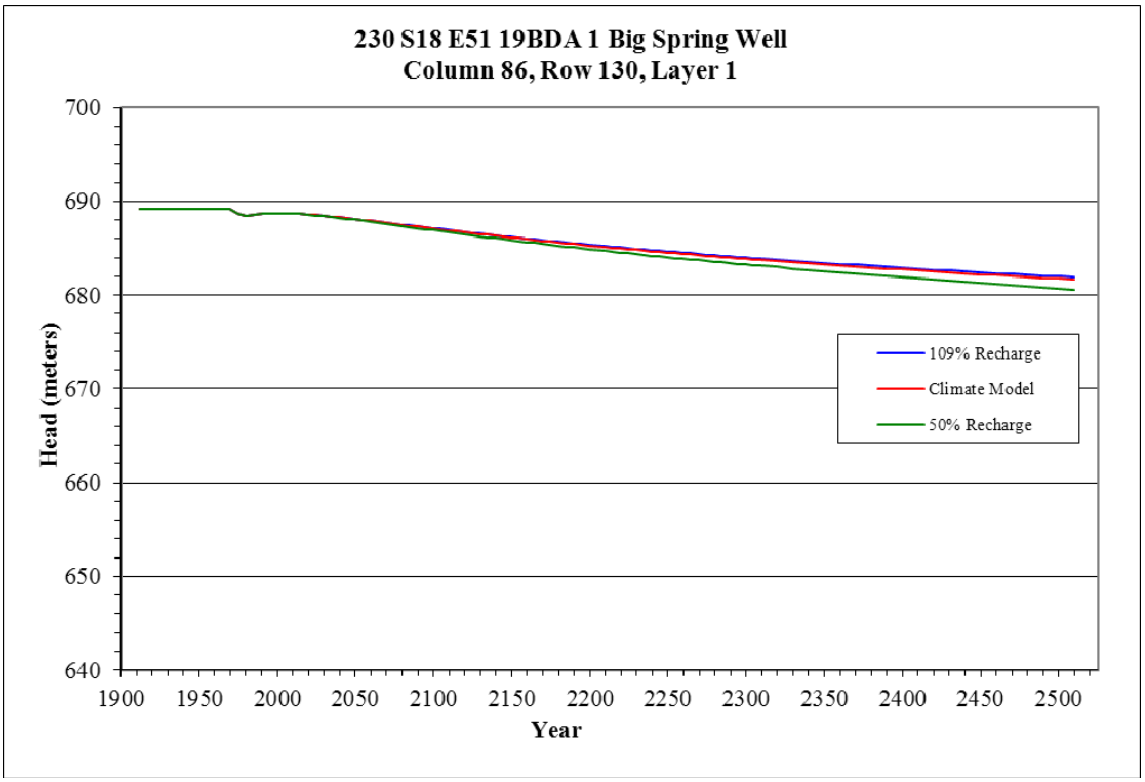

Figure B-48. Head Change in Column 86, Row 130, Layer 1

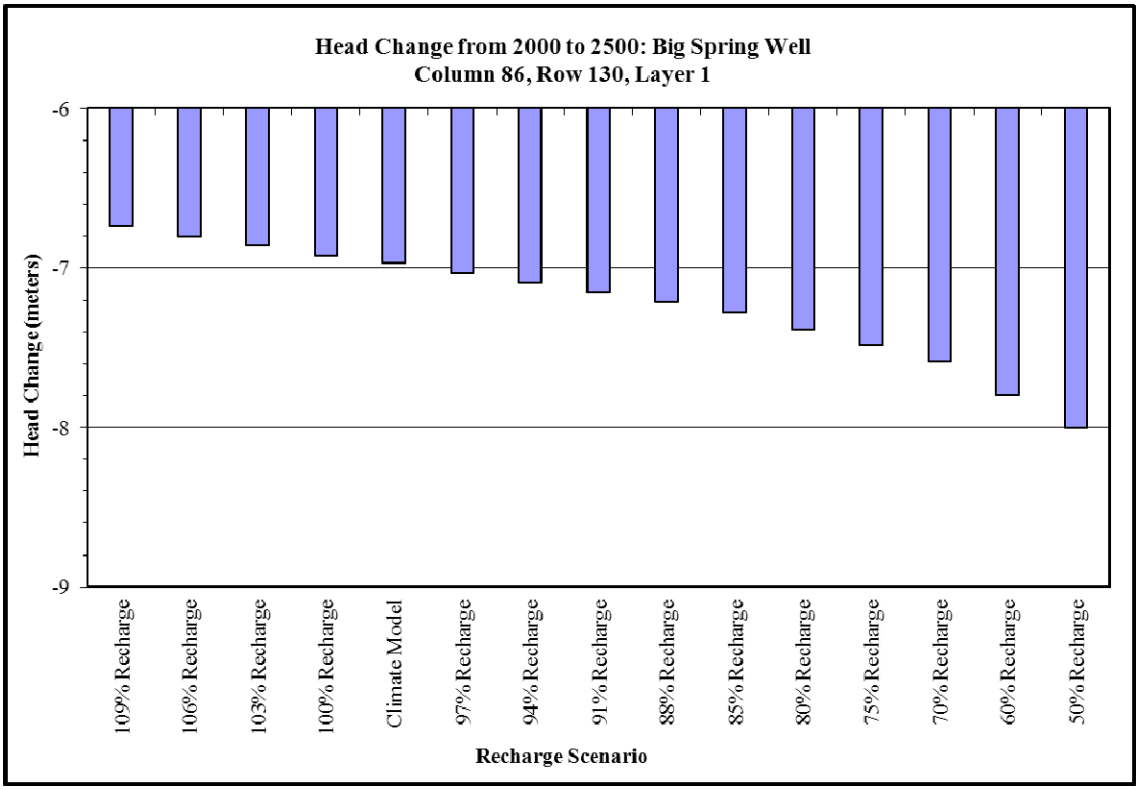

Figure B-49. Quantified Head Change in Column 86, Row 130, Layer 1

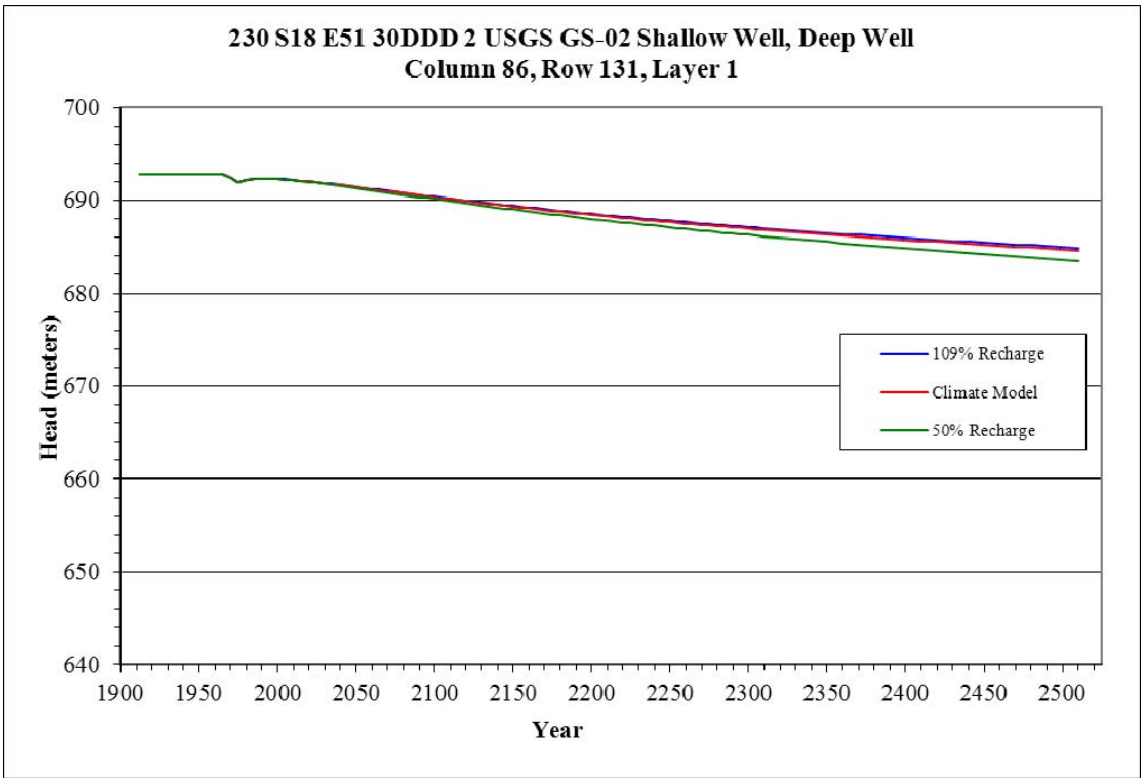

Figure B-50. Head Change in Column 86, Row 131, Layer 1

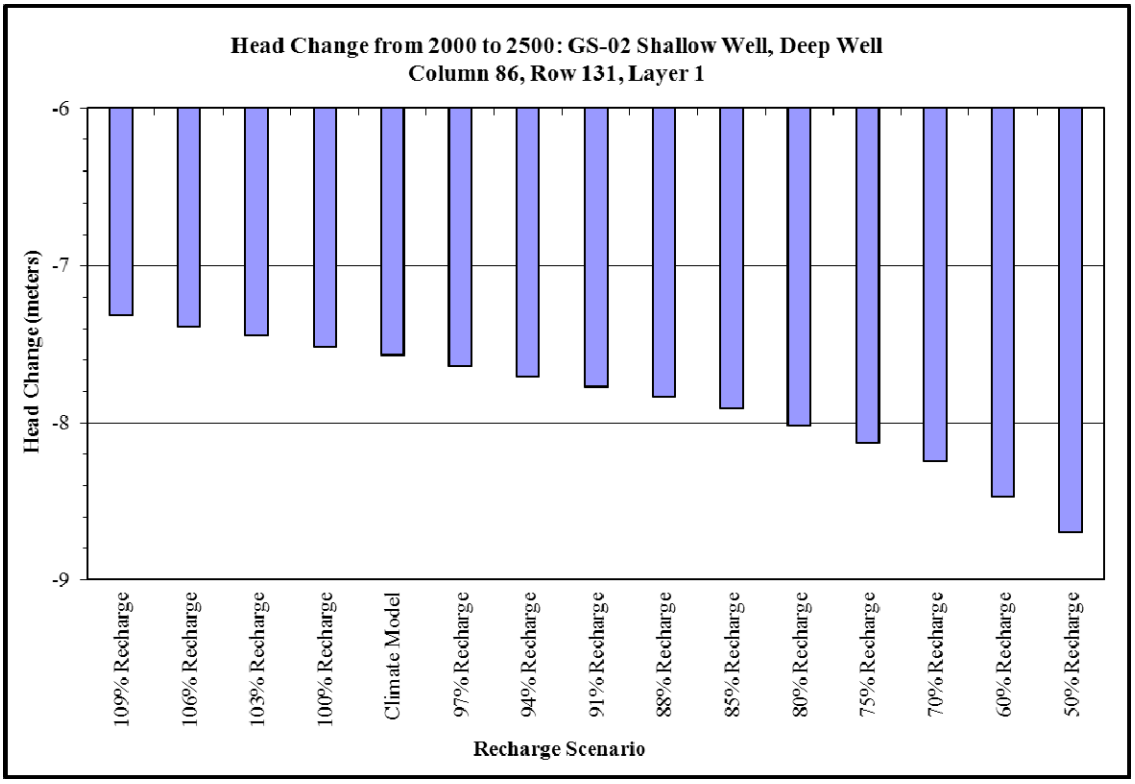

Figure B-51. Quantified Head Change in Column 86, Row 131, Layer 1

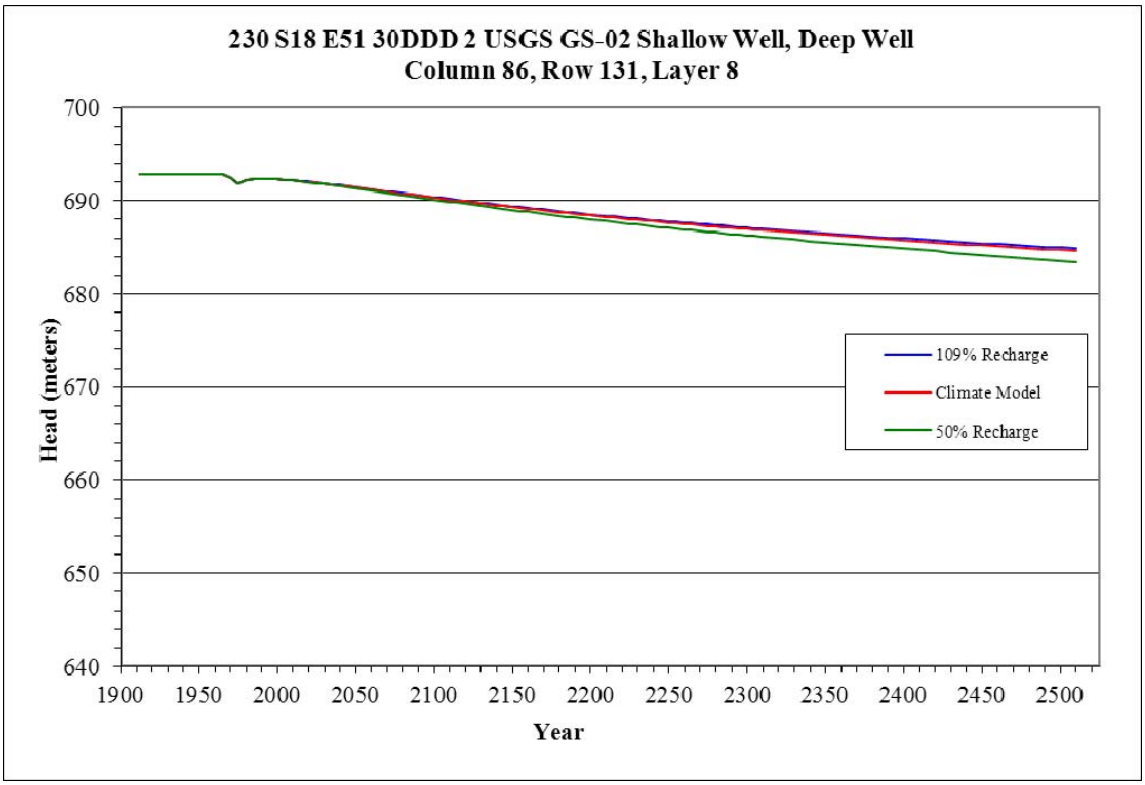

Figure B-52. Head Change in Column 86, Row 131, Layer 8

Amargosa Desert, Excluding Amargosa Farms Pumping Area and Ash Meadows

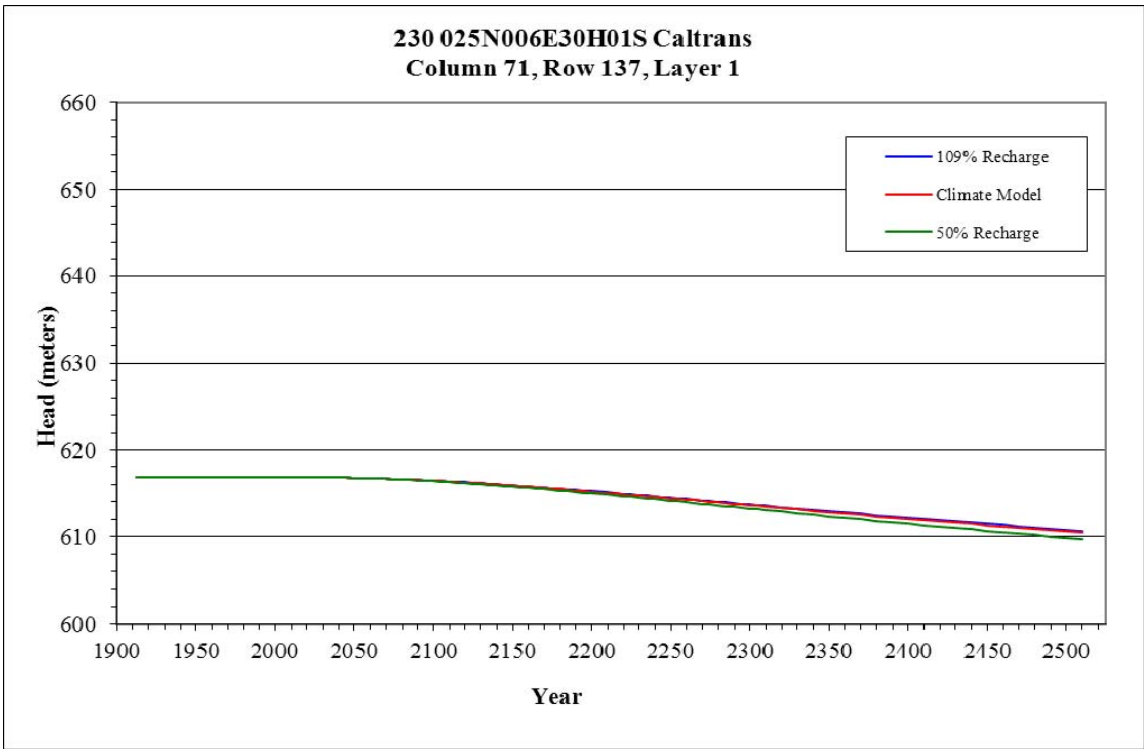

Figure B-53. Head Change in Column 71, Row 137, Layer 1

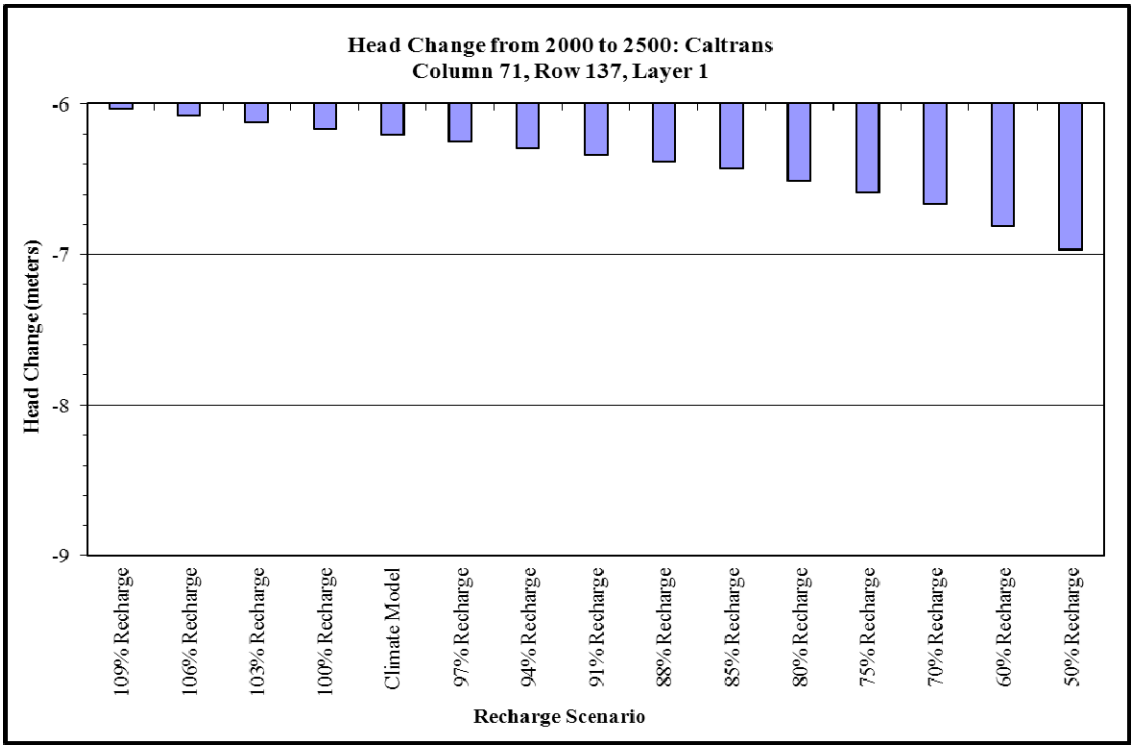

Figure B-54. Quantified Head Change in Column 71, Row 137, Layer 1

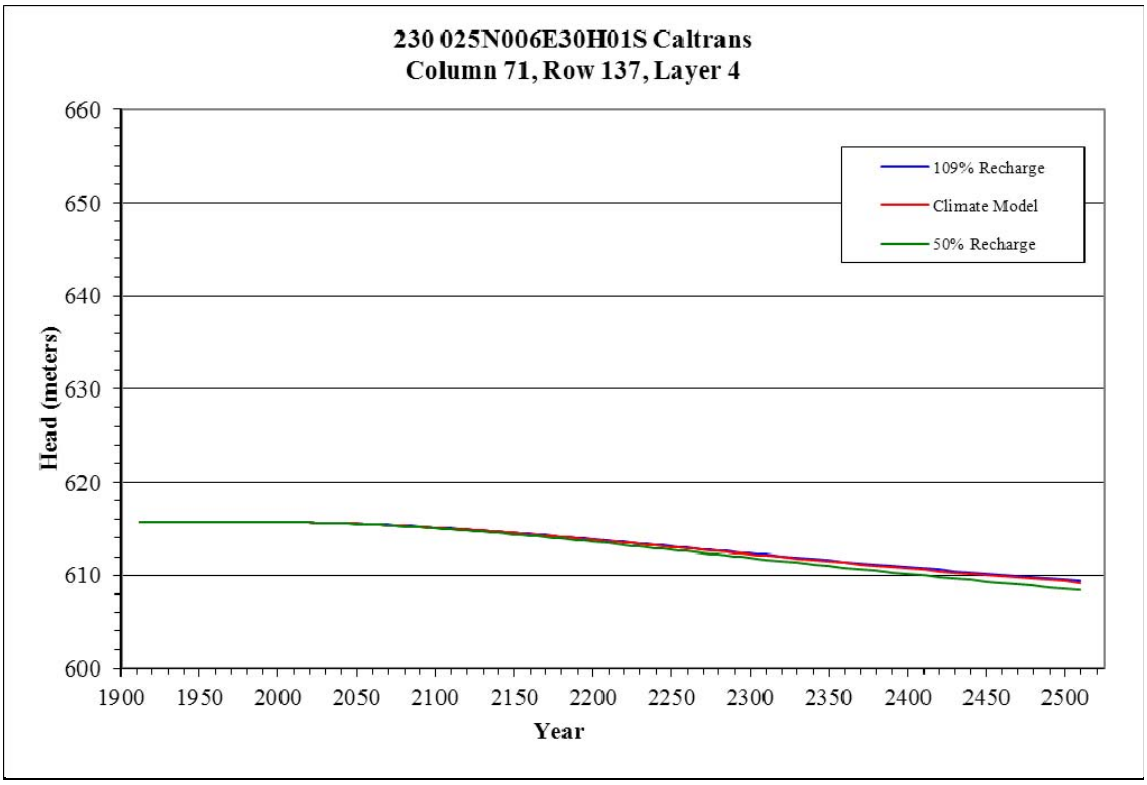

Figure B-55. Head Changes in Column 71, Row 137, Layer 4

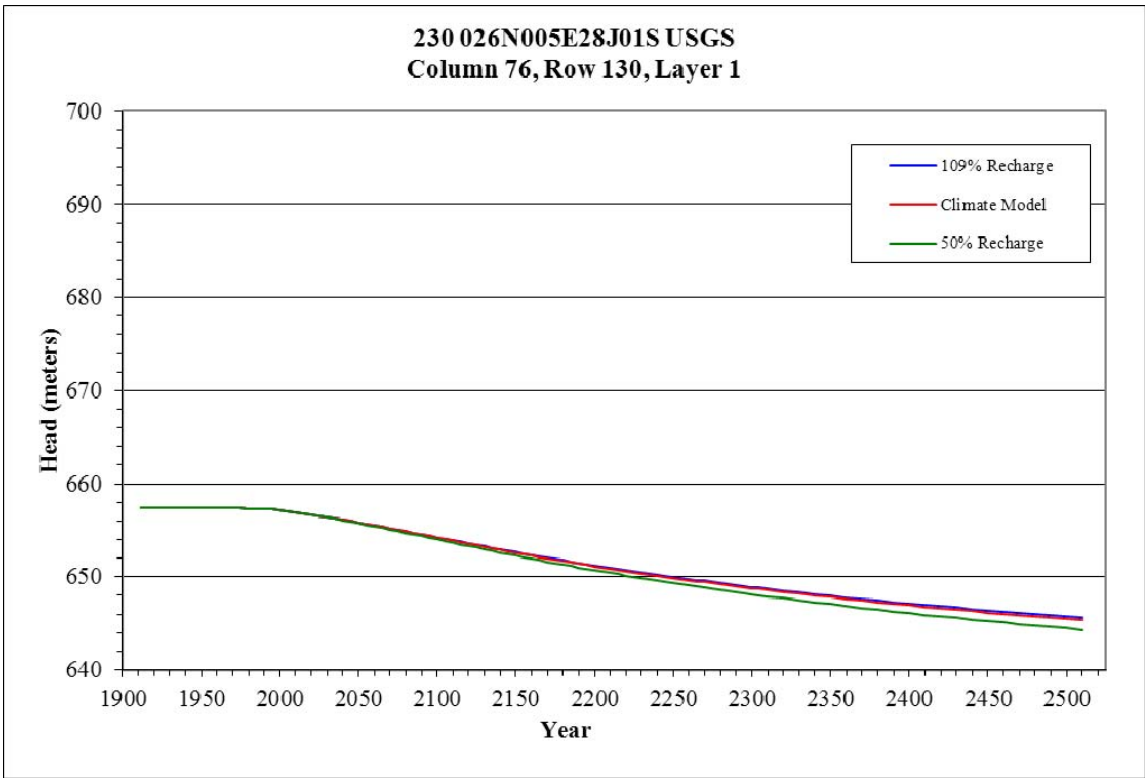

Figure B-56. Head Change in Column 76, Row 130, Layer 1

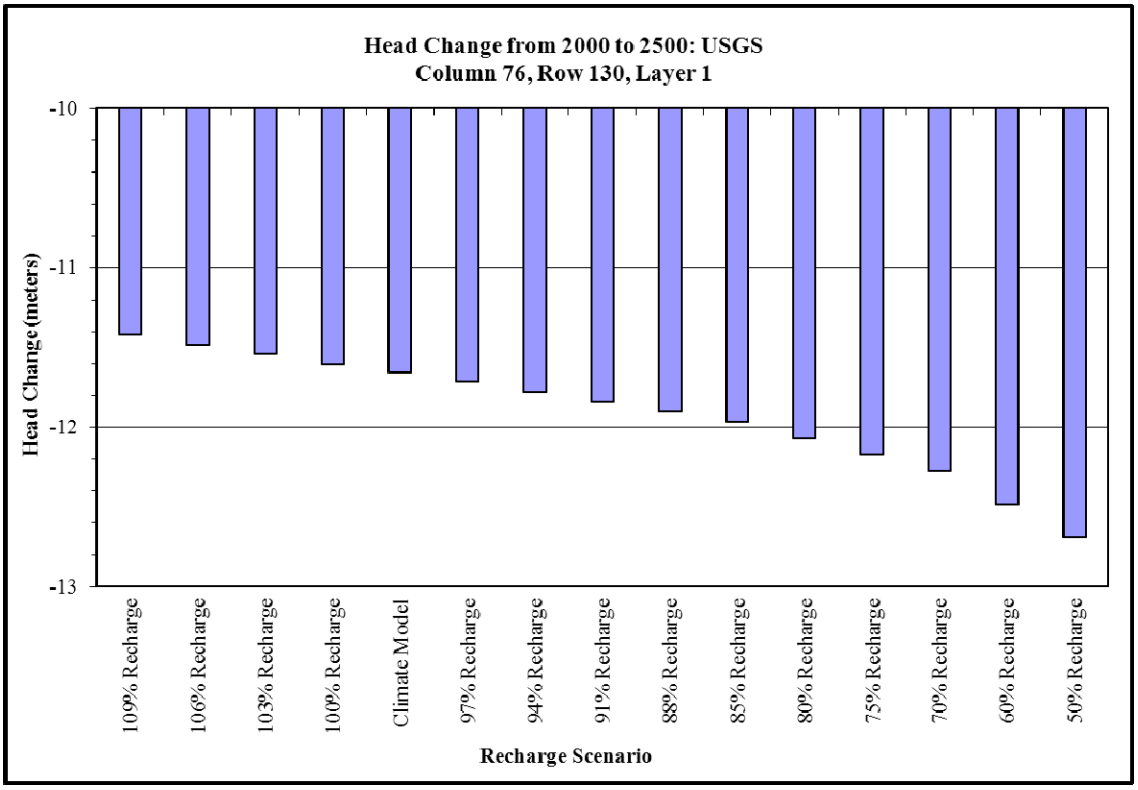

Figure B-57. Quantified Head Change in Column 76, Row 130, Layer 1

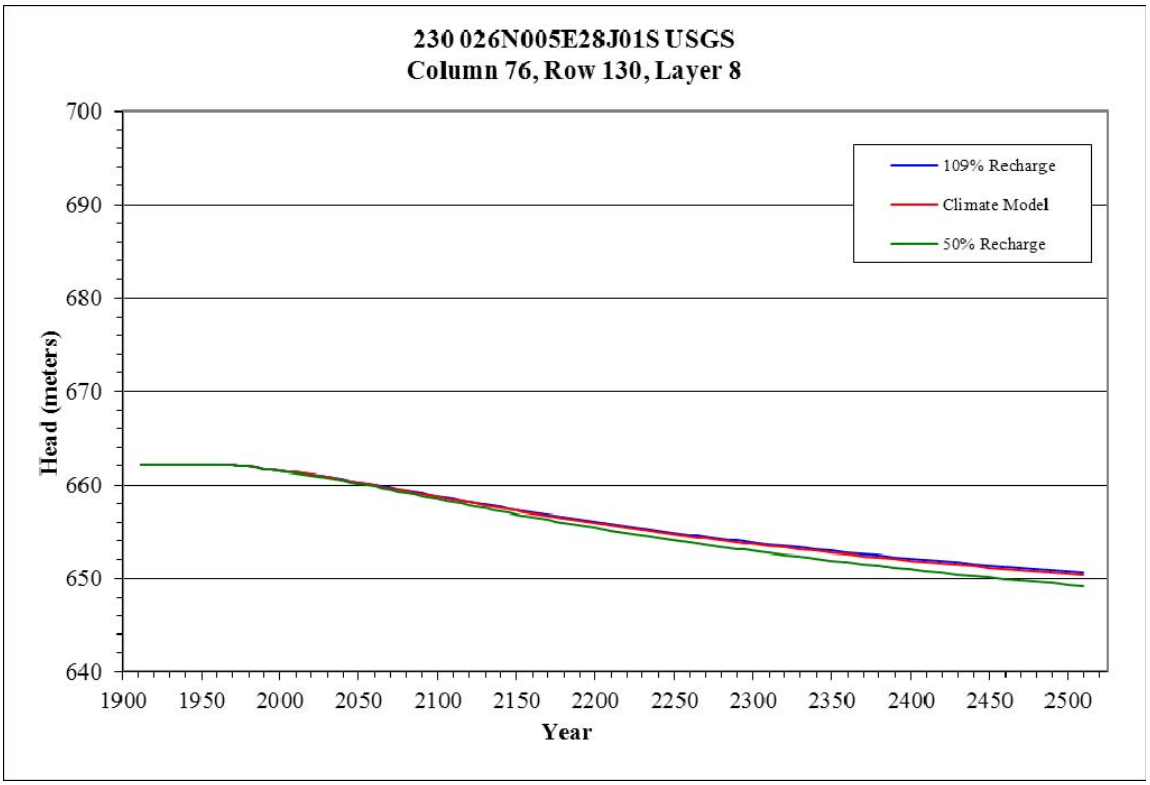

Figure B-58. Head Change in Column 76, Row 130, Layer 8

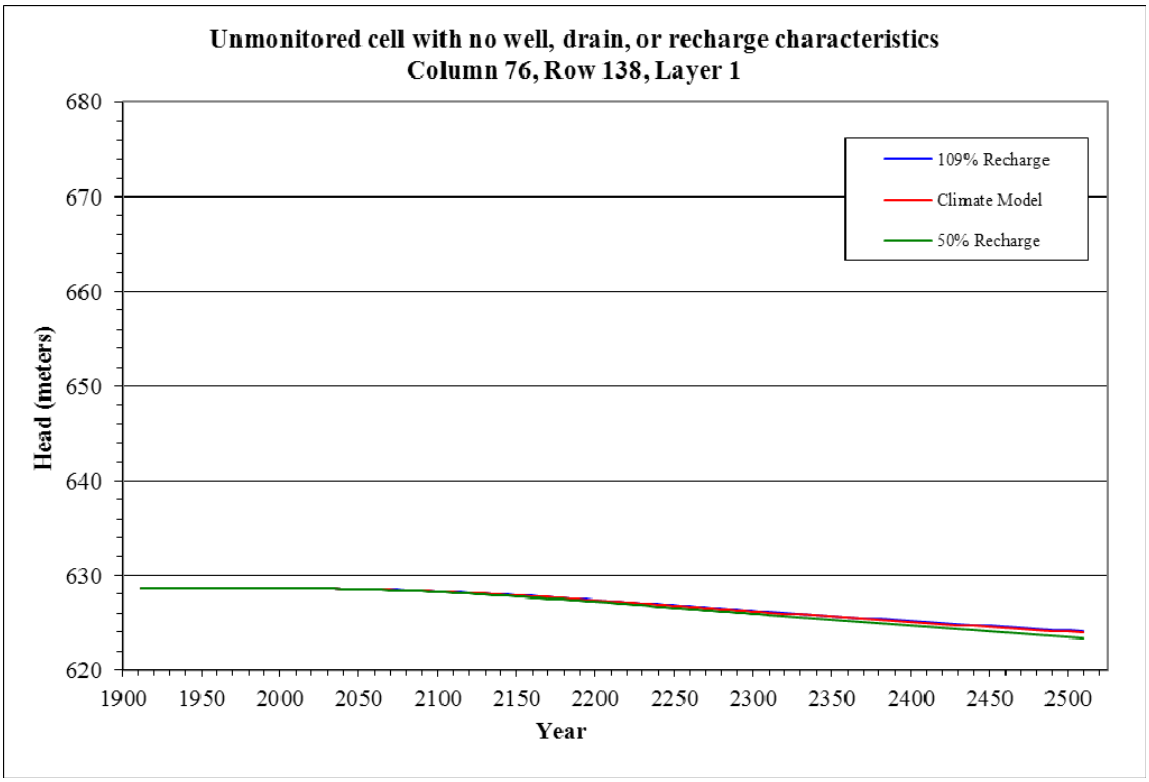

Figure B-59. Head Change in Column 76, Row 138, Layer 1

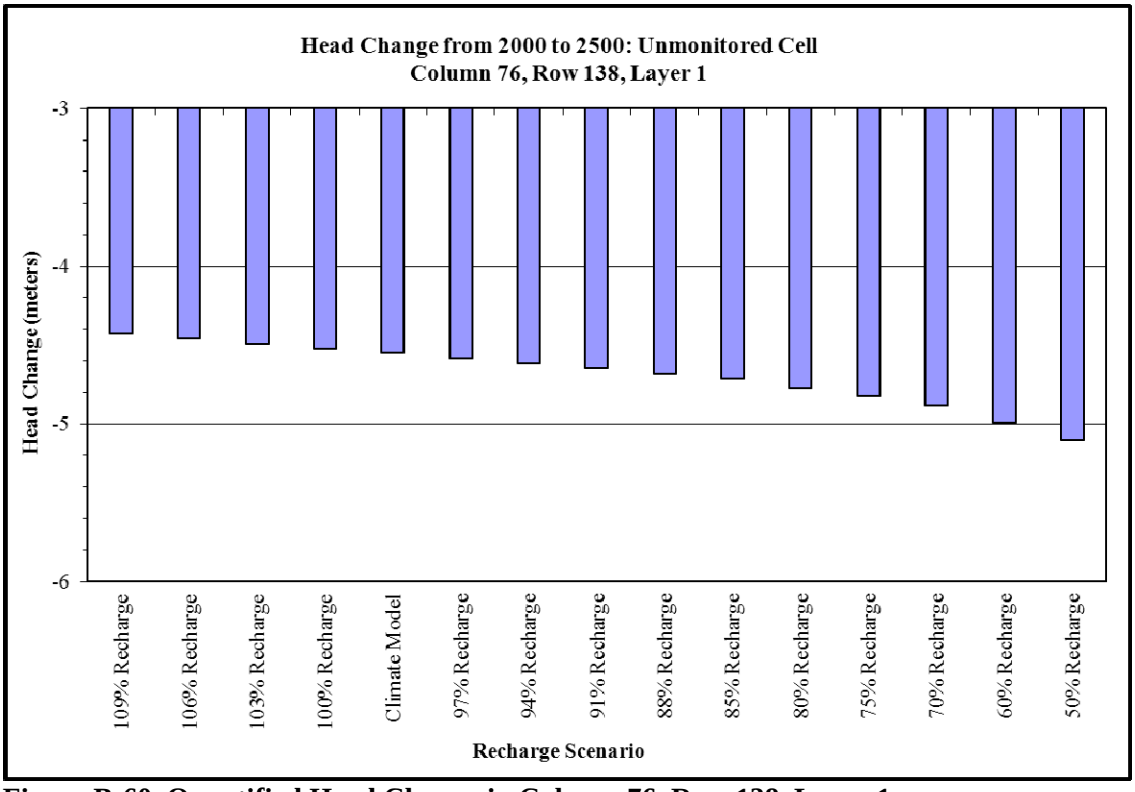

Figure B-60. Quantified Head Change in Column 76, Row 138, Layer 1

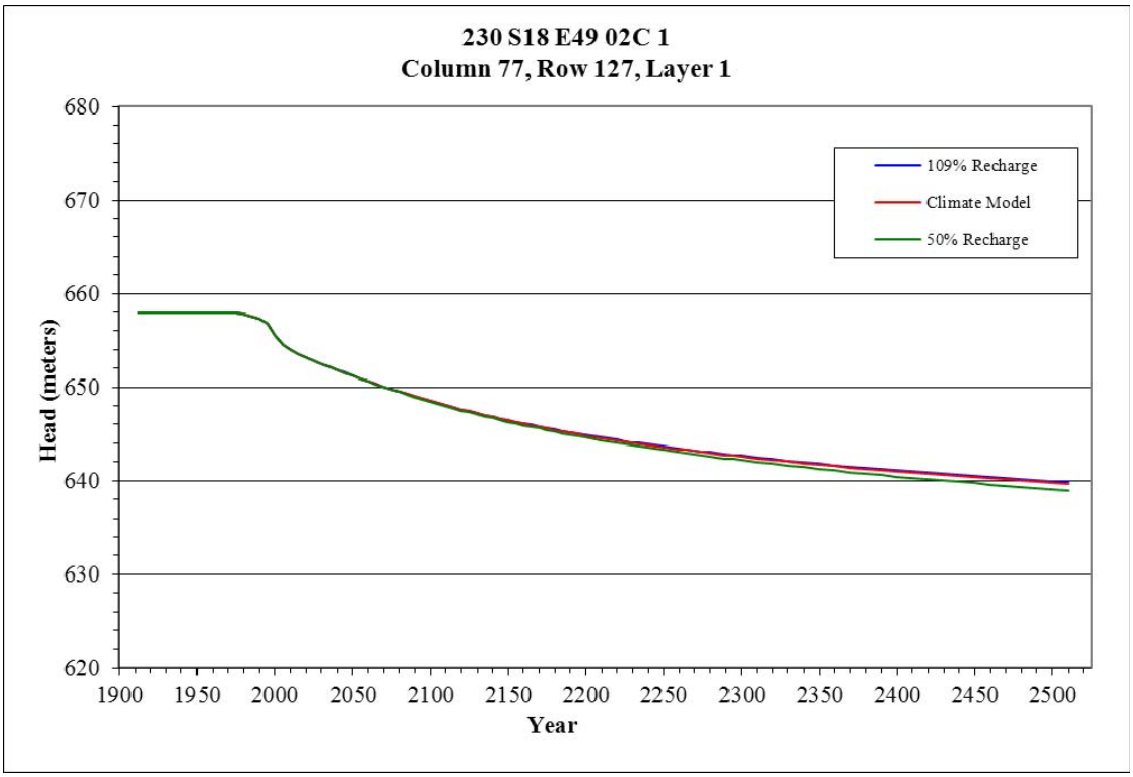

Figure B-61. Head Change in Column 77, Row 127, Layer 1

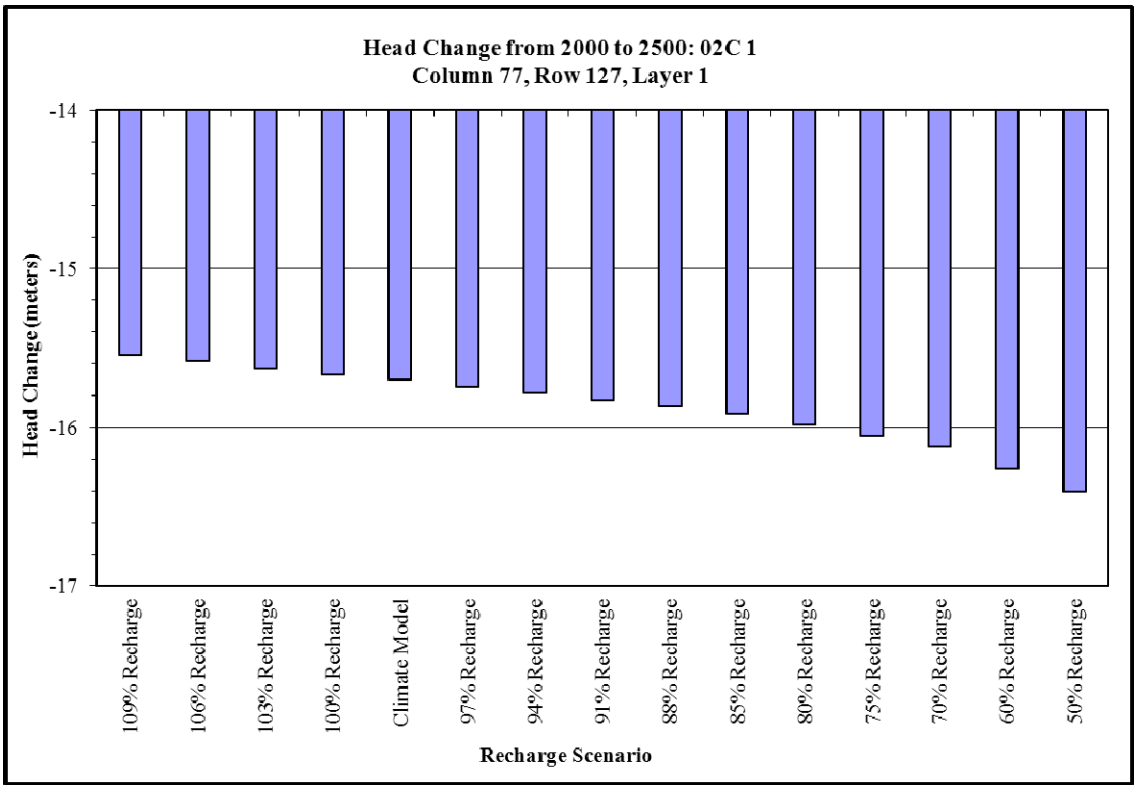

Figure B-62. Quantified Head Change in Column 77, Row 127, Layer 1

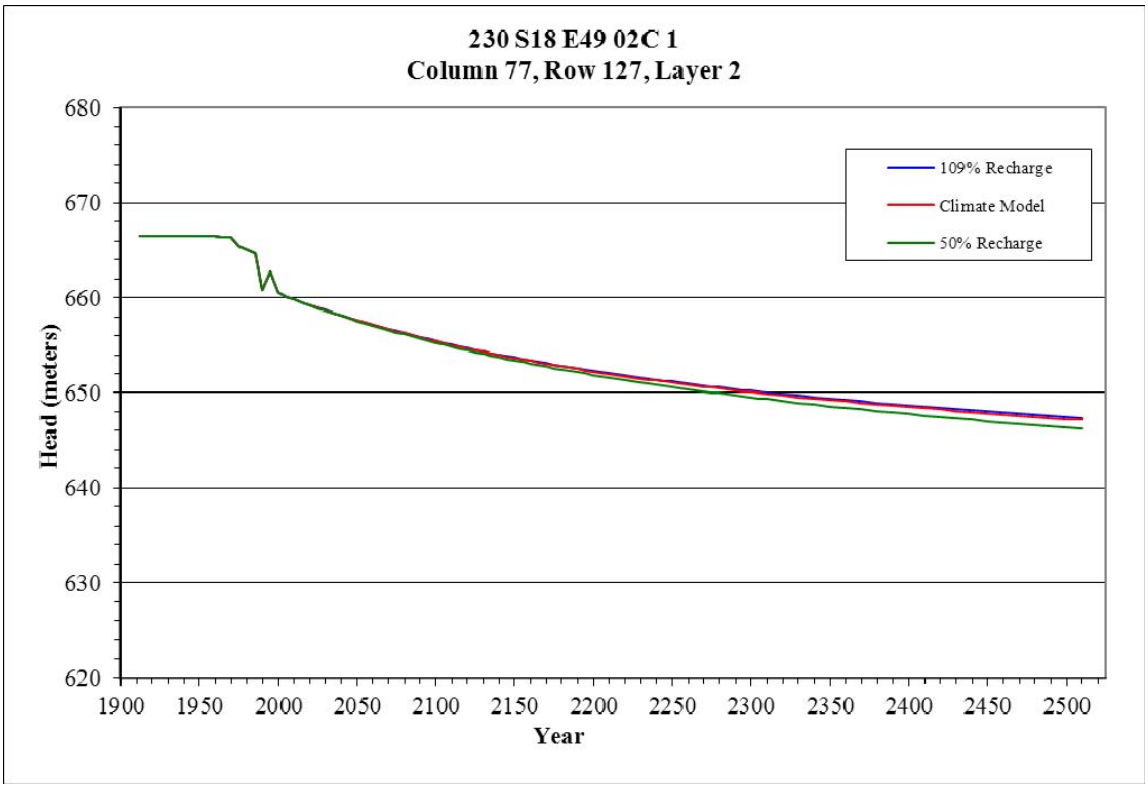

Figure B-63. Head Change in Column 77, Row 127, Layer 2

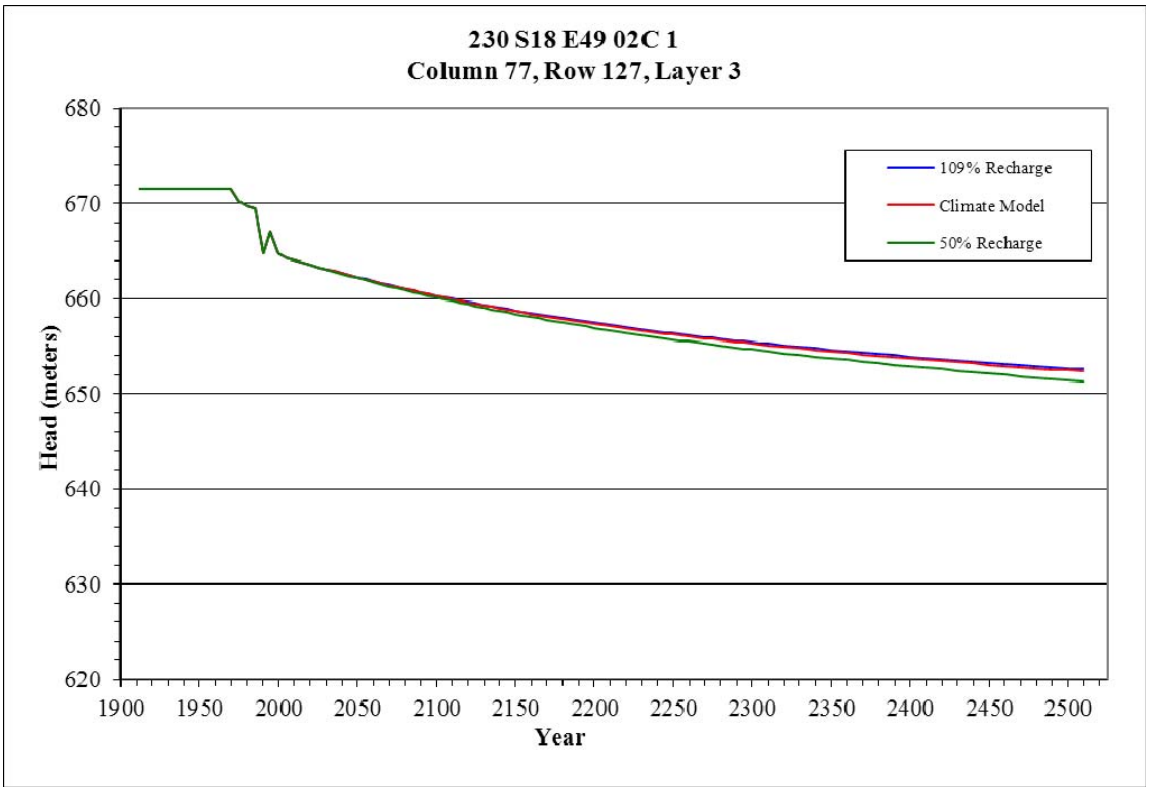

Figure B-64. Head Change in Column 77, Row 127, Layer 3

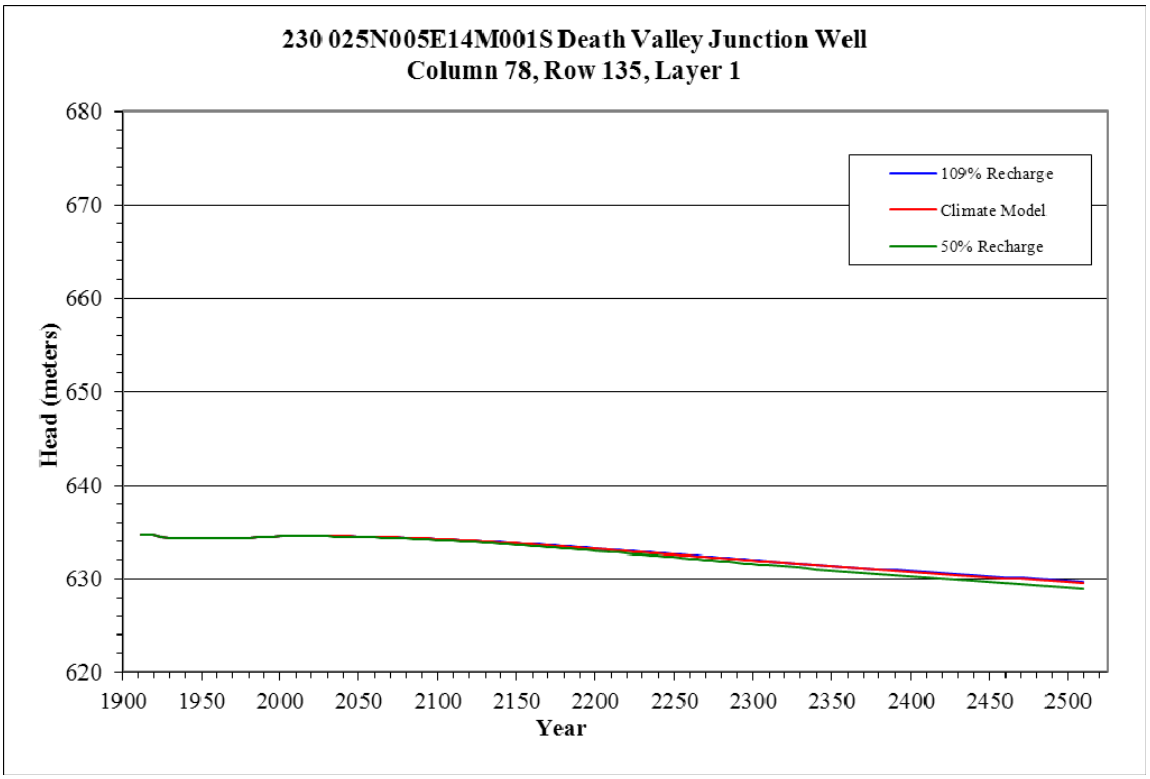

Figure B-65. Head Change in Column 78, Row 135, Layer 1

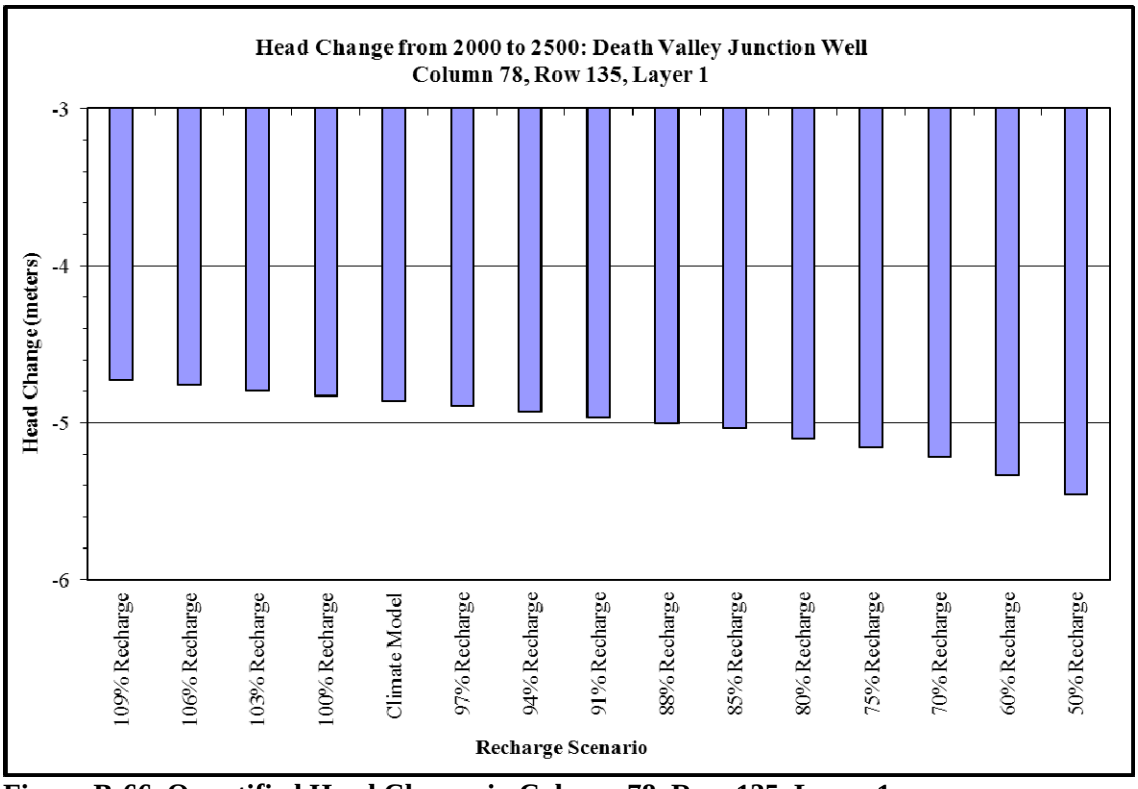

Figure B-66. Quantified Head Change in Column 78, Row 135, Layer 1

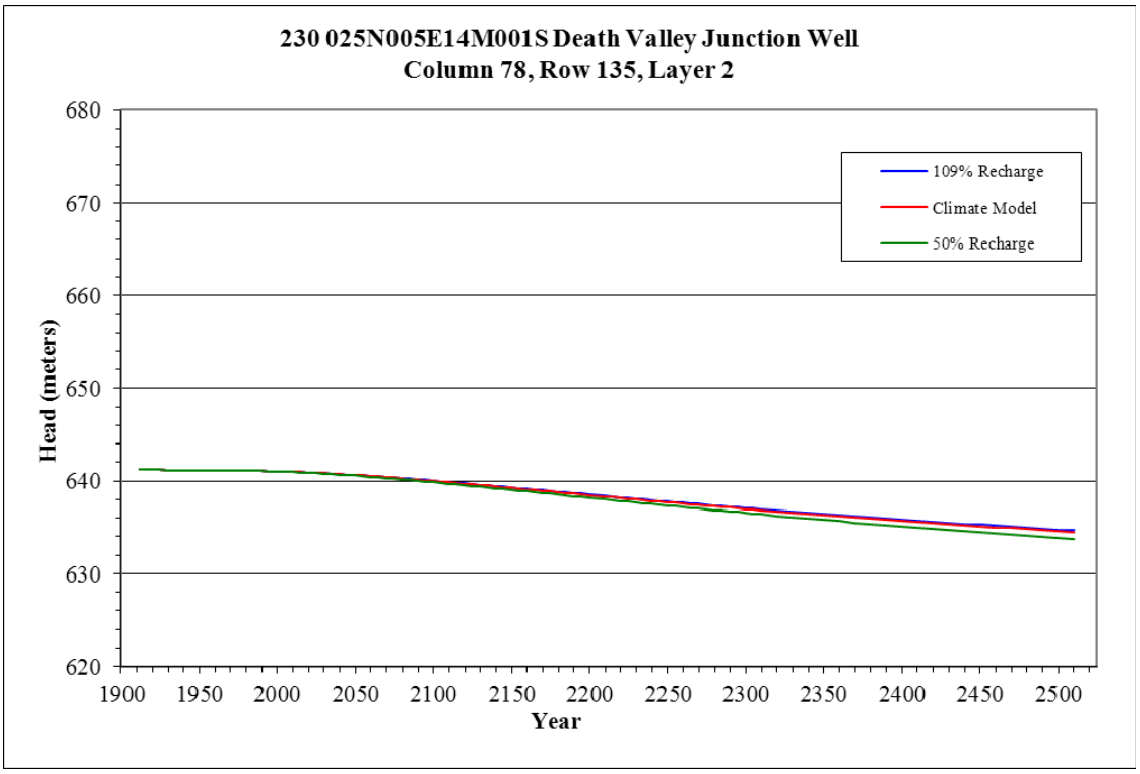

Figure B-67. Head Change in Column 78, Row 135, Layer 2

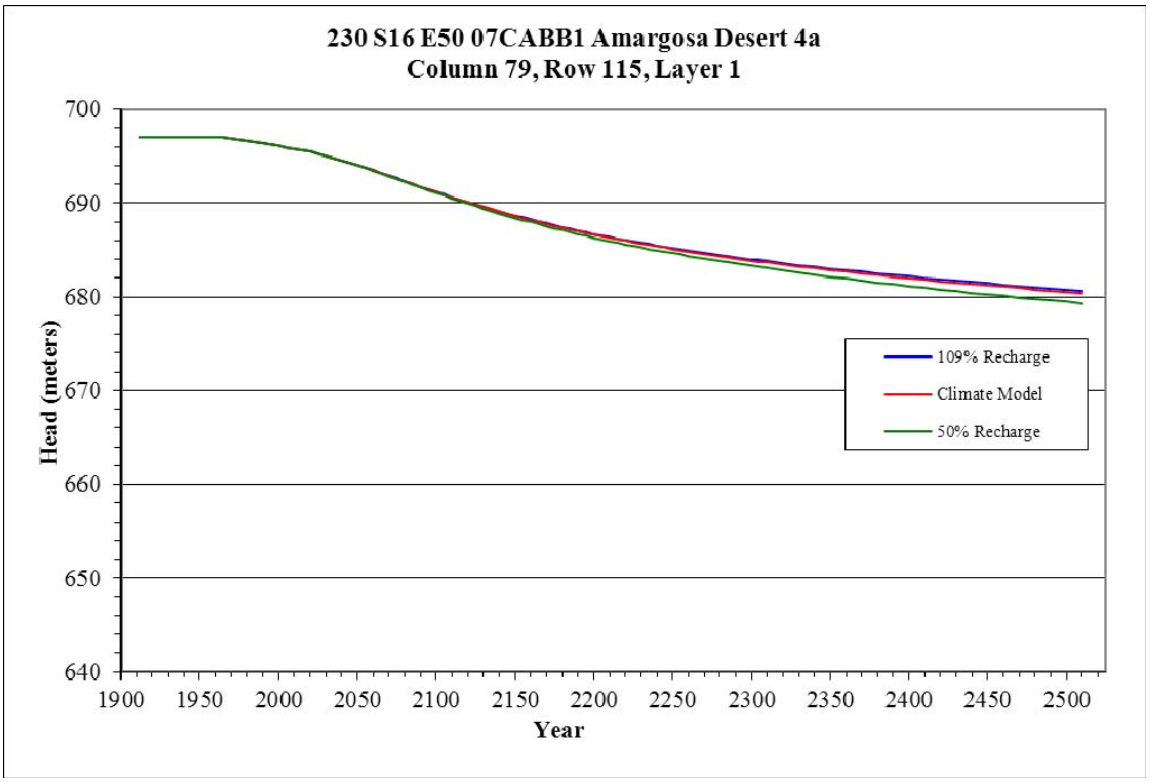

Figure B-68. Head Change in Column 79, Row 115, Layer 1

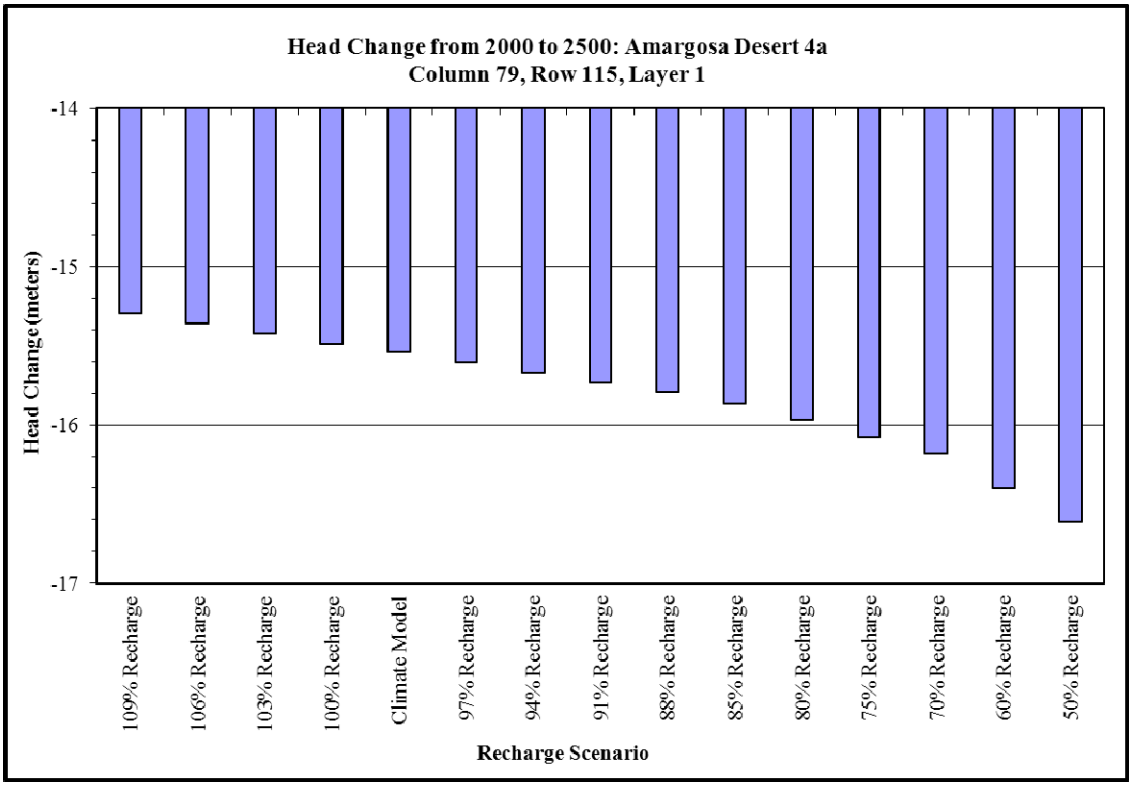

Figure B-69. Quantified Head Change in Column 79, Row 115, Layer 1

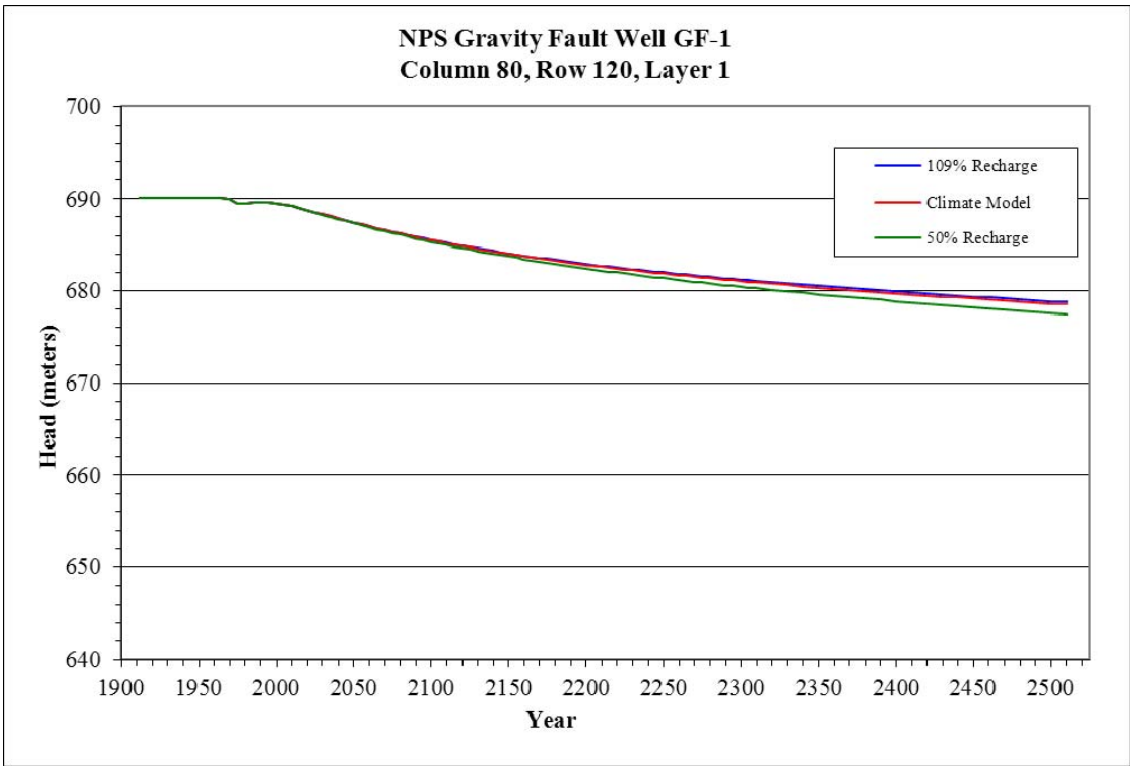

Figure B-70. Head Changes in Column 80, Row 120, Layer 1

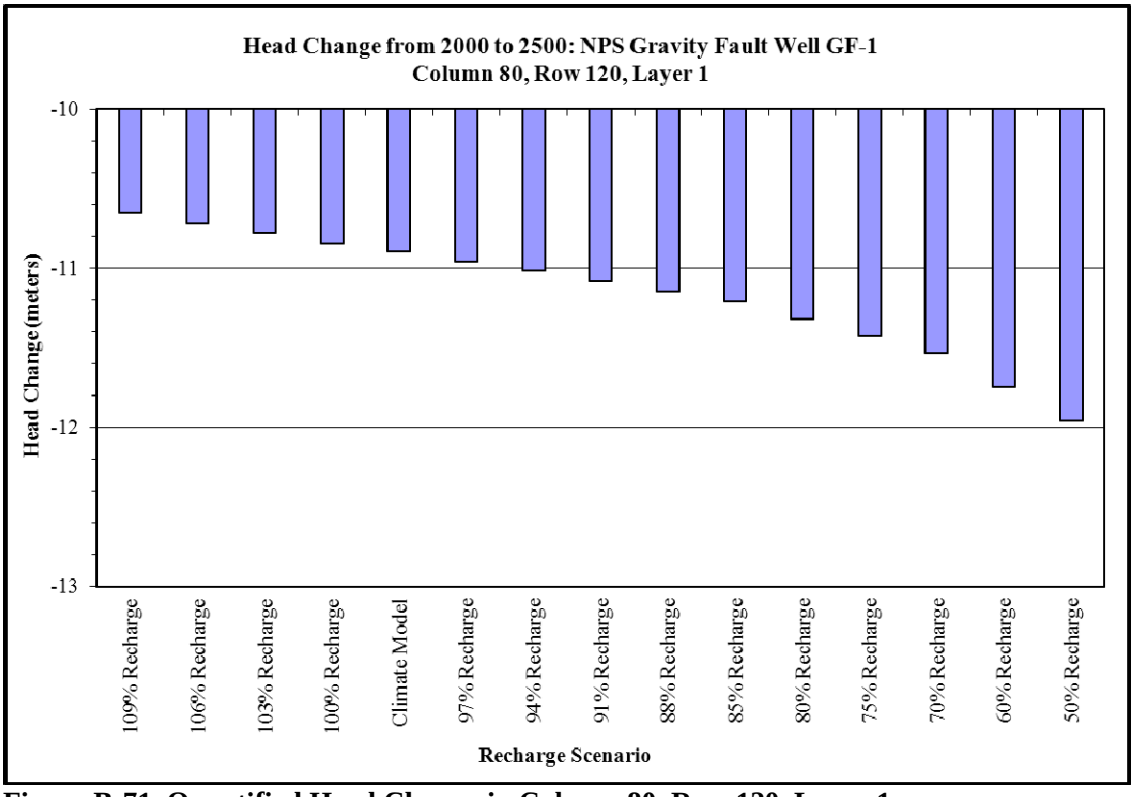

Figure B-71. Quantified Head Change in Column 80, Row 120, Layer 1

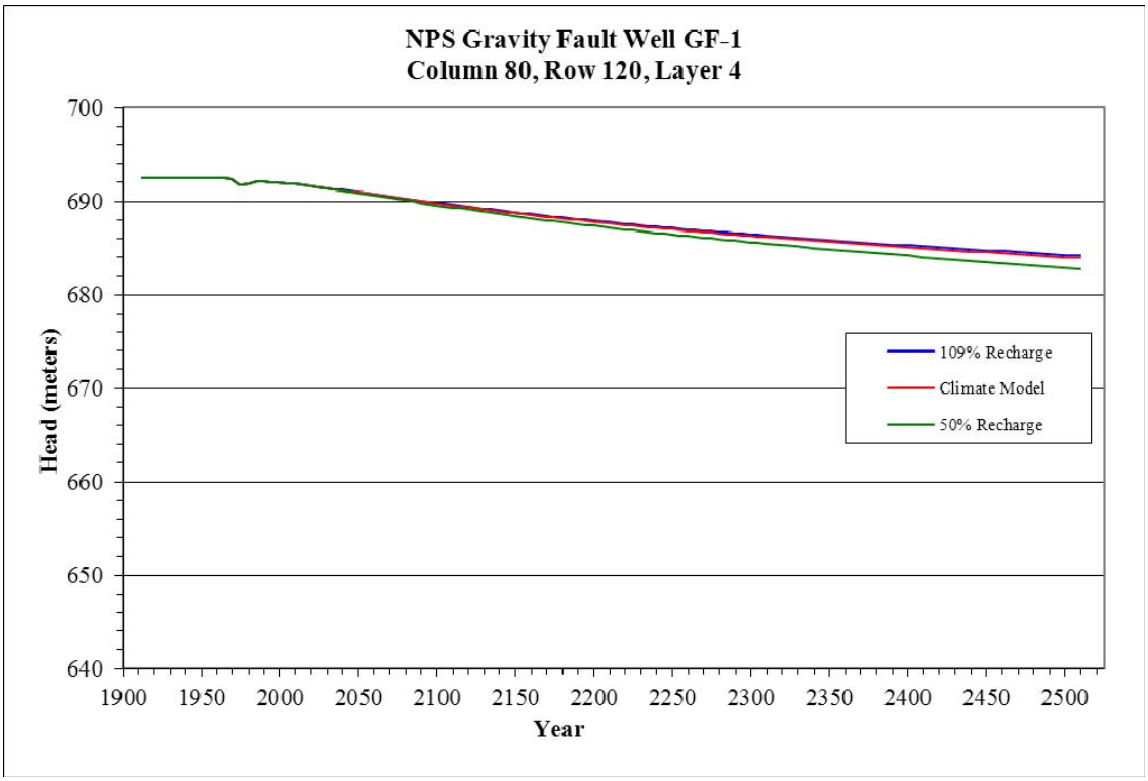

Figure B-72. Head Change in Column 80, Row 120, Layer 4

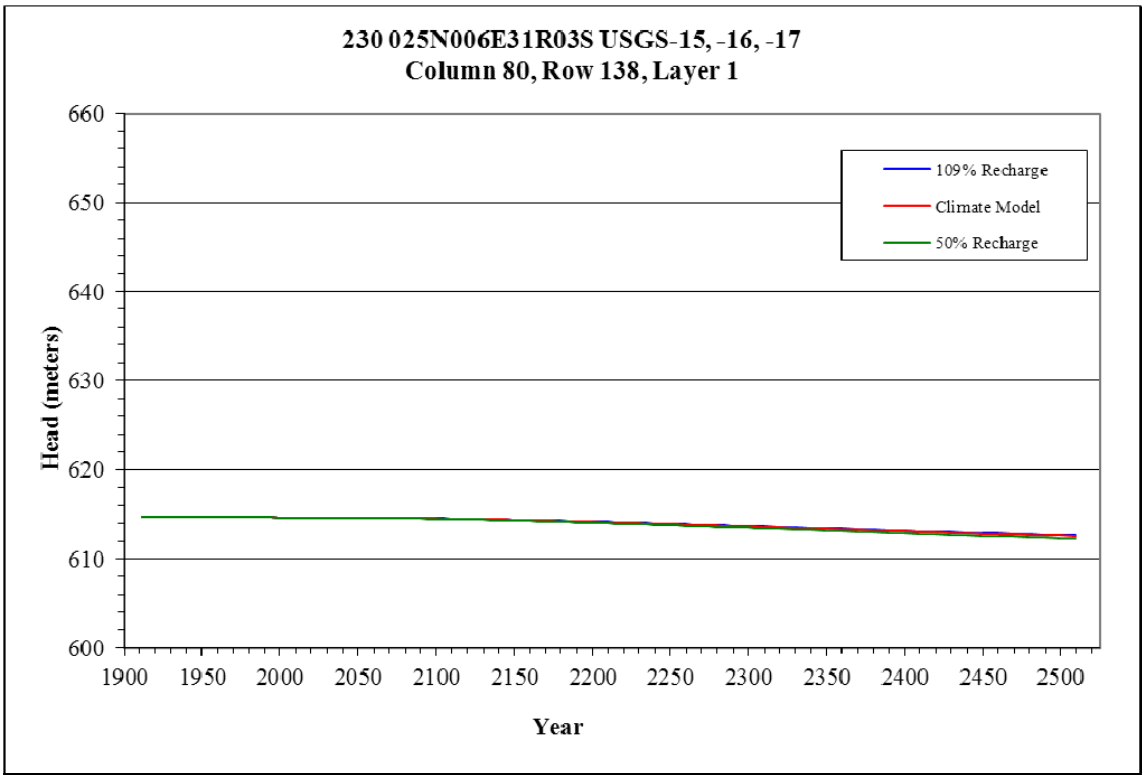

Figure B-73. Head Change in Column 80, Row 138, Layer 1

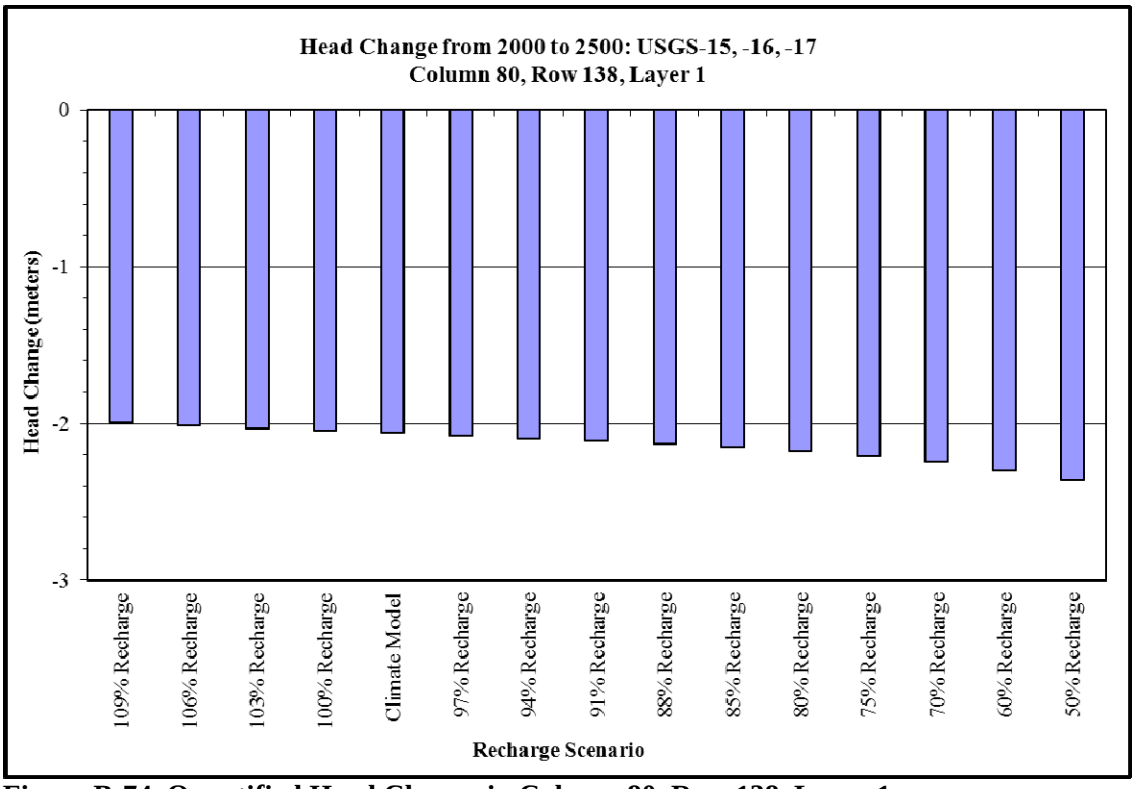

Figure B-74. Quantified Head Change in Column 80, Row 138, Layer 1

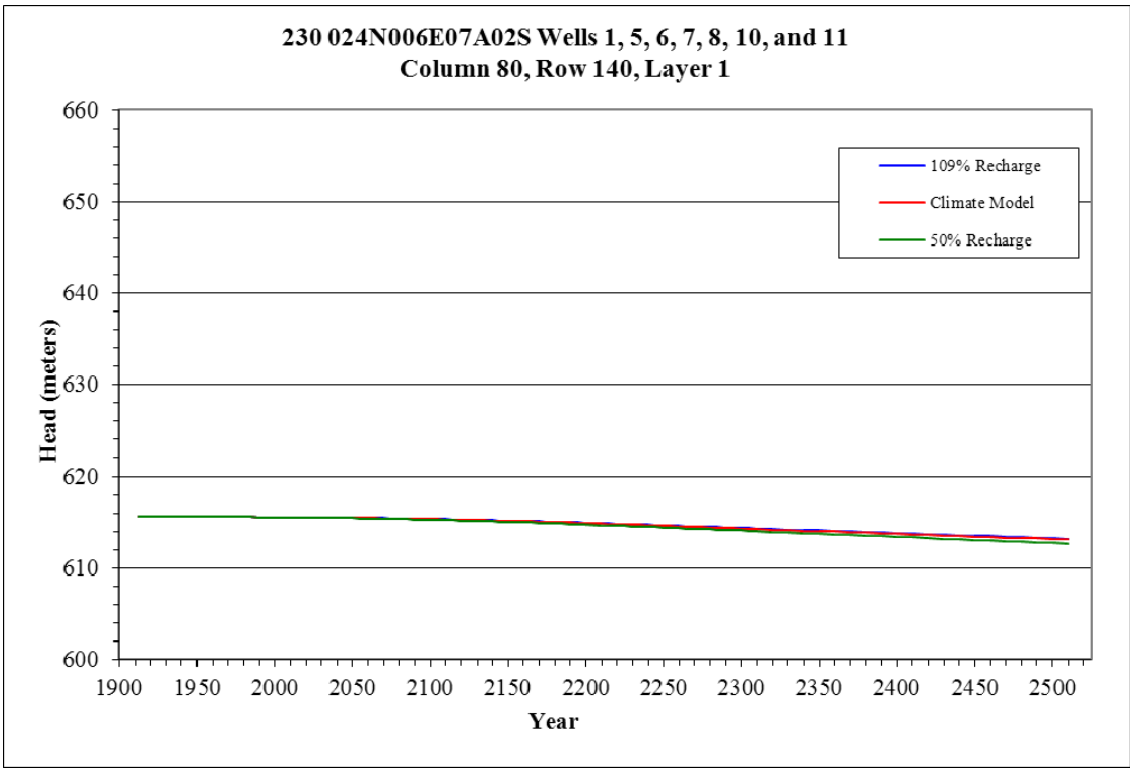

Figure B-75. Head Change in Column 80, Row 140, Layer 1

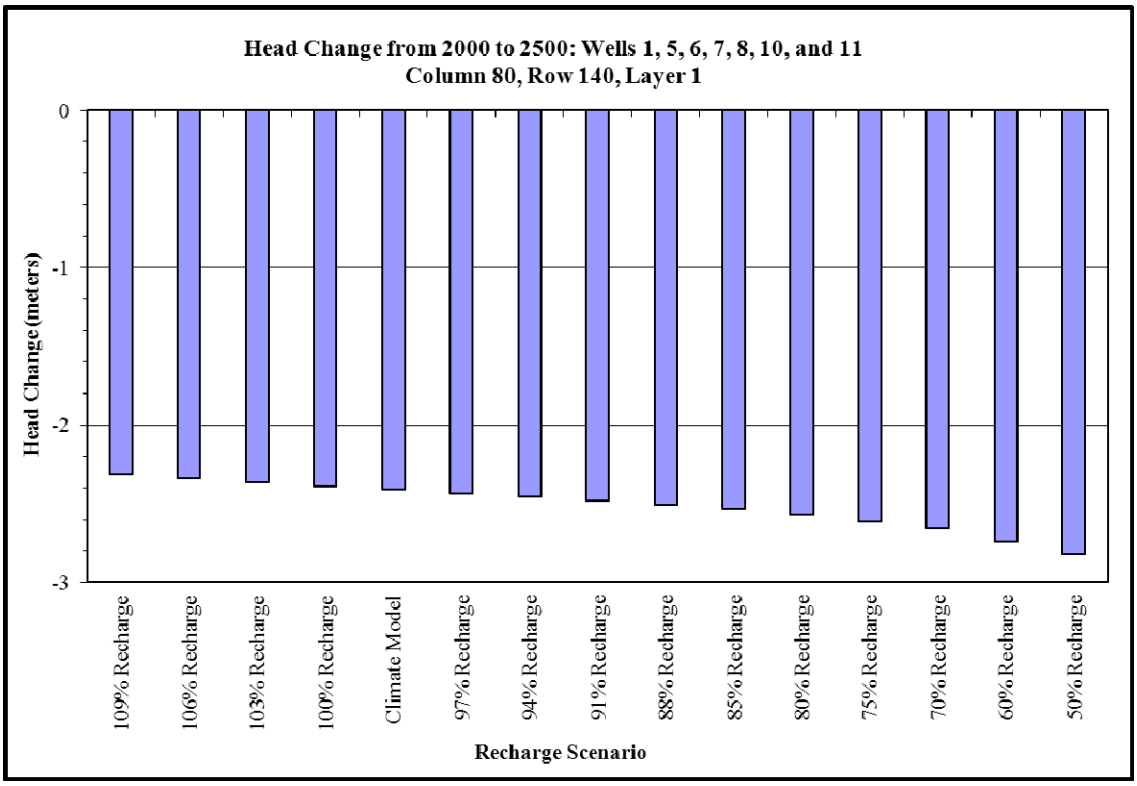

Figure B-76. Quantified Head Change in Column 80, Row 140, Layer 1

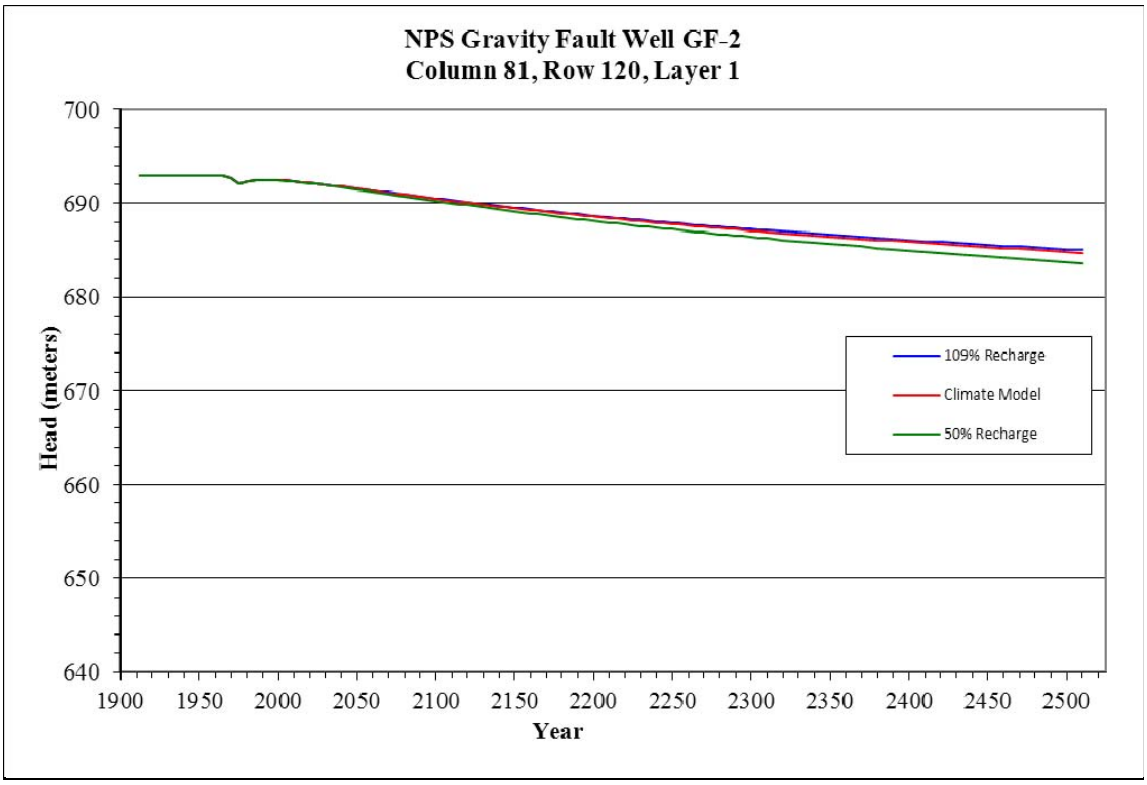

Figure B-77. Head Changes in Column 81, Row 120, Layer 1

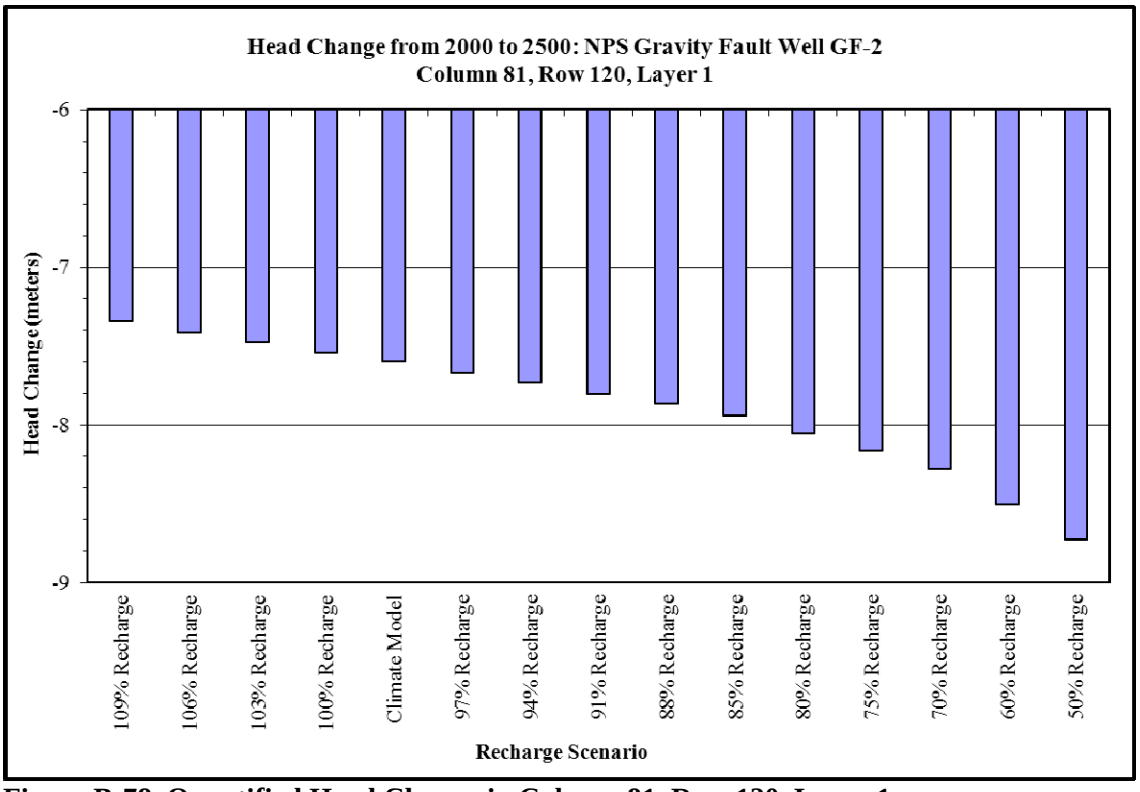

Figure B-78. Quantified Head Change in Column 81, Row 120, Layer 1

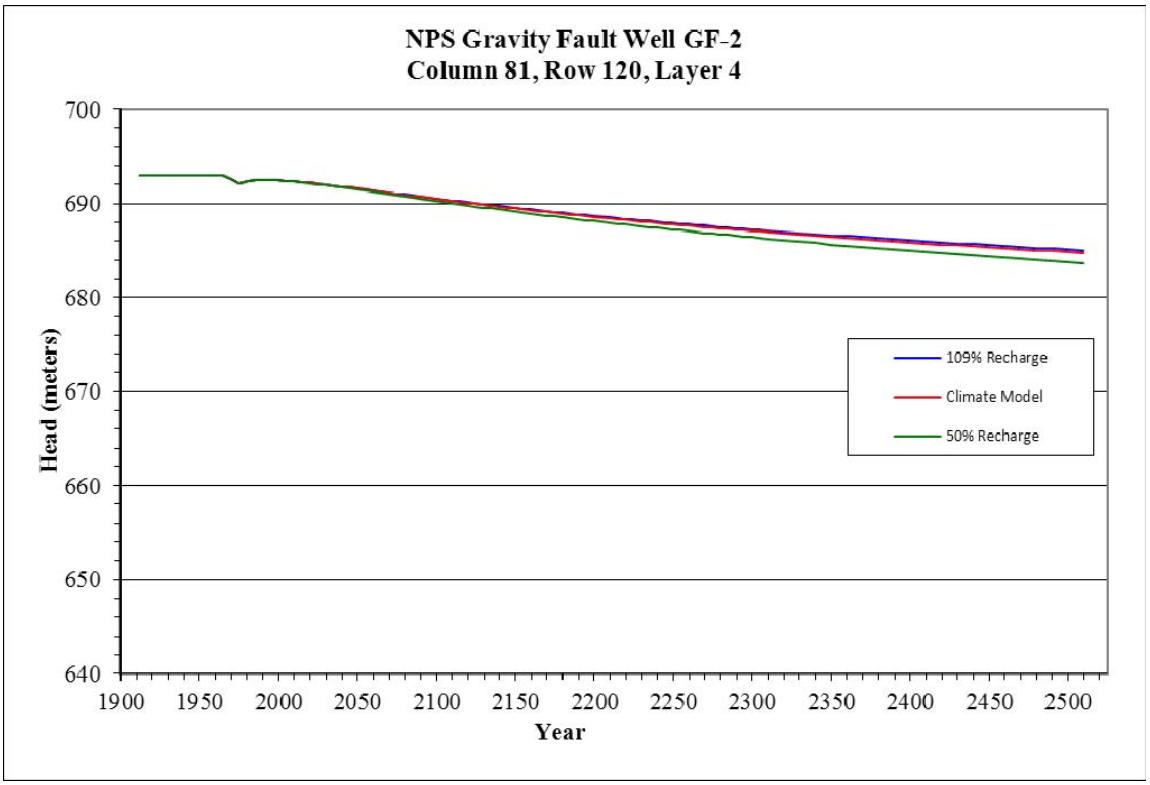

Figure B-79. Head Change in Column 81, Row 120, Layer 4

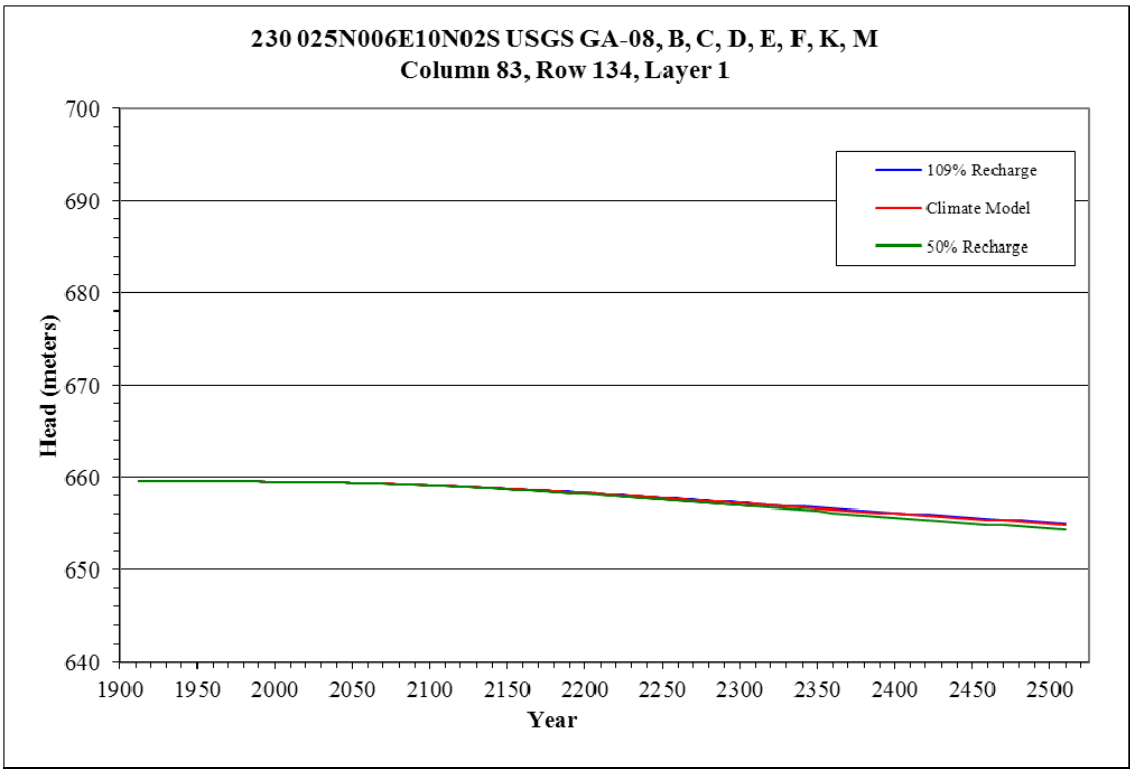

Figure B-80. Head Changes in Column 83, Row 134, Layer 1

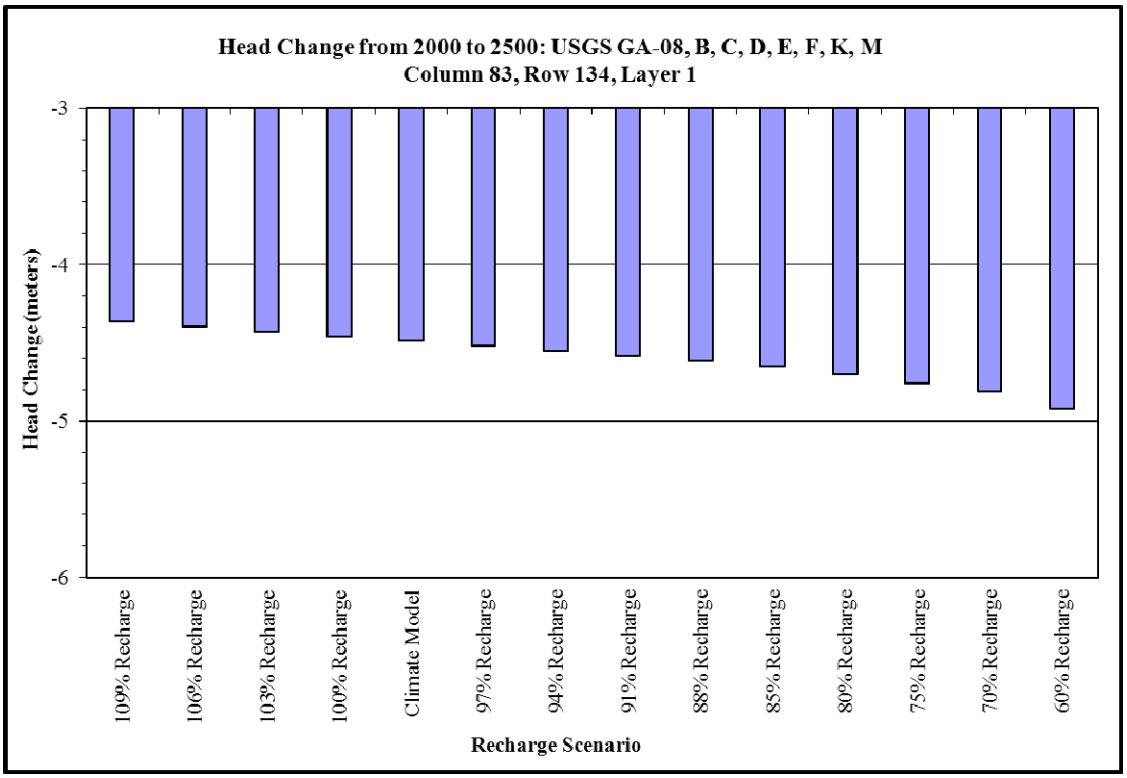

Figure B-81. Quantified Head Change in Column 83, Row 134, Layer 1

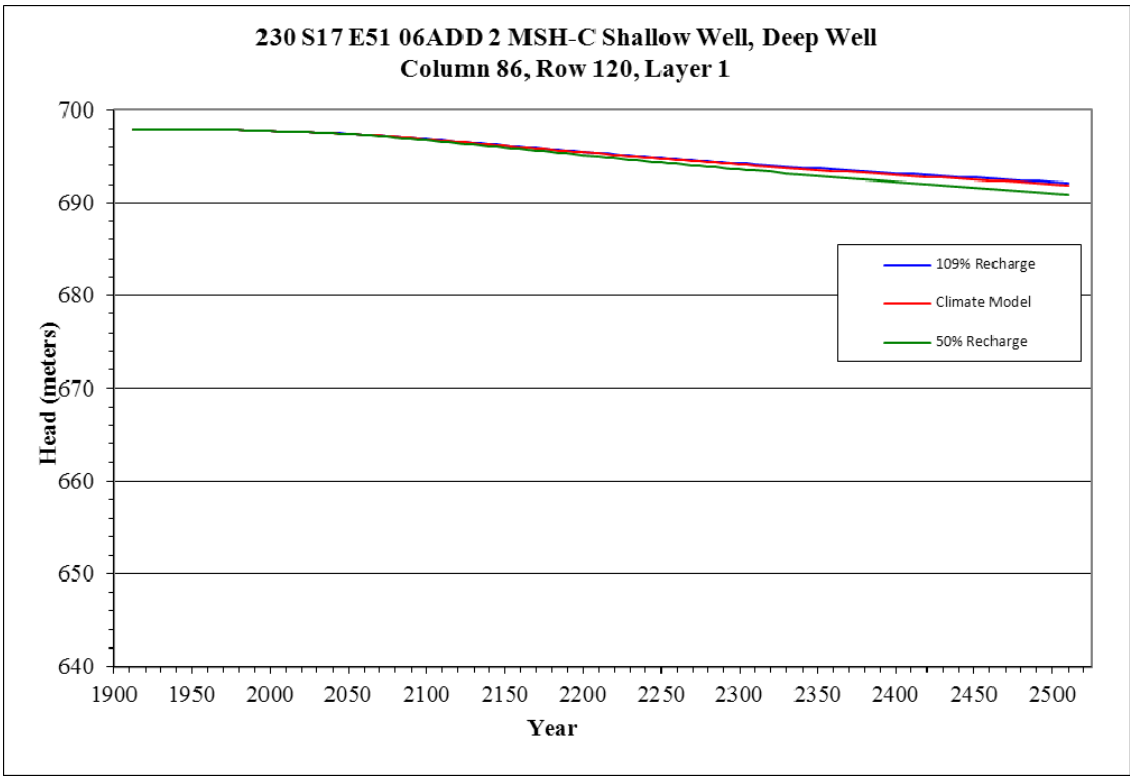

Figure B-82. Head Change in Column 86, Row 120, Layer 1

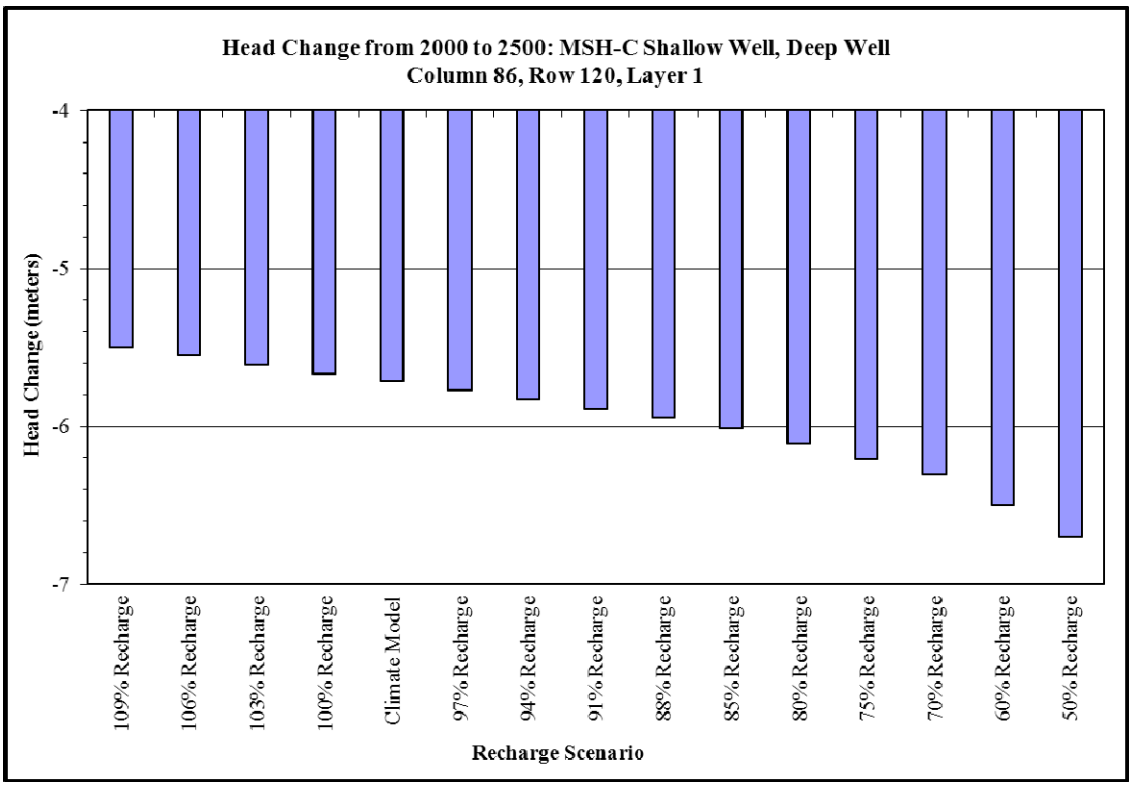

Figure B-83. Quantified Head Change in Column 86, Row 120, Layer 1

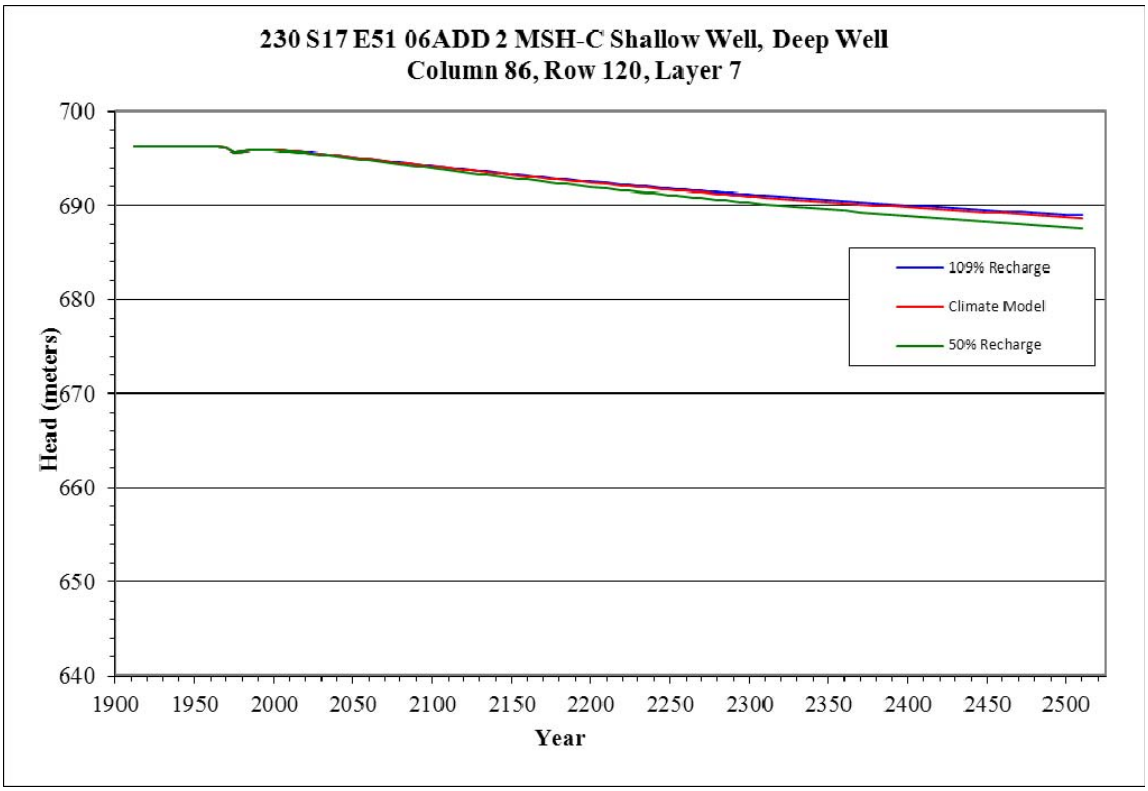

Figure B-84. Head Change in Column 86, Row 120, Layer 7

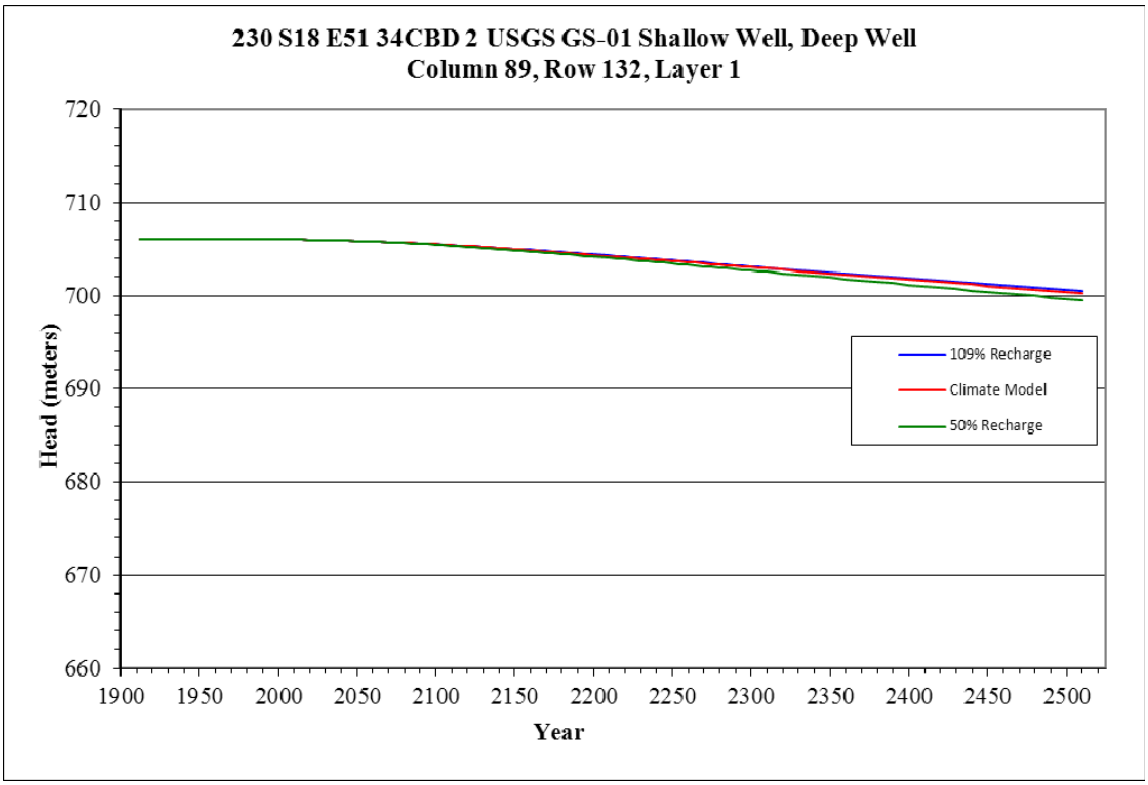

Figure B-85. Head Change in Column 89, Row 132, Layer 1

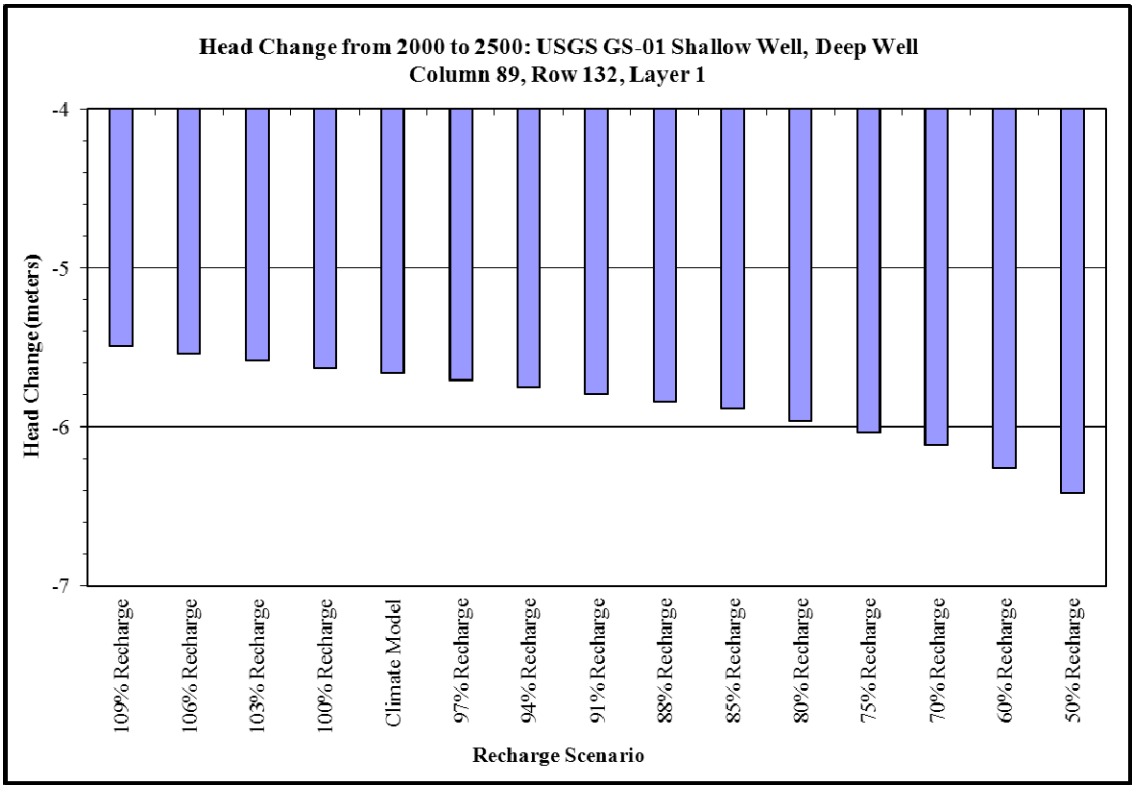

Figure B-86. Quantified Head Change in Column 89, Row 132, Layer 1

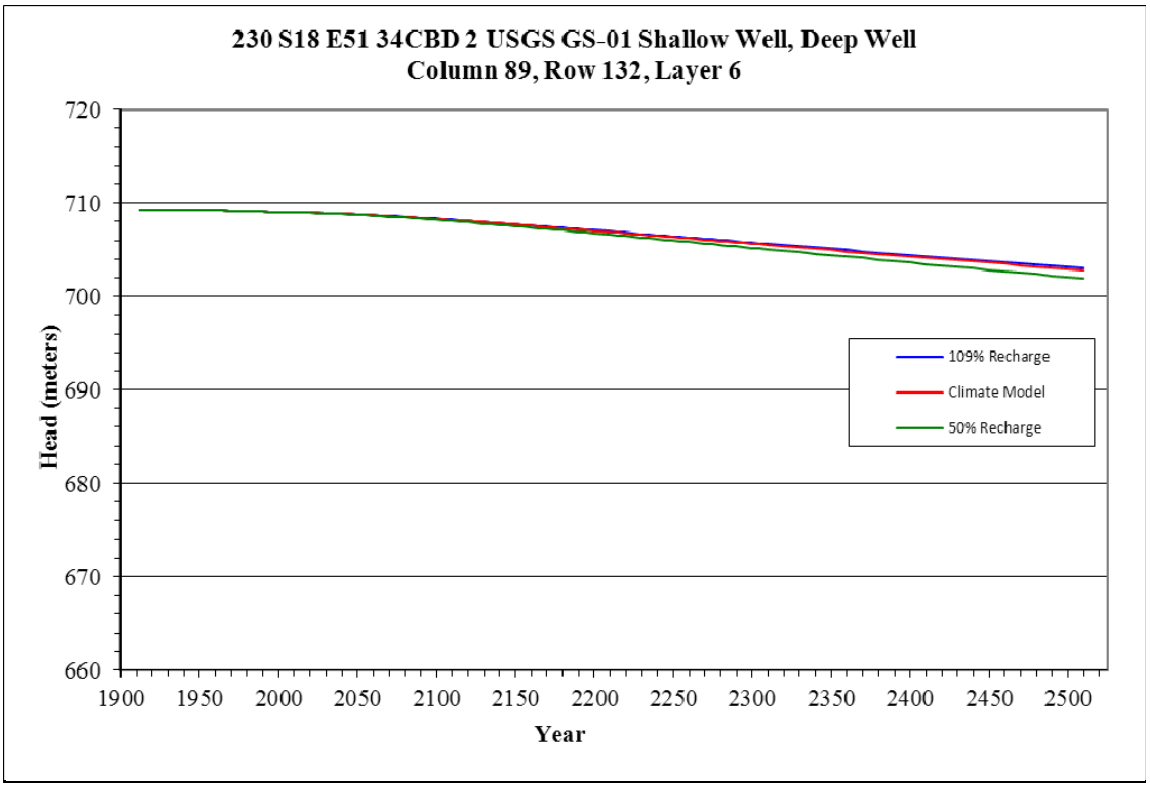

Figure B-87. Head Changes in Column 89, Row 132, Layer 6

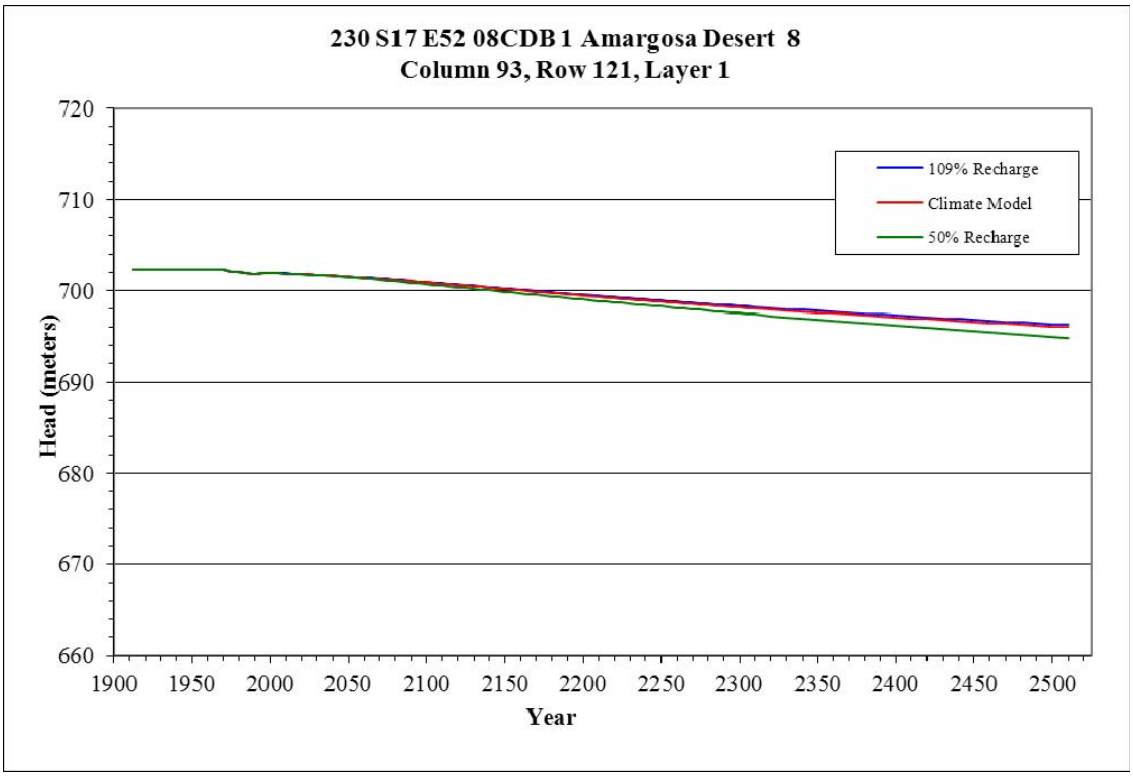

Figure B-88. Head Change in Column 93, Row 121, Layer 1

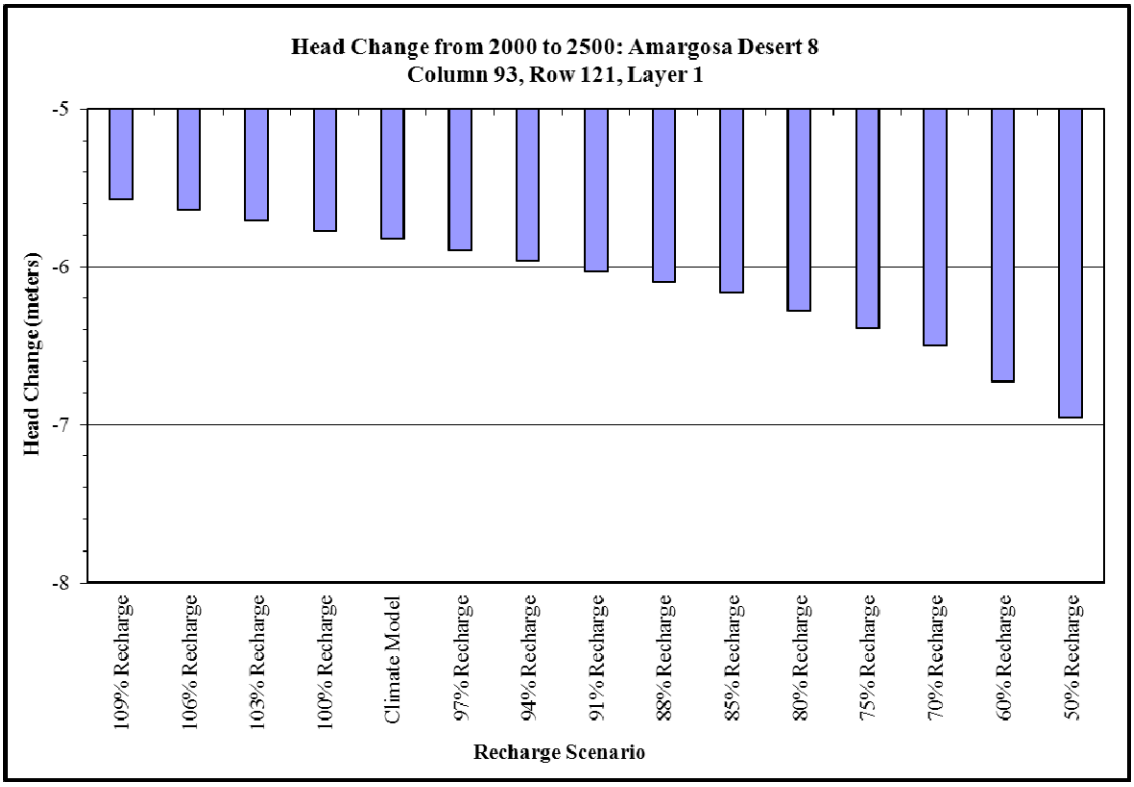

Figure B-89. Quantified Head Change in Column 93, Row 121, Layer 1

Death Valley

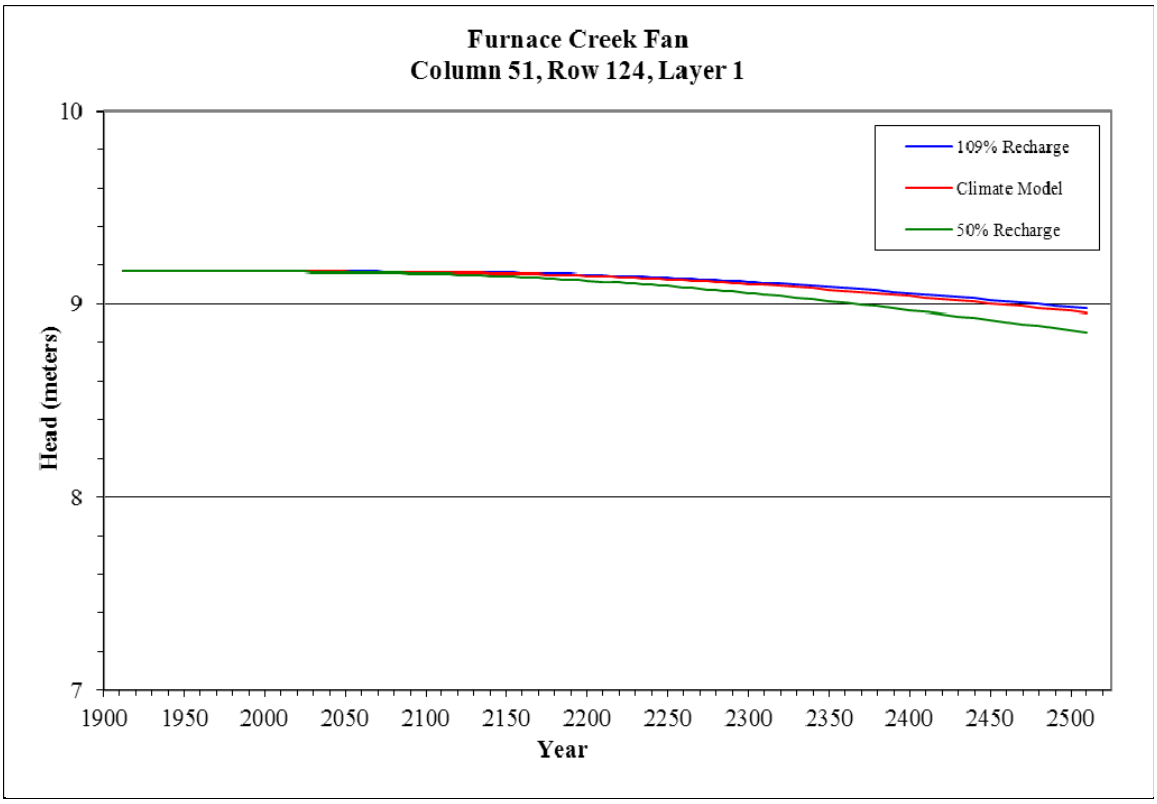

Figure B-90. Head Changes in Column 51, Row 124, Layer 1

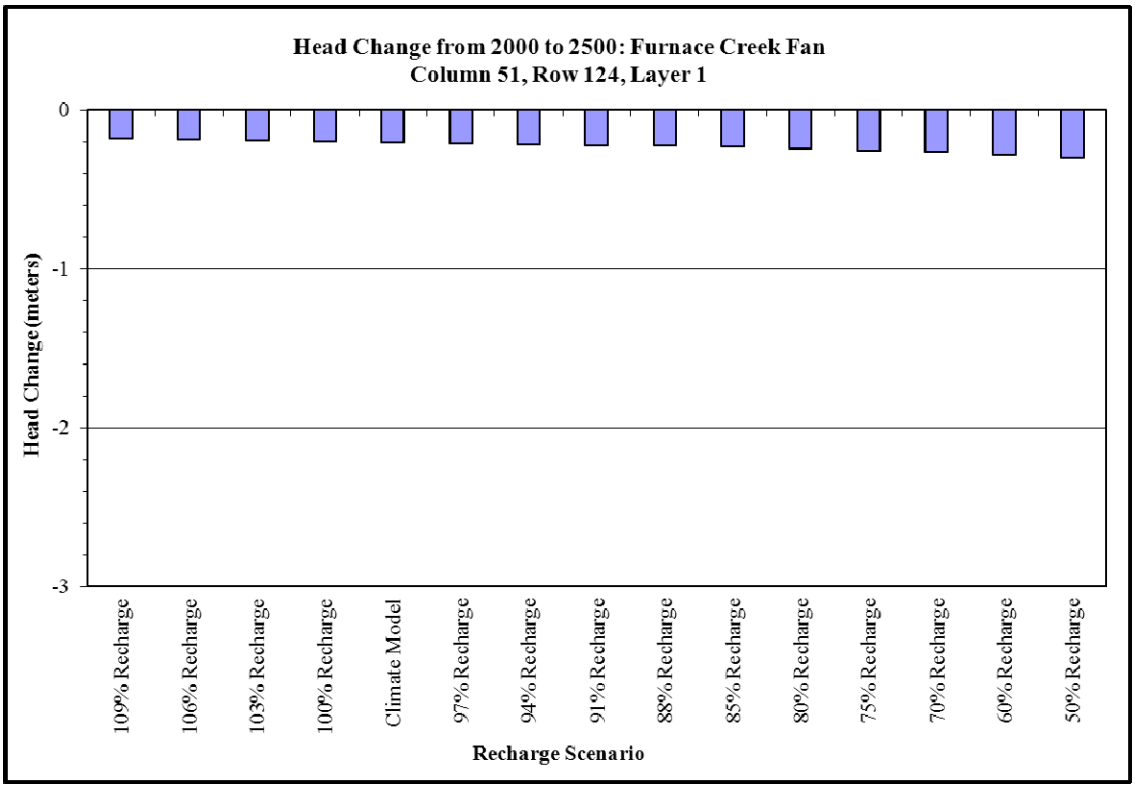

Figure B-91. Quantified Head Change in Column 51, Row 124, Layer 1

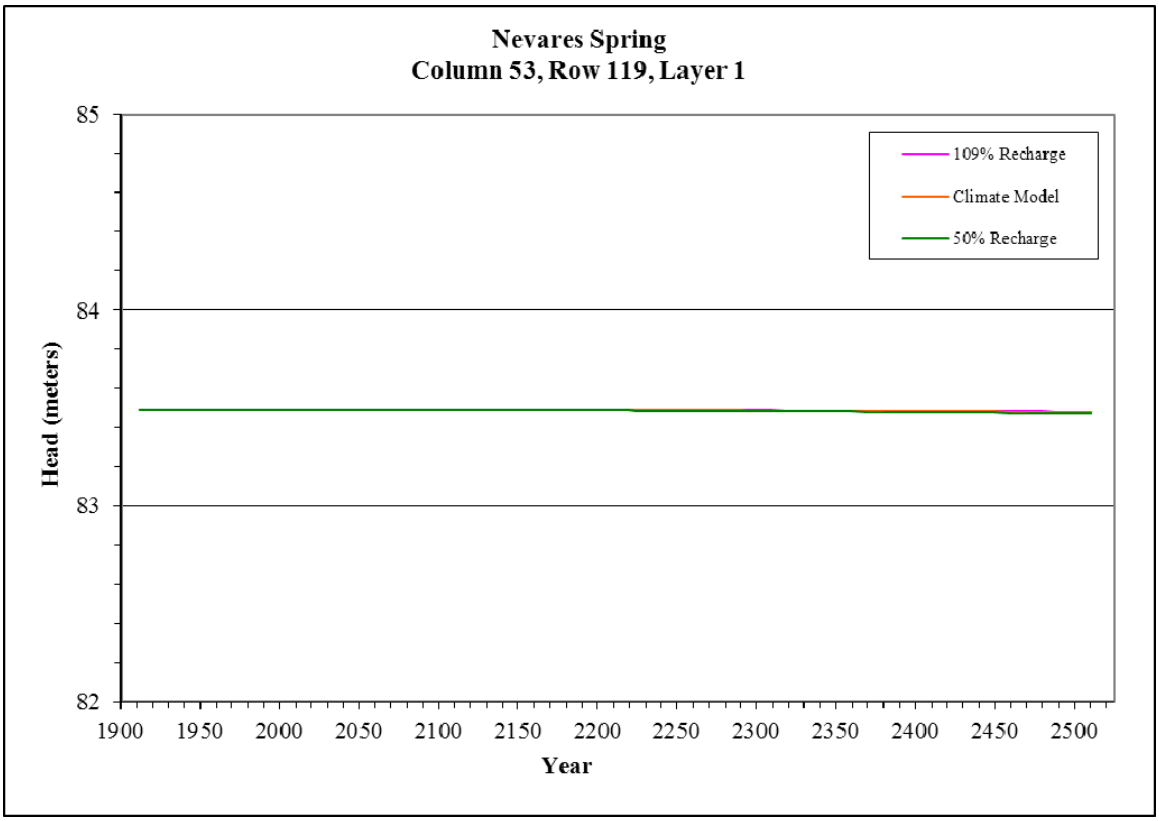

Figure B-92. Head Changes in Column 53, Row 119, Layer 1

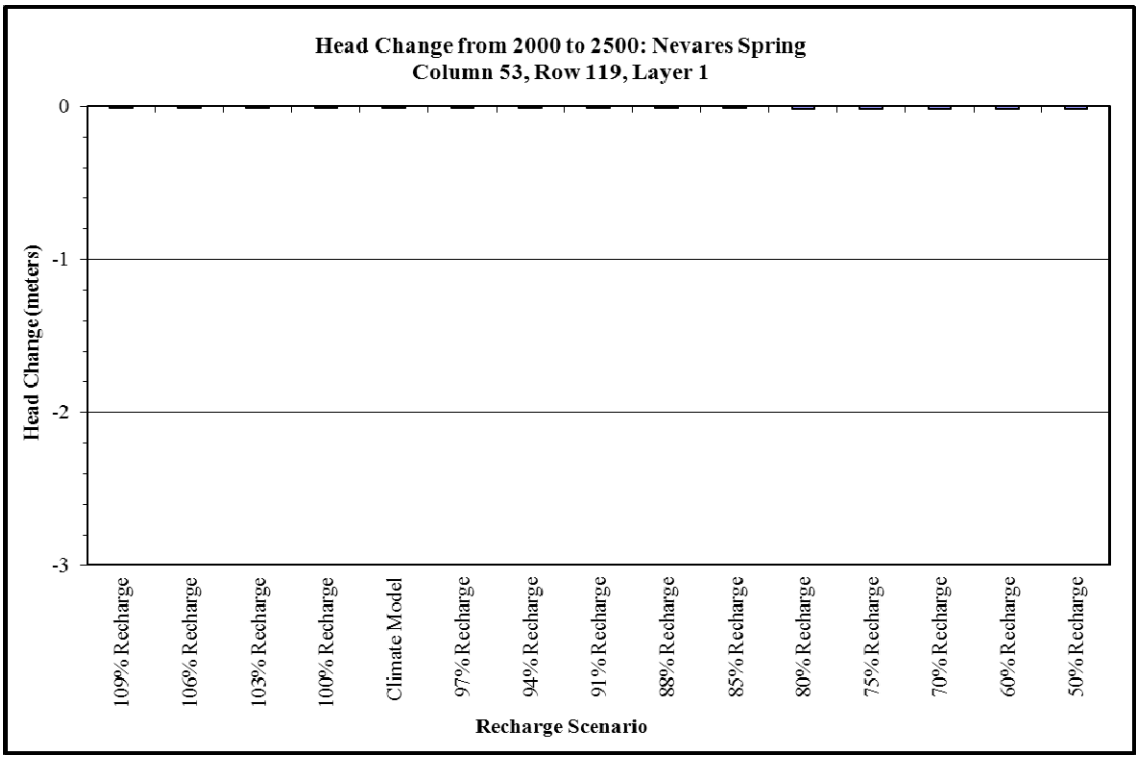

Figure B-93. Quantified Head Change in Column 53, Row 119, Layer 1

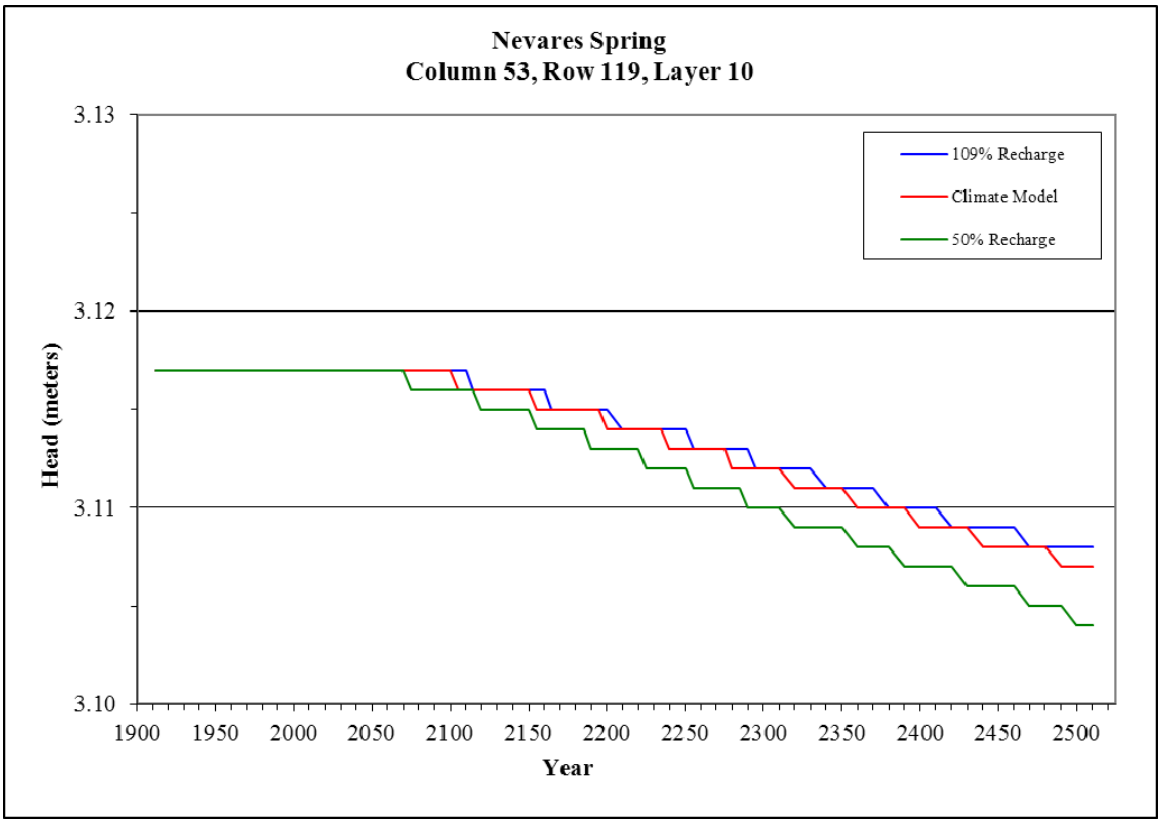

Figure B-94. Head Change in Column 53, Row 119, Layer 10

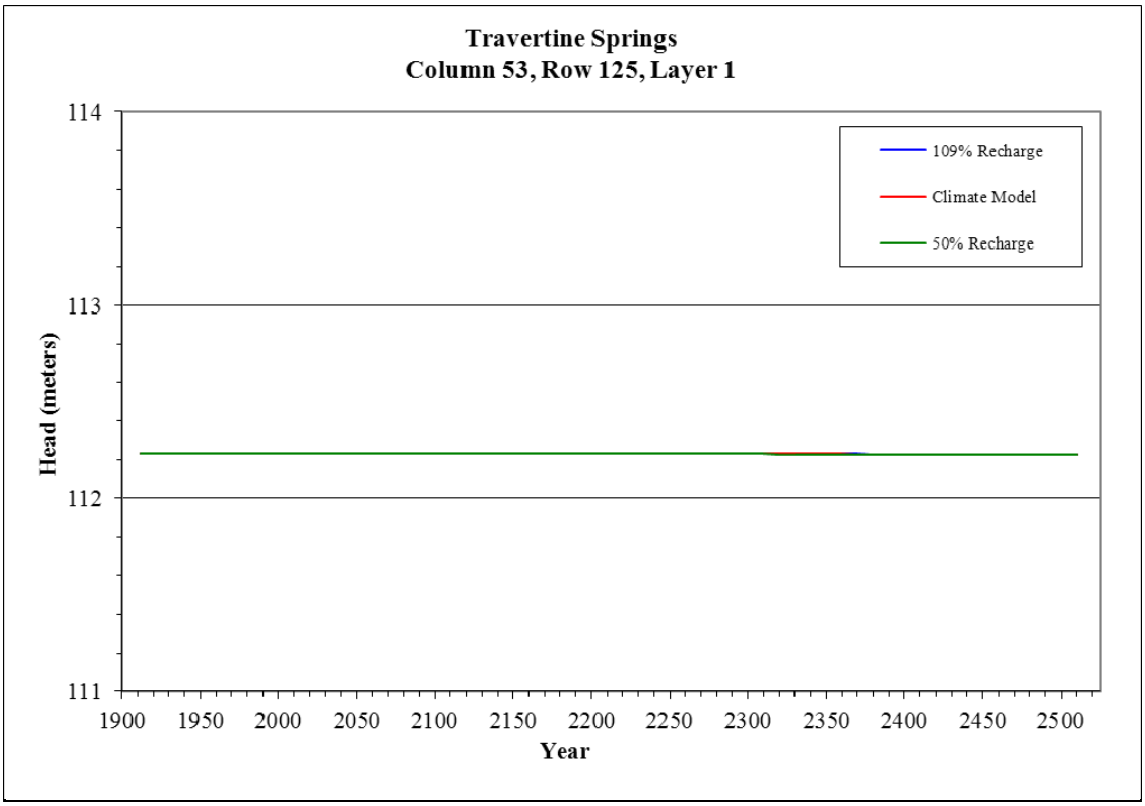

Figure B-95. Head Changes in Column 53, Row 125, Layer 1

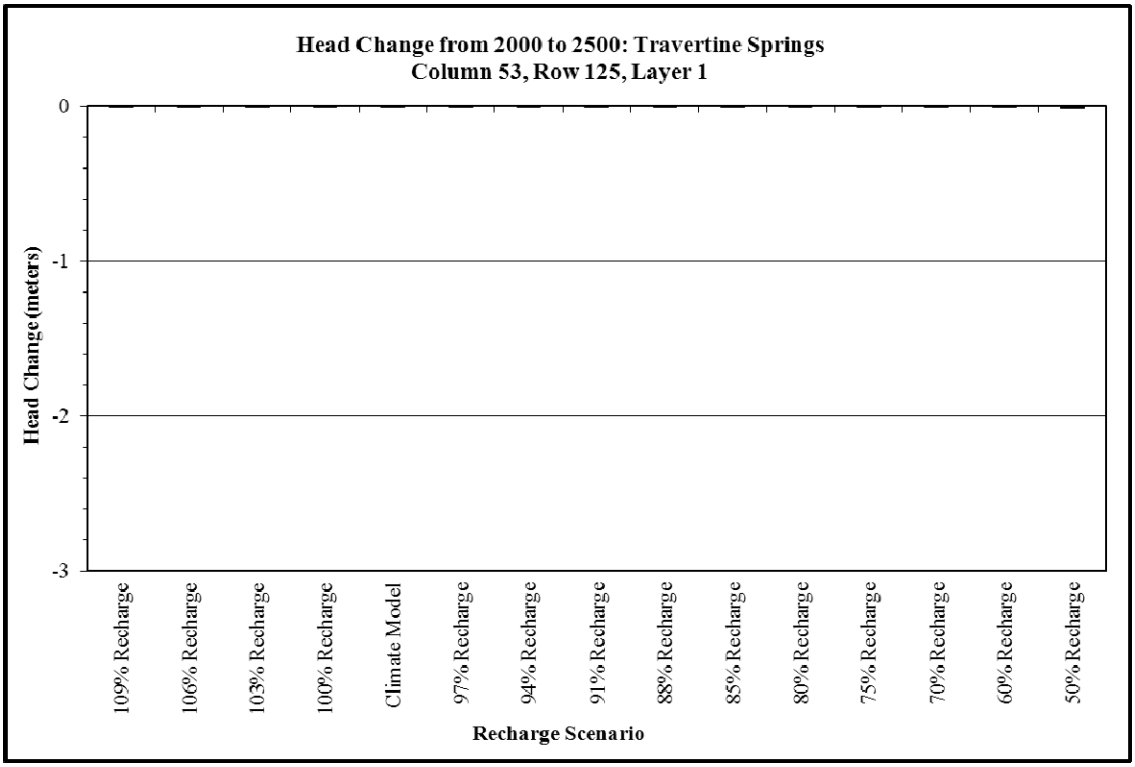

Figure B-96. Quantified Head Change in Column 53, Row 125, Layer 1

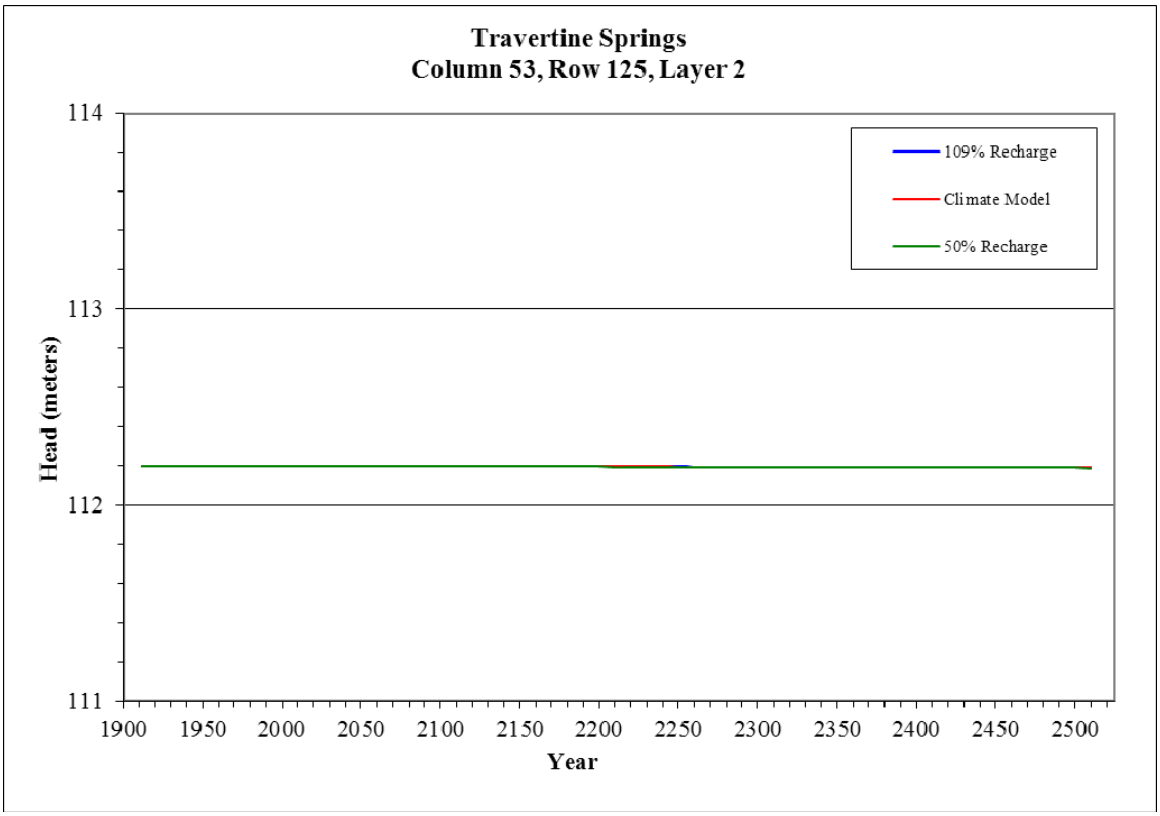

Figure B-97. Head Change in Column 53, Row 125, Layer 2

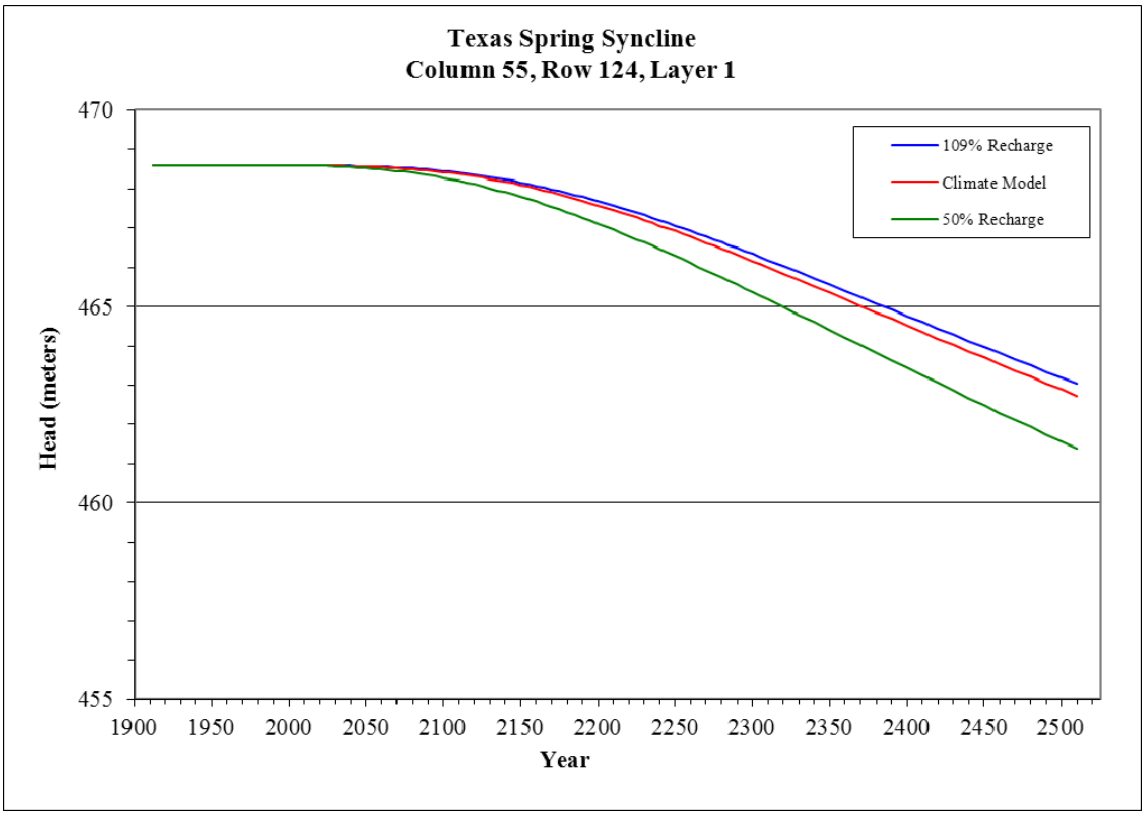

Figure B-98. Head Changes in Column 55, Row 124, Layer 1

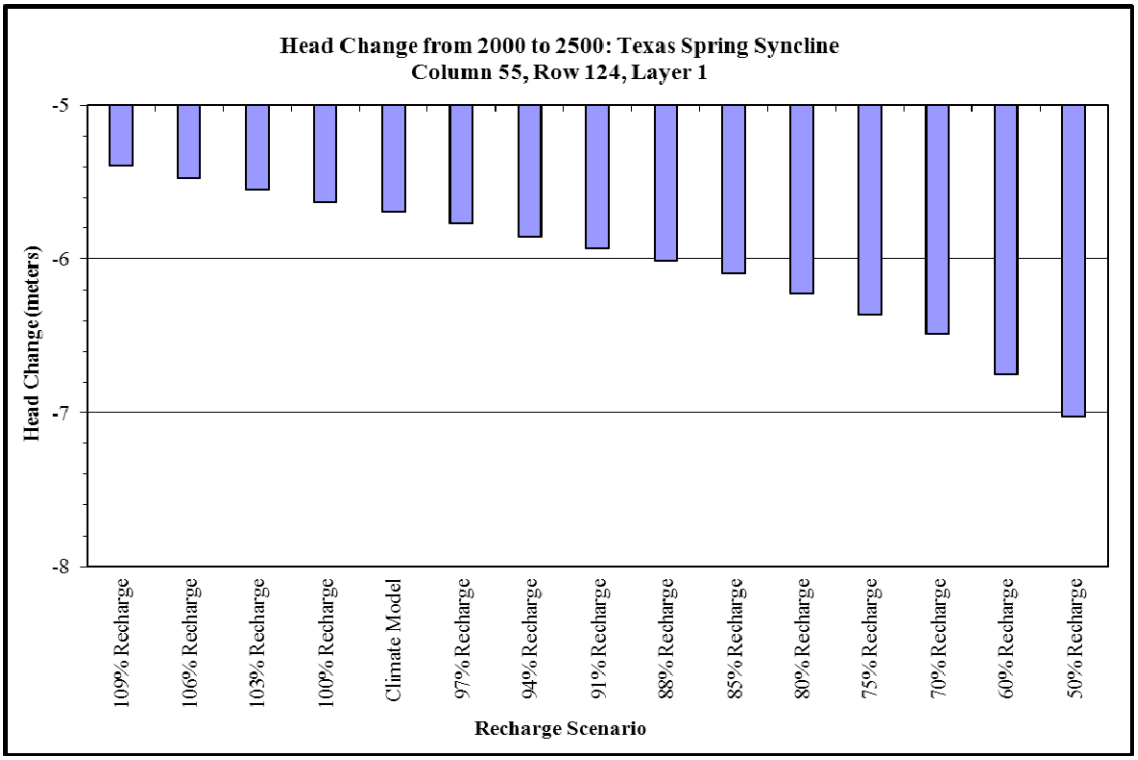

Figure B-99. Quantified Head Change in Column 55, Row 124, Layer 1

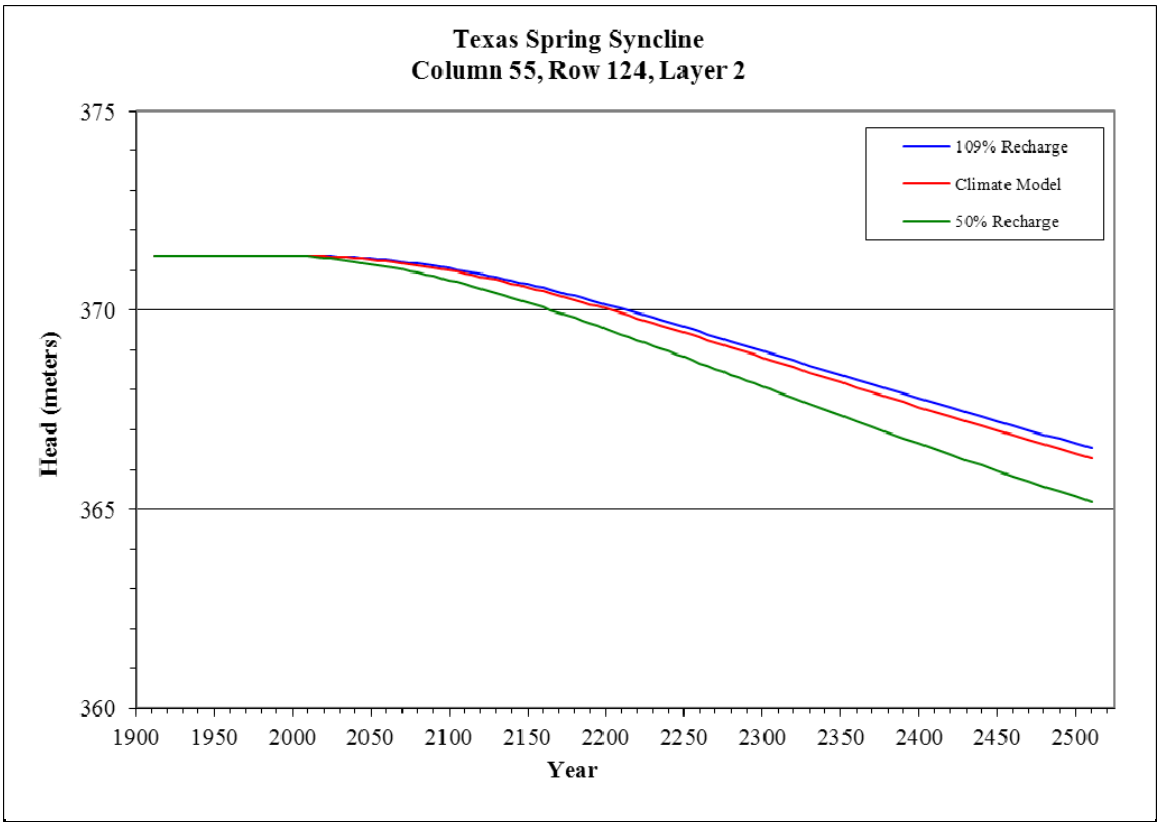

Figure B-100. Head Change in Column 55, Row 124, Layer 2

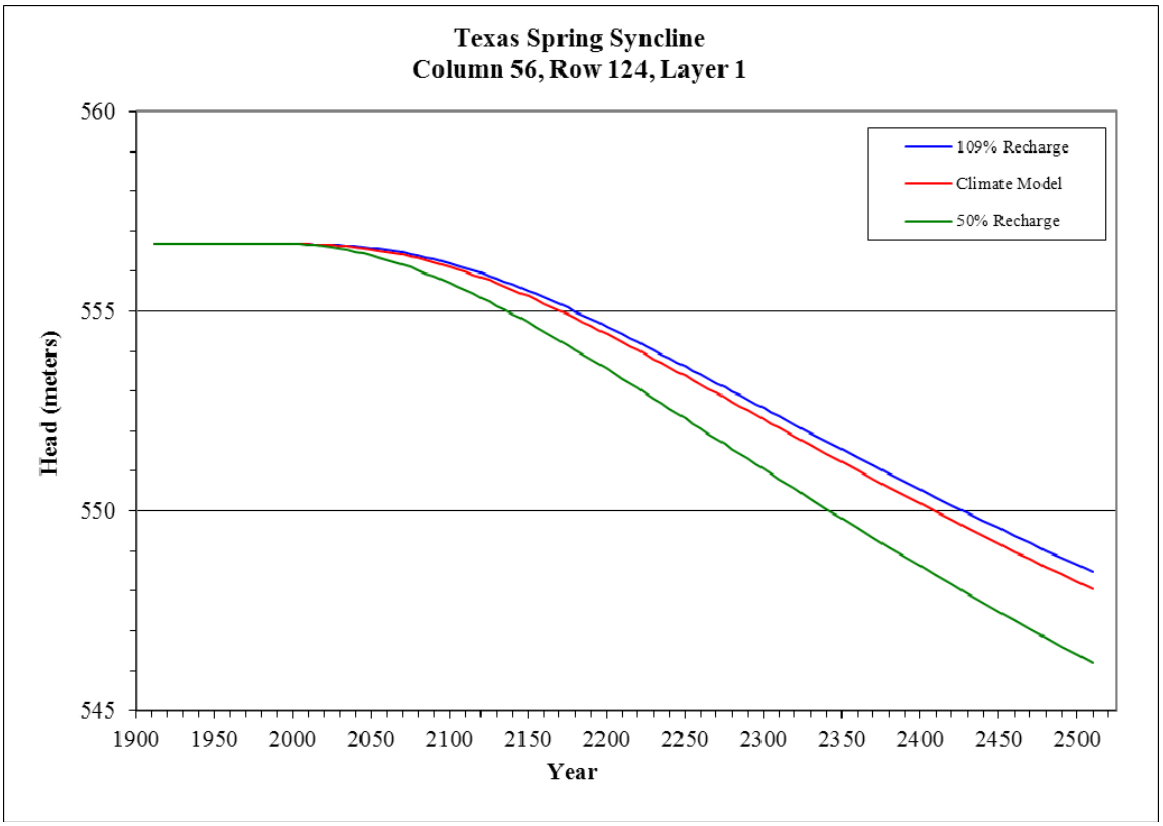

Figure B-101. Head Change in Column 56, Row 124, Layer 1

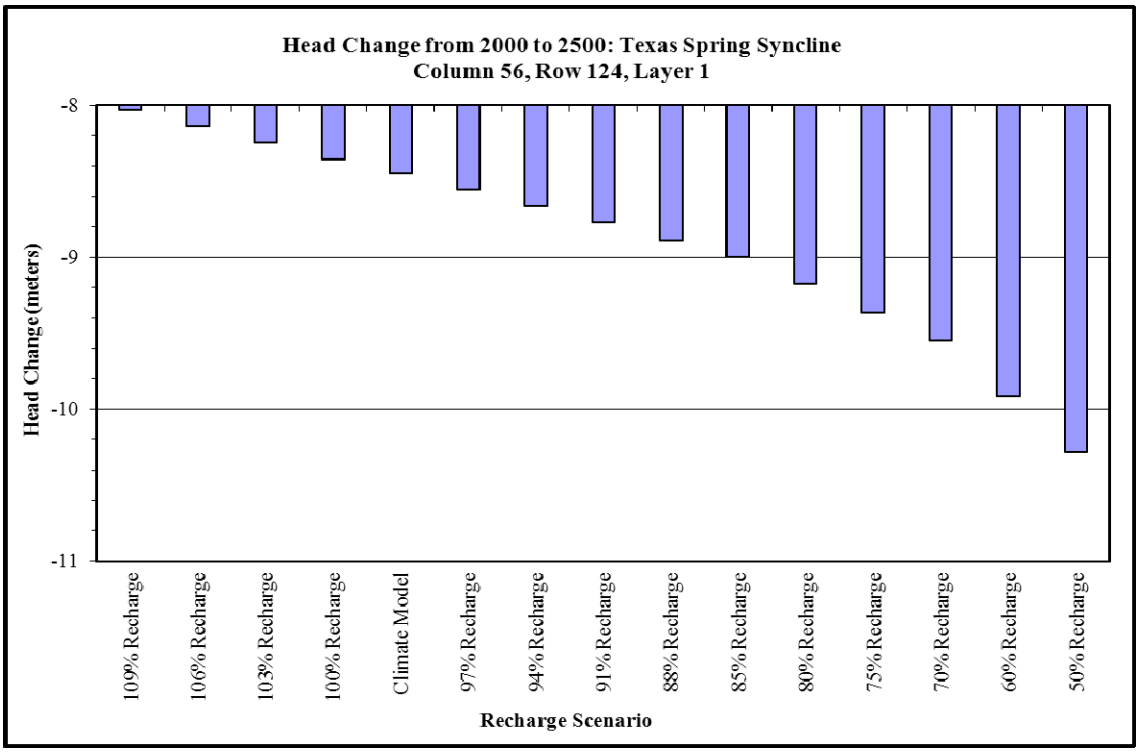

Figure B-102. Quantified Head Change in Column 56, Row 124, Layer 1

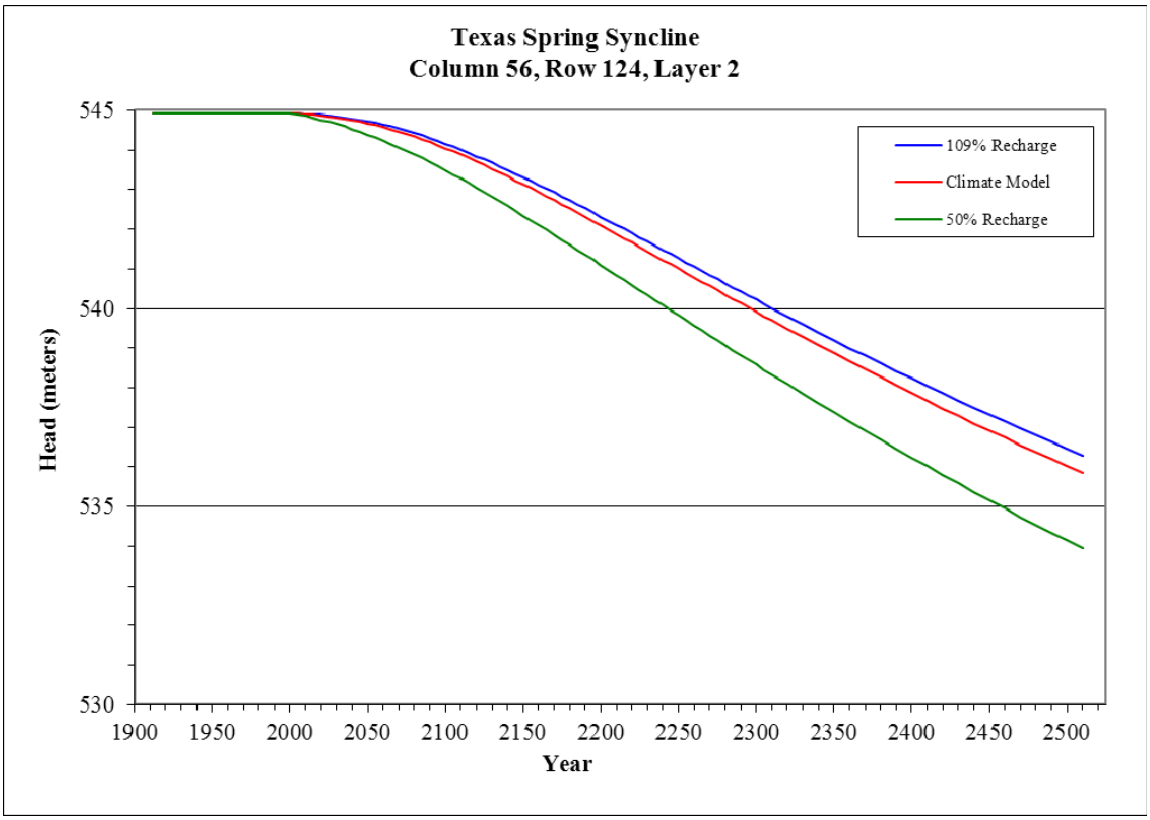

Figure B-103. Head Changes in Column 56, Row 124, Layer 2

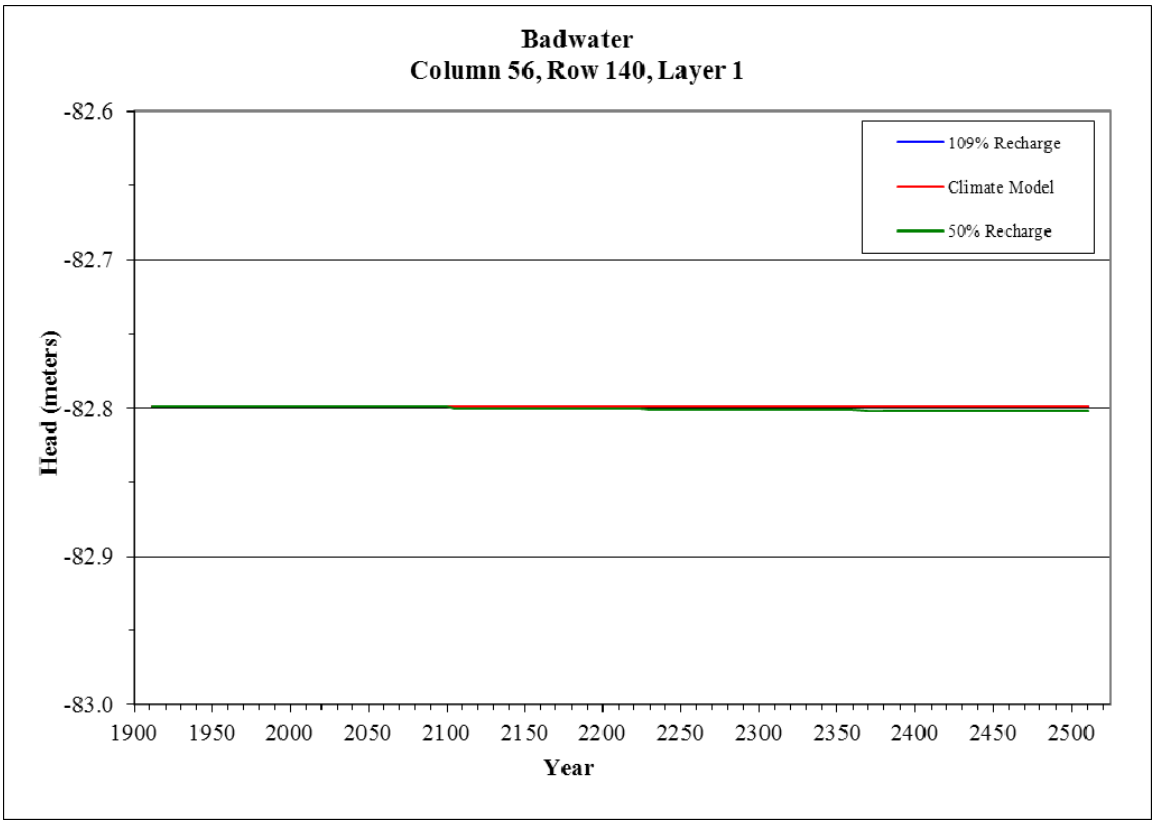

Figure B-104. Head Change in Column 56, Row 140, Layer 1

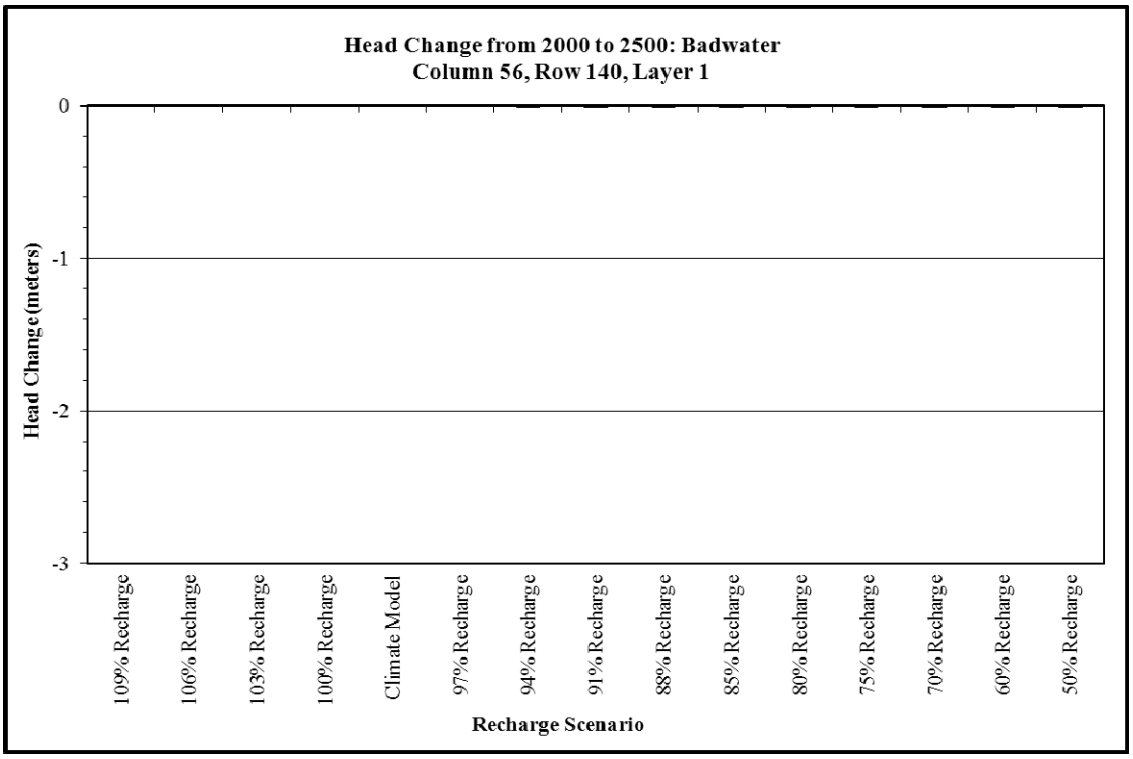

Figure B-105. Quantified Head Change in Column 56, Row 140, Layer 1

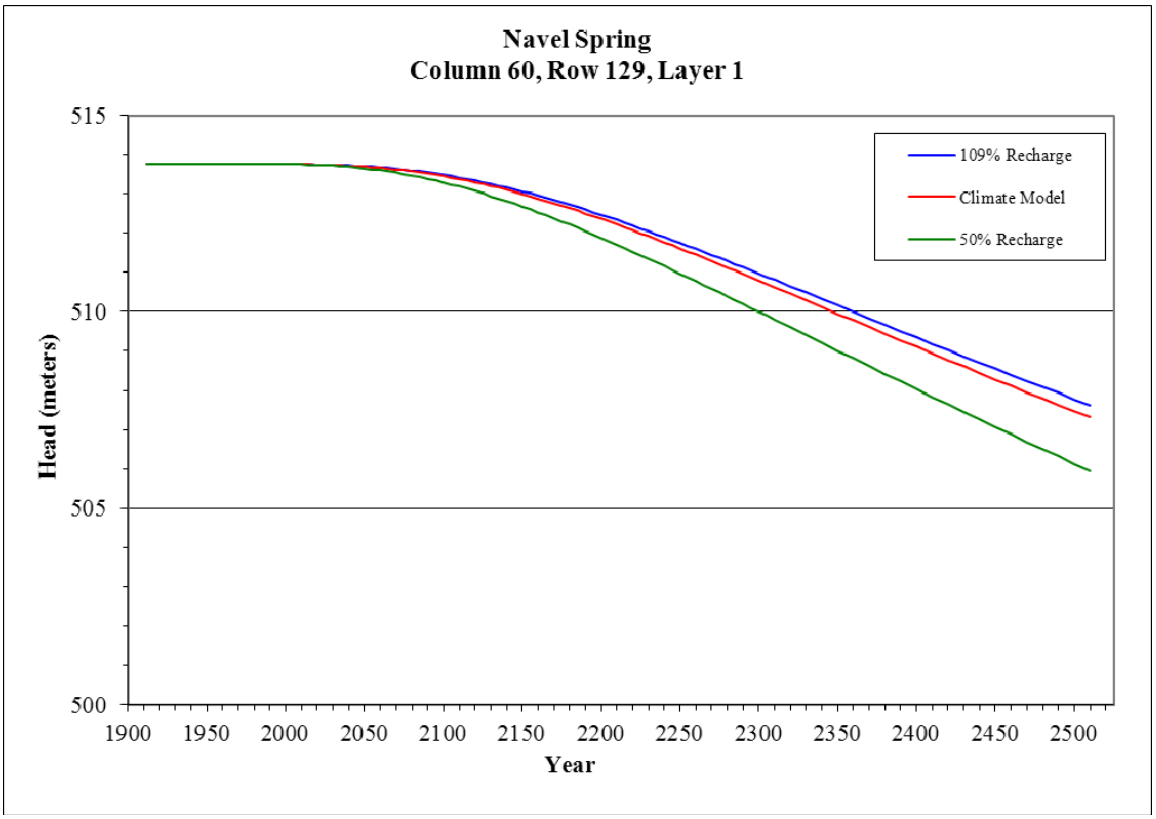

Figure B-106. Head Change in Column 60, Row 129, Layer 1

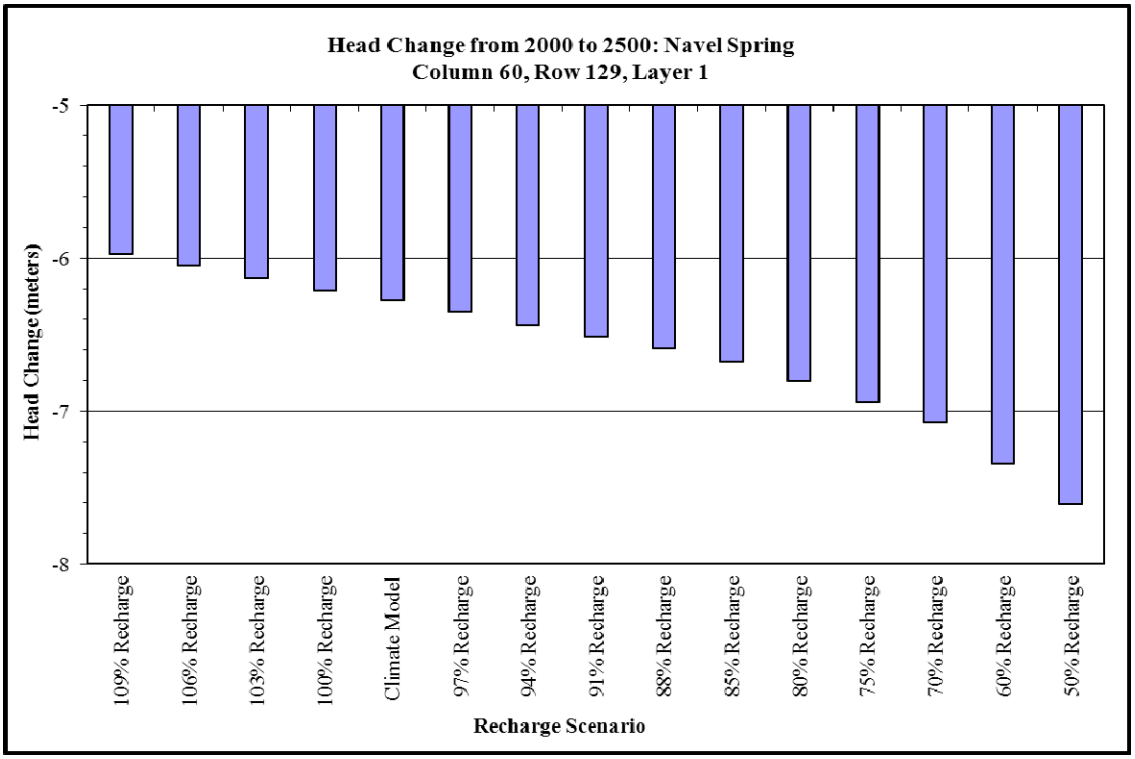

Figure B-107. Quantified Head Change in Column 60, Row 129, Layer 1

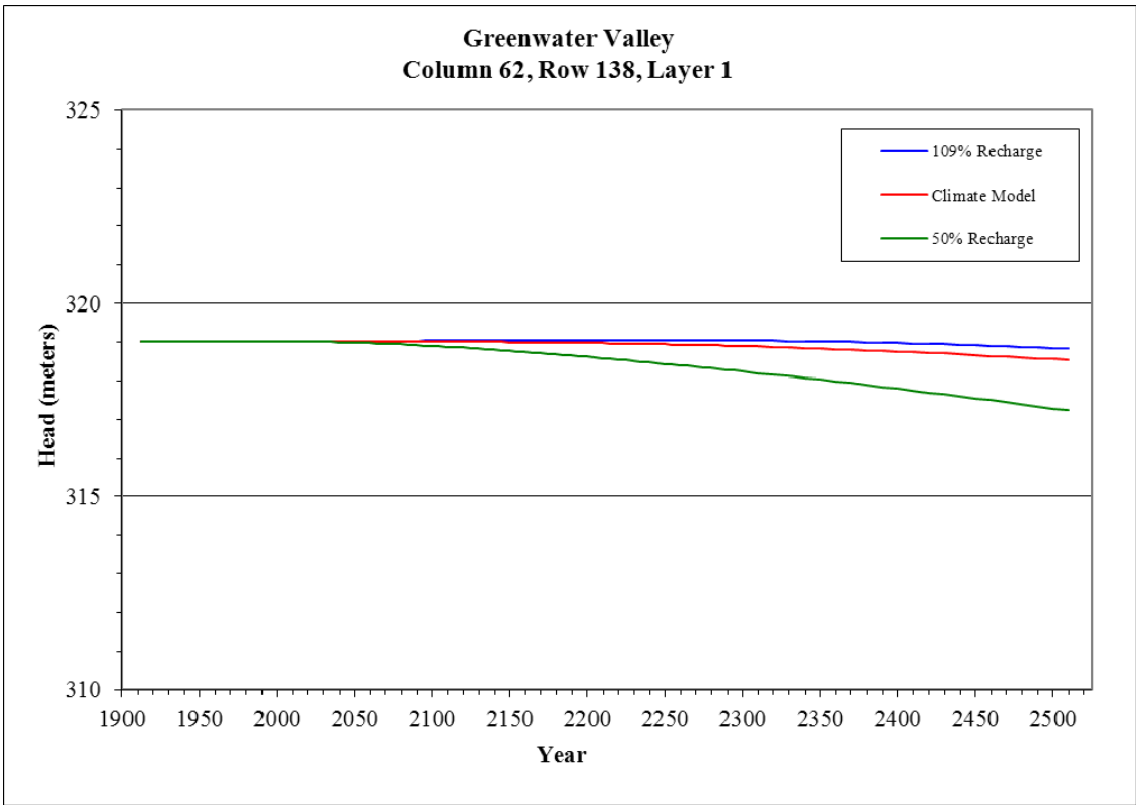

Figure B-108. Head Change in Column 62, Row 138, Layer 1

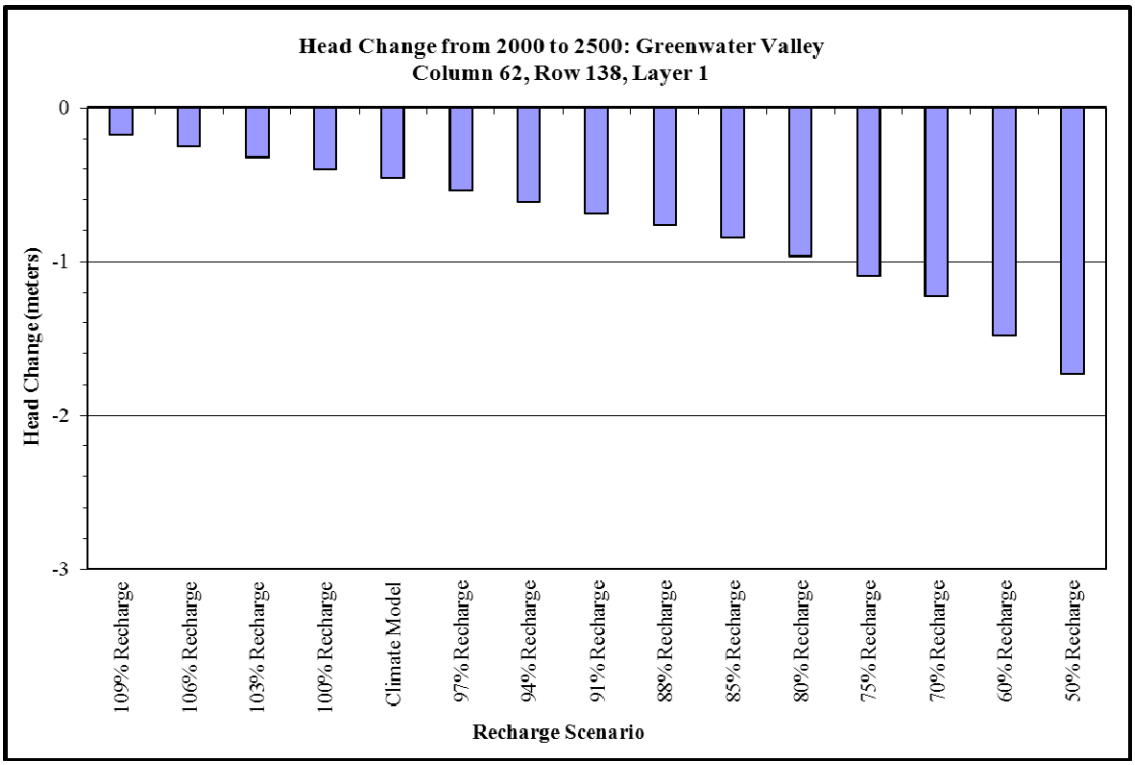

Figure B-109. Quantified Head Change in Column 62, Row 138, Layer 1

Effects of Pumping versus Recharge

The data summarized above suggest that a factor other than climate change is responsible for the simulated decline in head over time because (1) head declines occurred before recharge was simulated to be reduced, (2) heads decline in the simulations in which recharge is held at or increased relative to 20th Century levels, and (3) in many simulations the overall head decline is substantially greater than the range of decline caused by a change in recharge.

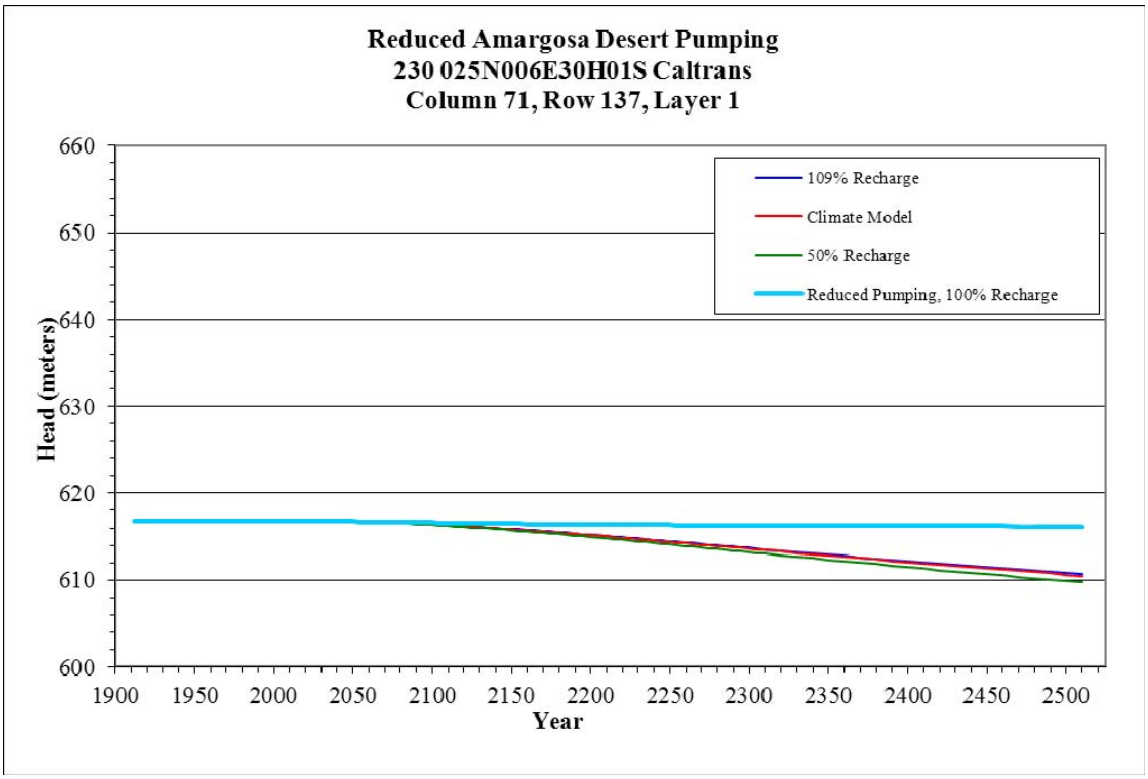

Figure B-110. Head Change with Pumping Minimized: Column 71, Row 137, Layer 1

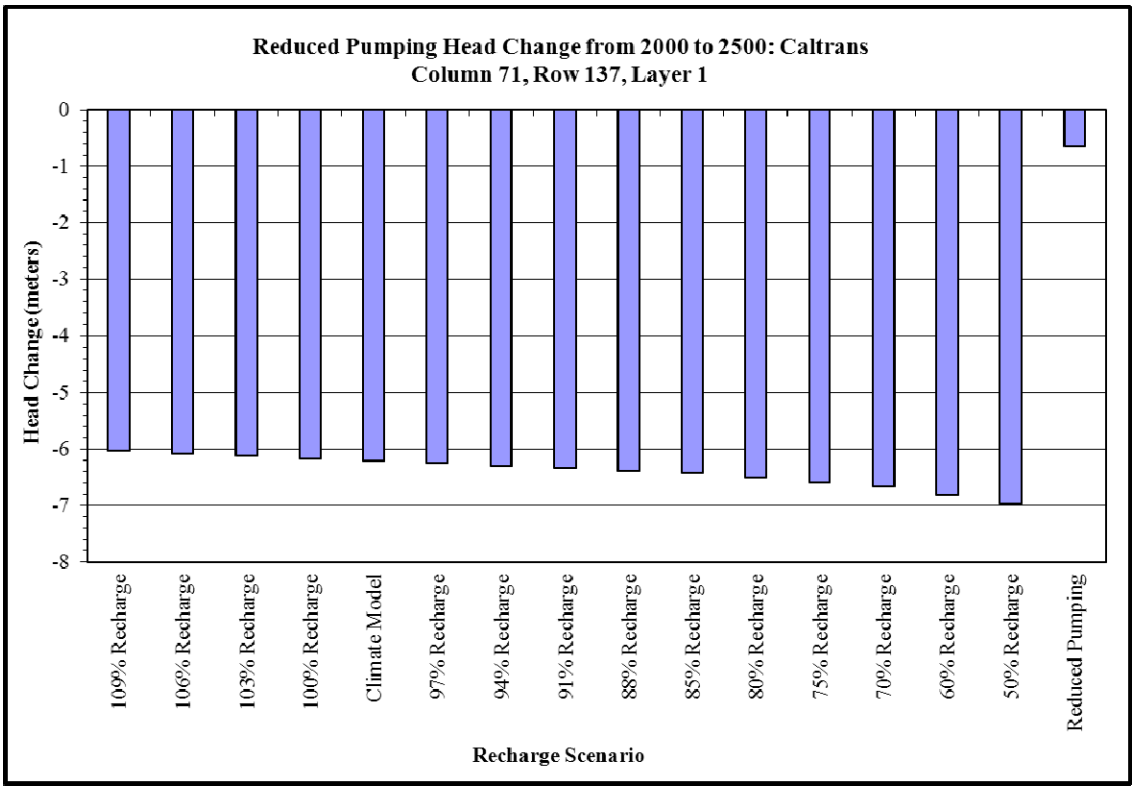

Figure B-111. Quantified Head Change: Pumping Minimized: Col 71, Row 137, Layer 1

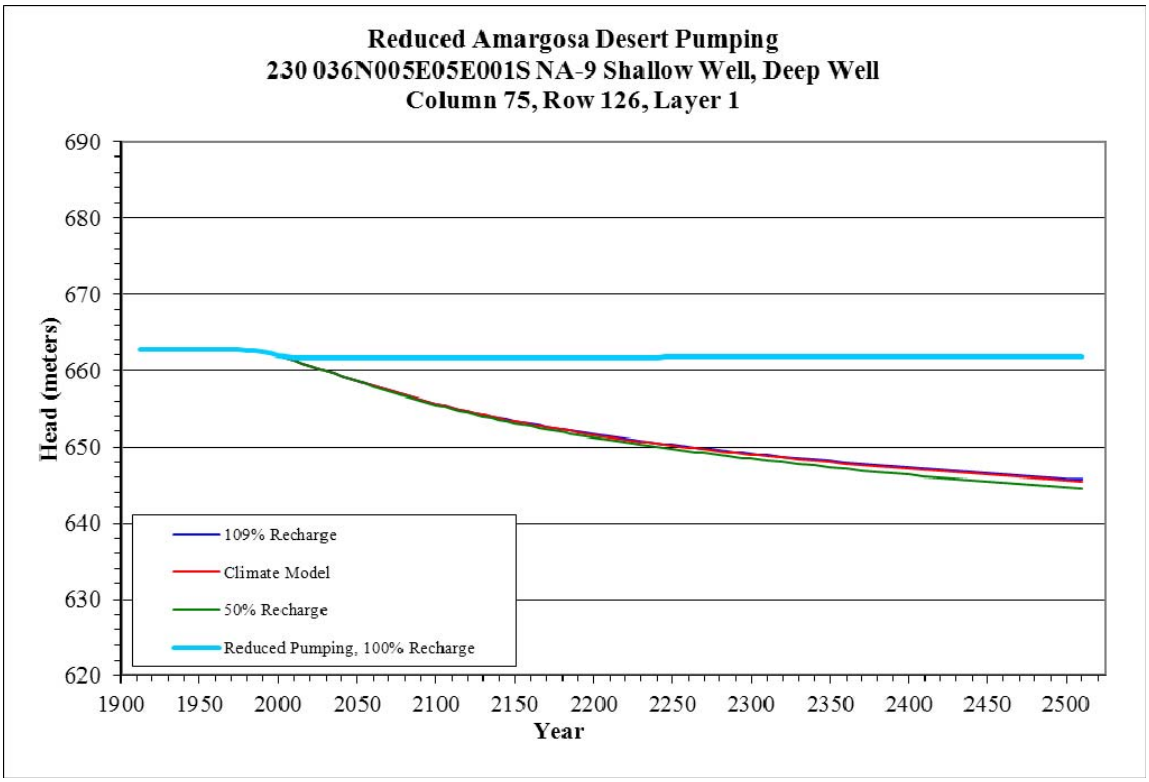

Figure B-112. Head Changes with Pumping Minimized: Column 75, Row 126, Layer 1

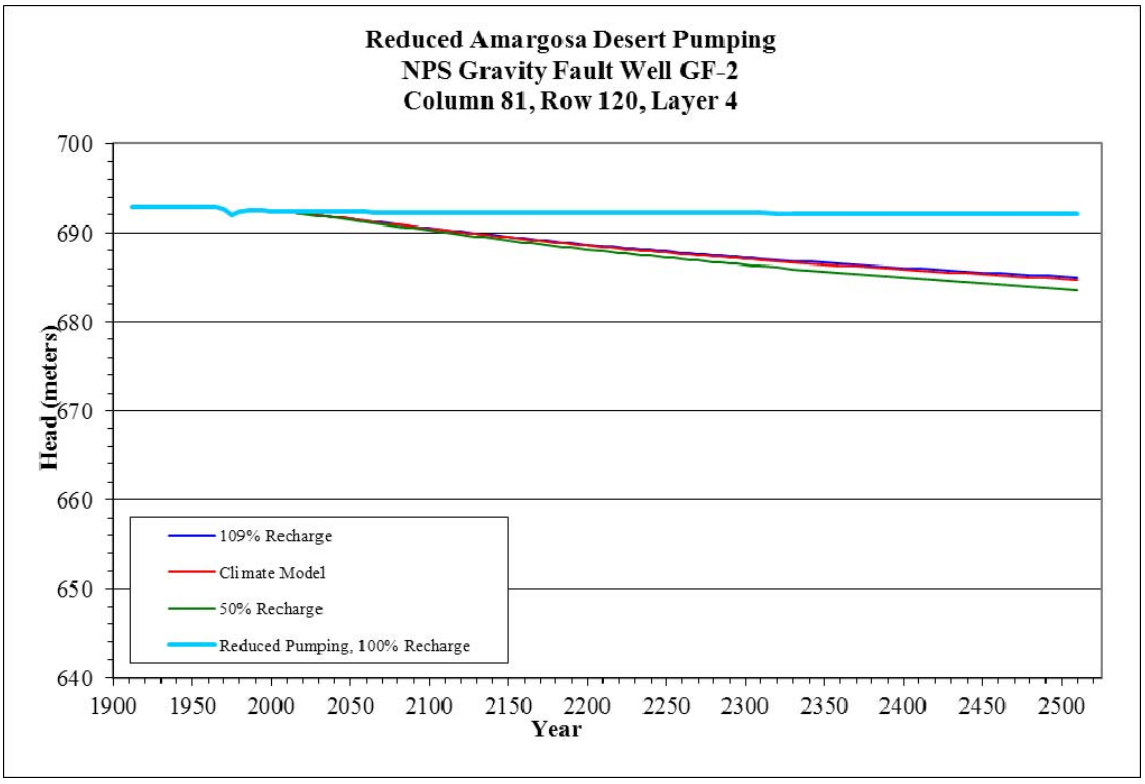

Figure B-113. Head Change with Pumping Minimized: Column 81, Row 120, Layer 4

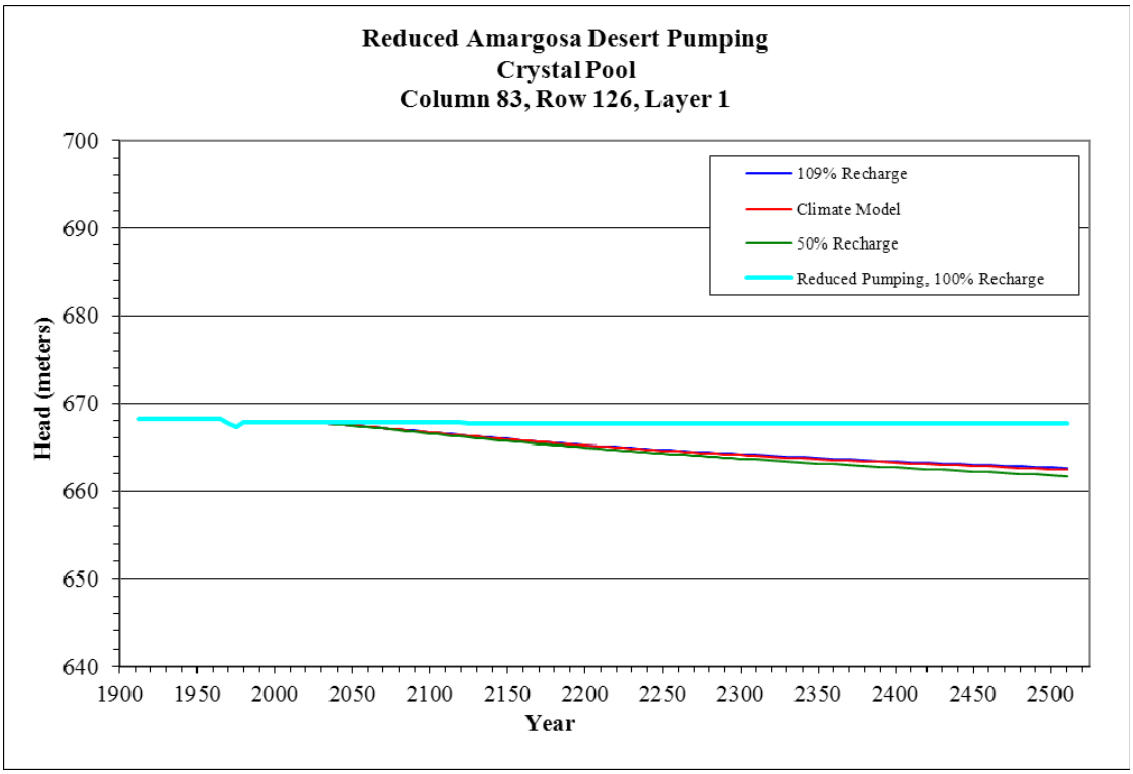

Figure B-114. Head Change with Pumping Minimized: Column 83, Row 126, Layer 1

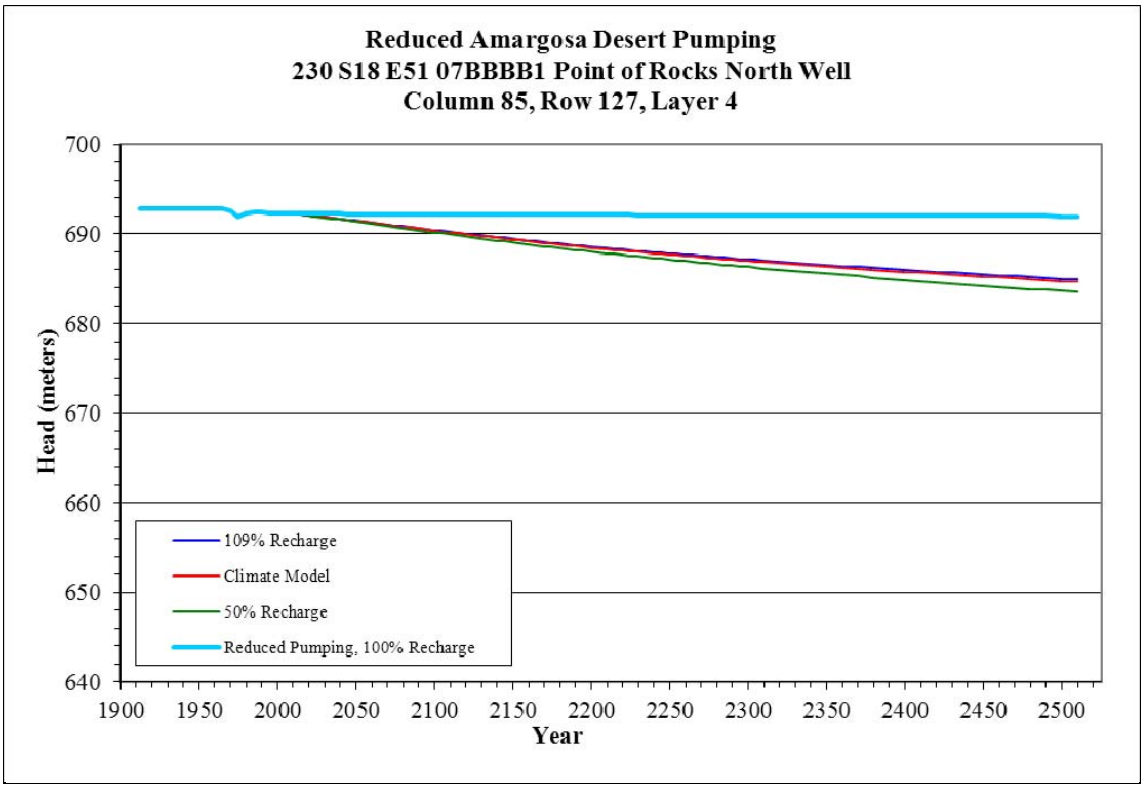

Figure B-115. Head Change with Pumping Minimized: Column 85, Row 127, Layer 4

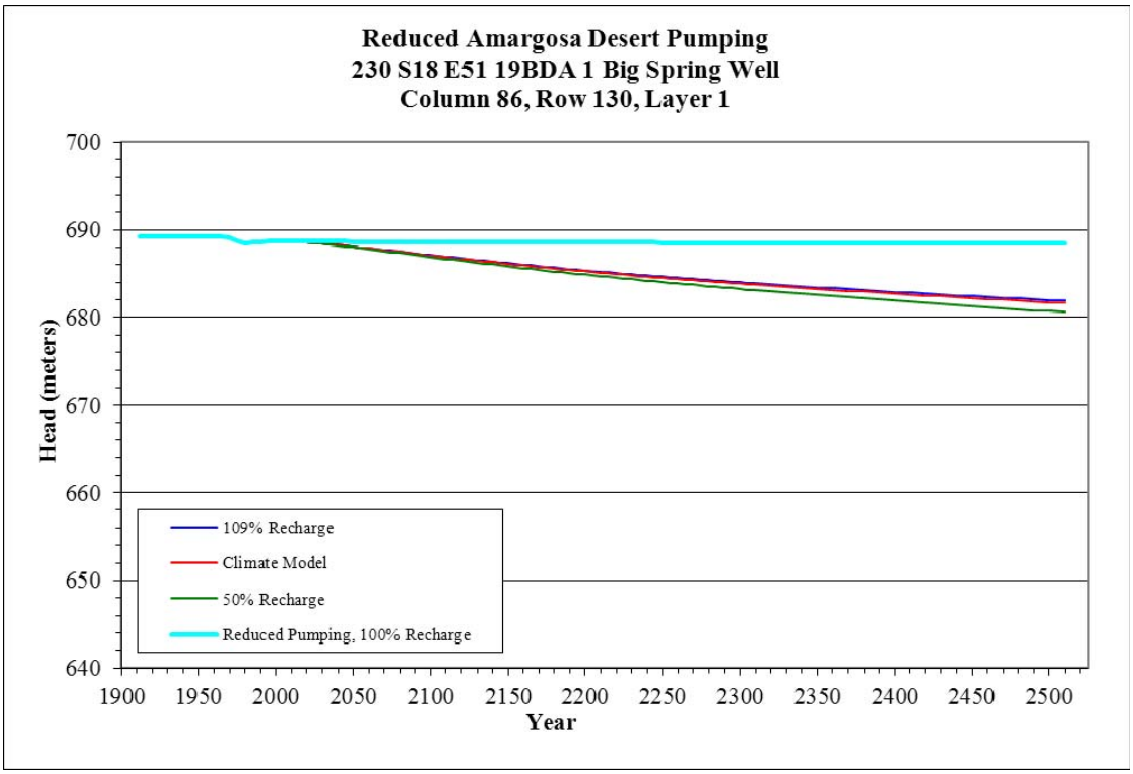

Figure B-116. Head Changes with Pumping Minimized: Column 86, Row 130, Layer 1

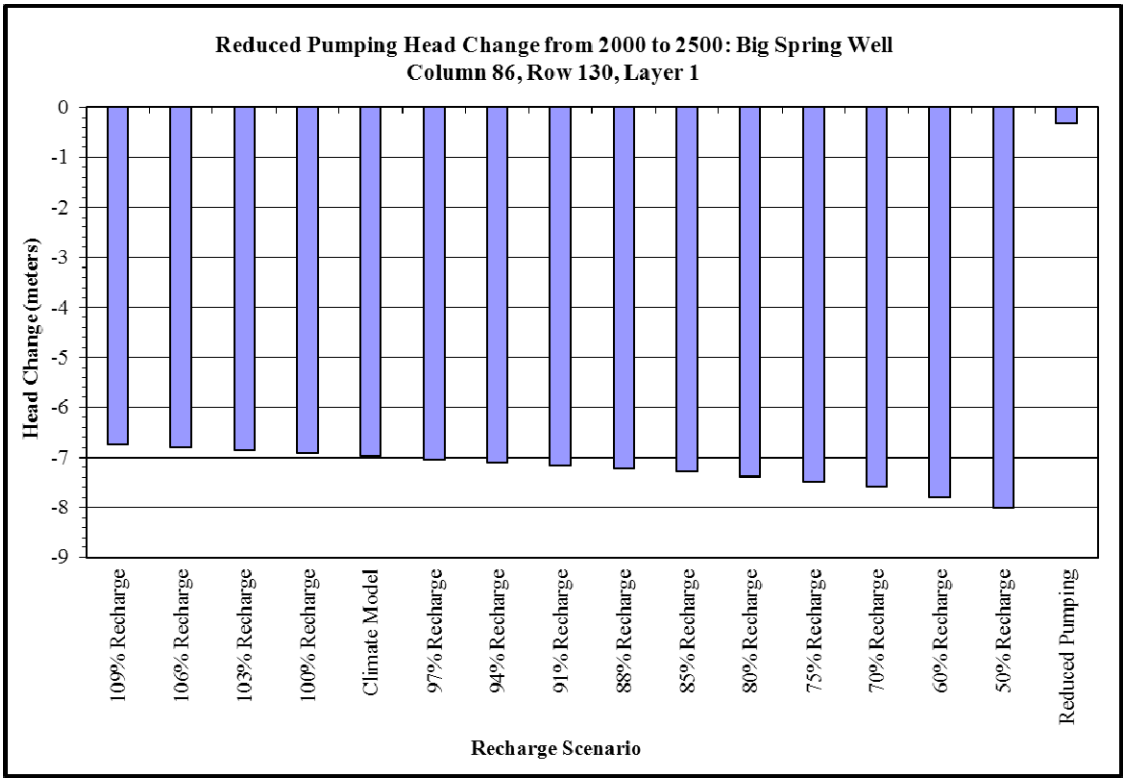

Figure B-117. Quantified Head Change: Pumping Minimized: Col 86, Row 130, Layer 1

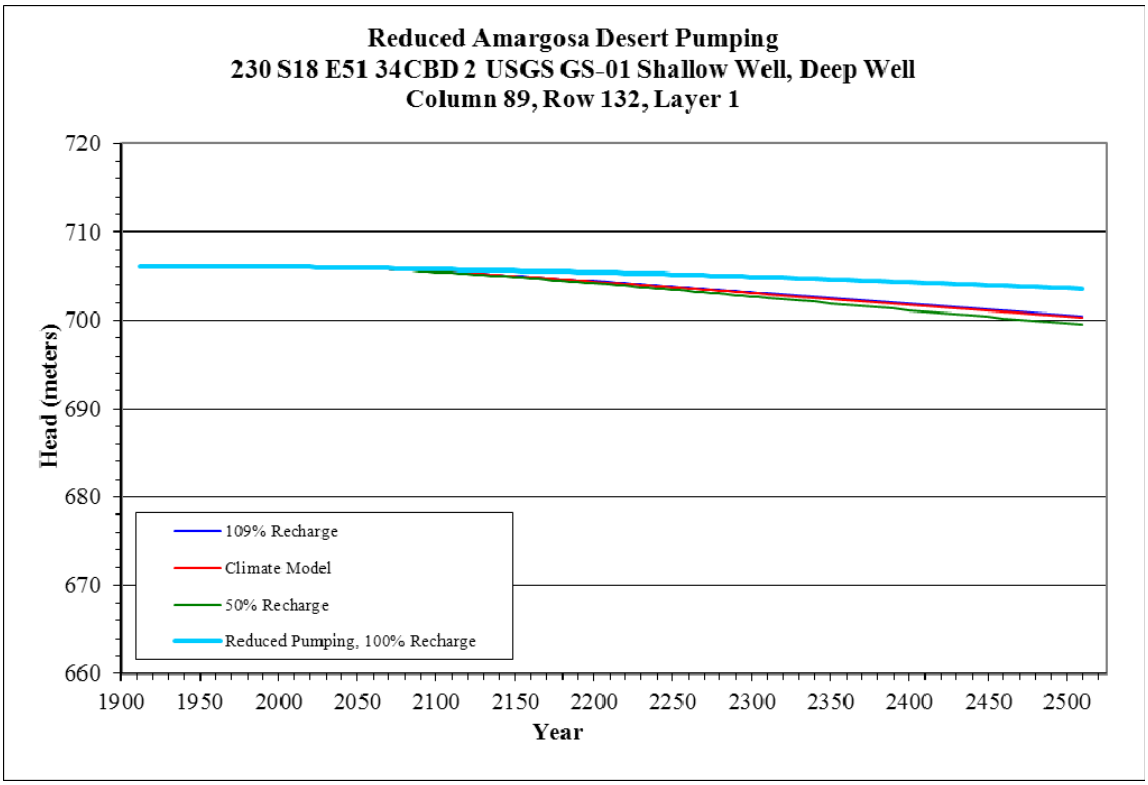

Figure B-118. Head Change with Pumping Minimized: Column 89, Row 132, Layer 1

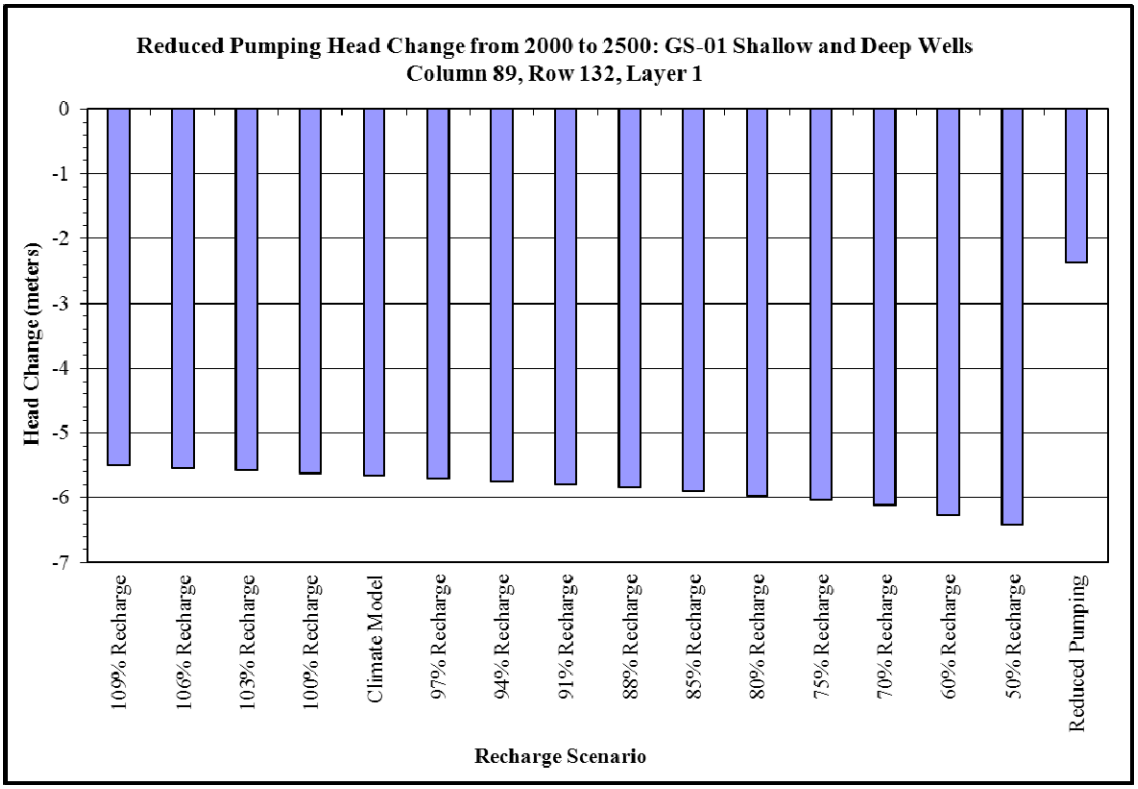

Figure B-119. Quantified Head Change: Pumping Minimized: Col 89, Row 132, Layer 1

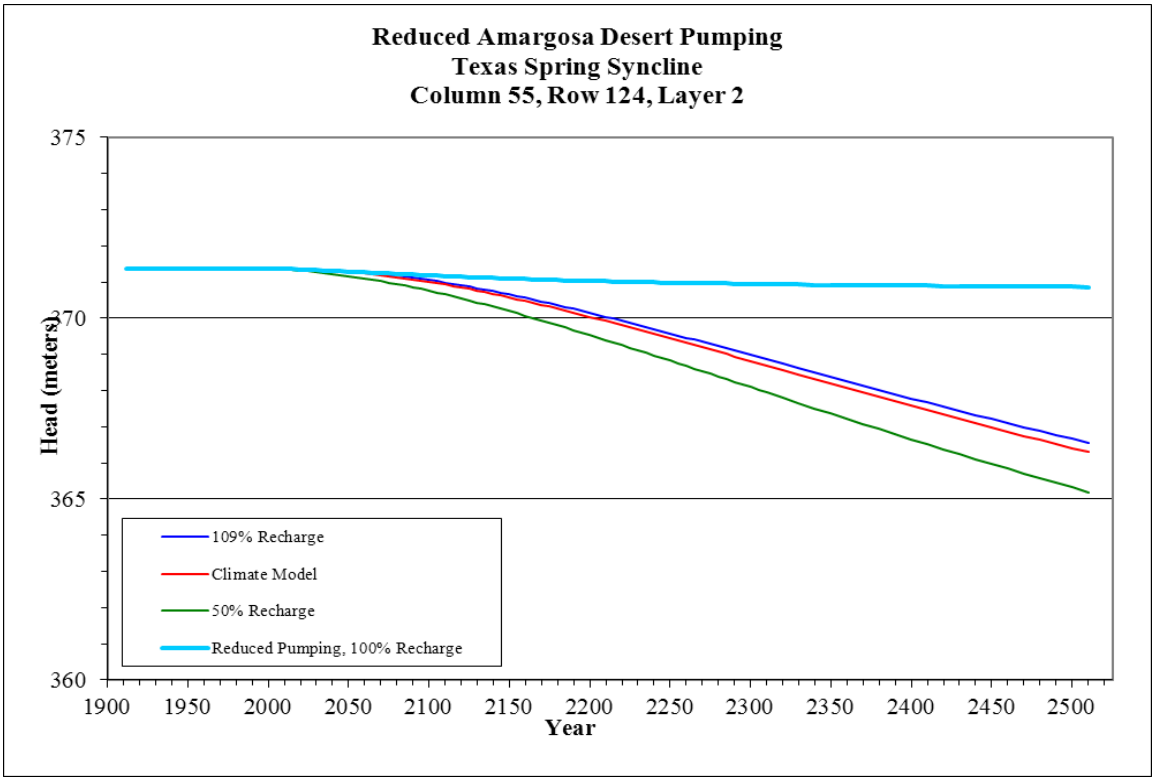

Figure B-120. Head Change with Pumping Minimized: Column 55, Row 124, Layer 2

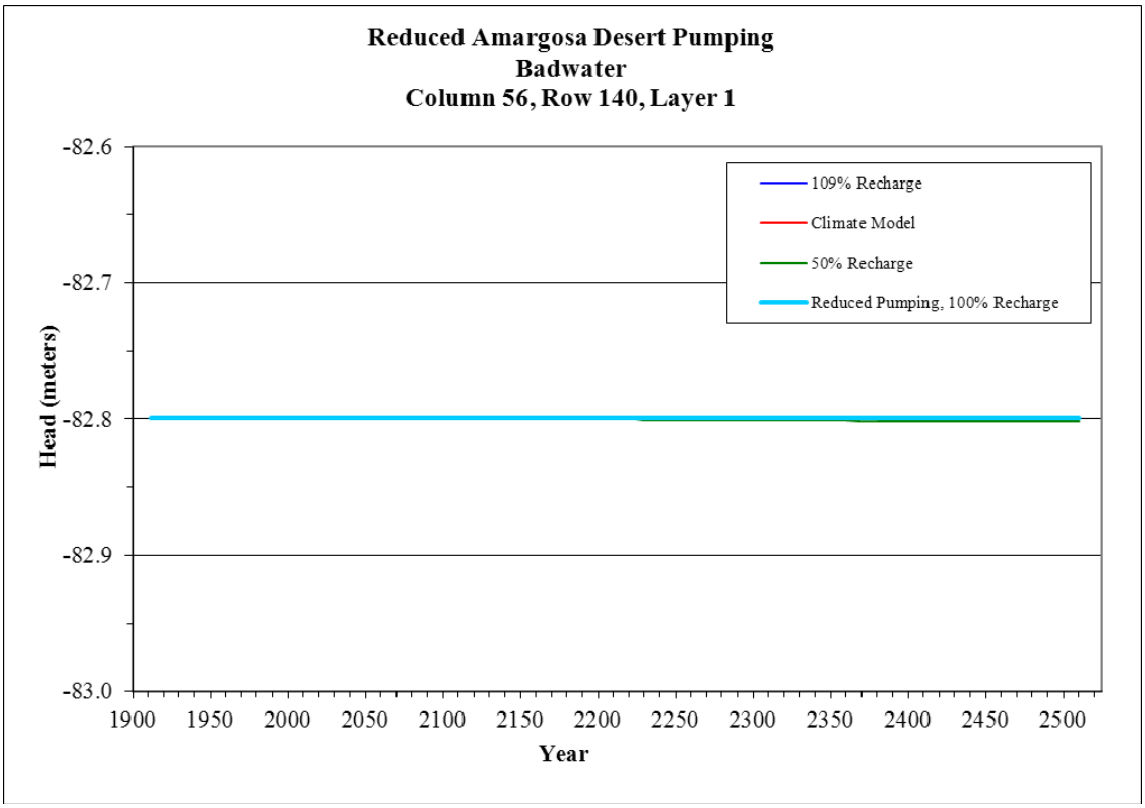

Figure B-121. Head Changes with Pumping Minimized: Column 56, Row 140, Layer 1

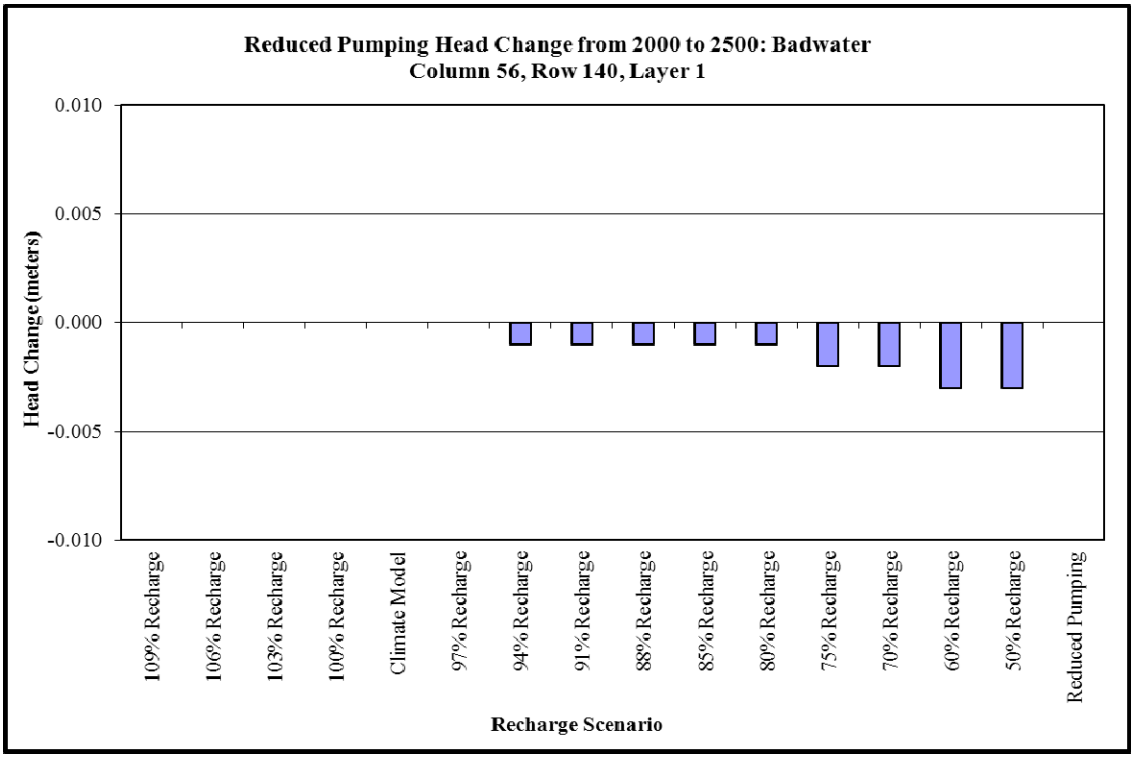

Figure B-122. Quantified Head Change: Pumping Minimized: Col 56, Row 140, Layer 1

Appendix C Model Layer 1 Contour Plots

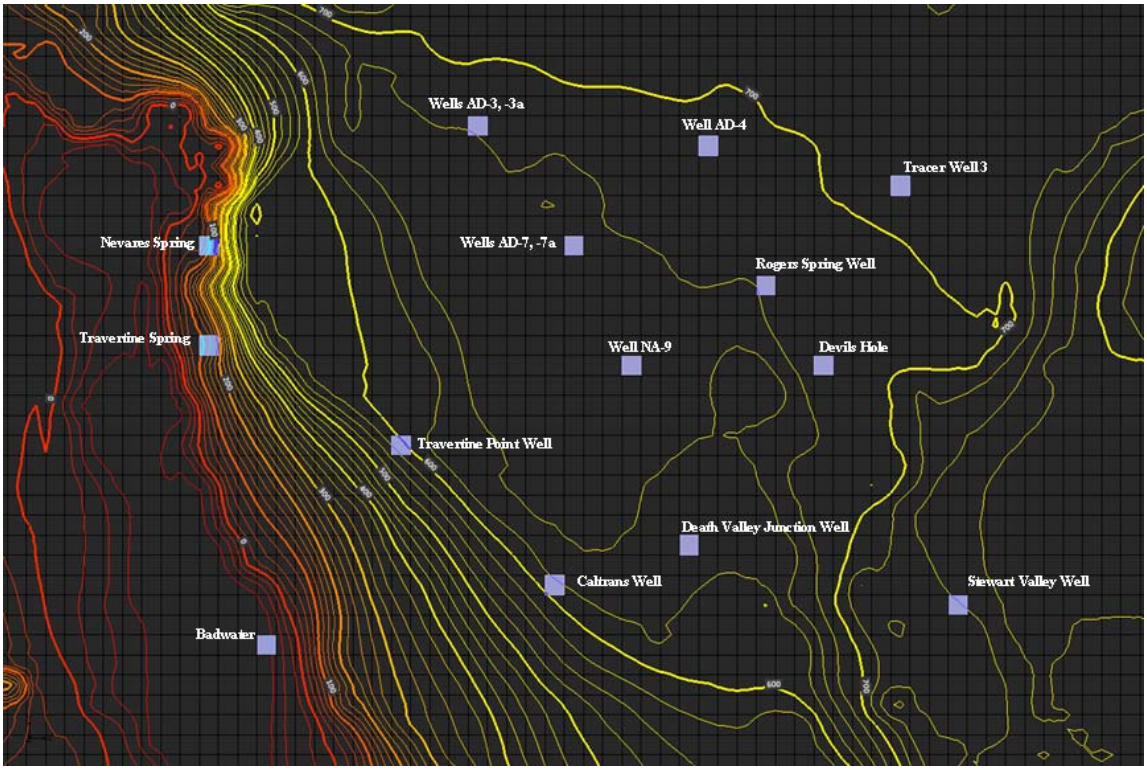

Figure C-130. Simulated Contours, Year 2000 Baseline Recharge

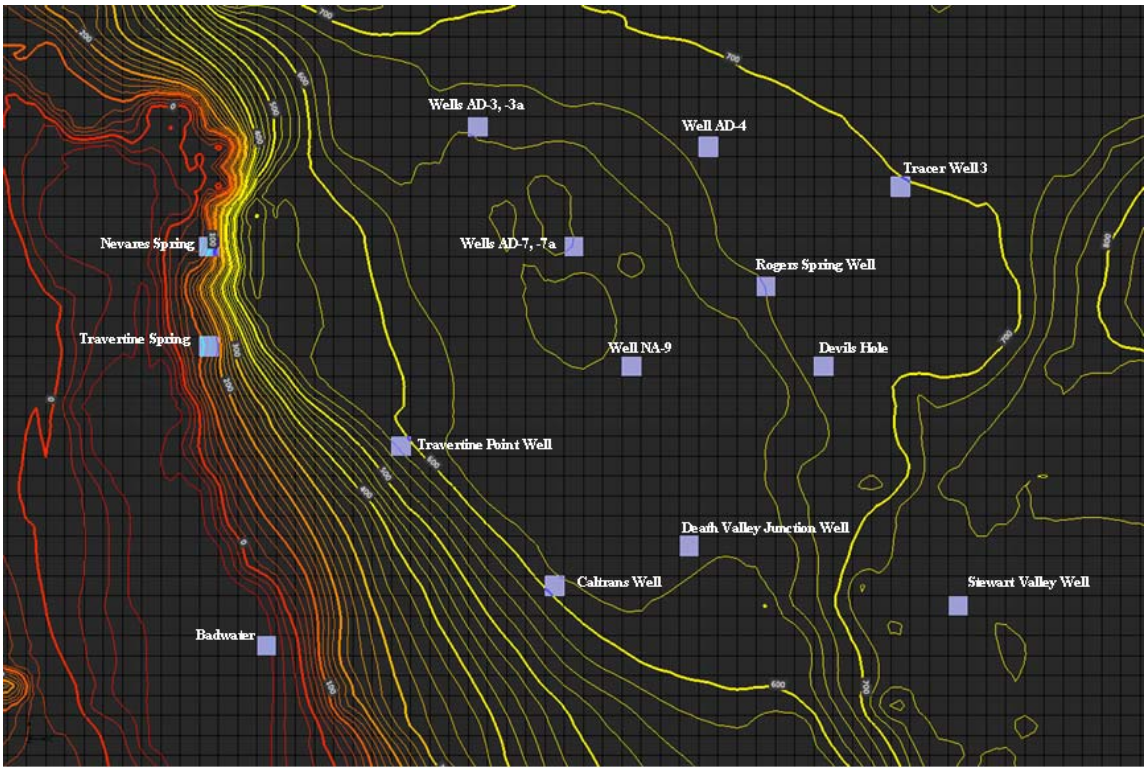

Figure C-131. Simulated Contours, Year 2500 with 109 % of Baseline Recharge

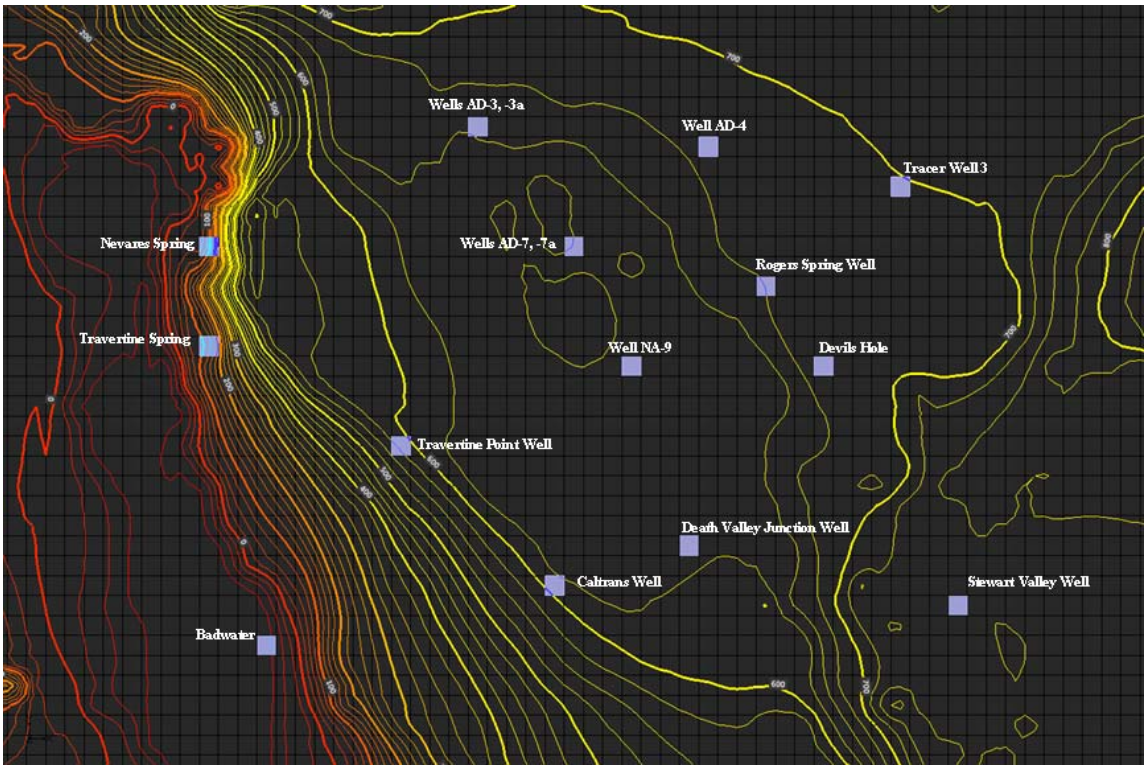

Figure C-132. Simulated Contours, Year 2500 with 106 % of Baseline Recharge

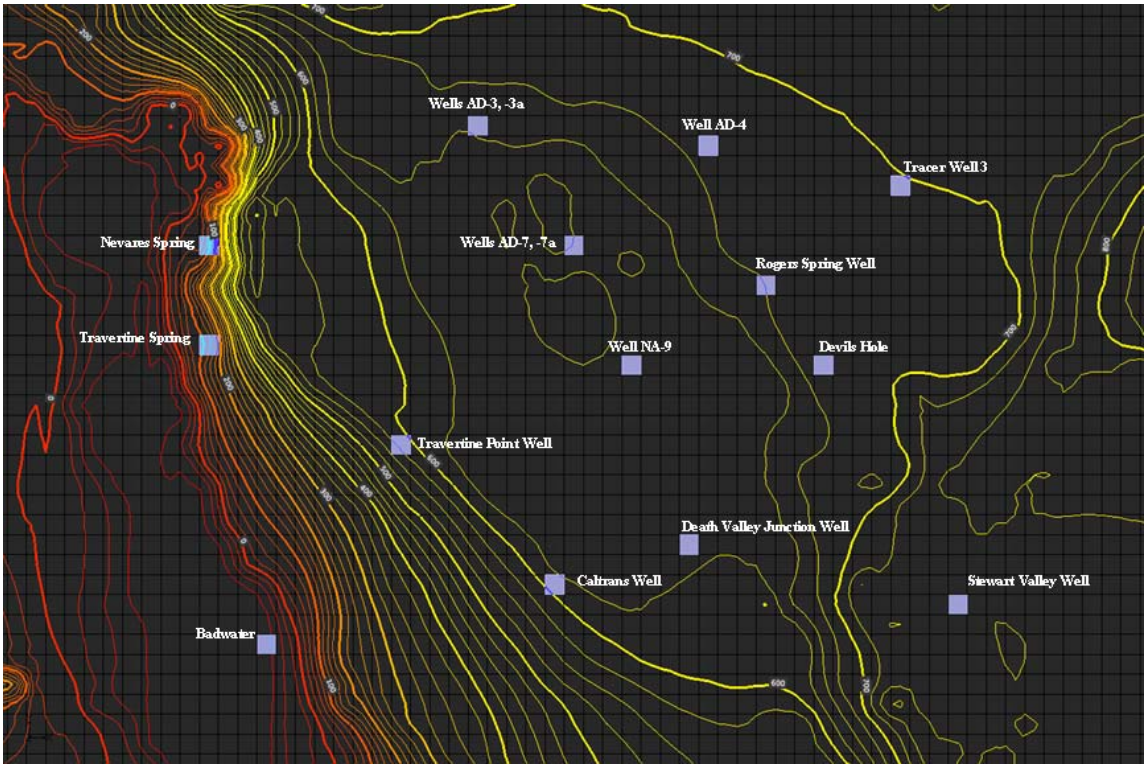

Figure C-133. Simulated Contours, Year 2500 with 103 % of Baseline Recharge

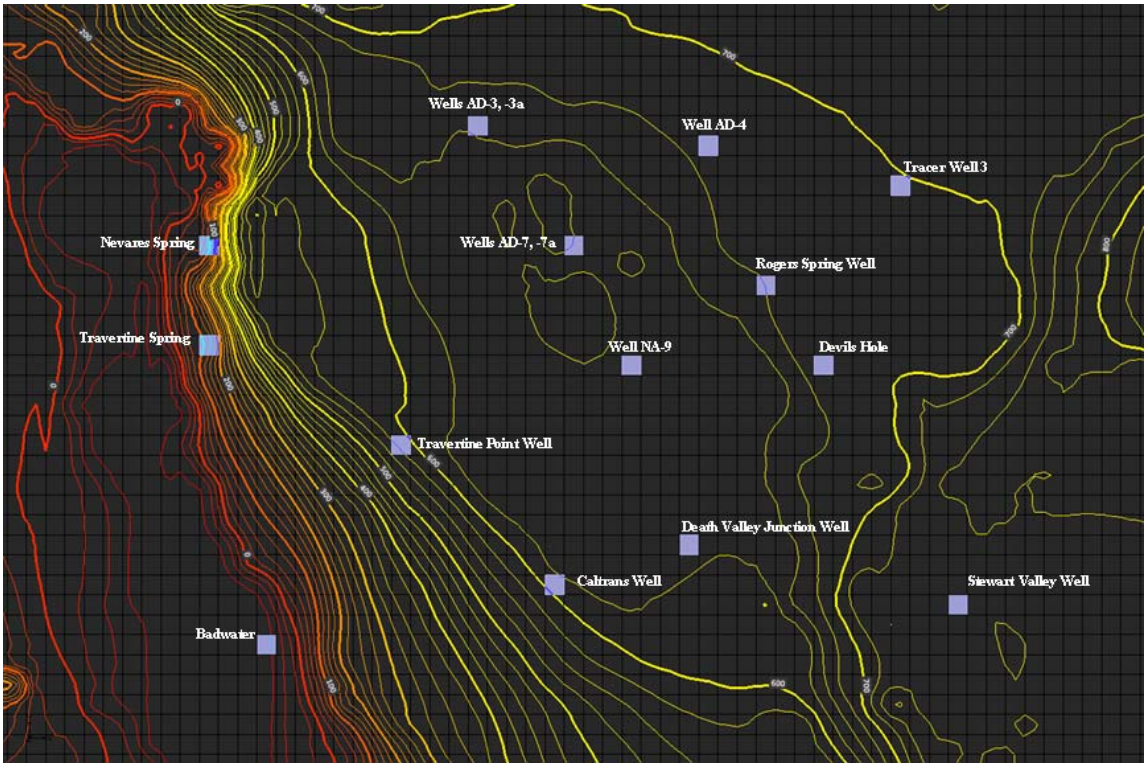

Figure C-134. Simulated Contours, Year 2500 with 100 % of Baseline Recharge

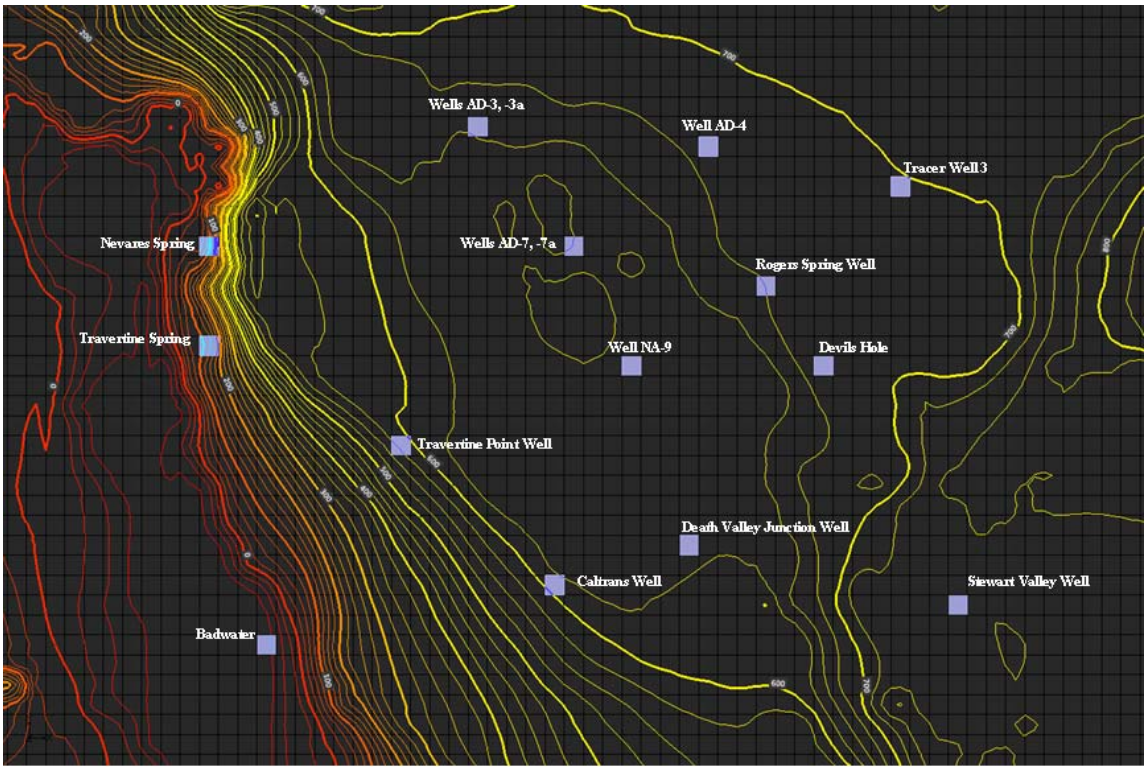

Figure C-135. Simulated Contours, Year 2500 Climate Model Recharge

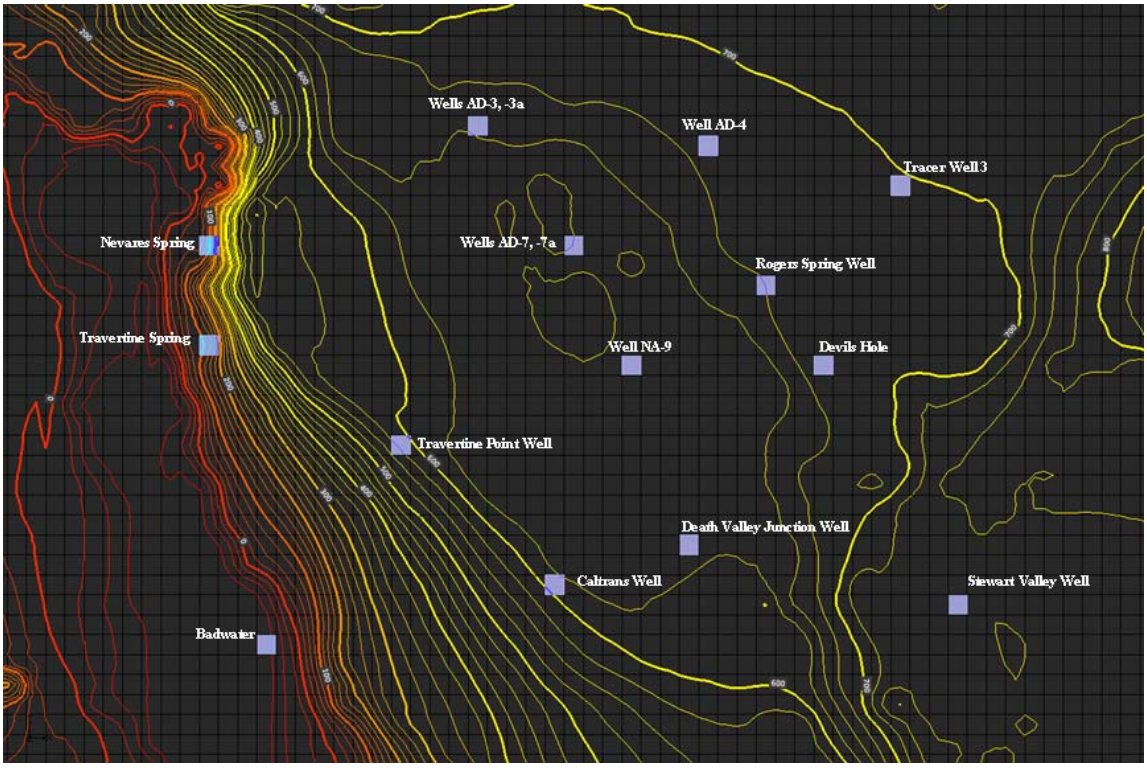

Figure C-136. Simulated Contours, Year 2500 with 97 % of Baseline Recharge

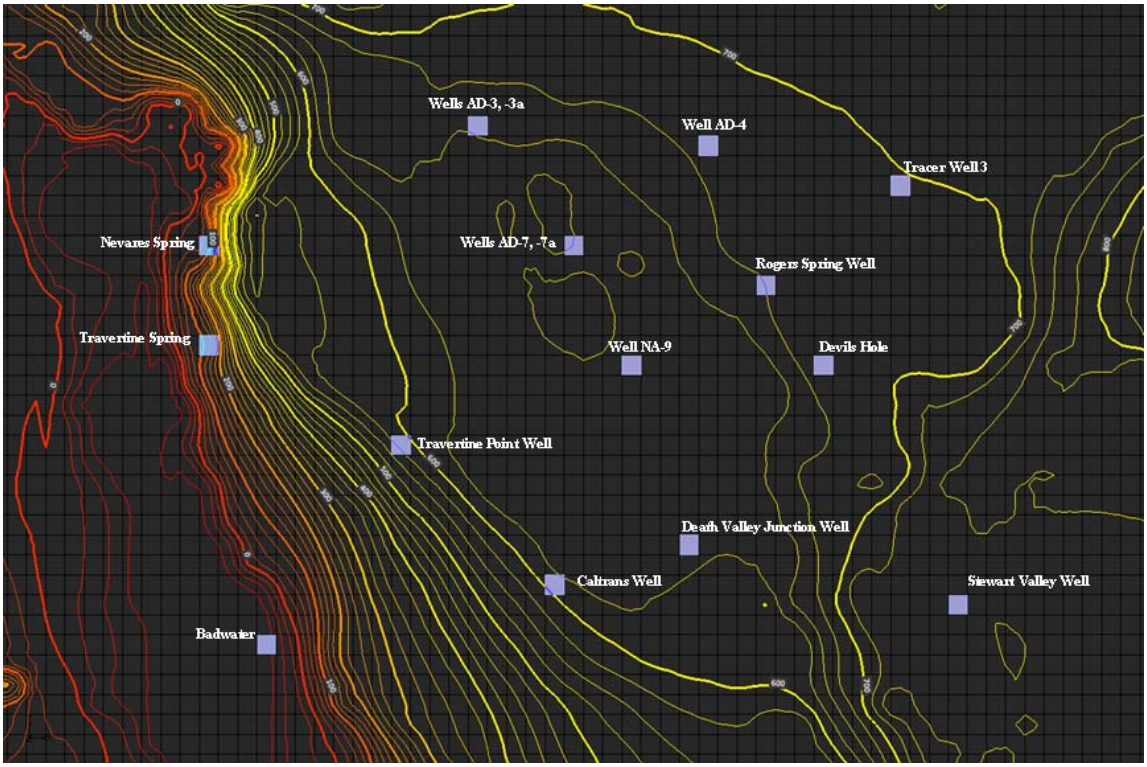

Figure C-137. Simulated Contours, Year 2500 with 94 % of Baseline Recharge

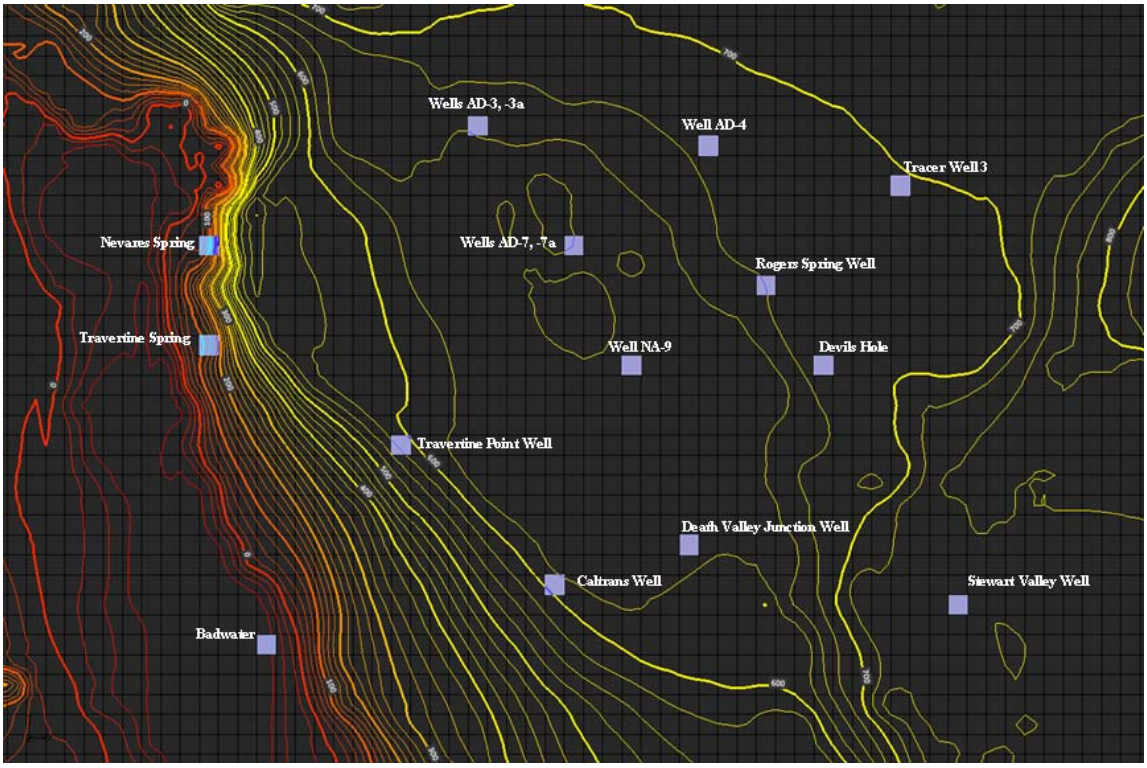

Figure C-138. Simulated Contours, Year 2500 with 91 % of Baseline Recharge

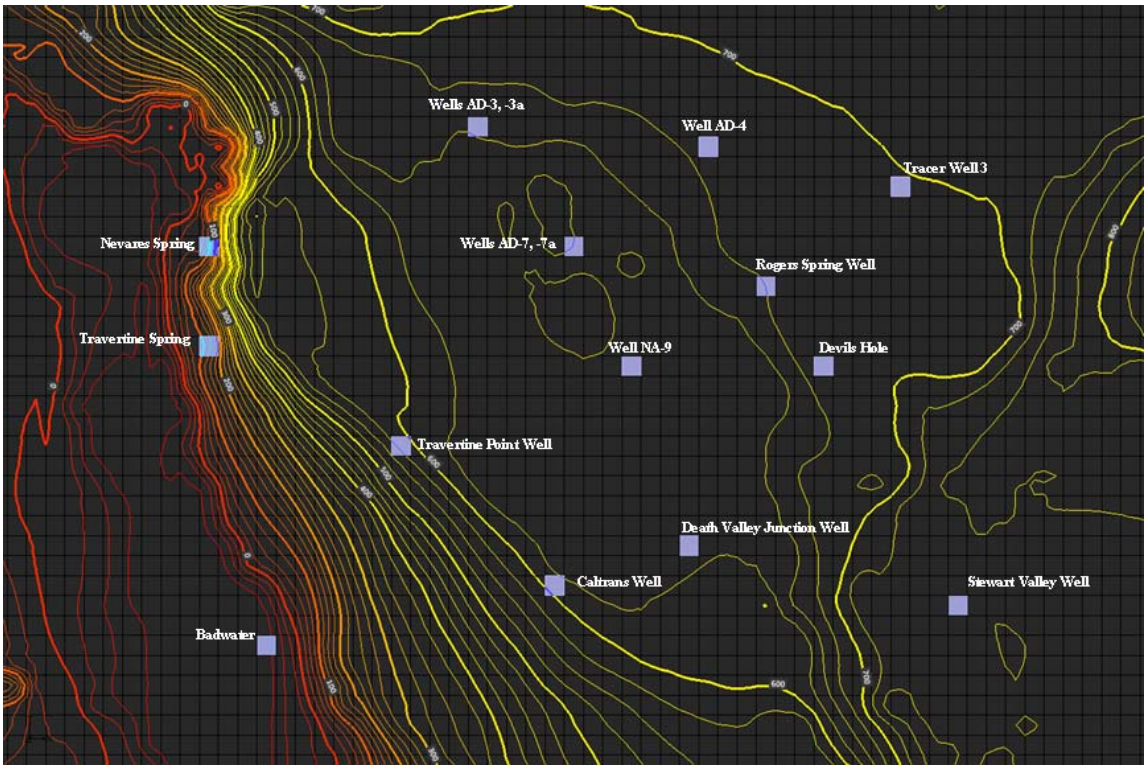

Figure C-139. Simulated Contours, Year 2500 with 88 % of Baseline Recharge

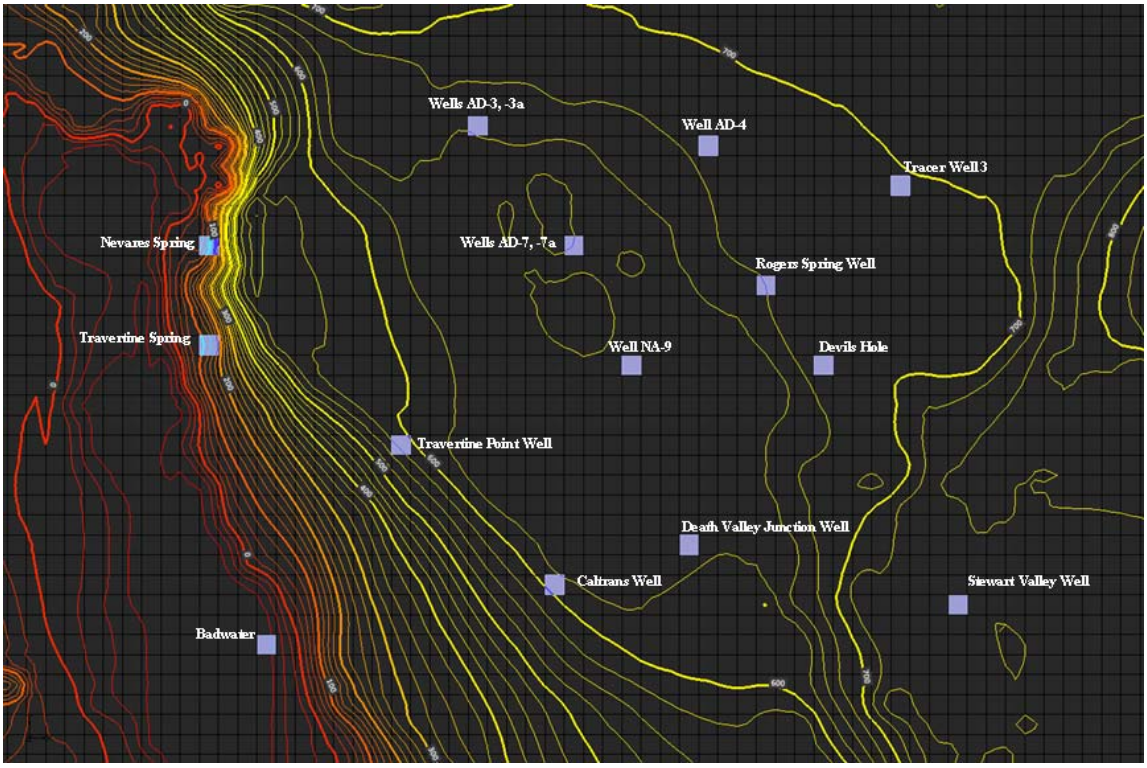

Figure C-140. Simulated Contours, Year 2500 with 85 % of Baseline Recharge

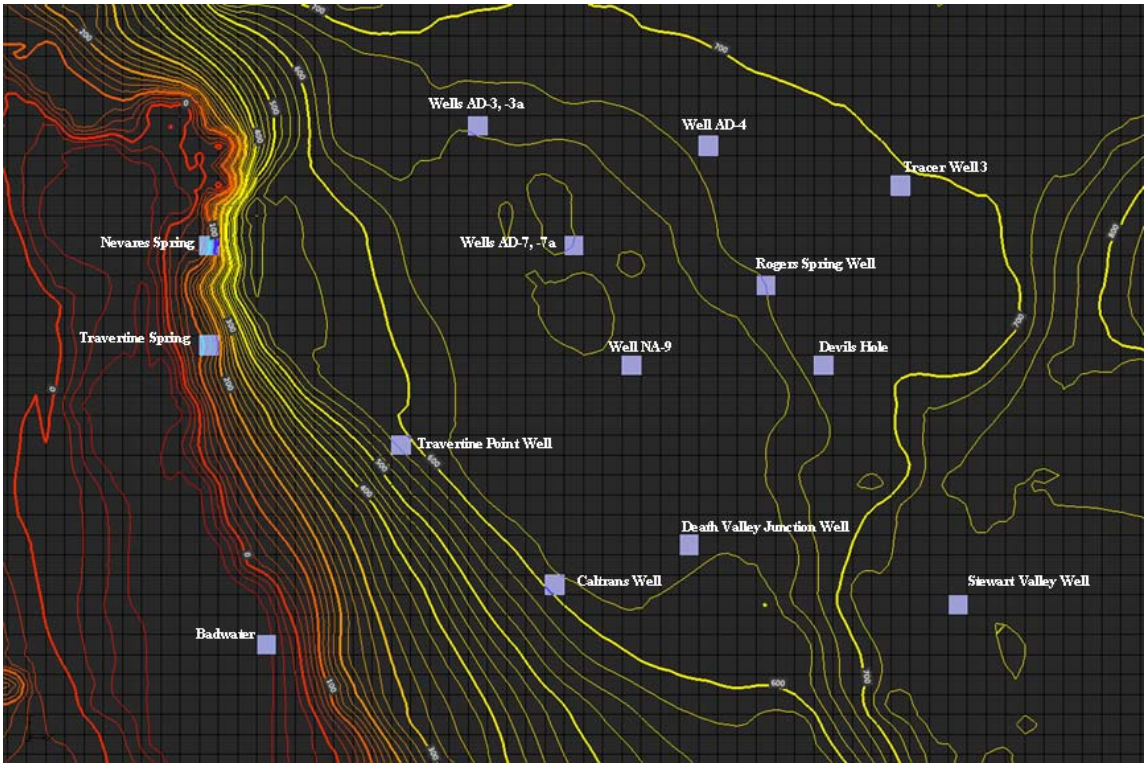

Figure C-141. Simulated Contours, Year 2500 with 80 % of Baseline Recharge

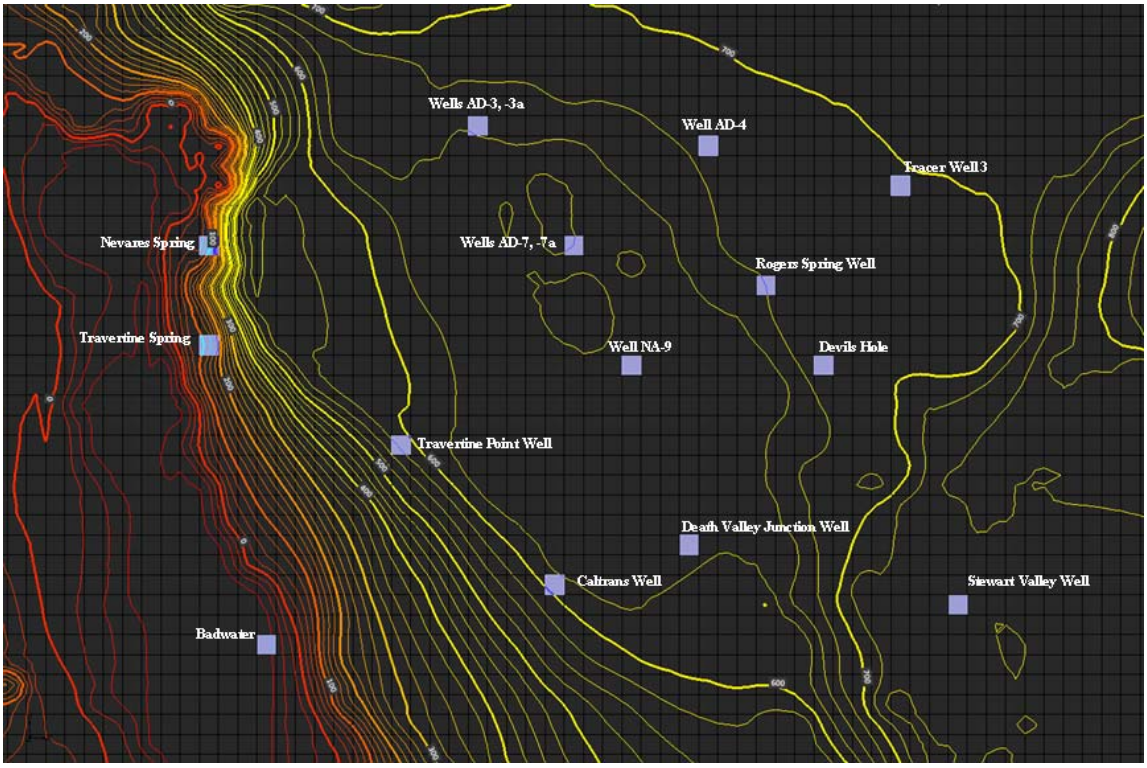

Figure C-142. Simulated Contours, Year 2500 with 75 % of Baseline Recharge

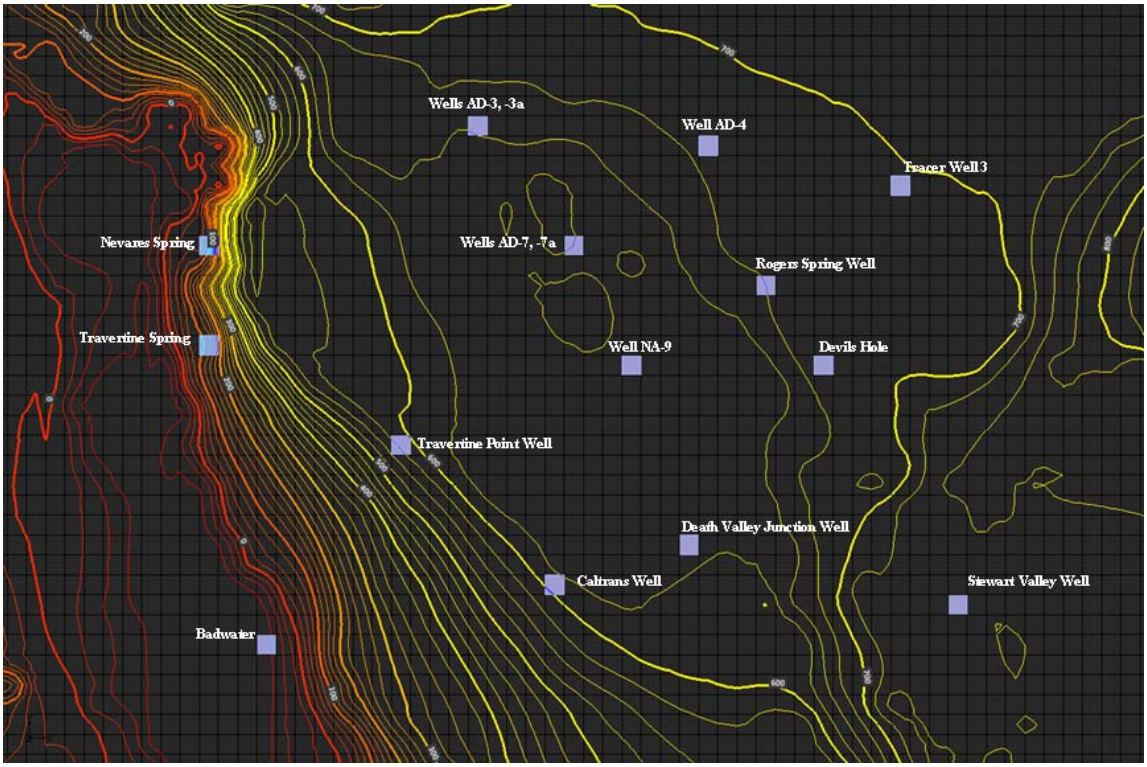

Figure C-143. Simulated Contours, Year 2500 with 70 % of Baseline Recharge

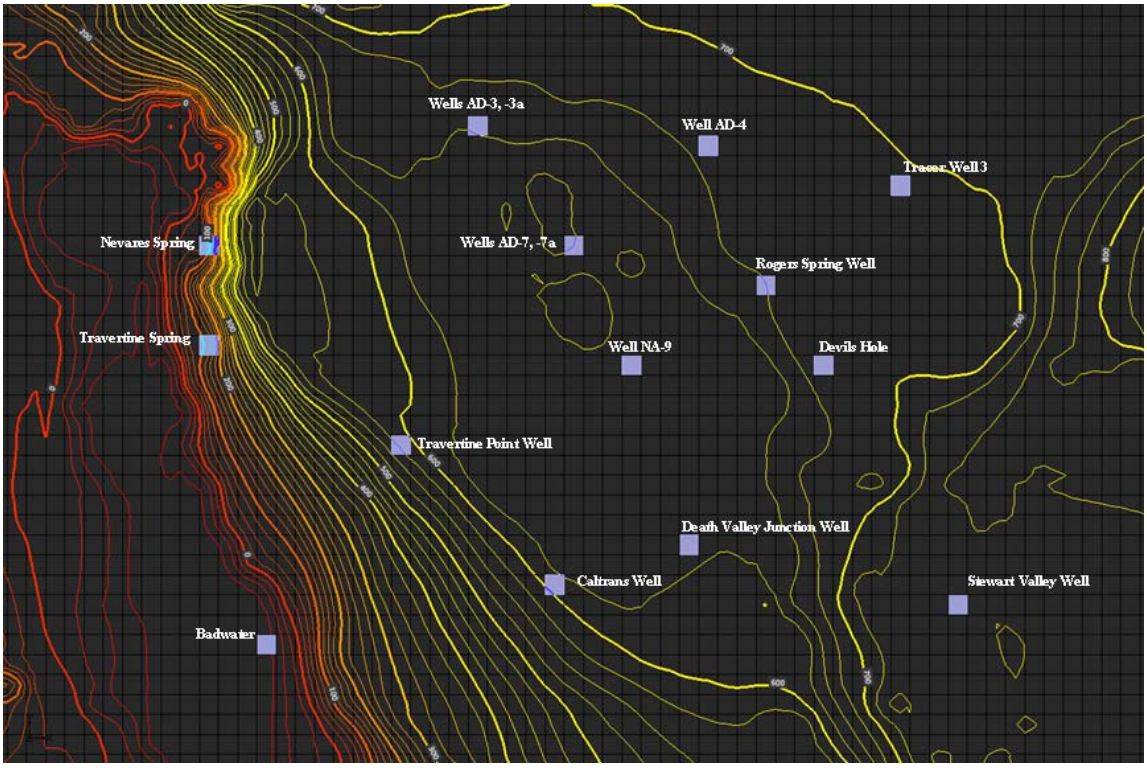

Figure C-144. Simulated Contours, Year 2500 with 60 % of Baseline Recharge

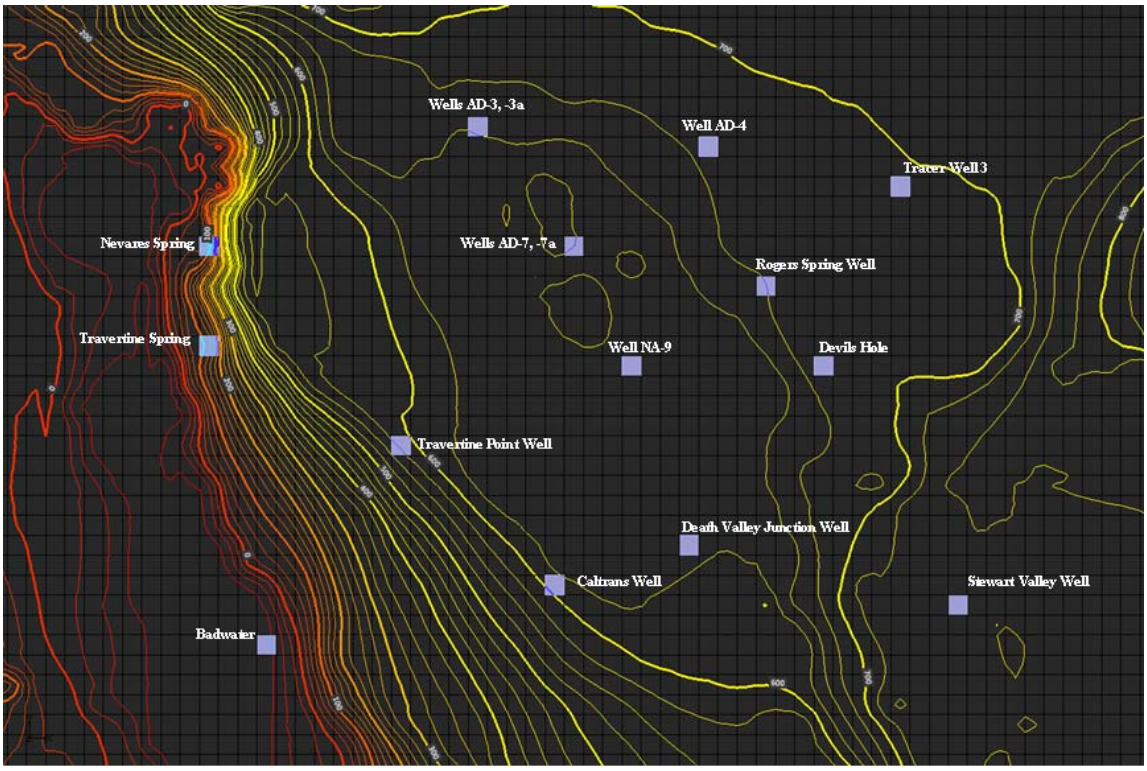

Figure C-145. Simulated Contours, Year 2500 with 50 % of Baseline Recharge

Appendix D Drain Cell Discharge Tables and Graphs

Simulation of 106 Percent of 20th Century Recharge

In the simulation with recharge at 106 percent of 20th Century rates, discharge from drain cells declined from 2000 to 2500 at all locations in the study area, except for the Badwater cell. Table D-1 presents the discharge data for selected years relative to the baseline recharge condition.

Table D-1. Drain Cell Discharge, 106 % of 20th Century Recharge (m^3/day)

Year	Model Domain	Study Area	Amargosa Desert	Ash Meadows South	Ash Meadows North	Stewart Valley	Big Spring	Amargosa Flat
1912	362,455	123,370	72,474	48,401	12,076	3,116	2,544	2,459
2000	345,347	122,580	71,688	47,924	11,926	3,070	2,521	2,380
2100	331,391	118,430	67,538	45,549	11,031	2,738	2,433	2,078
2200	323,043	114,280	63,413	43,263	10,291	2,395	2,349	1,601
2300	318,981	111,040	60,227	41,569	9,785	2,093	2,283	1,190
2400	316,057	108,440	57,695	40,244	9,401	1,822	2,230	869
2500	313,660	106,250	55,584	39,138	9,083	1,573	2,184	637
Total Change 2000 to 2500	-31,687	-16,330	-16,104	-8,786	-2,843	-1,497	-337	-1,743
% Change 2000 to 2500	-9.18%	-13.32%	-22.46%	-18.33%	-23.84%	-48.76%	-13.36%	-73.25%
Baseline (100% Recharge) Change	-32,438	-16,630	-16,341	-8,913	-2,880	-1,525	-343	-1,772
Difference Relative to Baseline	752	300	237	127	37	28	6	29

Year	Crystal Pool	Fairbanks Spring	Amargosa River	Death Valley	Travertine Springs	Nevares Spring	Badwater	Texas Spring
1912	1,543	1,120	546	50,896	3,415	2,728	1,665	1,455
2000	1,520	1,105	520	50,895	3,415	2,728	1,665	1,455
2100	1,433	1,048	329	50,895	3,410	2,727	1,665	1,454
2200	1,348	993	193	50,867	3,389	2,722	1,666	1,451
2300	1,282	950	107	50,815	3,358	2,716	1,666	1,447
2400	1,229	915	67	50,745	3,322	2,708	1,667	1,441
2500	1,183	885	35	50,666	3,285	2,700	1,667	1,435
Total Change 2000 to 2500	-337	-220	-485	-229	-131	-28	2	-20
% Change 2000 to 2500	-22.18%	-19.92%	-93.20%	-0.45%	-3.82%	-1.02%	0.13%	-1.36%
Baseline (100% Recharge) Change	-343	-224	-488	-287	-135	-29	-1	-21
Difference Relative to Baseline	6	4	3	58	4	1	3	1

The comparative change in discharge for each drain cell or group of drain cells evaluated for the 106 percent of 20th Century recharge simulation is shown in Figures D-1 through D-3.

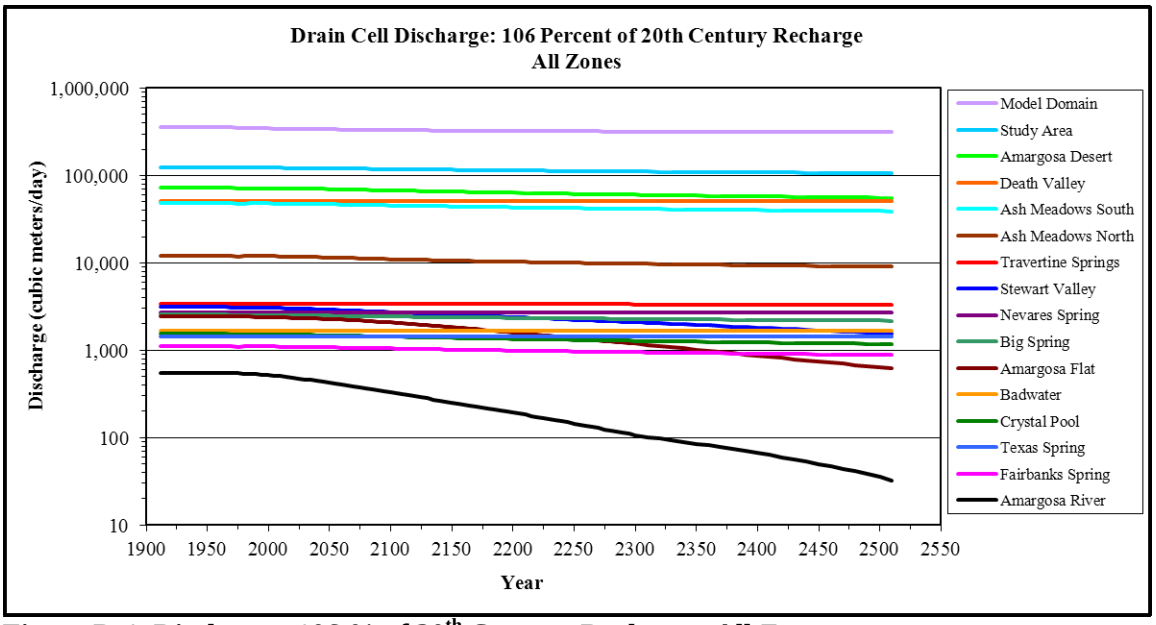

Figure D-1. Discharge: 106 % of 20th Century Recharge, All Zones

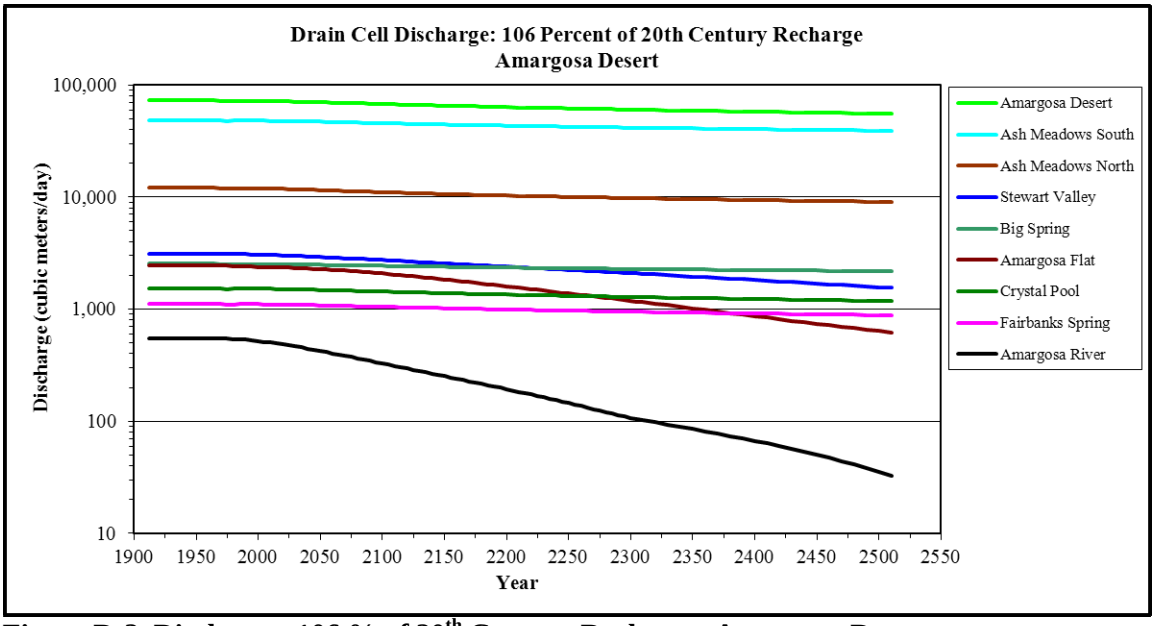

Figure D-2. Discharge: 106 % of 20th Century Recharge, Amargosa Desert

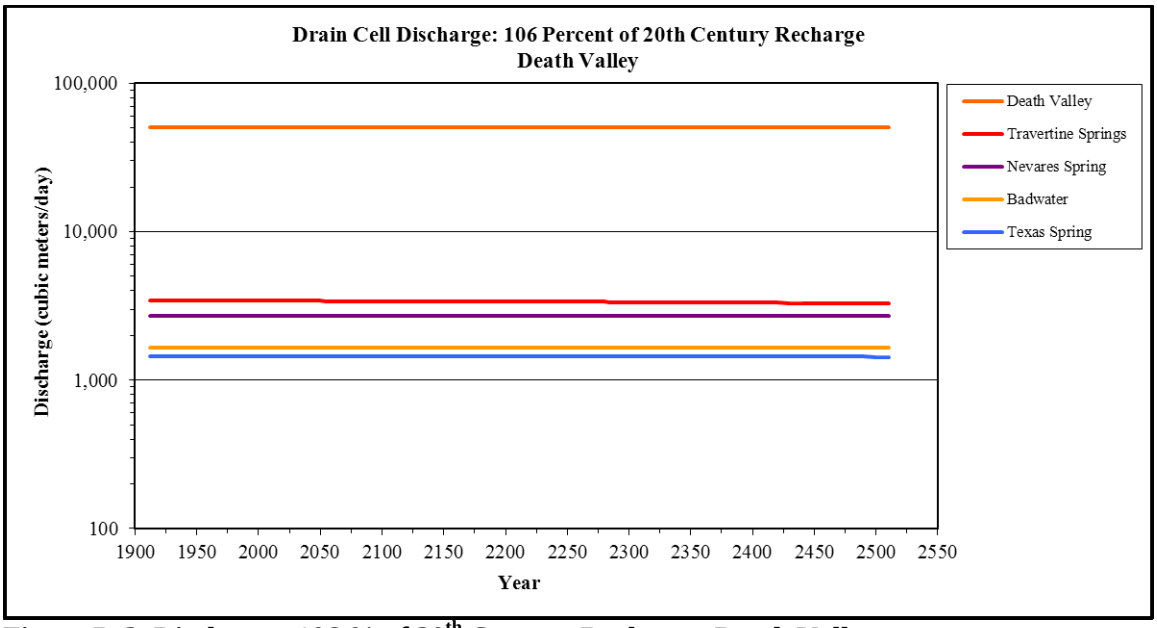

Figure D-3. Discharge: 106 % of 20th Century Recharge, Death Valley

Simulation of 103 Percent of 20th Century Recharge

In the simulation with recharge at 103 percent of 20th Century rates, discharge from drain cells declined from 2000 to 2500 at all locations in the study area, except for the Badwater cell. Table D-2 presents the discharge data for selected years relative to the baseline recharge condition.

Table D-2. Drain Cell Discharge, 103 % of 20th Century Recharge (m^3/day)

Year	Model Domain	Study Area	Amargosa Desert	Ash Meadows South	Ash Meadows North	Stewart Valley	Big Spring	Amargosa Flat
1912	362,455	123,370	72,474	48,401	12,076	3,116	2,544	2,459
2000	345,347	122,580	71,688	47,924	11,926	3,070	2,521	2,380
2100	331,294	118,410	67,516	45,539	11,027	2,734	2,433	2,075
2200	322,864	114,220	63,363	43,238	10,284	2,387	2,347	1,594
2300	318,742	110,950	60,155	41,533	9,774	2,083	2,281	1,179
2400	315,749	108,320	57,599	40,195	9,386	1,810	2,227	856
2500	313,290	106,110	55,471	39,078	9,066	1,559	2,181	623
Total Change 2000 to 2500	-32,057	-16,470	-16,217	-8,846	-2,861	-1,511	-340	-1,757
% Change 2000 to 2500	-9.28%	-13.44%	-22.62%	-18.46%	-23.99%	-49.21%	-13.47%	-73.83%
Baseline (100% Recharge) Change	-32,438	-16,630	-16,341	-8,913	-2,880	-1,525	-343	-1,772
Difference Relative to Baseline	381	160	124	67	20	14	3	15

Year	Crystal Pool	Fairbanks Spring	Amargosa River	Death Valley	Travertine Springs	Nevares Spring	Badwater	Texas Spring
1912	1,543	1,120	546	50,896	3,415	2,728	1,665	1,455
2000	1,520	1,105	520	50,895	3,415	2,728	1,665	1,455
2100	1,432	1,048	328	50,890	3,409	2,727	1,665	1,454
2200	1,347	992	192	50,856	3,388	2,722	1,665	1,451
2300	1,281	949	106	50,797	3,357	2,715	1,665	1,447
2400	1,227	913	65	50,722	3,320	2,708	1,665	1,441
2500	1,180	883	34	50,637	3,283	2,700	1,665	1,435
Total Change 2000 to 2500	-340	-222	-486	-258	-133	-28	1	-20
% Change 2000 to 2500	-22.35%	-20.09%	-93.48%	-0.51%	-3.89%	-1.04%	0.04%	-1.38%
Baseline (100% Recharge) Change	-343	-224	-488	-287	-135	-29	-1	-21
Difference Relative to Baseline	3	2	1	29	2	1	2	0

The comparative change in discharge for each drain cell or group of drain cells evaluated for the 103 percent of 20th Century recharge simulation is shown in Figures D-4 through D-6.

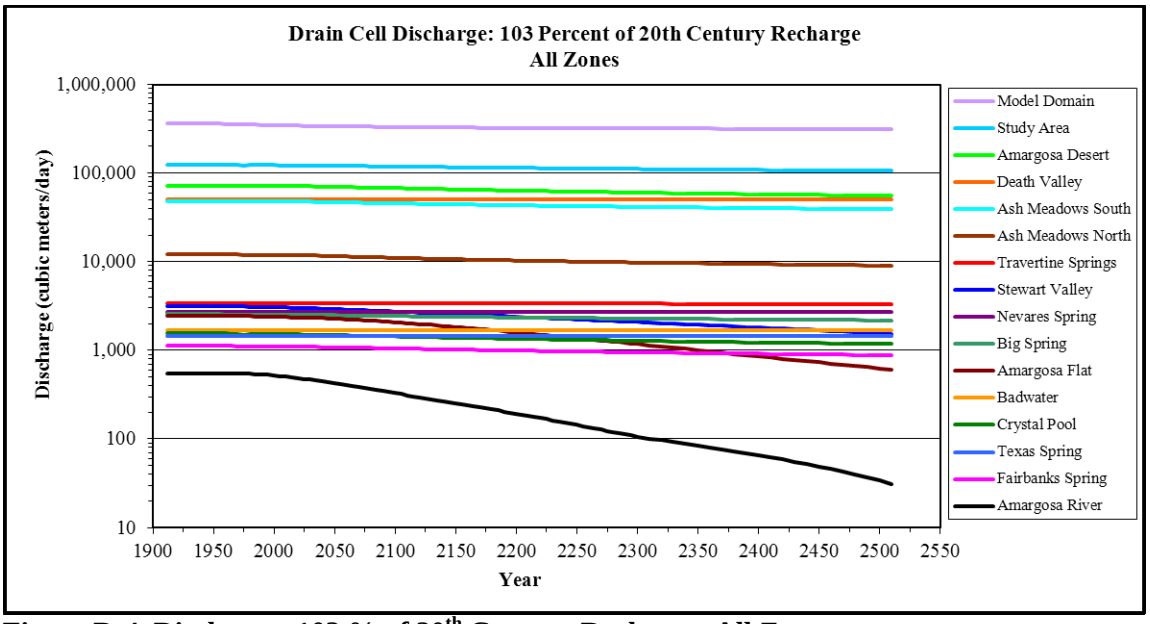

Figure D-4. Discharge: 103 % of 20th Century Recharge, All Zones

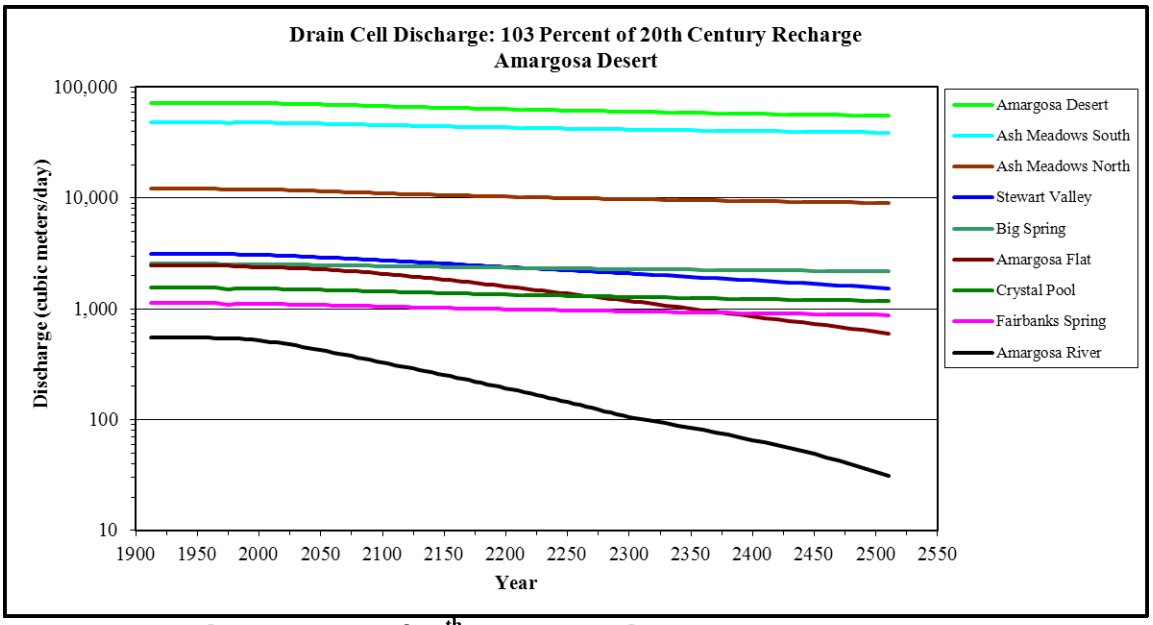

Figure D-5. Discharge: 103 % of 20th Century Recharge, Amargosa Desert

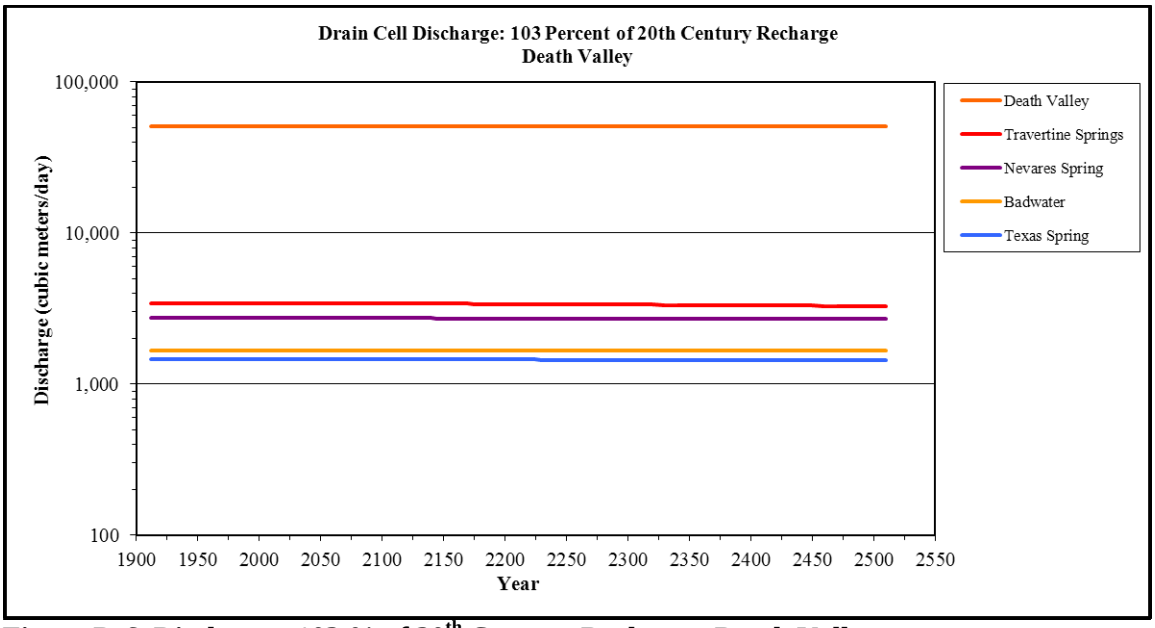

Figure D-6. Discharge: 103 % of 20th Century Recharge, Death Valley

Simulation of 97 Percent of 20th Century Recharge

In the simulation with recharge at 97 percent of 20th Century rates, discharge from drain cells declined from 2000 to 2500 at all locations in the study area. Table D-3 presents the discharge data for selected years relative to the baseline recharge condition.

Table D-3. Drain Cell Discharge, 97 % of 20th Century Recharge (m^3/day)

Year	Model Domain	Study Area	Amargosa Desert	Ash Meadows South	Ash Meadows North	Stewart Valley	Big Spring	Amargosa Flat
1912	362,455	123,370	72,474	48,401	12,076	3,116	2,544	2,459
2000	345,347	122,580	71,688	47,924	11,926	3,070	2,521	2,380
2100	331,056	118,340	67,464	45,513	11,020	2,724	2,432	2,070
2200	322,423	114,060	63,234	43,175	10,265	2,367	2,344	1,576
2300	318,078	110,690	59,945	41,425	9,743	2,055	2,276	1,150
2400	314,889	107,980	57,325	40,050	9,344	1,776	2,220	820
2500	312,234	105,690	55,129	38,893	9,012	1,520	2,172	583
Total Change 2000 to 2500	-33,113	-16,890	-16,559	-9,031	-2,915	-1,550	-348	-1,797
% Change 2000 to 2500	-9.59%	-13.78%	-23.10%	-18.84%	-24.44%	-50.50%	-13.82%	-75.52%
Baseline (100% Recharge) Change	-32,438	-16,630	-16,341	-8,913	-2,880	-1,525	-343	-1,772
Difference Relative to Baseline	-674	-260	-218	-118	-34	-25	-6	-25

Year	Crystal Pool	Fairbanks Spring	Amargosa River	Death Valley	Travertine Springs	Nevares Spring	Badwater	Texas Spring
1912	1,543	1,120	546	50,896	3,415	2,728	1,665	1,455
2000	1,520	1,105	520	50,895	3,415	2,728	1,665	1,455
2100	1,431	1,047	327	50,876	3,408	2,727	1,664	1,454
2200	1,343	990	190	50,826	3,386	2,722	1,664	1,451
2300	1,275	945	103	50,749	3,353	2,715	1,663	1,446
2400	1,220	909	62	50,657	3,315	2,707	1,662	1,440
2500	1,171	878	30	50,557	3,277	2,698	1,661	1,434
Total Change 2000 to 2500	-349	-228	-490	-338	-139	-30	-4	-21
% Change 2000 to 2500	-22.94%	-20.60%	-94.27%	-0.66%	-4.06%	-1.09%	-0.22%	-1.45%
Baseline (100% Recharge) Change	-343	-224	-488	-287	-135	-29	-1	-21
Difference Relative to Baseline	-6	-4	-3	-51	-4	-1	-3	-1

The comparative change in discharge for each drain cell or group of drain cells evaluated for the 97 percent of 20th Century recharge simulation is shown in Figures D-7 through D-9.

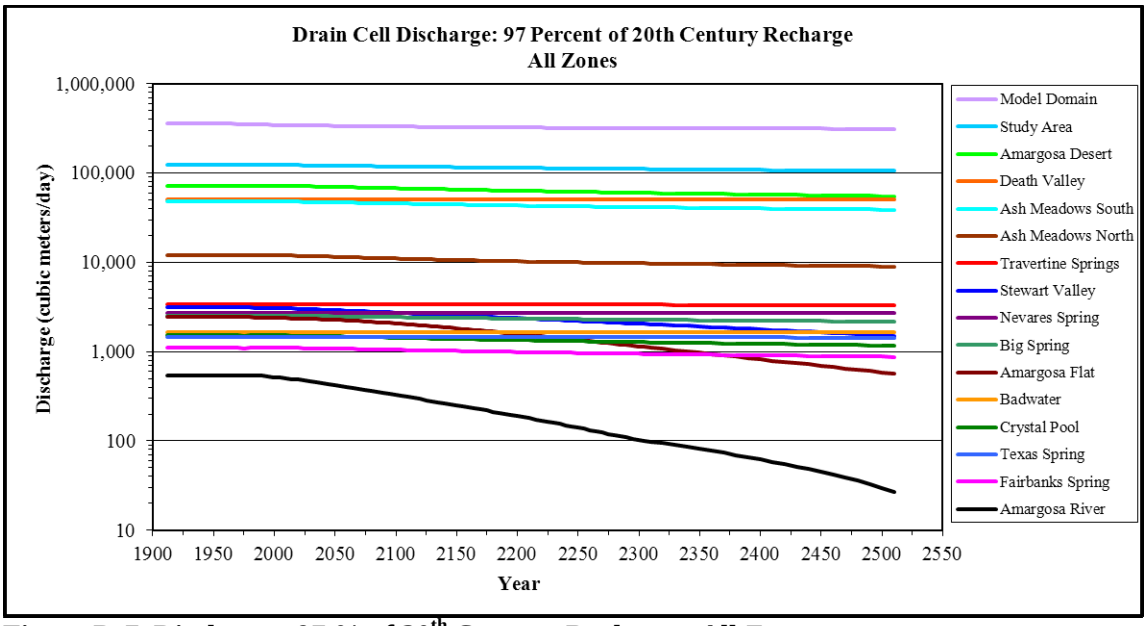

Figure D-7. Discharge: 97 % of 20th Century Recharge, All Zones

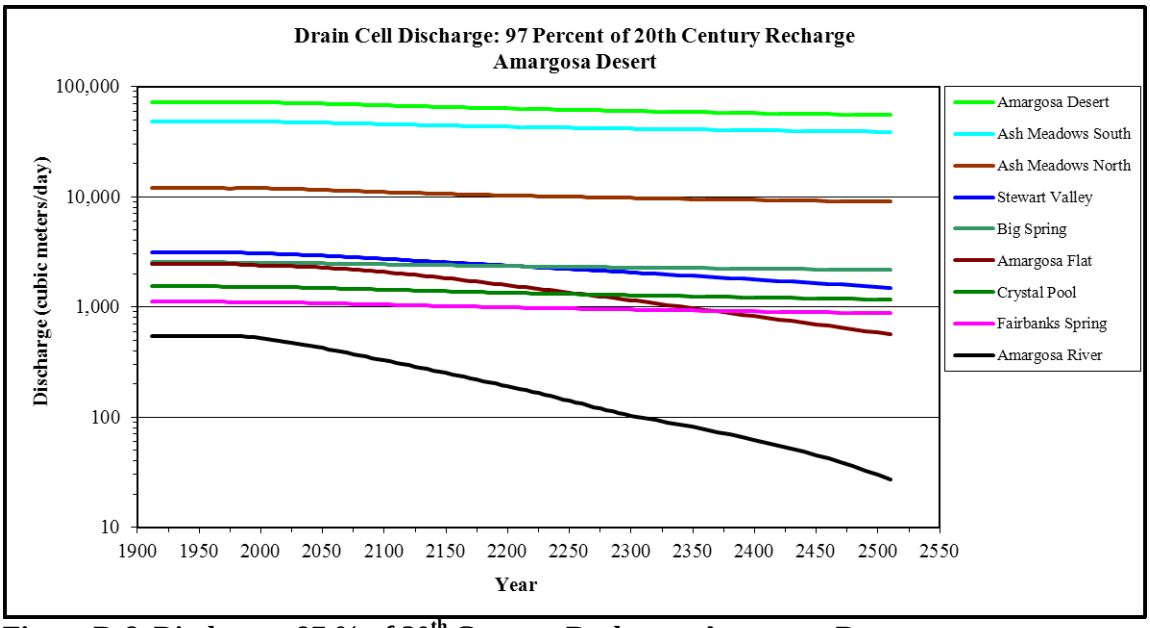

Figure D-8. Discharge: 97 % of 20th Century Recharge, Amargosa Desert

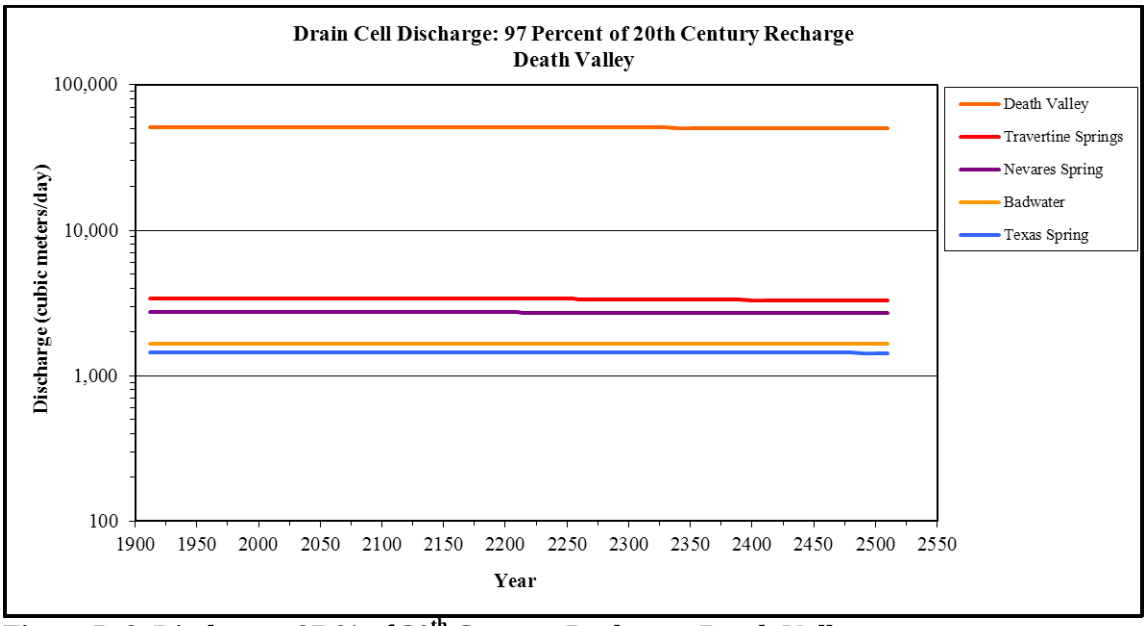

Figure D-9. Discharge: 97 % of 20th Century Recharge, Death Valley

Simulation of 94 Percent of 20th Century Recharge

In the simulation with recharge at 94 percent of 20th Century rates, discharge from drain cells declined from 2000 to 2500 at all locations in the study area. Table D-4 presents the discharge data for selected years relative to the baseline recharge condition.

Table D-4. Drain Cell Discharge, 94 % of 20th Century Recharge (m^3/day)

Year	Model Domain	Study Area	Amargosa Desert	Ash Meadows South	Ash Meadows North	Stewart Valley	Big Spring	Amargosa Flat
1912	362,455	123,370	72,474	48,401	12,076	3,116	2,544	2,459
2000	345,347	122,580	71,688	47,924	11,926	3,070	2,521	2,380
2100	330,959	118,310	67,442	45,503	11,017	2,720	2,431	2,067
2200	322,257	114,000	63,186	43,150	10,258	2,360	2,343	1,569
2300	317,837	110,600	59,870	41,387	9,732	2,045	2,274	1,140
2400	314,572	107,850	57,221	39,994	9,328	1,764	2,218	807
2500	311,859	105,540	55,011	38,830	8,993	1,506	2,169	568
Total Change 2000 to 2500	-33,488	-17,040	-16,677	-9,094	-2,933	-1,564	-351	-1,812
% Change 2000 to 2500	-9.70%	-13.90%	-23.26%	-18.98%	-24.59%	-50.96%	-13.94%	-76.12%
Baseline (100% Recharge) Change	-32,438	-16,630	-16,341	-8,913	-2,880	-1,525	-343	-1,772
Difference Relative to Baseline	-1,050	-410	-336	-181	-53	-39	-9	-40

Year	Crystal Pool	Fairbanks Spring	Amargosa River	Death Valley	Travertine Springs	Nevares Spring	Badwater	Texas Spring
1912	1,543	1,120	546	50,896	3,415	2,728	1,665	1,455
2000	1,520	1,105	520	50,895	3,415	2,728	1,665	1,455
2100	1,430	1,047	327	50,870	3,408	2,726	1,664	1,454
2200	1,342	989	189	50,814	3,386	2,721	1,663	1,451
2300	1,273	944	102	50,731	3,352	2,714	1,662	1,446
2400	1,217	907	61	50,633	3,314	2,706	1,661	1,440
2500	1,169	876	28	50,528	3,275	2,698	1,660	1,434
Total Change 2000 to 2500	-352	-230	-492	-367	-141	-30	-5	-22
% Change 2000 to 2500	-23.13%	-20.78%	-94.56%	-0.72%	-4.12%	-1.11%	-0.31%	-1.48%
Baseline (100% Recharge) Change	-343	-224	-488	-287	-135	-29	-1	-21
Difference Relative to Baseline	-9	-6	-4	-80	-6	-1	-4	-1

The comparative change in discharge for each drain cell or group of drain cells evaluated for the 94 percent of 20th Century recharge simulation is shown in Figures D-10 through D-12.

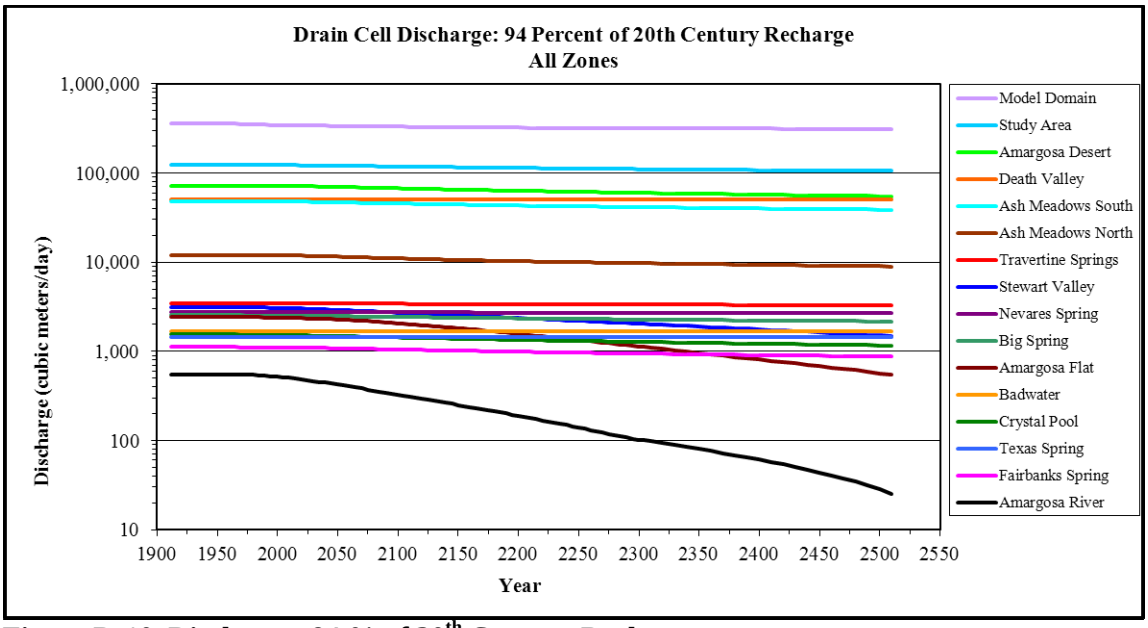

Figure D-10. Discharge: 94 % of 20th Century Recharge

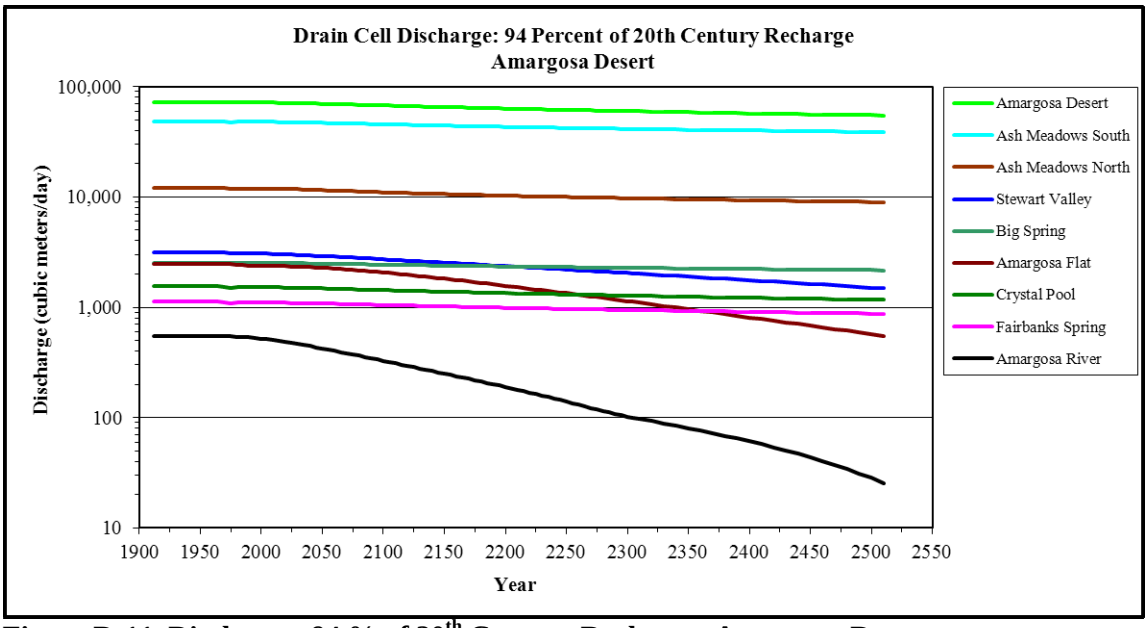

Figure D-11. Discharge: 94 % of 20th Century Recharge, Amargosa Desert

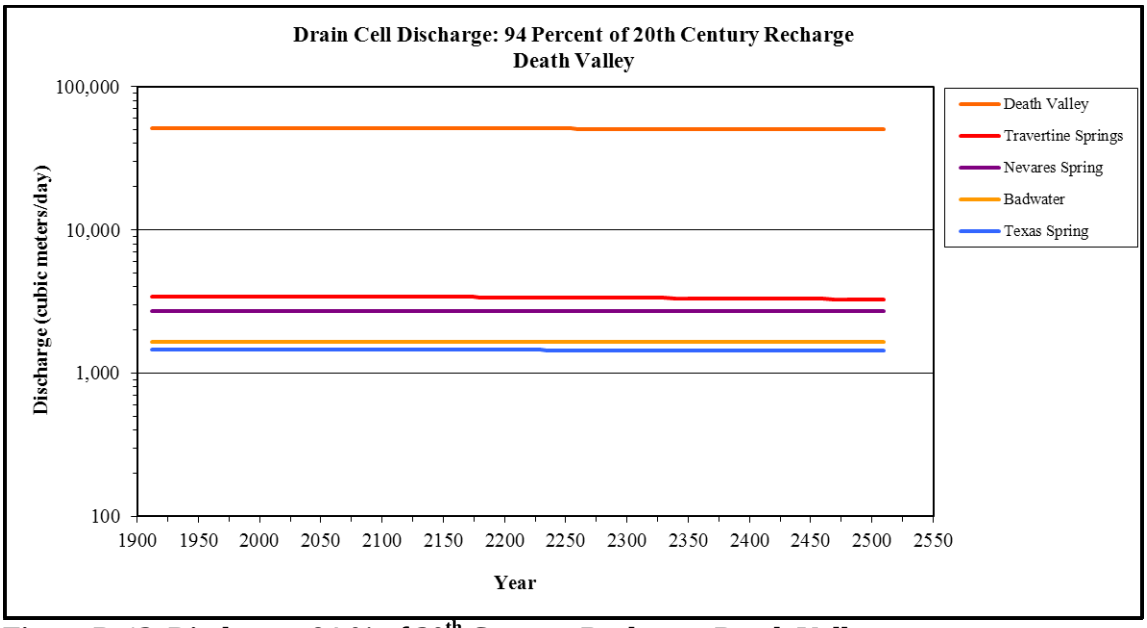

Figure D-12. Discharge: 94 % of 20th Century Recharge, Death Valley

Simulation of 91 Percent of 20th Century Recharge

In the simulation with recharge at 91 percent of 20th Century rates, discharge from drain cells declined from 2000 to 2500 at all locations in the study area. Table D-5 presents the discharge data for selected years relative to the baseline recharge condition.

Table D-5. Drain Cell Discharge, 91 % of 20th Century Discharge (m^3/day)

Year	Model Domain	Study Area	Amargosa Desert	Ash Meadows South	Ash Meadows North	Stewart Valley	Big Spring	Amargosa Flat
1912	362,455	123,370	72,474	48,401	12,076	3,116	2,544	2,459
2000	345,347	122,580	71,688	47,924	11,926	3,070	2,521	2,380
2100	330,862	118,280	67,420	45,492	11,014	2,716	2,430	2,065
2200	322,091	113,940	63,137	43,126	10,251	2,352	2,342	1,562
2300	317,596	110,510	59,796	41,349	9,720	2,035	2,272	1,129
2400	314,263	107,730	57,125	39,944	9,313	1,752	2,215	795
2500	311,479	105,390	54,888	38,764	8,974	1,492	2,166	554
Total Change 2000 to 2500	-33,868	-17,190	-16,800	-9,160	-2,952	-1,579	-354	-1,826
% Change 2000 to 2500	-9.81%	-14.02%	-23.43%	-19.11%	-24.76%	-51.42%	-14.06%	-76.73%
Baseline (100% Recharge) Change	-32,438	-16,630	-16,341	-8,913	-2,880	-1,525	-343	-1,772
Difference Relative to Baseline	-1,430	-560	-459	-247	-72	-54	-12	-54

Year	Crystal Pool	Fairbanks Spring	Amargosa River	Death Valley	Travertine Springs	Nevares Spring	Badwater	Texas Spring
1912	1,543	1,120	546	50,896	3,415	2,728	1,665	1,455
2000	1,520	1,105	520	50,895	3,415	2,728	1,665	1,455
2100	1,430	1,047	326	50,865	3,408	2,726	1,664	1,454
2200	1,341	988	188	50,803	3,385	2,721	1,662	1,451
2300	1,271	943	101	50,714	3,351	2,714	1,661	1,446
2400	1,214	906	60	50,609	3,312	2,706	1,659	1,440
2500	1,165	874	27	50,499	3,272	2,697	1,658	1,433
Total Change 2000 to 2500	-355	-232	-493	-396	-143	-31	-7	-22
% Change 2000 to 2500	-23.34%	-20.96%	-94.84%	-0.78%	-4.18%	-1.13%	-0.40%	-1.51%
Baseline (100% Recharge) Change	-343	-224	-488	-287	-135	-29	-1	-21
Difference Relative to Baseline	-12	-8	-6	-109	-8	-2	-6	-1

The comparative change in discharge for each drain cell or group of drain cells evaluated for the 91 percent of 20th Century recharge simulation is shown in Figures D-13 through D-15.

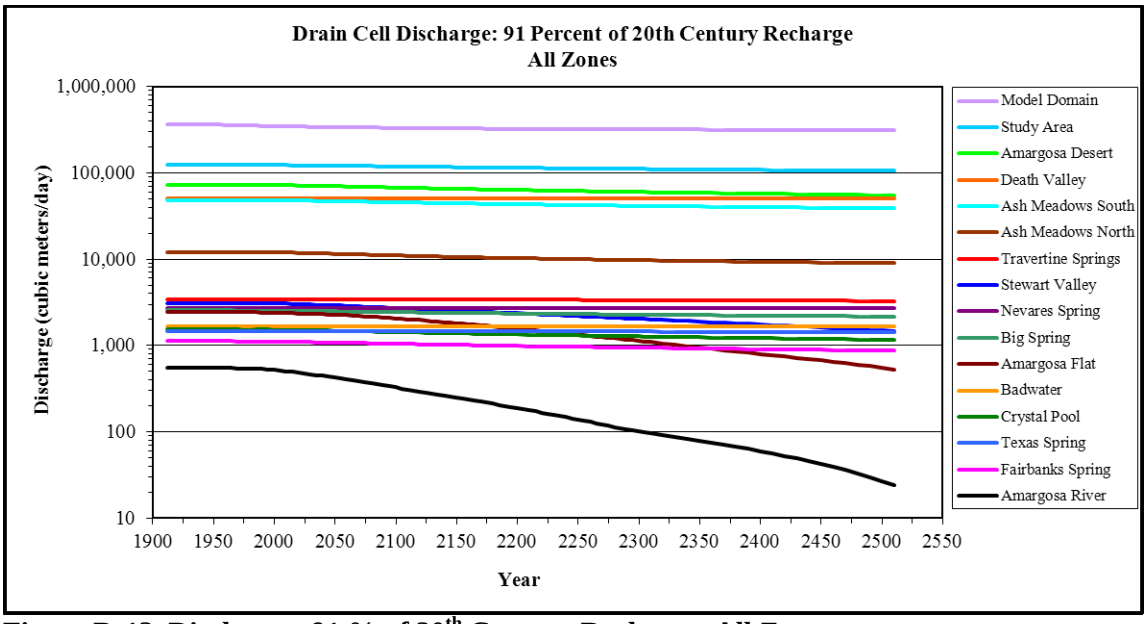

Figure D-13. Discharge: 91 % of 20th Century Recharge, All Zones

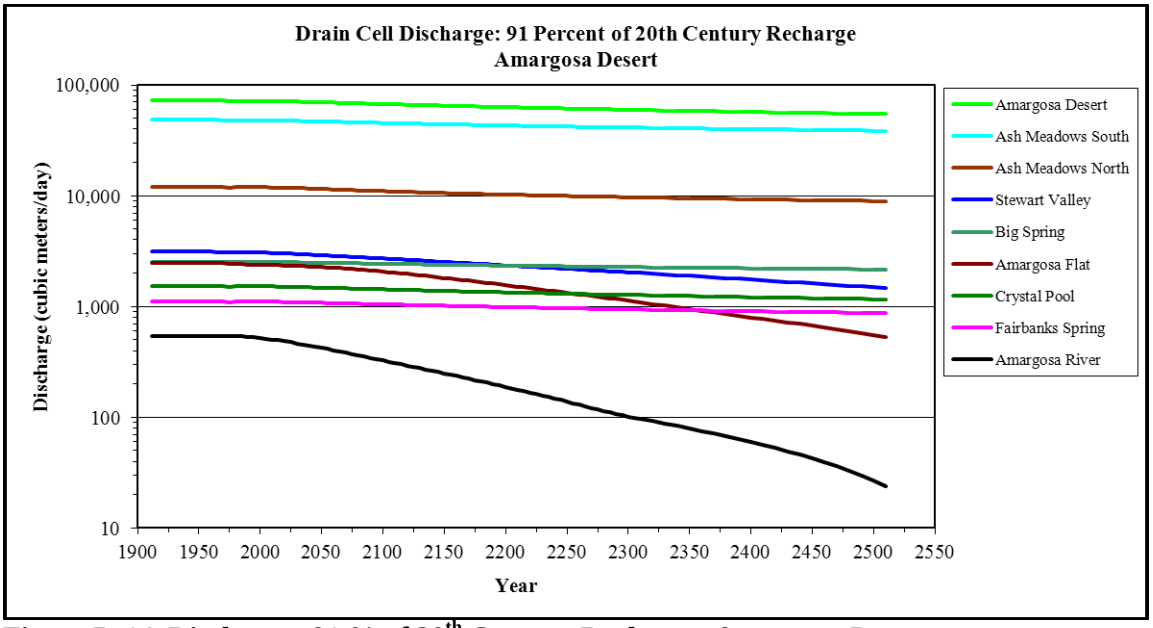

Figure D-14. Discharge: 91 % of 20th Century Recharge, Amargosa Desert

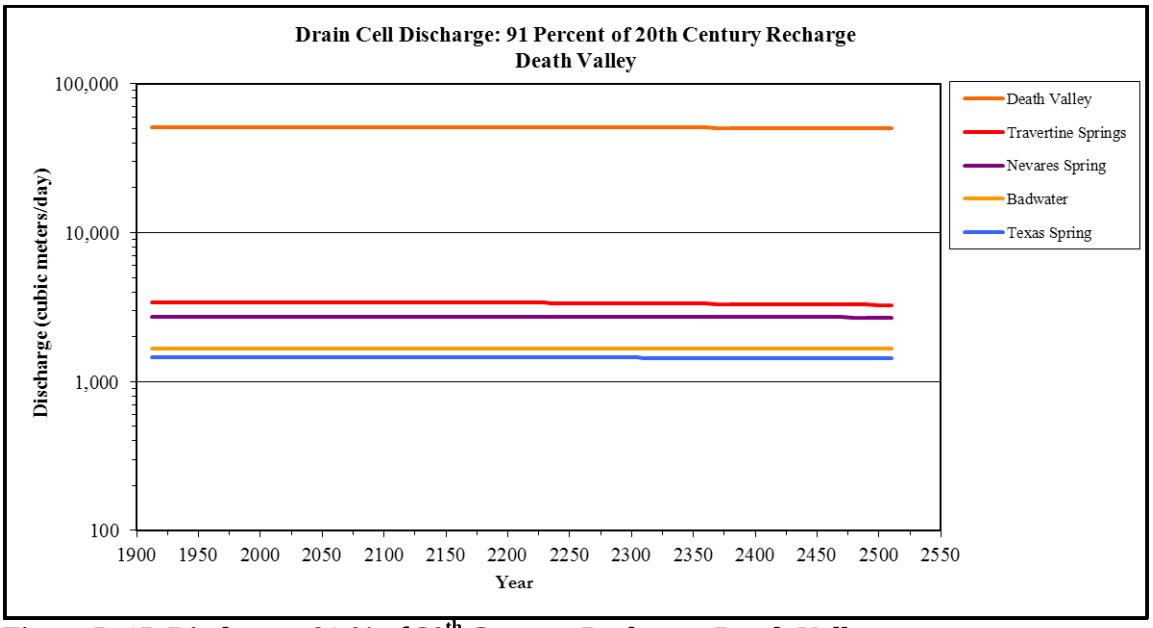

Figure D-15. Discharge: 91 % of 20th Century Recharge, Death Valley

Simulation of 88 Percent of 20th Century Recharge

In the simulation with recharge at 88 percent of 20th Century rates, discharge from drain cells declined from 2000 to 2500 at all locations in the study area. Table D-6 presents the discharge data for selected years relative to the baseline recharge condition.

Table D-6. Drain Cell Discharge, 88 % of 20th Century Recharge (m^3/day)

Year	Model Domain	Study Area	Amargosa Desert	Ash Meadows South	Ash Meadows North	Stewart Valley	Big Spring	Amargosa Flat
1912	362,455	123,370	72,474	48,401	12,076	3,116	2,544	2,459
2000	345,347	122,580	71,688	47,924	11,926	3,070	2,521	2,380
2100	330,765	118,260	67,398	45,482	11,011	2,711	2,430	2,062
2200	321,924	113,880	63,087	43,102	10,244	2,345	2,341	1,555
2300	317,356	110,420	59,723	41,312	9,710	2,025	2,270	1,118
2400	313,952	107,610	57,026	39,892	9,298	1,739	2,213	782
2500	311,107	105,240	54,774	38,703	8,956	1,477	2,163	540
Total Change 2000 to 2500	-34,240	-17,340	-16,914	-9,221	-2,970	-1,593	-357	-1,840
% Change 2000 to 2500	-9.91%	-14.15%	-23.59%	-19.24%	-24.90%	-51.88%	-14.17%	-77.32%
Baseline (100% Recharge) Change	-32,438	-16,630	-16,341	-8,913	-2,880	-1,525	-343	-1,772
Difference Relative to Baseline	-1,802	-710	-573	-308	-90	-68	-15	-68

Year	Crystal Pool	Fairbanks Spring	Amargosa River	Death Valley	Travertine Springs	Nevares Spring	Badwater	Texas Spring
1912	1,543	1,120	546	50,896	3,415	2,728	1,665	1,455
2000	1,520	1,105	520	50,895	3,415	2,728	1,665	1,455
2100	1,429	1,046	326	50,859	3,408	2,726	1,664	1,454
2200	1,340	987	187	50,791	3,384	2,721	1,662	1,451
2300	1,270	942	100	50,696	3,350	2,714	1,660	1,445
2400	1,212	904	59	50,586	3,310	2,705	1,658	1,439
2500	1,163	872	25	50,470	3,270	2,697	1,656	1,433
Total Change 2000 to 2500	-358	-233	-495	-425	-145	-31	-8	-22
% Change 2000 to 2500	-23.52%	-21.13%	-95.13%	-0.84%	-4.25%	-1.14%	-0.49%	-1.53%
Baseline (100% Recharge) Change	-343	-224	-488	-287	-135	-29	-1	-21
Difference Relative to Baseline	-15	-9	-7	-138	-10	-2	-7	-2

The comparative change in discharge for each drain cell or group of drain cells evaluated for the 88 percent of 20th Century recharge simulation is shown in Figures D-16 through D-18.

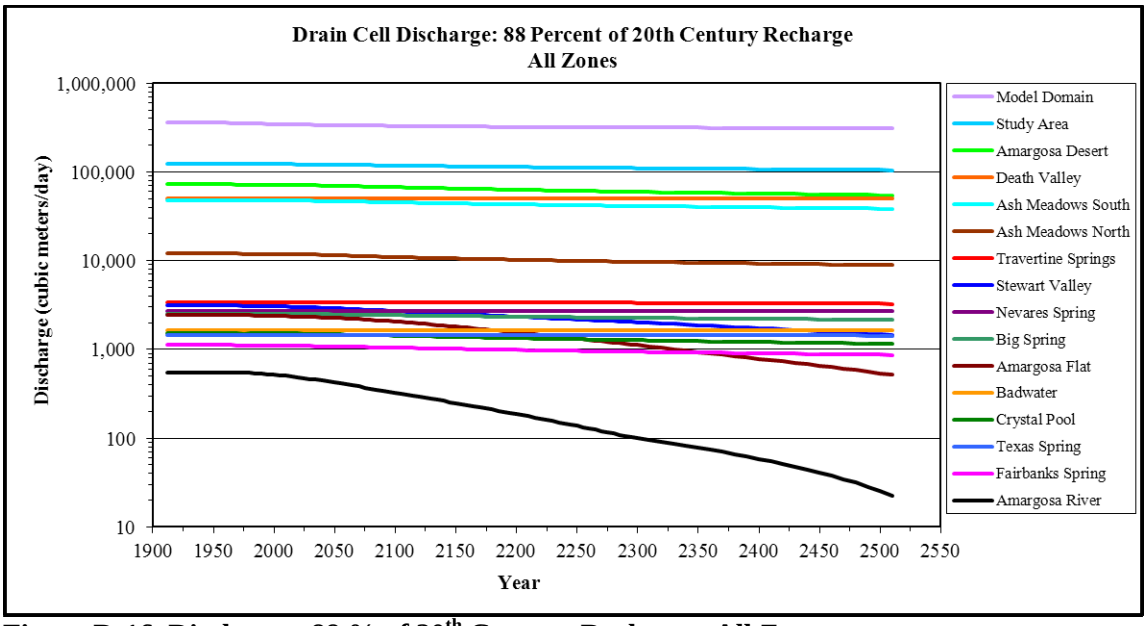

Figure D-16. Discharge: 88 % of 20th Century Recharge, All Zones

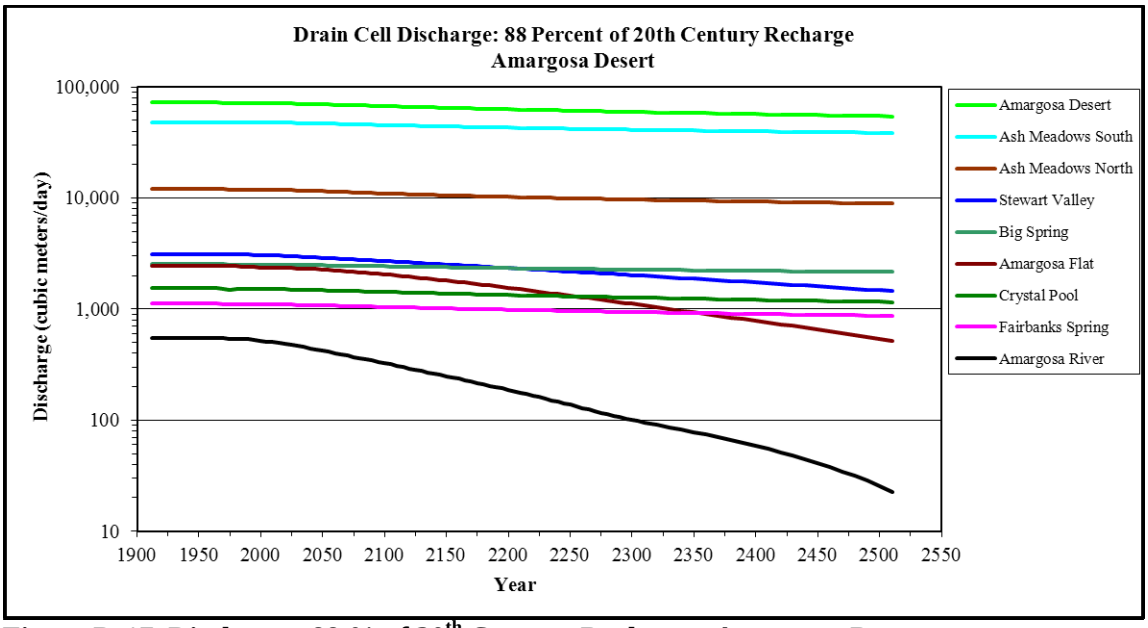

Figure D-17. Discharge: 88 % of 20th Century Recharge, Amargosa Desert

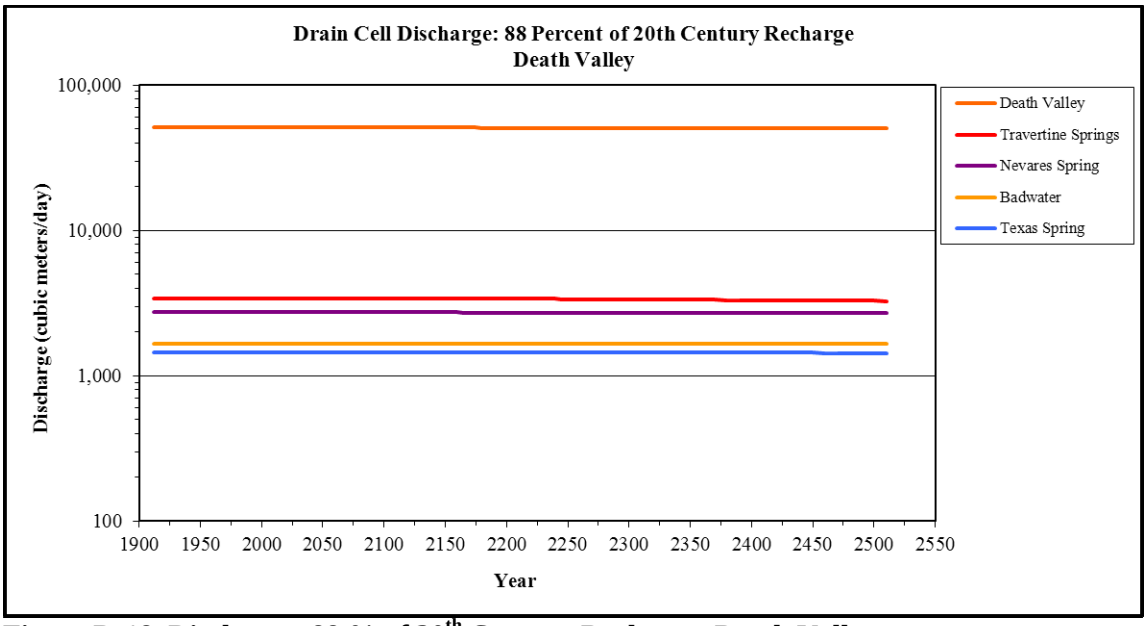

Figure D-18. Discharge: 88 % of 20th Century Recharge, Death Valley

Simulation of 85 Percent of 20th Century Recharge

In the simulation with recharge at 85 percent of 20th Century rates, discharge from drain cells declined from 2000 to 2500 at all locations in the study area. Table D-7 presents the discharge data for selected years and relative to the baseline recharge condition.

Table D-7. Drain Cell Discharge, 85 % of 20th Century Recharge (m^3/day)

Year	Model Domain	Study Area	Amargosa Desert	Ash Meadows South	Ash Meadows North	Stewart Valley	Big Spring	Amargosa Flat
1912	362,455	123,370	72,474	48,401	12,076	3,116	2,544	2,459
2000	345,347	122,580	71,688	47,924	11,926	3,070	2,521	2,380
2100	330,668	118,230	67,376	45,471	11,008	2,707	2,429	2,059
2200	321,758	113,820	63,039	43,077	10,237	2,337	2,339	1,548
2300	317,112	110,320	59,644	41,270	9,698	2,015	2,268	1,107
2400	313,640	107,490	56,927	39,839	9,282	1,727	2,210	769
2500	310,722	105,090	54,645	38,633	8,936	1,463	2,160	525
Total Change 2000 to 2500	-34,625	-17,490	-17,043	-9,291	-2,991	-1,607	-361	-1,855
% Change 2000 to 2500	-10.03%	-14.27%	-23.77%	-19.39%	-25.08%	-52.34%	-14.30%	-77.95%
Baseline (100% Recharge) Change	-32,438	-16,630	-16,341	-8,913	-2,880	-1,525	-343	-1,772
Difference Relative to Baseline	-2,187	-860	-702	-378	-110	-82	-18	-83

Year	Crystal Pool	Fairbanks Spring	Amargosa River	Death Valley	Travertine Springs	Nevares Spring	Badwater	Texas Spring
1912	1,543	1,120	546	50,896	3,415	2,728	1,665	1,455
2000	1,520	1,105	520	50,895	3,415	2,728	1,665	1,455
2100	1,429	1,046	326	50,854	3,407	2,726	1,663	1,454
2200	1,339	987	186	50,780	3,383	2,721	1,661	1,450
2300	1,268	940	99	50,678	3,348	2,714	1,659	1,445
2400	1,209	902	57	50,562	3,308	2,705	1,657	1,439
2500	1,159	870	24	50,441	3,268	2,697	1,655	1,433
Total Change 2000 to 2500	-361	-236	-496	-454	-147	-32	-10	-23
% Change 2000 to 2500	-23.74%	-21.32%	-95.42%	-0.89%	-4.31%	-1.16%	-0.58%	-1.55%
Baseline (100% Recharge) Change	-343	-224	-488	-287	-135	-29	-1	-21
Difference Relative to Baseline	-18	-12	-9	-167	-12	-3	-9	-2

The comparative change in discharge for each drain cell or group of drain cells evaluated for the 85 percent of 20th Century recharge simulation is shown in Figures D-19 through D-21.

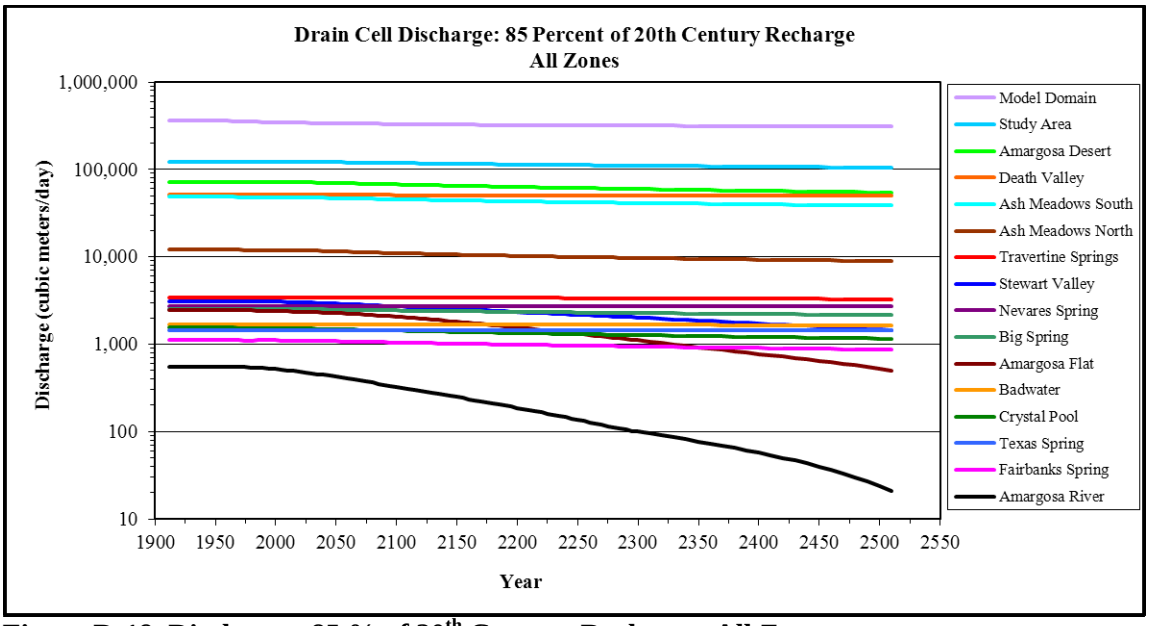

Figure D-19. Discharge: 85 % of 20th Century Recharge, All Zones

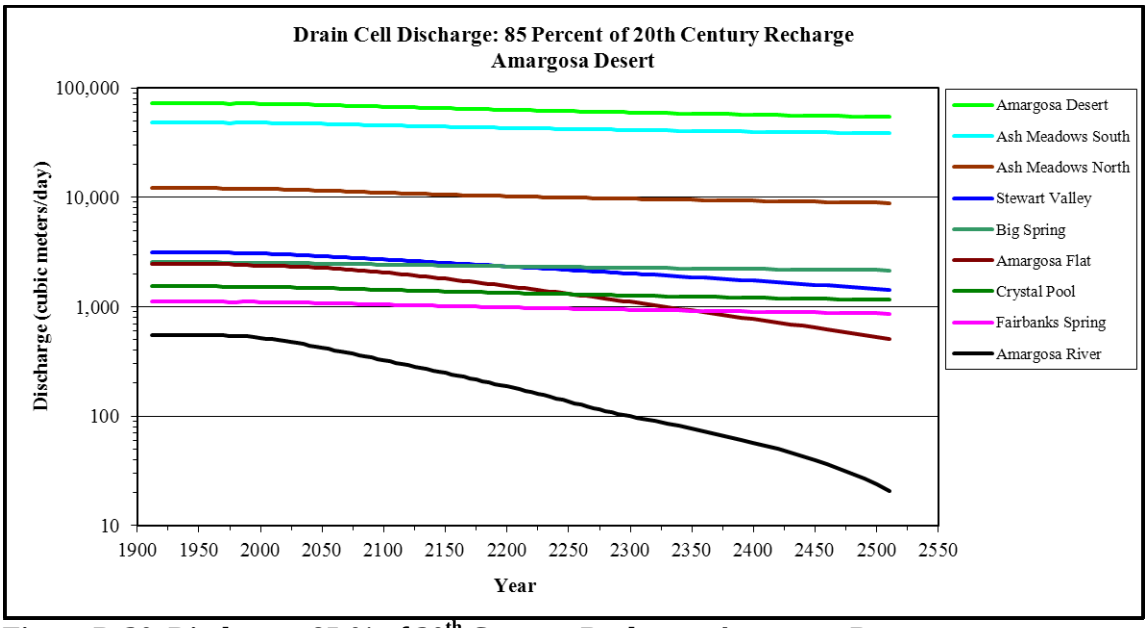

Figure D-20. Discharge: 85 % of 20th Century Recharge, Amargosa Desert

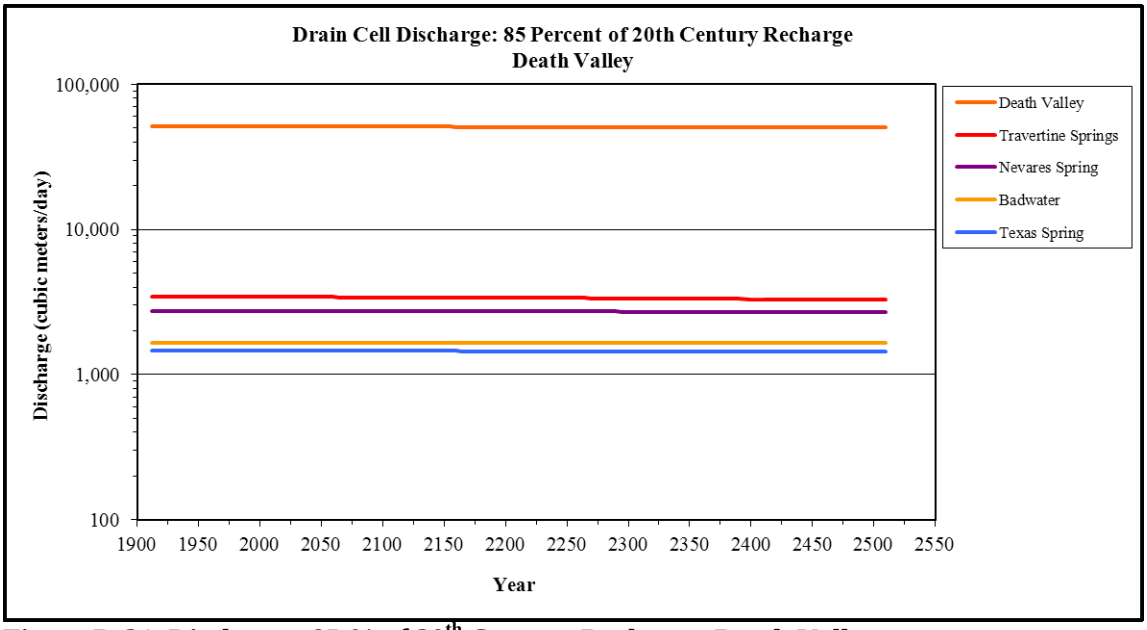

Figure D-21. Discharge: 85 % of 20th Century Recharge, Death Valley

Simulation of 80 Percent of 20th Century Recharge

In the simulation with recharge at 80 percent of 20th Century rates, discharge from drain cells declined from 2000 to 2500 at all locations in the study area. Table D-8 presents the discharge data for selected years relative to the baseline recharge condition.

Table D-8. Drain Cell Discharge, 80 % of 20th Century Recharge (m^3/day)

Year	Model Domain	Study Area	Amargosa Desert	Ash Meadows South	Ash Meadows North	Stewart Valley	Big Spring	Amargosa Flat
1912	362,455	123,370	72,474	48,401	12,076	3,116	2,544	2,459
2000	345,347	122,580	71,688	47,924	11,926	3,070	2,521	2,380
2100	330,507	118,180	67,340	45,453	11,003	2,700	2,428	2,055
2200	321,482	113,720	62,957	43,037	10,225	2,325	2,337	1,536
2300	316,717	110,170	59,525	41,211	9,680	1,999	2,266	1,090
2400	313,130	107,290	56,771	39,757	9,258	1,707	2,206	751
2500	310,093	104,840	54,444	38,524	8,904	1,440	2,155	502
Total Change 2000 to 2500	-35,254	-17,740	-17,244	-9,400	-3,022	-1,630	-366	-1,878
% Change 2000 to 2500	-10.21%	-14.47%	-24.05%	-19.61%	-25.34%	-53.10%	-14.51%	-78.90%
Baseline (100% Recharge) Change	-32,438	-16,630	-16,341	-8,913	-2,880	-1,525	-343	-1,772
Difference Relative to Baseline	-2,816	-1,110	-903	-487	-142	-105	-23	-106

Year	Crystal Pool	Fairbanks Spring	Amargosa River	Death Valley	Travertine Springs	Nevares Spring	Badwater	Texas Spring
1912	1,543	1,120	546	50,896	3,415	2,728	1,665	1,455
2000	1,520	1,105	520	50,895	3,415	2,728	1,665	1,455
2100	1,428	1,045	325	50,845	3,407	2,726	1,663	1,454
2200	1,337	985	185	50,761	3,382	2,721	1,660	1,450
2300	1,265	938	98	50,648	3,346	2,713	1,657	1,445
2400	1,206	900	55	50,523	3,306	2,704	1,655	1,438
2500	1,154	866	21	50,393	3,265	2,696	1,652	1,432
Total Change 2000 to 2500	-366	-239	-499	-502	-151	-33	-12	-23
% Change 2000 to 2500	-24.08%	-21.63%	-95.89%	-0.99%	-4.41%	-1.19%	-0.73%	-1.59%
Baseline (100% Recharge) Change	-343	-224	-488	-287	-135	-29	-1	-21
Difference Relative to Baseline	-23	-15	-11	-215	-16	-4	-11	-3

The comparative change in discharge for each drain cell or group of drain cells evaluated for the 80 percent of 20th Century recharge simulation is shown in Figures D-22 through D-24.

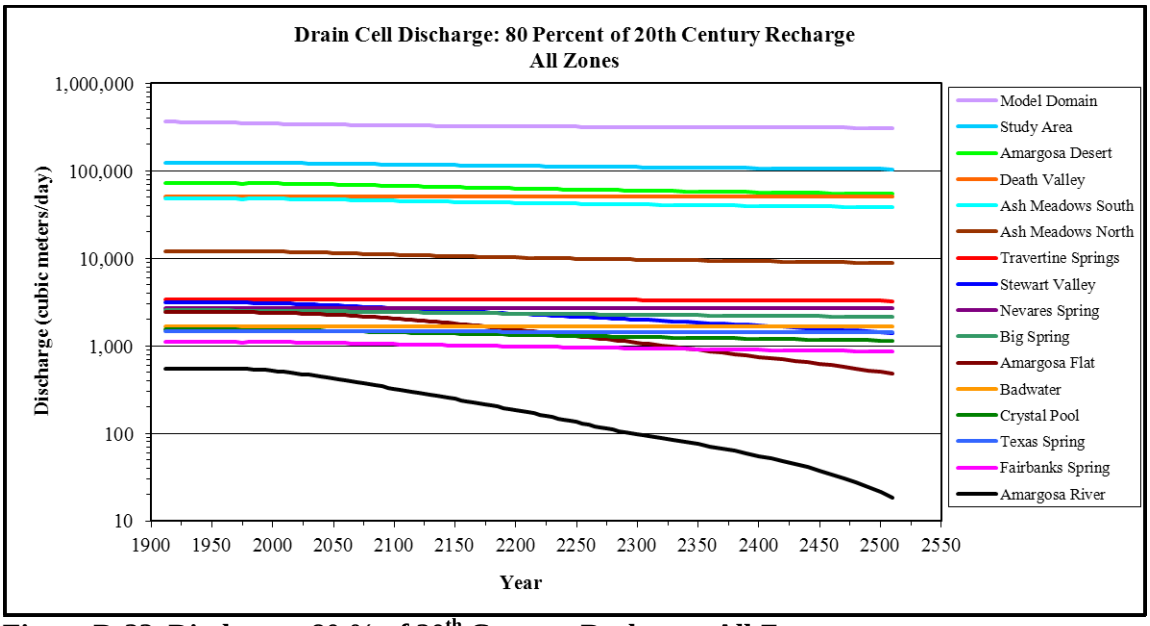

Figure D-22. Discharge: 80 % of 20th Century Recharge, All Zones

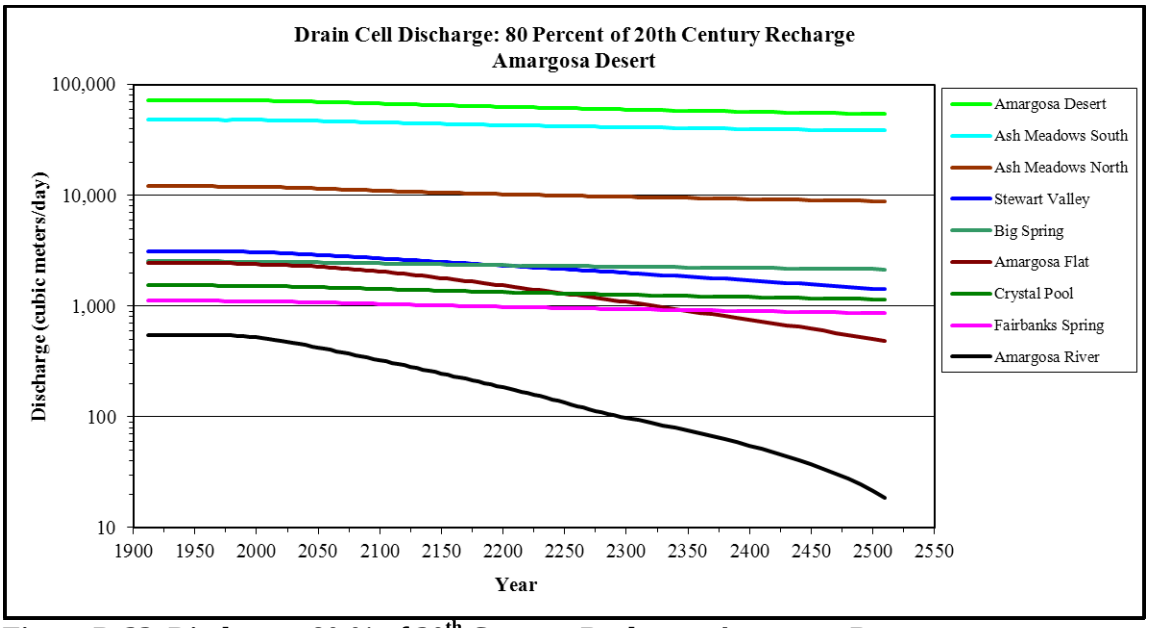

Figure D-23. Discharge: 80 % of 20th Century Recharge, Amargosa Desert

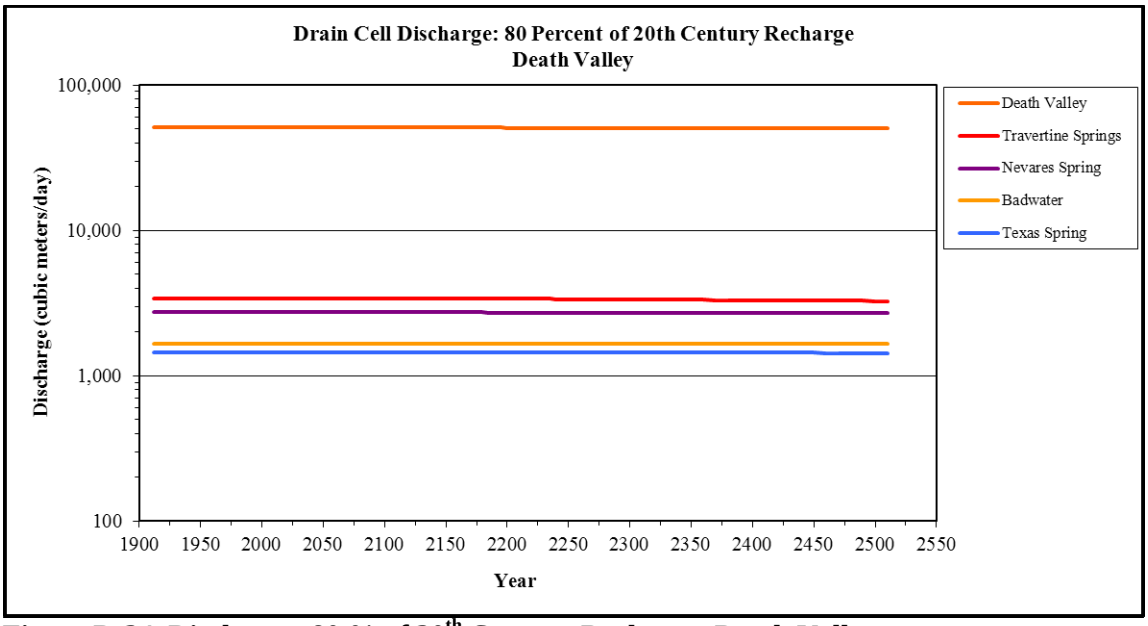

Figure D-24. Discharge: 80 % of 20th Century Recharge, Death Valley

Simulation of 75 Percent of 20th Century Recharge

In the simulation with recharge at 75 percent of 20th Century rates, discharge from drain cells declined from 2000 to 2500 at all locations in the study area. Table D-9 presents the discharge data for selected years relative to the baseline recharge condition.

Table D-9. Drain Cell Discharge, 75 % of 20th Century Recharge (m^3/day)

Year	Model Domain	Study Area	Amargosa Desert	Ash Meadows South	Ash Meadows North	Stewart Valley	Big Spring	Amargosa Flat
1912	362,455	123,370	72,474	48,401	12,076	3,116	2,544	2,459
2000	345,347	122,580	71,688	47,924	11,926	3,070	2,521	2,380
2100	330,345	118,140	67,304	45,436	10,998	2,693	2,427	2,051
2200	321,205	113,620	62,875	42,996	10,213	2,313	2,335	1,525
2300	316,314	110,020	59,397	41,144	9,661	1,982	2,262	1,072
2400	312,612	107,090	56,607	39,668	9,232	1,687	2,202	733
2500	309,471	104,590	54,250	38,419	8,873	1,416	2,150	480
Total Change 2000 to 2500	-35,876	-17,990	-17,438	-9,505	-3,053	-1,654	-371	-1,900
% Change 2000 to 2500	-10.39%	-14.68%	-24.32%	-19.83%	-25.60%	-53.87%	-14.70%	-79.82%
Baseline (100% Recharge) Change	-32,438	-16,630	-16,341	-8,913	-2,880	-1,525	-343	-1,772
Difference Relative to Baseline	-3,438	-1,360	-1,097	-592	-173	-129	-28	-128

Year	Crystal Pool	Fairbanks Spring	Amargosa River	Death Valley	Travertine Springs	Nevares Spring	Badwater	Texas Spring
1912	1,543	1,120	546	50,896	3,415	2,728	1,665	1,455
2000	1,520	1,105	520	50,895	3,415	2,728	1,665	1,455
2100	1,427	1,045	324	50,836	3,406	2,726	1,662	1,454
2200	1,335	984	183	50,741	3,381	2,720	1,659	1,450
2300	1,262	936	96	50,618	3,344	2,713	1,656	1,444
2400	1,201	897	53	50,483	3,303	2,704	1,653	1,438
2500	1,149	863	19	50,344	3,261	2,695	1,650	1,431
Total Change 2000 to 2500	-371	-242	-501	-551	-154	-33	-15	-24
% Change 2000 to 2500	-24.41%	-21.91%	-96.36%	-1.08%	-4.51%	-1.22%	-0.89%	-1.64%
Baseline (100% Recharge) Change	-343	-224	-488	-287	-135	-29	-1	-21
Difference Relative to Baseline	-28	-18	-14	-264	-19	-5	-14	-3

The comparative change in discharge for each drain cell or group of drain cells evaluated for the 75 percent of 20th Century recharge simulation is shown in Figures D-25 through D-27.

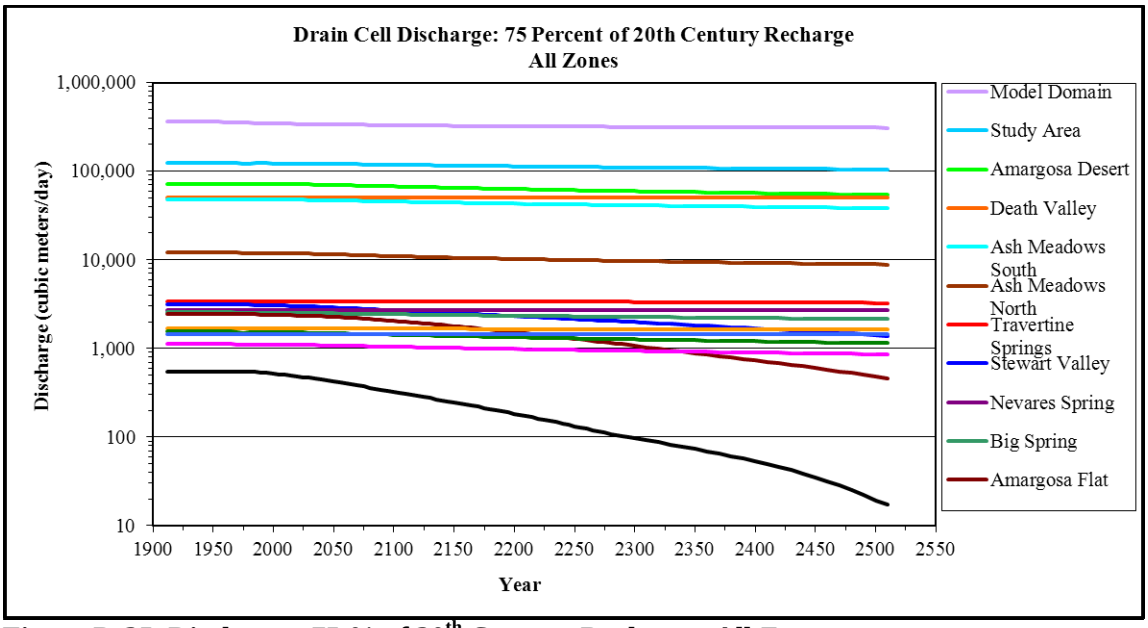

Figure D-25. Discharge: 75 % of 20th Century Recharge, All Zones

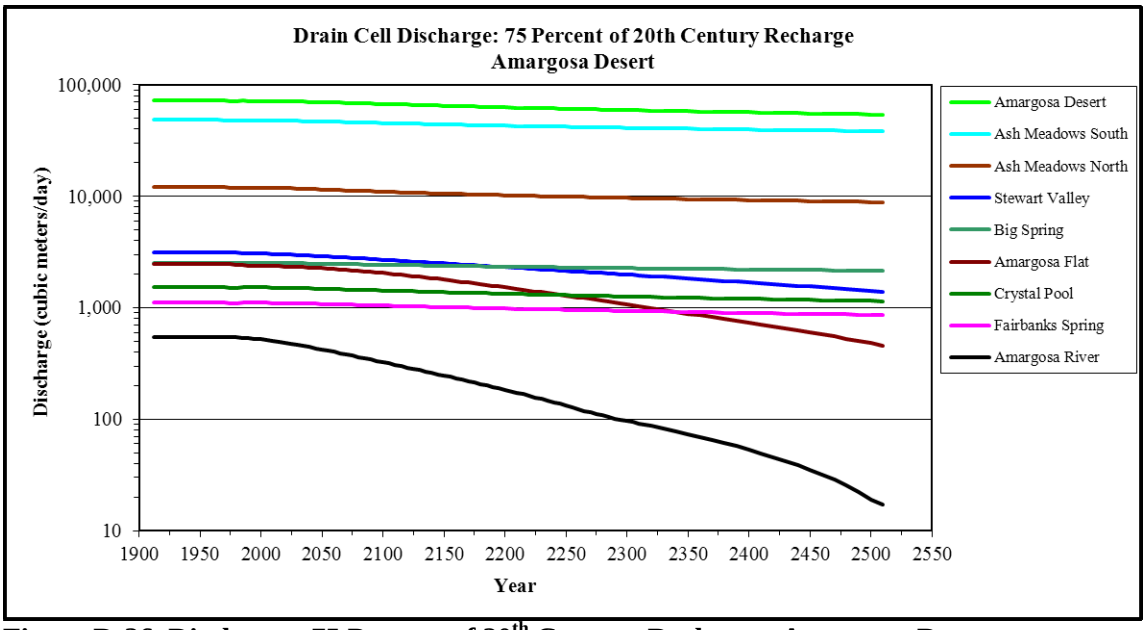

Figure D-26. Discharge: 75 Percent of 20th Century Recharge, Amargosa Desert

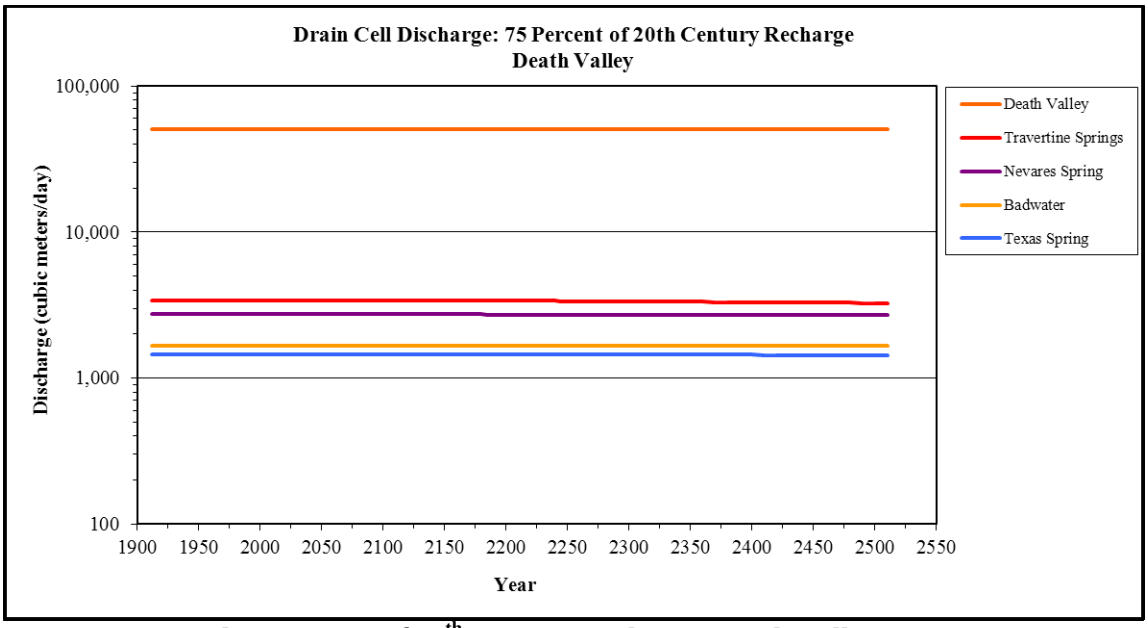

Figure D-27. Discharge: 75 % of 20th Century Recharge, Death Valley

Simulation of 70 Percent of 20th Century Recharge

In the simulation with recharge at 70 percent of 20th Century rates, discharge from drain cells declined from 2000 to 2500 at all locations in the study area. Table D-10 presents the discharge data for selected years relative to the baseline recharge condition.

Table D-10. Drain Cell Discharge, 70 % of 20th Century Recharge (m^3/day)

Year	Model Domain	Study Area	Amargosa Desert	Ash Meadows South	Ash Meadows North	Stewart Valley	Big Spring	Amargosa Flat
1912	362,455	123,370	72,474	48,401	12,076	3,116	2,544	2,459
2000	345,347	122,580	71,688	47,924	11,926	3,070	2,521	2,380
2100	330,184	118,090	67,267	45,418	10,992	2,687	2,426	2,047
2200	320,929	113,520	62,793	42,956	10,201	2,300	2,333	1,513
2300	315,915	109,860	59,274	41,081	9,642	1,965	2,259	1,055
2400	312,098	106,890	56,448	39,583	9,208	1,667	2,198	714
2500	308,841	104,340	54,048	38,308	8,841	1,393	2,145	458
Total Change 2000 to 2500	-36,506	-18,240	-17,640	-9,616	-3,086	-1,677	-376	-1,922
% Change 2000 to 2500	-10.57%	-14.88%	-24.61%	-20.07%	-25.87%	-54.63%	-14.91%	-80.74%
Baseline (100% Recharge) Change	-32,438	-16,630	-16,341	-8,913	-2,880	-1,525	-343	-1,772
Difference Relative to Baseline	-4,067	-1,610	-1,299	-703	-205	-152	-33	-150

Year	Crystal Pool	Fairbanks Spring	Amargosa River	Death Valley	Travertine Springs	Nevares Spring	Badwater	Texas Spring
1912	1,543	1,120	546	50,896	3,415	2,728	1,665	1,455
2000	1,520	1,105	520	50,895	3,415	2,728	1,665	1,455
2100	1,426	1,044	323	50,827	3,406	2,726	1,662	1,454
2200	1,333	983	182	50,722	3,379	2,720	1,658	1,450
2300	1,258	934	95	50,589	3,342	2,712	1,654	1,444
2400	1,197	894	51	50,444	3,300	2,703	1,651	1,438
2500	1,144	860	18	50,296	3,258	2,694	1,647	1,431
Total Change 2000 to 2500	-376	-246	-503	-599	-158	-34	-17	-24
% Change 2000 to 2500	-24.75%	-22.23%	-96.63%	-1.18%	-4.62%	-1.25%	-1.04%	-1.68%
Baseline (100% Recharge) Change	-343	-224	-488	-287	-135	-29	-1	-21
Difference Relative to Baseline	-33	-22	-15	-312	-23	-5	-16	-4

The comparative change in discharge for each drain cell or group of drain cells evaluated for the 70 percent of 20th Century recharge simulation is shown in Figures D-28 through D-30.

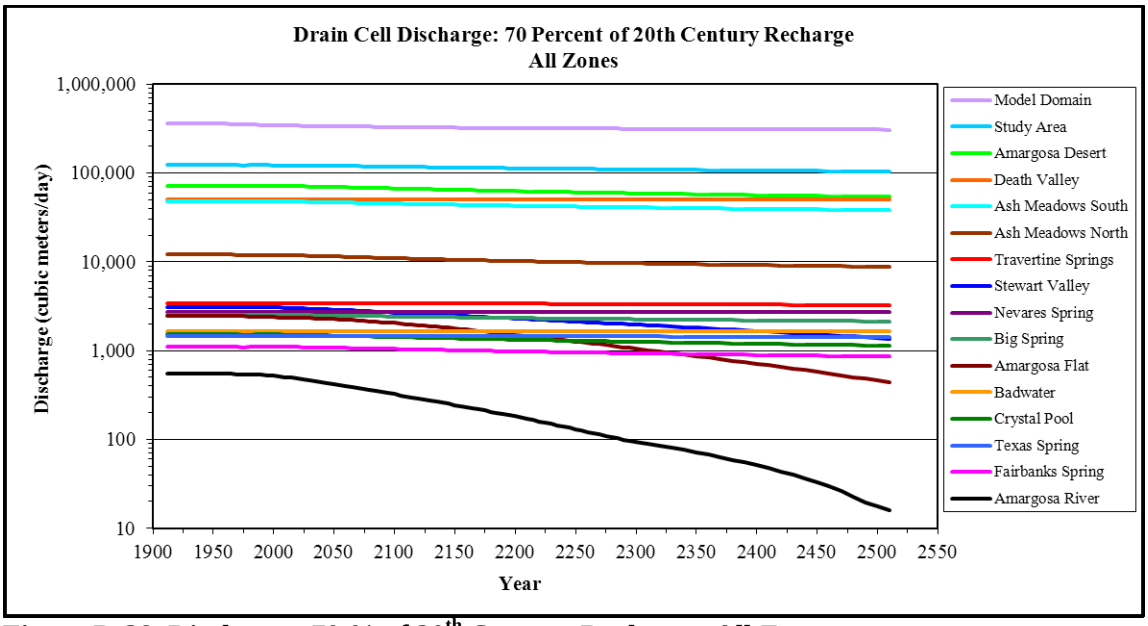

Figure D-28. Discharge: 70 % of 20th Century Recharge, All Zones

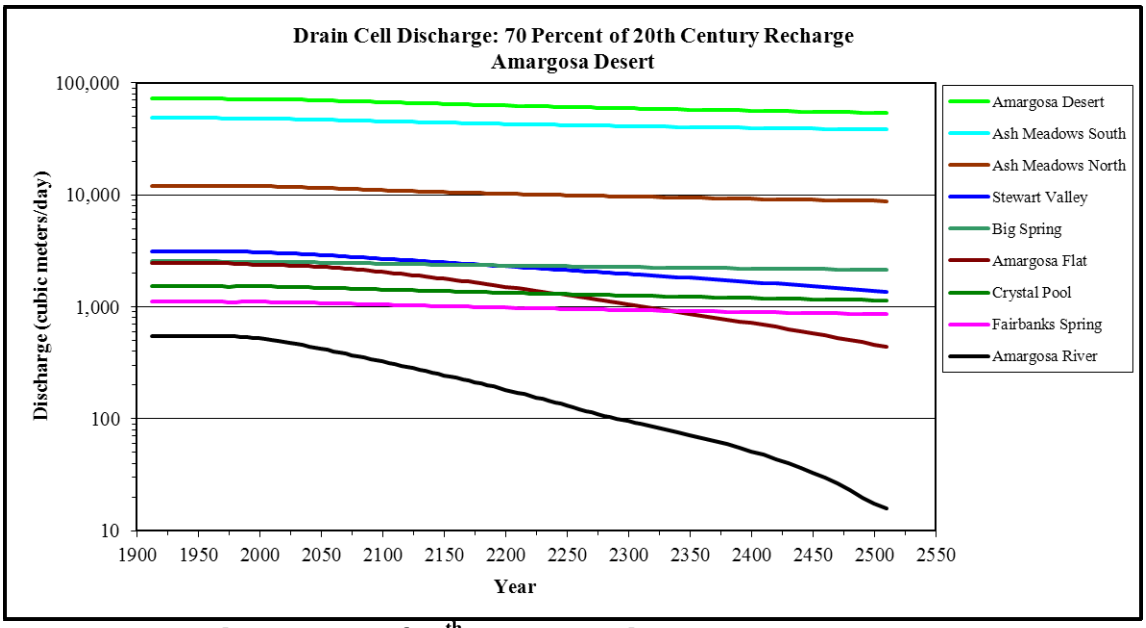

Figure D-29. Discharge: 70 % of 20th Century Recharge, Amargosa Desert

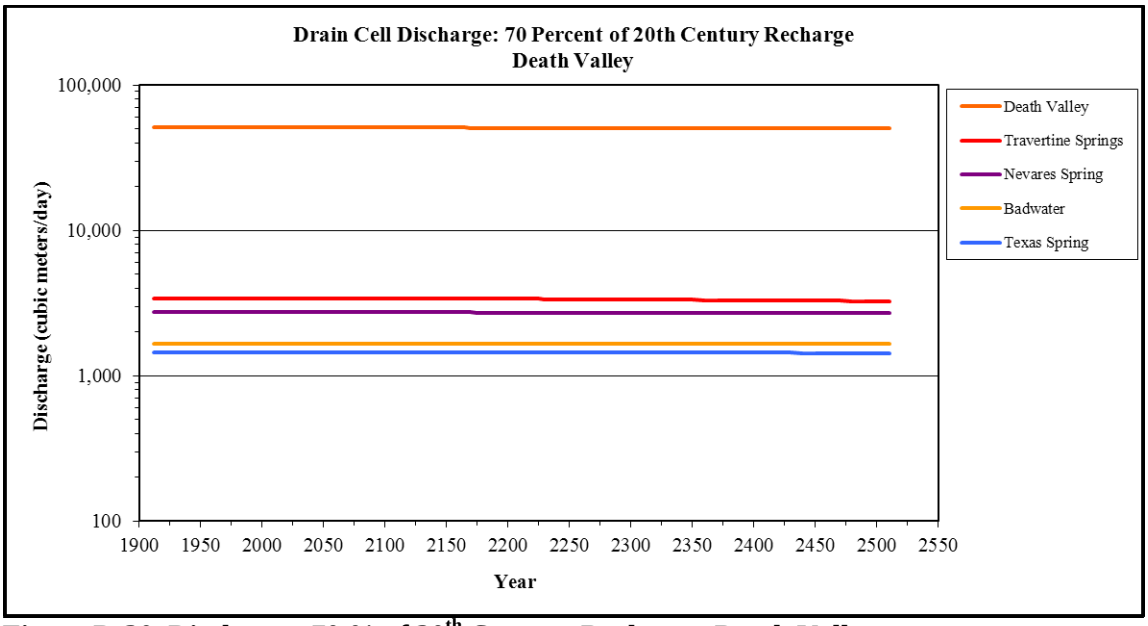

Figure D-30. Discharge: 70 % of 20th Century Recharge, Death Valley

Simulation of 60 Percent of 20th Century Recharge

In the simulation with recharge at 60 percent of 20th Century rates, discharge from drain cells declined from 2000 to 2500 at all locations in the study area. Table D-11 presents the discharge data for selected years relative to the baseline recharge condition.

Table D-11. Drain Cell Discharge, 60 % of 20th Century Recharge (m^3/day)

Year	Model Domain	Study Area	Amargosa Desert	Ash Meadows South	Ash Meadows North	Stewart Valley	Big Spring	Amargosa Flat
1912	362,455	123,370	72,474	48,401	12,076	3,116	2,544	2,459
2000	345,347	122,580	71,688	47,924	11,926	3,070	2,521	2,380
2100	329,861	118,000	67,195	45,383	10,982	2,673	2,425	2,038
2200	320,376	113,310	62,630	42,875	10,178	2,275	2,329	1,490
2300	315,113	109,550	59,023	40,953	9,605	1,932	2,253	1,020
2400	311,067	106,490	56,125	39,410	9,157	1,626	2,190	676
2500	307,585	103,850	53,647	38,089	8,777	1,346	2,134	414
Total Change 2000 to 2500	-37,762	-18,730	-18,041	-9,835	-3,150	-1,724	-386	-1,967
% Change 2000 to 2500	-10.93%	-15.28%	-25.17%	-20.52%	-26.41%	-56.16%	-15.33%	-82.62%
Baseline (100% Recharge) Change	-32,438	-16,630	-16,341	-8,913	-2,880	-1,525	-343	-1,772
Difference Relative to Baseline	-5,324	-2,100	-1,700	-922	-269	-199	-44	-195

Year	Crystal Pool	Fairbanks Spring	Amargosa River	Death Valley	Travertine Springs	Nevares Spring	Badwater	Texas Spring
1912	1,543	1,120	546	50,896	3,415	2,728	1,665	1,455
2000	1,520	1,105	520	50,895	3,415	2,728	1,665	1,455
2100	1,424	1,043	322	50,809	3,405	2,726	1,661	1,453
2200	1,328	980	179	50,684	3,377	2,719	1,656	1,449
2300	1,252	930	92	50,529	3,338	2,711	1,651	1,443
2400	1,189	889	47	50,365	3,294	2,702	1,646	1,437
2500	1,133	853	15	50,200	3,251	2,692	1,642	1,430
Total Change 2000 to 2500	-387	-252	-505	-695	-165	-36	-22	-26
% Change 2000 to 2500	-25.44%	-22.83%	-97.15%	-1.37%	-4.83%	-1.31%	-1.35%	-1.76%
Baseline (100% Recharge) Change	-343	-224	-488	-287	-135	-29	-1	-21
Difference Relative to Baseline	-44	-28	-18	-408	-30	-7	-22	-5

The comparative change in discharge for each drain cell or group of drain cells evaluated for the 60 percent of 20th Century recharge simulation is shown in Figures D-31 through D-33.

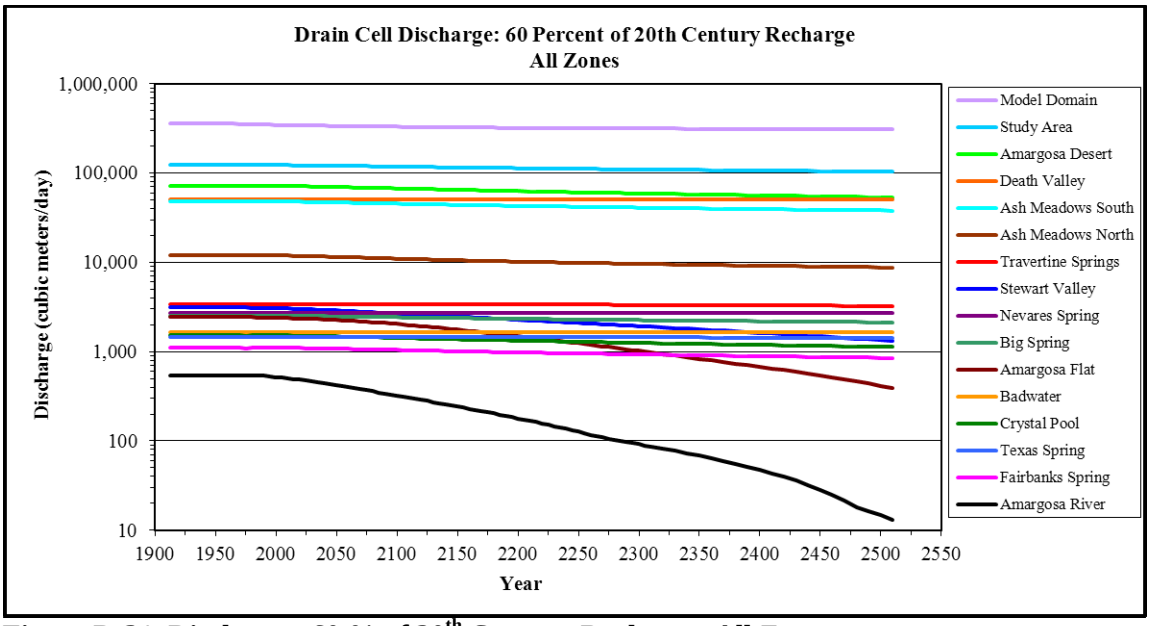

Figure D-31. Discharge: 60 % of 20th Century Recharge, All Zones

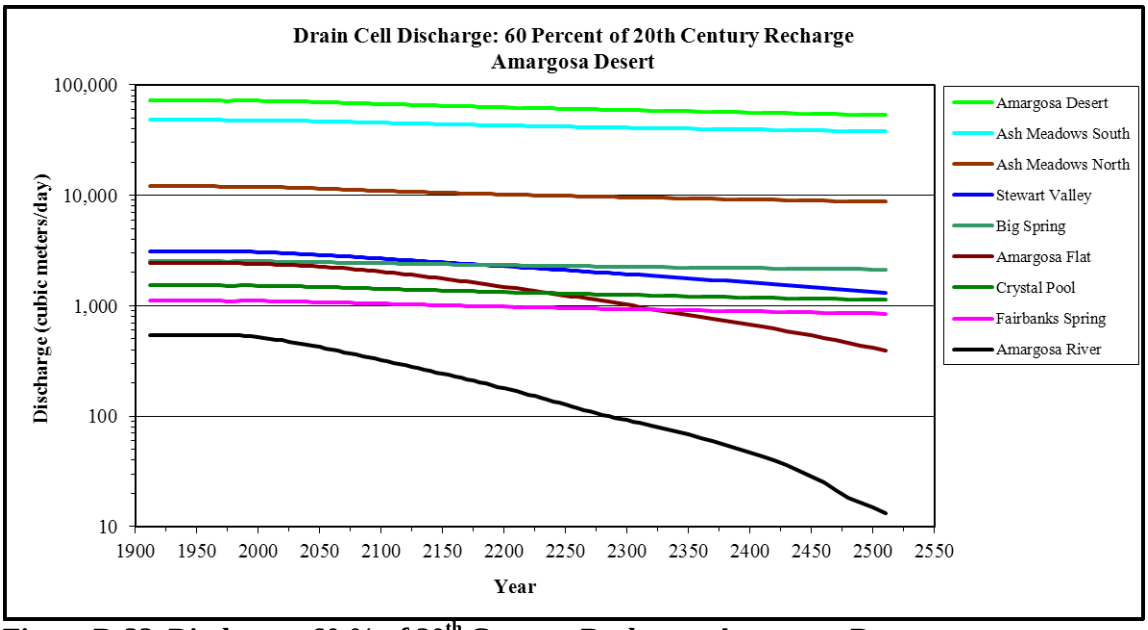

Figure D-32. Discharge: 60 % of 20th Century Recharge, Amargosa Desert

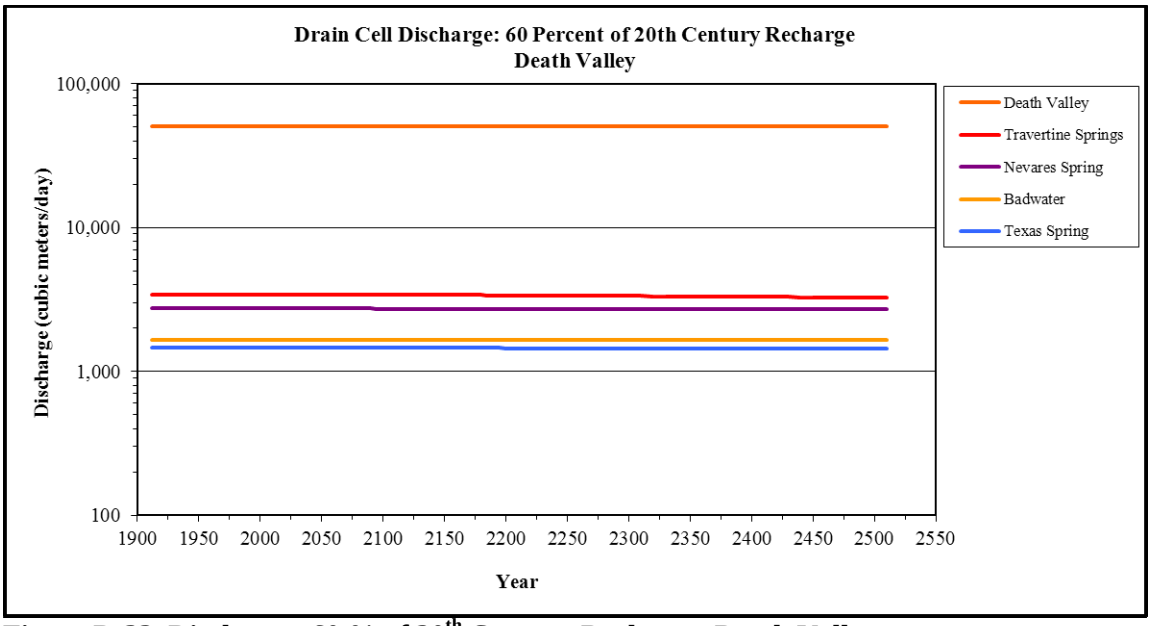

Figure D-33. Discharge: 60 % of 20th Century Recharge, Death Valley